

© 2021 Albert E. Patterson

MESO-SCALE FDM MATERIAL LAYOUT DESIGN STRATEGIES UNDER
MANUFACTURABILITY CONSTRAINTS AND FRACTURE CONDITIONS

BY

ALBERT E. PATTERSON

DISSERTATION

Submitted in partial fulfillment of the requirements
for the degree of Doctor of Philosophy in Industrial Engineering
in the Graduate College of the
University of Illinois Urbana-Champaign, 2021

Urbana, Illinois

Doctoral Committee:

Associate Professor James T. Allison, Chair, Director of Research
Professor Iwona M. Jasiuk, Co-Director of Research
Associate Professor Girish Krishnan
Associate Professor Pingfeng Wang

ABSTRACT

In the manufacturability-driven design (MDD) perspective, manufacturability of the product or system is the most important of the design requirements. In addition to being able to ensure that complex designs (e.g., topology optimization) are manufacturable with a given process or process family, MDD also helps mechanical designers to take advantage of unique process-material effects generated during manufacturing. One of the most recognizable examples of this comes from the scanning-type family of additive manufacturing (AM) processes; the most notable and familiar member of this family is the fused deposition modeling (FDM) or fused filament fabrication (FFF) process. This process works by selectively depositing uniform, approximately isotropic beads or elements of molten thermoplastic material (typically structural engineering plastics) in a series of pre-specified traces to build each layer of the part. There are many interesting 2-D and 3-D mechanical design problems that can be explored by designing the layout of these elements. The resulting structured, hierarchical material (which is both manufacturable and customized layer-by-layer within the limits of the process and material) can be defined as a manufacturing process-driven structured material (MPDSM). This dissertation explores several practical methods for designing these element layouts for 2-D and 3-D meso-scale mechanical problems, focusing ultimately on design-for-fracture. Three different fracture conditions are explored: (1) cases where a crack must be prevented or stopped, (2) cases where the crack must be encouraged or accelerated, and (3) cases where cracks must grow in a simple pre-determined pattern. Several new design tools, including a mapping method for the FDM manufacturability constraints, three major literature reviews, the collection, organization, and analysis of several large (qualitative and quantitative) multi-scale datasets on the fracture behavior of FDM-processed materials, some new experimental equipment, and the refinement of a fast and simple g-code generator based on commercially-available software, were developed and refined to support the design of MPDSMs under fracture conditions. The refined design method and rules were experimentally validated using a series of case studies (involving both design and physical testing of the designs) at the end of the dissertation. Finally, a simple design guide for practicing engineers who are not experts in advanced solid mechanics nor process-tailored materials was developed from the results of this project.

ACKNOWLEDGMENTS

I would like to express my gratitude first to my doctoral advisor, Dr. James T. Allison, for giving me the opportunity to pursue my Ph.D. at the University of Illinois, for being a great mentor by providing helpful guidance while also encouraging me to explore my interests wherever they may lead, and for being willing to learn new areas/fields with me as I conceptualized, explored, refined, and completed the research described in this dissertation. I would like to thank Dr. Iwona Jasiuk, my co-director of research, for her constant guidance, help, and mentorship and for always making time to help or talk to me (sometimes on very short notice) when I needed guidance on some technical aspects of my research. I would like to thank my other committee members Dr. Pingfeng Wang and Dr. Girish Krishnan for their help, guidance, and feedback throughout my dissertation research and writing process. I would like to thank my primary peer research partner and friend Charul Chadha for always being willing to explore new ideas, design/build new experimental equipment, work on tedious months-long literature reviews with me, and for giving me encouragement during stressful times and disappointments in my work.

I would like the Department of Industrial and Enterprise Systems Engineering at the University of Illinois at Urbana-Champaign for providing me a home base from where to complete my research, for several years of funding support that allowed me the freedom to explore my project fully, and for actively promoting my work. Of the other faculty in the ISE department and the Grainger College of Engineering in general, I would especially like to thank Dr. Bob Norris for his years of mentorship and guidance and for helping me learn how to write grant proposals and patent documents and Dr. Molly Goldstein for mentoring and supervising my teaching work and helping me grow and improve greatly as a teacher. I would also like to thank Dr. Henrique Reis, Dr. Harrison Kim, Dr. Yuhang Hu, Dr. John Lambros, Dr. Kai James, and Dr. Randy Ewoldt for their personal advice and helpful teaching which contributed to ideas and approaches for my dissertation research. I would like to thank current and former ISE department administrators Holly Kizer, Shawna Graddy, Aleta Lynch, Tracey Rich, Michael Adams, William Gillespie, Elise Lee, Julie Murphy, Lucas Osborn, and most especially Lauren Redman, for all their help, guidance, and patience helping me navigate the day-to-day paperwork, expectations, and questions that came up during my Ph.D. studies. I would like to thank Dr. Abigail Wooldridge and Dr. Rasoul Etesami specifically for their help and guidance on preparing my documents and application packages for

faculty job applications in the last year of my doctoral studies. I would also like to thank all those involved in my Mavis Future Faculty Fellowship award and my several College of Engineering conference travel awards.

I would like to thank my lab mates and the many excellent other graduate students I met while pursuing my Ph.D., especially those who I worked with or had frequent personal interactions with, including (in alphabetical order by last name): Rashid Anzoom, Madhav Arora, Saeid Bayat, Tonghui Cui, Tianshi Fu, Tinghao Guo, Bayan Hamdan, Dan Herber, Yong Hoon Lee, Rodra Hascaryo, Danny Lohan, Reza Maragheh, Hossein Matin, Tim Murray, Sreekalyan Patiballa, Satya Peddada, Akash Singh, Reza Soleymanifar, Dedy Suryadi, Vedant, and Simon Zhang. I would like to thank my undergraduate and MS student assistants who have worked with me in various capacities over the years at the University of Illinois at Urbana-Champaign, especially Kinga Wrobel, Nick Eikelberner, Lucas Semitka, Adam McCarthy, Bozun Wang, and Yang Yuan.

Finally, at the University of Illinois, I would like to thank the Department of Mechanical Science and Engineering and the Department of Materials Science and Engineering for making me feel welcome as I was pursuing my research, for giving me keys and building access, and for inviting me to seminars and to freely participate in department activities relevant to my research.

I would like to thank my many important professional mentors and supervisors from outside the University of Illinois for their significant professional and personal contributions to my success and/or my decision to pursue this Ph.D., especially Dr. Sherri Messimer, Dr. Christina Carmen, Dr. Phillip Farrington, Dr. Alanna Frost, Dr. Kip Kendrick, Dr. Keith Hollingsworth, Dr. Brad Hembree, Dr. Don Wallace, Dr. Paul Collopy, Dr. Sam Gholston, Harley Hollingsworth, Seth Thompson, Troy Skinner, Steve Collins, James Glenn, David LaChance, Jeff Sexton, Meredith Bain, and Elizabeth Peterson. I would like to thank some additional professionals who all provided some significant direct comments or advice on my work but whom I only interacted with a few times, including: Dr. Bill Bernstein, Dr. Katherine Matlack, Dr. Krishnan Suresh, and Dr. Niao He.

I would like to thank my personal friends who are also practicing engineers and other professionals and who provided me advice, expertise, encouragement, and support during this Ph.D. and/or the process leading me to do it, especially: Tais Rocha Pereira, Ben and Kaila Browning, Nasiha Muna, Taylor Bono, John Kendrick, Robby and Lauren Renz, Matt Mazurkavich, Matt Ray, James Lawler, Kayla Jarratt Henslee, Chad Jones, Phillip Reed, and Raghu Katragadda. I would also like to thank some personal friends and other people who had a positive impact on me during my PhD studies and who contributed to my success through encouragement,

kindness, and help unrelated to academics or work, especially (first names only, in alphabetical order): Alexis, Amber, Callie, Chris, Eric, Gregory, Haley, Jacinthe, Jonathan, James, Kathy, Kimberly, Kyle, Matthew, Mattison, Michael, Molly, Nathan, Nicole, Paul, Sadie, Sandra, Scott, Sheldon, Taylor, Thomas, Vincent, and everyone else not named here who has contributed something positive to my life the past several years.

I would like to thank my family (core, extended, and by marriage) for their support, both morale and financial, through the years I worked on this Ph.D. Thanks particularly to my amazing mom who has been there for me throughout the good and bad days of the past few years and was always there to encourage me in spite of having her own problems and worries to deal with at the time. I would also especially like to thank my aunt and uncle Anna and Joe Stallings for their essential support and constant encouragement. I would like to thank my uncle Dr. John Fair for his advice and encouragement related to becoming a professor, academic writing, and pursuing an academic job. Finally, I would most especially like to thank my maternal grandfather Joseph Abel for inspiring me to be an engineer and to pursue all these years of school and work. Without his example and encouragement throughout my life, I likely would not have attempted this career path.

Dedicated to Joseph Abel

*My brilliant grandfather whose success, encouragement, and example helped inspire me
to dedicate my life to the practice and profession of engineering*

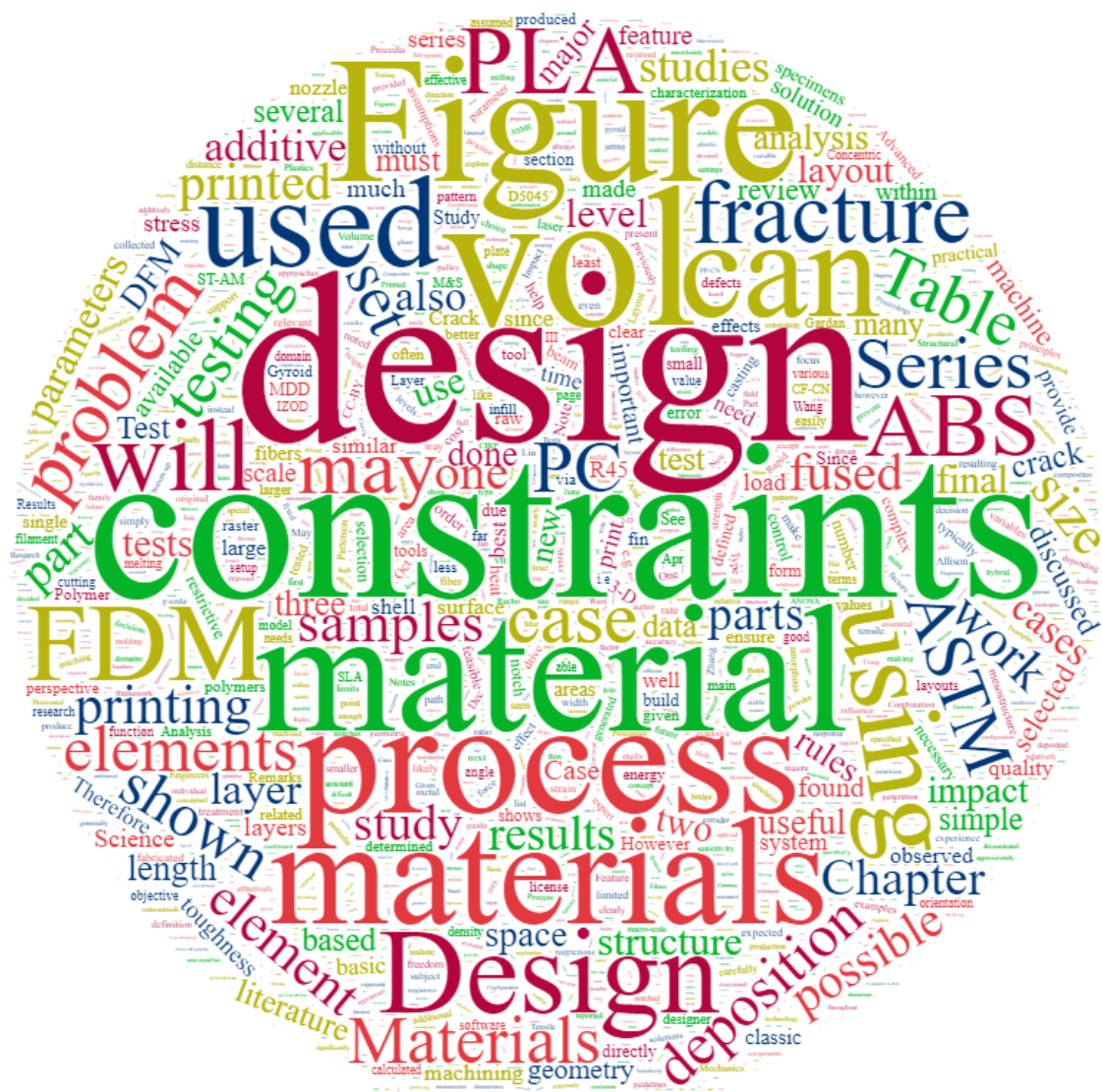
TABLE OF CONTENTS

Word Cloud.....	x
Nomenclature and Acronyms	xi
1. INTRODUCTION	1
1.1. Background and Motivations	1
1.2. Primary Research Objective Statement	4
1.3. Major Contributions	5
1.4. Research Approach	6
1.5. Chapter Outlines and Major Research Questions	9
Chapter 1 Bibliography	14
2. MANUFACTURABILITY CONSTRAINTS FOR MECHANICAL DESIGN	17
2.1. Introduction	17
2.2. Literature Review	20
2.3. MR-DFM Concept Development	41
2.4. General Design Problem Formulation	43
2.5. Constraint Restrictiveness and Dominance	51
2.6. General MR-DFM Framework	53
2.7. Case Studies	56
2.8. Remarks on Inputs and Practical Implementation	69
2.9. Closing Remarks	73
Chapter 2 Bibliography	79
3. FDM MECHANICS AND MANUFACTURABILITY CONSTRAINTS	98
3.1. Introduction	98
3.2. FDM Manufacturability Constraints: Concepts	102
3.3. FDM Material Selection	126
3.4. FDM Manufacturability Constraints: Determination	128

3.5. Case Studies	139
3.6. Closing Remarks	144
Chapter 3 Bibliography	146
4. FDM-DRIVEN STRUCTURED MATERIALS	157
4.1. Introduction	157
4.2. Manufacturability-Driven Design	161
4.3. Mechanics of FDM as Scanning-Type AM Process	165
4.4. Meso-Scale FDM-Driven MPDSMs	166
4.5. Case Studies	177
4.6. Closing Remarks	184
Chapter 4 Bibliography	186
5. FRACTURE MECHANICS AND DESIGN KNOWLEDGE	193
5.1. Introduction	193
5.2. Review: Fracture Methods, Materials, and Standards for FDM Materials	196
5.3. Design Information Gathering from Fracture Studies	207
5.4. Practical Implementation in Design	213
5.5. Closing Remarks	216
Chapter 5 Bibliography	218
6. FDM FRACTURE MECHANICS – PHYSICAL EXPERIMENTS.....	226
6.1. Introduction	226
6.2. Hardware, Equipment, and Software Used	229
6.3. Test Series I: Basic Characterization.....	234
6.4. Test Series II: FDM-Processed Fibers.....	238
6.5. Test Series III: FDM-Processed Films	245
6.6. Test Series IV: ASTM D5045 CT Sample Size Sensitivity	251
6.7. Test Series V: ASTM D5045 CT Notch Sensitivity.....	261
6.8. Test Series VI: Fracture Behavior vs Element Layout	267

6.9. Test Series VII: IZOD Impact Testing	272
6.10. Closing Remarks	283
Chapter 6 Bibliography	285
7. DESIGN RULE DEVELOPMENT FOR FRACTURE-DRIVEN FDM MPDSMS	288
7.1. Introduction	288
7.2. Design Rules under MDD	289
7.3. Fracture Driven FDM MPDSM Design Objectives	290
7.4. Design Knowledge Drivers	292
7.5. Design Rules	297
7.6. Closing Remarks	304
Chapter 7 Bibliography	306
8. DESIGN STUDIES.....	308
8.1. Introduction	308
8.2. Design Study 1: ASTM D5045 CT Layout using Cube Plot Optimization.....	310
8.3. Design Study 2: Plane Stress Field Trace.....	314
8.4. Design Study 3: 2-D Eccentric Beam Re-Design.....	316
8.5. Design Study 4: 3-D Beam Design under Bending and Torsion Load.....	321
Chapter 8 Bibliography	325
9. CONCLUSIONS AND FUTURE WORK.....	326
APPENDIX A: Preliminary Design Guide	328
APPENDIX B: Cura-Based G-Code Generator Tutorial	337
APPENDIX C: Converting G-Code Back to STL with Voxel Mesh	352
APPENDIX D: Calculation Process for K_Q and K_{1c} for Chapter 6	355
APPENDIX E: Experimental Data Sharing and Availability	358
APPENDIX F: Interesting Experimental Figures	359
APPENDIX G: Detailed Review Approaches for Chapter 2 and Chapter 5	366
APPENDIX H: Copyright Permissions for Previously Published Material	381

WORD CLOUD



Created using wordclouds.com

NOMENCLATURE AND ACRONYMS

ABS	Acrylonitrile butadiene styrene
AD	Anderson-Darling test (statistical tool)
AM	Additive manufacturing
ANOVA	Analysis of variance (statistical tool)
ASTM	American Society for Testing and Materials
BJ	Binder jetting
CAD	Computer-aided design
Classic DFM	DFM according to basic principles without adaptations or updates
CNC	Computer-numerical control
CT	Compact tension (experimental specimen)
CTOD	Crack tip opening displacement
DFAM	Design for additive manufacturing
DFM	Design-for-manufacturing or design-for-manufacturability
DoF	Degrees of freedom
DLP	Digital light processing
EBM	Electron beam melting
ED	Externally dominated (by a non-manufacturability constraint)
FDM	Fused deposition modeling
FEA	Finite element analysis
FFF	Fused filament fabrication
FM	Formative manufacturing
FoS	Factor of safety
INCOSE	International Council on Systems Engineering
ID	Internally dominated (by another manufacturability constraint)

ISO	International Organization for Standardization
ISRC.....	Identify-specify-rank-combine process for design requirements
K_{1c}	LEFM plane strain fracture toughness
K_q	Conditional fracture toughness
KW	Kruskal-Wallace test (statistical tool)
LBF	Laser powder bed fusion
LED.....	Light-emitting diode
LEFM.....	Linear elastic fracture mechanics
MDD	Manufacturability-driven design
MfG or Mfg.....	Manufacturing
MM-SC	Multi-material or structural composites (material configuration)
MPDSM	Manufacturing process-driven structured material
MR	Minimally-restrictive (constraints)
MR-DFM	Minimally-restrictive design-for-manufacturability
NASA.....	National Aeronautics and Space Administration
PA	Polyamide (another term to describe nylon)
PC.....	Polycarbonate
PLA	Polylactic acid
PM.....	Powder metallurgy
R45.....	Standard raster printed at $\pm 45^\circ$
R90.....	Standard raster printed at $0/90^\circ$
SENB	Single-edge notched bending (experimental specimen)
SLA	Laser-based stereolithography
SLM	Selective laser melting
SLS.....	Selective laser sintering
σ_y	Measured yield stress of a material

SM.....	Subtractive manufacturing
SMT	Structured material
ST-AM	Scanning-type AM (process mechanics)
TO	Topology optimization
V&V.....	Verification and validation
VV&C.....	Verification, validation, and certification

Chapter 1

INTRODUCTION

1.1 Background and Motivations

One of the most important issues currently in both mechanical design and manufacturing science is the (sometimes severe) mismatch between modern advanced design methods (e.g., topology optimization, optimal design, and generative design) and the existing and developing manufacturing processes [1–6]. Design and manufacturing methods for most common products were roughly equivalent in terms of refinement in the 1980s and 1990s after decades of development and refinement in design-for-manufacturability (DFM) principles [5–9]. Beginning in the late 1990s (and especially after about 2010) there has been an “arms race” of sorts to develop and refine new design methods based on new design knowledge development, the birth and spread of additive manufacturing (AM), better and cheaper computers and optimization tools, and other such real or perceived advances [10–21]. A major result of this is that the available manufacturing methods, including AM, cannot fabricate a large portion of modern designs.

There was a lot of hope and optimism that the advancement of AM would (eventually) help mitigate these issues and provide an advanced manufacturing paradigm worthy of the new world of advanced design methods [15–17, 22–24]. Sadly, this has not come to pass for a wide variety of reasons; it is becoming clear that AM is not only *not* the silver bullet for many difficult manufacturing problems but that in some ways it can be more limited and restrictive than traditional subtractive and formative processes. In realistic application, AM is another family of processes (many of them directly derivative from

traditional processes) which can offer an expanded range of manufacturing options and cover some areas previously not possible. It is very unlikely to replace much of the traditional manufacturing process catalog but will simply be a useful supplement to it. This is not to discount the impact and importance of AM; the advancement of AM has been a tremendous leap forward for engineering and technology. However the fact remains (even if it was more widely useful) that AM and other processes have not thus far been able to keep up with the rapidly advancing world of design methods. Therefore, the mis-match remains and must be accounted for. Figure 1.1 shows some examples of extremely complex designs which may or may not be manufacturable depending on the applied constraints and limitations.

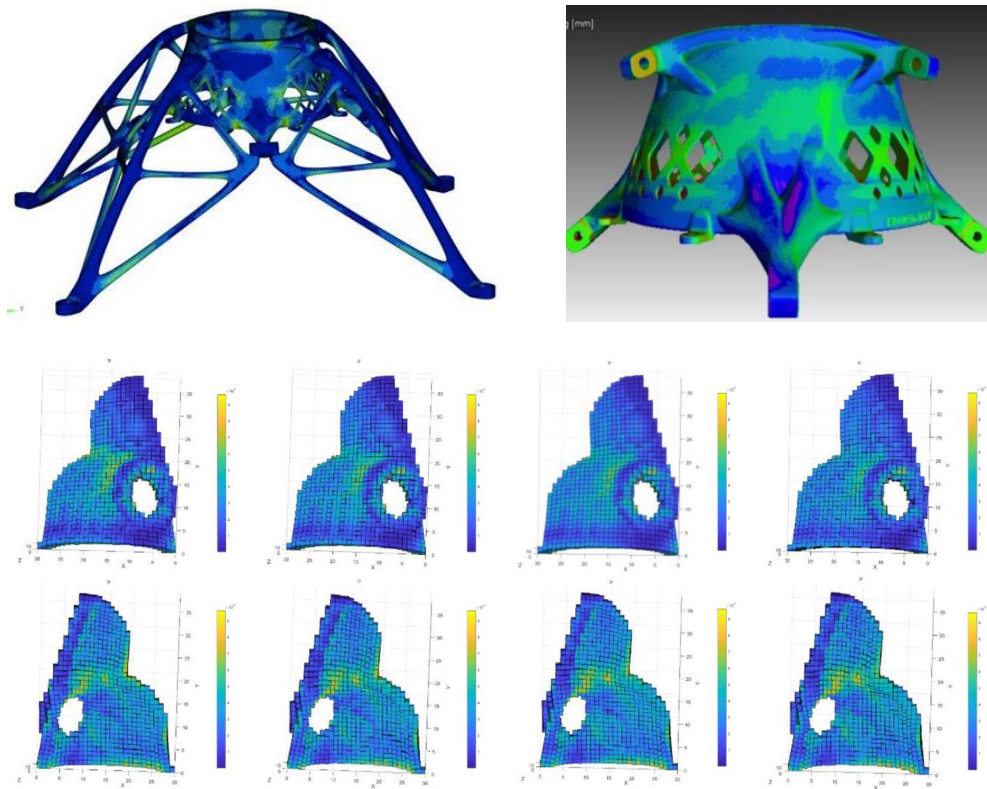


Figure 1.1: Examples of advanced designs which may or may not be manufacturing using the much more limited modern manufacturing technologies. Figures from [25, 26] and reproduced here under the terms of their original CC-BY open access license.

The major question on the table is how to account for the design-manufacturing mis-match and ensure manufacturability without erasing the advantages of modern design meth-

ods or promising unrealistic solutions from the manufacturing side. In general, classic design for manufacturability (DFM) methods strongly prioritize design simplification, liberal tolerances, the use of non-specialized materials, and similar goals [6–8, 11, 20, 27, 28]. In many cases, these goals are directly opposed to the goals and capability of many advanced design processes and so are not useful or desirable for this purpose. One promising method of dealing with this is to impose direct process-driven constraints in the design problem itself implicitly or explicitly in the problem formulation; this has been quite effective in some areas, particularly in topology optimization [1, 29–34].

This suggests the need for a new design perspective in which manufacturability is the prime or co-prime design requirement; in this dissertation, this concept is defined as *manufacturability-driven design* (MDD). The concept is simple: instead of generating a candidate design or set of candidates and then selecting from among the manufacturable ones, this simply restricts the initial design space to only manufacturable designs. Therefore, any candidate design produced (subject to the quality of the modeling and design space definition, of course) is manufacturable. Therefore, the designers can focus on generating or selecting the best design freely since manufacturability has already been accounted for. It is true that the set of design candidates after the design space restrictions will be smaller than one without the constraints; however, the final set of designs which are both desirable (as judged by the project requirements) and manufacturable should be approximately the same size using either approach in the end. However, the candidates which were not subject to any kind of manufacturability constraints early in the life cycle may have to be individually tested or evaluated for it. This can waste a significant amount of time and resources during the design life cycle, especially in one of those common cases where this evaluation can only happen at the prototyping stage or later.

It may seem at first glance that MDD could be extremely restrictive and counteract the advantages of modern design methods as much or more than DFM. However, in practice the opposite is true. Not only does it allow much more design complexity than classic DFM (by leaving open the entire manufacturable design space), but it allows process-material interactions to be observed clearly. Looking at scanning-type AM (ST-AM) processes (those which trace out layers as a collection of lines, versus processes which project entire layers at

once or sections like an inkjet printer), this benefit is especially clear. The process (which could be fused deposition modeling (FDM), laser powder bed processes (SLS, SLM, and similar), laser-based stereolithography (SLA), or a number of others) builds up the geometry using a series of material elements, each of which is approximately isotropic or transversely isotropic. These elements generally have a uniform cross section throughout a part and when laid out in a desired 2-D pattern, form a layer of the part which are then all collected into the whole part. The resulting 3-D structure at the macro-scale is highly anisotropic and can be thought of something like a collection of layers, each of which is a sort of dense truss made up of the fundamental elements. Thinking in terms of bottom-up design, if each of the elements are manufacturable, then then layers made up of them are also manufacturable. If the layers are manufacturable, the entire 3-D structure is manufacturable. Understanding these ST-AM processes from the MDD perspective allows a new design approach to be developed and refined here.

This dissertation explores this concept in depth and applies it to the design of meso-scale structured materials under MDD for which the mechanical load is fracture. They may be designed to stop or prevent cracks, accelerate cracks, or control the pattern of a crack as it forms. The design approach developed is valid for both 2-D and 3-D structures, as demonstrated in the case studies at the end. The manufacturing process used is fused deposition modeling (FDM) and the materials used are acrylonitrile butadiene styrene (ABS), polylactic acid (PLA), and polycarbonate (PC). ABS and PC are common engineering plastics derived from petroleum-based hydrocarbons, while PLA is a biomaterial sourced from renewable sources which as corn and sugar cane. All are thermoplastics and can be easily processed using FDM.

1.2 Primary Research Objective Statement

The primary research objective of this dissertation is to *develop a bottom-up design method based on MDD to build and fabricate manufacturable meso-scale thermoplastic structured materials under fracture conditions which will be fabricated via FDM*. This is mostly new work (previous work will be discussed in each chapter) and is built from the ground up based

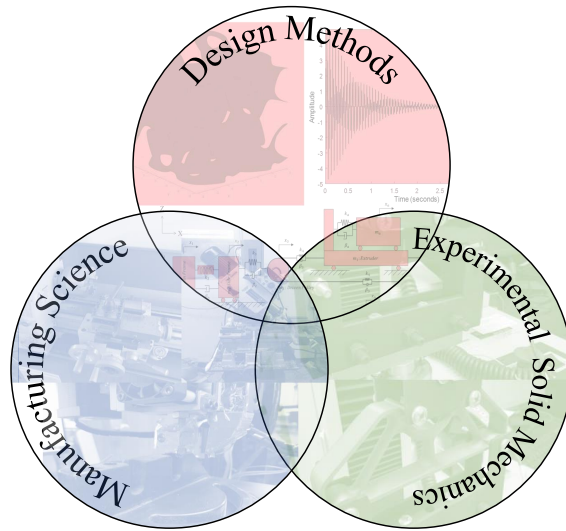


Figure 1.2: Relationship between design methods, manufacturing science, and experimental mechanics

on knowledge and observations from mechanical design principles and manufacturing process behavior. No similar design processes currently exist for reference, so the development from fundamental knowledge is necessary. This problem lies at the heart of the intersection between mechanical design, manufacturing science, and mechanics (Figure 1.2); knowledge and intuition toward its definition and refinement come from all three domains. Its solution will also benefit all three, helping to further illuminate and develop connections and synergies between them.

1.3 Major Contributions

This dissertation had seven major intellectual contributions, in addition to a variety of secondary ones addressed in each chapter. These major novel contributions are:

1. The completion of four major literature reviews on design under manufacturability constraints, the fracture testing of FDM materials, the mechanics and constraints related to FDM, and the basic principles and history of structured materials. This involved the review and synthesis of more than 500 unique papers. Three of the reviews were extensive and useful enough to be published on their own as articles in peer-reviewed academic journals.

2. The development of a general method for capturing and mapping manufacturability constraints for mechanical design problems, verified experimentally through several design studies.
3. The application of the mapping and manufacturability constraints method to the complete mapping of a new manufacturing process (FDM). This included developing and validating the full set of manufacturability constraints (which can now be used automatically).
4. The development and validation of a bottom-up design method for manufacturing process-driven structured materials (MPDSMs) for general structural problems. Design studies for this method used expert intuition, topology optimization, and other methods successfully.
5. The completion of a large course of fracture mechanics experiments, focusing on seven different major areas, and interpretation of the results relative to design.
6. The development and experimental validation of a set of rigorous design rules for the design of MPDSMs under fracture problems using several different objective functions and design approaches.
7. Most importantly, every new model, concept, tool, or design approach presented in the dissertation were experimentally validated, even if the demonstrated ideas were originally derived from experimental data.

In addition to the major academic contributions, several new conclusions related to fracture testing of FDM materials, some new experimental and design equipment, and a g-code generator based on Ultimaker[®] Cura[®] and Autodesk[®] Inventor[®] were developed.

1.4 Research Approach

In this dissertation, each of the major chapters contain their own research questions, objectives, intellectual contributions, and literature reviews (as appropriate), so these will not be

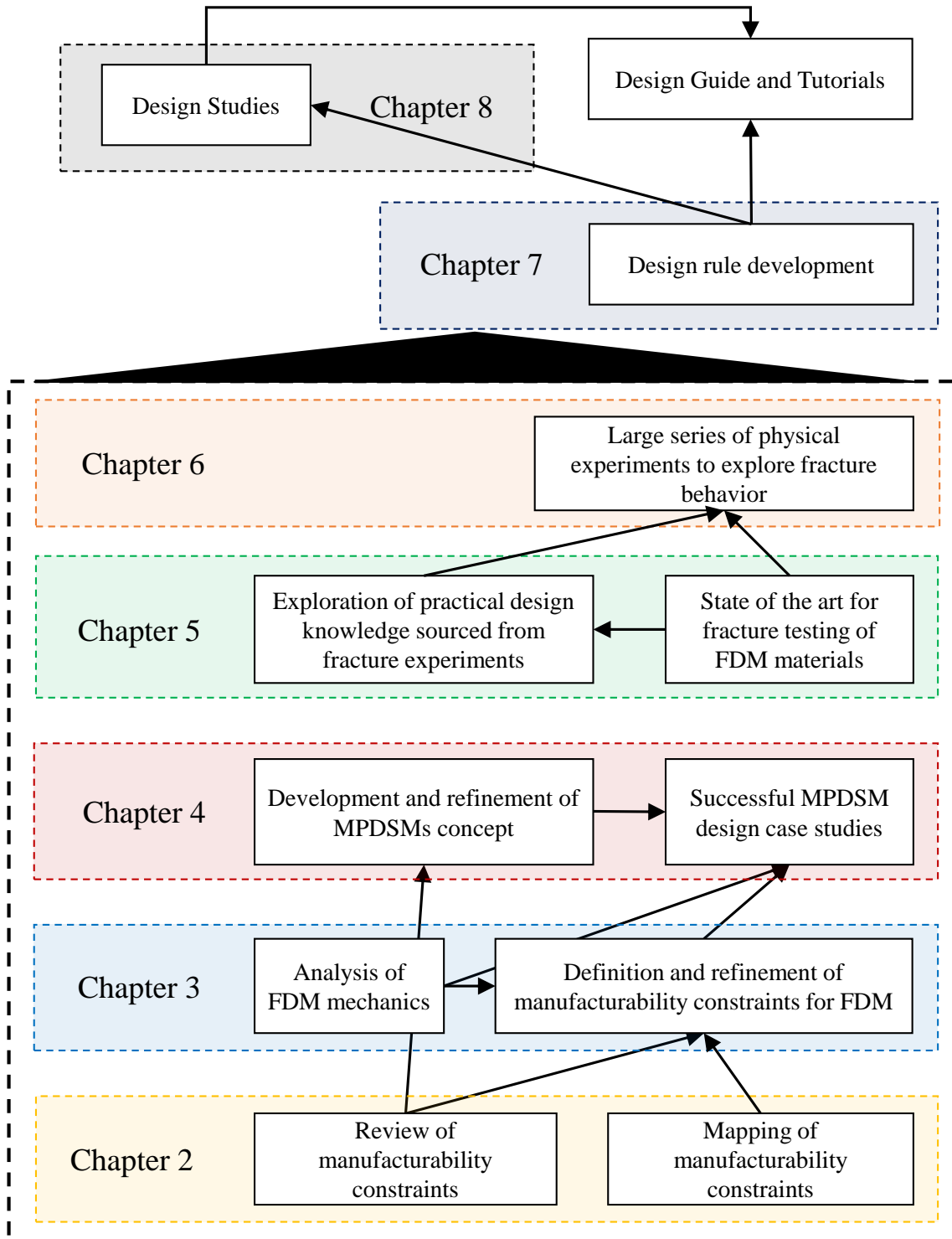


Figure 1.3: Organization and relationship of various topics and chapters in this dissertation

described in detail here. This section presents a general summary to demonstrate the approach taken and the ordered relationship of the topics covered. Two major requirements, unrelated to the dissertation directly but helping to guide its approach, were established in order to make the work useful for practicing engineers and designers who are not experts in the individual topics. There were:

1. Only commercially-available software tools available to practicing engineers and designers should be used if at all possible.
2. Simulations should be avoided and everything possible should be experimentally validated, from the full set of proposed design rules to the development of small tools to support the experiments.

The bottom-up development of the design approach described in the primary research objective was done in several major steps, as shown in Figure 1.3. Beginning with a very deep literature review on the topic of manufacturability constraints, the first effort develops a method for capturing and mapping this vital information. This is then applied to the FDM process, producing a very clear and well-defined set of manufacturability constraints for this process. Using the manufacturability constraint set and principles from classic structured materials, the idea of an MDD-driven structured material is introduced and developed. The various components, requirements, and implementation strategies are discussed for this new class of structured materials, known as manufacturing process-driven structured materials (MPDSMs). Up to this point, the concepts behind manufacturable FDM-driven structured materials had been described and refined. Next, a deep exploration of the literature on experimental fracture mechanics of FDM-processed materials was done and used to drive a large set of physical experiments to observe (both qualitatively and quantitatively) how these materials may behave under fracture conditions. The material and principles from all of the previous chapters were then used to develop a set of design rules for making and fabricating FDM MPDSMs under fracture conditions. These rules were then used to drive five major case studies on designing such structured materials, showing that they are manufacturable, and that the objectives of the design have been met in each case. Finally, a practical design guide and some helpful tutorials are presented in the appendices to ensure

that the developed method is useful for practicing engineers and designers who are not experts in fracture mechanics, AM, or structured materials.

1.5 Chapter Outlines and Major Research Questions

This dissertation can be divided into three major sections, as shown in Figure 1.4. The purpose of the first is to establish and refine the concept of structured materials which are subject to well-defined manufacturability constraints, the second explored fracture-driven design, and the third combined the manufacturable structured materials with a mechanical load driven by fracture and developed design rules and layout strategies for these cases. Summaries of the individual chapters are given below, including their major research questions.

- **Chapter 2** is focused on establishing the need for a general manufacturability constraint mapping method and proposing such a method. An extensive literature review is presented, covering the question from a variety of design perspectives and design scales. The information from this review is then used to assist in developing a general mapping method from basic manufacturing knowledge. The main contribution from this chapter to the other chapters was a refined method for finding and imposing the constraints necessary for manufacturable structured materials. Several design case studies were completed to demonstrate and validate the method. The major research questions were:

1. *How have manufacturability problems for complex modern designs been addressed in the past and how successful have those approaches been?* This question was answered through a literature review and implicitly in the design studies.
2. *Have the techniques used to ensure manufacturability severely restricted the design space or solution methods available to designers?* This question was answered through the literature review.
3. *Given that the literature shows overwhelming evidence that manufacturability constraints can be applied without major limitations on the designs themselves,*

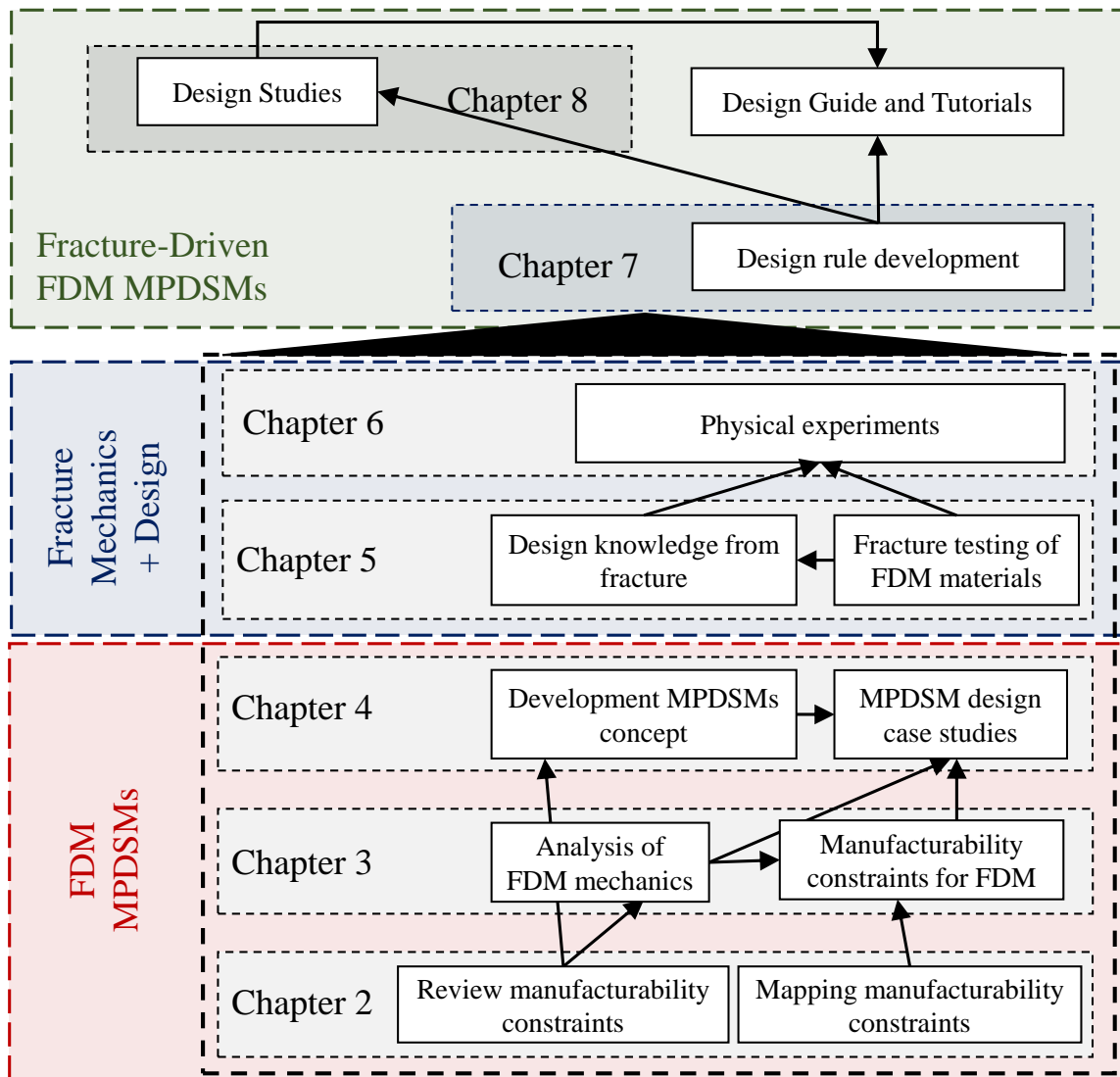


Figure 1.4: Basic sections and the chapters in each.

how might these constraints be collected, defined, and mapped for more general cases? This question was answered by development of the minimally-restrictive DFM (MR-DFM) technique.

4. How effective is the mapping and constraint imposition method for real-world problems? This question was answered through three large design studies, one using a single process, one using two processes in the same family, and one using two unrelated processes in a sequential hybrid configuration. In all cases, the designs were shown to fail without the manufacturability constraints and to be

successful on the first try with them imposed. The small trade-offs involved are also discussed.

- **Chapter 3** extends Chapter 2, but for a single process (fused deposition modeling (FDM)). Chapter 3 is focused on the careful application of the Chapter 2 principles to a specific process, collecting all the relevant manufacturing process knowledge and mapping this directly into a set of 54 well-defined and material-independent FDM manufacturability constraints. The constraints are further refined and subject to a sensitivity analysis once a set of materials (ABS, polycarbonate, and PLA) are selected for it. The constraints and approach are experimentally validated in a series of three major design studies which depend on the constraints for success. Since this chapter focused on application, there were no new specific research questions beyond those explored in Chapter 2.
- **Chapter 4** explores the concepts behind applying the MDD approach to the design of structured materials (SMs), especially those based on controllable process-material effects (such as those seen in most AM processes). The chapter includes a review of structured materials and SM design, helping to develop a simple but effective design framework for creating a new class of structured materials known as *manufacturing process-driven structured materials* (MPDSMs). After the framework is defined and methods established for imposing the FDM manufacturability constraints, a series of three major design studies are presented to demonstrate and validate the approach. The major research questions were:
 1. *How are structured materials defined?* This question was answered with a short literature review.
 2. *What does it mean for a structured material to be manufacturable and what design freedom trade-offs are necessary to accomplish this?* This was answered both by a literature review and conceptual development from basic technical definitions.
 3. *How can the manufacturability constraints from Chapter 2 and Chapter 3 be effectively applied and enforced?* This question was answered by developing an MDD-based bottom-up design framework.

4. *Given that the best design approach for MPDSMs is bottom-up, how can the basic material elements be described and defined in a way that is consistent with the current literature and SM design principles?* This question was answered via MDD-based model development and basic knowledge about the mechanics of FDM.
 5. *What types of mechanical loads can be used on these MPDSMs?* This question was not explored for every possible load, but the three most common failure modes (buckling, yielding, and fracture) were discussed within the development framework and used in the design studies.
- **Chapter 5** kicks off the fracture mechanics portion of the dissertation and was intended to be mainly a conceptual chapter to show why studying mechanical design from a fracture mechanics perspective is valuable. The chapter is mainly based on the review and deep analysis of a set of published fracture mechanics studies using FDM-processed materials. The main research questions were:
 1. *What are the fracture tests and standards that have been used to analyze FDM-processed materials and what materials have been tested?* This question was answered through a detailed literature review.
 2. *What types of design knowledge can be extracted from fracture studies, both qualitative and quantitative?* This was answered through a combination of literature review and conceptual analysis.
 3. *What approaches to testing might produce the most valuable design knowledge?* This was answered partially through the literature review and partially through deep analysis of the collected data.
 4. *How can fracture testing and its related tools and assumptions be improved to provide even more valuable design knowledge?* This was answered via deep analysis and critical appraisal of the collected studies.
 - **Chapter 6** continues the discussion from Chapter 5 about the role (both actual and potential) of fracture mechanics data in design. In Chapter 6, a series of major

experimental studies are undertaken to collect realistic data and make conclusions about the behavior of the FDM-printed materials.

1. Series I examined the basic mechanical properties of the macro-scale printed materials in order to collect baseline properties for each.
 2. Series II looked at the behavior of FDM-processed fibers (i.e., the essential building blocks of MPDSMs) from the perspectives of extruded individual fibers, deposited individual fibers, and series-printed fibers.
 3. Series III explored the behavior of films, meant to represent individual layers built from a series of fibers. Both notched and un-notched films were used.
 4. Series IV helped determine the impact of the sample size on the results, showing that the sample size (within the tested range) had no statistically significant impact on the fracture toughness of the materials.
 5. Series V looked at the sensitivity of the samples to notching and pre-cracking method used to prepare them.
 6. Series VI provided a qualitative and quantitative analysis of crack behavior relative to a series of pre-determined element layouts.
 7. Series VII examined the impact of element layout on the fracture properties under impact using a standard IZOD test.
- **Chapter 7** compiled the results and conclusions from the previous chapters and presented a series of designed rules and guidance for producing MPDSMs.
 - **Chapter 8** completed the research work for the dissertation by exploring four detailed design studies which used the derived design rules and other tools developed in the previous chapters.
 - **Chapter 9** wraps up the dissertation with some concluding remarks and suggestions for future research directions.

Chapter 1 Bibliography

- [1] S. L. Vatanabe, T. N. Lippi, C. R. de Lima, G. H. Paulino, and E. C. Silva, “Topology optimization with manufacturing constraints: A unified projection-based approach,” *Advances in Engineering Software*, vol. 100, pp. 97–112, 2016.
- [2] G. A. Adam and D. Zimmer, “Design for additive manufacturing - element transitions and aggregated structures,” *CIRP Journal of Manufacturing Science and Technology*, vol. 7, no. 1, pp. 20–28, 2014.
- [3] Y. Reich, S. L. Konda, S. N. Levy, I. A. Monarch, and E. Subrahmanian, “New roles for machine learning in design,” *Artificial Intelligence in Engineering*, vol. 8, no. 3, pp. 165–181, 1993.
- [4] A. Sutradhar, J. Park, P. Haghghi, J. Kresslein, D. Detwiler, and J. J. Shah, “Incorporating manufacturing constraints in topology optimization methods: A survey,” in *Volume 1: 37th Computers and Information in Engineering Conference*, ASME, 2017.
- [5] B. S. Blanchard and W. J. Fabrycky, *Systems Engineering and Analysis (4th Edition)*. Prentice Hall, 2005.
- [6] J. G. Bralla, *Design for Manufacturability Handbook (2nd Edition)*. McGraw-Hill Education, 1998.
- [7] G. Boothroyd, “Product design for manufacture and assembly,” *Computer-Aided Design*, vol. 26, no. 7, pp. 505–520, 1994.
- [8] G. Pahl, W. Beitz, J. Feldhusen, and K. H. Grote, *Engineering Design: A Systematic Approach (3rd Edition)*. Springer, 2007.
- [9] T. T. Pullan, M. Bhasi, and G. Madhu, “Application of concurrent engineering in manufacturing industry,” *International Journal of Computer Integrated Manufacturing*, vol. 23, no. 5, pp. 425–440, 2010.
- [10] J. W. Herrmann, J. Cooper, S. K. Gupta, C. C. Hayes, K. Ishii, D. Kazmer, P. A. Sandborn, and W. H. Wood, “New directions in design for manufacturing,” in *Volume 3d: 8th Design for Manufacturing Conference*, ASME, 2004.

- [11] P. Barnawal, M. C. Dorneich, M. C. Frank, and F. Peters, “Evaluation of design feedback modality in design for manufacturability,” *Journal of Mechanical Design*, vol. 139, no. 9, p. 094503, 2017.
- [12] S. J. Hu, “Evolving paradigms of manufacturing: From mass production to mass customization and personalization,” *Procedia CIRP*, vol. 7, pp. 3–8, 2013.
- [13] C. R. Duguay, S. Landry, and F. Pasin, “From mass production to flexible/agile production,” *International Journal of Operations & Production Management*, vol. 17, no. 12, pp. 1183–1195, 1997.
- [14] A. Gelsey, M. Schwabacher, and D. Smith, “Using modeling knowledge to guide design space search,” *Artificial Intelligence*, vol. 101, no. 1-2, pp. 35–62, 1998.
- [15] N. Guo and M. C. Leu, “Additive manufacturing: technology, applications and research needs,” *Frontiers of Mechanical Engineering*, vol. 8, no. 3, pp. 215–243, 2013.
- [16] I. Gibson, D. Rosen, and B. Stucker, *Additive Manufacturing Technologies: 3D Printing, Rapid Prototyping, and Direct Digital Manufacturing*. Springer, 2016.
- [17] M. K. Thompson, G. Moroni, T. Vaneker, G. Fadel, R. I. Campbell, I. Gibson, A. Bernard, J. Schulz, P. Graf, B. Ahuja, and F. Martina, “Design for additive manufacturing: Trends, opportunities, considerations, and constraints,” *CIRP Annals*, vol. 65, no. 2, pp. 737–760, 2016.
- [18] T. Simpson, J. Peplinski, P. Kock, and J. Allen, “Metamodels for computer-based engineering design: Survey and recommendations,” *Engineering with Computers*, vol. 17, pp. 129–150, 2001.
- [19] P. Y. Papalambros and D. J. Wilde, *Principles of Optimal Design: Modeling and Computation (2d Edition)*. Cambridge University Press, 2000.
- [20] W.-S. Chu, M.-S. Kim, K.-H. Jang, J.-H. Song, H. Rodrigue, and et al., “From design for manufacturing (DFM) to manufacturing for design (MFD) via hybrid manufacturing and smart factory: A review and perspective of paradigm shift,” *International Journal of Precision Engineering and Manufacturing-Green Technology*, vol. 3, no. 2, pp. 209–222, 2016.
- [21] J. Vallhagen, O. Isaksson, R. Söderberg, and K. Wärmefjord, “A framework for producibility and design for manufacturing requirements in a system engineering context,” *Procedia CIRP*, vol. 11, pp. 145–150, 2013.
- [22] A. Gebhardt and J.-S. Hotter, *Additive Manufacturing: 3D Printing for Prototyping and Manufacturing*. Hanser Publications, 2016.
- [23] S. H. Huang, P. Liu, A. Mokasdar, and L. Hou, “Additive manufacturing and its societal impact: a literature review,” *The International Journal of Advanced Manufacturing Technology*, vol. 67, no. 5-8, pp. 1191–1203, 2012.

- [24] M. Baumers, P. Dickens, C. Tuck, and R. Hague, “The cost of additive manufacturing: machine productivity, economies of scale and technology-push,” *Technological Forecasting and Social Change*, vol. 102, pp. 193–201, 2016.
- [25] M. Orme, I. Madera, M. Gschweidl, and M. Ferrari, “Topology optimization for additive manufacturing as an enabler for light weight flight hardware,” *Designs*, vol. 2, p. 51, Nov. 2018.
- [26] H. Sun and L. Ma, “Generative design by using exploration approaches of reinforcement learning in density-based structural topology optimization,” *Designs*, vol. 4, p. 10, May 2020.
- [27] E. Lutters, F. J. van Houten, A. Bernard, E. Mermoz, and C. S. Schutte, “Tools and techniques for product design,” *CIRP Annals*, vol. 63, no. 2, pp. 607–630, 2014.
- [28] L. Howard and H. Lewis, “The development of a database system to optimise manufacturing processes during design,” *Journal of Materials Processing Technology*, vol. 134, no. 3, pp. 374–382, 2003.
- [29] A. M. Mirzendehtdel and K. Suresh, “Support structure constrained topology optimization for additive manufacturing,” *Computer-Aided Design*, vol. 81, pp. 1–13, 2016.
- [30] M. Iyengar and A. Bar-Cohen, “Design for manufacturability of SISE parallel plate forced convection heat sinks,” *IEEE Transactions on Components and Packaging Technologies*, vol. 24, no. 2, pp. 150–158, 2001.
- [31] H. Li, P. Li, L. Gao, L. Zhang, and T. Wu, “A level set method for topological shape optimization of 3d structures with extrusion constraints,” *Computer Methods in Applied Mechanics and Engineering*, vol. 283, pp. 615–635, 2015.
- [32] S. Mantovani, I. L. Presti, L. Cavazzoni, and A. Baldini, “Influence of manufacturing constraints on the topology optimization of an automotive dashboard,” *Procedia Manufacturing*, vol. 11, pp. 1700–1708, 2017.
- [33] J. K. Guest and M. Zhu, “Casting and milling restrictions in topology optimization via projection-based algorithms,” in *Volume 3: 38th Design Automation Conference, Parts A and B*, ASME, 2012.
- [34] N. Morris, A. Butscher, and F. Iorio, “A subtractive manufacturing constraint for level set topology optimization,” *Structural and Multidisciplinary Optimization*, vol. 61, pp. 1573–1588, Feb. 2020.

Chapter 2

MANUFACTURABILITY CONSTRAINTS FOR MECHANICAL DESIGN

Collaborator Acknowledgement: The author gratefully acknowledges the contributions, advice, direction, and feedback from the following people on the work presented in this chapter: **Dr. James T. Allison** (help with mathematical formulation and design automation perspective); **Dr. Yong Hoon Lee** (collaborator on literature review); **Dr. Bill Bernstein** and **Dr. Dan Herber** (extensive informal feedback on mapping concepts); **Dr. Sherri Messimer**, **Dr. Katherine Matlack**, **Dr. Danny Lohan**, **Dr. Krishnan Suresh**, and **Dr. Niao He** (challenging discussion and feedback on concept development).

This chapter may contain previously published text and figures, which are reproduced with the permission of the copyright holders. See the copyright statement and list of references at the end of the chapter

2.1 Introduction

Recent years have seen much advancement in the sophistication of mechanical design methods, both for the design of individual parts and integrated assemblies/systems. Many of these new techniques for design genesis focus on design automation, in which large areas

of a given design space can be explored in a quick and efficient way and a large number of candidate designs can be compared quickly. Some good examples are the development of generative design [1, 2], topology optimization [3, 4], candidate architecture analysis for mechanical systems [5, 6], and machine learning for analyzing and selecting potential designs [7, 8]. Such methods are steadily increasing in their level of maturity, but problems remain which restrict their usefulness in final product design. A particular concern that has not yet been fully addressed is the manufacturability of the final designs. While these and other advanced design methods can produce very sophisticated and nearly-ideal parts in terms of performance and other metrics, the designs are often extremely complex and not easily manufacturable using conventional fabrication methods, including with additive manufacturing techniques [9–12]. This is the case for both macro-level user products and design problems at smaller scales (e.g., structured material design, micro-scale design features, and similar areas of interest).

Realization of the final design is one of the most important considerations of a product lifecycle but it is often overlooked or deprioritized by designers, especially at the earlier stages and in requirements definition [13, 14]. When the manufacturing process can be selected after the completion of the design, this can speed up the design process and reduce the number of design requirements; however, this presents the risk of mis-match between the final product and any available fabrication processes [9, 13, 15, 16]. When this mis-match is encountered, the final design may need to be sent back for additional iterations. This generally increases the cost and schedule risk significantly and may, in extreme cases, require revising the requirements from scratch [17, 18].

The mis-match risk may be low if the product is simple (e.g., an injection molded plastic cup) or is a member of an established product family that was shown to work well in the past (e.g., a set of socket wrenches). However, when the design is relatively complex, the risk can be high that the product is completely un-manufacturable with any available process [9, 10, 16]. Traditionally, this problem was addressed using design-for-manufacturability (DFM) principles; these principles were developed as a set of guidelines or heuristics to simplify the manufacturing requirements to the point where several processes could be feasible and the risk of mis-match is low [16, 19–21]. However, these rules can be

very vague and simplistic and often require expert judgement (and experience) to apply effectively to particular design problems. Therefore, traditional DFM rules often clash with design automation objectives. According to Bralla [16] and Boothroyd [18], traditional DFM can be summarized in five basic rules:

1. Prioritize geometric simplicity whenever possible
2. Select the most common, cost-effective, and easily-processed materials available which will function acceptably
3. Avoid designing new parts for a system and use as many existing parts (e.g., fasteners or gears) as possible
4. Make the tolerances for the parts as loose as possible while ensuring acceptable performance and reliability when used in an assembly or other system
5. Make sure that the experiences and opinions of manufacturing personnel are considered when making design decisions

In principle, DFM rules are process- and material-independent, and are designed to be generally-applicable to most design-production problems [16, 19, 22]. The classic DFM approach has proven very effective when creating simple, mass-produced products, but tends to be far too restrictive for complex or specialized products, prioritizing simplicity over optimal configuration or performance [16, 23, 24].

In the past couple of decades, partially aided by emerging advanced design and production methods and a renewed focus on user-centered design, the traditional mass-production focus has been shifting to a mass-customization environment [25–27]. In such an environment with small-batch, high-value part production, it is vital for designers to have access to as much of the product design space as possible in order to produce useful designs for complex problems such as those encountered in the medical and aerospace industries [28–31]. Therefore, it is necessary for a DFM technique to be developed and used which guarantees (or at least better ensures) manufacturability while restricting the design space as little as possible; this will allow more rigorous problem formulations and will prevent missing potentially feasible regions of the design space. In this context, the *design space* is the set

of feasible solutions for a given design problem which satisfy the constraints and objectives of the problem.

To accomplish this, traditional DFM must be refined or replaced with well-defined, manufacturing-process-driven design constraints which can be customized for each design problem or even each design feature. This would involve explicitly imposing the manufacturability constraints in the problem formulation or requirements definition, instead of simply checking manufacturability post-design or simplifying the design the point of low-risk manufacturing. This concept can be referred to as *minimally-restrictive design-for-manufacturability* or MR-DFM and is the subject of this chapter. Significant work has been invested into developing MR-DFM approaches for some very specific problems, but any kind of general process- and solver-independent method for defining, mapping, and enforcing these constraints does not yet exist. Section 2.2 presents an extensive literature review on this question. Taking lessons learned from the literature review and fundamental knowledge of the design life cycle process, Section 2.3 explores MR-DFM from a conceptual perspective. From here, Section 2.4 outlines a general problem formulation approach for capturing and mapping the manufacturability constraints. Section 2.5 examines the restrictiveness and dominance of different kinds of constraints and attempts to classify them for convenience during mapping. A general framework for applying MR-DFM is presented in Section 2.6, followed by three extensive case studies to demonstrate the process in Section 2.7. Finally, some remarks on inputs and practical implementation of MR-DFM and future work needed are given in Sections 2.8 and 2.9, respectively.

2.2 Literature Review

This section presents an extensive literature review on manufacturability constraints and MR-DFM concepts (as defined in Section 2.1). This review had four main objectives: (1) Collect definitions for relevant technologies and concepts, (2) find the state-of-the-art related to manufacturability constraints, their formulation, and their enforcement, (3) ensure that the MR-DFM concept for general mechanical design was feasible and novel, and (4) identify holes and gaps in the current literature related to this problem. More details related to the review approach and performance are given in Appendix G.

2.2.1 Basic Definitions

Any manufacturing process can be said to be subject to a set of natural *manufacturing constraints* which affect its use domain and which must be considered in the design process. In addition, it is necessary to consider *manufacturability constraints*, which are on the design or product itself and are in response to the manufacturing constraints. For example, a machined aluminum part design (Figure 2.1) would be constrained by the tool size, speed, and feed of the mill [32], the level of position error/vibration, and the heat dissipation rate of the selected material (manufacturing constraints). Driven by these constraints, a minimum feature size is necessary to ensure that the part could dissipate the heat and force of machining without warping [33,34] (manufacturability constraint); in addition, the minimum size of corner radii is also determined by tool choice. The design “ownership” in each domain (which determine the most appropriate decision makers) is different, with production engineers best understanding the manufacturing constraints. This requires excellent communication between the production team and the designers, a task that is not always performed effectively [10,14,16,19,20].

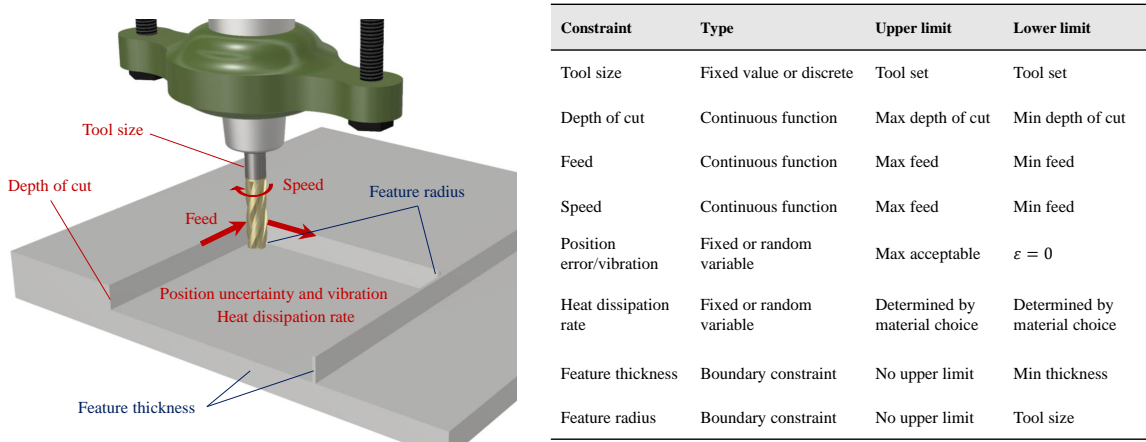


Figure 2.1: Example of manufacturing and manufacturability constraints for a machined aluminum component, with constraint type and source of limits demonstrated.

Table 2.1: Common subtractive, additive, and formative manufacturing processes and some of the common manufacturing constraints discussed in the manufacturing literature. Blank cells indicate that the constraint generally does not apply to a specific process. In the case of AM processes, the tool/work feed refers to the raw material deposition method. Figure 2.1 gives an example of how these constraints appear in practice for a milling process.

Common Processes		Common Manufacturing Constraints													Refs			
		Cutting speed	Tool size (Standard)	Depth of cut	Tool/work feed	Feature access	Specialized jigs needed	Heat dissipation	Work area size	Residual stresses	Anisotropy from process	Support material	Post-processing	Limited part size		Specialized tooling	Poor raw tolerances	Vibration/position error
Subtractive	Turning/Facing																	[35, 36]
	Milling																	[37, 38]
	Drilling/reaming																	[39, 40]
	Planing																	[41, 42]
	Broaching																	[43, 44]
	Grinding/polishing																	[45, 46]
	Sawing																	[47, 48]
	Hobbing																	[49, 50]
	Punching/blanking																	[51, 52]
Additive	Powder bed fusion																	[53, 54]
	Material extrusion																	[55, 56]
	Photopolymerization																	[57, 58]
	Material jetting																	[59, 60]
	Binder jetting																	[61, 62]
	DED/LENS																	[63, 64]
	Sheet lamination																	[65, 66]
Formative	Forging																	[67, 68]
	Sand casting																	[69, 70]
	Injection molding																	[71, 72]
	Investment casting																	[73, 74]
	Metal forming																	[75, 76]
	Blow molding																	[77, 78]
	Die casting																	[79, 80]
	Powder metallurgy																	[81, 82]

2.2.2 Manufacturing Processes and Constraints

Most standard (non-hybrid) manufacturing processes fall into one of three major families, namely *subtractive*, *additive*, and *formative* [32]. Table 2.1 shows some of the most commonly used processes in each family and an example subset of manufacturing constraints for each one. These were taken from the manufacturing literature and are not a complete set of the possible constraints that can be encountered during design and process selection.

Therefore, it is vital for the designers to understand the processes very well when using these; generally, this takes the form of expert intuition but it could also come from rigorous process models, digital twins, and design catalogs for specific processes.

2.2.2.1 Overview of Processes and Families

Subtractive manufacturing (SM) processes form geometry by cutting material away from a block or billet which is larger than the desired final shape [32, 83–85]. SM requires little custom tooling besides fixtures and jigs [86], but the design geometry is restricted to that which can be reached by standardized cutting tools; the features must also be large enough to resist the machining force and allow sufficient heat transfer since the tools produce friction heat [33, 34, 87]. For appropriate designs, SM is a very cheap, repeatable, and efficient manufacturing approach; it can be very wasteful, however, due to the large amount of material cut off in processing [88] in many cases. On the other hand, additive manufacturing (AM) builds up the desired geometry in layers, allowing great design freedom and highly complex parts [89]. The raw material can take many forms, as long as it can be layered and fused onto a surface in some fashion [90, 91]. Ideally, the process generates very little waste but most designs require a fixed build surface and support material [92]. AM requires almost no custom tooling and is generally complexity-agnostic in terms of material and production cost. However, it can be extremely slow and expensive in some cases [89, 93, 94]. Finally, formative manufacturing (FM) has the largest diversity of processes, as the only requirement to be a formative process is that material needs to be shaped or formed into the final part, usually keeping the same volume as the starting material (or producing easily reusable waste). The raw material may be a cold billet, molten metal, powder, resin, or one of many other options. As with AM, FM produces little to no waste; however, it requires a large amount of custom tooling to produce parts, and the geometry is restricted to the shape and quality of the molds and other tooling [32, 85, 95–98].

2.2.2.2 Manufacturing Constraints: Process-Limited Design Complexity

In general, SM processes tend to have the most restriction on the types of part features that can be created due to the essential requirement that cutting tools be able to reach

all of the part surfaces from some force point (commonly a rotating spindle) [99–101]. AM, by definition, does not have tooling-related complexity restrictions, but there are some restrictions due to support material removal [102,103], natural material anisotropy [104,105], and process mechanics [89,90]; however, the possible design complexity is very high for most of the AM processes [89,90,106]. Conversely, FM is almost entirely dependent on the tooling used and is limited to the tooling complexity. In the most common case, the tooling (molds, forging tools, and similar) must be made using some SM process, which limits its complexity to that which can be cut or machined [32,95–98]. However, some FM processes can use free-form or shell molds (for example, investment casting) which strongly enhances the possible part complexity [85,107–109].

2.2.2.3 Manufacturing Constraints: Material Selection

Of the three major domains, AM has the widest range of available materials when all of the major families are considered; the various AM processes can use almost any material which can somehow be applied in a layer and fused with a previous layer [89,90,110]. AM materials are most commonly in the form of filament, resin, or powder, but may be as diverse as water (ice prototyping [111]) or rolled metal sheets (ultrasonic consolidation [112]). In general, SM materials are limited to those which can easily be cut with a tool and can tolerate the associated heat load, usually ductile metals and hard polymers [32,85]. On the other hand, FM materials are limited to those that can be stably melted or cold-formed to conform with some tooling [32,95,97]. This is less restrictive than SM, being able to process various bulk and molten materials, resins, and metal powders, but less free than AM because of the dependence on tooling.

2.2.2.4 Manufacturing Constraints: Production System Considerations

Due to the need only for standard clamps and fixtures [32,85,86] for single parts, SM tends to be able to produce one-off parts relatively cheaply compared to AM and FM. However, it can be more expensive to mass-produce parts using SM because of the need for jigs and higher quality cutting tools than needed for one-off parts [32,85]. The cost for one-off AM parts is high due to the expensive nature of the processing equipment and materials, as well

as the generally slow processing speed; unlike SM, AM can be relatively cheaper to perform mass production for some (not all) complex designs since the manufacturing time and cost is mostly dependent on total part volume and not complexity [90,113]. The supply chain for AM, within the available set of processes and materials, is also often more efficient and less prone to blockages [89,90]. Finally, FM is very expensive for single parts and very cheap for mass production, making it ideal for many products. The reason for the high up-front cost is the tooling initial cost, but this goes down quickly as the tool is used more [32,85]; the raw materials for FM are generally much cheaper than those for SM and AM (since they will be formed or melted during processing, high quality finish and precision in the materials is usually not necessary), the supply chain is very efficient, and one good set of tooling may last for hundreds of thousands of parts [32,97,98].

2.2.3 Manufacturability Constraints: Design Perspectives

In the preceding section, the three major classes of manufacturing processes and their common constraints were explored. Careful consideration of these constraints and their potential impact on design allows the development of customized design/manufacturing approaches for specific problems; this, in turn, allows the designer to restrict the available design space just enough to ensure manufacturability. This section examines the various specific DFM methodologies developed within three essential design perspectives or viewpoints in which DFM or MR-DFM has been applied effectively. These are (1) the system design (top-down) perspective, (2) the product design (bottom-up) perspective, and (3) the case where a specific manufacturing process is required.

2.2.3.1 System Design (Top-Down) Perspective

In the system (top-down) design perspective, the goal is to consider the construction of a system or subsystem (including interfaces) and is less concerned with the optimal design of individual parts; while optimization of each part is important, it is more important in top-down design for each part of the system to be optimal relative to overall system utility [13, 17, 114, 115]. In terms of practical manufacturability constraints, the focus is generally to make the manufacturing process selection such that the parts are manufacturable in an

efficient way, and such that the materials and tolerances are compatible. The business case for considering a DFM or other constraint technique is easy to make, as it prevents re-design and resulting delays, as well as ensuring that the potential design space is as large as possible [116–119]. The most obvious application within this domain is the improvement of any general lifecycle design technique, such as those proposed by NASA [15], INCOSE [114], Pahl *et al.* [17], and Blanchard and Fabrycky [13]. Within such a design engine, more general DFM approaches usually work the best. This allows easier application of classic DFM principles during the design process with a low risk of mis-match with the set of available manufacturing processes [16, 20]. While the general engine does not necessarily need customized DFM methods (especially if the design is very simple), when the lifecycle design approach is applied to a particular domain, the use of minimal-DFM can be very valuable.

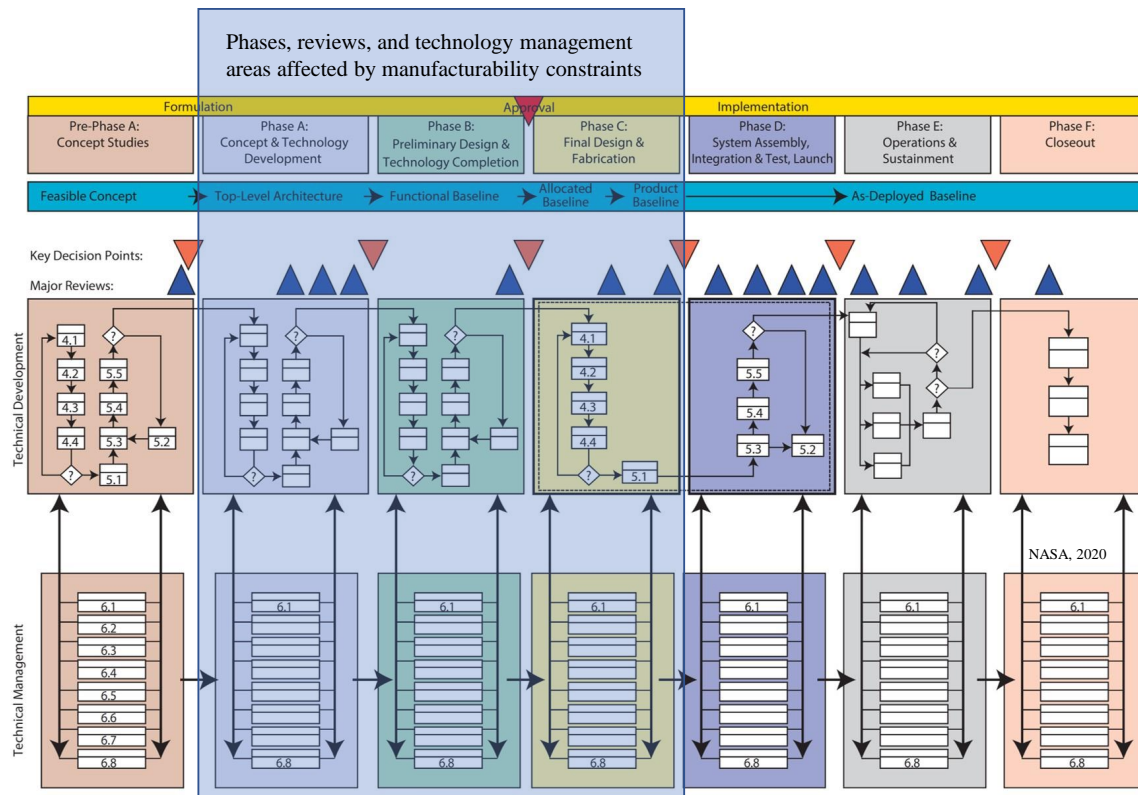


Figure 2.2: Example NASA systems engineering engine [15], demonstrating milestones, design reviews, and technical development and management phases. Highlighted areas mainly affected by manufacturability considerations. (Image from a US government document and not subject to copyright in the United States.)

Figure 2.2 shows a version of the NASA systems engineering engine [15], where the main phases affected by manufacturing decisions are highlighted. It can be assumed that little manufacturing knowledge is certainly needed in the conceptual design phase (Pre-Phase A) but it will be needed (in any design scenerio) in the final design and fabrication (Phase C). When DFM is used (especially when defining and imposing manufacturability constraints), Phase A (technology development) and Phase B (preliminary design) will also be heavily affected. In fact, if a proper DFM process is followed in Phase A and Phase B, the risk to Phase C could be greatly reduced [15–17, 114]. This systems engineering model could be used for relatively simple systems and assemblies and has been used successfully for large NASA programs.

This value can be especially apparent in previous work done on aircraft design. Generally, aircraft parts have very tight tolerances, need to be very lightweight, and need to be highly consistent, which dramatically limits the available manufacturing processes for these parts [116, 117, 120]. The set-based concurrent design technique proposed by Vallhagen et al. [120] uses a type of custom DFM technique to eliminate clearly infeasible manufacturing processes early in the design and allows the accommodation of process constraints at several points in the lifecycle. A similar approach focused on ensuring that all of the parts have compatible tolerances and that the various system interfaces are producible was developed by Barbosa and Carvalho [117]. Electronics and mechatronics design is an important application of DFM at the system level. The 2003 study by Bajaj *et al.* [121] explored this in detail, developing a rule-based system for finding and imposing the relevant constraints (of several options available from the system to the designer) to accomplish a good quality design. Several studies by W.H. Wood [122, 123], Shetty *et al.* [124], Berselli *et al.* [125], and Lee *et al.* [126] discussed some of the major issues when designing mechatronic systems and presented a framework for considering formal (mathematical) and heuristic manufacturability constraints related to both the mechanical and electronics sides of the design.

2.2.3.2 General Product Design (Bottom-Up) Perspective

The design perspective with the most direct benefit from the use of minimally-restrictive DFM is design of individual parts. When the design focus is bottom-up (i.e., the system

is built from several products individually developed) and each part must be optimized individually, the largest possible expansion of the design space is needed. It is assumed in this case that a specific manufacturing process has not been required by the customer and the designer is free to select the one that provides the least restrictive manufacturing profile and design space. Manufacturability constraints in this case are generally geometric in nature, driven by both the needs of the design, the capabilities of the manufacturing process selected, and the limits and nature of the material.

In most of the DFM studies found on part design, a specific manufacturing process was defined in the problem statement and so it was not true bottom-up design (where it is assumed that performance is the primary goal and several production processes may be possible) [127,128]; these cases will be discussed in the proceeding section. The work found in this area was primarily in the domain of decision analysis, where the manufacturability requirements or guidelines are discovered and fed back into the design process as it developed. Works by Barnawal *et al.* [22] and Budinoff *et al.* [129] analyzed this in detail, showing that effective communication of the constraints and manufacturing expectations was the key to ensuring product manufacturability; this was shown to be true for both heuristic, experienced-based constraints and formal mathematical manufacturability constraints. Mirzendehtdel *et al.* [130] showed that sometimes this required delaying the actual optimization or design of a part as long as possible while exploring constraint trade-offs. While this is a valid approach for many different types of constraints, ensuring manufacturability (relative to other constraints) is one of the main applications.

A large and detailed case study on the mathematical definition and enforcement of manufacturability constraints was completed by Iyengar and Bar-Cohen [131] in which a side-inlet-side-exit (SISE) parallel plate heat exchanger was developed using constraint sets for eight different processes (extrusion, two types of die casting, bonding, folding, forging, skiving, and machining); it was found that feasible solutions for the design existed under each process constraint set, but the constraints were clearly active and provided very different optimal solutions based on the process selected.

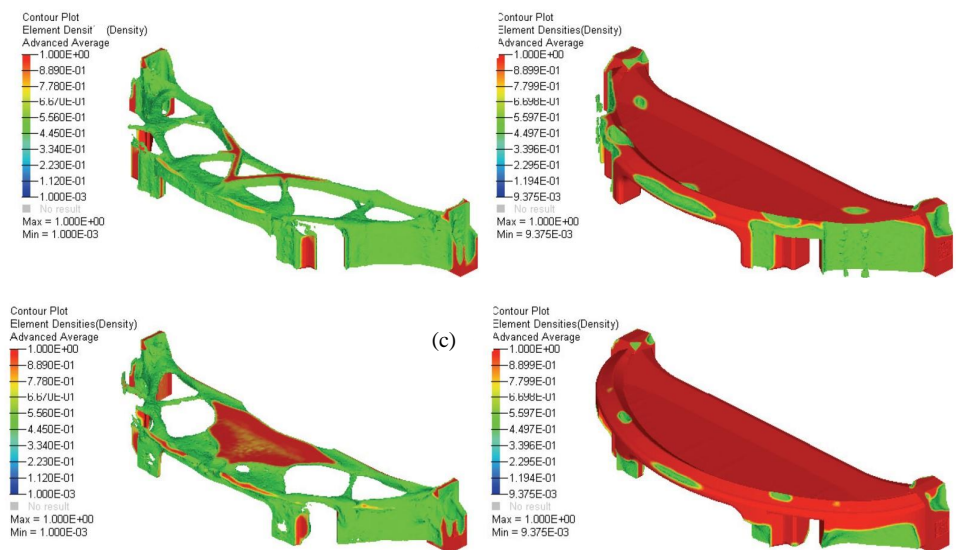
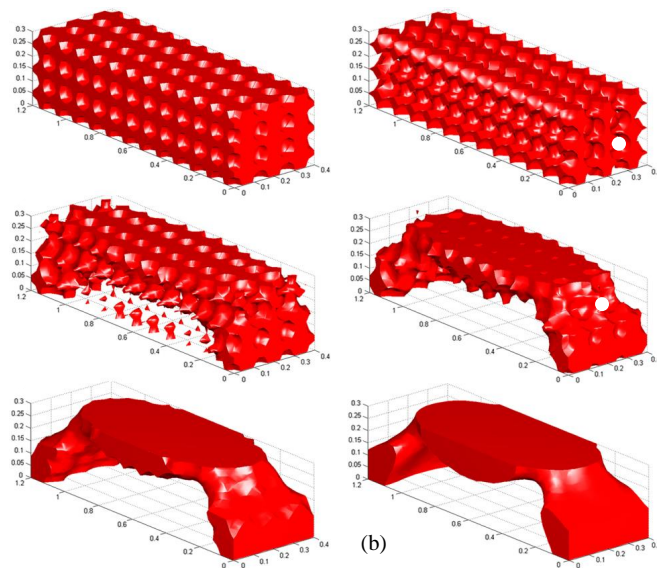
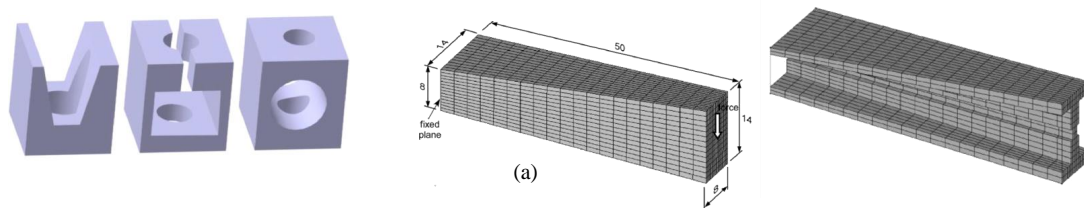


Figure 2.3: Some significant successful examples of bottom-up design methods with integrated manufacturability constraints, including (a) shape optimization [9] and (b) small-scale [132] and (c) large-scale [133] topology optimization. (Panels (a) and (b) © Elsevier Ltd. and reproduced with permission. Panel (c) published under CC-BY 4.0 license.)

Several studies by Vatanabe *et al.* [9] (Figure 2.3a), Guest and Zhu [134], Li *et al.* [132] (Figure 2.3b), Mantovani *et al.* [133] (Figure 2.3c), Zuo *et al.* [135], and Reddy *et al.* [136] have examined the impact of manufacturability constraints on shape and topology optimization (TO) solutions. Several of these studies compared the results for several different manufacturing processes simultaneously, with outcomes similar to the heat exchanger problem described above. Since TO is an algorithm-based design process, the manufacturability constraints are usually enforced inside of the algorithm. For example, the study by Vatanabe *et al.* (Figure 2.3a) applied manufacturability constraints for six different processes (casting, milling, turning, extrusion, rolling, and forging), producing a variety of different topologies under these constraints. The constraints were enforced in the form of topology constraints, such as minimum feature sizes, symmetry, and avoiding undercuts, within the formulation of the problem.

2.2.3.3 Manufacturing Process Perspective

This section continues the discussion from the previous section on product design, with a manufacturing process specified in the design requirements. In this case, one or more specific processes must be selected in advance, requiring special consideration of the relevant constraints. In general, machining requires a careful tool-path planning to ensure that all of the geometry can be cut with the tools [137]; this is true for both manual and computer-controlled machines. For example, Monge *et al.* [138] proposed a three-step process for designing turbine blades by generating an optimal shape based on a combined set of constraints from a computational fluid dynamics (CFD) model and an optimal tool-path generator; the solution found produced both an improved design and one that was manufacturable using a machining process.

More general solutions were developed by Kang *et al.* [139], Deja and Siemiatkowski [140], and Gupta and Nau [141], which are based on feature clustering and checking the optimality of a series of cutting path plans which open the design space as much as possible. Conversely, Mirzendehtdel *et al.* [142] defined an “off-limits” region to represent the areas which would not be reachable with a cutting tool; this method was also shown to converge more easily than many other TO-based methods with machining constraints. In addition to path plan-

ning for conventionally-designed parts, machining constraints have been developed for use in TO-generated designs as well. Projection-based TO can be very effectively constrained for machining, as it is based on continuous geometric constraints and interfaces well with a toolpath, as shown by Guest and Zhu [134]. Specific machining and milling-related constraints have also been developed for a few cases within the level-set TO approach [143–145], as well as heavyside projection, gradient, and hybrid methods [135, 146]. Some examples solutions from the study by Liu *et al.* are shown in Figure 2.4a.

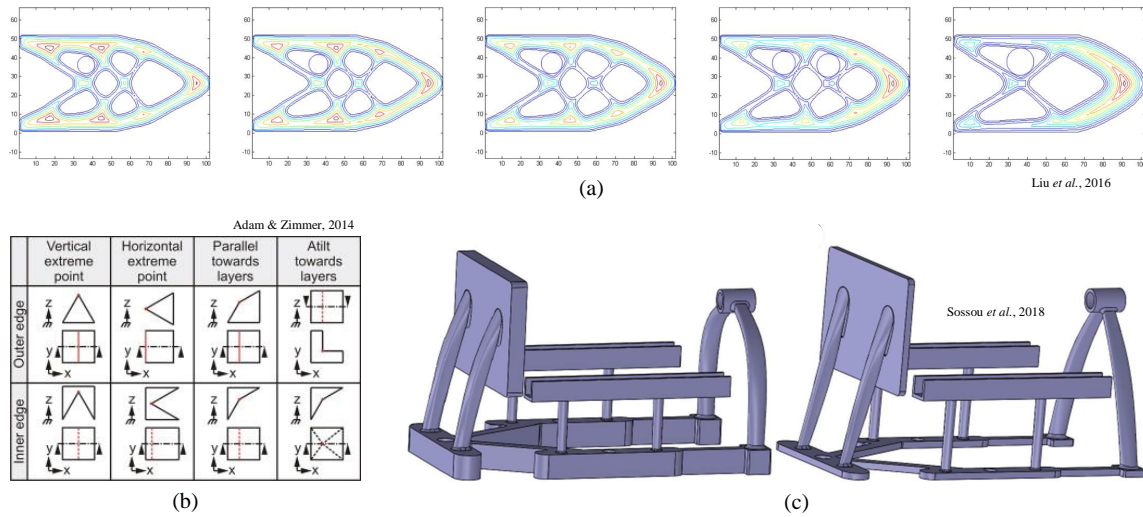


Figure 2.4: Successful examples of process-driven design under manufacturability constraints. (a) topology optimization under machining radii constraints [144], design feature catalog for AM parts [147], and (c) design of a mechanical assembly under AM manufacturability constraints [148]. (Panels (a) and (b) © Elsevier Ltd. and reproduced with permission. Panel (c) published under CC-BY 4.0 license.)

Most of the work done so far in establishing and enforcing manufacturability constraints for AM processes has been for the development of design rules, some for general AM and some for specific processes. The focus of extensive studies by Jee and Withereil [149], Adam and Zimmer [147, 150] (Figure 2.4b), Bin Maidin *et al.* [151], and Kranz *et al.* [152] was on the development of standardized feature databases in which the AM manufacturing constraints could be applied to standard common part features to ensure manufacturability. The designer could then select the features from the database that are best for the design at hand while ensuring manufacturability. In a more focused effort, Tang *et al.* [153] presented a method for developing a unit structure-performance database to al-

low discrete optimization of light-weight housings via selective laser melting; this technique for arranging small standard features to optimize a design is useful and complementary with the feature catalogs developed in the previously-mentioned works.

Using the results from an extensive literature survey, Pradel *et al.* [154] proposed a framework for mapping of AM process knowledge for product design. They describe the need for more “practical” application of AM in design and suggest several methods for achieving this for general processes. Some work has been performed to establish AM constraints in TO [155, 156], similar to those discussed in the previous section, but this is still an immature area and needs additional attention. Thompson *et al.* [103] point out that many of the process limitations in AM come from the modeling and software used to drive the processes, but that this is an area where progress is being made. The design of mechanical assemblies under AM manufacturability constraints was explored by Sossou *et al.* [148]. Some of the results from this study are shown in Figure 2.4c.

In addition to more general AM constraints (minimal feature size [157], overhangs [102], surface roughness, avoidance of stress concentrations [105], material anisotropy [104], support material removal [158], among other things), some processes have more specific constraints which must be considered. While many of these are not well characterized, much work has been done for some of the very common processes. For example, Utley *et al.* [159], Thomas [160], and Kranz and Herzog [152] proposed a series of manufacturability constraints for the selective laser melting (SLM) process directly driven by the process characteristics. These SLM constraints are things such as delamination, laser heat deformation, potential oxidation between the material layers, and scan pattern constraints specific to laser scanning processes such as SLM. Similar work has been done for selective laser sintering (SLS) [161, 162] (such as shown in Figure 2.5a) and electron beam melting (EBM) [163–165], which have similar manufacturing constraints, with EBM generally being less restrictive than SLS/SLM due to the use of a heated chamber.

Other specific processes for which process-specific design rules have been developed include fused deposition modeling (FDM) [166–169], stereolithography (SLA) [170–172], material jetting [173], and binder jetting [174]. The general design limitations cited from FDM are in the area of minimal feature size (more strict than standard AM constraints),

support material design, and surface accuracy and finish. FDM, material jetting, and SLA have similar manufacturability constraints, with the exception that SLA and material jetting have less strict minimal feature size restrictions. Binder jetting, which uses powder as the raw material, has constraints similar to those of the powder bed processes (SLM, SLS, EBM) mentioned above except for those related to heat warping.

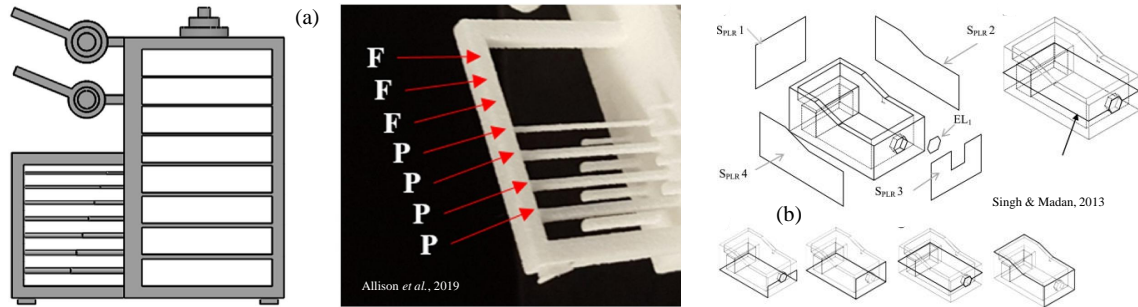


Figure 2.5: Successful examples of process-driven design cases for (a) design of a structure under additive manufacturing [162] and (b) parting line design for die cast parts [175]. (Figures © Elsevier Ltd. and reproduced with permission.)

An area of significant interest in MR-DFM has been in the use of casting processes to fabricate complex geometry generated by topology optimization (TO) algorithms. In the major studies reviewed, this is done by mapping the major casting/FM constraints [176] into the design within level-set [177,178], gradient [179], and projection [9,134,180] methods to generate a topology that is cast-able. Casting constraints are well-suited for TO, since they are much less strict than those for machining processes, and can be defined simply in terms of thickness and a requirement that the geometry be continuous; these constraints ensure that the liquefied material can flow into the mold and reach all features, can dissipate the heat, and that a parting line can be established. While relatively simple to design, in practice even simple casting constraints need careful assessment. For example, correctly predicting the amount of time available to fill the cavity before the molten metal solidifies is extremely important both for the production of good products but also for the life of the tooling. Consideration of directional solidification is another important factor for the effective DFM of most FM methods, especially for sand casting [16,32].

Some work has also been completed on the TO-based design of parts to be fabricated

using an extrusion or drawing process. The manufacturability constraints for extrusion are much more simple than those for casting. When using a projection-based TO method, as done by Vatanabe *et al.* [9], the constraints are simply applied to a “slice” of the part; the domain is automatically continuous in an extrusion process, so the manufacturability constraints consist mainly of avoiding features that are too delicate to survive being pushed or drawn through a die. Li *et al.* [132] and Sutradhar *et al.* [10] showed that this can also be done using a type of internal projection within a level-set TO method.

In addition to DFM-based TO solutions in casting and extrusion, some work has gone into finding conventional (non-TO) design rules for closed-tooling processes, particularly injection molding, die casting, and powder metallurgy. Injection molding is typically limited to plastics (e.g., ABS or silicone), die casting to ductile metals (e.g., zinc or aluminum), and powder metallurgy to metal powder (sometimes mixed with a binder); manufacturability analysis within the appropriate tooling is focused primarily on being able to quickly and efficiently fill the mold with material and eject it safely. The manufacturability constraints then are in the form of feature restrictions (they must fit into and be easily removable from the tool), usually with a two-part tool, and the location of the tool parting line [175, 181–183] (Figure 2.5b shows one of the design results from Singh and Madan [175]). From a simple design perspective, powder metallurgy is often the least restrictive [32, 184], as it can sometimes use a multi-part tool instead of the standard two-part used in injection molding and die casting. However, it is possible to include cores with injection molding/die casting, which is generally not possible with PM. It is also possible to have multi-part tools for injection molding and die casting in some applications. These practical advances in tooling technology allow more complex geometries to be fabricated; this, however, comes at a high design cost due to complex constraints involved, as well as the special tooling. Extensive work has gone into simulation of these processes in order to better understand how the material can flow into the tool and solidify in the way intended by the designer [185–189]; these simulations can be used to guide designs but generally are used just to check manufacturability and plan the process after the completion of the design.

2.2.4 Manufacturability Constraints: View of Design Scales and Levels

The design of features and part details can be completed at different design levels, each of which requires different kinds of manufacturability constraints. The main difference, from a design perspective, of each of the levels is the scale of feature sizes created within each domain. The macro-level is defined as containing features at least a millimeter in size, while meso-level features may range from a few hundred micrometers to one millimeter, the micro-level may range from one to a few hundred micrometers, and sub-micro-scale is less than one micrometer in size. A visual comparison for each can be seen in Figure 2.6.

Macro	Length scale: $> 1\text{ mm}$
Meso	Length scale: $100\ \mu\text{m} - 1\text{ mm}$
Micro	Length scale: $1\ \mu\text{m} - 100\ \mu\text{m}$
Sub-Micro	Length scale: $< 1\ \mu\text{m}$

Figure 2.6: Design-related process characteristics for SM, AM, and FM, shown with examples of common processes and common manufacturing constraints for processes within each domain.

2.2.4.1 Macro-Level Design

One of the major tasks when designing at this level is the generation and refinement of macro-level structures and aggregates such as lattices, overhangs, mounting bosses, and similar features. Design at this level is generally straight-forward, and is usually done using design rules and feature catalogs which provide manufacturable features [147, 150, 190]. Definition of these rules for most traditional manufacturing processes (such as machining and injection molding) is based on simple DFM principles [16, 18]. Figure 2.7a shows an injection-molding caliper case, which is an example of a standard product with macro-scale features.

Fabrication of macro-scale features for AM processes is more complex due to the layered nature of the resulting material and the presence of natural voids, stress concentrations, and residual stresses [105, 193]. While it is important to use feature catalogs and feature families, the manufacturability constraints will be more strict than they would for more simple processes. Research has been performed specifically for AM processes; for example,

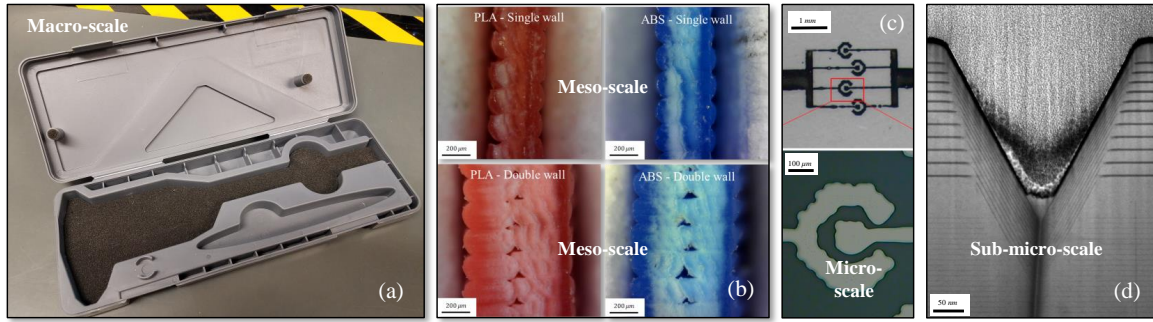


Figure 2.7: Examples of design features at various levels. (a) macro-scale injection-molded caliper case, (b) meso-scale 3-D printed thin-walled structures, (c) micro-scale electrodes [191], and (d) sub-micro-scale LED pits [192]. (Panels (c) and (d) reproduced under CC-BY 4.0 license.)

the studies by Adam and Zimmer [147, 150] and Bin Maidin *et al.* [151] developed a list of macro-level standard design features and their transitions. The rules presented are developed for several specific AM processes and incorporate process knowledge directly from these processes into the design of edges, wall thicknesses, gap heights, and other design features. Some AM processes (such as SLM) require the ability of the material to transfer heat rapidly during processing and small features need to be adjusted for this, including controlling the porosity [194]. Maximum length scale constraints for structural and fluid topology optimization is another important application; it can limit the size flow channels and structural members as needed, as shown by Guest [195] and Lazerov and Wang [196].

2.2.4.2 Meso-Level Design

The primary applications found for meso-level design were in the design of meso-scale features which act as a controllably-anisotropic material. Since, in most cases, the material for parts made using SM and FM process is approximately isotropic, this design level has been applied mainly to additively-fabricated parts. The use of AM to design and build meso-level materials structures was the topic of several studies; Chu *et al.* [197], Yu *et al.* [198], Garcia *et al.* [199] and Florea *et al.* [200] developed different theoretical frameworks for single- and multi-material problems, while Sivapuram *et al.* [201], Gopsill *et al.* [202], and Gardan *et al.* [203] explored the practical implications and requirements for using AM to build meso-scale tailored materials. Examples of some AM-generated mesostructured materials are shown in Figure 2.7b.

2.2.4.3 Micro-Level Design

Manufacturing constraints derived for micro-scale features and parts (Figure 2.7c) could be more restrictive than larger-scale designs due to the small length scales involved. Most conventional manufacturing processes, including casting, forging, machining, and additive manufacturing, do not have the capacity to fabricate extremely small geometry; therefore, it is vital that a production process be selected and considered at the design stage to ensure that the final product is manufacturable.

The small number of manufacturing processes that can reliably fabricate at the micro-scale are well-understood, so it is relatively straight-forward to find and enforce the manufacturability constraints in most cases. For example, Ashman and Kandlikar [204] examined several types of manufacturing processes for fabricating heat exchangers with hydraulic diameter of less than 200 micrometers. Etsion [205] presented a comprehensive review on micro-level laser surface texturing (LST) in connection with hydrodynamic lubrication and wear reduction as well as surface texturing in general. Romig *et al.* [206] discussed issues in association with micro-electro-mechanical systems (MEMS) design and fabrication, including materials, manufacturability, performance, and reliability. AM-based fabrication has been discussed by Frazier *et al.* [207] and Dede *et al.* [4]; while AM offers great potential for micro-scale fabrication, there are clear problems with the processes that need to be addressed before they can be effectively used for micro-scale fabrication. Current challenges include material defects, anisotropic properties (which affect the fabrication more for smaller geometries), inconsistent cooling, residual stresses, complex material behavior, and other related concerns.

In addition to feature size restrictions, design topologies and shapes also should have specific constraints when fabricated at this scale. As an example, considering a micro-milling process with a ball end mill, Lee *et al.* [208] applied a spline-interpolated smooth free surface with a maximum slope angle as a manufacturability constraint in the surface texture design-for-lubrication problem. Even though the target design size is larger than micro-level, features in the design may still be smaller than those which can be fabricated at this level by certain processes. Specifically, keeping the feature size larger than the manufacturing resolution should not be overlooked in topology and shape optimization. Sigmund [209,

[210] showed examples of manufacturing failure due to feature size, and introduced robust topology optimization frameworks that can filter out infeasibly small features.

2.2.4.4 Sub-Micro-Level Design

An example of a feature at this scale is a nano-scale LED pit, as shown in Figure 2.7d. This is an extremely important design scale and many important applications require designed features at this scale. Some of these applications include friction and wear reduction [211, 212], nano-electro-mechanical systems (NEMS) [213], and superhydrophobic surfaces [214]. Sub-micro-level surface treatment using micro- and nano-texturing and surface modification strategies are similar to those discussed for other scales, except that the tolerances are much tighter and the manufacturability constraints are very restrictive. Sub-micro-scale surface texturing and treatment methods for corrosion and wear resistance often involve combinations of thermal, electrochemical, and mechanical processes, which alter surface electrochemical and molecular properties, mechanical shapes and patterns, or sometimes material itself [215]. Often, sub-micro-level features and parts are manufactured using the same or similar techniques that are applied to fabricated nano-scale structures; these fabrication techniques can be typically classified into two categories: top-down and bottom-up approaches.

Top-down fabrication approaches mostly utilize nanolithography, deposition, and etching processes. This approach is commonly used in the semiconductor industries, but the usage is expanding to more intricate applications, including NEMS, sensors and actuators, optoelectronics, as it is capable of fabricating structures down to nanometer resolution [213]. Due to the layered nature of fabrication processes, the top-down approach is mainly limited to 2D or 2.5D structures in manufacturing. Structures can be fabricated by repeated material deposition and removal processes, supporting very accurate manufacturing, but present manufacturability problems when the length scale is less than a few nanometers [216, 217]. The bottom-up approach places material at the desired locations, similar to 3-D printing processes. Currently, a direct-write nano-deposition (specifically, two-photon polymerization, 2PP) method is available to fabricate structures smaller than the micrometer level easily, and at its limits down to a length scale of approximately 50 *nm* [218, 219]. This ap-

proach has similar characteristics and constraints to what is commonly seen in 3D printing; however, even with the wide freedom in shape and topologies that AM enables, postprocessing of structures fabricated using nanoscale AM via 2PP is still challenging. The main challenge is the removal of support structure and any extra raw material, as this is very difficult or impossible when dealing with extremely small parts [220].

2.2.4.5 Literature Review Conclusions and Closing Remarks

The purpose of this survey was to explore the generation and imposition of process-driven manufacturability constraints for product design problems. The four main take-aways from the review are:

- The information collected in this survey and discussion demonstrated a wide variety of design problems involving (explicit and implicit) manufacturability constraints. These problems, formulations, and solutions can provide a basis for solving new problems related to manufacturability and design.
- This survey looked at a number of design perspectives and levels, making it more useful as a guide for specific problems.
- This survey exposed the need for a general formulation method which is design-method-independent and which works with very complex problems, as well as methods for several areas of little to no coverage in the existing literature.
- It is clear from the existing literature that manufacturability considerations (explicit or implicit) are required for most design problems.

In addition to the larger take-aways, some important observations and conclusions were made after reviewing the collected literature on the topic:

- Significant progress has been made in the effort to include relevant manufacturability constraints (both explicit and implicit) in specific domains and design scales. The representation of different methods is very uneven, with topology optimization of metal AM and FM parts being the most over-represented. On the other hand, there are considerable gaps in the literature; some of the affected areas were observed to

be sheet metal forming, forging and rolling, traditional casting and plastic injection molding (where classic FDM is typically used), and most subtractive processes beyond simple milling and turning.

- Specific comparison with classic DFM was very rarely found during the survey. In future studies, this practice should be adopted to better justify using specific constraints instead of classic DFM ones.
- Throughout all of the design perspectives and levels, clear dependencies exist between the choice of process and the manufacturability limitations for specific designs.
- The impact of trade-offs between the manufacturability and the performance of the final design was not addressed in most of the found studies.
- The processes for finding and enforcing manufacturability constraints depends heavily on which domain (SM, AM, FM) the process in question belongs to. For most SM and FM studies found, the essential constraints were tool access and minimum feature size.
- The established manufacturability constraints for SM processes tend to be related to surface topography, while AM constraints generally relate to part cross-section and material behavior, and FM constraints seem to be driven primarily by material behavior when interacting with and being removed from the tooling. This is an important consideration during early design efforts when the ideal manufacturing method may not be selected.
- If it can be shown that all the manufacturability constraints are inactive, it is very likely that the design is manufacturable without the constraints. This is the ideal case for many problems, as a smaller number of design constraints will usually result in less expensive decision making processes and a larger design space.
- The smaller the design scale, the more restrictive the manufacturability constraints become and the fewer process types are capable of fabrication.

- Research involving different design scales is dominated by specific types of manufacturing processes. This appears to be largely the choice of researchers (e.g., studies at micro- or sub-micro scales tend to rely more on AM processes) based on what is most practical for a specific problem. In the future, this will need to be expanded to include a wider variety of processes.
- Parts conventionally-designed (i.e., not designed using an algorithm) under several common FM and SM processes do not appear to have formally-defined methods for ensuring manufacturability of the parts beyond visual observation and rules-of-thumb. Especially noted were investment casting, blanking/coining/stamping, turning/facing processes, rolling, and forging processes.
- The design of conventional sand and shell casting parts seem to be completed using mainly rule-based design and traditional DFM principles (i.e., "make it simple").
- In top-down (system-level) design, the manufacturability constraints need to consider global as well as local manufacturability problems.
- In bottom-up (component) design, the same product can have vastly different final designs from the same starting point when active manufacturability constraints for different processes are considered.

Further work on developing a general DFM or MR-DFM method, especially that in the following sections of this chapter, should aim to address each of these issues.

2.3 MR-DFM Concept Development

A general framework for applying rigorous (i.e., repeatable, as complex or simple as needed, and with low uncertainty) manufacturability constraints in design practice requires development in three domains, namely (1) process and material behavior modeling, (2) mapping and problem formulation, and (3) practical implementation, including verification and validation strategies. Figure 2.8 shows some of the major technical knowledge areas within each domain. The first, the process and material modeling domain, is mostly concerned

with mechanics and materials science and includes rigorous process and material modeling and definition. The second domain is concerned with collecting and mapping design knowledge and formulating useful and rigorous problem formulations. The third is the practical implementation, consisting mainly of design method (to solve the problems formulated in Domain 2), automation, and verification, validation, certification, and standards development for the design problem or problem family under consideration. Much previous work has been completed in the first and third domains, but very little in the second domain. Hence, there is a clear and specific need for a MR-DFM concept which is general and can serve as the connection from the process/material modeling and practical design application.

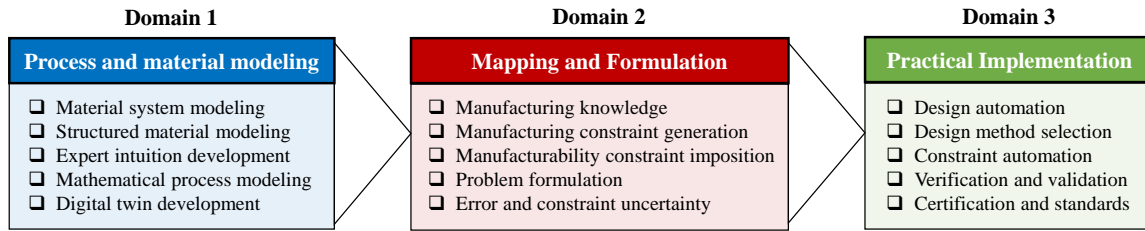


Figure 2.8: Domains of technical and design knowledge required for effective design under manufacturability constraints. The present study focused on Domain 2: Mapping and Formulation.

As with classic DFM, this framework is agnostic to the design solution, manufacturing process or processes, and materials selected. This method is based on a simple, direct mapping of the “practical” knowledge from the selected manufacturing processes (and by extension the materials) into a set of mathematical manufacturability constraints which can be imposed in the design problem formulation or requirements, or only selected features. Whether these constraints actually restrict the design space more than the other design constraints in the problem may be established during the mapping process or after a preliminary solution is found (depending mainly on the complexity and form of the constraints). In an ideal situation, all of the non-constant constraints are linear or at least monotonic and there is only one for each design variable over the entire space. Realistic problems are unlikely to be so simple, but effort should be made to impose the smallest possible number of these constraints and ensure that they are as minimally-restrictive (hence MR-DFM) as possible while ensuring a significant increase of manufacturability under the conditions established by the stakeholders/designers. The “minimally-restrictive” nature

of the constraints generated refers only to their restrictiveness on the domains of the design variables, not to minimization (optimality) in the mathematical sense, and does not establish a “tolerance” on the design variables (the concept of tolerance allocation has been extensively explored elsewhere [221–224]). It should be further noted that the constraints may be approximate, depending on the conditions of the problem and the quality of the problem inputs (from Domain 1 - Figure 2.8).

2.4 General Design Problem Formulation

In the standard formulation of a design problem, the decision objective or objectives must be specified, as well as any needed or desired constraints on any of the variables in the problem. Whether this takes the form of a set of practical, experience-based general design rules or a formal optimization problem, it is vital that the designers specify the design objectives and constraints in a way that is clear and easily understood by all the stakeholders and easily communicated within an interdisciplinary design team. One way to express this mathematically, assuming that the design decisions can be represented using real continuous variables, is:

$$f : \mathbb{R}^n \rightarrow \mathbb{R} \text{ over } S \subset \mathbb{R}^n \quad (2.1)$$

where $f(\cdot)$ denotes some objective function (usually formulated such that the minimum value is the desired solution) and S denotes the set of feasible solutions to this function. In formal design optimization terminology:

$$\begin{aligned} \min_{\mathbf{x}} \quad & f(\mathbf{x}) \\ \text{subject to} \quad & g_i(\mathbf{x}) \leq 0, \quad i = 1, \dots, n \\ & h_i(\mathbf{x}) = 0, \quad i = 1, \dots, m \end{aligned} \quad (2.2)$$

where $g_i(\cdot)$ are the inequality constraints on \mathbf{x} , $h_i(\cdot)$ are the equality constraints, and $\mathbf{x} \in \mathbb{R}^n$ is the vector of decision variables which represent the design. The constraints bound the design space to feasible regions [225]. In the context of this study, the feasible domain only includes manufacturable designs that also satisfy failure modes, packaging, and other design constraints.

2.4.1 Mapping the Manufacturability Constraints

Three related levels of analysis can be defined to map the practical knowledge from process mechanics into enforceable manufacturability constraints. These are the *manufacturing considerations* (basic mechanical knowledge about the processes and materials), *manufacturing constraints* (constraints on the process), and *manufacturability constraints* (design constraints imposed by the choice of manufacturing process). The levels of analysis, the design ownership (i.e., primary decision makers or technical experts for stakeholders), and the relative sizes of the domains are shown in Figure 2.9.

2.4.1.1 Manufacturing Considerations

Three things can be gained at this level: (1) process advantages (which expand the design space), (2) process limitations (which restrict the design complexity), and best-practices or guidelines for proper use of the process. This is the broadest level of analysis and the applicability may be to an entire industry or family of manufacturing processes. Technical ownership at this level belongs to technicians and process engineers who have the most practical knowledge about manufacturing processes. The use of DFM generally implies that a specific process has been selected early in the design lifecycle; if the process is not yet specified, the manufacturing considerations level would be the most appropriate place to compare processes to aid in the selection process. An example of manufacturing considerations (for a machining process) is the requirement that all features in the design be (1) reachable by the cutting tools and (2) able to dissipate the friction heat and stress from the cutting without damaging the product.

2.4.1.2 Manufacturing Constraints

Mapped from the design considerations, these are natural constraints on the use of the process in question and are typically not changeable within a particular process. In most cases, incompatible manufacturing constraints necessitate the selection of a different manufacturing process to fabricate the design in question. The level of analysis is moderate in scope, being restricted to a single manufacturing process or several very similar processes within

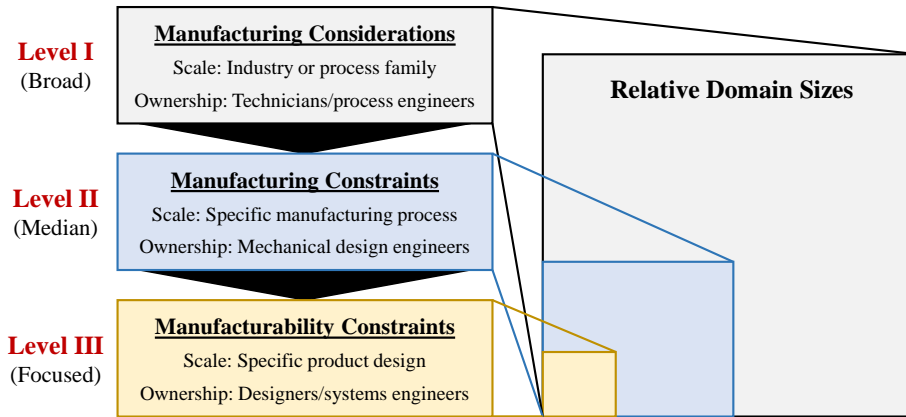


Figure 2.9: Basic mapping domains with scales and design ownership (i.e., primary decision makers) for each.

the same family. It should be noted that manufacturing constraints, by their nature, are more likely to be equality constraints and may take the form of discrete or combinatorial functions (such as a list of available machining tools for milling). The constraints generated here can be redundant or inactive, so it is important to consider some kind of refinement at this level in order to facilitate the formal constraint definition once mapped to the design itself. Following the example manufacturing considerations from the previous step, the equivalent manufacturing constraints would be (1) the quantification of the cutting tool range and (2) the limitation of machining to features strong and thick enough to withstand the associated heat and stress.

2.4.1.3 Manufacturability constraints

These constraints are mapped from the manufacturing constraints and are constraints on the design, not on the process. There are different methods of enforcing these, depending on the nature of the problem, but in most cases they can be described mathematically and imposed onto the problem via mathematical constraints for typical mechanical design problems (as shown in Eq.(2.2)). Carrying on the example from the previous two steps, the manufacturability constraints on a design to be made using a machining process would be the (1) maximum complexity allowed considering the type of tool used and (2) the minimum feature thickness required for the machining loads. Note that the design space could be expanded through use of higher fidelity constraints, such as feature thickness constraints

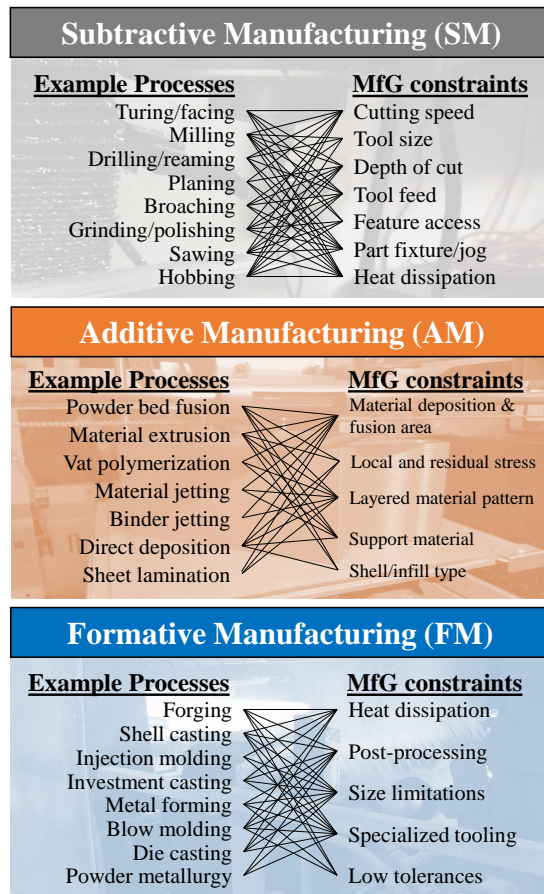


Figure 2.10: Fundamental manufacturing process families with common processes and their commonly-encountered manufacturing constraints shown within each. Note that these are housed within Level II in Figure 2.9 and refer to constraints on the processes.

that depend on neighboring geometry instead of a uniform limit, but this trades off with the effort required to create and use constraints in the design problem.

2.4.1.4 High-Level Mapping Scheme

Figure 2.11 shows the conceptual mapping process, with each of the levels shown relative to each other.

1. First (Figure 2.11a), the process advantages, disadvantages, and best-practices are analyzed and then mapped to manufacturing constraints (Figure 2.11b). The needed domain-specific knowledge here is a fundamental understanding of the manufacturing process or processes that may be used.

2. These constraints are then subject to a refinement process (Figure 2.11b), where they are identified, specified carefully, ranked in terms of importance, and combined when possible to reduce the number of them that need to be mapped to the design domain (Figure 2.11c). Knowledge about the mechanics of manufacturing processes is needed for this step, but most of the technical data will carry over from the first step.
3. Finally, the manufacturing constraints are mapped onto the design domain, where the focus shifts from the process mechanics to the details of the design (Figure 2.11c).

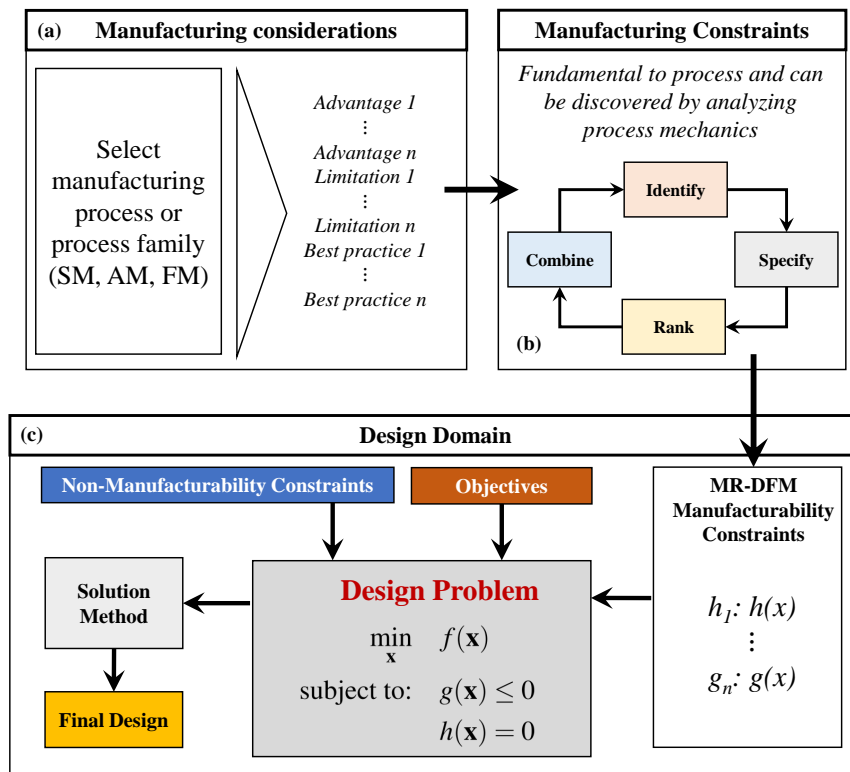


Figure 2.11: Mapping concept for imposing MR-DFM constraints from practical manufacturing knowledge.

Once these constraints and the other problem constraints imposed by the stakeholders (material constraints, cost constraints, technology limitations, performance and reliability, etc.) are applied and enforced, the remaining design space is available for the designers to explore. This mapping method ensures that all of the important manufacturing process information is used in the design process, while restricting the design space as little as possible.

2.4.2 Constraint Representation and Uncertainty

One of the major concerns remaining with the derived manufacturability constraints is the quality of representation and level of uncertainty for them. Classic DFM tends to provide a very flexible design representation, proxy comparison metrics, and a highly simplified system representation. Therefore, the classic DFM constraints tend to be very general and simple. On the other hand, MR-DFM gives a much more structured design representation, a higher-fidelity system representation, and more realistic metrics. Figure 2.12 shows the design formulation space for classic DFM and MR-DFM [226]. This is heavily dependent on the inputs from Domain 1 (Figure 2.8) and uncertainties in the location and effect of the constraints certainly may come from uncertainties in process and problems modeling. This is especially true in the cases where expert intuition are used to determine the constraints.

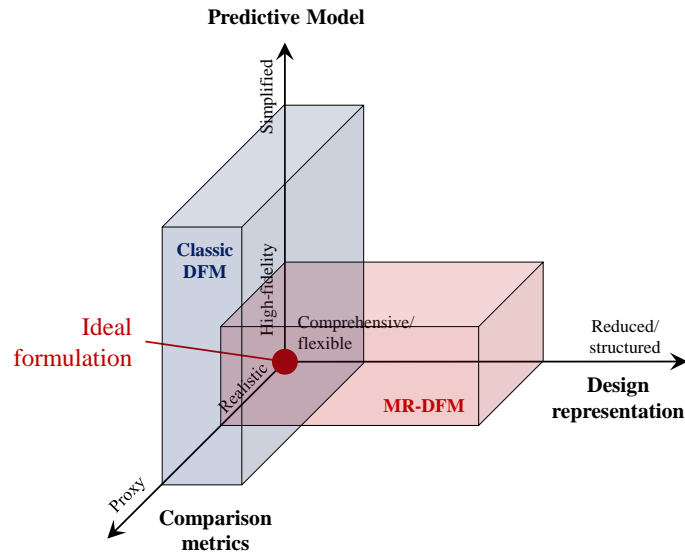


Figure 2.12: Formulation spaces for classic DFM and MR-DFM.

When defining classic DFM constraints on design problems, it is common to give very general guidelines such as “simplify as much as possible”. This simply limits general design complexity, often resulting in a feasible region similar to the one shown in Figure 2.13a. In the case where MR-DFM is used, more complex but tight constraints can be used, as shown in Figure 2.13b. These cases are far more simplified than most design problems and only represent level sets for two variables; however, they illustrate the benefit of using MR-DFM.

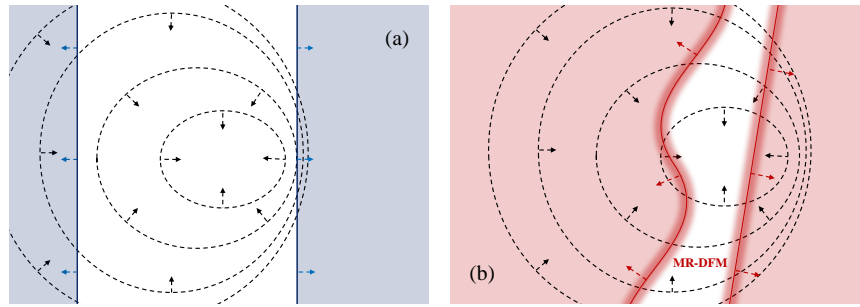


Figure 2.13: Simple level sets demonstrating possible constraint forms for (a) classic DFM and (b) MR-DFM.

Most product and system design problems have many local optima, so these represent what could happen around only one of the available solutions.

Note that the MR-DFM constraints in Figure 2.13b are “fuzzy” and less well-defined than those for classic DFM. This represents the uncertainties that come from simplifications in process and material modeling and possible errors when using expert intuition to derive the constraints. However, it should be noted that often the MR-DFM constraints still provide a significant benefit even if there is some uncertainty about their exact location and path.

One of the expected outcome from this kind of problem formulation is that a large set of constraints will be derived, most of which will likely not be active. However, at the formulation phase of the problem (in the form of Eq. (2.2)) it is difficult to determine activity [225]. For problems which are convex, have a small number of variables, or have a clear and obvious solution within the original feasible domain, this is not difficult to accomplish. For very simple problems with 2-3 variables, visual analysis (such as plots or level sets) may be effective. However, these kinds of design problems most likely have large design domains and a number of local optima that need to be examined. In the case of multi-objective problems, this could become even more complicated and difficult to address.

2.4.3 Relationship to Classic DFM

This proposed method of identifying and using manufacturing knowledge in design is distinct from (and potentially complementary to) classic DFM in several major ways. Specifically,

- MR-DFM uses the basic DFM principles and modifies them using specific manufactur-

ing process knowledge and problem formulation techniques from classic and modern optimal design methods.

- In contrast to classic DFM (which generally relies on generic design rules which the designer or other stakeholders then apply to a problem), MR-DFM provides a clear, clean, screened/sorted set of constraints which can be directly integrated into a design problem; this point will be discussed further in later sections of this paper.
- Both classic DFM and MR-DFM focus on constraint generation. However, classic DFM can also be used to drive objective functions and solutions method selection.
- Using the classic definitions [9, 16, 17, 19], DFM forces a general design simplification (typically as a heuristic requirement or tool for decision making after the initial design is completed). This tends to be too strict for many modern design methods, especially those which can be formulated as a mathematical program, where imposition of the constraints is a simple task once they are known. As shown in the previous section and in Figures 2.12 and 2.13, MR-DFM works to create the smallest possible restriction on the design space for each individual design problem by identifying realistic constraints.
- Due to the restrictiveness and focus on simplicity, classic DFM does not work well on topology optimization and similar problems. Successful constraining of these designs to the manufacturable domain requires process-specific and carefully-formulated constraints [9, 131, 134, 147, 150, 177, 179, 227].
- MR-DFM is better suited to complex and computationally expensive design problems (e.g., many problems in the aerospace, automotive, and medical devices industries), while classic DFM is best for simple problems and products which are well-established (e.g., consumer goods and part/product families with relatively simple designs).
- Classic DFM is based mainly on expert intuition and decision-making processes derived from it [13, 16, 18]. MR-DFM may be based on expert intuition or may be based on explicit or implicit mathematics, depending on the form and needs of the problems. This makes the MR-DFM method design method independent and able to handle many different types (and mixes) of input data.

- As shown in Figure 2.12, the problem formulation space (i.e., the approach for how design problems should be formulated) for MR-DFM is very different from classic DFM since it is a distinct method with different goals. Specifically, classic DFM relies on a very simple predictive model (i.e., as much as possible, everything is primitive shapes and as simple as can be made), proxy comparison methods (necessary since DFM is usually very generic unless applied carefully to a specific problem), and a very flexible application (also since the principles are typically generic). On the other hand, MR-DFM relies on a higher-fidelity predictive model (i.e., the manufacturing knowledge), a more structured design representation, and more realistic comparison methods (since the constraints are directly mapped).
- Once a set of data about a specific process is collected and mapped, this mapping can generally be used again for other designs with small or no modifications needed. This helps open the door to easier automation of the process.

While not a definite new contribution in itself, it is easier for practicing engineers and students to apply this method, as it is far more specific and knowledge-driven than classic DFM. A final major contribution that can be attributed to this method is that applying it does not take many years of developed expert intuition to apply like most DFM methods do. It does require knowledge about a specific process (or family of processes) and their effects on materials during processing; this is typically a much smaller domain than intuitively understanding the complexities between design and manufacturing on a general level. Therefore, the designer does not need as much practical experience or developed judgement to successfully apply MR-DFM.

2.5 Constraint Restrictiveness and Dominance

Let G be the set of all possible manufacturability constraints (active and inactive) on the set of all possible design variables X (including those that may be defined as constants). Assuming that the potentially useful set of constraints $\bar{g} \in G$ on the set of selected design variables $\bar{x} \in X$ is defined and ordered after mapping (Figure 2.11) and that the non-manufacturability constraints are known, screening can begin. The exact screening process

will depend on the nature of the problem, but the general goal is to evaluate each of the manufacturability constraints for each design variable and determine if this constraint $g_i \in G$ restricts the design space in any way for that variable $x_i \in X$. If so, it should be classified as a “restrictive” constraint and kept in the initial set. After a set of potentially useful manufacturability constraints is defined, they need to be screened (in a sequence as done in previous steps) for duplication, redundancy, and dominance. After all the screening steps, the manufacturability constraints could be classified into five categories:

1. Restrictive: The manufacturability constraint restricts the design space to feasible designs for a specific process [131]. These constraints are potentially active but their status will need to be established during the problem solution [225,228–230]. Inactive constraints can be removed from the model once activity can be tested mathematically. However, this does not affect the initial formulation and restrictive constraints are useful in estimating the feasible design space without unnecessarily restricting it. An example of a useful and restrictive constraint could be the minimum feature thickness on a manufactured part to be designed for minimum mass.
2. Not Useful/Inactive: The constraint is either non-restrictive in the defined design space or it is obviously inactive for the problem. An example of a non-useful constraint would be a maximum feature size constraint when the objective function seeks to minimize mass or size; in this case, an upper bound on the size is obviously not an active constraint and can be safely removed. Depending on the needs of the designer, this determination may be made based on expert intuition or may be easily automated. In cases of doubt, the designer may decline to reject the constraint and retain it in the restrictive category.
3. Duplicate: The constraint applied is mathematically or effectively identical to one that was already imposed and is therefore not needed at all. This is relatively common for manufacturability problems, as lower or upper bound values for the design may be identical for several constraint sources (for example, heat dissipation and minimum thickness-to-height ratio to withstand force of machining may produce identical lower bounds on wall thickness for a machined part).

4. Internally dominated (ID): The constraint was restrictive when added to the model but later found to be less restrictive to another manufacturability constraint (it is assumed here that the list of constraints will be examined in a sequence) and therefore is a dominated constraint and no longer necessary.
5. Externally dominated (ED): Identical to ID but dominated by a non-manufacturability constraint

This process can be easily automated in many cases, with the possible exception of determining some of the rejected constraints for the “not useful” category since these may need to be determined by expert opinion. However, if the resources are available to retain questionable constraints until their activity can be established (to avoid mistakenly rejecting active constraints and opening up the design to manufacturing process mismatch), automation of the process can still be done, even if not as efficiently as with a smaller number of constraints. When possible, defining constraints as bounds or low-order functions will prevent this problem. In the case where a hybrid manufacturing process is selected or it is necessary to consider more than one process, it should be noted that constraints may be different in different stages of the process. Depending on the problem, this could be a significantly more difficult problem or may be leveraged to improve the design (for example, if a sequential hybrid process [11] is used the order of the processes may affect the constraints significantly).

2.6 General MR-DFM Framework

Combining the discussion from the previous two sections, a general framework for generating, mapping, and screening the set of MR-DFM constraints can be formulated for use within a general mechanical design process; this framework is shown in Figure 2.14. The inputs consist of stakeholder preferences, the selection of a manufacturing process to use, and any needed non-manufacturability constraints imposed or potentially imposed on the system. The first step (Block 1) is to collect the manufacturing considerations, which can then be directly translated to manufacturing constraints. It is assumed that the stakeholders specify a manufacturing process or feasible set of processes in the design requirements,

but if this is not the case, several processes can be compared at this step to see which are the least restrictive within the desired domain. It is necessary, however, to select a process or small set of processes before going any further.

Table 2.2: Input and outputs for MR-DFM mapping and screening framework activity blocks.

Activity Block	Input	Output
1	Given from stakeholders	Raw set of manufacturing considerations
2	Raw set of manufacturing considerations	Ranked, ordered, and specified manufacturing constraints
3	Full set of manufacturing constraints	Raw set of manufacturability constraints
4	Raw set of manufacturability constraints	Set of restrictive or possibly restrictive manufacturability constraints
5	Set of restrictive or possibly restrictive manufacturability constraints	Screened set of restrictive or possibly restrictive constraints with redundant and dominated constraints removed

Once a preliminary set of manufacturing constraints are defined, they are subjected to the identify, specify, rank, and combine (I-S-R-C) process (as discussed previously) (Block 2). The output of this process is a set of manufacturing constraints which are well-defined, clearly-specified, ranked in order of importance, and combined into the smallest practical number of constraints. This is then mapped onto a set of manufacturability constraints (Block 3). After the potential set of manufacturability constraints is defined (set $C1$), the constraints are then individually screened to determine if they are restrictive or obviously not restrictive. Uncertain constraints at this point should be retained in the set. The collection of restrictive or potentially restrictive constraints then make up set $C2 \subseteq C1$ (Block 5). This this set is then screened as a set for redundant and dominated constraints, which are rejected from the set. Note that this includes comparison with known non-manufacturability constraints as well.

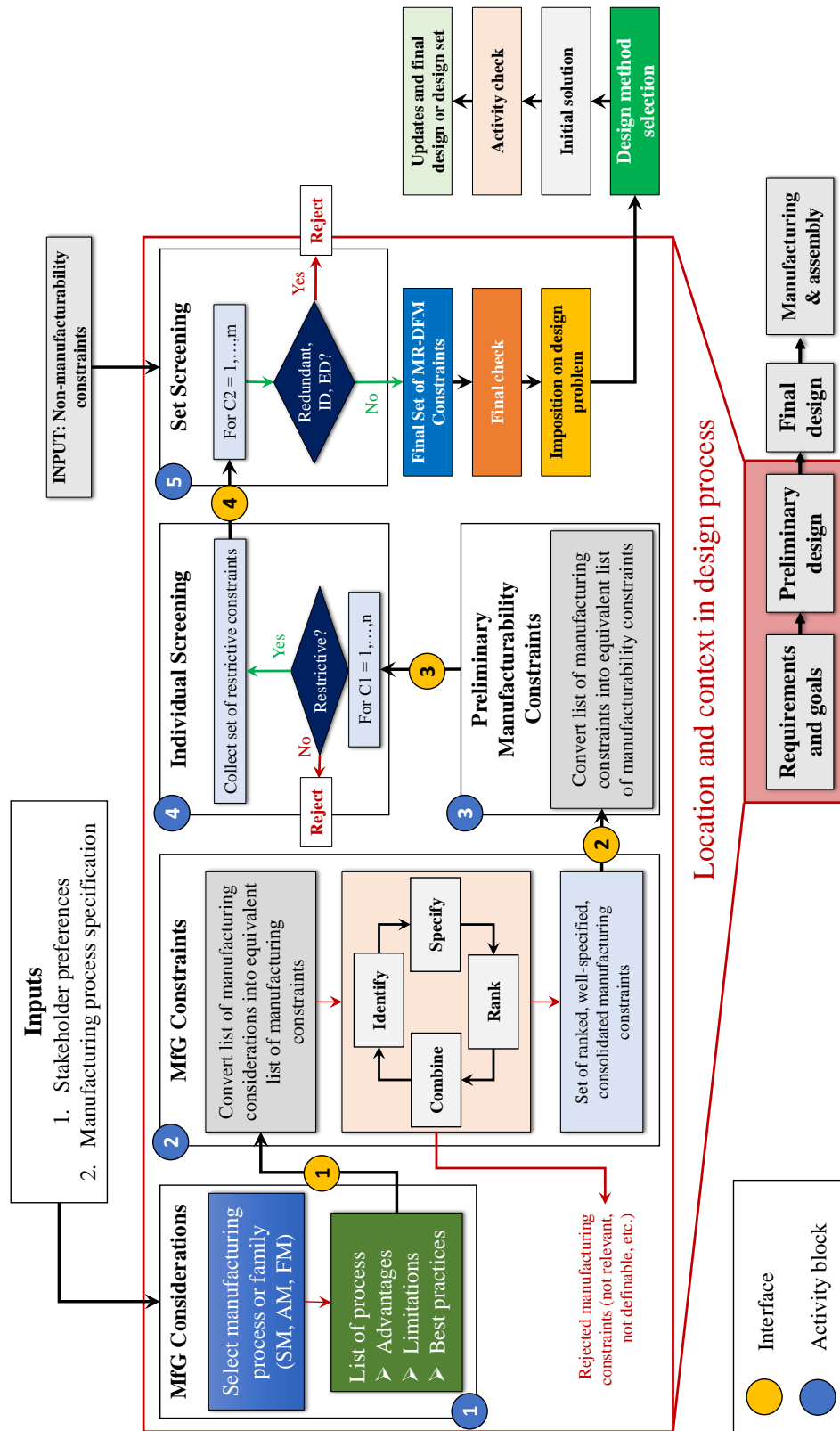


Figure 2.14: Proposed mapping and screening MR-DFM framework.

The set C_{final} should consist of the smallest possible number of manufacturability constraints, which can then be effectively imposed into the design problem, restricting the design space only just enough to ensure manufacturability (i.e., “minimally-restrictive”) and leaving as much of it as possible for the designer to explore. Mathematical activity is not clearly established in this set, as the problem has only been formulated and not yet solved. After building the set of useful and possibly useful constraints, they can be fed into a solution method (classic optimization techniques, topology optimization, procedure/rule-based design, etc.) and the initial solution should give needed information about the activity of the constraints. At this point, the formulation can be finalized and a set of feasible designs generated for the stakeholders to examine.

The data that is mapped could take a variety of forms and the mapping may be explicit, implicit, or manual depending on the needs and formulation of the problem. This may depend on the processes involved of the form of the design problems. In the most common case, it is anticipated that the design problem will involve geometric constraints related to manufacturability; in this case, the mapping could be based on primitive shapes (squares, circles, triangles, etc), nodes in a mesh, points or lines on a shell model, a toolpath (i.e., g-code), or similar. The form of this will be one of the decisions made by the stakeholders when using MR-DFM very early in the design lifecycle.

2.7 Case Studies

2.7.1 Case 1: Milled Aluminum Heat Exchanger Fin

This case study explores a design problem using a single well-defined manufacturing process as the basis for the manufacturability constraints. A heat exchanger fin in a natural-convection environment must be machined from 6061 aluminum (Figure 2.15a). To fit into its defined space, the fin must be 50 *mm* wide and 20 *mm* tall, but the thickness can be adjusted. The design objective was to minimize the total volume of the fin required to dissipate $\dot{Q} = 25 \text{ W}$ of thermal power (Figure 2.15b) with a maximum fin base temperature of 70°C to avoid melting its plastic (polylactic acid) enclosure. The fin base was insulated and so all heat transfer from the 25 *W* source was dissipated by the fin itself. The fin was also

a structural member and required to support a static load of 100 N without buckling. The manufacturability constraint will be the minimum thickness of the fin needed to withstand a conventional milling process (with cutting fluid) using a 7/16 in TiN-coated steel end mill running at 1760 RPM with a feed of 200 mm/min and a cut of up to 0.5 mm per tool pass.

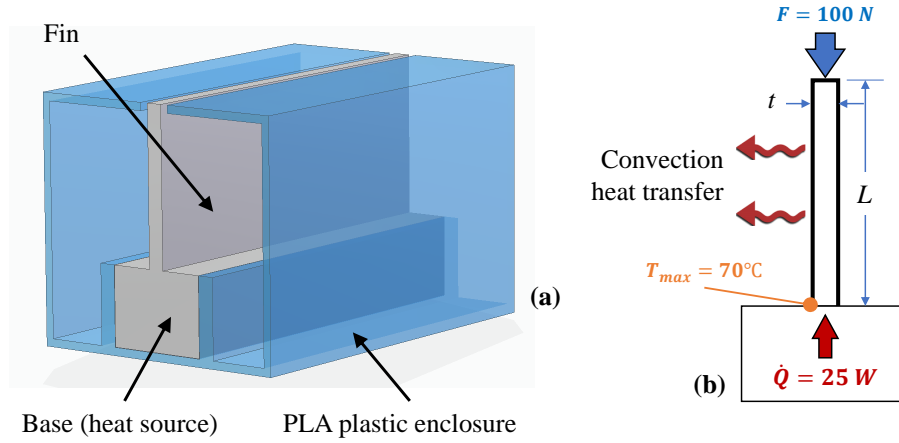


Figure 2.15: Case Study 1 (a) configuration and (b) applied loads.

First, the minimum thickness for the needed heat dissipation (by natural convection) was calculated in order to act as the baseline for the buckling load requirement. This is a performance requirement and not directly related to the manufacturing, but it is necessary in order to judge the effectiveness and need for manufacturability constraints. The heat transfer rate in a finite-length fin heat-transferring (i.e., non-insulated tip) fin is

$$\dot{Q} = \sqrt{hPkA_c}T_{base} \frac{\sinh(mL) + \frac{h}{mk} \cosh(mL)}{\cosh(mL) + \frac{h}{mk} \sinh(mL)} \quad (2.3)$$

where all of the variables are known from the problem statement except for the values of A_c and P , but these are both functions of the fin thickness t . Assuming that $h = h_{air} = 100 \text{ W/m}^2$, $T_{base} = 70^\circ\text{C}$, $k_{AL} = 200 \text{ W/mK}$, and

$$A_c = 50t \text{ mm} \quad (2.4)$$

$$P = 100 + 2t \text{ mm} \quad (2.5)$$

$$m = \sqrt{\frac{hP}{kA_c}} \quad (2.6)$$

the required value of t can be found. Calculating it numerically using MATLAB[®], the minimum value of t to satisfy the heat transfer performance requirement was found to be $t = 0.85 \text{ mm}$. As shown in Figure 2.15b, the fin can be modeled as a column with one fixed end and the maximum allowable compressive force is

$$F = \nu\pi^2 \frac{EI}{L^2} \quad (2.7)$$

where the force F , the length x , the elastic modulus E , and height L of the column are known. Since the fin is fixed at one end and free at the other, $\nu = 0.25$. The value of I is a function of t and can be described by

$$I = \frac{t^3 x}{12} = \frac{50t^3}{12} \quad (2.8)$$

where $x = 50 \text{ mm}$ is the width of the fin. It is clear from inspection of the variable magnitudes that the required thickness of the fin for buckling under the 100 N load is much, much smaller than the thickness needed for heat transfer. Therefore, the heat transfer constraint is restrictive and the fin can be assumed to be able to withstand the load.

Mapping the manufacturability constraints (Table 2.3) for this problem, it is necessary to consider three aspects of the milling process: (1) heat transfer from the end mill to the feature, (2) bending force on the fin from during processing, and (3) vibration and compliance in the machine. Since the mill used in this case study had a large cast iron base and was in good condition, it was assumed that the effect from (3) was negligible. The exact cutting force for a standard milling machine is difficult to measure and is dependent on several factors; a good average peak cutting force value of 200 N was found by Rubeo and Schmitz [231] after extensive modeling and experimentation for aluminum milling, and this value was used for the present case study. Treating the fin as a cantilever beam, a minimum thickness t_{mach} must be used to prevent excessive deflection during machining. A maximum allowable deflection (and resulting dimensional error) δ of 0.1% of the fin thickness was specified; this allowable value was chosen based on the milling experience of

the authors. Therefore, the minimum value of the fin thickness t_{mach} for machining to be successful under the machining force is 1.17 mm .

The heat-of-machining can also be calculated for specific operations, but for this case study the mean value of $\Delta T = 70^\circ\text{C}$ on each cutting pass found by Denkena et al. [232] was used. The heat transfer rate from this temperature differential (assuming only steady-state conductive heat transfer and using the previously-described variables), was

$$\dot{Q} = \frac{kA_c}{L} \Delta T \quad (2.9)$$

In this case, the amount of energy which needs to be dissipated during machining was approximately 40 W . The original fin design (without manufacturability constraints) sized for 40 W would require a fin 1.27 mm thick. In this case study, it was assumed that, for safe operation of the milling process and avoiding any heat warping, the fin was not allowed to reach a temperature higher than its designed operating temperature during processing. Therefore, the fin thickness constraint of 1.27 mm was the minimally-restrictive constraint that ensured manufacturability under the selected processing conditions; this implies that the fin was not manufacturable without the imposition of these constraints, where the heat-of-machining constraint dominates the deflection constraint. Screening the resulting set of manufacturability constraints, it is clear that the 1.27 mm constraint is restrictive and that the 1.17 mm constraint is ID and can be rejected, leaving only the single manufacturability constraint. Both of the non-manufacturability constraints are also dominated and can be removed from the problem.

Table 2.3: Manufacturing consideration, manufacturing constraints, manufacturability constraints, and non-manufacturability constraints for Case Study 1.

Mfg Considerations	Mfg Constraints	Manufacturability Constraints
Heat of machining	Heat of machining $Q = 40 \text{ W}$	$t \geq 1.17 \text{ mm}$ for cutting force
Machining force	Cutting force $F = 200 \text{ N}$	$t \geq 1.27 \text{ mm}$ for heat during machining
Compliance/vibration		
Non-Manufacturability Constraints		$t \geq 0.85 \text{ mm}$ for thermal performance
		$t \geq \text{negligible } (\mathcal{O} \leq \mu\text{m})$ for buckling

Figures 2.16a and 2.16b show the final designs (with and without manufacturability constraints, respectively), while Figures 2.16c and 2.16d present the final manufactured designs. It can be clearly observed that the thin (0.85 mm) fin has numerous manufacturing defects (Figure 2.16e), while the one with the manufacturability constraint was successfully fabricated. In this unconstrained (thin) fin, three major defects were observed: (1) (Note [A]) the fin thickness was inconsistent, with the bottom of the fin being the nominal thickness and the top being 20% thinner, (2) (Note [B]) the top corner was chipped by the end mill during a cutting pass due to its flexibility under cutting force, and (3) (Note [C]) the top of the fin displayed a jagged, almost “scalloped” surface finish. It was observed that all of these defects were caused by the fin deflecting under the load from the end mill, with the top thinning implying that the deflection was at least 10% of the fin thickness, 100 times the allowable deflection. While the temperature of the part was not directly measured during machining, it was also observed that the 0.85 mm fin became hot enough during machining that the cutting fluid (Viper Venom cutting oil, Grizzly Inc.) began to produce smoke, suggesting a temperature over 200°C .

None of the fin surface defects or thinning or extreme heating were observed in the machining of the 1.27 mm fin under identical manufacturing conditions, showing that the imposed constraints were restrictive and effective in ensuring manufacturability. Note that the cost of manufacturability and accuracy was a 33% increase in the mass of the fin. However, this study showed that this was the least-restrictive constraint under which the fin can be effectively fabricated using the specified conditions and process assumptions. It should be noted that this particular case study could have been completed using a variety of design methods, including classic DFM and MR-DFM (as shown). If classic DFM had been used, it is likely that the original thickness based on performance would have been calculated and a factor of safety applied. Using a typical factor of safety of 2.0 for a problem like this, the fin thickness would have been about 1.7 mm thick - in this case, it would both perform correctly and be manufacturable, but the design would be inferior (i.e., be heavier) than the one produced using MR-DFM. Since MR-DFM provided more detailed constraints directly derived from the manufacturing process, a thinner fin that was both manufacturable and functional was able to be produced.

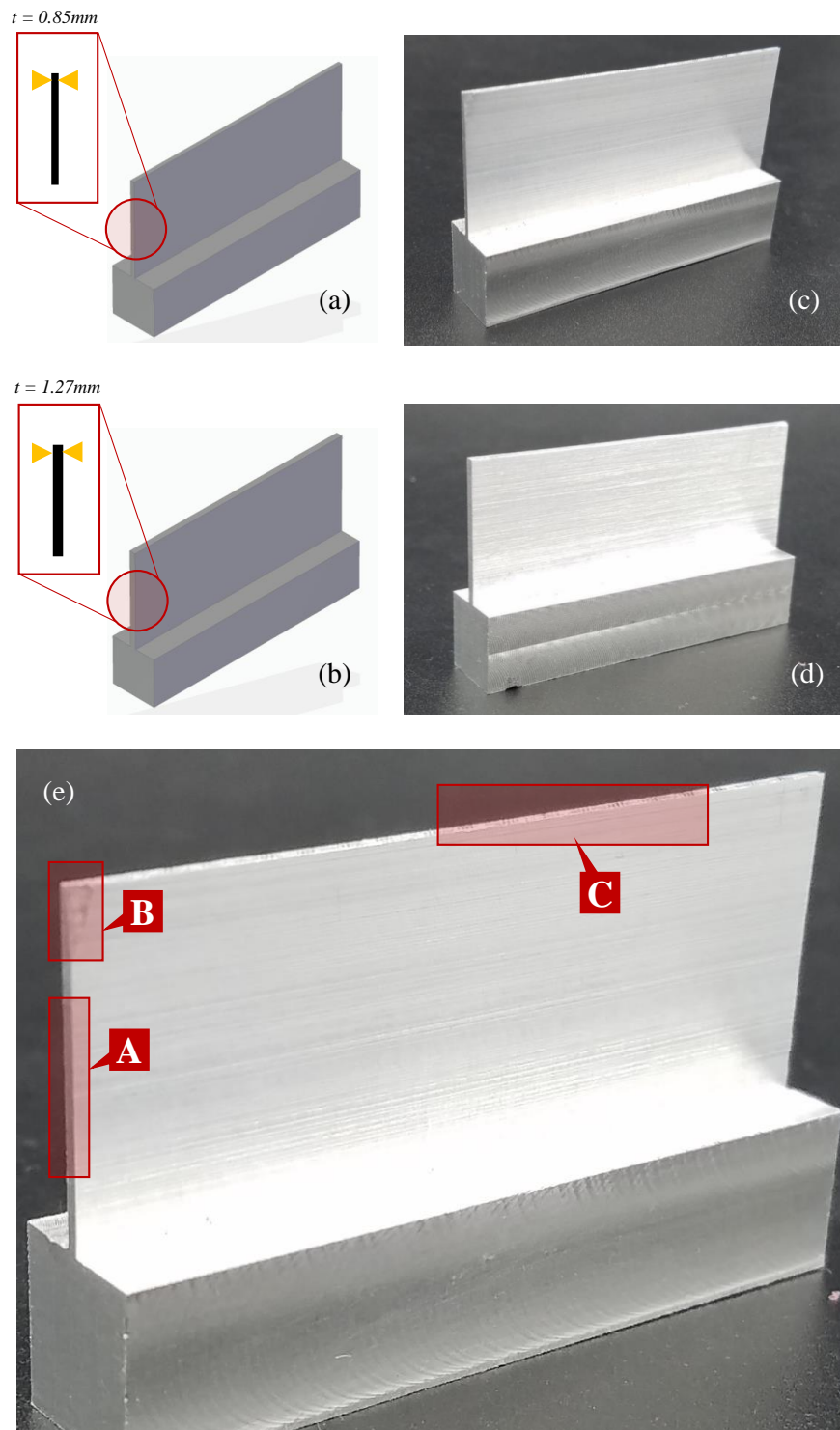


Figure 2.16: (a) original design, (b) design with manufacturability constraints, (c) (failed) manufactured original design, (d) (successful) manufactured constrained design, and (e) details of failed unconstrained design. Note [A]: inconsistent fin thickness, Note [B]: chipped edge from machining, and Note [C]: poor surface finish on fin tip from vibration.

2.7.2 Case 2: FDM/SLA TO Cantilever Beam

This case study used a design problem that must consider the constraints from two manufacturing processes from the same family, unlike Case Study 1 which used only a single process. In this problem, a simple symmetric cantilever beam was to be designed via topology optimization (TO) for minimum mass and minimum compliance (i.e., maximum stiffness). The final design was required to be symmetric along the length and thickness directions. As shown in Figure 2.17a, the beam was 40 mm long by 20 mm tall by 4 mm thick, fixed at one end, and subjected to a 20 N load on the free end. The stakeholders required that the part be made from non-conductive plastic and be both light-weight and stiff, with a final mass fraction goal of 50% and directions to simply “minimize compliance” while maintaining a factor of safety above 1.0. Since only a small number of beams were needed, it was not economical to produce tooling for a molding process, and it was therefore a good candidate for additive manufacturing. The PARETO[®] (Sciartsoft Inc.) TO method and software were used to produce the final geometry and generate the STL files for manufacturing. Since TO requires geometric constraints to be imposed in the problem formulation, they cannot be added later as was done in Case Study 1.

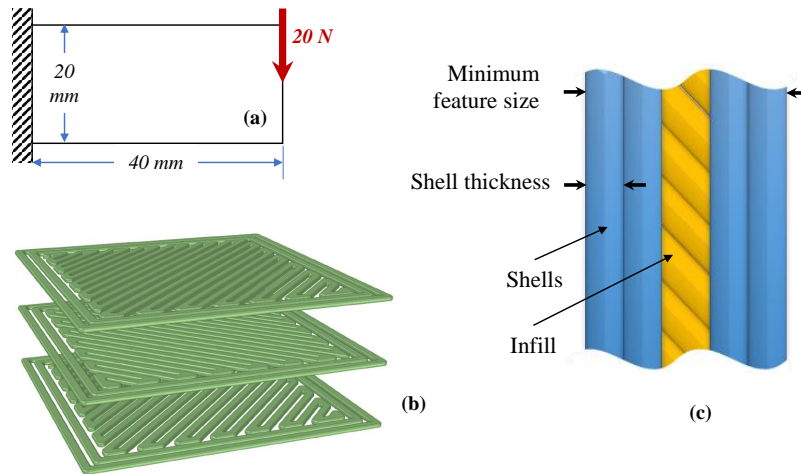


Figure 2.17: (a) Case Study 2 cantilever beam, (b) FDM/scanning SLA material pattern for several layers [167], and (c) detail showing shell and infilled regions of the material.

Two major AM processes were available for production, fused deposition modeling (FDM) and stereolithography (SLA). Neither was preferred by the stakeholders in the re-

quirements; both have different advantages and disadvantages in terms of material properties and performance, so it was decided to formulate the TO solution so that the stakeholders could viably use either one to produce the resulting design. In AM-TO problems, the primary manufacturability constraint is the minimum feature size (i.e., the length scale) that can be produced using a particular process. Both are scanning-type processes, with FDM laying down beads of material selectively to form layer cross-sections, while SLA selectively hardens resin in layers using a laser. In terms of process mechanics, FDM is more restrictive since the bead of material is much wider than the laser spot from SLA. Therefore, if it is possible to manufacture using FDM, it will be possible to fabricate using SLA as well; however, the inverse is not necessarily true. The basic material arrangement is shown in Figure 2.17b and 2.17c.

For both FDM and scanning-type SLA, material is built using shells and infill regions (Figure 2.17c). The minimum resolution for each line is the laser spot width for SLA and the extrusion nozzle diameter for FDM, but there can be some variability depending on the material behavior. In the experience of the authors, single-shelled round or sharp FDM features (such as those produced in 3-D TO solutions) are typically unstable and riddled with defects (due to rapid, un-dissipated local material shrinkage during cooling), so a double shell is required for good-quality prints. It is much less of a concern for parts with thick bead deposition widths or geometries that have mainly straight-line shells, so the designer should be careful when imposing the manufacturability constraint to choose the minimum feature size which ensures manufacturability while minimally restricting the design space. SLA is more forgiving since no material melting is involved, but still requires a shell and some amount of infill for a stable print. Typical values of the material line widths are 0.4 *mm* for FDM and 0.2 *mm* for SLA, so these values were used.

For this case study, a complex 3-D TO solution was expected within a relatively small geometric space (Figure 2.17a). Therefore, to ensure that all of the generated features were manufacturable, it is required to use two shells for the FDM parts and one shell for the SLA parts. This fundamentally translates into the minimum feature size allowed in the TO algorithm of 2 *mm* for the FDM parts and 1 *mm* for the SLA parts. Figures 2.18a and 2.18b show the resulting geometry for each case. The use of the 1 *mm* minimum

length scale allowed the 0.50 mass fraction target to be reached, while the imposition of the FDM manufacturability constraint was able to reach a minimum mass fraction of 0.53. The factor of safety constraint was simply set in the software and did not require any special imposition or monitoring. Screening of the constraints was not needed in this case study, as the minimum number of constraints possible were used from the beginning.

Table 2.4: Manufacturing consideration, manufacturing constraints, manufacturability constraints, and non-manufacturability constraints for Case Study 2

Mfg Considerations	Mfg Constraints	Manufacturability Constraints
Shell/infill print pattern	Two shells + infill for FDM	Minimum length scale for FDM is 2 <i>mm</i>
FDM = 0.4 <i>mm</i> /line	One shells + infill for SLA	Minimum length scale for SLA is 1 <i>mm</i>
SLA = 0.2 <i>mm</i> /line		
Non-Manufacturability Constraints		Mass fraction $\approx 50\%$
		Factor of safety ≥ 1 for TO
		Beam design symmetry

The PARETO method was used to generate the topology under the given conditions and constraints, using a voxel count of 500,000. Figure 2.18c shows an attempt to fabricate the 1 *mm* length scale solution using FDM (Hatchbox ABS, $\delta = 0.15$ *mm*, $230^{\circ}C$, $v = 30$ *mm/s*), resulting in numerous major manufacturing defects and missing features (highlighted yellow regions) since the features were too small for the process to accurately create with the 0.4 *mm* bead size. In contrast, the FDM fabrication was successful for the 2 *mm* length scale solution (Figure 2.18d). Both geometries were successfully produced by the SLA process (Formlabs[®] Form 1+, using Formlabs[®] FLGPK04 resin, $\delta = 0.05$ *mm*), as shown in Figures 2.18e and 2.18f. The PARETO software did not allow the use of a zero-thickness minimum feature size constraint, so it was not possible to generate a topology that was not manufacturable using SLA with this method at the small part size involved. However, the manufacturability constraints imposed clearly had a major impact on the part geometry and were clearly restrictive at least for the FDM fabrication. As with Case Study 1, this implies that the generated designs were not manufacturable under the specified conditions without the use of the manufacturability constraints. The use of the 2 *mm* manufacturability constraint resulted in a 3% mass increase over the 1 *mm* length scale solution, but the resulting final design met the design requirements and was manufacturable using both processes.

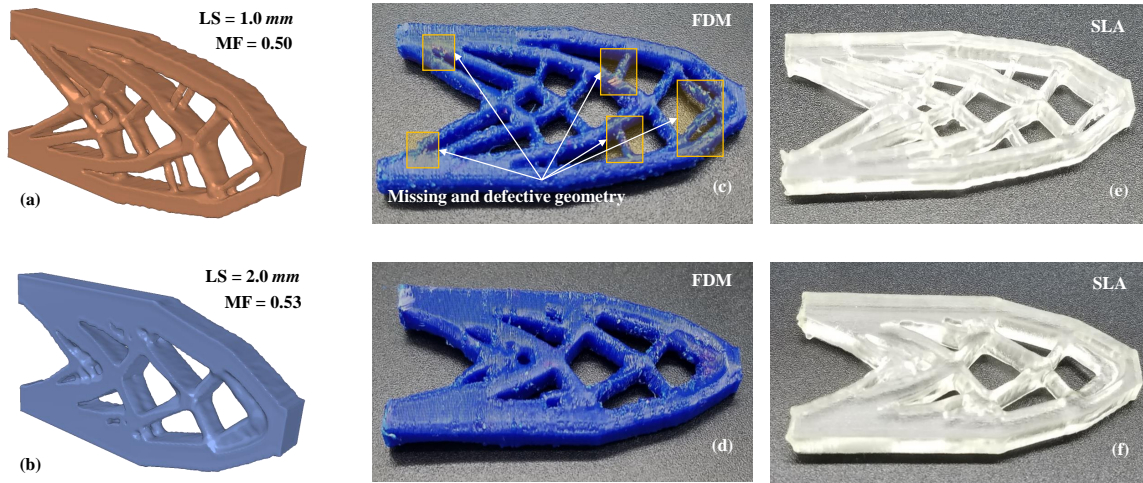


Figure 2.18: (a) TO solution with $LS = 1\text{ mm}$, (b) TO solution with $LS = 2\text{ mm}$, (c) (failed) FDM fabrication of the $LS = 1\text{ mm}$ case, (d) (successful) FDM fabrication of the $LS = 2\text{ mm}$ case, (e) (successful) SLA fabrication of $LS = 1\text{ mm}$ case, and (f) (successful) SLA fabrication of $LS = 2\text{ mm}$ case. Highlighted regions of (c) show the severe manufacturing defects such as missing features. Note that the successful FDM part (d) shows some surface roughness fundamental to FDM, but careful analysis under a microscope showed that all features were fabricated and no dimensional error larger than the print resolution of $150\ \mu\text{m}$ were present.

2.7.3 Case 3: Hybrid AM/SM PLA Pulley

The final case study presented is an updated solution approach to the generator pulley problem presented by Patterson and Allison [11]. In this problem, a belt-drive pulley for a generator was designed and required to be manufactured from PLA plastic (biodegradable polylactic acid) using a combined additive-subtractive hybrid manufacturing process. Therefore, this is also a two-process problem but with the processes in different families. As shown in Figure 2.19, the pulley needs to be driven by twin belts and be able to be stopped in an emergency by a pneumatic brake without damaging the generator. A radial encoder for tracking position is affixed to the side of the pulley, which is then mounted in a frame independent of the generator so that the assembly will not fly apart if the pulley should fail during braking.

The pulley is assumed to be subjected to a running torque load of 5 Nm during operation. During an emergency braking, it is preferred for the web to break instead of the generator or belts, so that should be the weakest point in the pulley. The stakeholders decided that the pulley needed to be lighter than the original design (Figure 2.19a and 2.19b),

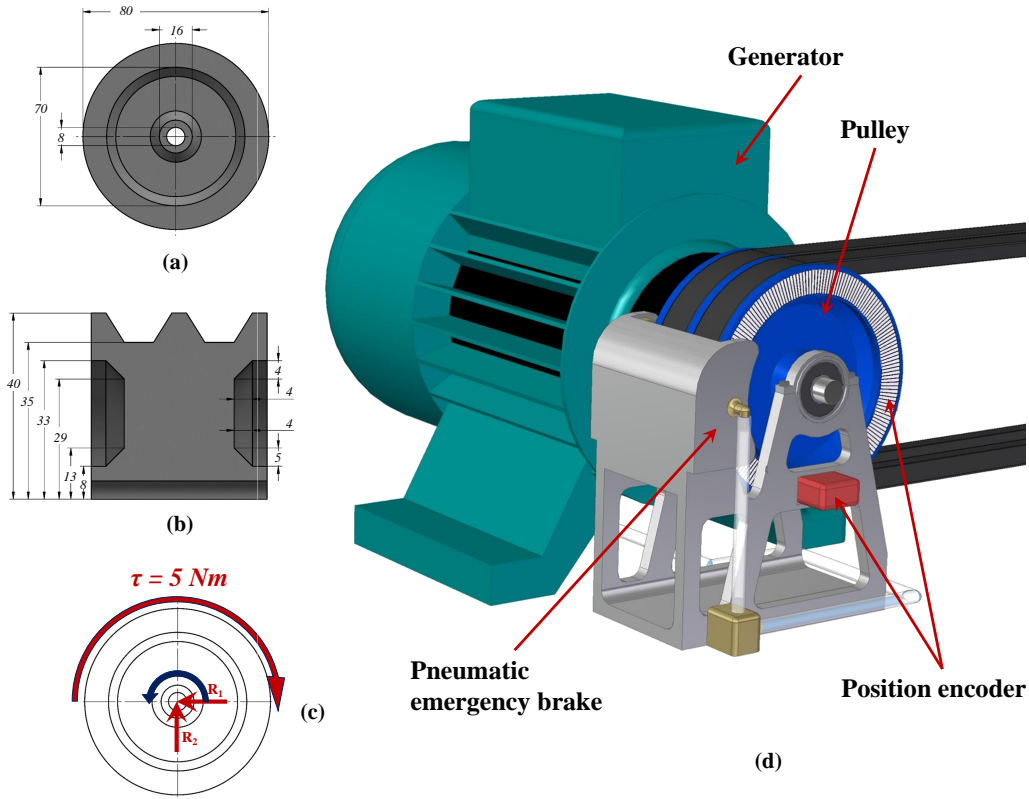


Figure 2.19: (a) original pulley design, (b) original pulley cross-section, (c) free-body diagram, and (d) problem setup

but that the basic interfaces, external shape, and size were not changeable and needed to be smooth and flat on the final part. The web of the pulley could be optimized to remove material as long as the compliance of the pulley remained less than $10 \text{ mm}/\text{KN}$. The solution method selected was a local topology optimization (TO) (PARETO method) with the shaft, brake, and belt interfaces fixed and not subjected to optimization. Given the solution method, it was decided to manufacture the basic web-optimized pulley using fused deposition modeling (deltabot machine, 3-D Solutech[®] PLA, 225°C , bead of 0.6 mm , $\delta = 0.25 \text{ mm}$, $v = 50 \text{ mm}/\text{s}$) and to use a turning process (Grizzly[®] G0602 lathe with indexable carbide cutting tools, 300 RPM) in a sequential hybrid AM-SM process [11]. The basic geometry was created using the AM process, which was then used to face the brake interface and the external edges of the pulley (areas not covered by belts in Figure 2.19d); the contact area for the belts was not to be turned down, as it was not necessary and only increased the manufacturing cost.

Given that (1) a hybrid process is needed, (2) the material will be anisotropic, and (3) the subtractive process involves turning and facing the part, there will be several major manufacturing constraints imposed, only some of which will be restrictive when translated to manufacturability constraints. The minimum feature size should be addressed by imposing a minimum length scale, while symmetry and build orientation are inherent on the AM process. The workholding constraint does not impact the manufacturability since the overall external size of the pulley did not change during the design. After completing the full screening process, it can be seen that the only definite manufacturability constraints which must be imposed in the part are the minimum feature size and the shell thickness. From the experience of the authors, it is necessary to remove at least 1 *mm* of material from PLA parts in a turning operation in order to generate chips and obtain a good surface finish. Considering the required printing parameters, it was determined that a minimum of five shells were required to be used to ensure both good quality printing and stable lathe operations. The minimum feature size for FDM was discussed extensively in Case Study 2, so it was not revisited fully. Since the bead width for this problem is 50% wider, PLA is less sensitive than ABS to residual stresses, and since pulley web lines are generally straight and cut-through, the same minimum size of 2 *mm* was determined to apply to this study as well.

Table 2.5: Manufacturing consideration, manufacturing constraints, manufacturability constraints, and non-manufacturability constraints for Case Study 3

Mfg Considerations	Mfg Constraints	Manufacturability Constraints
Hybrid process	Two shells + infill for FDM	Minimum length scale for FDM is 2 <i>mm</i>
AM + SM in sequence	Print orientation	Minimum shell count = 5
FDM + lathe	Shell thickness	Minimum roof layer count = 5
Anisotropic material	Part base/roof thickness	Minimum base layer count = 5
	Work holding	Maximum size \leq lathe chuck jaw diameter
Non-Manufacturability Constraints		Factor of safety \geq 1 for TO
		Pulley design symmetry

Based on the requirements, a series of TO solutions were found (PARETO TO, three million voxels), with the solution selected being the minimum-mass solution found before no more feasible designs were found (Figure 2.20a); the final design (Figure 2.20b) had a

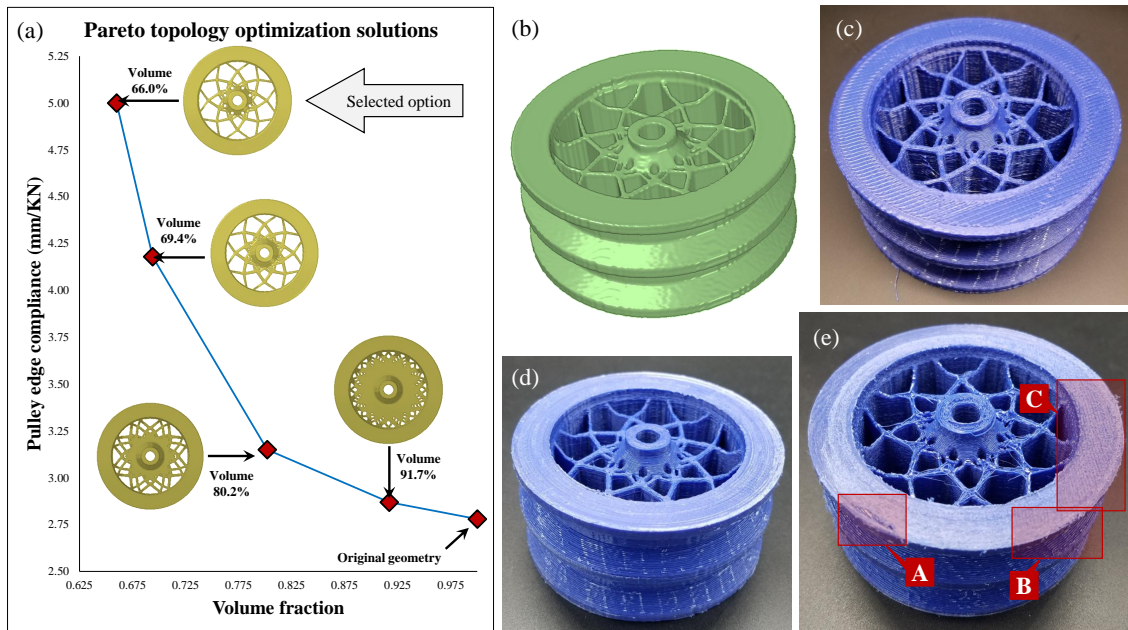


Figure 2.20: (a-b) selected solution from Pareto curve, (c) as-printed, and (d) successful and (e) failed pulleys. Note [A]: torn surface, Note [B] melted surface areas, Note [C] delamination.

mass fraction of 0.66 and a compliance of about $5.00 \text{ mm}/KN$, well within the maximum allowed. Figure 2.20c shows the printed pulley before lathe operations, while Figure 2.20d is the successful finished pulley. To show that the manufacturability constraints are restrictive, a second pulley was produced using the same TO solution, but which used only two shells; the activity of the minimum feature size constraint was established in Case Study 2, so only the shell constraint was tested here. Figure 2.20e illustrates the results for the 2-shell pulley, which was clearly a failure. Several areas of surface tearing, layer delamination, and plastic melting were observed, as highlighted in the figure. Unlike the other two case studies, the restrictive manufacturability constraints did not increase the mass of the final design, but they did increase the manufacturing time; shells are typically the slowest features on a printed part to create, so adding shells can slow down the process. It was observed for this case study that the 5-shell part required approximately 35 minutes more production time to fabricate than the 2-shell pulley. Clearly the extra shells were required, so the cost of the constraint is in manufacturing time and not in performance.

2.8 Remarks on Inputs and Practical Implementation

The approach presented in this article focused on mapping and formulation of mechanical design problems under MR-DFM constraints. As discussed in the introduction (Figure 2.8), a full design process under manufacturability constraints (whether classic DFM or MR-DFM) requires three major domains of knowledge. This article extensively discussed Domain 2 (mapping and formulation) to better develop the concepts and approach. However, some important remarks should be made regarding the other two domains in the context of the discussion thus far. It is necessary to carefully consider the impact of the other two for the work presented here to be useful in actual design. MR-DFM will not be useful or applicable to every design problem and may be quite expensive even in some cases where it is useful. The decision to use it should be made by the stakeholders and justified by its ability to provide a superior design or set of designs within an acceptable cost point. If the designers are looking for a “good enough” solution that simply fits within the minimum requirements, the additional work may not be practical. It is anticipated that this method will be most useful for high-value complex products and systems (such as aircraft and medical devices) in which excellent design quality is paramount and the designers need the largest possible feasible design space.

2.8.1 Process and Material Modeling

One of the most important mantras, reinforced throughout this article, of MR-DFM is that the quality of the constraints depends heavily on the quality of the inputs. In design, it is very common to use simplified representations of process and material models in order to reduce computational cost. While this may be useful in many cases, this could be the source of significant error in the formulation of MR-DFM constraints and should be avoided when possible. It is best to use direct experimental results to generate the constraints whenever possible via a fitted model or random variable generation. In both cases, the estimated uncertainty and potential errors may be calculated and documented. With these, the amount of “fuzziness” (Figure 2.13b) can be estimated to ensure that the calculated constraints are actually useful for the design at hand. An important area of future research

should be to find how much uncertainty is allowable in these constraints before the method fails to provide a design superior to one generated using classic DFM.

2.8.2 Constraint Automation and Design Trade-Offs

An obvious consideration with the MR-DFM method is that it can rapidly become unmanageable for a single designer or decision maker as the problem size increases. The case studies presented are reasonably complex for academic studies but when dozens of features are to be considered or system constraints must be considered (i.e., interfaces, tolerances, and reliability) it can become impossible to implement manually. Therefore, the mapping and enforcement should be automated as far as possible. This should be relatively easy to do for most manufacturability problems, as many DFM and MR-DFM constraints can be reasonably defined as boundaries and simple polynomial constraints, with some binary and discrete functions on occasion. However, as the method and computational methods improve in capacity, more accurate models of interactions between geometry and considerations such as temperature, stress, and deformation during manufacturing can be used. These higher-fidelity constraints can expand the design space even more (in many cases) but only are worth pursuing where the increase in design quality is worth the investment of time and resources.

With this in mind, it is clear that the complexity of the used constraints is at least partially under the control of the designer; if the constraint set is too complex, the stakeholders may wish to simplify the constraint set or define some design variables as constants. As long as the simplified MR-DFM constraints provide a larger design space than traditional DFM (or conversely, are shown to not be necessary at all), then this trade-off could still provide a superior solution or larger set of feasible designs to select from. Exactly how the automation should be done is beyond the scope of this paper; however, feature catalogs, general constraints that may repeat several times (e.g., minimum wall thickness for machining may be identical for several features in the design), and node-point maps for defining geometry (in which all geometry constraints can be defined as simple distances) are potentially helpful tools for this. In the case of more procedure-based design problems, the manufacturability constraints could be directly tied to the stakeholder requirements. Some

practical considerations for automating the constraint generation are:

- For explorations and for mapping new processes and process-material combinations, the mapping will likely involve a significant amount of manual or mathematical work. However, the mapping should be stable and consistent for each process so the mappings can be cataloged.
- These catalogs of mappings and constraints can be used as the starting place for automating constraints.
- Once a set of mappings are completed (e.g., for the 10 most common manufacturing processes), design automation studies can begin. Similarities and differences can be identified and some mappings combined or simplified in the ideal case.
- It is very important at the beginning of the design process to identify or specify the data type (mathematical functions, points in a mesh, etc.) to be used in the mapping. Consistent application of this will aid in automating the constraints.
- A future work direction may be to see if a new data type is needed to map these constraints, but this may not be necessary for general mechanical design problems. In formulating most mechanical design problems, most of the relevant constraints will be geometric and will be in the form of distances, thicknesses, norms between points, and similar.
- A very helpful technology that can support MR-DFM is digital twins of manufacturing processes. When properly developed and verified, this may be able to replace actual manufacturing processes and make the identification of manufacturing considerations much easier.
- From the other perspective, MR-DFM and other constraint/formulation methods may help drive the development and refinement of these digital twins. It would be especially useful if digital twin models could be developed and formulated so that they provide the manufacturing considerations and constraints as default outputs.

Clearly, there will be design trade-offs when using this methods as there are with classic FDM and other methods. The most important considerations for most problems would be:

- Cost, both in terms of labor during initial mappings or explorations and in terms of computational expense once automated.
- Different classes of manufacturing processes will have drastically different costs associated with using them in design. For example, simple geometric constraints based on a die casting tool will be far less expensive than designing a free-form lattice structure with different location densities.
- As previously discussed, MR-DFM is far more focused and based on technical knowledge instead of expert intuition. For simple problems and those with few or no active manufacturability constraints, the flexibility offered by using expert-intuition-driven DFM could provide better design outcomes.
- Continuing from the last point, not every mechanical design problem will have active manufacturability constraints and discovering this after using MR-DFM could waste time and resources. Design problems which are convex in nature are less likely to require many (or any) manufacturability constraints due to the fact that only a single global solution is possible.

2.8.3 Expert Intuition

For any DFM or MR-DFM method, some level of expert intuition will be necessary. For classic DFM, several excellent guides are available but still require interpretation and application to the problem at hand. With MR-DFM, the ability to capture process knowledge (manufacturing considerations) and experience is one of the strengths of the presented method; this allows more realistic constraints and a wider design space. However, there will always be some uncertainty in the collected information. To minimize this, the design team should be careful to collect only the most reliable information and make an effort to communicate well with the expert, who will often be a technician and not a researcher or engineer. Respect for the experience of the expert (who will not necessarily have advanced degrees), inclusion of the expert in design decisions, and real effort at partnership with the design team will be vital for collecting the best quality design knowledge. When practical, it would also be very useful for at least some members of the design team to have some

degree of practical knowledge and experience with the selected manufacturing process or processes. Whether this involved hiring designers with hands-on experience (of which there are very few in most industries), providing additional coursework, or some kind of hands-on training will depend on the type problem being solved and the desired outcomes.

2.8.4 Design Method Selection

The presented framework is design-method agnostic and can provide useful constraints for a wide variety of problems. However, the design method may affect the formulation of the problem and this should be expected for any design method outside of classic optimization methods. The formulation that comes from using this technique will be in the form of Eq. (2.2) and may need to be reformulated for a specific solution method. Therefore, care should be taken that the final model (objective function and constraints) are as mathematically rigorous and clear as possible to avoid any mistakes or misunderstandings during any needed reformulation. All variables should be distinct and clearly and consistently defined in a way that is easily understandable by someone not in the original design team.

2.8.5 Verification, Validation, and Certification

As with all design methods (all three domains in Figure 2.8), the final step and ultimate success metric is the completion of the verification, validation, and certification (VV&C) process. While this is largely independent of the specific constraint formulation, it may be necessary to have the constraints very clearly specified for VV&C. Therefore, it is vital that everything be well-documented during the entire process and, when possible, a calculation of the expected uncertainty and error in the placement of the constraints.

2.9 Closing Remarks

In this work, a conceptual framework and approach was developed for generating and imposing minimally-restrictive manufacturability constraints (MR-DFM) for mechanical design problems. The technique is based on mapping of practical manufacturing knowledge into enforceable manufacturability constraints; these can be screened and eliminated as needed to ensure that the imposed constraints restrict the design space only enough to guarantee

(or at least greatly improve) manufacturability while leaving as much as possible intact for design exploration.

The method was shown to be straight-forward and useful in three case studies, all of which were not manufacturable using the specified manufacturing conditions without the additional constraints. Note that the case studies made some simplifying assumptions, clearly stated within each problem, which may impact the validity of the case studies if the conditions were changed. The reader should keep in mind these assumptions when following the case studies and applying the approach to other (similar) problems. The impact of using simplifying assumptions for generating manufacturability constraints is the risk of false positives (the generated constraints are not sufficient to guarantee manufacturability) and false negatives (the constraints exclude more of the design space than actually required); care should be taken to avoid this when applying the method.

The case studies presented covered three different types of mechanical design problems under manufacturability: (1) design under a single process, (2) design under two different but related processes, and (3) design under a hybrid of two dissimilar processes. In terms of design problems,

- The design focus of case study 1 was to find the least restrictive constraint on the fin thickness such that it could both meet its design requirements and be manufacturable. This involved modeling and testing several aspects of the design (heat transfer, beam bending, and buckling) using a common design variable; the constraint found was the least-restrictive one which was applicable to all of the problems encountered containing the design variable.
- Case study 2 explored the formulation of a algorithmic design problem (topology optimization) under two possible manufacturing processes, requiring constraints which were valid for the entire problem. This also captured the potential scenario in which uncertainty exists in the selection of the process and so the design must allow some flexibility.
- Finally, case study 3 explored the complexity of a hybrid manufacturing problem, where a larger number of manufacturability constraints needed to be considered even

for a just two design variables. This problem also clearly demonstrated the way that the constraints can be quickly tested and eliminated when not useful.

Thus this proposed technique was shown to be valid for different mechanical design domains. The method is process-, material-, and solution method-independent, as derived and as demonstrated in the case studies. As presented, this method makes seven important assumptions:

1. That the design requirements for the product being designed are well-defined and relatively fixed at the time of planning
2. That expert intuition is sufficient to judge the impacts of the manufacturing processes and complete the mappings
3. That the manufacturing process selection happens during or before the conceptual design phase
4. The problem is small enough so that a relatively limited number of manufacturability constraints can be tracked and enforced by the designers. A few dozen design variables is likely to be the practical limit for this method without automation of constraint selection and enforcement.
5. The designers have enough basic manufacturing knowledge to complete the mappings or have access to manufacturing experts who are willing to assist
6. That a manufacturing process or set of candidate processes can be selected during requirements definition
7. In the case where several processes need to be compared during the manufacturing considerations phase, the decision can be fixed before defining the manufacturing constraints and not need to be revised later in the design process.

This method is applicable for any mechanical design problems in which the physical design constraints (part architecture and performance) can be defined and understood in terms of its manufacturing processes in some way. Future work will focus on refinement of the method and extension of it to other design domains, such as design of tailored

materials, on the automation of the process for larger problems, tolerance allocation along with the constraints, the use of simulations and experiments to establish the limits of problem complexity, and examining the impact of the expert intuition assumption on the proposed framework.

Copyright Acknowledgement: As of April 10, 2021, most of the work presented in this chapter has been published (or copyright assigned) in the following papers and is reproduced here with permission of the current copyright holder (if applicable) - see any needed official copyright permission forms attached in the supplemental materials.

Patterson, A.E., Lee, Y-H., Allison, J.T. (2021). Generation and enforcement of process-driven manufacturability constraints: A survey of methods and perspectives for product design. *Journal of Mechanical Design* (not yet assigned to an issue). DOI: 10.1115/1.4050740.

Patterson, A.E., Allison, J.T. (2019). Generation and mapping of minimally-restrictive manufacturability constraints for mechanical design problems. ASME IDETC - 24th ASME Design for Manufacturing and the Life Cycle Conference, August 18-21, 2019, Anaheim, CA, USA. DOI: 10.1115/DETC2019-97386.

Patterson, A.E., Lee, Y-H., Allison, J.T. (2019). Overview of the development and enforcement of process-driven manufacturability constraints in product design. ASME IDETC -24th ASME Design for Manufacturing and the Life Cycle Conference, August 18-21, 2019, Anaheim, CA, USA. DOI: 10.1115/DETC2019-97384.

Patterson, A.E., Allison, J.T. (2018). Manufacturability constraint formulation for design under hybrid additive-subtractive manufacturing. ASME IDETC - 23rd ASME Design for Manufacturing and the Life Cycle Conference, August 26-29, 2018, Quebec City, QC, Canada. DOI: 10.1115/DETC2018-85637.

In addition to the papers that make up the bulk of the text in the chapter, the following figures were also separately copyrighted. As with the papers above, official permission of

the copyright holders was obtained before reproducing them in this chapter.

- Figure 2.3a © Elsevier B.V. and reproduced with permission. The official copyright permission form can be found in the supplemental materials.
- Figure 2.3b © Elsevier B.V. and reproduced with permission. The official copyright permission form can be found in the supplemental materials.
- Figure 2.4a © Elsevier B.V. and reproduced with permission. The official copyright permission form can be found in the supplemental materials.
- Figure 2.4b © Elsevier B.V. and reproduced with permission. The official copyright permission form can be found in the supplemental materials.
- Figure 2.5a © Elsevier B.V. and reproduced with permission. The official copyright permission form can be found in the supplemental materials.
- Figure 2.5b © Elsevier B.V. and reproduced with permission. The official copyright permission form can be found in the supplemental materials.
- All other figures in this chapter are covered under the ASME copyright permissions, were originally published under a CC-BY license and appropriately cited, or were from official US Government documents and therefore not subject to copyright in the United States.

Chapter 2 Bibliography

- [1] S. Krish, “A practical generative design method,” *Computer-Aided Design*, vol. 43, no. 1, pp. 88–100, 2011.
- [2] A. Khetan, D. J. Lohan, and J. T. Allison, “Managing variable-dimension structural optimization problems using generative algorithms,” *Structural and Multidisciplinary Optimization*, vol. 52, no. 4, pp. 695–715, 2015.
- [3] K. Suresh, “A 199-line matlab code for pareto-optimal tracing in topology optimization,” *Structural and Multidisciplinary Optimization*, vol. 42, no. 5, pp. 665–679, 2010.
- [4] E. M. Dede, S. N. Joshi, and F. Zhou, “Topology optimization, additive layer manufacturing, and experimental testing of an air-cooled heat sink,” *Journal of Mechanical Design*, vol. 137, no. 11, p. 111403, 2015.
- [5] D. R. Herber, T. Guo, and J. T. Allison, “Enumeration of architectures with perfect matchings,” *Journal of Mechanical Design*, vol. 139, p. 051403, Apr. 2017.
- [6] D. R. Herber and J. T. Allison, “A problem class with combined architecture, plant, and control design applied to vehicle suspensions,” in *Volume 2A: 44th Design Automation Conference*, American Society of Mechanical Engineers, Aug. 2018.
- [7] Y. Reich, S. L. Konda, S. N. Levy, I. A. Monarch, and E. Subrahmanian, “New roles for machine learning in design,” *Artificial Intelligence in Engineering*, vol. 8, no. 3, pp. 165–181, 1993.
- [8] M. Fuge, B. Peters, and A. Agogino, “Machine learning algorithms for recommending design methods,” *Journal of Mechanical Design*, vol. 136, no. 10, p. 101103, 2014.
- [9] S. L. Vatanabe, T. N. Lippi, C. R. de Lima, G. H. Paulino, and E. C. Silva, “Topology optimization with manufacturing constraints: A unified projection-based approach,” *Advances in Engineering Software*, vol. 100, pp. 97–112, 2016.
- [10] A. Sutradhar, J. Park, P. Haghighi, J. Kresslein, D. Detwiler, and J. J. Shah, “Incorporating manufacturing constraints in topology optimization methods: A survey,” in *Volume 1: 37th Computers and Information in Engineering Conference*, ASME, 2017.

- [11] A. E. Patterson and J. T. Allison, “Manufacturability constraint formulation for design under hybrid additive-subtractive manufacturing,” in *ASME IDETC: Volume 4: 23rd Design for Manufacturing and the Life Cycle Conference*, ASME, 2018.
- [12] R. Lynn, C. Saldana, T. Kurfess, N. Reddy, T. Simpson, K. Jablokow, T. Tucker, S. Tedia, and C. Williams, “Toward rapid manufacturability analysis tools for engineering design education,” *Procedia Manufacturing*, vol. 5, pp. 1183–1196, 2016.
- [13] B. S. Blanchard and W. J. Fabrycky, *Systems Engineering and Analysis (4th Edition)*. Prentice Hall, 2005.
- [14] E. Lutters, F. J. van Houten, A. Bernard, E. Mermoz, and C. S. Schutte, “Tools and techniques for product design,” *CIRP Annals*, vol. 63, no. 2, pp. 607–630, 2014.
- [15] NASA, *NASA Systems Engineering Handbook: NASA/Sp-2016-6105 Rev2 - Full Color Version*. 12th Media Services, 2017.
- [16] J. G. Bralla, *Design for Manufacturability Handbook (2nd Edition)*. McGraw-Hill Education, 1998.
- [17] G. Pahl, W. Beitz, J. Feldhusen, and K. H. Grote, *Engineering Design: A Systematic Approach (3rd Edition)*. Springer, 2007.
- [18] G. Boothroyd, “Product design for manufacture and assembly,” *Computer-Aided Design*, vol. 26, no. 7, pp. 505–520, 1994.
- [19] J. W. Herrmann, J. Cooper, S. K. Gupta, C. C. Hayes, K. Ishii, D. Kazmer, P. A. Sandborn, and W. H. Wood, “New directions in design for manufacturing,” in *Volume 3d: 8th Design for Manufacturing Conference*, ASME, 2004.
- [20] T. T. Pullan, M. Bhasi, and G. Madhu, “Application of concurrent engineering in manufacturing industry,” *International Journal of Computer Integrated Manufacturing*, vol. 23, no. 5, pp. 425–440, 2010.
- [21] L. Howard and H. Lewis, “The development of a database system to optimise manufacturing processes during design,” *Journal of Materials Processing Technology*, vol. 134, no. 3, pp. 374–382, 2003.
- [22] P. Barnawal, M. C. Dorneich, M. C. Frank, and F. Peters, “Evaluation of design feedback modality in design for manufacturability,” *Journal of Mechanical Design*, vol. 139, no. 9, p. 094503, 2017.
- [23] S. J. Hu, “Evolving paradigms of manufacturing: From mass production to mass customization and personalization,” *Procedia CIRP*, vol. 7, pp. 3–8, 2013.

- [24] C. R. Duguay, S. Landry, and F. Pasin, "From mass production to flexible/agile production," *International Journal of Operations & Production Management*, vol. 17, no. 12, pp. 1183–1195, 1997.
- [25] W.-S. Chu, M.-S. Kim, K.-H. Jang, J.-H. Song, H. Rodrigue, and et al., "From design for manufacturing (DFM) to manufacturing for design (MFD) via hybrid manufacturing and smart factory: A review and perspective of paradigm shift," *International Journal of Precision Engineering and Manufacturing-Green Technology*, vol. 3, no. 2, pp. 209–222, 2016.
- [26] J. Jiao and M. M. Tseng, "Customizability analysis in design for mass customization," *Computer-Aided Design*, vol. 36, no. 8, pp. 745–757, 2004.
- [27] M. Tseng, R. Jiao, and C. Wang, "Design for mass personalization," *CIRP Annals*, vol. 59, no. 1, pp. 175–178, 2010.
- [28] G. A. Hazelrigg, "A framework for decision-based engineering design," *Journal of Mechanical Design*, vol. 120, no. 4, p. 653, 1998.
- [29] M. Gries, "Methods for evaluating and covering the design space during early design development," *Integration, the VLSI Journal*, vol. 38, no. 2, pp. 131–183, 2004.
- [30] I. Y. Kim and B. M. Kwak, "Design space optimization using a numerical design continuation method," *International Journal for Numerical Methods in Engineering*, vol. 53, no. 8, pp. 1979–2002, 2002.
- [31] A. Gelsey, M. Schwabacher, and D. Smith, "Using modeling knowledge to guide design space search," *Artificial Intelligence*, vol. 101, no. 1-2, pp. 35–62, 1998.
- [32] J. T. Black and R. A. Kohser, *DeGarmo's Materials and Processes in Manufacturing (11th Edition)*. Wiley, 2011.
- [33] A. Archenti, T. Osterlind, and C. M. Nicolescu, "Evaluation and representation of machine tool deformations," *Journal of Machine Engineering*, vol. 11, no. 4, pp. 105–117, 2011.
- [34] J. Mayr, J. Jedrzejewski, E. Uhlmann, M. A. Donmez, W. Knapp, F. Härtig, K. Wendt, T. Moriwaki, P. Shore, R. Schmitt, C. Brecher, T. Würz, and K. Wegener, "Thermal issues in machine tools," *CIRP Annals*, vol. 61, no. 2, pp. 771–791, 2012.
- [35] A. E. Diniz and R. Micaroni, "Cutting conditions for finish turning process aiming: the use of dry cutting," *International Journal of Machine Tools and Manufacture*, vol. 42, pp. 899–904, June 2002.
- [36] J. Zhou, M. Andersson, and J. Ståhl, "Identification of cutting errors in precision hard turning process," *Journal of Materials Processing Technology*, vol. 153-154, pp. 746–750, Nov. 2004.

- [37] J. Yan and L. Li, “Multi-objective optimization of milling parameters – the trade-offs between energy, production rate and cutting quality,” *Journal of Cleaner Production*, vol. 52, pp. 462–471, Aug. 2013.
- [38] F. Jiang, J. Li, L. Yan, J. Sun, and S. Zhang, “Optimizing end-milling parameters for surface roughness under different cooling/lubrication conditions,” *The International Journal of Advanced Manufacturing Technology*, vol. 51, pp. 841–851, May 2010.
- [39] N. Tosun, “Determination of optimum parameters for multi-performance characteristics in drilling by using grey relational analysis,” *The International Journal of Advanced Manufacturing Technology*, vol. 28, pp. 450–455, May 2005.
- [40] A. Bezerra, A. Machado, A. Souza, and E. Ezugwu, “Effects of machining parameters when reaming aluminium–silicon (SAE 322) alloy,” *Journal of Materials Processing Technology*, vol. 112, pp. 185–198, May 2001.
- [41] P. Albertelli, S. Elmas, M. R. Jackson, G. Bianchi, R. M. Parkin, and M. Monno, “Active spindle system for a rotary planing machine,” *The International Journal of Advanced Manufacturing Technology*, vol. 63, pp. 1021–1034, Feb. 2012.
- [42] M. R. Jackson, P. Hynek, and R. M. Parkin, “On planing machine engineering characteristics and machined timber surface quality,” *Proceedings of the Institution of Mechanical Engineers, Part E: Journal of Process Mechanical Engineering*, vol. 221, pp. 17–32, Feb. 2007.
- [43] J. Sutherland, E. Salisbury, and F. Hoge, “A model for the cutting force system in the gear broaching process,” *International Journal of Machine Tools and Manufacture*, vol. 37, pp. 1409–1421, Oct. 1997.
- [44] R. K. Cholpadi and A. Kuttan, “Mechanistic force modeling for broaching process,” *International Journal of Manufacturing Engineering*, vol. 2014, pp. 1–10, 2014.
- [45] Z. B. Hou and R. Komanduri, “On the mechanics of the grinding process – part i. stochastic nature of the grinding process,” *International Journal of Machine Tools and Manufacture*, vol. 43, pp. 1579–1593, Dec. 2003.
- [46] H. Tönshoff, J. Peters, I. Inasaki, and T. Paul, “Modelling and simulation of grinding processes,” *CIRP Annals*, vol. 41, no. 2, pp. 677–688, 1992.
- [47] V. Nasir and J. Cool, “A review on wood machining: characterization, optimization, and monitoring of the sawing process,” *Wood Material Science & Engineering*, vol. 15, pp. 1–16, Apr. 2018.
- [48] M. Sarwar, M. Persson, H. Hellbergh, and J. Haider, “Measurement of specific cutting energy for evaluating the efficiency of bandsawing different workpiece materials,” *International Journal of Machine Tools and Manufacture*, vol. 49, pp. 958–965, Oct. 2009.

- [49] Q. Fan, “Computerized modeling and simulation of spiral bevel and hypoid gears manufactured by gleason face hobbing process,” *Journal of Mechanical Design*, vol. 128, pp. 1315–1327, Dec. 2005.
- [50] K.-D. Bouzakis, S. Kombogiannis, A. Antoniadis, and N. Vidakis, “Gear hobbing cutting process simulation and tool wear prediction models,” *Journal of Manufacturing Science and Engineering*, vol. 124, pp. 42–51, Mar. 2001.
- [51] S. Maiti, A. Ambekar, U. Singh, P. Date, and K. Narasimhan, “Assessment of influence of some process parameters on sheet metal blanking,” *Journal of Materials Processing Technology*, vol. 102, pp. 249–256, May 2000.
- [52] W. Klingenberg and U. Singh, “Finite element simulation of the punching/blanking process using in-process characterisation of mild steel,” *Journal of Materials Processing Technology*, vol. 134, pp. 296–302, Mar. 2003.
- [53] E. Olakanmi, R. Cochrane, and K. Dalgarno, “A review on selective laser sintering/melting (SLS/SLM) of aluminium alloy powders: Processing, microstructure, and properties,” *Progress in Materials Science*, vol. 74, pp. 401–477, Oct. 2015.
- [54] H. Lee, C. H. J. Lim, M. J. Low, N. Tham, V. M. Murukeshan, and Y.-J. Kim, “Lasers in additive manufacturing: A review,” *International Journal of Precision Engineering and Manufacturing-Green Technology*, vol. 4, pp. 307–322, July 2017.
- [55] O. A. Mohamed, S. H. Masood, and J. L. Bhowmik, “Optimization of fused deposition modeling process parameters: a review of current research and future prospects,” *Advances in Manufacturing*, vol. 3, pp. 42–53, Feb. 2015.
- [56] M. Guvendiren, J. Molde, R. M. Soares, and J. Kohn, “Designing biomaterials for 3d printing,” *ACS Biomaterials Science & Engineering*, vol. 2, pp. 1679–1693, Apr. 2016.
- [57] F. P. Melchels, J. Feijen, and D. W. Grijpma, “A review on stereolithography and its applications in biomedical engineering,” *Biomaterials*, vol. 31, pp. 6121–6130, Aug. 2010.
- [58] Q. Mu, L. Wang, C. K. Dunn, X. Kuang, F. Duan, Z. Zhang, H. J. Qi, and T. Wang, “Digital light processing 3d printing of conductive complex structures,” *Additive Manufacturing*, vol. 18, pp. 74–83, Dec. 2017.
- [59] R. Singh, “Process capability study of polyjet printing for plastic components,” *Journal of Mechanical Science and Technology*, vol. 25, pp. 1011–1015, Apr. 2011.
- [60] N. Beltrán, F. Carriles, B. Álvarez, D. Blanco, and J. Rico, “Characterization of factors influencing dimensional and geometric errors in PolyJet manufacturing of cylindrical features,” *Procedia Engineering*, vol. 132, pp. 62–69, 2015.

- [61] S. Gaytan, M. Cadena, H. Karim, D. Delfin, Y. Lin, D. Espalin, E. MacDonald, and R. Wicker, "Fabrication of barium titanate by binder jetting additive manufacturing technology," *Ceramics International*, vol. 41, pp. 6610–6619, June 2015.
- [62] P. K. Gokuldoss, S. Kolla, and J. Eckert, "Additive manufacturing processes: Selective laser melting, electron beam melting and binder jetting - Selection guidelines," *Materials*, vol. 10, p. 672, June 2017.
- [63] L. Wang, S. D. Felicelli, and P. Pratt, "Residual stresses in LENS-deposited AISI 410 stainless steel plates," *Materials Science and Engineering: A*, vol. 496, pp. 234–241, Nov. 2008.
- [64] M. Izadi, A. Farzaneh, M. Mohammed, I. Gibson, and B. Rolfe, "A review of laser engineered net shaping (LENS) build and process parameters of metallic parts," *Rapid Prototyping Journal*, Mar. 2020. DOI: 10.1108/RPJ-04-2018-0088.
- [65] P. M. Bhatt, A. M. Kabir, M. Peralta, H. A. Bruck, and S. K. Gupta, "A robotic cell for performing sheet lamination-based additive manufacturing," *Additive Manufacturing*, vol. 27, pp. 278–289, May 2019.
- [66] X. Zhong, Y. S. and J. Feng, "Experimental study on ultrasonic consolidation process parameters of Ti-Al metal foil," *Journal of Advanced Mechanical Design, Systems, and Manufacturing*, vol. 13, no. 2, p. 24, 2019.
- [67] A. Łukaszek-Solek, J. Krawczyk, T. Śleboda, and J. Grelowski, "Optimization of the hot forging parameters for 4340 steel by processing maps," *Journal of Materials Research and Technology*, vol. 8, pp. 3281–3290, May 2019.
- [68] W. Zhuang, L. Hua, and X. Han, "Influences of key forging parameters on gear-tooth deviation of cold forged spur bevel gear," *Procedia Manufacturing*, vol. 15, pp. 504–510, 2018.
- [69] J. Zheng, B. Huang, and X. Zhou, "A low carbon process design method of sand casting based on process design parameters," *Journal of Cleaner Production*, vol. 197, pp. 1408–1422, Oct. 2018.
- [70] S. Kumar, P. S. Satsangi, and D. R. Prajapati, "Optimization of green sand casting process parameters of a foundry by using taguchi's method," *The International Journal of Advanced Manufacturing Technology*, vol. 55, pp. 23–34, Dec. 2010.
- [71] C. Shen, L. Wang, and Q. Li, "Optimization of injection molding process parameters using combination of artificial neural network and genetic algorithm method," *Journal of Materials Processing Technology*, vol. 183, pp. 412–418, Mar. 2007.
- [72] X.-P. Dang, "General frameworks for optimization of plastic injection molding process parameters," *Simulation Modelling Practice and Theory*, vol. 41, pp. 15–27, Feb. 2014.

- [73] S. Pattnaik, D. B. Karunakar, and P. Jha, “Developments in investment casting process—a review,” *Journal of Materials Processing Technology*, vol. 212, pp. 2332–2348, Nov. 2012.
- [74] D. O'Mahoney and D. J. Browne, “Use of experiment and an inverse method to study interface heat transfer during solidification in the investment casting process,” *Experimental Thermal and Fluid Science*, vol. 22, pp. 111–122, Sept. 2000.
- [75] T. B. Stoughton, “A general forming limit criterion for sheet metal forming,” *International Journal of Mechanical Sciences*, vol. 42, pp. 1–27, Jan. 2000.
- [76] J.-J. Park and Y.-H. Kim, “Fundamental studies on the incremental sheet metal forming technique,” *Journal of Materials Processing Technology*, vol. 140, pp. 447–453, Sept. 2003.
- [77] J. P. McEvoy, C. G. Armstrong, and R. J. Crawford, “Simulation of the stretch blow molding process of PET bottles,” *Advances in Polymer Technology*, vol. 17, no. 4, pp. 339–352, 1998.
- [78] F. Thibault, A. Malo, B. Lanctot, and R. Diraddo, “Preform shape and operating condition optimization for the stretch blow molding process,” *Polymer Engineering & Science*, vol. 47, no. 3, pp. 289–301, 2007.
- [79] G. Syrcos, “Die casting process optimization using taguchi methods,” *Journal of Materials Processing Technology*, vol. 135, pp. 68–74, Apr. 2003.
- [80] L. Wang, M. Makhlof, and D. Apelian, “Aluminium die casting alloys: alloy composition, microstructure, and properties-performance relationships,” *International Materials Reviews*, vol. 40, pp. 221–238, Jan. 1995.
- [81] Y. Liu, L. Chen, H. Tang, C. Liu, B. Liu, and B. Huang, “Design of powder metallurgy titanium alloys and composites,” *Materials Science and Engineering: A*, vol. 418, pp. 25–35, Feb. 2006.
- [82] B. Neville and A. Rabiei, “Composite metal foams processed through powder metallurgy,” *Materials & Design*, vol. 29, pp. 388–396, Jan. 2008.
- [83] H. El-Hofy, *Fundamentals of Machining Processes*. CRC Press, 2013.
- [84] J. P. Davim, *Machining: Fundamentals and Recent Advances*. Springer London, 2008.
- [85] S. Kalpakjian and S. R. Schmid, *Manufacturing Engineering and Technology (4th ed.)*. Prentice-Hall: Upper Saddle River, NJ, USA, 2001.
- [86] K. Li, R. Liu, G. Bai, and P. Zhang, “Development of an intelligent jig and fixture design system,” in *2006 7th International Conference on Computer-Aided Industrial Design and Conceptual Design*, IEEE, 2006.
- [87] K.-M. Li and S. Y. Liang, “Modeling of cutting temperature in near dry machining,” *Journal of Manufacturing Science and Engineering*, vol. 128, no. 2, p. 416, 2006.

- [88] F. Pusavec, P. Krajnik, and J. Kopac, "Transitioning to sustainable production - part i: application on machining technologies," *Journal of Cleaner Production*, vol. 18, no. 2, pp. 174–184, 2010.
- [89] I. Gibson, D. Rosen, and B. Stucker, *Additive Manufacturing Technologies: 3D Printing, Rapid Prototyping, and Direct Digital Manufacturing*. Springer, 2016.
- [90] N. Guo and M. C. Leu, "Additive manufacturing: technology, applications and research needs," *Frontiers of Mechanical Engineering*, vol. 8, no. 3, pp. 215–243, 2013.
- [91] B. Mueller, "Additive manufacturing technologies - rapid prototyping to direct digital manufacturing," *Assembly Automation*, vol. 32, no. 2, 2012.
- [92] S. H. Huang, P. Liu, A. Mokasdar, and L. Hou, "Additive manufacturing and its societal impact: a literature review," *The International Journal of Advanced Manufacturing Technology*, vol. 67, no. 5-8, pp. 1191–1203, 2012.
- [93] M. Baumers, P. Dickens, C. Tuck, and R. Hague, "The cost of additive manufacturing: machine productivity, economies of scale and technology-push," *Technological Forecasting and Social Change*, vol. 102, pp. 193–201, 2016.
- [94] E. Atzeni and A. Salmi, "Economics of additive manufacturing for end-usable metal parts," *The International Journal of Advanced Manufacturing Technology*, vol. 62, no. 9-12, pp. 1147–1155, 2012.
- [95] J. Beddoes and M. Bibby, *Principles of Metal Manufacturing Processes*. Butterworth-Heinemann: Oxford, UK, 1999.
- [96] J. Campbell, *Complete Casting Handbook: Metal Casting Processes, Metallurgy, Techniques, and Design (2nd ed.)*. Butterworth-Heinemann: Oxford, UK, 2015.
- [97] A. B. Strong, *Plastics: Materials and Processing (3rd ed.)*. Pearson: London, 2005.
- [98] B. Datta, *Powder Metallurgy: An Advanced Technique of Processing Engineering Materials*. Prentice-Hall: Upper Saddle River, NJ, USA, 2014.
- [99] I. Nishida, R. Sato, and K. Shirase, "Process planning system of 5-axis machining center considering constraint condition," in *2016 International Symposium on Flexible Automation (ISFA)*, IEEE, 2016.
- [100] K. Xu, J. Wang, C.-H. Chu, and K. Tang, "Cutting force and machine kinematics constrained cutter location planning for five-axis flank milling of ruled surfaces," *Journal of Computational Design and Engineering*, vol. 4, no. 3, pp. 203–217, 2017.
- [101] Y. Zhang, D. Zhang, and B. Wu, "An approach for machining allowance optimization of complex parts with integrated structure," *Journal of Computational Design and Engineering*, vol. 2, no. 4, pp. 248–252, 2015.

- [102] J. Jiang, X. Xu, and J. Stringer, "Support structures for additive manufacturing: A review," *Journal of Manufacturing and Materials Processing*, vol. 2, no. 4, p. 64, 2018.
- [103] M. K. Thompson, G. Moroni, T. Vaneker, G. Fadel, R. I. Campbell, I. Gibson, A. Bernard, J. Schulz, P. Graf, B. Ahuja, and F. Martina, "Design for additive manufacturing: Trends, opportunities, considerations, and constraints," *CIRP Annals*, vol. 65, no. 2, pp. 737–760, 2016.
- [104] S.-H. Ahn, M. Montero, D. Odell, S. Roundy, and P. K. Wright, "Anisotropic material properties of fused deposition modeling ABS," *Rapid Prototyping Journal*, vol. 8, no. 4, pp. 248–257, 2002.
- [105] A. E. Patterson, S. L. Messimer, and P. A. Farrington, "Overhanging features and the SLM/DMLS residual stresses problem: Review and future research need," *Technologies*, vol. 5, no. 2, p. 15, 2017.
- [106] R. E. Rebong, K. T. Stewart, A. Utreja, and A. A. Ghoneima, "Accuracy of three-dimensional dental resin models created by fused deposition modeling, stereolithography, and polyjet prototype technologies: A comparative study," *The Angle Orthodontist*, vol. 88, no. 3, pp. 363–369, 2018.
- [107] S. Jones and C. Yuan, "Advances in shell moulding for investment casting," *Journal of Materials Processing Technology*, vol. 135, no. 2-3, pp. 258–265, 2003.
- [108] A. S. Sabau and S. Viswanathan, "Material properties for predicting wax pattern dimensions in investment casting," *Materials Science and Engineering: A*, vol. 362, no. 1-2, pp. 125–134, 2003.
- [109] W. Jiang, Z. Fan, D. Liu, D. Liao, X. Dong, and X. Zong, "Correlation of microstructure with mechanical properties and fracture behavior of a356-t6 aluminum alloy fabricated by expendable pattern shell casting with vacuum and low-pressure, gravity casting and lost foam casting," *Materials Science and Engineering: A*, vol. 560, pp. 396–403, 2013.
- [110] ASTM, *ASTM F2792-12a: Standard Terminology for Additive Manufacturing Technologies*. ASTM International, 2012.
- [111] C. Feng, S. Yan, R. Zhang, and Y. Yan, "Heat transfer analysis of rapid ice prototyping process by finite element method," *Materials & Design*, vol. 28, no. 3, pp. 921–927, 2007.
- [112] R. Friel and R. Harris, "Ultrasonic additive manufacturing - a hybrid production process for novel functional products," *Procedia CIRP*, vol. 6, pp. 35–40, 2013.
- [113] D. Thomas, "Costs, benefits, and adoption of additive manufacturing: a supply chain perspective," *The International Journal of Advanced Manufacturing Technology*, vol. 85, no. 5-8, pp. 1857–1876, 2015.

- [114] INCOSE, *INCOSE Systems Engineering Handbook: A Guide for System Life Cycle Processes and Activities*. Wiley, 2015.
- [115] S. Bix and P. Witt, “Introducing constraints to improve new product development performance,” *Research-Technology Management*, vol. 63, pp. 29–37, Sept. 2020.
- [116] W. Knight, “Design for manufacture analysis: Early estimates of tool costs for sintered parts,” *CIRP Annals*, vol. 40, no. 1, pp. 131–134, 1991.
- [117] G. Barbosa and J. Carvalho, “Design for manufacturing and assembly methodology applied to aircrafts design and manufacturing,” *IFAC Proceedings Volumes*, vol. 46, no. 7, pp. 116–121, 2013.
- [118] I. Ferrer, J. Rios, and J. Ciurana, “An approach to integrate manufacturing process information in part design phases,” *Journal of Materials Processing Technology*, vol. 209, no. 4, pp. 2085–2091, 2009.
- [119] I. Ferrer, J. Rios, J. Ciurana, and M. Garcia-Romeu, “Methodology for capturing and formalizing DFM knowledge,” *Robotics and Computer-Integrated Manufacturing*, vol. 26, no. 5, pp. 420–429, 2010.
- [120] J. Vallhagen, O. Isaksson, R. Söderberg, and K. Wärmefjord, “A framework for producibility and design for manufacturing requirements in a system engineering context,” *Procedia CIRP*, vol. 11, pp. 145–150, 2013.
- [121] M. Bajaj, R. Peak, M. Wilson, I. Kim, T. Thurman, M. Jothishankar, M. Benda, P. Ferreira, and J. Stori, “Towards next-generation design-for-manufacturability (DFM) frameworks for electronics product realization,” in *IEEE/CPMT/SEMI 28th International Electronics Manufacturing Technology Symposium, 2003. IEMT 2003.*, IEEE, 2003.
- [122] H. Dong and W. H. Wood, “Issues in integration of design and manufacturing for mechatronics,” in *ASME IDETC: Volume 3a: 8th Design for Manufacturing Conference*, ASME, 2003.
- [123] W. H. Wood and A. M. Agogino, “Decision-based conceptual design: Modeling and navigating heterogeneous design spaces,” *Journal of Mechanical Design*, vol. 127, no. 1, p. 2, 2005.
- [124] D. Shetty, N. Poudel, and E. Ososanya, “Design of robust mechatronics embedded systems by integration of virtual simulation and mechatronics platform,” in *Volume 2B: Advanced Manufacturing*, ASME, 2015.
- [125] G. Berselli, G. Borghesan, M. Brandi, C. Melchiorri, C. Natale, G. Palli, S. Pirozzi, and G. Vassura, “Integrated mechatronic design for a new generation of robotic hands,” *IFAC Proceedings Volumes*, vol. 42, no. 16, pp. 8–13, 2009.

- [126] F. C. Lee, S. Wang, and Q. Li, “Next generation of power supplies-design for manufacturability,” *IEEE Journal of Emerging and Selected Topics in Power Electronics*, pp. 1–1, 2020. In press: DOI [10.1109/jestpe.2020.3002857](https://doi.org/10.1109/jestpe.2020.3002857).
- [127] M. Fathianathan and J. H. Panchal, “Modelling an ongoing design process utilizing top-down and bottom-up design strategies,” *Proceedings of the Institution of Mechanical Engineers, Part B: Journal of Engineering Manufacture*, vol. 223, no. 5, pp. 547–560, 2008.
- [128] M. Thomas and F. McGarry, “Top-down vs. bottom-up process improvement,” *IEEE Software*, vol. 11, no. 4, pp. 12–13, 1994.
- [129] H. D. Budinoff, S. McMains, and A. Rinaldi, “An interactive manufacturability analysis and tolerance allocation tool for additive manufacturing,” in *Volume 2A: 44th Design Automation Conference*, ASME, 2018.
- [130] A. M. Mirzendehtdel, M. Behandish, and S. Nelaturi, “Exploring feasible design spaces for heterogeneous constraints,” *Computer-Aided Design*, vol. 115, pp. 323–347, Oct. 2019.
- [131] M. Iyengar and A. Bar-Cohen, “Design for manufacturability of SISE parallel plate forced convection heat sinks,” *IEEE Transactions on Components and Packaging Technologies*, vol. 24, no. 2, pp. 150–158, 2001.
- [132] H. Li, P. Li, L. Gao, L. Zhang, and T. Wu, “A level set method for topological shape optimization of 3d structures with extrusion constraints,” *Computer Methods in Applied Mechanics and Engineering*, vol. 283, pp. 615–635, 2015.
- [133] S. Mantovani, I. L. Presti, L. Cavazzoni, and A. Baldini, “Influence of manufacturing constraints on the topology optimization of an automotive dashboard,” *Procedia Manufacturing*, vol. 11, pp. 1700–1708, 2017.
- [134] J. K. Guest and M. Zhu, “Casting and milling restrictions in topology optimization via projection-based algorithms,” in *Volume 3: 38th Design Automation Conference, Parts A and B*, ASME, 2012.
- [135] K.-T. Zuo, L.-P. Chen, Y.-Q. Zhang, and J. Yang, “Manufacturing- and machining-based topology optimization,” *The International Journal of Advanced Manufacturing Technology*, vol. 27, no. 5-6, pp. 531–536, 2005.
- [136] S. N. R. K., V. Maranan, T. W. Simpson, T. Palmer, and C. J. Dickman, “Application of topology optimization and design for additive manufacturing guidelines on an automotive component,” in *Volume 2A: 42nd Design Automation Conference*, ASME, 2016.
- [137] Y. A. Lu, Y. Ding, C. Wang, and L. Zhu, “Tool path generation for five-axis machining of blisks with barrel cutters,” *International Journal of Production Research*, pp. 1–15, 2018.

- [138] J. Monge, C. Vezzaz, F. Avellan, and C. Tournier, "Integration of machining constraints in design optimization of a guide vane cascade," in *10th International Conference on Computer Aided Design, Jun 2013, Bergamo, Italy.*, 2013.
- [139] M. Kang, J. Han, and J. Moon, "An approach for interlinking design and process planning," *Journal of Materials Processing Technology*, vol. 139, no. 1-3, pp. 589–595, 2003.
- [140] M. Deja and M. S. Siemiatkowski, "Feature-based generation of machining process plans for optimised parts manufacture," *Journal of Intelligent Manufacturing*, vol. 24, no. 4, pp. 831–846, 2012.
- [141] S. K. Gupta and D. S. Nau, "Systematic approach to analysing the manufacturability of machined parts," *Computer-Aided Design*, vol. 27, no. 5, pp. 323–342, 1995.
- [142] A. M. Mirzendehtdel, M. Behandish, and S. Nelaturi, "Topology optimization with accessibility constraint for multi-axis machining," *Computer-Aided Design*, vol. 122, p. 102825, May 2020.
- [143] J. Liu and Y. S. Ma, "3d level-set topology optimization: a machining feature-based approach," *Structural and Multidisciplinary Optimization*, vol. 52, no. 3, pp. 563–582, 2015.
- [144] J. Liu, H. Yu, and Y. Ma, "Minimum void length scale control in level set topology optimization subject to machining radii," *Computer-Aided Design*, vol. 81, pp. 70–80, 2016.
- [145] N. Morris, A. Butscher, and F. Iorio, "A subtractive manufacturing constraint for level set topology optimization," *Structural and Multidisciplinary Optimization*, vol. 61, pp. 1573–1588, Feb. 2020.
- [146] J. Liu and Y. Ma, "A survey of manufacturing oriented topology optimization methods," *Advances in Engineering Software*, vol. 100, pp. 161–175, 2016.
- [147] G. A. Adam and D. Zimmer, "Design for additive manufacturing - element transitions and aggregated structures," *CIRP Journal of Manufacturing Science and Technology*, vol. 7, no. 1, pp. 20–28, 2014.
- [148] G. Sossou, F. Demoly, G. Montavon, and S. Gomes, "An additive manufacturing oriented design approach to mechanical assemblies," *Journal of Computational Design and Engineering*, vol. 5, no. 1, pp. 3–18, 2018.
- [149] H. Jee and P. Witherell, "A method for modularity in design rules for additive manufacturing," *Rapid Prototyping Journal*, vol. 23, no. 6, pp. 1107–1118, 2017.
- [150] G. A. O. Adam and D. Zimmer, "On design for additive manufacturing: evaluating geometrical limitations," *Rapid Prototyping Journal*, vol. 21, no. 6, pp. 662–670, 2015.
- [151] S. B. Maidin, I. Campbell, and E. Pei, "Development of a design feature database to support design for additive manufacturing," *Assembly Automation*, vol. 32, no. 3, pp. 235–244, 2012.

- [152] J. Kranz, D. Herzog, and C. Emmelmann, “Design guidelines for laser additive manufacturing of lightweight structures in TiAl6v4,” *Journal of Laser Applications*, vol. 27, no. S1, p. S14001, 2015.
- [153] L. Tang, Q. Zhang, K. Liang, X. Zhao, and Z. Zhang, “Discrete optimization of internal part structure via SLM unit structure-performance database,” *Metals*, vol. 8, no. 1, p. 45, 2018.
- [154] P. Pradel, Z. Zhu, R. Bibb, and J. Moultrie, “A framework for mapping design for additive manufacturing knowledge for industrial and product design,” *Journal of Engineering Design*, vol. 29, no. 6, pp. 291–326, 2018.
- [155] K. Mhapsekar, M. McConaha, and S. Anand, “Additive manufacturing constraints in topology optimization for improved manufacturability,” *Journal of Manufacturing Science and Engineering*, vol. 140, no. 5, p. 051017, 2018.
- [156] H. Rezayat, J. R. Bell, A. J. Plotkowski, and S. S. Babu, “Multi-solution nature of topology optimization and its application in design for additive manufacturing,” *Rapid Prototyping Journal*, 2018. DOI 10.1108/rpj-01-2018-0009.
- [157] B. Weiss, O. Diegel, D. Storti, and M. Ganter, “A process for estimating minimum feature size in selective laser sintering,” *Rapid Prototyping Journal*, vol. 24, no. 2, pp. 436–440, 2018.
- [158] A. M. Mirzendehtel and K. Suresh, “Support structure constrained topology optimization for additive manufacturing,” *Computer-Aided Design*, vol. 81, pp. 1–13, 2016.
- [159] E. Utley, “Designing for 3D printing: direct metal laser sintering,” in *Laser 3D Manufacturing V* (H. Helvajian, A. Piqué, and B. Gu, eds.), SPIE, 2018.
- [160] D. Thomas, *The development of design rules for selective laser melting*. PhD thesis, Cardiff Metropolitan University, Cardiff, UK, 2009. Available at <https://repository.cardiffmet.ac.uk/handle/10369/913>.
- [161] C. Seepersad, “Design rules for selective laser sintering,” tech. rep., University of Texas-Austin, Austin, Texas, USA, 2012. Available at <https://www.me.utexas.edu/~ppmmlab/files/designers.guide.sls.pdf>.
- [162] J. Allison, C. Sharpe, and C. C. Seepersad, “Powder bed fusion metrology for additive manufacturing design guidance,” *Additive Manufacturing*, vol. 25, pp. 239–251, 2019.
- [163] B. Cheng and Y. K. Chou, “Overhang support structure design for electron beam additive manufacturing,” in *Volume 2: Additive Manufacturing Materials*, ASME, 2017.
- [164] W. Ameen, A. Al-Ahmari, M. Mohammed, and S. Mian, “Manufacturability of overhanging holes using electron beam melting,” *Metals*, vol. 8, no. 6, p. 397, 2018.

- [165] S. L. Sing, J. An, W. Y. Yeong, and F. E. Wiria, “Laser and electron-beam powder-bed additive manufacturing of metallic implants: A review on processes, materials and designs,” *Journal of Orthopaedic Research*, vol. 34, no. 3, pp. 369–385, 2015.
- [166] R. J. Urbanic and R. Hedrick, “Fused deposition modeling design rules for building large, complex components,” *Computer-Aided Design and Applications*, vol. 13, no. 3, pp. 348–368, 2016.
- [167] S. Messimer, T. Pereira, A. Patterson, M. Lubna, and F. Drozda, “Full-density fused deposition modeling dimensional error as a function of raster angle and build orientation: Large dataset for eleven materials,” *Journal of Manufacturing and Materials Processing*, vol. 3, no. 1, p. 6, 2019.
- [168] E. Kouhi, S. Masood, and Y. Morsi, “Design and fabrication of reconstructive mandibular models using fused deposition modeling,” *Assembly Automation*, vol. 28, no. 3, pp. 246–254, 2008.
- [169] J. V. Carstensen, “Topology optimization with nozzle size restrictions for material extrusion-type additive manufacturing,” *Structural and Multidisciplinary Optimization*, vol. 62, pp. 2481–2497, June 2020.
- [170] D. T. Pham and C. Ji, “Design for stereolithography,” *Proceedings of the Institution of Mechanical Engineers, Part C: Journal of Mechanical Engineering Science*, vol. 214, no. 5, pp. 635–640, 2000.
- [171] A. Davoudinejad, L. C. Diaz-Perez, D. Quagliotti, D. B. Pedersen, J. A. Albajez-García, J. A. Yagüe-Fabra, and G. Tosello, “Additive manufacturing with vat polymerization method for precision polymer micro components production,” *Procedia CIRP*, vol. 75, pp. 98–102, 2018.
- [172] G. Campana and M. Mele, “An application to stereolithography of a feature recognition algorithm for manufacturability evaluation,” *Journal of Intelligent Manufacturing*, vol. 31, pp. 199–214, Aug. 2018.
- [173] N. Meisel and C. Williams, “An investigation of key design for additive manufacturing constraints in multimaterial three-dimensional printing,” *Journal of Mechanical Design*, vol. 137, no. 11, p. 111406, 2015.
- [174] J. Gardan, “Method for characterization and enhancement of 3D printing by binder jetting applied to the textures quality,” *Assembly Automation*, vol. 37, no. 2, pp. 162–169, 2017.
- [175] R. Singh and J. Madan, “Systematic approach for automated determination of parting line for die-cast parts,” *Robotics and Computer-Integrated Manufacturing*, vol. 29, no. 5, pp. 346–366, 2013.

- [176] L. Harzheim and G. Graf, “A review of optimization of cast parts using topology optimization. II-Topology optimization with manufacturing constraints,” *Structural and Multidisciplinary Optimization*, vol. 31, no. 5, pp. 388–399, 2005.
- [177] G. Allaire, F. Jouve, and G. Michailidis, “Casting constraints in structural optimization via a level-set method,” in *10th World Congress on Structural and Multidisciplinary Optimization, Orlando, FL, USA*, 2013.
- [178] Y. Wang and Z. Kang, “Structural shape and topology optimization of cast parts using level set method,” *International Journal for Numerical Methods in Engineering*, vol. 111, no. 13, pp. 1252–1273, 2017.
- [179] A. R. Gersborg and C. S. Andreasen, “An explicit parameterization for casting constraints in gradient driven topology optimization,” *Structural and Multidisciplinary Optimization*, vol. 44, no. 6, pp. 875–881, 2011.
- [180] J. K. Guest, J. H. Prévost, and T. Belytschko, “Achieving minimum length scale in topology optimization using nodal design variables and projection functions,” *International Journal for Numerical Methods in Engineering*, vol. 61, no. 2, pp. 238–254, 2004.
- [181] R. A. Bidkar and D. A. McAdams, “Methods for automated manufacturability analysis of injection-molded and die-cast parts,” *Research in Engineering Design*, vol. 21, no. 1, pp. 1–24, 2009.
- [182] A. Fagade and D. Kazmer, “Economic design of injection molded parts using dfm guidelines - a review of two methods for tooling cost estimation,” in *Proceedings of ANTEC98, Society of Plastic Engineers, Atlanta, GA, USA*, pp. 869–873, SPE, 1998.
- [183] M. Fu, J. Fuh, and A. Nee, “Generation of optimal parting line direction based on undercut features in injection molded parts,” *IIE Transactions*, vol. 31, no. 10, pp. 947–955, 1999.
- [184] L. N. Smith, “A knowledge based system for optimum and concurrent design, and manufacture by powder metallurgy technology,” *International Journal of Production Research*, vol. 37, no. 1, pp. 125–137, 1999.
- [185] R. Spina, M. Spekowius, and C. Hopmann, “Multiphysics simulation of thermoplastic polymer crystallization,” *Materials & Design*, vol. 95, pp. 455–469, 2016.
- [186] S.-J. Choi and S. K. Kim, “Multi-scale filling simulation of micro-injection molding process,” *Journal of Mechanical Science and Technology*, vol. 25, no. 1, pp. 117–124, 2011.
- [187] D. Niedziela, J. Tröltzsch, A. Latz, and L. Kroll, “On the numerical simulation of injection molding processes with integrated textile fiber reinforcements,” *Journal of Thermoplastic Composite Materials*, vol. 26, no. 1, pp. 74–90, 2011.

- [188] H. Tercan, A. Guajardo, J. Heinisch, T. Thiele, C. Hopmann, and T. Meisen, “Transfer-learning: Bridging the gap between real and simulation data for machine learning in injection molding,” *Procedia CIRP*, vol. 72, pp. 185–190, 2018.
- [189] J. Shi, Z. Cheng, T. Barriere, B. Liu, and J. C. Gelin, “Multiphysic coupling and full cycle simulation of microwave sintering applied to a ceramic compact obtained by ceramic injection moulding,” *Powder Metallurgy*, vol. 60, no. 5, pp. 404–414, 2017.
- [190] S. An, P. Martinez, M. Al-Hussein, and R. Ahmad, “Automated verification of 3d manufacturability for steel frame assemblies,” *Automation in Construction*, vol. 118, p. 103287, Oct. 2020.
- [191] V.-T. Tran, Y. Wei, W. Liau, H. Yang, and H. Du, “Preparing of interdigitated microelectrode arrays for AC electrokinetic devices using inkjet printing of silver nanoparticles ink,” *Micromachines*, vol. 8, no. 4, p. 106, 2017.
- [192] S.-W. Chen, H. Li, C.-J. Chang, and T.-C. Lu, “Effects of nanoscale v-shaped pits on GaN-based light emitting diodes,” *Materials*, vol. 10, no. 2, p. 113, 2017.
- [193] H. Eiliat and J. Urbanic, “Visualizing, analyzing, and managing voids in the material extrusion process,” *The International Journal of Advanced Manufacturing Technology*, vol. 96, no. 9-12, pp. 4095–4109, 2018.
- [194] M. Brandt, S. J. Sun, M. Leary, S. Feih, J. Elambasseril, and Q. C. Liu, “High-value SLM aerospace components: From design to manufacture,” *Advanced Materials Research*, vol. 633, pp. 135–147, 2013.
- [195] J. K. Guest, “Imposing maximum length scale in topology optimization,” *Structural and Multidisciplinary Optimization*, vol. 37, no. 5, pp. 463–473, 2008.
- [196] B. S. Lazarov and F. Wang, “Maximum length scale in density based topology optimization,” *Computer Methods in Applied Mechanics and Engineering*, vol. 318, pp. 826–844, 2017.
- [197] C. Chu, G. Graf, and D. W. Rosen, “Design for additive manufacturing of cellular structures,” *Computer-Aided Design and Applications*, vol. 5, no. 5, pp. 686–696, 2008.
- [198] H. Z. Yu, S. R. Cross, and C. A. Schuh, “Mesostucture optimization in multi-material additive manufacturing: a theoretical perspective,” *Journal of Materials Science*, vol. 52, no. 8, pp. 4288–4298, 2017.
- [199] D. Garcia, M. E. Jones, Y. Zhu, and H. Z. Yu, “Mesoscale design of heterogeneous material systems in multi-material additive manufacturing,” *Journal of Materials Research*, vol. 33, no. 01, pp. 58–67, 2017.

- [200] V. Florea, M. Pamwar, B. Sangha, and I. Y. Kim, “3d multi-material and multi-joint topology optimization with tooling accessibility constraints,” *Structural and Multidisciplinary Optimization*, vol. 60, pp. 2531–2558, July 2019.
- [201] R. Sivapuram, P. D. Dunning, and H. A. Kim, “Simultaneous material and structural optimization by multiscale topology optimization,” *Structural and Multidisciplinary Optimization*, vol. 54, no. 5, pp. 1267–1281, 2016.
- [202] J. A. Gopsill, J. Shindler, and B. J. Hicks, “Using finite element analysis to influence the infill design of fused deposition modelled parts,” *Progress in Additive Manufacturing*, vol. 3, no. 3, pp. 145–163, 2017.
- [203] J. Gardan, A. Makke, and N. Recho, “Improving the fracture toughness of 3d printed thermoplastic polymers by fused deposition modeling,” *International Journal of Fracture*, vol. 210, no. 1-2, pp. 1–15, 2017.
- [204] S. Ashman and S. G. Kandlikar, “A review of manufacturing processes for microchannel heat exchanger fabrication,” in *Proceedings of the ASME 4th International Conference on Nanochannels, Microchannels, and Minichannels, Parts A and B*, no. ICNMM2006-96121, (Limerick, Ireland), pp. 855–860, 2006.
- [205] I. Etsion, “State of the art in laser surface texturing,” *Journal of Tribology*, vol. 127, no. 1, pp. 248–253, 2005.
- [206] A. D. Romig Jr., M. T. Dugger, and P. J. McWhorter, “Materials issues in microelectromechanical devices: science, engineering, manufacturability and reliability,” *Acta Materialia*, vol. 51, no. 19, pp. 5837–5866, 2003.
- [207] W. E. Frazier, “Metal additive manufacturing: a review,” *Journal of Materials Engineering and Performance*, vol. 23, no. 6, pp. 1917–1928, 2014.
- [208] Y. H. Lee, J. K. Schuh, R. H. Ewoldt, and J. T. Allison, “Enhancing full-film lubrication performance via arbitrary surface texture design,” *Journal of Mechanical Design*, vol. 139, no. 5, p. 053401, 2017.
- [209] O. Sigmund, “Morphology-based black and white filters for topology optimization,” *Structural and Multidisciplinary Optimization*, vol. 33, no. 4-5, pp. 401–424, 2007.
- [210] O. Sigmund, “Manufacturing tolerant topology optimization,” *Acta Mechanica Sinica*, vol. 25, no. 2, pp. 227–239, 2009.
- [211] A. F. S. Baharin, M. J. Ghazali, and J. A. Wahab, “Laser surface texturing and its contribution to friction and wear reduction: a brief review,” *Industrial Lubrication and Tribology*, vol. 68, no. 1, pp. 57–66, 2016.

- [212] R. A. Gittens, T. McLachlan, R. Olivares-Navarrete, Y. Cai, S. Berner, R. Tannenbaum, Z. Schwartz, K. H. Sandhage, and B. D. Boyan, “The effects of combined micron-/submicron-scale surface roughness and nanoscale features on cell proliferation and differentiation,” *Bio-materials*, vol. 32, no. 13, pp. 3395–3403, 2011.
- [213] S. K. Dew and M. Stepanova, “Directions in nanofabrication,” in *Nanofabrication: Techniques and Principles* (M. Stepanova and S. K. Dew, eds.), ch. 1, pp. 3–8, Wien: Springer-Verlag, 2012.
- [214] T. Onda, S. Shibuichi, N. Satoh, and K. Tsujii, “Super-water-repellent fractal surfaces,” *Langmuir*, vol. 12, no. 9, pp. 2125–2127, 1996.
- [215] W. Zhao, L. Wang, and Q. Xue, “Influence of micro/nano-textures and chemical modification on the nanotribological property of au surface,” *Colloids and Surfaces A: Physicochemical and Engineering Aspects*, vol. 366, no. 1-3, pp. 191–196, 2010.
- [216] C. Chiang and J. Kawa, *Design for Manufacturability and Yield for Nano-Scale CMOS*. Integrated Circuits and Systems, Dordrecht: Springer, 2007.
- [217] M. J. Kelly, “Intrinsic top-down unmanufacturability,” *Nanotechnology*, vol. 22, p. 245303, 2011.
- [218] S. Maruo, O. Nakamura, and S. Kawata, “Three-dimensional microfabrication with two-photon-absorbed photopolymerization,” *Optics Letters*, vol. 22, no. 2, pp. 132–134, 1997.
- [219] G. de Miguel, G. Vicidomini, B. Harke, and A. Diaspro, “Linewidth and writing resolution,” in *Three-Dimensional Microfabrication Using Two-photon Polymerization*, pp. 190–220, Elsevier, 2016.
- [220] S. Waheed, J. M. Cabot, N. P. Macdonald, T. Lewis, R. M. Guijt, B. Paull, and M. C. Breadmore, “3d printed microfluidic devices: enablers and barriers,” *Lab on a Chip*, vol. 16, no. 11, pp. 1993–2013, 2016.
- [221] N. Lyu, A. Shimura, and K. Saitou, “Optimal tolerance allocation of automotive pneumatic control valves based on product and process simulations,” in *ASME IDETC: Volume 1: 32nd Design Automation Conference, Parts A and B*, ASME, 2006.
- [222] H.-G. R. Choi, M.-H. Park, and E. Salisbury, “Optimal tolerance allocation with loss functions,” *Journal of Manufacturing Science and Engineering*, vol. 122, no. 3, p. 529, 2000.
- [223] Y. M. Huang and C.-S. Shiau, “Optimal tolerance allocation for a sliding vane compressor,” *Journal of Mechanical Design*, vol. 128, no. 1, p. 98, 2006.
- [224] P. Muthu, V. Dhanalakshmi, and K. Sankaranarayanan, “Optimal tolerance design of assembly for minimum quality loss and manufacturing cost using metaheuristic algorithms,”

The International Journal of Advanced Manufacturing Technology, vol. 44, no. 11-12, pp. 1154–1164, 2009.

- [225] P. Y. Papalambros and D. J. Wilde, *Principles of Optimal Design: Modeling and Computation (2d Edition)*. Cambridge University Press, 2000.
- [226] S. Luan, D. L. Thurston, M. Arora, and J. T. Allison, “Developing and comparing alternative design optimization formulations for a vibration absorber example,” in *Volume 4: 22nd Design for Manufacturing and the Life Cycle Conference; 11th International Conference on Micro- and Nanosystems*, American Society of Mechanical Engineers, Aug. 2017.
- [227] L. Harzheim and G. Graf, “A review of optimization of cast parts using topology optimization,” *Structural and Multidisciplinary Optimization*, vol. 30, no. 6, pp. 491–497, 2005.
- [228] J. N. Hooker, “Logic, optimization, and constraint programming,” *INFORMS Journal on Computing*, vol. 14, pp. 295–321, Nov. 2002.
- [229] H. Bernau, “Active constraint strategies in optimization,” in *Geophysical Data Inversion Methods and Applications*, pp. 15–31, Vieweg+Teubner Verlag, 1990.
- [230] F. Facchinei, A. Fischer, and C. Kanzow, “On the accurate identification of active constraints,” *SIAM Journal on Optimization*, vol. 9, pp. 14–32, Jan. 1998.
- [231] M. A. Rubeo and T. L. Schmitz, “Milling force modeling: A comparison of two approaches,” *Procedia Manufacturing*, vol. 5, pp. 90–105, 2016.
- [232] B. Denkena, J. Brüning, D. Niederwestberg, and R. Grabowski, “Influence of machining parameters on heat generation during milling of aluminum alloys,” *Procedia CIRP*, vol. 46, pp. 39–42, 2016.

Chapter 3

FDM MECHANICS AND MANUFACTURABILITY CONSTRAINTS

Collaborator Acknowledgement: The author gratefully acknowledges the contributions, advice, direction, and feedback from the following people on the work presented in this chapter: **Tais Rocha Pereira** (help with process modeling and lead of dimensional accuracy study); **Dr. Sherri Messimer** (extensive advice on realistic FDM constraints and assumptions and help with dimensional accuracy study); **Dr. James T. Allison** (help with process modeling and understanding of system dynamics, which helped drive some of the constraint mapping as well as helpful discussion on the sensitivity analysis for major assumptions); **Nasiha Muna** (help with developing Case Study 3).

This chapter may contain previously published text and figures, which are reproduced with the permission of the copyright holders. See the copyright statement and list of references at the end of the chapter.

3.1 Introduction

One of the most well-developed and mature additive manufacturing (AM) processes designed for polymer and polymer-composite materials is the fused deposition modeling (FDM) pro-

cess; this process is also sometimes called fused filament fabrication (FFF) or simply materials extrusion AM. The process works by extruding a molten bead (sometimes also called a “road”) of thermoplastic material into elements to selectively trace out the layers of the part. The fusion between the previous layer and the neighboring elements is accomplished via a polymer melt reaction [1–5]. The extruder position and path is driven using g-code (similar to a CNC milling machine); the process is typically monitored by an open-loop control system based on stepper motor position encoders, but other control systems exist [3,4,6–8]. The essential hardware components of an FDM machine are the extruder (for melting and depositing the molten raw material), the frame, and the build plate (Figure 3.1). A number of configurations are available (some examples shown in Figure 3.2a–3.2d), each with its own set of advantages and disadvantages; there are others (such as delta robots and robotic arm printers), but the ones shown are the most common 3-degree-of-freedom configurations. For the purposes of this chapter, it is assumed that the design process for printed parts is the same regardless of the hardware configuration.

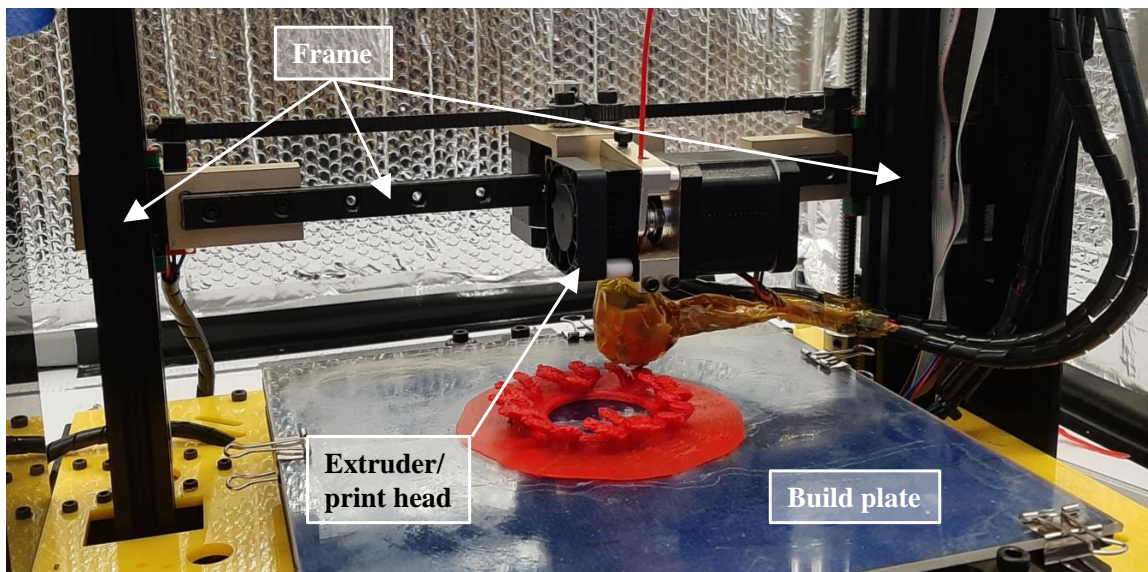


Figure 3.1: Typical hardware for the FDM process.

FDM is a scanning-type AM (ST-AM) process, building each layer as a series of elements laid out in a pattern, typically bounded by a solid shell of elements printed on the outside boundary of each layer. The final bulk material contains small voids/inclusions

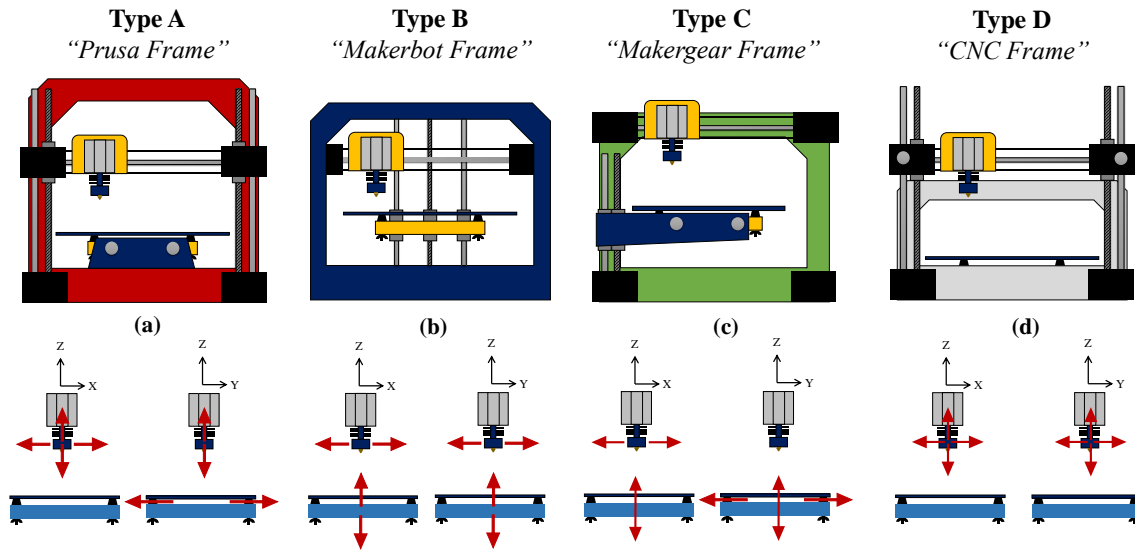


Figure 3.2: Common hardware configurations, with the degrees of freedom for the extruder and build plate shown in each case. These are the most common 3-degree-of-freedom (3DoF) configurations, but others exist such as those built around delta robots and higher-DoF robotic arms.

and is highly anisotropic [37]; however, the pattern of the laid out elements is designable, allowing FDM to be used to create structured and tailored materials by controlling or optimizing the layout of the elements [11, 38–40]. Effective design of the FDM structure requires knowledge and control of a variety of parameters, the most commonly studied of which are the nominal density, element layout (typically raster angle), layer thickness, print orientation, deposition speed, and processing temperature. A sampling of 30 recent papers related to FDM and discussing manufacturing parameters was collected to determine which parameters are most often considered; the results are shown in Table 3.1. Material choice was not considered as a parameter in this table, as the best ranges and limits on parameters are dependent on material choice. In most FDM studies, the materials under considerations are treated as separate problems since each material will have different optimal parameters and constraints. Some FDM materials are amorphous (such as acrylonitrile butadiene styrene (ABS) and polycarbonate) and some are semi-cystalline (such as polylactic acid (PLA) and polyamides (nylon)).

This chapter explores the mechanics and manufacturability constraints for the FDM process, with the purpose of creating a set of assumptions and design constraints that will be used to drive future chapters. First, the mapping technique (MR-DFM) developed in

Table 3.1: Example parameter control/optimization studies from a review of 30 recent papers on FDM.

Refs.	Parameters from Sampled Literature								
	Density	Infill pattern	Print speed	Print temp	Layer height	Orientation	Nozzle size	Shells	Variance compensation
[9]	■	■	■	■					
[10]		■							
[11]	■	■	■	■	■	■			
[12]	■	■		■	■				
[13]	■								
[14]	■	■			■				
[15]	■	■			■				
[16]	■	■				■			
[17]	■			■	■	■			
[18]	■		■	■	■		■	■	
[19]	■	■					■		
[20]	■	■			■		■		
[21]		■	■		■	■			
[22]	■	■			■			■	
[23]	■	■			■	■		■	
[24]		■				■			
[25]	■			■	■				
[26]		■				■			
[5]		■				■			
[2]	■	■			■	■	■	■	
[27]		■	■	■	■				
[28]	■	■			■	■	■		
[29]		■				■			
[30]			■		■				■
[31]			■	■	■			■	
[32]		■							
[33]	■	■	■		■	■	■		■
[34]	■	■			■		■		
[35]			■	■	■		■		
[36]			■		■				■

Chapter 2 is used in Section 3.2 to derive the basic set of manufacturability constraints specifically for the FDM process. Next, a set of materials to be used for the work reported in this dissertation are selected and discussed (Section 3.3). Given that a set of materials were selected, Section 3.4 refines the constraint set relative to these materials; this included experimental determination of some of the constraints and sensitivity analysis on the stated assumptions. Finally, three case studies are presented in Section 3.5 and some final remarks are offered in Section 3.6.

Table 3.2: Example constraints for the general parameters found during the survey presented in Table 3.1.

Parameter	Example Simple Constraints
Nominal density	Maximum realistic density ($< 100\%$), minimum stable density
Raster angle	Minimum and maximum raster angle
Print speed	Minimum and maximum print speed for polymer rheology, minimum and maximum print speed for hardware stability/vibration, limits on motor performance
Extruder temperature	Minimum and maximum temperature for polymer rheology, minimum and maximum temperature for proper hardware function
Layer thickness	Minimum and maximum layer thickness for polymer rheology, minimum and maximum thickness for print time requirements, minimum and maximum thickness for surface quality
Printing orientation	Printing orientation limited by the number of degrees of freedom (DoF) for printing hardware (most printers limited to three DoF)
Nozzle size	Maximum nozzle size \leq filament size, minimum nozzle size dependent on polymer melt behavior and temperature
Number of shells/contours	Minimum number of shells = minimal stable layer boundary, maximum number of shells \leq smallest layer dimension divided by $2 \times$ nozzle size
Compensation for filament	Minimum = no compensation, maximum extra material that will not disturb surface finish or create nodules/strings during printing

3.2 FDM Manufacturability Constraints: Concepts

3.2.1 Parameters versus Constraints

The printing parameters, being the main drivers for the final material properties for FDM-processed materials, can provide design variables and aid in the development of objective functions [9, 15, 17] during design. However, the constraints on and between these parameters is an important area which has received little to no attention in the AM literature thus far. Simple example constraints for the parameters shown in Table 3.1 are given in Table 3.2. Others certainly exist (including some complex equality constraints that describe relationships between the parameters); however, these provide excellent conceptual examples to demonstrate some kind of relationship between manufacturing parameters and manufacturability constraints. The realistic constraints that will be explored by this concept paper will be far more detailed and specific than the examples shown in Table 3.2.

As discussed in Chapter 2, the proper formulation of any design problem requires at least one design objective and a design space to explore for answers which satisfy the objective [41]. In most problem formulations, this involves the identification of decision or design variables, formulation of an objective function, and definition of the design space via a set of constraints. Some toy problems and cases with obvious optima do not need constraints [42, 43], but most practical problems will. While the objective function will always be a function of the decision variables, the constraints may take two forms: (1) a function of decision variables or (2) simple bounds on the possible values of each decision variable. For manufacturing-related problems, the bounds will be more commonly encountered [40, 44–46]. As previously discussed, the various manufacturing parameters provide excellent objective functions and design variables, but do not provide rigorous constraints. In order to avoid manufacturability problems with the final designs [45, 47, 48] and to avoid simplifying the design too much (as is often done in traditional design-for-manufacturing techniques [49–51]), it is vital that accurate and useful constraints be generated.

3.2.2 Mapping Manufacturing Knowledge to Design Constraints

The advantages, limitations, and best practices related to specific manufacturing processes are vital considerations during product design. This is especially true when using complex design methods (e.g., those generated using algorithms, such as topology optimization), as the final design may not actually be manufacturable without the imposition of the manufacturability constraints. This requires a rigorous process of mapping the useful manufacturing knowledge into design-focused manufacturability constraints; the purpose of these is to limit the design candidates to those which are manufacturable using a particular process or series of processes [52–57]. This design perspective and approach was the focus of Chapter 2. Different design scales must also be considered during this mapping; the basic scales referred to in this dissertation are defined in Figure 3.3.

Manufacturing processes can be classified according to type (subtractive, additive, formative), family (e.g., machining processes), and individual process mechanics [58]. At each of these classifications, a list of process characteristics can be made; the items on this list may overlap heavily with other processes of the same type or family or may be unique

Design perspective on structured material (SM) levels

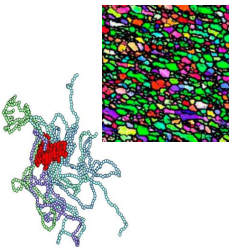
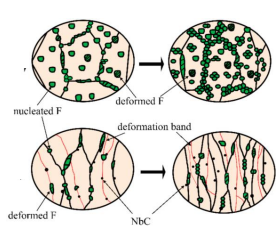
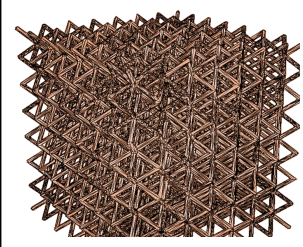

Natural material		Source of Dominant Properties		Structure and processing	
					
Sub-microstructure	Microstructure	Mesostructure	Macrostructure		
<ul style="list-style-type: none"> <input type="checkbox"/> Natural material structure on atomic, crystal, or molecular level <input type="checkbox"/> May be influenced by processing conditions <input type="checkbox"/> Examples: Polymer chains, grain structure details in metals 	<ul style="list-style-type: none"> <input type="checkbox"/> Structure observable using an optical microscope, heavily influential on macro-scale properties <input type="checkbox"/> Strongly influenced by processing conditions <input type="checkbox"/> Examples: Porosity, metal grain layout, scan structure in 3-D printed materials 	<ul style="list-style-type: none"> <input type="checkbox"/> Designed or patterned structure, may be generated by element layout or designed inclusions/defects/voids <input type="checkbox"/> Solid, homogeneous materials do not have a mesostructure <input type="checkbox"/> Examples: Honeycomb structure, metamaterial, unit cell-based lattice 	<ul style="list-style-type: none"> <input type="checkbox"/> In design, typically the “useful level” <input type="checkbox"/> Generally the final component or product that is to be made from the designed material <input type="checkbox"/> For homogeneous solid materials, microstructure drives macrostructure properties (no mesostructure) 		

Figure 3.3: Design scales for materials and parts/products referred to throughout this dissertation. The mesostructure level will be the most often used and discussed. This chart shows examples of non-polymer materials for completeness, but it should be noted that all of the materials covered in this dissertation are hard polymers.

to a single process. These characteristics can be divided into advantages, disadvantages, and best practices. The advantages provide some kind of clear cost or schedule benefit or open up the list of possible designs and design features the process can fabricate. The disadvantages do the opposite, helping decrease the size of the design space or increasing cost and schedule issues. Best practices are effectively “soft constraints” which could be either an advantage or disadvantage in particular cases and must be evaluated. The list of manufacturing considerations can cover a very large domain, as shown in Figure 3.4.

Once the set of manufacturing considerations is established (at least conceptually), a set of manufacturing constraints arise naturally. For example, a manufacturing consideration for a machining process is that the cutting tool will generate both force and heat during operation. This naturally implies two manufacturing constraints: (1) that a machined feature must be thick enough to withstand the cutting force from the tool and (2) a feature must be large enough to dissipate heat without damaging the feature or material microstructure. The manufacturing constraints should be more formal than the manufacturing considerations and may require some expert intuition and experience, extensive

experimental data, or accurate enough simulations (if used) to fully translate in some cases. The manufacturing constraints are also related to the material choice, but whether they are depending on the material selection or vice-versa will depend on the problem at hand. Since these constraints are based on a specific process and specific set of conditions, the domain is contained within but significantly smaller than that of the manufacturing considerations (Figure 3.4).

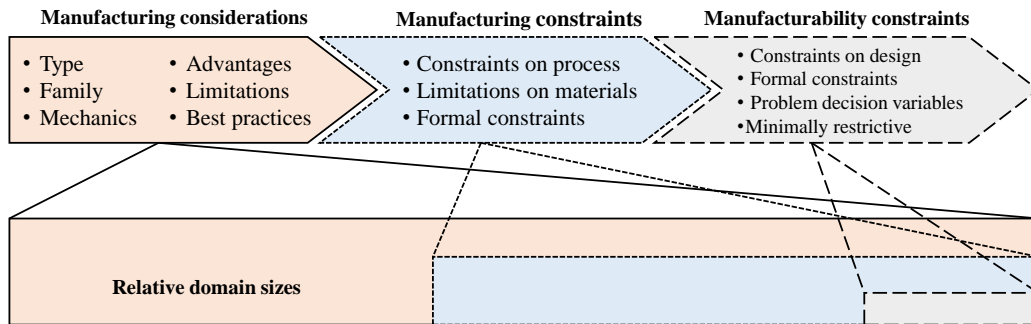


Figure 3.4: Basic mapping and domain sizes for general manufacturing processes.

The term “manufacturing” can have a variety of meanings, but one that is widely used and relevant to this work is the definition given by *DeGarmo’s Materials and Processes in Manufacturing*. Paraphrased, manufacturing is the performance of a series of operations on a product, raw material, or other item such that the successful completion of each operation or step increases its utility or monetary value [58]. With this in mind, the steps to manufacture a product will require a subset of the possible steps a particular process or set of processes are capable of. Therefore, the domain (Figure 3.4) for the manufacturability constraints (imposed on the design, not the manufacturing process) will be the smallest of the three; this makes sense when considering that the set of relevant constraints bounds the design space for a specific design or design family. In summary,

- The manufacturing considerations are observed or collected by designers and/or experts in manufacturing science. These may be quite conceptual and may be at the level of process type (SM, AM, FM), process family, or specific process and material combination. Manufacturing considerations may provide advantages (e.g., AM increases possible design complexity over machining), limitations (e.g., in machining,

features must be reachable by cutting tools), or guidelines/soft constraints (e.g., it is better to machine metal and mold engineering plastics when possible).

- The manufacturing considerations can (typically) be easily converted into manufacturing constraints (i.e., bounds on the applicability of the process).
- The manufacturability constraints on the design itself result directly from the limitations of the manufacturing process and material used.

3.2.3 FDM: Manufacturing Considerations

The four basic levels of analysis (system, extruder, element design, and element extrusion/fusion) for the FDM process are shown in Figure 3.5, from which the basic manufacturing considerations can be collected. Assuming a standard FDM machine design with three degrees of freedom, eight essential manufacturing considerations apply (Figure 3.6):

1. *MCR1 - ST-AM*: FDM is a scanning-type AM process, where each layer is built from a series of elements (typically of uniform cross-section) which do not fully merge into each other and form an anisotropic material with natural voids and inclusions which may be designed or optimized (Figures 3.5a, 3.5d, and 3.5e) [5, 13, 37–40, 46, 59, 60]
2. *MCR2 - Selective Deposition*: Deposition of the raw material is accomplished by extruding a filament through a heated die and selectively depositing it to form the essential elements (Figures 3.5b, 3.5c, 3.5d, and 3.5e) [13, 37, 46, 60–62]
3. *MCR3 - Polymer Melting*: The fusion is accomplished via polymer melting (Figure 3.5b, 3.5c, and 3.5d) [60, 63–69]
4. *MCR4 - Thermal Cycling*: The bulk material is subjected to uneven thermal cycling during operations (Figure 3.5b) [63–65, 67, 70, 71]
5. *MCR5 - Isotropic Elements*: Each element is approximately isotropic or transversely isotropic in terms of mechanical properties (Figure 3.5b, 3.5c, and 3.5d) [37, 60, 72–77]

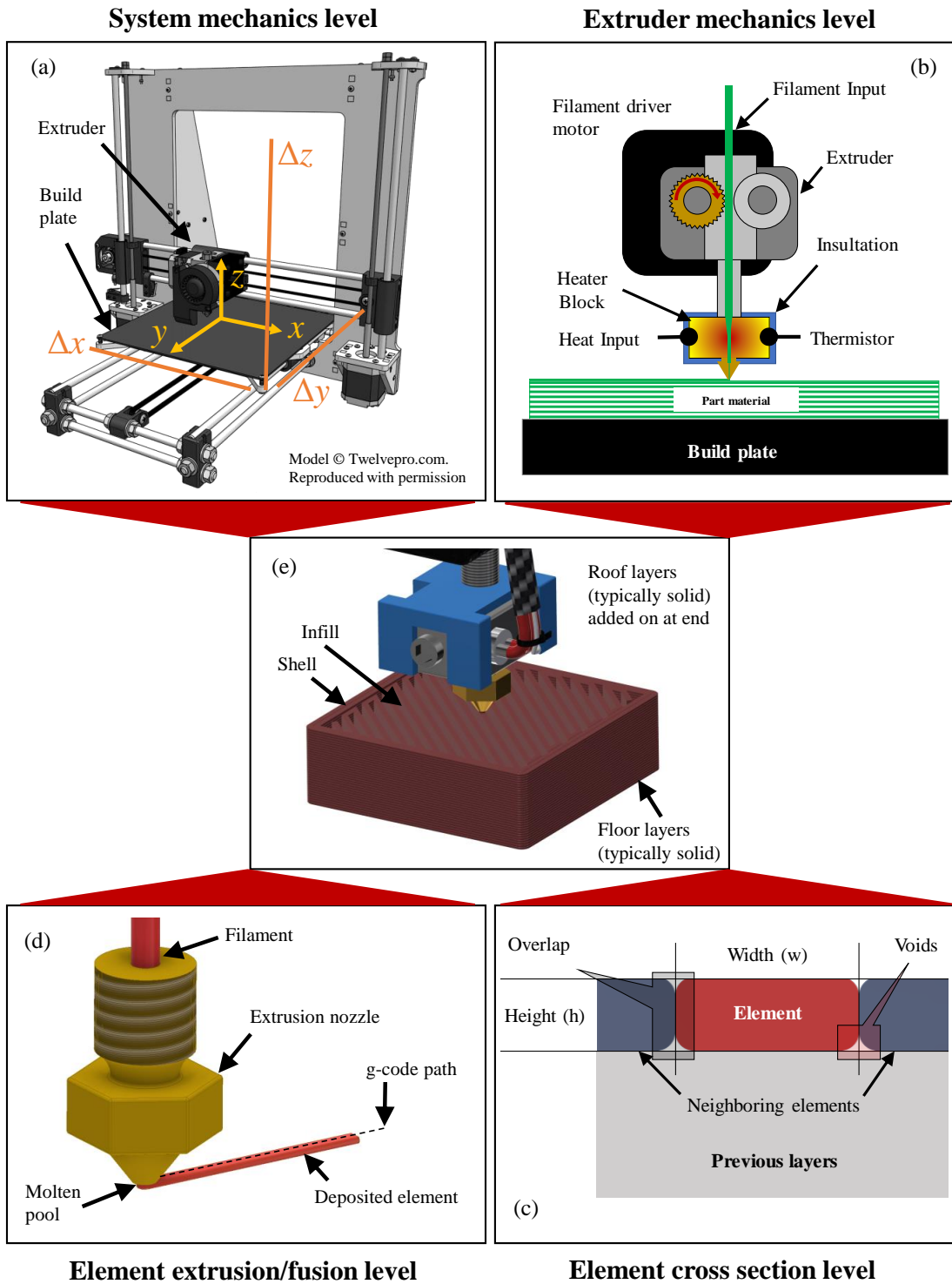


Figure 3.5: Levels of analysis for FDM. (a) System level, (b) extruder level, (c) element geometry level, and (d) element deposition/fusion level. Panel (e) shows the full process.

6. *MCR6 - G-Code Control*: The extruder die is controlled (generally using an open-loop controller or step counting in the motors) using g-code (Figure 3.5a and 3.5d) [37, 46, 60, 64, 78–81]
7. *MCR7 - X/Y Motion*: Motion of the extruder in X or Y directions builds each layer (Figure 3.5a) (definition for standard 3 DoF system)
8. *MCR8 - Z Motion*: Motion of the extruder in Z adds more layers (Figure 3.5a) (definition for standard 3 DoF system)

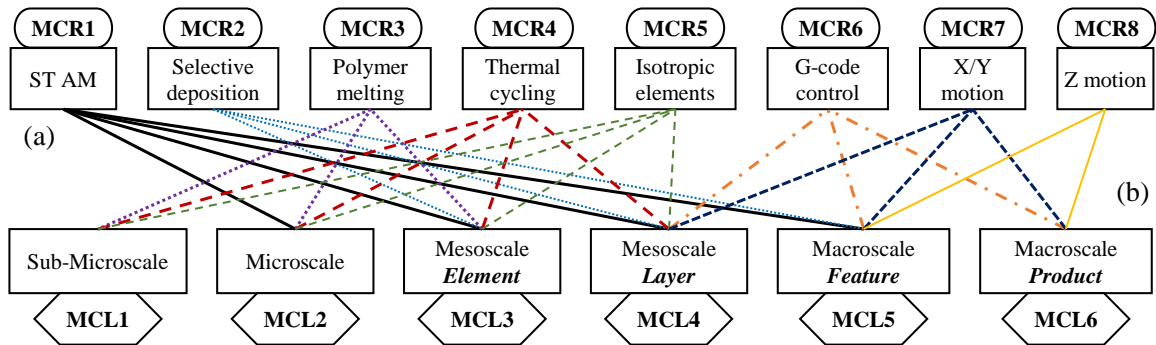


Figure 3.6: Mapping from the (a) basic eight manufacturing considerations to the (b) six sets of manufacturing constraints at each level of analysis for FDM.

3.2.4 FDM: Manufacturing Constraints

Given the manufacturing considerations from the previous section, the manufacturing constraints may be derived. In order to do this in a consistent and useful way, it is important to recognize that the bulk parts or products fabricated via FDM are structured materials, whether or not they are designed [13, 37–39, 59, 60]. As such, it is necessary to examine FDM at several scales, which correspond to specific levels of analysis shown in Figure 3.3. As demonstrated in Figure 3.6, FDM can be analyzed at the macro-level (e.g., a whole part or large feature), the meso-level (e.g., the “structured” level of the part or product), the micro-level, and the sub-micro-level. It is assumed in this section that the reader has a basic understanding of polymer material behavior and the mechanics of the FDM process. In case of doubt, refer to an earlier section of the paper or one of the references.

3.2.4.1 Sub-Microstructure Level

At the sub-micro level, the basic material properties of the polymers in use determine the manufacturing constraints (Figure 3.7). The homogeneity of the local material units (driven often by the quality of the filament used) and the rheology of the polymer determine the manufacturing constraints at this level. These things in general must be determined experimentally for each polymer or polymer composite used and limited choices are currently available since most FDM materials are thermoplastics. It is difficult to impossible to design the specific properties at this level, so the designer is typically required to consider these as fixed parameters (if a material is specified) or criteria for material selection (if not pre-selected). The rheological parameters (including the polymerization behavior and state) are mainly determined by the operating temperature for thermoplastics at this level [1, 82], so temperature must be carefully specified or established when taking property data or observing behavior. At the sub-micro level, the processing conditions have little to no direct influence, so the experiments used do not have to be directly related to FDM to draw useful conclusions. As shown in Figure 3.7, seven basic manufacturing constraints directly from FDM can be mapped from the manufacturing considerations at this level.

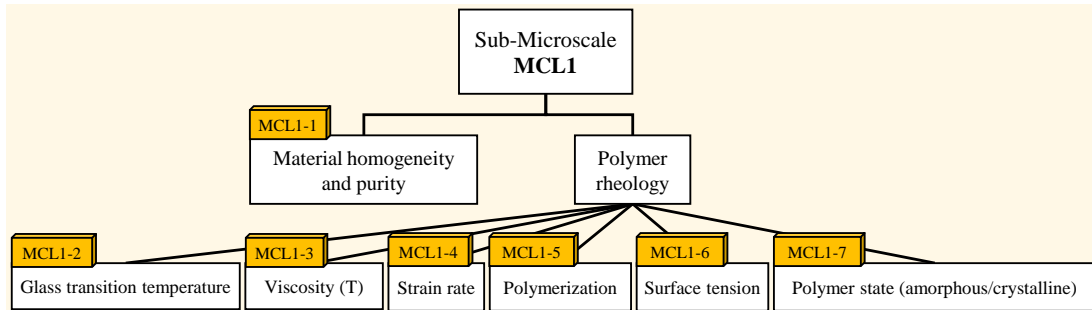


Figure 3.7: Essential manufacturing constraints at the sub-microscale level.

3.2.4.2 Microstructure Level

For the micro level (Figure 3.8), the material properties and processing conditions both influence the manufacturing constraints. Things such as the quality of the polymer chain reformulation (i.e., bonding) after extrusion and fusion, the amount of residual stress in

and between each element, the state of the polymer chain (amorphous or semi-crystalline), and the amount of shrinkage (which may be related to residual stresses) after cooling drive the manufacturing constraints at this level. As with the sub-micro level, the values of the resulting manufacturing constraints must be determined experimentally.

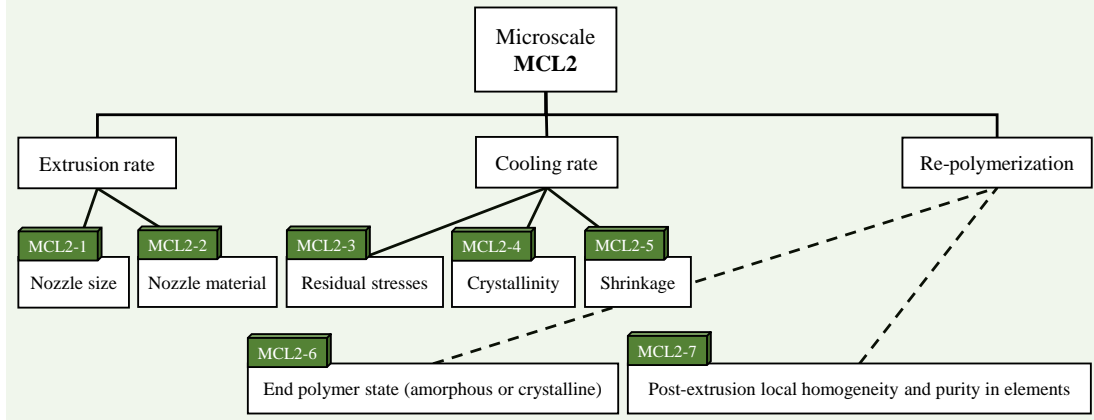


Figure 3.8: Essential manufacturing constraints at the microscale level.

3.2.4.3 Mesostructure Level

Using the definition for “meso level” given in Figure 3.3, FDM will have two levels of mesostructure, one at the individual element level (Figure 3.9) and one at the layer level (Figure 3.10). This is due to its nature as a scanning-type AM (ST-AM) process (Figure 3.5) and the fact that both the element geometry and the layout of the elements (i.e., the layer) can be designed in a simple mechanical way. These two sub-levels will have the largest set of manufacturing constraints of all the levels, but most of these will be simple bounds and inequality constraints. For these levels, the processing conditions and layout of the elements has a much larger impact on the final bulk properties of the part or product than the basic material properties. Of course, the constraints from the sub-micro and micro levels also impact the problem at the meso level through the properties of each element.

- *Single element mesostructure:* As seen in Figure 3.5c, the element cross section and length can be designed in a similar way to a simple beam or truss member. The major manufacturing constraints at this level (Figure 3.9) are the selected geometry, height-to-width ratio, minimum length, minimum corner radius, minimum connection

length with the last layer and neighboring elements, and a number of other constraints including the various dimensional errors. Given that FDM elements are produced via extrusion, are selectively laid out, and are approximately isotropic or transversely isotropic, they can often be seen and treated similar to beams in design problems.

- *Single layer mesostructure*: Similar to the single element mesostructure, the single layer element layout can be designed to have controllable (to some degree) mechanical properties. The most important of the manufacturing constraints for this level are restrictions on layer geometry, print direction, position accuracy uncertainties, element packing density, minimum useful layer thickness, the number of shells (“contours” in some literature), and the ratio of the shell area to the infill area for the layer. There are a number of others, as shown in Figure 3.10, which may be relevant. Following on from the discussion concerning the treatment of elements as beams in design problems, the layers may often be designed similar to 2-D or 2.5D truss problems in practice.

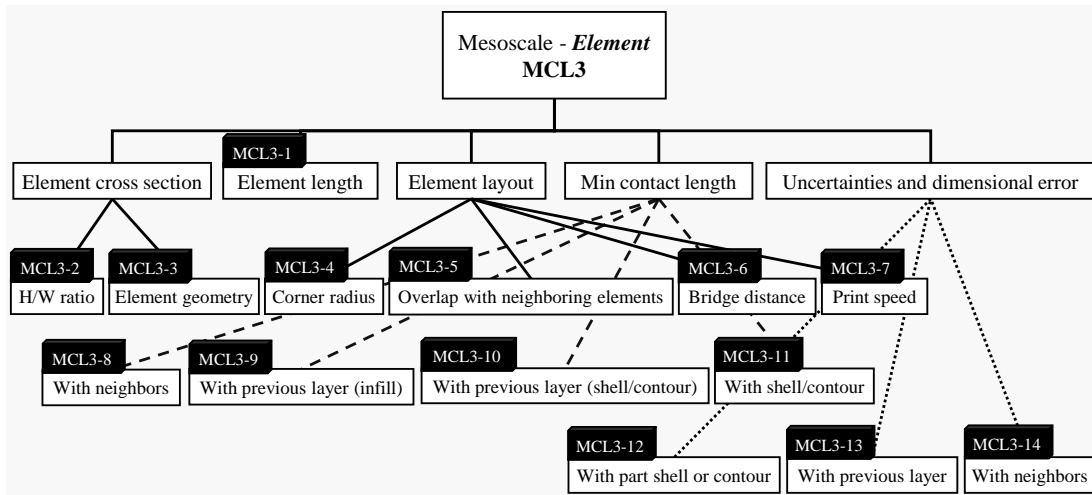


Figure 3.9: Essential manufacturing constraints at the single element mesoscale level.

3.2.4.4 Macrostructure Level

At the macro (“useful”) level, it is assumed that many layers of printed material are present. The size of macroscale features can range from an individual feature to the whole final part or product. In the case of FDM, this level can be further divided into two regions:

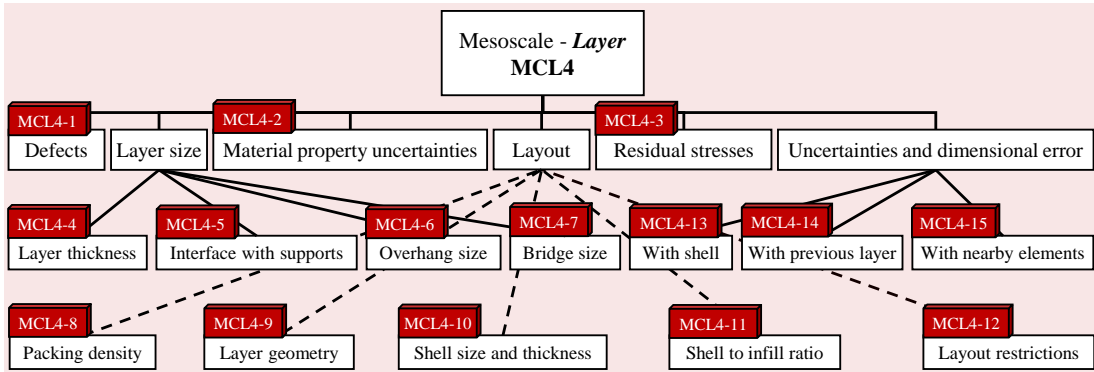


Figure 3.10: Essential manufacturing constraints at the single layer mesoscale level.

- *Feature-level macrostructure*: Manufacturing constraints at this level include things like the printing orientation, the minimum layers to be printed, the roof and flood thickness, and interfaces with support material and other features on the part or product. Most of the existing feature catalogs and feature-level design for additive manufacturing guidelines focus on this level; examples include [83–88].

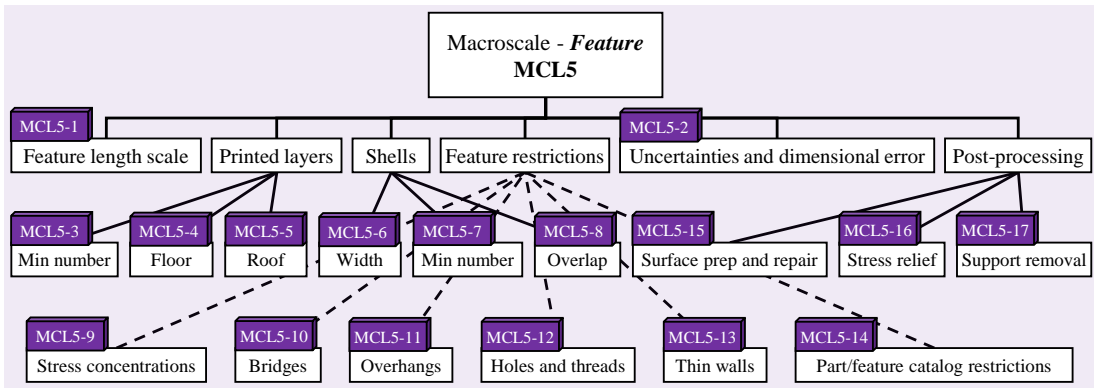


Figure 3.11: Essential manufacturing constraints at the macroscale (feature) level.

- *Part/product-level macrostructure*: This level is the one that will be directly observed or tested by most users and product/part designers and so the manufacturing constraints are mainly concerned with final appearance, post-processing, dimensional accuracy, and interfaces with other parts. General product design and success criteria mainly apply to this level. If the additively manufactured product is to be post-processed, it will typically be done with the product-level macroscale in mind.

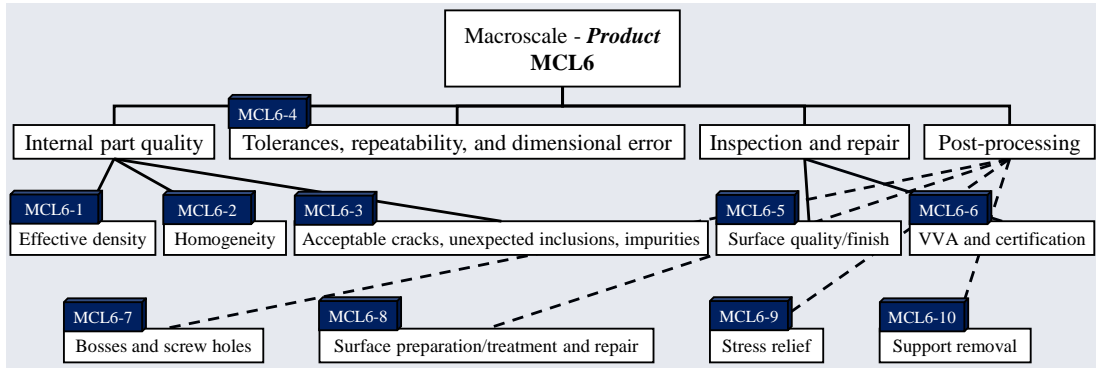


Figure 3.12: Essential manufacturing constraints at the macroscale (product) level.

3.2.5 FDM: Manufacturability Constraints

Given the large set of derived manufacturing constraints (i.e., limits on the process capabilities) explored in the previous section, a set of manufacturability constraints (i.e., on the design of a product to be fabricated using FDM) can be found. The step of mapping from the process limits to the design limits is a much more simple task than defining or finding all of the relevant process limits. Essentially, for each limit or set of limits, an equivalent design limit must exist to accommodate the parent process limit(s). These design limits (manufacturability constraints) can be used directly in design problems to guarantee (or at least better ensure) that the final product is indeed manufacturable using FDM.

Compiling all of the process constraints discussed in Section 3.2.4 (and combining/refining as needed), the set of design constraints at each level can be found as shown in Table 3.3. Finding these constraints are fairly straight-forward given the information from Section 3.2.4 and no special processes are required. In most cases, each of the manufacturability constraints will have more than one parent manufacturing constraint; likewise, a manufacturing constraint may drive more than one manufacturability constraint. For thermoplastic FDM, all of the constraints directly drive the design decisions; however, in practice some of the constraints simply drive the selection of materials, some of them limit the printing parameters, and some directly impact the design. Notes are given in the table for each case. Note that exact constraints cannot be derived without selecting a material and possibly collecting some experimental data, due to the different behavior of each of the FDM polymers. In addition, the constraints may not be independent of each other.

The mapped conceptual manufacturability constraints for FDM are shown in Table 3.3. A total of 54 were identified, but not all of them will apply to all design problems. The large majority of these fall into two categories when not used as constraints:

1. *Build parameters*: Designated as “PP-CN” type constraints in Table 3.3, these may be used as print parameters or constraints, depending on the objectives and needs of the design. In practice, a mix of constraints and parameters will likely be used.
2. *Confounding factors*: Confounding factors are those which have some influence on a model or system but the influence is not necessarily known or understood when these are not directly controlled. Designated as “CF-CN” type constraints in Table 3.3, these could be considered to be largely “noise” variables in FDM processes but could also be controlled or used as constraints in design problems.

The remaining constraints (“CN” in Table 3.3) are simple constraints (generally generated by the stakeholders as part of the project requirements). The *type* and *form* of the constraints should be considered separately in order to best formulate and use them effectively in the design problem at hand. Just as the type of constraint may be *simple* (CN), *parameter* (PP-CN), or *confounding factor* (CF-CN), the form of the constraints may also be divided into three major categories (Table 3), depending on its main source.

1. *Build parameters* (BP): Constraints directly on the build parameters. These will almost always be simple bounds (e.g., minimum and maximum raster angle) on the parameter in question.
2. *Material selection* (MS): Constraints either driven by or driving material selection (depending on the progress of the design process). These may take the form of bounds, inequality constraints, and equality constraints, depending on what is considered. In the experience of the authors, the more complex constraint equations (e.g., the equality constraints) can be simplified dramatically by setting some variable values to fixed parameters.
3. *Geometric constraints* (GS): These constraints may be driven by design rules (e.g., [84, 85]) or by looking at geometric relationships in the design. While any non-bound

functions are likely to be simple continuous functions, the possibility of having both inequality and equality constraints often necessitates simplification, similar to what is done for material selection.

The realistic determination of the constraints may be done in eight major ways in practice (Table 3.3), namely:

1. *Stakeholder decision* (SD): A value or limit decided and enforced by the designers and other stakeholders. These constraints typically deal with things such as manufacturing time, cost, safety, aesthetics and ergonomics, and the final verification/validation and accreditation process for the part or system being designed. These constraints may have little to no input directly from the process mechanics or material selection.
2. *Observation* (OB): For parameters and constraints that are difficult to control (or simply not of interest to control for the present design problem - the ambient air temperature is a good example), simple observation may provide the needed values.
3. *Partial observation* (PO): Similar to observation but when only partial or incomplete information is available to the designer and other stakeholders. Good examples would be the properties of proprietary filaments with unknown dyes and additives and the exact parameters for proprietary “plug and play” FDM systems.
4. *Formal experiments* (FE): The vast majority of the constraint values and relationships for FDM can be found from simple formal experiments or from reviewing the experimental literature for some common materials.
5. *Modeling and simulation* (M&S): Some of the boundaries and relationships needed can be found using modeling and simulation (for example, finding unhelpful stress concentrations using finite element modeling).
6. *Hardware limitations* (HL): Hardware limitations can be a major source of constraints for FDM and these can usually be observed or measured easily.
7. *Calculations* (CA): Some constraints may be able to be calculated directly, such as ratios and relationships between geometric elements.

8. *Geometry check* (GC): Given the numerous excellent sets of design feature catalogs and experimental testing methods, checking that geometry meets the constraints is not difficult to accomplish. This may be done automatically during design or the check may be formulated as a constraint.

Table 3.3: Manufacturability constraints mapped from the manufacturing constraints and manufacturing consideration for the FDM process. These constraints are subject to three major assumptions: (1) The system has three degrees of freedom, (2) the extruder has a fixed round extrusion nozzle, and (3) the printer hardware is properly tuned

Constraint	Type	Form	Parent(s)	Method	Notes
1. Acceptable material purity and quality	CN	MS	MCL1-1	SD	Usually need the highest quality material possible, but may be traded off for some other objective such as cost or order time
2. Filament additives and colors	CF-CN	MS	MCL1-1 MCL2-6 MCL2-7	PO ¹	For most open-source materials, the presence of additives and dyes is not a major concern, with the exception of PLA [89]. Most commercial or proprietary filaments contain additives which may or may not be known to the designer. Flag 1: It is often only possible to obtain partial information regarding this constraint.
3. Environmental conditions	PP-CN	BP	MCL1-1 MCL2-6 MCL2-7	OB	Standard environmental conditions such as temperature, humidity, and air pressure
4. Minimum and maximum extruder temperature	PP-CN	BP	MCL1-2 MCL1-3 MCL1-4 MCL1-5 MCL1-6 MCL4-3	FE, M&S, HL	Common printing parameter that can be used as a constraint. The minimum temperature cannot be lower than the glass transition temperature or higher than the boiling point of the polymer material. However, typically much more narrow range in which the material flows effectively and can re-polymerize quickly once deposited.

Continued on next page

Table 3.3 – *Continued from previous page*

Constraint	Type	Form	Parent(s)	Method	Notes
5. Ambient temperature	CF-CN	BP	MCL1-2 MCL1-3 MCL1-4 MCL1-5 MCL1-6 MCL4-3	OB	The ambient temperature may be the temperature around the working environment or may be the local surrounding temperature only (in the case where an enclosure is used).
6. Minimum and maximum print speed	PP-CN	BP	MCL1-2 MCL1-3 MCL1-4 MCL1-5 MCL1-6 MCL3-7 MCL4-3	FE, M&S, HL	Common printing parameter that can be used as a constraint. Print speed is a function of the system dynamics and the molten polymer rheology. In general, faster print speed will result in faster completion but also rougher surface finish, lower dimensional accuracy, and increased incidences of defects in the final part. This is a trade-off that must be found for every material used.
7. Minimum and maximum build plate temperature	PP-CN	BP	MCL1-2 MCL1-3 MCL1-4 MCL1-5 MCL1-6 MCL4-3	FE, M&S, HL	Common printing parameter that can be used as a constraint. For many materials (particularly amorphous glassy polymers such as ABS and polycarbonate), the build plate heater helps keep a large section of the part at a temperature close to (but below) that of the glass transition temperature of the material. This helps to naturally dissipate residual stresses (for polymer materials) and prevent warping and premature bed detachment. Heating above glass transition temperature can cause melting/drooping of features and reduce dimensional accuracy.
8. Jerk and acceleration settings	CF-CN	BP	MCL1-2 MCL1-3 MCL1-4 MCL1-5 MCL1-6 MCL3-7 MCL4-3	SD, FE, CA, HL	Jerk and acceleration settings are not commonly considered by designers but are the best way to control/mitigate system vibration without modifying the basic hardware. Higher settings allow faster printing but decrease dimensional accuracy and increase the probability of print defects.

Continued on next page

Table 3.3 – Continued from previous page

Constraint	Type	Form	Parent(s)	Method	Notes
9. Crystallinity after printing	CF-CN	MS/BP ²	MCL1-7 MCL4-3	FE, M&S	<p>The final polymer structure of the engineering plastic used has a lot of influence on the final mechanical properties, the degree of anisotropy, and the recyclability of the material. For many crystalline and semi-crystalline polymers, this can be controlled by controlling the cooling rate and with additives.</p> <p>Flag 2: Typically an amorphous or naturally semi-crystalline material will be selected for use, but can also be partially controlled when setting the printing parameters, so could be defined in the form of either material selection or build parameters.</p>
10. Maximum % shrinkage allowed on cooling	CF-CN	MS	MCL2-3 MCL2-4 MCL2-5	SD, FE, M&S, CA	Stakeholder requirement
11. Defect % tolerance	CF-CN	BP	MCL4-1 MCL6-2 MCL6-3	SD	Stakeholder requirement
12. Degree of homogeneity in structure	CF-CN	BP/MS ³	MCL6-1 MCL6-2	FE, M&S	<p>The higher the degree of homogeneity, the lower the anisotropy in the final part [90,91].</p> <p>Flag 3: Usually going to be determined by the build parameters but material choice may also have a significant influence.</p>
13. Realistic minimum and maximum element packing density	PP-CN	BP/MS ⁴	MCL4-8 MCL2-3 MCL2-4 MCL2-5 MCL2-6 MCL2-7 MCL4-3 MCL6-1	FE, M&S	<p>Flag 4: Typically set using a combination of density and overlap parameters during printing setup, but can also be dependent on material choice. For example, amorphous materials such as ABS and PC can have regular packing densities greater than 99% while the same print settings produce 94-95% density for PLA [29]</p>

Continued on next page

Table 3.3 – *Continued from previous page*

Constraint	Type	Form	Parent(s)	Method	Notes
14. Support available when needed?	PP-CN	GS	MCL4-5 MCL5-17 MCL6-10	GC	Basic requirement
15. Support removable?	PP-CN	GS	MCL4-5 MCL5-17 MCL6-10	GC	Basic requirement
16. Support does not interfere with function?	PP-CN	GS	MCL4-5 MCL5-17 MCL6-10	GC	Basic requirement
17. Minimum and maximum extruder nozzle size	PP-CN	BP	MCL1-3 MCL1-4 MCL1-6 MCL2-1	HL, FE, M&S	Common printing parameter that can be used as a constraint.
18. Nozzle material	CF-CN	BP ⁵	MCL2-2	SD, FE	Nozzle material is often a confounding factor that is not considered during print setup. However, the choice of nozzle material (typically brass or stainless steel, but can include others) can influence how much heat is retained in the immediate area of the extrusion, which can affect the rheological properties of the melt pool. Flag 5: Really can only be controlled as a build parameter.
19. Minimum and maximum deposited element width	PP-CN	BP	MCL3-2 MCL3-3	HL, FE, M&S	In most pre-processing software packages such as Ultimaker [®] Cura [®] , the element width can be varied significantly by over- or under-extruding out of the given nozzle. While calculating the nozzle diameter and the air gap/overlap between elements is the best way (in general) to lay out the elements, varying the element width here can be useful for materials which shrink rapidly (such as PLA with metal powder). This can also be used to improve the effective packing density (and homogeneity) in a part.

Continued on next page

Table 3.3 – Continued from previous page

Constraint	Type	Form	Parent(s)	Method	Notes
20. Minimum and maximum layer/element height	PP-CN	BP	MCL3-2 MCL4-4	HL, FE, M&S	Common printing parameter that can be used as a constraint.
21. Variability in layer height	CF-CN	GS ⁶	MCL3-2 MCL4-4	SD, HL, FE, CA	<p>Generally, the layer height is consistent for a single part or at least within each layer. However, this is not necessary since some freedom is available here even when using a standard 3 DoF system.</p> <p>Flag 6: It probably is better to consider this a geometric constraint (due to its influence on the rest of the part) instead of a printing parameter even though it can be accomplished with custom g-code.</p>
22. [Element] Height to width ratio	CN	GS	MCL3-2	FE, M&S	Function of the layer height and nozzle size in most cases. The ideal ratio depends on the material choice but should never be larger than $H/W = 2/3$ in the experience of the authors. When higher print speed is not available or too risky (due to vibration) using larger elements will decrease manufacturing time; however, this may require a trade-off with surface finish and internal void size.
23. [Element] Element layout restrictions (for non-raster infill layout)	PP-CN	BP/GS ⁷	MCL3-4 MCL3-5 MCL3-6 MCL4-9 MCL4-12	HL, FE, M&S, GC	<p>When not using a raster-based layout for the infill, various constraints may be necessary to ensure that the infill is stable. Generally, this will include all of the parameters as a raster-based layout (gaps/overlaps, max and min element lengths, element size, etc.) except the minimum and maximum raster angles.</p> <p>Flag 7: Depending on the layout and parameters, this could be considered either a printing parameter constraint or a geometric constraint.</p>

Continued on next page

Table 3.3 – Continued from previous page

Constraint	Type	Form	Parent(s)	Method	Notes
24. [Element] Minimum and maximum raster angle (for raster layout)	PP-CN	BP	MCL4-9 MCL4-12	HL, FE, M&S, GC	Common printing parameter that can be used as a constraint. It is almost always set as part of the build parameters.
25. [Element] Minimum stand-alone element length	CF-CN	GS/BP ⁸	MCL3-1	HL, FE, M&S	The minimum length of a single element so that it is stable and does not warp or curl. It may or may not be attached to another polymer element. Flag 8: This may be a geometric constraint (i.e., determine the minimum length scale for the part or feature) or may be set during the printing parameters.
26. [Element] Minimum and maximum element corner/turn radius	CF-CN	GS/BP ⁸	MCL3-4	HL, FE, M&S	The minimum turn radius of a single element so that it is stable and does not warp or curl. It may or may not be attached to another polymer element. See #25, Table 3.3 for flag.
27. [Element] Minimum contact length with shell/contour	CF-CN	GS/BP ⁸	MCL3-11	HL, FE, M&S	Same as #25 except based on single element in contact with other printed material. See #25, Table 3.3 for flag.
28. [Element] Minimum contact length with previous layer (infill)	CF-CN	GS/BP ⁸	MCL3-9	HL, FE, M&S	Same as #25 except based on single element in contact with other printed material. See #25, Table 3.3 for flag.
29. [Element] Minimum contact length with previous layer (shell/contour)	CF-CN	GS/BP ⁸	MCL3-10	HL, FE, M&S	Same as #25 except based on single element in contact with other printed material. See #25, Table 3.3 for flag.
30. [Element] Limits on overlap or air gap with neighboring elements	PP-CN	BP	MCL3-5	HL, FE, M&S	Common printing parameter that can be used as a constraint. Generally, positive values represent air gaps and negative values represent overlaps.
31. [Element] Maximum bridge distance	CF-CN	GS	MCL3-6	HL, FE, M&S	The maximum distance that a single element can bridge an unsupported gap without collapsing.

Continued on next page

Table 3.3 – *Continued from previous page*

Constraint	Type	Form	Parent(s)	Method	Notes
32. Shell thickness	PP-CN	BP	MCL4-10 MCL5-6 MCL5-7 MCL5-8	SD, HL, FE, M&S	Common printing parameter that can be used as a constraint. May be a single shell with a fixed width or several shells with an overlap or air gap between them. Two times the minimum shell thickness plus the minimum infill distance for a design defines the lower bound on the length scale for a feature.
33. Shell-infill ratio	CF-CN	GS ⁹	MCL4-11	SD, FE, M&S	Common printing parameter that can be used as a constraint. The shell-infill ratio will determine the directional strengths in the FDM structure, especially in cases with large gaps or low-density infill. Flag 9: Best considered a geometric constraint. If control of this is desired during the design, the ratio between the two areas will be specified instead of being automatically generated based on build parameters.
34. [Layer] Maximum bridge distance	CF-CN	GS	MCL4-7	HL, FE, M&S	The maximum unsupported distance between two edges which can be bridged by a single layer.
35. [Layer] Max overhang distance	CF-CN	GS	MCL4-6	HL, FE, M&S	The maximum unsupported overhang distance from a single edge. This is heavily dependent on the material properties and rheology of the polymer, as well as the printing parameters [92]. The overhang angle is important as well, but usually addressed by Constraint #40, Table 3.3 and similar.
36. Minimum number of layers	PP-CN	BP	MCL5-3	HL, FE, M&S	Standard build parameter which may be used as a constraint

Continued on next page

Table 3.3 – Continued from previous page

Constraint	Type	Form	Parent(s)	Method	Notes
37. Minimum floor and roof thickness	PP-CN	BP	MCL5-4	HL, FE, M&S	Standard build parameter which may be used as a constraint. Only relevant if (1) the infill used is not the same density as the roof and floor or (2) a different infill pattern is used. If 100% density is used and/or a consistent infill pattern is used throughout the printed height, the floor and roof are not needed.
38. Feature geometry: Stress concentrations	CF-CN	GS	MCL5-9 MCL5-14	M&S, GC	Geometric constraints based on modeling, material properties, and design rules developed for specific AM processes. For example, sets of rules which would govern such a feature can be found in works by [84–86,93]
39. Feature geometry: Bridges	CF-CN	GS	MCL5-10 MCL5-14	M&S, GC	See #38, Table 3.3.
40. Feature geometry: Overhangs	CF-CN	GS	MCL5-11 MCL5-14	M&S, GC	See #38, Table 3.3.
41. Feature geometry: Holes and threads	CF-CN	GS	MCL5-12 MCL5-14 MCL6-7	M&S, GC	See #38, Table 3.3.
42. Feature geometry: Thin walls	CF-CN	GS	MCL5-13 MCL5-14	M&S, GC	See #38, Table 3.3.
43. Dimensional error [Element with shell or contour]	CF-CN	BP	MCL3-12	HL, FE, CA	Allowable dimensional error could be based on the size of the part being made, the expected tolerances and repeatability, and other considerations. This is an important consideration for design and one that may drive build parameters and design decisions directly. One of the weaknesses of FDM is the vibration during mechanical motion, as well as the open-loop position control system. The exact amount of error can be calculated using simple experiments for a specific machine and material, but may also include effects from material shrinkage and software/g-code errors [5,94–96].

Continued on next page

Table 3.3 – Continued from previous page

Constraint	Type	Form	Parent(s)	Method	Notes
44. Dimensional error [Layer with shell or contour]	CF-CN	BP	MCL4-13	HL, FE, CA	See #43, Table 3.3.
45. Dimensional error [Element with previous layer]	CF-CN	BP	MCL3-13	HL, FE, CA	See #43, Table 3.3.
46. Dimensional error [Layer with previous layer]	CF-CN	BP	MCL4-14	HL, FE, CA	See #43, Table 3.3.
47. Dimensional error [Element with neighboring element]	CF-CN	BP	MCL3-14	HL, FE, CA	See #43, Table 3.3.
48. Dimensional error [Layer with other out-of-layer elements]	CF-CN	BP	MCL4-15	HL, FE, CA	See #43, Table 3.3.
49. Dimensional error [Features]	CF-CN	BP	MCL5-2	HL, FE, CA	See #43, Table 3.3.
50. Allowable uncertainty in essential material properties	CF-CN	MS	MCL4-2	SD, FE	Stakeholder decision which may be the driver of some disparity between modeled and realistic performance for some parts.
51. Min feature length scale to dissipate heat/stress stably	CN	GS	MCL5-1 MCL4-3 MCL2-3 MCL2-4 MCL2-5 MCL5-1	FE, GC	For many design problems using FDM, this is the most important but most different constraint to figure out. In most cases it is best to use physical experiments to determine the smallest length scale [91,97,98]. In general, the smaller the length scale, the more larger the possible design space becomes. The rule of thumb (in the experience of the authors) is to use two shells around a feature plus a single shell-width worth of infill; given a nozzle size of 0.5 mm, the length scale is then 2.5 mm for any standard features. In some cases, particularly when using well-supported thin walls [99–101], it may be much smaller and still be stable.

Continued on next page

Table 3.3 – Continued from previous page

Constraint	Type	Form	Parent(s)	Method	Notes
52. Surface prep and repair access	CN	GS	MCL5-15 MCL6-5 MCL6-8	M&S, GC	Basic requirement
53. Allowable surface roughness	CF-CN	BP/MS ¹⁰	MCL5-15 MCL6-5 MCL6-8	SD, HL, FE, M&S	Basic requirement. Flag 10: Typically would be controlled via the build parameters (and post-processing, if needed), but could also be influenced by material selection.
54. Inspection, VV&A + Certification	CF-CN	MS/GS ¹¹	MCL6-5 MCL6-6	SD, OB, HL, FE, M&S, CA, GC	Basic requirement for any part that will be used for a practical or real use beyond a prototype. Flag 11: In most cases, with require consideration of both material choice and geometric constraints; for a complete job, both destructive and non-destructive evaluation methods are need.

To be useful in design, the constraints must be formulated in terms of the problem requirements. For mathematical optimization problems, these could be formulated as mathematical inequality and equality constraints and included in the problem directly. For other kinds of design problems, the constraints may be used to develop or refine design rules, guide requirement definition, and help drive success criteria for the project. Using the generated constraints in Table 3 as a checklist, an effective approach to formulating and using valuable FDM manufacturability constraints is:

1. *Collection:* Note all of the relevant manufacturability constraints, their type, and their form. Formulate or define them in the same form as the rest of the problem.
2. *Refinement:* Decide which constraints may be simplified and which require additional information (such as material properties or machine performance behavior)
3. *Completion:* For the constraints which require additional information, perform the tests or collect data from the published literature

4. *Condensation*: Remove all the duplicate, redundant, and inactive constraints
5. *Application*: Apply to the problem at hand
6. *Sensitivity analysis*: For any simplifications or assumptions, a sensitivity analysis should be done in some form.

3.3 FDM Materials Selection

Before the design process can proceed, it is necessary to identify the constraints in more detail. In most cases, this involved selecting a material or set of materials and deriving the constraints for each. For the work presented in this dissertation, three materials will be used throughout: (a) Acrylonitrile butadiene styrene (ABS), (b) polycarbonate (PC), and (c) polylactic acid (PLA). The selection process for materials focused on several major selection criteria. The main needs were:

1. The materials needed to be common enough so that there was some information about their printing behavior and final properties
2. The materials needed to be able to print smoothly and reliably at the meso-scale
3. The selected materials needed to be pure (as far as possible) and not contain any major additives or composite materials (such as carbon fibers or metal powder)
4. The materials needed to be considered at least somewhat brittle in the AM literature and experience of the author
5. The materials needed to be able to be printed using the existing equipment with a basic enclosure (discussed in more depth in the Materials and Methods section of Chapter 5) limited to an extrusion temperature of 250° C.

In addition to the three main materials selected for use, other materials were investigated, primarily polyamide (nylon), high-impact polystyrene (HIPS), polyethylene terephthalate glycol (PETG) but were found to be infeasible during the initial investigation. Figure 3.13

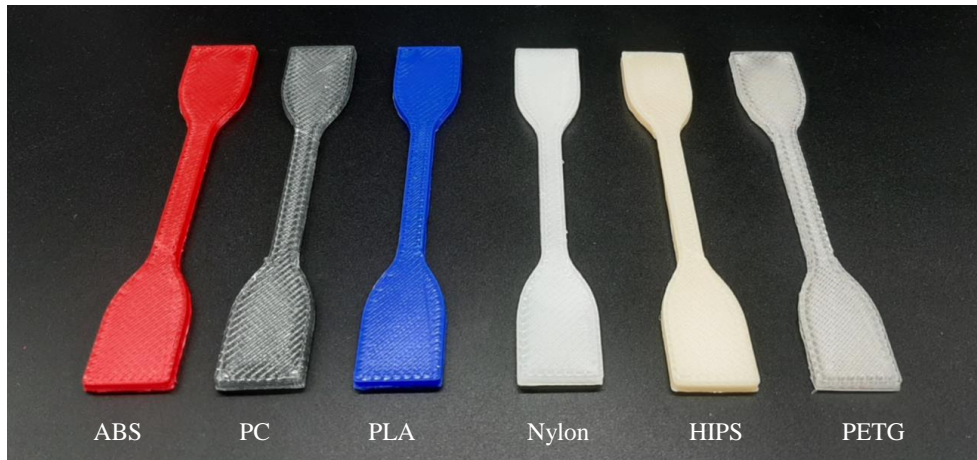


Figure 3.13: Tensile testing samples of the six materials considered for the work presented in this dissertation. ABS, PC, and PLA were selected for use while the others were removed from consideration, as described in Section 3.3. and Chapter 5.

shows samples of the six materials printed from the same rolls of filament and using the same printing hardware as the experimental samples shown in Chapter 6.

The environmental conditions in central Illinois during the Fall 2020 and Spring 2021 semesters were not appropriate for processing nylons due to wide and unpredictable variations in temperature and humidity, even within air conditioned (but old) buildings. The campus access limitations due to the University’s COVID-19 response during part of this time also caused some delays. Nylon is known to be extremely sensitive to environmental conditions [5, 29, 102–105] and the brand purchased for this work (natural eSun[®] ePA-175-N) was very much so. During screening experiments, the material behaved erratically and unpredictably making it unsuitable for the current design applications. Several different approaches to mitigate this were tried, including conditioning samples in three different buildings of various ages (the author’s home, the basement of the Mechanical Engineering Laboratory, and a top-floor lab in the Transportation Building) and using a dehydrating chamber to prepare and store the samples. All conditioning was done in an air conditioned environment with a steady temperature of 23 – 24° C (with an observed humidity ranging from 10% to 70% with rapid changes - this is discussed further in Chapter 6). After extensive testing (~60 samples) and discussion with advisors, it was decided that nylon would not be a feasible material for the current research effort.

The HIPS was found during some initial tests to be too soft and flexible for the planned

work. Thinking that there were some similar effects in HIPS as observed with the nylon, samples were conditioned and dehydrated, but to little effect. In addition, no information in the AM literature beyond what was already published by the author [5,29,71] was found, so independently-set expectations of behavior were not possible. Since this material did not meet the selection criteria, it was rejected early in the planning process.

The other main material that was considered when setting up the work described in this dissertation was PETG, a glassy thermoplastic which is considered both amorphous and semi-crystalline depending on the processing conditions. It was considered to be a good choice; however, at the time when the materials for this research were purchased not enough of the material was available at reasonable price to complete the planned experiments. After it became widely available again from a good quality brand, the work with the other materials was already well underway. Therefore, it was decided to place work based on PETG into the planned future work and proceed with three good materials.

3.4 FDM Manufacturability Constraints: Determination

3.4.1 General Constraint Set

Now that materials have been selected, Table 3.4 shows the 54 identified constraints and how they are or can be satisfied using a mixture of assumptions, literature review, and physical experiments on the materials to be used.

Table 3.4: FDM manufacturability constraint set based on material selection and design approach for printed parts in this dissertation. Note that the geometric constraints were more easily established since the printed parts for this work primarily consist of simple standard fracture specimens. Some of the case studies in Chapter 6 will expand several of these constraints further than what is discussed here.

Constraint	Values/How Met
1. Acceptable material purity and quality	For the work presented in this dissertation, only pure ABS, PC, and PLA sourced from Hatchbox were used for all the studies. Based on long history of use by the author, these were considered to be the best quality raw materials available within the initial budget for the work. Up to four 1-kg rolls of each material were used for the work presented here and in Chapters 5 and 6; care was taken to use the same color, same settings, and same storage technique for all the rolls. When possible, rolls were purchased in groups to reduce possible batch variability.

Continued on next page

Table 3.4 – *Continued from previous page*

Constraint	Values/How Met
2. Filament additives and colors	See #1, Table 3.4
3. Environmental conditions	As noted in the FDM Materials Selection section, the environmental conditions during this research were sometimes hard to control. When possible the limits for polymer materials from typical ASTM standards (e.g., 22–24° C and 40-60% relative humidity) were followed. Possible violations of this constraint are discussed in for individual experiments in Chapter 5.
4. Minimum and maximum extruder temperature	The maximum extruder temperature was one of the material selection criteria for this work. The highest printing temperature available was 250° C. Since extruder temperature was not a design variable for this work, it was considered a parameter and set to fixed values. See Chapter 5 for further details.
5. Ambient temperature	See #3, Table 3.4. All printing was done inside of an enclosure which was not heated directly but provided a more consistent environment. See Chapter 5 for more details on the design of the enclosure.
6. Minimum and maximum print speed	Similarly to the extrusion temperature, the values were fixed and so constraints were not necessary.
7. Minimum and maximum build plate temperature	Like the extrusion temperature and print speed, the build plate temperature was defined to be a print parameter and so was not subject to constraints for the present work.
8. Jerk and acceleration settings	Jerk and acceleration settings were treated as fixed parameters for all of the materials.
9. Crystallinity after printing	Of the three materials used to complete the work presented in this dissertation, ABS and PC are known to be amorphous, while PLA can vary from partially amorphous to semi-crystalline depending on the printing parameters [106–111]. One of the themes which will be explored in Chapter 5 will be the difference in mechanical behavior between the amorphous and semi-crystalline materials. Therefore, it was important that the PLA be as close to semi-crystalline as possible. To accomplish this, a heated bed was used for the PLA and it was printed inside of an enclosure to allow it to cool as slowly as possible during printing.
10. Maximum % shrinkage allowed on cooling	The manufacturer of the filament used in the presented studies promised an error of less than 2.86% including cooling-related shrinkage. The true rate of shrinkage will be explored in terms of dimensional accuracy later in this section and in Chapter 5. The true rate of shrinkage should be the value given by the manufacturer or less.
11. Defect % tolerance	Since all of the main studies in this dissertation involve fully-dense printed parts that have notches for testing, it was considered to not be an important constraint. The likelihood that a printing defect will dominate the notch for each case is very low. In the few cases in Chapters 5 and 6 where defect presence could be a major issue, this will be discussed for individual cases.

Continued on next page

Table 3.4 – *Continued from previous page*

Constraint	Values/How Met
12. Degree of homogeneity in structure	Since all of the explored case (except some case studies in Chapter 4 which is for illustrative purposes) were printed fully dense. Therefore, the degree of homogeneity is as much as it can be naturally; ideally, all variations in homogeneity are designed and contribute to the properties of the architected materials.
13. Realistic minimum and maximum element packing density	The packing density should be no less than 95% for the amorphous materials and 90% for semi-crystalline materials (stakeholder choice). This parameter will be experimentally determined in Chapter 5 during the basic material characterization.
14. Support available when needed?	Support material will not be used for the work presented in this dissertation.
15. Support removable?	See #14, Table 3.4
16. Support does not interfere with function?	See #14, Table 3.4
17. Minimum and maximum extruder nozzle size	The constraint for this was set by the available nozzle sizes, which ranged from 0.2 mm to 1.0 mm in increments of 0.05 mm. The nozzles selected for use were 0.6 mm and 0.8 mm, depending on need for each experiment. The choice of nozzle sizes will be explored in more depth in Chapter 5.
18. Nozzle material	This parameter was fixed. Only tool steel nozzles were used. More information about nozzle selection is provided in Chapter 5.
19. Minimum and maximum deposited element width	In the experience of the author, the element width can be up to 0.05 mm wider or more narrow than the nozzle size on each side of the element without affecting printability. In the present work, every effort was made when tuning the FDM machine to use a realistic deposited element width equal to that of the nozzle.
20. Minimum and maximum layer (and element) height	For the materials in use, experience of the author and common best practice directs that the element height-to-width ratio should not be larger than 2/3. Element width is determined mainly the nozzle size, so layer height should be selected accordingly.
21. Variability in layer height	Since the machine for use in this dissertation was essentially new, good quality, and was carefully tuned, this was not considered a significant factor for printing quality.
22. [Element] Height to width ratio	See #20, Table 3.4
23. [Element] Element layout restrictions (for non-raster infill layout)	For the present work with dense printed materials with designed layouts, no specific layout restrictions were anticipated beyond what will be imposed by other constraints.
24. [Element] Minimum and maximum raster angle (for raster layout)	Raster angle for the work described in this dissertation was limited to range from 0° to 90°. However the only raster angles used in this work were 0° and 45°. More information about this decision is provided in Chapter 5.
25. [Element] Minimum stand-alone element length	Minimum element print distance for stable print on a clean polished glass plate with no adhesive or contact with other polymer material. Experimentally determined, see Section 3.4.2

Continued on next page

Table 3.4 – *Continued from previous page*

Constraint	Values/How Met
26. [Element] Minimum and maximum element corner/turn radius	Since the radius will be determined by the mechanics of the process and not the adhesion to the build plate, this value is assumed to be valid for first-layer print and printing on top of existing polymer materials. Experimentally determined, see Section 3.4.2
27. [Element] Minimum contact length with shell/-contour	Measured as the minimum printed distance needed to ensure stable printing on top of existing polymer material. Experimentally determined, see Section 3.4.2
28. [Element] Minimum contact length with previous layer (infill)	Since the printing is being done on top of existing material, it is assumed that this value will be the same as that determined for #27, Table 3.4
29. [Element] Minimum contact length with previous layer (shell/contour)	Since the printing is being done on top of existing material, it is assumed that this value will be the same as that determined for #27, Table 3.4
30. [Element] Limits on overlap or air gap with neighboring elements	Since almost all of the printed parts presented in this dissertation are presented full-density, the maximum air gap will be zero. A small 2% overlap was used for all printing.
31. [Element] Maximum bridge distance	Assumed to be the same as the maximum bridge length for a layer or better. See #34, Table 3.4
32. Shell thickness	Unless otherwise stated, all of the prints shown in this dissertation will have only one shell. This is to minimize the impact of the shell itself and save printing time.
33. Shell-infill ratio	See #32, Table 3.4
34. [Layer] Maximum bridge distance	Experimentally determined, see Section 3.4.2
35. [Layer] Max overhang distance	It is not expected that any overhangs will be used in any of the geometries presented in this dissertation. If necessary, it is reasonable to assume that the maximum unsupported overhangs with the three materials in question is zero; for a supported overhang, the support material would create a bridge and so would not longer be an overhang design problem.
36. Minimum number of layers	Based on the experience of the author, a minimum of 5 layers should be printed for structural parts. Soft constraint for most FDM cases.
37. Minimum floor and roof thickness	With the designed element layouts for most of the work presented in this dissertation, floor and roof layers will not be used. However when they are it is best to use at least three layers for each in the experience of the author.
38. Feature geometry: Stress concentrations	No major stress concentrations exist in the printed parts for this work except those designed for fracture testing.
39. Feature geometry: Bridges	See #34, Table 3.4.2
40. Feature geometry: Overhangs	See #35, Table 3.4.2

Continued on next page

Table 3.4 – *Continued from previous page*

Constraint	Values/How Met
41. Feature geometry: Holes and threads	Since no toleranced holes and no threads will be used in the present work, this constraint is not relevant.
42. Feature geometry: Thin walls	Since no thin walls will be used in the present work, this constraint is not relevant.
43. Dimensional error [Element with shell or contour]	It is assumed for this work that the expected dimensional error will be the same percentage as that which was experimentally determined for macro-scale features. See #49, Table 3.4
44. Dimensional error [Layer with shell or contour]	It is assumed for this work that the expected dimensional error will be the same percentage as that which was experimentally determined for macro-scale features. See #49, Table 3.4
45. Dimensional error [Element with previous layer]	It is assumed for this work that the expected dimensional error will be the same percentage as that which was experimentally determined for macro-scale features. See #49, Table 3.4
46. Dimensional error [Layer with previous layer]	It is assumed for this work that the expected dimensional error will be the same percentage as that which was experimentally determined for macro-scale features. See #49, Table 3.4
47. Dimensional error [Element with neighboring element]	It is assumed for this work that the expected dimensional error will be the same percentage as that which was experimentally determined for macro-scale features. See #49, Table 3.4
48. Dimensional error [Layer with other out-of-layer elements]	It is assumed for this work that the expected dimensional error will be the same percentage as that which was experimentally determined for macro-scale features. See #49, Table 3.4
49. Dimensional error [Features]	Experimentally determined, see Section 3.4.2.
50. Allowable uncertainty in essential material properties	See #1, #2, and #3, Table 3.4.
51. Min feature length scale to dissipate heat/stress stably	Based on author experience and previous work [5, 53, 54], the minimum macro-scale feature scale should be 2.5 times the nozzle diameter for any parts which are taller than the part length scale. An exception to this is for thin-walled structures which do not need the same support due to geometry which keeps the part stable during printing [99] or 2.5D parts with stable features.
52. Surface prep and repair access	Not relevant to the present work
53. Allowable surface roughness	Not relevant to the present work
54. Inspection, VV&A + Certification	Not relevant to the present work

3.4.2 Detailed Constraint Determination

In this section, the experimental determination of constraints 25, 26, 27, 31, 34, and 35 is presented. In addition, dimensional error (constraints 10 and 49) analysis on a previously published dataset [5] is completed to find the values and confidence intervals for the material used in this work. Note that the equipment used in this section is the same as used to produce samples tested in Chapter 5 and the case studies presented in Chapters 3, 4, and 6. In all cases, the print bed was heated (80°C for ABS and PC and 60°C for PLA - pre-heated for 10 minutes before printing). The extrusion temperatures were 230°C for ABS, 250°C for PC, and 210°C for PLA).

3.4.2.1 Minimum Element Length on Glass Plate

In order to establish the minimum printed element length needed to securely print on a non-polymer surface, a series of prints were made on a clean, polished glass plate (Figure 3.14a). The length of any curled or separated material was measured. The test was repeated four times for each material, with the results shown in Figure 3.14b. The element width was 0.6 mm and height was 0.2 mm. No adhesive or other aid was used on the bed; the only treatment was a careful cleaning with isopropyl alcohol between runs. Note the significant difference in performance between the amorphous and semi-crystalline materials.

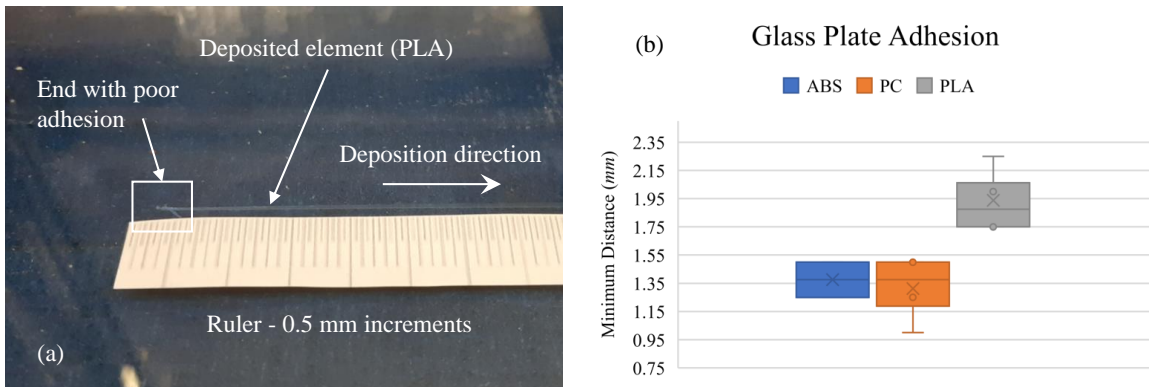


Figure 3.14: (a) Printed element on glass plate (PLA shown) and (b) minimum printed distance needed for adhesion to glass plate.

3.4.2.2 Minimum Element Corner Radius

To identify the minimum corner radius possible with the FDM, a 25-mm square film consisting of two printed layers and a single shell printed at 50 mm/s was examined under a microscope. Each corner of each film was examined, for a total of four observations for each material. The results are shown in Figure 3.16; it was observed for all cases that the corner radii were approximately the same size as the nozzle radii; therefore, a reasonable conclusion is that the lower limit of corner radii is the width of the extrusion nozzle. The element width was 0.6 mm and height was 0.2 mm.

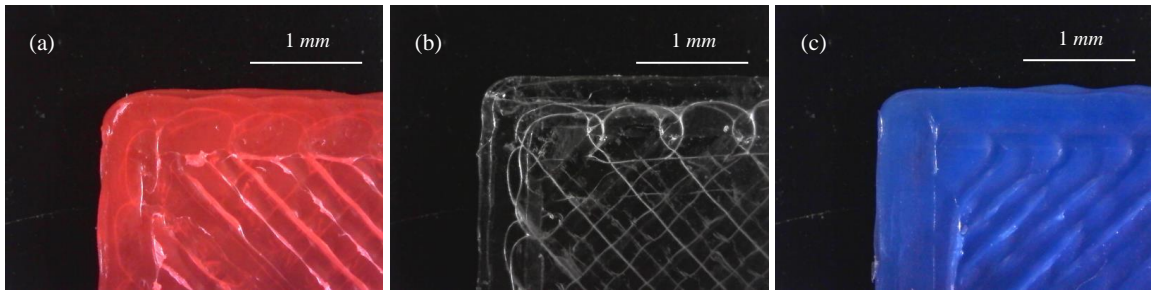


Figure 3.15: Example corners for printed samples of (a) ABS, (b) PC, and (c) PLA.

3.4.2.3 Minimum Element Length on Previous Material

A single thin wall 25-mm high and wide was printed to estimate the minimum length of adhesion between the deposited and previously printed material. In all cases, the adhesion was excellent and any observed error was much smaller than the nozzle with (Figure 3.16). The element width was 0.6 mm and height was 0.2 mm.

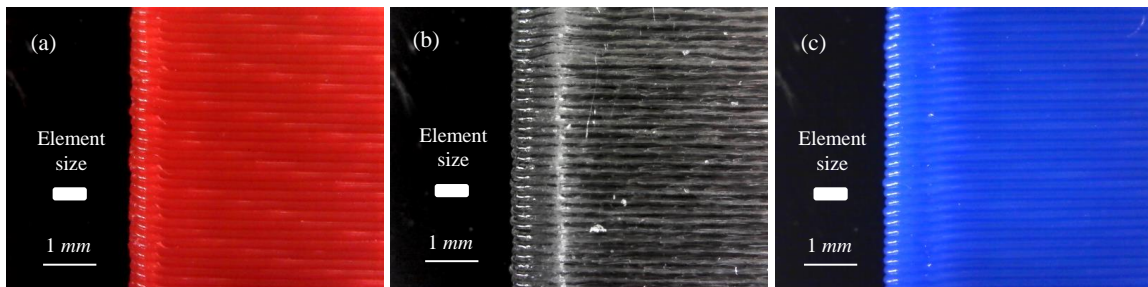


Figure 3.16: Edge samples to estimate the gap (if any) at the end of each layer of (a) ABS, (b) PC, and (c) PLA.

From the presented cases, it is reasonable to conclude that setting the minimum polymer-polymer contact length to be the nozzle width would give a conservative constraint. For the specific materials here, a value 0.10-0.25 times the nozzle width would also likely be a valid constraint.

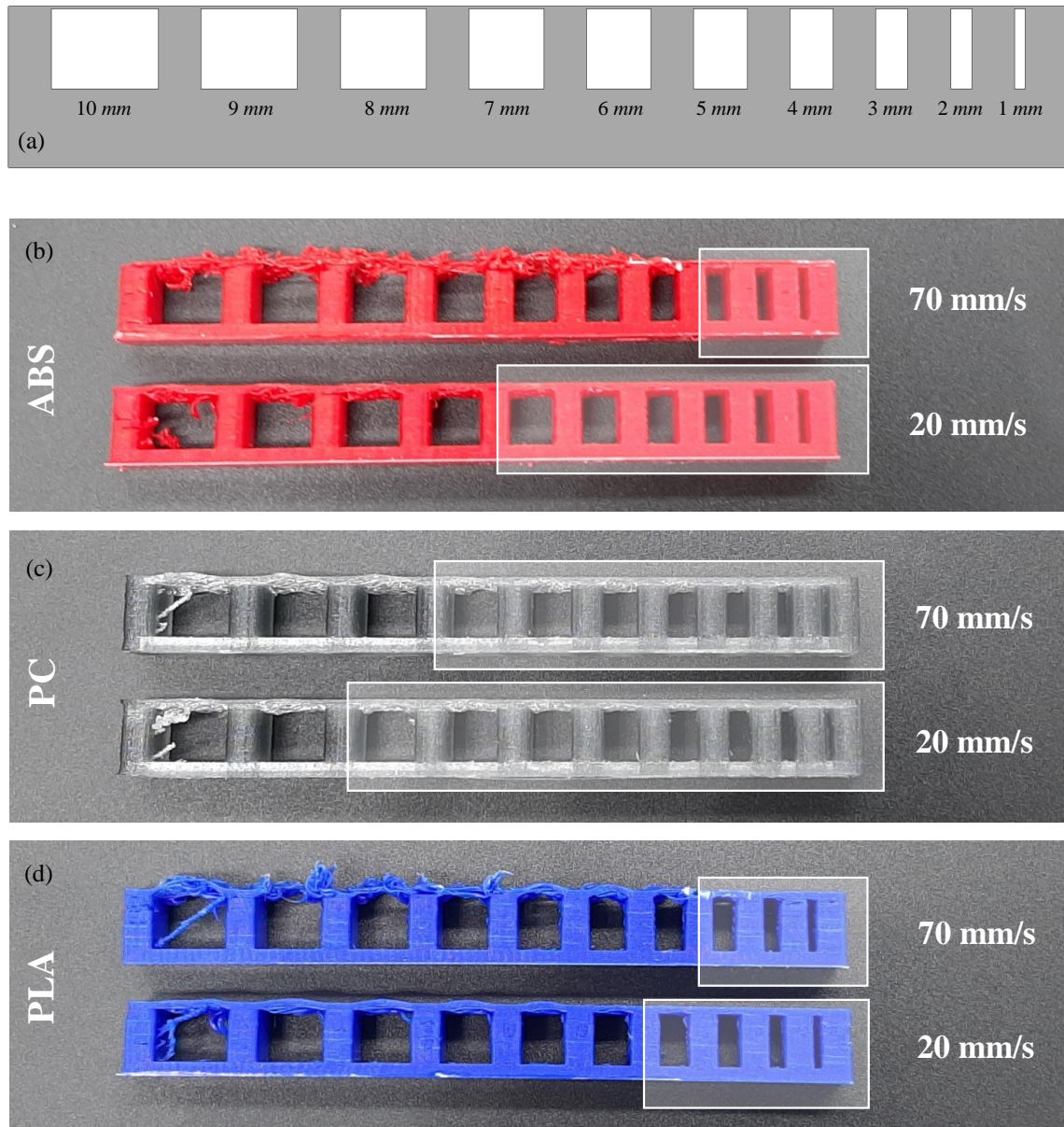


Figure 3.17: Bridge length test setup and results. (a) Sample geometry, (b) results for ABS, (c) results for PC, and (d) results for PLA.

Table 3.5: Some reported bridge lengths from the FDM literature compared with results found in this work. Note that only PLA-based studies were found in the literature, while studies for all three materials under consideration were completed.

Study	Material	Stable Bridge Length
[112]	PLA	0.5-5.5 mm
[113]	PLA	0.5-4.0 mm
[114]	PLA	0.5-5.5 mm
Current (70 mm/s)	ABS	3.0 mm
Current (70 mm/s)	PC	7.0 mm
Current (70 mm/s)	PLA	3.0 mm
Current (20 mm/s)	ABS	6.0 mm
Current (20 mm/s)	PC	8.0 mm
Current (20 mm/s)	PLA	4.0 mm

3.4.2.4 Maximum Element Bridge Distance

The maximum element bridge distance was estimated using the geometry shown in Figure 3.17a, where the gap varied from 1 mm to 10 mm in 1-mm increments. Two different print speeds were used (10 mm/s and 50 mm/s) for each material. The bridge length has been examined in several studies, which were reviewed in Table 3.5 in order to compare with the results found here. Note the very wide variance between materials, even when controlling for the print speed. As seen in Figure 3.17, the longest stable bridge was taken as the maximum approximate bridge length for that material/speed combination.

3.4.2.5 Dimensional Error

To find the expected dimensional error, a dataset published previously by the author and colleagues [5, 115] was analyzed (Figure 3.18). Note that this data analysis is new and was not part of the original studies that reported the dataset. It was based on the measurement of ASTM-specified IZOD testing samples with the nominal Z, C, and E dimensions coming from ASTM-D256-10(2018) (Figure 3.18). Note that the printing parameters were slightly different (most importantly, the element width was 0.4 mm with a height of 0.2 mm) from what is used elsewhere in this dissertation, but it is assumed that the error between what is reported in this study and the current conditions is trivial; see the discussion on sensitivity analysis later in this chapter. For the three materials examined, the observed errors (both raw and root mean squared (RMS) error) were equal to or smaller than the nozzle size.

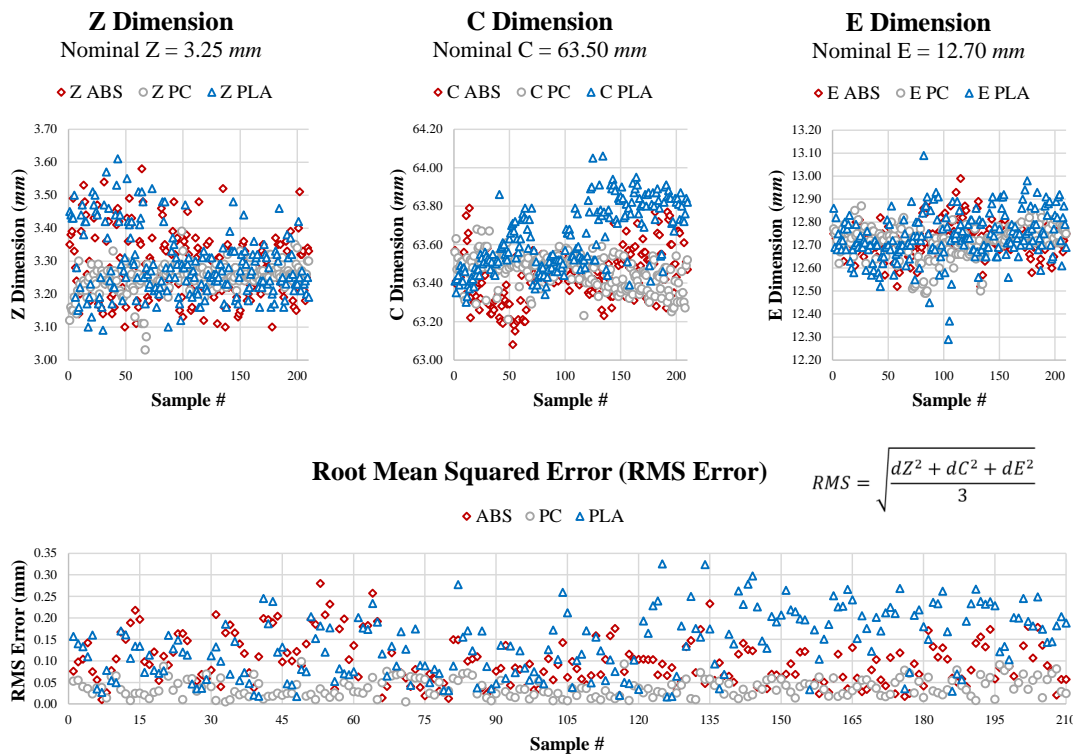


Figure 3.18: True versus nominal dimensions for Z, C, and E as well as the root mean squared error [5, 115].

3.4.3 Sensitivity Analysis

In this sensitivity analysis (Table 3.6), the assumptions and simplifications from Table 3.4 and elsewhere in this chapter are formally laid out. In each case, the consequences and impact of a particular assumption or simplification being incorrect or poor is presented.

Table 3.6: Sensitivity analysis on assumptions for the presented constraint set to be applied to the work in this dissertation. If a mitigation strategy has been put in place for the work presented in this dissertation, it will be specified. If not (mitigation not needed or not possible), the entry for that assumption will be "None".

Assumption	Risk if Wrong	Likelihood	Mitigation
1. The material used in this work is of good, consistent quality	Small increase in variability and error in the final results of any study	Low to moderate	Select material colors and brands with good historical behavior

Continued on next page

Table 3.6 – *Continued from previous page*

Assumption	Risk if Wrong	Likelihood	Mitigation
2. Using the same color and brand of filament for all cases in this dissertation will eliminate or minimize dye and manufacturing impacts on the rolls of raw filament	Small increase in uncertainty about measured properties	Low	None
3. Environmental conditions required for standardized printing and testing can be accomplished	Increase in uncertainty concerning measured properties and behavior	Moderate	Careful conditioning of specimens and monitoring of environmental conditions
4. Jerk and acceleration can be treated as parameters and controlled during process	Effects on material placement, increase of dimensional error, poorer surface finish, more uncertainty in final material properties	Low	Careful settings and regular setting checks during printing
5. Amorphous materials will not fundamentally change their structure before and after printing	Material properties can change and become unpredictable	Very low	None
6. Semi-crystalline materials will not fundamentally change their structure before and after printing	Material properties can change and become unpredictable	Moderate to high	Careful process parameter selection, as well as full description of risk to reader of described results.
7. The expected shrinkage of the material on cooling is no more than that reported by the filament manufacturer	Less control over element geometry and repeatability and lower effective bulk density	Low	The manufacturer-given value is likely conservative, so no mitigation taken in this work.
8. There is no statistically significant variability in layer height unless specifically designed into the final g-code	Decreased control of structure and increased likelihood of cracks forming between layers	Low	Careful machine tuning, with regular lubrication and bearing and belt inspections.
9. The minimum print stable print length on any existing material is the same as estimated for a single element in Section 3.4.2.3	Less control over material structure and increased chance of unplanned voids and cracks	Very low	None
10. Bridge and overhang distances are similar for both individual elements and whole layers	Failed bridges and overhangs	Low	None

Continued on next page

Table 3.6 – *Continued from previous page*

Assumption	Risk if Wrong	Likelihood	Mitigation
11. For fracture testing samples, no significant stress concentrations exist except those specifically designed into the structure to produce a controlled fracture	Unpredictable and unstable testing results	Very low	All parts and specimens inspected for obvious defects before being tested
12. Expected dimensional error (in terms of %) the same for all parts, scales, and areas of print	Reduced control of element geometry and placement	Moderate	Print with internal overlap of 2%, carefully maintain hardware, and reduce print speed and jerk when possible.
13. Roof and floor thickness should be at least three layers	Wasted material and print time	Low to moderate	None
14. Minimum length scale (for part or feature) is 2.5 times nozzle diameter (except self-supporting thin walled structures) to allow for two shells and some infill	Slightly reduced design freedom, wasted material, and longer printing time	Low to moderate	None

3.5 Case Studies

In addition to Case Study 2 and Case Study 3 in Chapter 2, where FDM manufacturability constraints are used to ensure that the final design can be fabricated, three more case studies are presented here to demonstrate the constraints and how they can be used explicitly.

3.5.1 Case 1: 2.5D Designs with Stable Features

The first case study explores three simple problems (Figure 3.19) that could be represented as 2-D or 2.5-D (2-D + thickness) design representations subject to the constraints developed in this chapter. In the first case, (Designs 1a and 1b), a simple fan cover was designed with manually laid out features. For Design 1a, a deposition nozzle of $w = 0.4$ mm was used with a layer thickness of $h = 0.2$ mm ($h/w = 0.5$), with each of the thicker features being two elements wide for stability and one element wide for the smaller features. For design 1b, a nozzle of $w = 1.0$ mm ($h/w = 0.2$) was used, with resulting changes in the design.

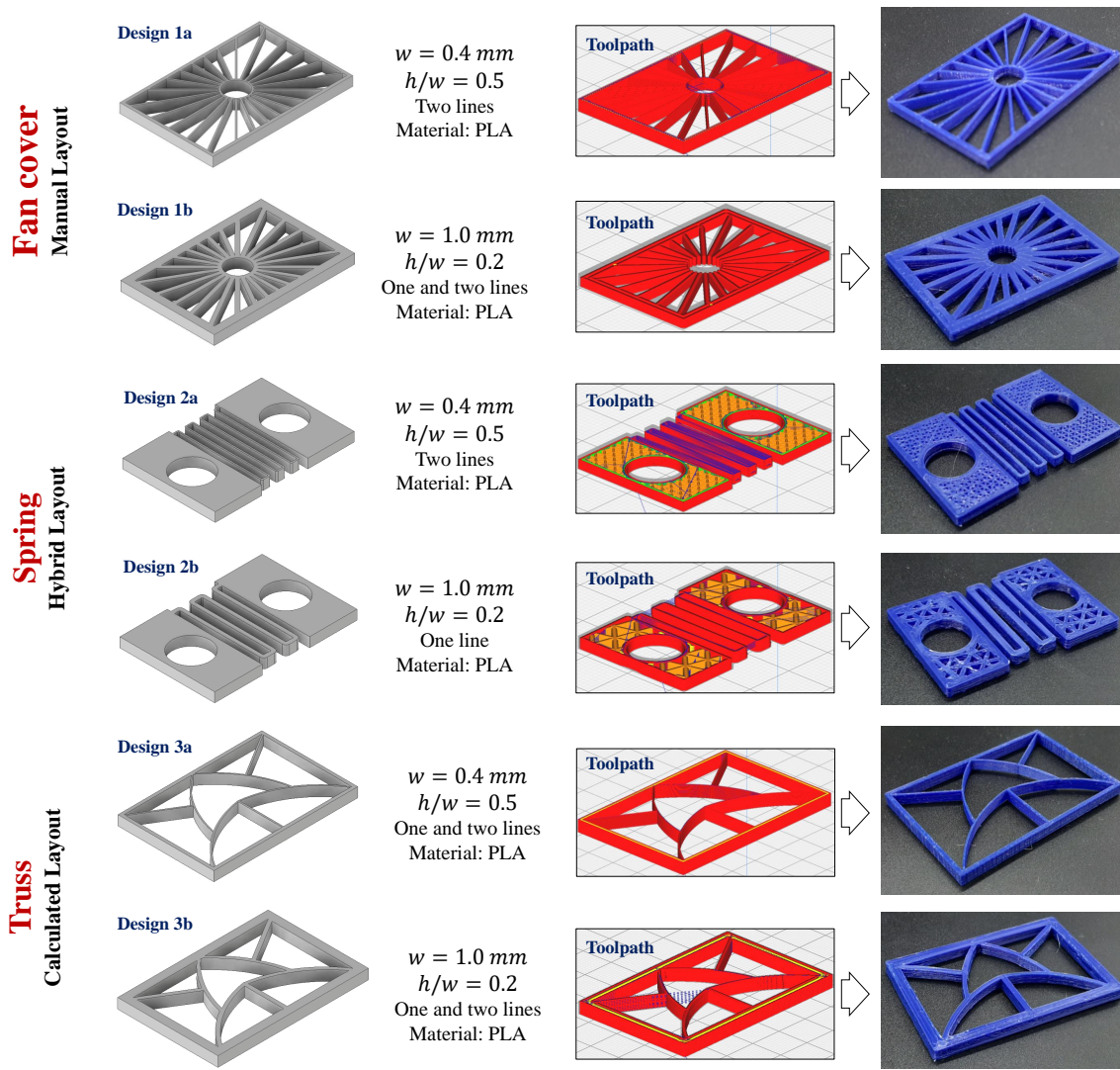


Figure 3.19: Results of Case Study 1.

In the case of Design 2, a hybrid design method was used, with the spring coil being manually laid out and the infill for the solid area being calculated and laid out in a series of triangles. The last problem dealt with a truss, where the layout could be calculated in response to a specific mechanical problem. This case study demonstrated that the imposition of effective constraints on the parameters heavily influenced the designs. In addition, it showed that all of the constrained designs, regardless of complexity, were manufacturable on the first attempt.

3.5.2 Case 2: Designed Infill Geometry in Defined Space

In this case study, the computational layout of a 20-mm cubic shell with a low-density designed core was generated using Ultimaker[®] Cura[®] from PLA. All of the FDM constraints generated in this chapter were applied to ensure manufacturability, even on areas with bridges and very thin features. In addition to the objectives (lay out the elements efficiently based on inputs) and constraints, the major design inputs to the software tool were:

1. The geometry within the shell was only allowed to be a single element thick, so the designed core only presented one level of designable mesostructure.
2. The deposition nozzle used was 0.5 mm in diameter and the deposition width was defined as 0.505 mm to account for material shrinkage. This setting was found to be the best for the transparent PLA used in the study after several trials.
3. The w/h ratio was selected to be 5/2. An overlap setting was not needed, since the designed area was only allowed to be one element thick.

Four basic layouts were selected, specifically 3D cross, quarter cubic, gyroid, and standard raster lines. Figure 3.20 shows the layouts for Layer 10, Layer 25, Layer 50, and Layer 90 for each of the cases. Only the gyroid contained an unsupported bridge, so a maximum unsupported bridge length was set at 3 mm (see Section 3.4.2.4) before the design generation. Since it was impractical to use support material for these designs, this was used to limit the size of the gyroid elements. The layouts were driven by the requirement that the 3-D cross and quarter cubic cases were to occupy a total of 10% of the open space, the gyroid was to be close to 15% dense with the bridge requirement (so the density is slightly higher), and the elements in raster case were to have a diagonal (corner-to-corner) length of approximately 4 mm. Note that all of the cases could easily have been printed without the outer shell (or had the shell removed after printing). Including the shell was a design choice, as the concept could be explored with or without the shell.

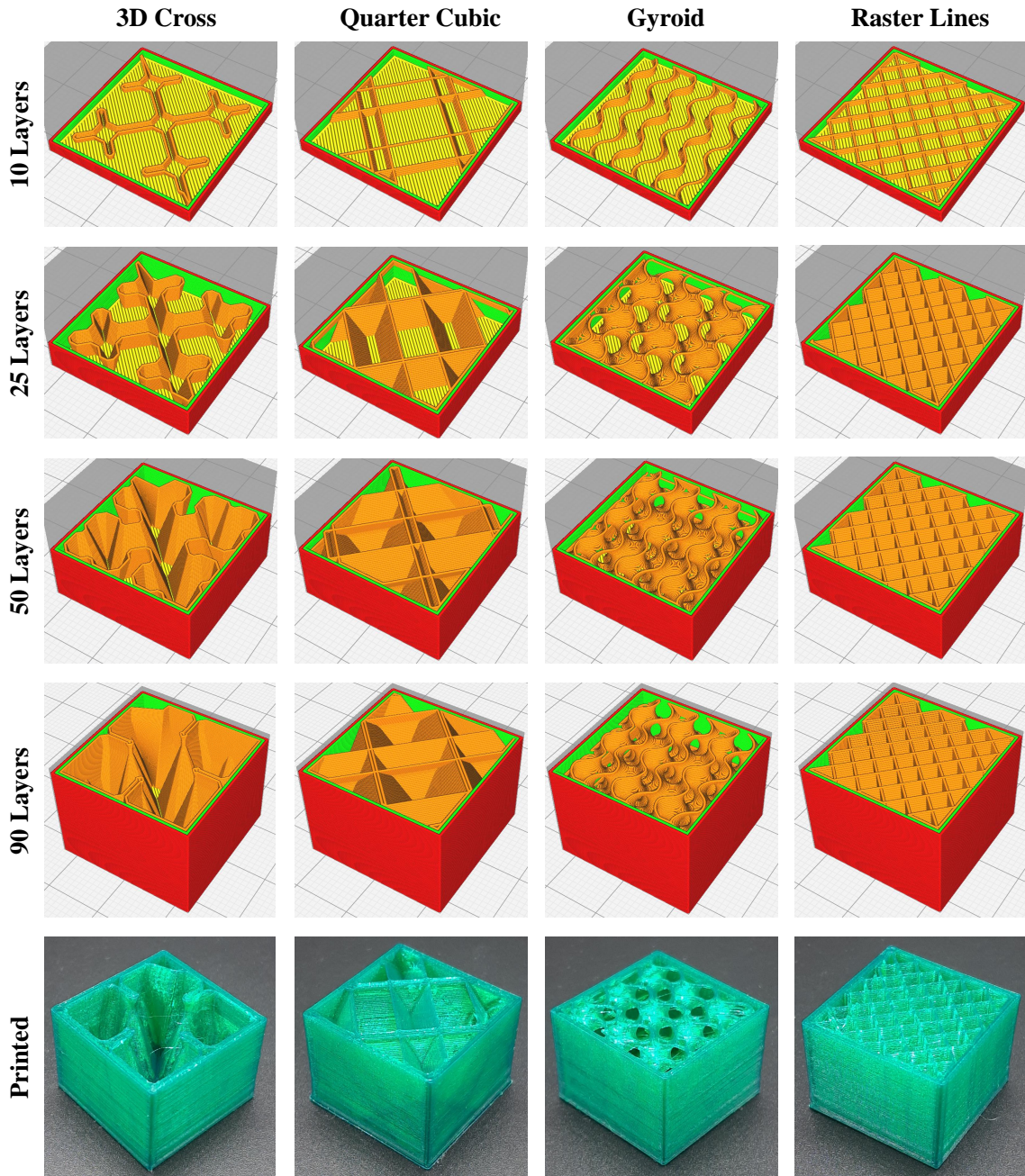


Figure 3.20: Results of Case Study 2.

This case study did not solve a specific design problem and was focused on demonstrating that the designed structures (with several different layouts, including those that varied significantly between layers) could be accurately manufactured since the design parameters were based on the mechanics of the selected process. As shown in Figure 3.20,

the manufacturing was successful, with no significant manufacturing defects noted upon examination under a microscope.

3.5.3 Case 3: Minimal Surfaces with Second Mesostructure

In this case study, the design of two mesostructure levels is explored for two basic minimal surfaces (gyroid - a triply-periodic surface and a Scherk tower - a singly-periodic structure) which are given a wall thickness. The internal structure (the lower mesostructure level) for each case is designed the same way as described in Case Study 2.

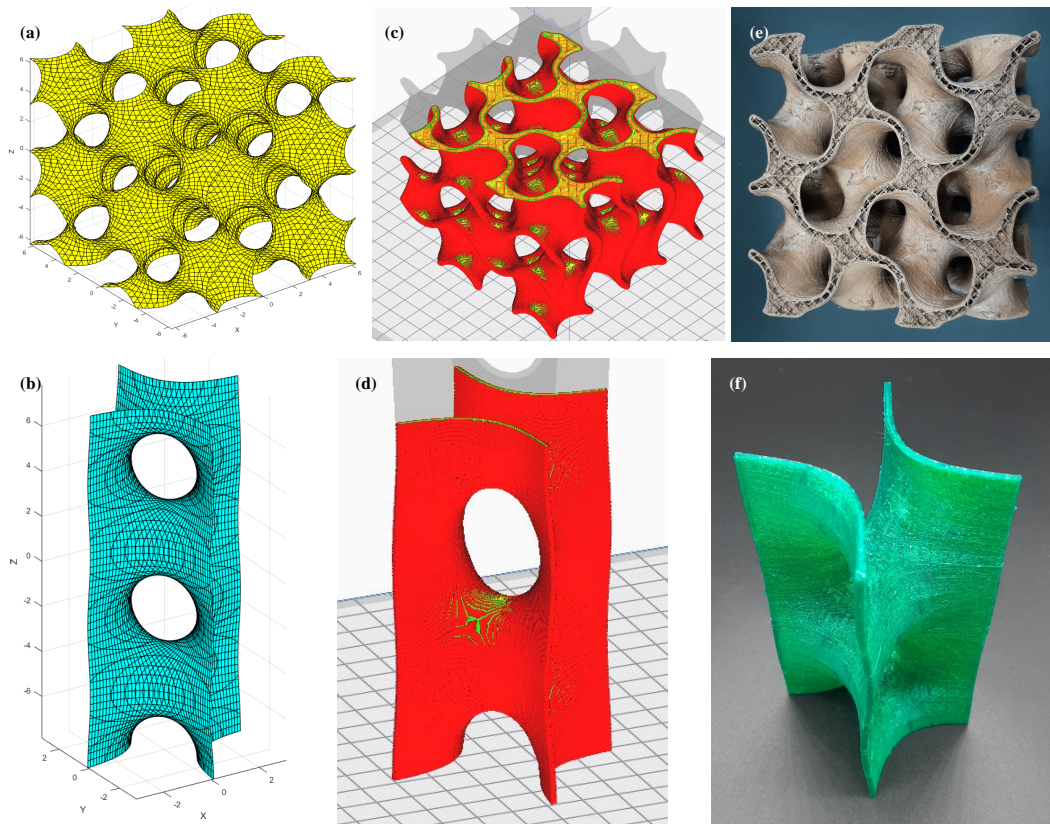


Figure 3.21: Results of Case Study 3.

In these cases, the gyroid (defined within a 125-mm cubic design space) is given a wall thickness of 5 mm, while the Scherk surface is given a wall thickness of 2 mm and calculated within a design space with a 50-mm square base and 160-mm height (Figure 3.21). The basic surface figures, generating functions, and MATLAB[®] code for generating the surfaces came

from a technical report on generating minimal surface models by Muna & Patterson [116]. There are numerous ways to translate the surface model into a solid STL file, the best of which is to use the SURF2SOLID tool in MATLAB[®] with the surface generation code published in Ref [116]. The functions used to generate the minimal surfaces were:

$$f_{gyroid} = \sin(x) \cos(y) + \sin(y) \cos(z) + \sin(z) \cos(x) \quad [x, y, z \in [0, 125] \text{ mm}] \quad (3.1)$$

$$f_{scherk} = \sinh(x) \sinh(y) - \sinh(z) \quad [x, y \in [0, 50] \text{ mm}, z \in [0, 160] \text{ mm}] \quad (3.2)$$

Example surfaces are shown in Figures 3.21a-b, while the g-code for the generated surfaces for this case study can be seen in Figures 3.21c-d. Partial prints (to show the internal mesostructure) of each can be seen the last two panels of the figure. Both were printed from PLA using FDM and used the same settings as Case Study 1, with the exceptions that the Scherk surface was printed at nearly 100% density (so only natural voids determined meso-scale properties). In this case, the internal mesostructure was a series of concentric rings. The internal mesostructure for the gyroid (clearly seen in Figure 3.21e), was identical to that of the raster case in Case Study 2, with the exception that the diagonal dimension of the resulting squares was 5 mm.

3.6 Closing Remarks

In this chapter, the mechanics and manufacturability constraints for FDM were explored and established in clear terms. This chapter will provide perspective, assumptions, and the constraint set for future chapters in this dissertation. These constraints and the mechanical knowledge here will be essential for the effective derivation of design rules related to manufacturing process-driven structured material (MPDSM) design, the beginning of which will be explored in the next chapter.

Copyright Acknowledgement: As of April 10, 2021, most of the work presented in this chapter has been published (or is under review) in the following papers and is reproduced here with permission of the copyright holder (if applicable) - see any needed official copyright permission forms attached in the supplemental materials.

Patterson, A.E., Chadha, C., Jasiuk, I.M. (2021). Identification and mapping of manufacturability constraints for extrusion-based additive manufacturing. *Journal of Manufacturing and Materials Processing*, 5(2): 33.

This paper was published open-access under a CC-BY license with the author retaining the copyright and full distribution rights for the work presented in this chapter. The CAD model reproduced in Figure 3.5a is owned by Twelvepro.com and reproduced with permission.

Chapter 3 Bibliography

- [1] O. A. Mohamed, S. H. Masood, and J. L. Bhowmik, “Experimental investigations of process parameters influence on rheological behavior and dynamic mechanical properties of FDM manufactured parts,” *Materials and Manufacturing Processes*, vol. 31, pp. 1983–1994, Dec. 2015.
- [2] O. A. Mohamed, S. H. Masood, and J. L. Bhowmik, “Optimization of fused deposition modeling process parameters for dimensional accuracy using i-optimality criterion,” *Measurement*, vol. 81, pp. 174–196, Mar. 2016.
- [3] B. N. Turner and S. A. Gold, “A review of melt extrusion additive manufacturing processes: II. materials, dimensional accuracy, and surface roughness,” *Rapid Prototyping Journal*, vol. 21, pp. 250–261, Apr. 2015.
- [4] B. N. Turner, R. Strong, and S. A. Gold, “A review of melt extrusion additive manufacturing processes: I. process design and modeling,” *Rapid Prototyping Journal*, vol. 20, pp. 192–204, Apr. 2014.
- [5] S. Messimer, T. Pereira, A. Patterson, M. Lubna, and F. Drozda, “Full-density fused deposition modeling dimensional error as a function of raster angle and build orientation: Large dataset for eleven materials,” *Journal of Manufacturing and Materials Processing*, vol. 3, no. 1, p. 6, 2019.
- [6] S. Hongyao, Y. Xiaoxiang, and F. Jianzhong, “Research on the flexible support platform for fused deposition modeling,” *The International Journal of Advanced Manufacturing Technology*, vol. 97, pp. 3205–3221, May 2018.
- [7] C. Kim, D. Espalin, A. Cuaron, M. A. Perez, E. MacDonald, and R. B. Wicker, “A study to detect a material deposition status in fused deposition modeling technology,” in *2015 IEEE International Conference on Advanced Intelligent Mechatronics (AIM)*, IEEE, July 2015.
- [8] Y. Wang, J. Huang, Y. Wang, S. Feng, T. Peng, H. Yang, and J. Zou, “A CNN-based adaptive surface monitoring system for fused deposition modeling,” *IEEE/ASME Transactions on Mechatronics*, vol. 25, pp. 2287–2296, Oct. 2020.

- [9] C. Abeykoon, P. Sri-Amphorn, and A. Fernando, “Optimization of fused deposition modeling parameters for improved PLA and ABS 3d printed structures,” *International Journal of Lightweight Materials and Manufacture*, vol. 3, pp. 284–297, Sept. 2020.
- [10] A. Ahmed and L. Susmel, “Additively manufactured PLA under static loading: strength/cracking behaviour vs. deposition angle,” *Procedia Structural Integrity*, vol. 3, pp. 498–507, 2017.
- [11] A. Alafaghani, A. Qattawi, B. Alrawi, and A. Guzman, “Experimental optimization of fused deposition modelling processing parameters: A design-for-manufacturing approach,” *Procedia Manufacturing*, vol. 10, pp. 791–803, 2017.
- [12] A. Alafaghani and A. Qattawi, “Investigating the effect of fused deposition modeling processing parameters using taguchi design of experiment method,” *Journal of Manufacturing Processes*, vol. 36, pp. 164–174, Dec. 2018.
- [13] K. Álvarez, R. F. Lagos, and M. Aizpun, “Investigating the influence of infill percentage on the mechanical properties of fused deposition modelled ABS parts,” *Ingeniería e Investigación*, vol. 36, p. 110, Dec. 2016.
- [14] O. Carneiro, A. Silva, and R. Gomes, “Fused deposition modeling with polypropylene,” *Materials & Design*, vol. 83, pp. 768–776, Oct. 2015.
- [15] S. N. Cerda-Avila, H. I. Medellín-Castillo, and D. F. de Lange, “Analysis and numerical simulation of the structural performance of fused deposition modeling samples with variable infill values,” *Journal of Engineering Materials and Technology*, vol. 141, Dec. 2018.
- [16] H. K. Dave, N. H. Patadiya, A. R. Prajapati, and S. R. Rajpurohit, “Effect of infill pattern and infill density at varying part orientation on tensile properties of fused deposition modeling-printed poly-lactic acid part,” *Proceedings of the Institution of Mechanical Engineers, Part C: Journal of Mechanical Engineering Science*, p. 095440621985638, June 2019.
- [17] A. Dey, D. Hoffman, and N. Yodo, “Optimizing multiple process parameters in fused deposition modeling with particle swarm optimization,” *International Journal on Interactive Design and Manufacturing (IJIDeM)*, vol. 14, pp. 393–405, Oct. 2019.
- [18] L. F. C. S. Durão, R. Barkoczy, E. Zancul, L. L. Ho, and R. Bonnard, “Optimizing additive manufacturing parameters for the fused deposition modeling technology using a design of experiments,” *Progress in Additive Manufacturing*, vol. 4, pp. 291–313, Feb. 2019.
- [19] A. Gebisa and H. Lemu, “Investigating effects of fused-deposition modeling (FDM) processing parameters on flexural properties of ULTEM 9085 using designed experiment,” *Materials*, vol. 11, p. 500, Mar. 2018.

- [20] M. S. Hossain, D. Espalin, J. Ramos, M. Perez, and R. Wicker, “Improved mechanical properties of fused deposition modeling-manufactured parts through build parameter modifications,” *Journal of Manufacturing Science and Engineering*, vol. 136, Oct. 2014.
- [21] B. Huang, S. Meng, H. He, Y. Jia, Y. Xu, and H. Huang, “Study of processing parameters in fused deposition modeling based on mechanical properties of acrylonitrile-butadiene-styrene filament,” *Polymer Engineering & Science*, vol. 59, pp. 120–128, Apr. 2018.
- [22] U. Khaleeq uz Zaman, E. Boesch, A. Siadat, M. Rivette, and A. A. Baqai, “Impact of fused deposition modeling (FDM) process parameters on strength of built parts using taguchi’s design of experiments,” *The International Journal of Advanced Manufacturing Technology*, vol. 101, pp. 1215–1226, Nov. 2018.
- [23] A. Khatri and A. Adnan, “Effect of raster orientation on fracture toughness properties of 3D printed ABS materials and structures,” in *Volume 9: Mechanics of Solids, Structures and Fluids; NDE, Diagnosis, and Prognosis*, American Society of Mechanical Engineers, Nov. 2016.
- [24] P. Lanzillotti, J. Gardan, A. Makke, and N. Recho, “Strengthening in fracture toughness of a smart material manufactured by 3D printing,” *IFAC-PapersOnLine*, vol. 51, no. 11, pp. 1353–1358, 2018.
- [25] J. Lyu and S. Manoochchri, “Modeling machine motion and process parameter errors for improving dimensional accuracy of fused deposition modeling machines,” *Journal of Manufacturing Science and Engineering*, vol. 140, Oct. 2018.
- [26] T. D. McLouth, J. V. Severino, P. M. Adams, D. N. Patel, and R. J. Zaldivar, “The impact of print orientation and raster pattern on fracture toughness in additively manufactured ABS,” *Additive Manufacturing*, vol. 18, pp. 103–109, Dec. 2017.
- [27] F. Ning, W. Cong, Y. Hu, and H. Wang, “Additive manufacturing of carbon fiber-reinforced plastic composites using fused deposition modeling: Effects of process parameters on tensile properties,” *Journal of Composite Materials*, vol. 51, pp. 451–462, July 2016.
- [28] S. K. Padhi, R. K. Sahu, S. S. Mahapatra, H. C. Das, A. K. Sood, B. Patro, and A. K. Mondal, “Optimization of fused deposition modeling process parameters using a fuzzy inference system coupled with taguchi philosophy,” *Advances in Manufacturing*, vol. 5, pp. 231–242, Aug. 2017.
- [29] A. E. Patterson, T. R. Pereira, J. T. Allison, and S. L. Messimer, “IZOD impact properties of full-density fused deposition modeling polymer materials with respect to raster angle and print orientation,” *Proceedings of the Institution of Mechanical Engineers, Part C: Journal of Mechanical Engineering Science*, p. 095440621984038, Apr. 2019.
- [30] A. Peng, X. Xiao, and R. Yue, “Process parameter optimization for fused deposition modeling using response surface methodology combined with fuzzy inference system,” *The International*

- Journal of Advanced Manufacturing Technology*, vol. 73, pp. 87–100, Apr. 2014.
- [31] M. Pérez, G. Medina-Sánchez, A. García-Collado, M. Gupta, and D. Carou, “Surface quality enhancement of fused deposition modeling (FDM) printed samples based on the selection of critical printing parameters,” *Materials*, vol. 11, p. 1382, Aug. 2018.
- [32] K. M. Rahman, T. Letcher, and R. Reese, “Mechanical properties of additively manufactured PEEK components using fused filament fabrication,” in *Volume 2A: Advanced Manufacturing*, American Society of Mechanical Engineers, Nov. 2015.
- [33] R. V. Rao and D. P. Rai, “Optimization of fused deposition modeling process using teaching-learning-based optimization algorithm,” *Engineering Science and Technology, an International Journal*, vol. 19, pp. 587–603, Mar. 2016.
- [34] C. M. Vicente, T. S. Martins, M. Leite, A. Ribeiro, and L. Reis, “Influence of fused deposition modeling parameters on the mechanical properties of ABS parts,” *Polymers for Advanced Technologies*, vol. 31, pp. 501–507, Nov. 2019.
- [35] P. Wang, B. Zou, H. Xiao, S. Ding, and C. Huang, “Effects of printing parameters of fused deposition modeling on mechanical properties, surface quality, and microstructure of PEEK,” *Journal of Materials Processing Technology*, vol. 271, pp. 62–74, Sept. 2019.
- [36] J. W. Zhang and A. H. Peng, “Process-parameter optimization for fused deposition modeling based on taguchi method,” *Advanced Materials Research*, vol. 538-541, pp. 444–447, June 2012.
- [37] S.-H. Ahn, M. Montero, D. Odell, S. Roundy, and P. K. Wright, “Anisotropic material properties of fused deposition modeling ABS,” *Rapid Prototyping Journal*, vol. 8, no. 4, pp. 248–257, 2002.
- [38] J. Gardan, A. Makke, and N. Recho, “A method to improve the fracture toughness using 3D printing by extrusion deposition,” *Procedia Structural Integrity*, vol. 2, pp. 144–151, 2016.
- [39] J. Gardan, “Method for characterization and enhancement of 3D printing by binder jetting applied to the textures quality,” *Assembly Automation*, vol. 37, no. 2, pp. 162–169, 2017.
- [40] R. Rezaie, M. Badrossamay, A. Ghaie, and H. Moosavi, “Topology optimization for fused deposition modeling process,” *Procedia CIRP*, vol. 6, pp. 521–526, 2013.
- [41] P. Y. Papalambros and D. J. Wilde, *Principles of Optimal Design: Modeling and Computation (2d Edition)*. Cambridge University Press, 2000.
- [42] N. Andrei, “An unconstrained optimization test function collection,” *Advanced Modeling and Optimization*, vol. 10, pp. 147–161, 2008.
- [43] P. E. Gill and W. Murray, “Quasi-newton methods for unconstrained optimization,” *IMA Journal of Applied Mathematics*, vol. 9, no. 1, pp. 91–108, 1972.

- [44] N. Morris, A. Butscher, and F. Iorio, “A subtractive manufacturing constraint for level set topology optimization,” *Structural and Multidisciplinary Optimization*, vol. 61, pp. 1573–1588, Feb. 2020.
- [45] S. L. Vatanabe, T. N. Lippi, C. R. de Lima, G. H. Paulino, and E. C. Silva, “Topology optimization with manufacturing constraints: A unified projection-based approach,” *Advances in Engineering Software*, vol. 100, pp. 97–112, 2016.
- [46] J. V. Carstensen, “Topology optimization with nozzle size restrictions for material extrusion-type additive manufacturing,” *Structural and Multidisciplinary Optimization*, vol. 62, pp. 2481–2497, June 2020.
- [47] A. Sutradhar, J. Park, P. Haghghi, J. Kresslein, D. Detwiler, and J. J. Shah, “Incorporating manufacturing constraints in topology optimization methods: A survey,” in *Volume 1: 37th Computers and Information in Engineering Conference*, ASME, 2017.
- [48] E. Lutters, F. J. van Houten, A. Bernard, E. Mermoz, and C. S. Schutte, “Tools and techniques for product design,” *CIRP Annals*, vol. 63, no. 2, pp. 607–630, 2014.
- [49] J. G. Bralla, *Design for Manufacturability Handbook (2nd Edition)*. McGraw-Hill Education, 1998.
- [50] W. ElMaraghy, H. ElMaraghy, T. Tomiyama, and L. Monostori, “Complexity in engineering design and manufacturing,” *CIRP Annals*, vol. 61, no. 2, pp. 793–814, 2012.
- [51] B. S. Blanchard and W. J. Fabrycky, *Systems Engineering and Analysis (4th Edition)*. Prentice Hall, 2005.
- [52] A. E. Patterson and J. T. Allison, “Manufacturability constraint formulation for design under hybrid additive-subtractive manufacturing,” in *ASME IDETC: Volume 4: 23rd Design for Manufacturing and the Life Cycle Conference*, ASME, 2018.
- [53] A. E. Patterson and J. T. Allison, “Generation and mapping of minimally-restrictive manufacturability constraints for mechanical design problems,” in *Volume 4: 24th Design for Manufacturing and the Life Cycle Conference; 13th International Conference on Micro- and Nanosystems*, American Society of Mechanical Engineers, Aug. 2019.
- [54] A. E. Patterson, Y. H. Lee, and J. T. Allison, “Overview of the development and enforcement of process-driven manufacturability constraints in product design,” in *Volume 4: 24th Design for Manufacturing and the Life Cycle Conference; 13th International Conference on Micro- and Nanosystems*, American Society of Mechanical Engineers, Aug. 2019.
- [55] Borgue, Müller, Leicht, Panarotto, and Isaksson, “Constraint replacement-based design for additive manufacturing of satellite components: Ensuring design manufacturability through tailored test artefacts,” *Aerospace*, vol. 6, p. 124, Nov. 2019.

- [56] O. Borgue, F. Valjak, M. Panarotto, and O. Isaksson, "Supporting additive manufacturing technology development through constraint modeling in early conceptual design: A satellite propulsion case study," *Proceedings of the Design Society: DESIGN Conference*, vol. 1, pp. 817–826, May 2020.
- [57] J. R. Müller, O. Borgue, M. Panarotto, and O. Isaksson, "Mapping the design space in function and geometry models supporting redesign for additive manufacturing," *J. of Design Research*, vol. 18, no. 1/2, p. 37, 2020.
- [58] J. T. Black and R. A. Kohser, *DeGarmo's Materials and Processes in Manufacturing (11th Edition)*. Wiley, 2011.
- [59] J. Gardan, A. Makke, and N. Recho, "Improving the fracture toughness of 3d printed thermoplastic polymers by fused deposition modeling," *International Journal of Fracture*, vol. 210, no. 1-2, pp. 1–15, 2017.
- [60] A. Cattenone, S. Morganti, G. Alaimo, and F. Auricchio, "Finite element analysis of additive manufacturing based on fused deposition modeling: Distortions prediction and comparison with experimental data," *Journal of Manufacturing Science and Engineering*, vol. 141, Nov. 2018.
- [61] A. Bellini, S. Guçeri, and M. Bertoldi, "Liquefier dynamics in fused deposition," *Journal of Manufacturing Science and Engineering*, vol. 126, pp. 237–246, May 2004.
- [62] N. Shadvar, E. Foroozmehr, M. Badrossamay, I. Amouhadi, and A. S. Dindarloo, "Computational analysis of the extrusion process of fused deposition modeling of acrylonitrile-butadiene-styrene," *International Journal of Material Forming*, Dec. 2019.
- [63] V. Srinivas, C. S. van Hooy-Corstjens, and J. A. Harings, "Correlating molecular and crystallization dynamics to macroscopic fusion and thermodynamic stability in fused deposition modeling: a model study on polylactides," *Polymer*, vol. 142, pp. 348–355, Apr. 2018.
- [64] T. J. Coogan and D. O. Kazmer, "In-line rheological monitoring of fused deposition modeling," *Journal of Rheology*, vol. 63, pp. 141–155, Jan. 2019.
- [65] J. Zhang, X. Z. Wang, W. W. Yu, and Y. H. Deng, "Numerical investigation of the influence of process conditions on the temperature variation in fused deposition modeling," *Materials & Design*, vol. 130, pp. 59–68, Sept. 2017.
- [66] Y. Zhou, T. Nyberg, G. Xiong, and D. Liu, "Temperature analysis in the fused deposition modeling process," in *2016 3rd International Conference on Information Science and Control Engineering (ICISCE)*, IEEE, July 2016.
- [67] Y. Zhang and V. Shapiro, "Linear-time thermal simulation of as-manufactured fused deposition modeling components," *Journal of Manufacturing Science and Engineering*, vol. 140, Apr.

2018.

- [68] C. Bellehumeur, L. Li, Q. Sun, and P. Gu, “Modeling of bond formation between polymer filaments in the fused deposition modeling process,” *Journal of Manufacturing Processes*, vol. 6, pp. 170–178, Jan. 2004.
- [69] S. Costa, F. Duarte, and J. Covas, “Estimation of filament temperature and adhesion development in fused deposition techniques,” *Journal of Materials Processing Technology*, vol. 245, pp. 167–179, July 2017.
- [70] Y. Kim, D. Alcantara, and T. I. Zohdi, “Thermal state estimation of fused deposition modeling in additive manufacturing processes using kalman filters,” *International Journal for Numerical Methods in Engineering*, Aug. 2020.
- [71] S. L. Messimer, A. E. Patterson, N. Muna, A. P. Deshpande, and T. R. Pereira, “Characterization and processing behavior of heated aluminum-polycarbonate composite build plates for the FDM additive manufacturing process,” *Journal of Manufacturing and Materials Processing*, vol. 2, p. 12, Feb. 2018.
- [72] J. F. Rodríguez, J. P. Thomas, and J. E. Renaud, “Mechanical behavior of acrylonitrile butadiene styrene fused deposition materials modeling,” *Rapid Prototyping Journal*, vol. 9, pp. 219–230, Oct. 2003.
- [73] M. Shofner, F. Rodriguez-Macias, R. Vaidyanathan, and E. Barrera, “Single wall nanotube and vapor grown carbon fiber reinforced polymers processed by extrusion freeform fabrication,” *Composites Part A: Applied Science and Manufacturing*, vol. 34, pp. 1207–1217, Dec. 2003.
- [74] G. Alaimo, S. Marconi, L. Costato, and F. Auricchio, “Influence of meso-structure and chemical composition on FDM 3D-printed parts,” *Composites Part B: Engineering*, vol. 113, pp. 371–380, Mar. 2017.
- [75] N. P. Levenhagen and M. D. Dadmun, “Interlayer diffusion of surface segregating additives to improve the isotropy of fused deposition modeling products,” *Polymer*, vol. 152, pp. 35–41, Sept. 2018.
- [76] S. Lin, L. Xia, G. Ma, S. Zhou, and Y. M. Xie, “A maze-like path generation scheme for fused deposition modeling,” *The International Journal of Advanced Manufacturing Technology*, vol. 104, pp. 1509–1519, July 2019.
- [77] A. Bellini and S. Güçeri, “Mechanical characterization of parts fabricated using fused deposition modeling,” *Rapid Prototyping Journal*, vol. 9, pp. 252–264, Oct. 2003.
- [78] E. G. Gordeev, A. S. Galushko, and V. P. Ananikov, “Improvement of quality of 3d printed objects by elimination of microscopic structural defects in fused deposition modeling,” *PLOS ONE*, vol. 13, p. e0198370, June 2018.

- [79] H. H. Nadiyapara and S. Pande, "A review of variable slicing in fused deposition modeling," *Journal of The Institution of Engineers (India): Series C*, vol. 98, pp. 387–393, June 2016.
- [80] E. C. Balta, D. M. Tilbury, and K. Barton, "Control-oriented modeling and layer-to-layer stability for fused deposition modeling: A kernel basis approach," in *2019 American Control Conference (ACC)*, IEEE, July 2019.
- [81] D. Aksoy, E. C. Balta, D. M. Tilbury, and K. Barton, "A control-oriented model for bead cross-sectional geometry in fused deposition modeling," in *2020 American Control Conference (ACC)*, IEEE, July 2020.
- [82] R. Prabhu and A. Devaraju, "Recent review of tribology, rheology of biodegradable and FDM compatible polymers," *Materials Today: Proceedings*, Oct. 2020.
- [83] P. Pradel, Z. Zhu, R. Bibb, and J. Moultrie, "A framework for mapping design for additive manufacturing knowledge for industrial and product design," *Journal of Engineering Design*, vol. 29, no. 6, pp. 291–326, 2018.
- [84] G. A. Adam and D. Zimmer, "Design for additive manufacturing - element transitions and aggregated structures," *CIRP Journal of Manufacturing Science and Technology*, vol. 7, no. 1, pp. 20–28, 2014.
- [85] G. A. O. Adam and D. Zimmer, "On design for additive manufacturing: evaluating geometrical limitations," *Rapid Prototyping Journal*, vol. 21, no. 6, pp. 662–670, 2015.
- [86] S. B. Maidin, I. Campbell, and E. Pei, "Development of a design feature database to support design for additive manufacturing," *Assembly Automation*, vol. 32, no. 3, pp. 235–244, 2012.
- [87] M. K. Thompson, G. Moroni, T. Vaneker, G. Fadel, R. I. Campbell, I. Gibson, A. Bernard, J. Schulz, P. Graf, B. Ahuja, and F. Martina, "Design for additive manufacturing: Trends, opportunities, considerations, and constraints," *CIRP Annals*, vol. 65, no. 2, pp. 737–760, 2016.
- [88] S. Liu, Q. Li, W. Chen, L. Tong, and G. Cheng, "An identification method for enclosed voids restriction in manufacturability design for additive manufacturing structures," *Frontiers of Mechanical Engineering*, vol. 10, no. 2, pp. 126–137, 2015.
- [89] B. Wittbrodt and J. M. Pearce, "The effects of PLA color on material properties of 3-d printed components," *Additive Manufacturing*, vol. 8, pp. 110–116, Oct. 2015.
- [90] F. Arbeiter, M. Spoerk, J. Wiener, A. Gosch, and G. Pinter, "Fracture mechanical characterization and lifetime estimation of near-homogeneous components produced by fused filament fabrication," *Polymer Testing*, vol. 66, pp. 105–113, Apr. 2018.

- [91] J. Allum, A. Gleadall, and V. V. Silberschmidt, “Fracture of 3D-printed polymers: Crucial role of filament-scale geometric features,” *Engineering Fracture Mechanics*, vol. 224, p. 106818, Feb. 2020.
- [92] G. Cicala, D. Giordano, C. Tosto, G. Filippone, A. Recca, and I. Blanco, “Polylactide (PLA) filaments a biobased solution for additive manufacturing: Correlating rheology and thermo-mechanical properties with printing quality,” *Materials*, vol. 11, p. 1191, July 2018.
- [93] H. Jee and P. Witherell, “A method for modularity in design rules for additive manufacturing,” *Rapid Prototyping Journal*, vol. 23, no. 6, pp. 1107–1118, 2017.
- [94] U. Yaman, “Shrinkage compensation of holes via shrinkage of interior structure in FDM process,” *The International Journal of Advanced Manufacturing Technology*, vol. 94, pp. 2187–2197, Sept. 2017.
- [95] A. Manmadhachary, Y. R. Kumar, and L. Krishnanand, “Finding of correction factor and dimensional error in bio-AM model by FDM technique,” *Journal of The Institution of Engineers (India): Series C*, vol. 99, pp. 293–300, June 2016.
- [96] K. Tong, S. Joshi, and E. A. Lehtihet, “Error compensation for fused deposition modeling (FDM) machine by correcting slice files,” *Rapid Prototyping Journal*, vol. 14, pp. 4–14, Jan. 2008.
- [97] H. Rahman, T. John, M. Sivadasan, and N. Singh, “Investigation on the scale factor applicable to ABS based FDM additive manufacturing,” *Materials Today: Proceedings*, vol. 5, no. 1, pp. 1640–1648, 2018.
- [98] J. Liu, Y. Ma, A. J. Qureshi, and R. Ahmad, “Light-weight shape and topology optimization with hybrid deposition path planning for FDM parts,” *The International Journal of Advanced Manufacturing Technology*, vol. 97, pp. 1123–1135, Apr. 2018.
- [99] T. Rocha Pereira, A. E. Patterson, and S. L. Messimer, “Buckling strength of 3-d printed thermoplastic thin shells: Notes on an exploratory study of as-printed and reinforced cases,” *Applied Sciences*, vol. 10, p. 5863, Aug. 2020.
- [100] I. Skawiński and T. Goetzendorf-Grabowski, “FDM 3d printing method utility assessment in small RC aircraft design,” *Aircraft Engineering and Aerospace Technology*, vol. 91, pp. 865–872, June 2019.
- [101] X. Fu, X. Zhang, and Z. Huang, “Axial crushing of nylon and al/nylon hybrid tubes by FDM 3d printing,” *Composite Structures*, vol. 256, p. 113055, Jan. 2021.
- [102] M. Vishwas, C. Basavaraj, and M. Vinyas, “Experimental investigation using taguchi method to optimize process parameters of fused deposition modeling for ABS and nylon materials,” *Materials Today: Proceedings*, vol. 5, no. 2, pp. 7106–7114, 2018.

- [103] C. K. Basavaraj and M. Vishwas, “Studies on effect of fused deposition modelling process parameters on ultimate tensile strength and dimensional accuracy of nylon,” *IOP Conference Series: Materials Science and Engineering*, vol. 149, p. 012035, Sept. 2016.
- [104] S. Guessasma, S. Belhabib, and H. Nouri, “Effect of printing temperature on microstructure, thermal behavior and tensile properties of 3d printed nylon using fused deposition modeling,” *Journal of Applied Polymer Science*, vol. 138, p. 50162, Nov. 2020.
- [105] R. Singh and S. Singh, “Development of nylon based FDM filament for rapid tooling application,” *Journal of The Institution of Engineers (India): Series C*, vol. 95, pp. 103–108, Apr. 2014.
- [106] K. Pal, V. Panwar, S. Friedrich, and M. Gehde, “An investigation on vibration welding of amorphous and semicrystalline polymers,” *Materials and Manufacturing Processes*, vol. 31, pp. 372–378, Mar. 2015.
- [107] M. A. Dundar and G. S. Dhaliwal, “Investigation for impact behavior of acrylonitrile-butadiene-styrene amorphous thermoplastic,” *Polymer Testing*, vol. 89, p. 106624, Sept. 2020.
- [108] K. Neki and P. H. Geil, “Morphology-property studies of amorphous polycarbonate,” *Journal of Macromolecular Science, Part B*, vol. 8, pp. 295–341, Oct. 1973.
- [109] P. Zoller, “A study of the pressure-volume-temperature relationships of four related amorphous polymers: Polycarbonate, polyarylate, phenoxy, and polysulfone,” *Journal of Polymer Science: Polymer Physics Edition*, vol. 20, pp. 1453–1464, Aug. 1982.
- [110] Q. Fang and M. A. Hanna, “Rheological properties of amorphous and semicrystalline polylactic acid polymers,” *Industrial Crops and Products*, vol. 10, pp. 47–53, June 1999.
- [111] E. Piorkowska, Z. Kulinski, A. Galeski, and R. Masirek, “Plasticization of semicrystalline poly(l-lactide) with poly(propylene glycol),” *Polymer*, vol. 47, pp. 7178–7188, Sept. 2006.
- [112] J. Jiang, J. Stringer, and X. Xu, “Support optimization for flat features via path planning in additive manufacturing,” *3D Printing and Additive Manufacturing*, vol. 6, pp. 171–179, June 2019.
- [113] J. Jiang, X. Xu, and J. Stringer, “Optimization of process planning for reducing material waste in extrusion based additive manufacturing,” *Robotics and Computer-Integrated Manufacturing*, vol. 59, pp. 317–325, Oct. 2019.
- [114] J. Jiang, G. Hu, X. Li, X. Xu, P. Zheng, and J. Stringer, “Analysis and prediction of printable bridge length in fused deposition modelling based on back propagation neural network,” *Virtual and Physical Prototyping*, vol. 14, pp. 253–266, Feb. 2019.

- [115] F. Drozda, T. Rocha Pereira, and A. Patterson, “End-user manufacturing with FDM/FFF: Interfaces, tolerances, repeatability, and dimensional accuracy,” in *2020 Institute of Industrial and Systems Engineers (IISE) Annual Conference and Exhibition*, IISE, 2020.
- [116] N. Muna and A. Patterson, “Simple 3-D visualization of some common mathematical minimal surfaces using MATLAB,” tech. rep., IDEALS - University of Illinois at Urbana-Champaign, 2018. Accessed Jan 3, 2020. Available at <http://hdl.handle.net/2142/101899>.

Chapter 4

FDM-DRIVEN STRUCTURED MATERIALS

Collaborator Acknowledgement: The author gratefully acknowledges the contributions, advice, direction, and feedback from the following people on the work presented in this chapter: **Charul Chadha** (help with some initial concept development and early case studies); **Dr. Sreekalyan Patiballa** (extensive discussion on concepts and presentation).

4.1 Introduction

A topic of great interest in recent years is the design and fabrication of structured materials (SMTs), including lattices, functionally graded materials, and metamaterials. These are designed synthetic forms which provide properties, attributes, or behavior distinct from basic materials [1–3]. While the fundamental material properties (from the base material) have some influence on the behavior of the structure, the bulk properties are driven partially or fully by the arrangement of material elements. This effect can range from strong directional anisotropy (e.g., some solid metal parts made using a laser-based additive manufacturing (AM) process) to cases where the dominant material properties come from the structure (in the case of cellular materials and metamaterials). The material structural elements can vary significantly in scale, ranging from atomic-scale lattices to bridge-sized truss structures.

SMTs are typically studied at four different structural scales, namely the sub-microstructure, the microstructure, the mesostructure, and the macrostructure (Figure 4.1) [4–9].

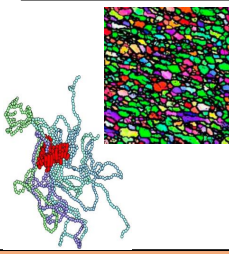
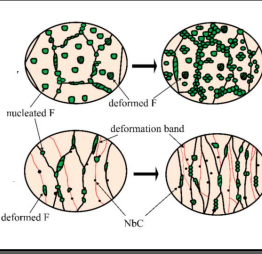
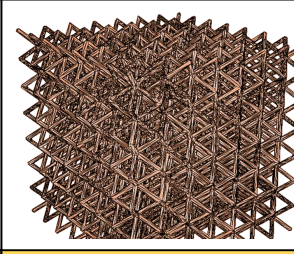

Design perspective on structured material (SM) levels			
Natural material	Source of Dominant Properties		Structure and processing
			
Sub-microstructure	Microstructure	Mesostructure	Macrostructure
<ul style="list-style-type: none"> <input type="checkbox"/> Natural material structure on atomic, crystal, or molecular level <input type="checkbox"/> May be influenced by processing conditions <input type="checkbox"/> Examples: Polymer chains, grain structure details in metals 	<ul style="list-style-type: none"> <input type="checkbox"/> Structure observable using an optical microscope, heavily influential on macro-scale properties <input type="checkbox"/> Strongly influenced by processing conditions <input type="checkbox"/> Examples: Porosity, metal grain layout, scan structure in 3-D printed materials 	<ul style="list-style-type: none"> <input type="checkbox"/> Designed or patterned structure, may be generated by element layout or designed inclusions/defects/voids <input type="checkbox"/> Solid, homogeneous materials do not have a mesostructure <input type="checkbox"/> Examples: Honeycomb structure, metamaterial, unit cell-based lattice 	<ul style="list-style-type: none"> <input type="checkbox"/> In design, typically the “useful level” <input type="checkbox"/> Generally the final component or product that is to be made from the designed material <input type="checkbox"/> For homogeneous solid materials, microstructure drives macrostructure properties (no mesostructure)

Figure 4.1: Basic structured material (SMT) hierarchical levels of organization [10]. Each basic level may have more than one effective level of organization in practice. The source of the dominant material properties depends on the level, ranging from primarily natural properties to mostly structure-based properties.

While the exact nature of each level (as well as the appropriate length scales for each case) will vary, the following definitions generally hold true for all SMTs:

1. *Sub-microstructure*: Atomic, crystal, or molecular level structure, such as polymer chains, crystalline/amorphous polymer configurations, and grain structures in metals
2. *Microstructure*: Structure observed in the material on a microscopic level, such as porosity or grain arrangement, which is driven by the processing conditions of the material
3. *Mesostructure*: In an SMT, the level at which the material is “designed”, such as the case of a unit cell, 3-D printed infill layout, or metamaterial
4. *Macrostructure*: Depending on the problem, the definition may vary but in general it is the “useful” scale and represents a final part or product

The mesostructure is typically the one that is designed to provide the required properties or performance [2, 11]. In some cases, there may be more than four basic levels of organization. Most commonly this takes the form of two or more levels of mesostructure; in these cases, one or more could be held fixed or they could all be designed to provide more control over the structure to the designer. It should also be noted that in this dissertation, the term “structured material” indicates a designed material with a structure composed of only a single base material; it does not include composites or infiltrated materials. One of the main points of value or utility for SMTs (behind the control and design of specific properties as in metamaterial design) is the ability to gain a desired property using a standard or cheap base material. This does not require the design and chemical yield of new materials with uncertain properties and often unknown environmental and safety effects. For structured or architected materials, a standard base can be used to create material elements or units which provide the desired properties within the limits of the base materials.

Classic structured materials were originally developed to deal with electrical, optical, and acoustic problems [1, 12, 13], as the architectures allow waves and energy to be guided through the material. These often consist of repeating simple patterns and minimal surfaces which can be designed intuitively or computationally, depending on the needs of the problem and the preferences of the stakeholders. A more recent, but no less important, area of progress has been the development of SMTs for mechanical applications; these generally fit into two major categories, namely arranged structural materials (e.g., for lightweighting aerospace parts) and mechanical metamaterials [1, 12]. The second provide a wide range of unique properties, including negative Poisson ratio, higher shear modulus, negative thermal expansion, and other behaviors not available from basic materials. These properties can enhance fracture and impact toughness, allow higher energy absorption, and offer other desirable synthetic properties. Structures can include large and small-scale 2-D, 3-D, and 2.5-D cellular materials [14–16] (Figure 4.2a-b), origami structures [17] (Figure 4.2c), bones [18, 19], structurally-graded materials [20, 21], single-material 4-D structures [22, 23], AM-processed materials with patterned voids (Figure 4.2d) [24, 25], solid or semi-solid materials with strong designed anisotropy [26, 27], and classic SMTs such as chiral (Figure 4.2e) and gyroid (Figure 4.2f) structures [1, 28, 29].

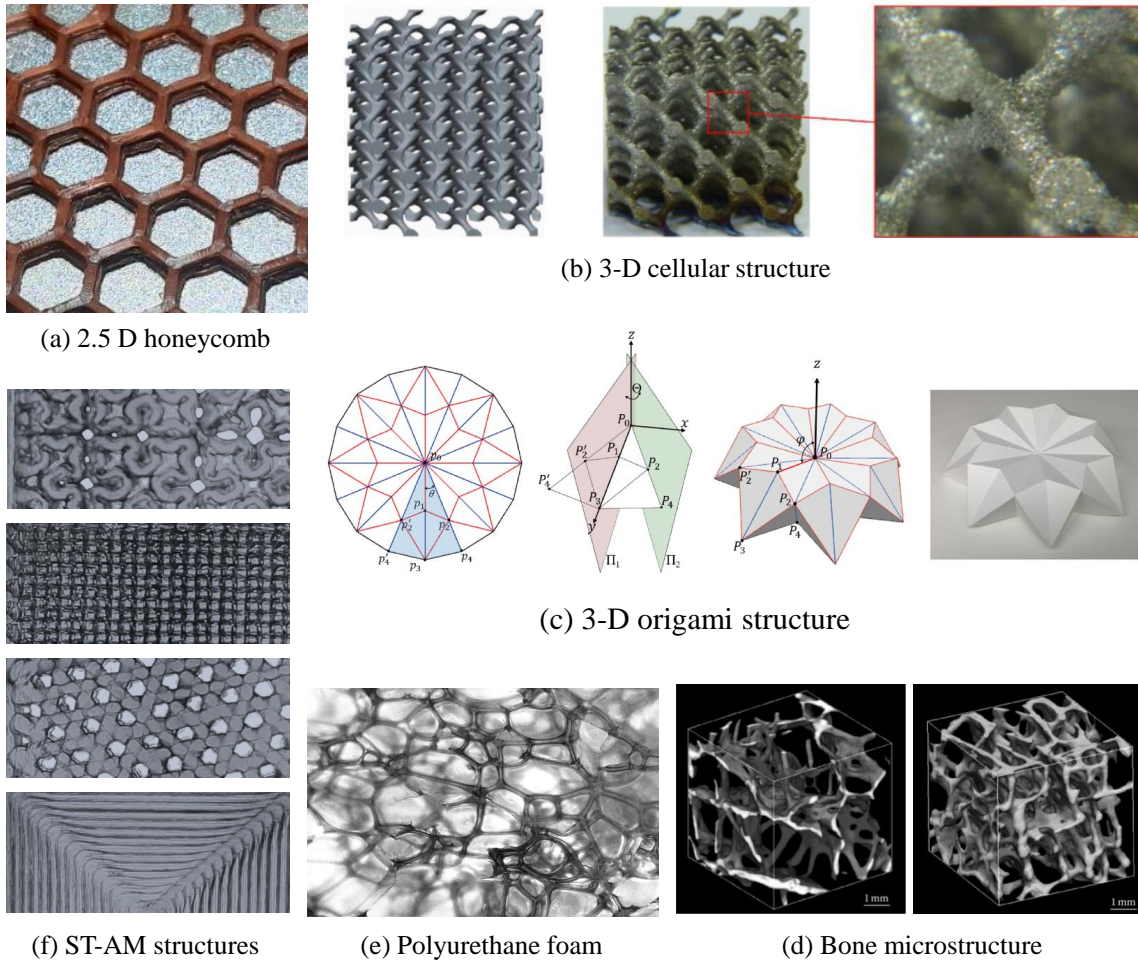


Figure 4.2: Examples of structured materials, including (a) 2.5-D and (b) 3-D [16] cellular materials, (c) origami structures [17], (d) bone microstructure [30], (e) foam structure, and (f) designed material element layouts for ST-AM. All figures original or reproduced under CC-BY 4.0 license.

Design methods used to create the SMTs can vary significantly, depending on the design objectives and requirements. Classic design methods for standard SMTs are beyond the scope of this dissertation, with the exception of the case (manufacturability-driven design (MDD)) where manufacturability is the prime or a co-prime requirement. This is a design perspective that can be used in any area of mechanical design, not just in the area of structured materials. However, prioritizing manufacturability provides two major benefits for the design of structured/architected materials:

1. Final designs are manufacturable with a selected process or set of processes (within the limits of the problem modeling and assumptions)

2. The unique characteristics and material-processing effects of each process can be captured during the design process and lead to new and better approaches for design

For the second point specifically, various AM processes provide great opportunities for exploration in this area. Chapters 2 and 3 addressed this in depth so it will not be repeated here. While MDD provides both more freedom to explore the design space, offers more design methods, and improves the manufacturability of the final designs, there is a definite trade-off. The increased complexity in design can come with a higher design cost (computational, space exploration, etc.); in addition, the exploration of the design space is limited to designs which are manufacturable for a specific process or family of processes (Chapter 2).

This chapter explores the design of structured materials under prime manufacturability requirement for fused deposition modeling (FDM) (examined carefully in Chapter 3). Several steps are required for this exploration, beginning with a discussion and definition of MDD (Section 4.2). A quick summary of the results found in Chapter 3 are then provided in the context of MDD in Section 4.3. Section 4.4 defines a new class of architected materials produced under MDD, known as manufacturing process-driven structured materials (MPDSMs). Some illustrative case studies and closing remarks are given in Sections 4.5 and 4.6, respectively.

4.2 Manufacturability-Driven Design

4.2.1 General Concepts

In order to ensure that the designed structures can be produced properly, it will be necessary to identify and impose manufacturability constraints on the design candidates. Constraint definition and enforcement can be done effectively using a design-for-manufacturability (DFM) [31, 32] approach when the design requirements are clearly established, and the constraints simply restrict the design space to manufacturable options. However, it is also possible for the selected process to drive the design from the conceptualization stage and determine the available design space before requirements (e.g., aesthetics, performance, reliability, and similar) are established. This design space will be a design representation

that may either implicitly or explicitly account for the manufacturing process mechanics. This approach, using manufacturability as the prime or co-prime requirement, can be called *manufacturability-driven design* (MDD). Like most high-level design requirements, MDD provides tools and information for the development of both objective functions and constraint sets. A conceptual comparison of MDD and classic DFM is shown in Figure 4.3.

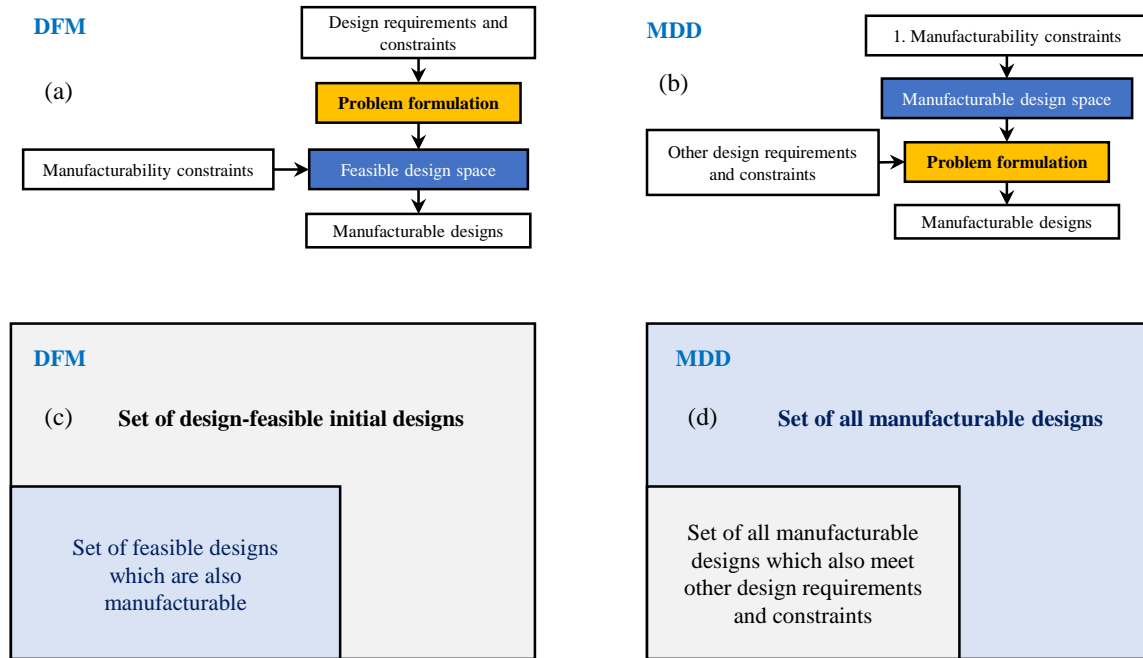


Figure 4.3: Design problem formulation approach for (a) classic DFM and (b) MDD and design space representations for (c) classic DFM and (d) MDD.

It should be noted that the mapping concept (MR-DFM) [7, 33] for problem formulation developed in Chapter 2 is fully compatible with either MDD or classic DFM. MR-DFM would supply the manufacturability constraints used in the problem formulation, regardless of the order and form of the problem statement. The two main benefits of using the MDD approach with mapped manufacturability constraints are:

1. Any generated candidate designs are guaranteed to be manufacturable (subject to any uncertainties in the process modeling and stakeholder inputs). The search for feasible designs will be more targeted and provide less noise for the stakeholders making design decisions. The practical application range for MDD is smaller than general design with manufacturability constraints imposed (since the set of nominally

feasible candidate designs is smaller). However, those designs which are produced can be more confidently used since they are unlikely to be un-manufacturable (within the limits of the process modeling and assumptions mapped to the problem formulation).

2. Any unique process characteristics can potentially be leveraged very early in the design life cycle in order to better drive the design. Using the mapping process developed in Chapter 2 will contribute to this, since the process to be used will be well-understood by the designers prior to making the final design requirements.

4.2.2 MDD Applied to SMTs

Due to the extreme sensitivity of SMTs to geometry and material defects, ensuring that all the potential solutions are manufacturable before design initiation has several essential benefits, namely:

- The unique advantages, limitations, and soft constraints (“best practices”) inherent in each manufacturing process can be used to help determine more realistic design requirements.
- When the manufacturability domain is established first, this can enable design exploration that is both more guided and more unstructured; while the boundaries may be stricter, the designer will be freer to explore the design space within these boundaries. A (non-exhaustive) list of examples of where this has been done successfully for manufacturing problems can be seen in the studies by Vatanabe *et al.* [34] and Li *et al.* [35] (topology optimization), Ferrer *et al.* [36] and Gries [37] (design thinking process), and Iyengar & Bar-Cohen [38] (design quality comparison based on process selection). The results of these studies can be viewed within the contexts of either classic DFM or MDD.
- Based on specific manufacturing processes, new design methods and structures can be explored that may not have been considered before. Since most AM process mechanics are relatively new in the world of engineering design, many opportunities exist in this domain. This is true both for the development of new processes and the more effective use of their unique characteristics.

- When used with ST-AM, the basic elements or units (each of which is manufacturable) can be used as the building blocks for a bottom-up design approach for creating SMTs
- When the AM process used is controlled and well-understood, this enables the possibility of having more than one designable level of structure (i.e., mesostructure) in the material. This can complexify the design process but also greatly expand the design space by adding one more or more additional levels of layout control. This is a form of the classic design trade-off between formulation effort and solution cost, where representation, solution accuracy, computational cost, and other considerations must be balanced for the specific problem at hand.

While this approach has much value for the practical design of new and useful SMTs, it does restrict the conceptual design freedom significantly and so the produced structures are limited to what a pre-specified manufacturing process can fabricate. A class of structured materials, *manufacturing process-driven structured materials* (MPDSMs) can be defined based on this concept. The exact design criteria and constraints will vary based on the process and material selected, but all MPDSMs will have three essential properties or characteristics:

1. MPDSMs are manufacturable regardless of the complexity of the final structure (subject to the quality of the process modeling and assumptions, of course)
2. MPDSM structure is dependent on the "abilities" of the process selected to fabricate it. The structure may have constraints or limitations which are more strict than those imposed by performance requirements since by definition, MPDMS.
3. Like most structured materials, the specialized or custom properties will depend on the structure more than on the base material. Since the structure consists of manufacturable elements, lattices, unit cells, etc., it is feasible to explore using a cheaper or more common material than one that may have otherwise been selected if more uncertainty existed in the true macro-scale properties.

4.3 Mechanics of FDM as Scanning-Type AM Process

The characteristics and mechanics of the FDM process were discussed in depth in Chapter 3. FDM is the most well-known of the scanning-type AM (ST-AM) processes, a family which includes any processes having the following characteristics:

1. For each layer of the part, the cross-section geometry of the layer is traced out using a series of elements, typically with a uniform cross-section and width.
2. The layout of the elements is driven by g-code or some other kind of toolpath
3. Fusion of the new layer with the previously printed material is accomplished using some energy input during the trace of each element, fusing each with the previous layer and any neighboring elements in the current layer.
4. With the exception of traditional laser-based stereolithography and some rare ceramic deposition processes, all of the common ST-AM processes use some kind of re-processable material (typically metals and thermoplastic polymers) which helps support the scanning without destroying the part.
5. Many ST-AM processes have severe local temperature gradients in the structure during processing, which can lead to residual stress formulation [39–46].
6. Most ST-AM-processed parts contain natural meso-scale inclusions and voids left from the processing [39, 47–51]
7. In most cases, the elements deposited by ST-AM processes are homogeneous and approximately isotropic or transversely isotropic, so most of the anisotropy in the macro-scale final part comes from the structure of the elements [11, 52–61]
8. In most cases, the elements and their layout for ST-AM processes are designable, producing 2.5-D of design freedom in an individual layer and 3-D (with some limitations, as discussed in Section 4.2 and Section 4.4) [53, 62–64]

Other common ST-AM processes are the various laser powder bed processes (such as polymer and metal selective laser sintering (SLS), selective laser melting (SLM)), laser-based

stereolithography (SLA), electron beam melting (EBM), direct deposition processes (such as laser engineered net shaping (LENS) and wire/weld-deposition), and useful variations of these processes. ST-AM processes tend to be rather slow in their processing speed, but also tend to provide far better final properties than many non-ST-AM processes (including projection-type (PT-AM) (such as digital light processing (DLP)) and inkjet-type (IT-AM) (such as material jetting (Polyjet) or binder-jetting)). Therefore, most of the processes that have been considered for end-user products have been ST-AM processes.

All AM processes are potentially useful for manufacturing SMTs [3, 14, 15, 22, 26, 28, 65–68], but the scanning nature of ST-AM processes allows selective placement of the fused material beyond the basic design of each layer. Therefore, ST-AM processes can produce multiple levels of mesostructure (such as the example demonstrated in Figure 4) and this can present new design opportunities not available elsewhere. In the case shown, the lattice structure itself (red) is one level of mesostructure that can be designed. When this architecture is manufactured using ST-AM, the elements themselves can be built of patterned element layouts (yellow), providing a second mesostructure that can potentially be designed. In the case where only the first (lattice) structure is of interest to the stakeholders, the potential architecture from the printing can be optimized for things like minimal print time, slight reductions of mass, and similar useful objectives that do not necessarily contribute to the mechanical design of the overall structure.



Figure 4.4: Example of unit cell lattice structure with two levels of designable mesostructure. Level 1 is the arrangement of the unit cells (red) and Level 2 is the shell-infill structure (yellow) within each unit cell element.

4.4 Meso-Scale FDM-Driven MPDSMs

The essential workflow FDM-driven MPDSMs is demonstrated in Figure 4.5. After a process (and equivalent material) is selected, the element cross-section or set of cross-sections will

be designed. A layout strategy will then be selected for laying out the designed elements; this may be automated, manual, or a combination of both. The set of layouts (essentially the set of layers for the part) are then combined to build the final designed part or product.

4.4.1 Basic Concepts

Given a design problem (such as a structural or other mechanical design problem) including objectives and constraints and a selected material, elements can be designed around the mechanics of a specific ST-AM process (FDM in this case, as shown in Figure 4.6a). These elements will be laid out in a series of 2.5D (i.e., 2-D + non-trivial thickness) or 3-D layers (ranging from under 10 μm to more than 1 mm thick, depending on the process and material selected) and the resulting layers fused together to form the final geometry. As shown in Figure 4.5, the general workflow for accomplishing this (regardless of material and process) should have three major steps, the second of which (Figure 4.5b) is mainly concerned with element design. Proper design of the elements is essential, as the process must be able to fabricate them accurately and consistently if they are to be useful for the building of MPDSMs (Figure 4.6). In general, the layout of the elements themselves will be accomplished computationally (driven by manufacturability constraints and selected printing parameters) and does not require direct design by the user; various slicing and path generation software tools (e.g., Cura, Preform, RepliSLS3D) do this easily for various processes. However, it is possible (and often desirable) to manually design the layout. A good example of this is the fracture toughening method developed by Gardan *et al.* [62] where the elements were laid out such that they traced out the calculated stress field around a crack tip and helped arrest the crack growth. The design perspective outlined in Figure 4.5 allows for either manual or automatic layout calculation or a hybrid of both. In general, all of the elements within each layer (and often within the whole part) will have a consistent cross section geometry (Figure 4.6b and 4.6c); however, this is not required if another configuration is needed but it should be noted that the fabrication will be much more complex (and potentially require additional controls or hardware) than if standard ST-AM processes are used.

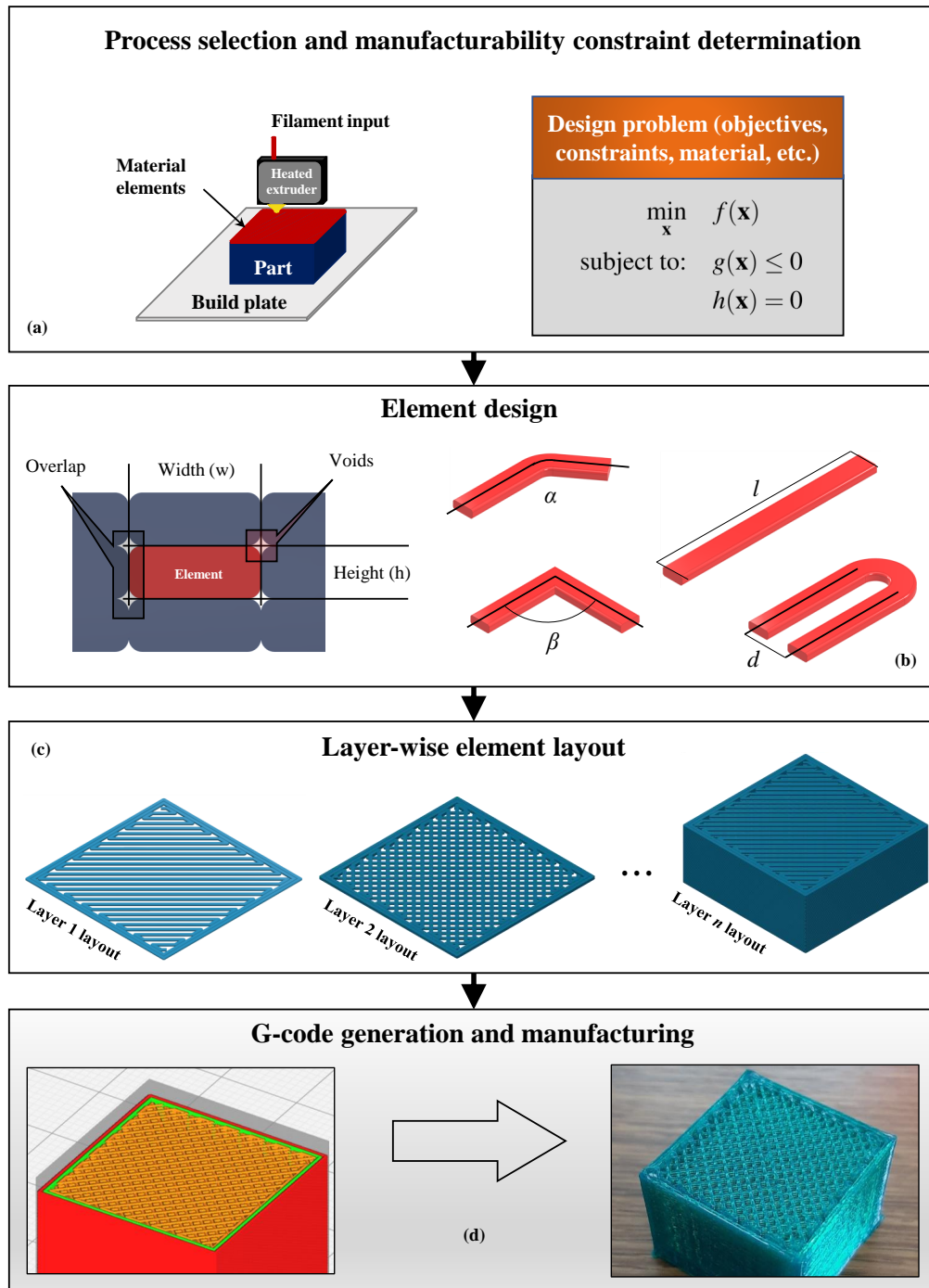


Figure 4.5: Design and fabrication workflow under ST-AM with a designed mesostructure and layered construction. Given a design problem (including a set of objectives and non-manufacturability constraints and a selected material), (a) an ST-AM process is selected (FDM, SLA, and SLS are three common examples but not an exhaustive list) to generate manufacturability constraints. From here, (b) material elements are designed and (c) laid out in a series of layers.

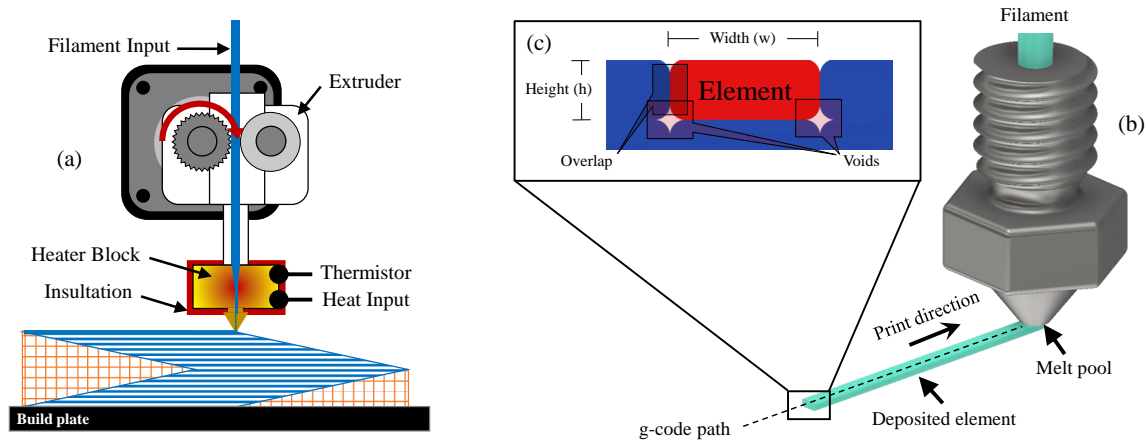


Figure 4.6: Fused deposition modeling/fused filament fabrication (FDM/FFF) process overview. (a) Essential process mechanics, (b) extrusion mechanics to deposit material element, and (c) element cross-section design and parameters

4.4.2 Design of Element Cross Section

For the element cross-section design (Figure 4.6b and 4.6c), the most important parameters are the element width w , the element height h , and the overlap percentage with neighbor elements. All of these are settings that must be selected by the designer and are subjected to the manufacturability constraints of the selected process. For FDM, the width is determined by the extruder diameter and the thermal shrinkage of the material (discussed extensively in Chapter 3), while the height is a free variable that is generally defined as “layer thickness”; however, a w/h ratio of less than $3/2$ tends to produce weak parts due to the large size of the resulting voids and the smaller contact area between elements. This can be addressed by overlapping the elements, but this can waste material, reduce dimensional accuracy (via a rougher surface), and subject the part to unnecessary thermal stress. In general, the higher the w/h ratio, the stronger and denser the final part is but the slower the printing is. For FDM, the element width and w/h ratio are design variables that should be selected as part of the design requirements and used to generate the final layout. The rheology of the polymer used will also determine the ranges of available extruder sizes and this should be considered when selecting a material.

4.4.3 Intralayer Element Layout Design

After the design of the element cross-section, the individual element layout parameters should be selected. This is related only to the design of the elements as they are laid out and is not the design of the final MPDSM. While not an exhaustive list, some of the most useful and common layout parameters for individual elements are:

- The angle of a gradual turn (smooth corner) for which the extrusion or fusion process will not stop during the turn (represented by α in Figure 4.5b). This can be defined as a fixed value, a range with limits (inequality constraint), or a function related to other elements (equality constraint).
- The angle of a sharp corner where the process stopped and was restarted (β in Figure 4.5b). Like α , β can be defined as a fixed value (most commonly 90°), a range with limits (inequality constraint), or a function related to other elements (equality constraint).
- The minimum straight length of an element without any turns or corners, described by l in Figure 4.5b. This setting is directly enforceable in many 3-D printing software tools and can often be defined as either a minimum distance or a minimum printing time. Curves can be defined as a sum of small-length straight elements, where the minimum length is defined by the resolution of the printed file and can be in the path generation software.
- The distance between elements, illustrated by d in Figure 4.5b. This can be defined as either a fixed distance or density of the layer regardless of whether the layer is designed or laid out automatically. For high- or full-density parts or features, the distance may be very small. In cases where two or more levels of mesostructure are present, the elements may be very dense in some areas, with significant distance between sets of elements in others. This is clearly demonstrated in Figure 4.4.
- The option to overlap the ends of elements in corners or against the part shell to better control gaps within the structure. This is generally only needed when the resulting MPDSM needs to be very dense. Once the layout parameters (and other printing

settings) are established, it is a simple matter to automate their enforcement. The last two (minimum printing distance or time and distance between elements) are two fundamental constraints that are set by the user during pre-processing and slicing of the models to be printed. These software settings are usually not focused on creation of a specific material layout and generally focus on minimizing printing time or printer operations; however, they are very useful settings when specific layouts are needed.

4.4.4 Bottom-Up Design of MPDSMs

While the concept of material element layout is well-defined, the literature thus far (outlined in Section 4.1) has focused mostly on the macroscale behavior of the materials or the effects of the architecture on the full part (i.e., top-down perspectives). The workflow introduced in this chapter (Figure 4.5) begins with the basic elements as the “building blocks” (Sections 4.2-4.4) for MPDSMs and uses them to fill the available design space in layers - a *bottom-up* design approach. As previously discussed, these elements may take the form of straight lines, curves, elbows, and other shapes and may be laid out manually, automatically, or a hybrid of the two. This is conceptually similar to other methods which use building-block approaches for design. Some examples of this design technique in the literature exist for common design areas, such as architecture [69], compliant mechanisms [70,71], vehicle design [72], and small customized consumer products [73]. The method presented here is primarily concerned with manufacturability, so the available design complexity is lower than available in some other building-block design studies. Essentially, *the complexity of the MPDSM is dependent on the complexity of the fabrication and assembly of its constituent elements* (Figure 4.7).

In spite of the limited design space, the focus on manufacturability has several significant benefits - both for general design problems and structured materials in particular:

1. The shape, size, and quality of the material elements are determined by the process and material selected. Unlike the study of macro-scale properties of AM materials, the study and characterization of individual material elements is relatively straightforward to accomplish. The elements are approximately isotropic or transversely

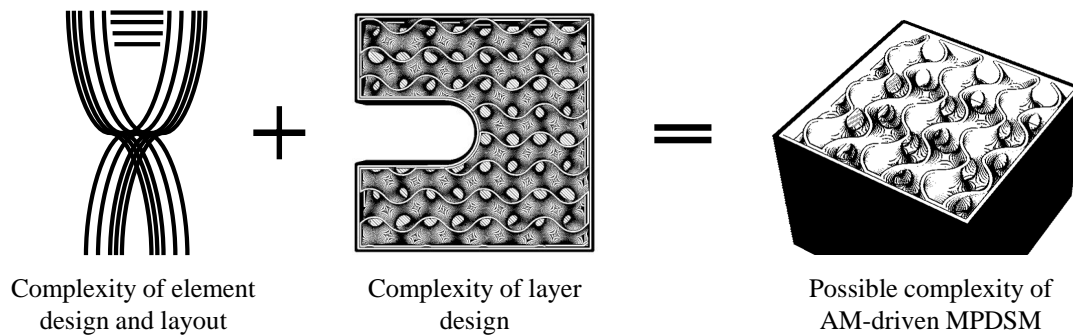


Figure 4.7: The possible design complexity for an AM-driven MPDSM is the sum of the complexity/design freedom of the elements and layers. If each element is manufacturable, it is assumed that each layer will be manufacturable (as long as the elements are non-interfering). If each layer is manufacturable, the final MPDSM is also directly manufacturable.

isotropic on the microstructural level (as previously discussed) and so modeling them can rely more heavily on standard/catalogued properties and not on the direction-specific properties usually attributed to AM-processed materials. Since the elements are generally small compared to the final product, predictable in shape, and ideally do not contain voids (i.e., voids exist between and at the intersection of elements, not in the elements themselves), it is also easier to define their properties and dimensions as probability distributions when needed.

2. The bottom-up approach to designing MPDSMs with well-defined AM-produced elements is similar in approach to designing trusses and other structural systems (where the elements can be understood as structural members in many problem formulations) and so a new design paradigm is not required for most cases.
3. Since the elements are driven by the selected process, they are guaranteed to be manufacturable as long as the constituent elements are manufacturable and non-interfering (subject to modeling and measurement errors and process uncertainties). An ideal objective is that no un-manufacturable design candidates will be produced, so the design team can focus only on the performance metrics of the manufacturable design solutions. In the cases where the problem may be able to be formulated around a convex design space, a global solution can be found which will save time and resources during the life cycle process.

4. When the goal of the design problem is actual manufacturing and not modeling of the SMT behavior, the process-driven nature of the elements under ST-AM allows them to directly be translated into g-code or other build path definitions for building the part. This can dramatically decrease the computational cost involved in realizing the final design and make it extremely simple to translate directly from final design to manufactured product.

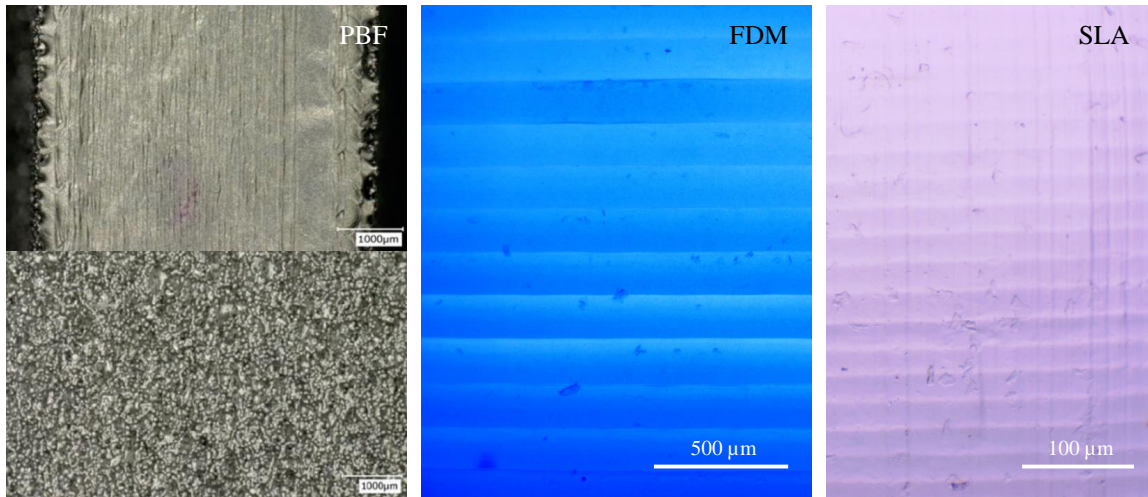


Figure 4.8: Experimentally-found element stacking textures for PBF (specifically electron beam melting (EBM) [74], FDM, and SLA. All views normal to layer stacking direction. PBF panel published under CC-BY-4.0 license. FDM and SLA panels original to the present work.

While the benefits of using MPDSMs based on AM processes are clear, there are some general limitations that must be considered as well:

1. The layout of the elements is limited to a layer-based configuration and true 3-D packing of the individual elements under ST-AM is impossible under most conditions. 3-D structures can be easily built within the MPDSM, but this will consist of several or many individual elements stacked (Figure 4.8 shows examples for a metal powder bed process, FDM, and SLA, three common ST-AM processes) to form it.
2. The layout of the elements in layers requires a length scale limit on design features (generally two shells and intralayer material, in the experience of the authors, for any ST-AM process). This does not necessarily apply if the design level for the problem

is the individual elements stacked in single-wall or thin-wall configurations but would certainly apply in cases where two or more levels of mesostructure exist (as shown in Figure 4.4).

3. The 3-D structure that is produced after the layers are assembled will exhibit an AM-driven surface roughness which may affect the mechanical properties (Figure 4.8). For more solid or large MPDSMs, this effect is likely trivial compared to the effects from the mesostructure(s), but this could have a very large impact on very thin or small features and when using more brittle materials.

4.4.5 MPDSMs and FDM Manufacturability Constraints

A good and clear set of manufacturability constraints is absolutely essential for effective design of the MPDSMs. The full set for FDM were derived and refined in Chapter 3, so they do not need to be reproduced here. A total of 54 constraints were identified, plus any geometry limitations on the final parts or their features.

4.4.6 Final Framework

So far in this article, ST-AM processes have been carefully defined (focusing on FDM), the necessary manufacturability constraints have been derived, and the basic concepts of material element design and layout have been developed. Using these elements, a high-level framework (Figure 8) can be derived which is process- and material-agnostic. Given a proposed design problem, it must first be screened to make sure that the MPDSM approach is best or at least feasible; the main screening criteria are the considerations discussed in Section 4.4.4. If it does not pass the screening, another design method should be used. If all the concerns are satisfied, then the process and material should be selected, and the design problem should be defined relative to them. The next step is to design the elements.

The elements are then laid out using the preferred design method, layer by layer until the full set of layers has been designed. From here, the layers may be converted into g-code and sent to the printer for manufacturing or may be digitally assembled and used for simulations (see Appendix C). In general, the design problem (in the Inputs box) will

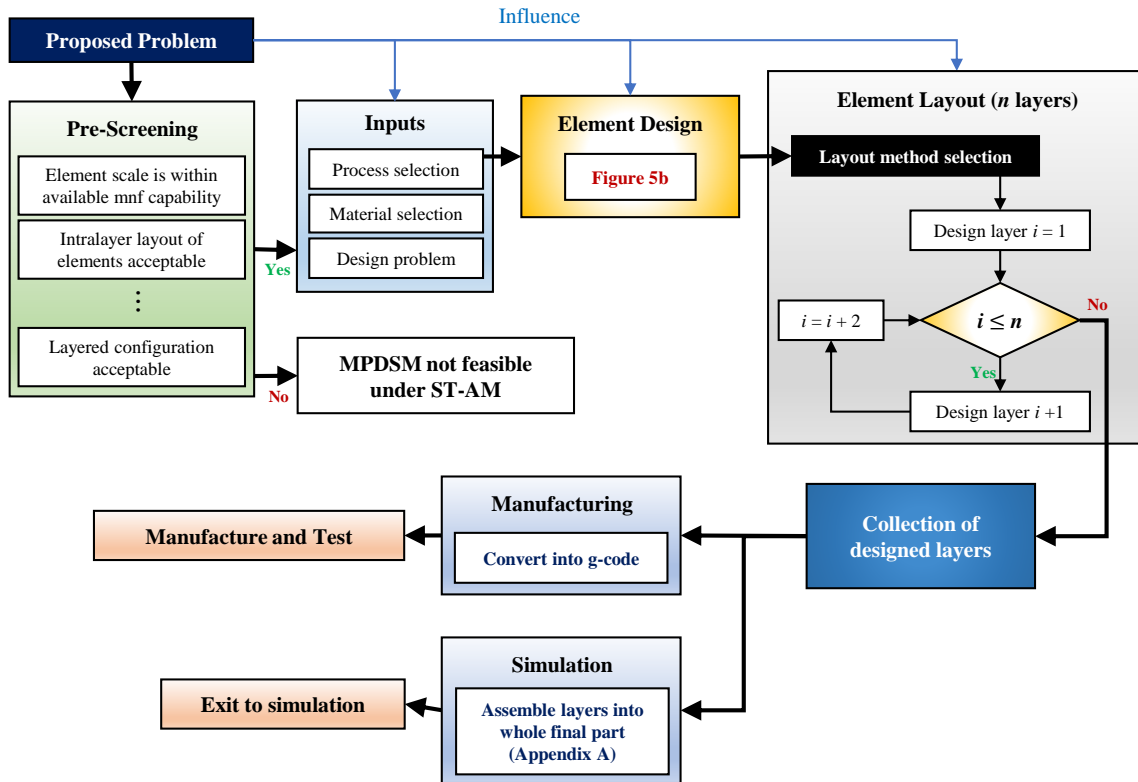


Figure 4.9: General MPDSM design and manufacturing framework (material- and process-agnostic within ST-AM). Choice of manufacturability constraints and layout method will apply this approach to FDM.

consist of a finite element model or other primitive geometry describing the problem that must be designed for (such as a crack arrest or an overhanging beam problem). This model (or at least its stress/strain distributions) must be segmented into “slices” representing each layer to be manufactured. This is not always necessary when the design is consistent throughout the thickness of the final part. This segmentation is relatively easy to do or automate using various mesh tools and slicing software packages. Each of these will be a model which drives the element layouts, considering both the stresses and strains within the slice, and also those from neighboring slices. Therefore, when the part is manufactured and each layer re-assembled, the final product will represent a useful and manufacturable solution to the design problem. The proposed problem should influence, but not directly control, the decisions made in the Inputs, Element Design, and Element Layout steps.

4.4.7 Layout Methods

Numerous layout methods could be applied to the design and fabrication of MPDSMs, using automated or manual approaches or a hybrid of each. As previously discussed, when the elements are not in contact with each other, they behave like beam elements (isotropic, uniform cross-section, designed by length and angle, etc.) and the layers behave like trusses. Treating each layer this way, it is possible to create 3-D FDM-driven MPDSMs easily. When the desired outcome is a fully-dense MPDSM, the design becomes more complex but follows the same principles. While manual layout is certainly feasible (and may even be desirable in some cases), automating the design as much as possible is usually best. Figure 4.10 shows two example layouts, one dense and the other more sparse.

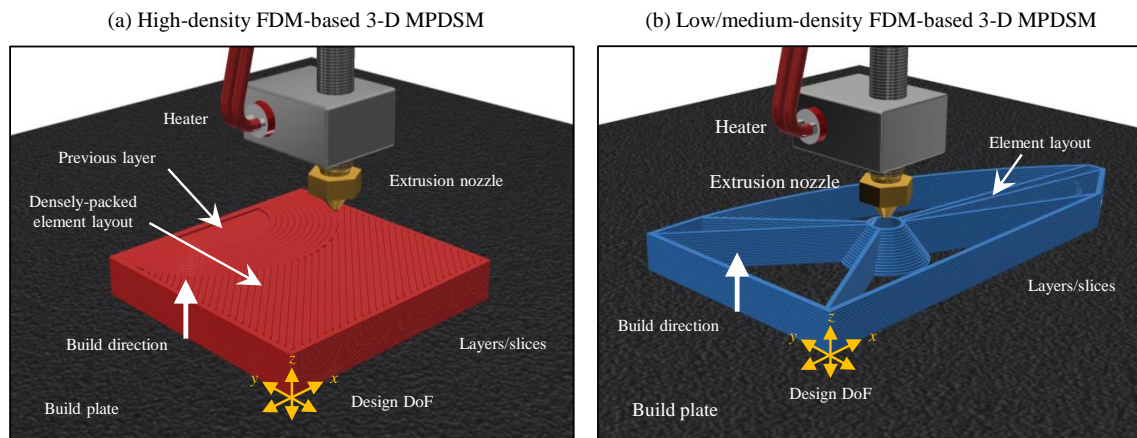


Figure 4.10: (a) Applied to low/medium density MPDSMs and (b) applied to high density MPDSMs.

Fortunately, design tools exist which can be adapted for this purpose, so automated layout methods do not have to be designed from scratch. In particular for design under FDM, there are numerous truss design and topology optimization methods for which the truss elements can be defined as manufacturable FDM-deposited elements. For more dense structures, the layout of elements in FDM pre-processing software such as Ultimaker[®] Cura[®] can be controlled locally using a wide variety of settings. The regions which need to be redesigned must be determined, the element properties must be well-defined, and the type of pattern must be defined. In general for dense FDM-driven MPDSMs, a layout following the contours of a stress/strain field or feature is the best approach. A detailed

tutorial on how to input all of the design parameters and instructions into Cura (assisted by Autodesk[®] Inventor[®] for some problems) is given in Appendix B of this dissertation. All of the design settings, layout parameters, etc. must be put into Cura or a similar software but designed carefully prior to input. Note that *Cura does not complete the design process, but simply automates what the designer inputs (in terms of objectives and constraints) and defines for the design.* The main design work is done by the designer prior to automated application in Cura or other software packages.

4.5 Case Studies

4.5.1 Case 1: Manual 2-D Truss Layout Design

The first and most basic application of the MPDSMs concept is the manual layout of elements for a particular design, especially for a simple case with only a few elements. Figure 4.11 shows an example of this approach, specifically a printed layer in the form of a truss (made from PLA). In this case, it is assumed that the designer determined the layout of the nodes and size of the elements using some calculations (or other method) and so the implementation as a sparse MPDSM is manually completed by the designer.

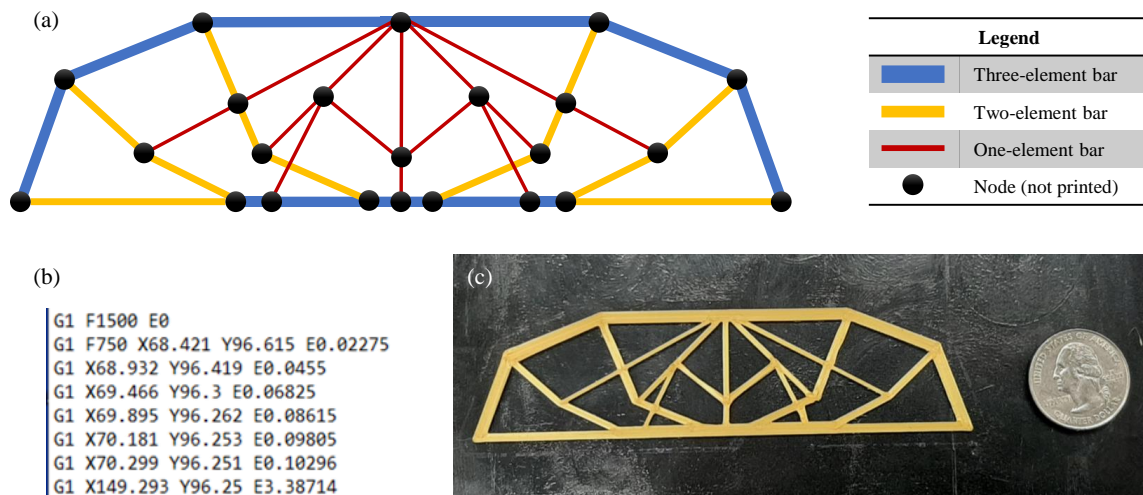


Figure 4.11: Case study 1 (a) manual layout of sparse MPDSM in the form of a truss, presenting a printed layer of a solid part, (b) example (real) g-code, and (c) directly-manufacturable outcome. The final product was made using PLA and each bar element was 0.6 mm wide and 0.2 mm tall.

The g-code (Figure 4.11b) was driven by the elements themselves and could have been manually or automatically created, depending on the pre-processing tools used. This manual layout may represent the entire MPDSM, it could represent a simple truss, or it may represent only a single layer in a larger part. Essentially, it was designed manually from a series of manufacturable elements and therefore meets the definition of a manually-laid out MPDSM.

4.5.2 Case 2: Beam Reinforcement via 3-D Element Layout

A simple PLA beam (5 mm thick) is supported by two pinned joints 130 mm apart and subject to a center load of 50 N (Figure 4.12a). It can be reinforced (increasing both load capacity and toughness) by selectively arranging the elements that make up the beam. The beam is to be made via FDM from PLA (0.6 mm nozzle with 0.2 mm layer height). In order to identify where the elements may be re-arranged to improve performance (with the smallest practical change in the structure), the shape generator tool in Autodesk[®] Inventor Professional[®] 2020 was used to find the areas where the stress is highest under the given load. The highlighted areas in Figure 4.12 show the regions that were preserved from material removal during the problem setup. This was done to prevent any unnecessary stress concentrations in the design.

The settings for this topology optimization (TO) tool allowed the input of the important manufacturability constraints from Chapter 3, ensuring that the solution itself was manufacturable using FDM; this portion of the problem is similar to case studies reported in Chapter 2 and in [33]. Two solutions were generated, one (Figure 4.12b) using a minimum length scale of 1.2 mm and using a 0.03 mm minimum mesh size. This one was meant to represent the new layout within the primitive, so requiring a thick wall on its own was not required, simplifying the solution. As shown in Figures 4.12 and 4.13, its performance was also tested on its own. The second (Figure 4.12c) was meant to be explored and testing on its own as a sort of sensitivity analysis (and additional demonstration of a sparse MPDSM, if desired). It used a much finer mesh (minimum element size of 0.005 mm) and required much more time (35 minutes versus 4 minutes for case 1) to process on a standard desktop computer. The second case was also given the recommended length scale constraint (2.4 mm

in this case - see Chapter 3). For both cases, the objective function was to increase stiffness and to attempt to remove 60% of the material; in both cases, the solution converged at the desired 40% mass function. Note that both TO solutions were 3-D, even with the simple problem loading, so each layer of the resulting parts (and later MPDSM) was unique.

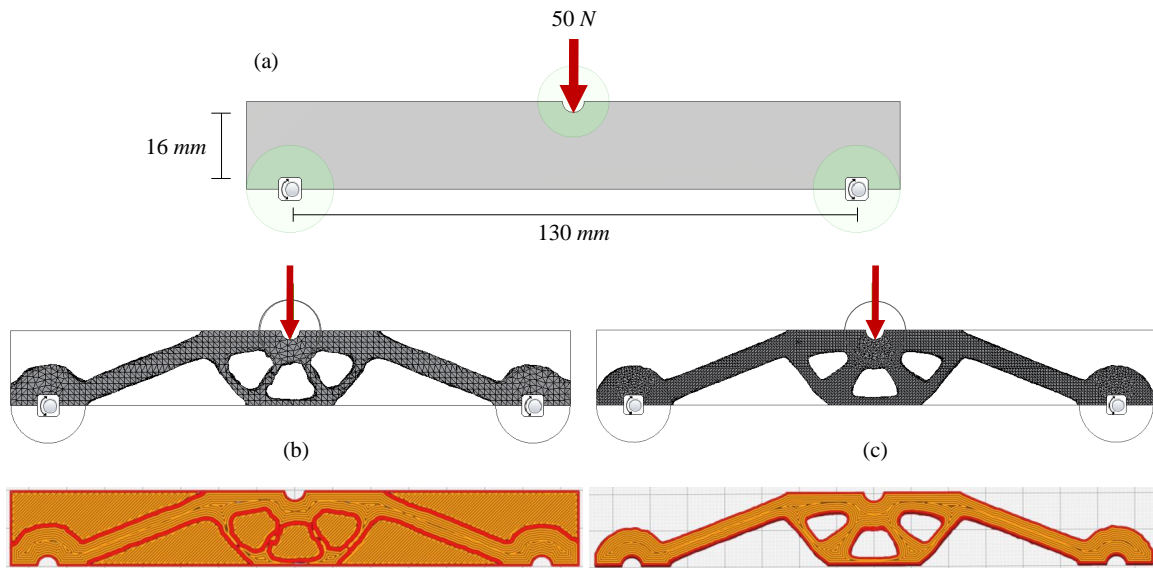


Figure 4.12: Case study 2 (a) problem definition, (b) TO solution with length scale = 1.2 mm and larger mesh, including embedded layout design, and (c) TO solution for length scale = 2.4 mm and finer mesh.

Figures 4.13 a-d show the basic primitive, the TO solution under the 2.4 mm length scale, the TO solution under the 1.2 mm length scale, and the final MPDSM, respectively. The primitive with arranged elements embedded was the focus of this case study, with the other designs contributing to its creation. As discussed previously in this chapter, Cura was used to lay out the elements given the two regions and the manufacturability constraints. The standard raster-45° pattern was used for both the primitive (Figure 4.13a) and the non-optimized regions (Figure 4.12b and Figure 4.13d) of the designed MPDSM. To maximize stiffness and toughness, a concentric pattern was used for the TO-solution area.

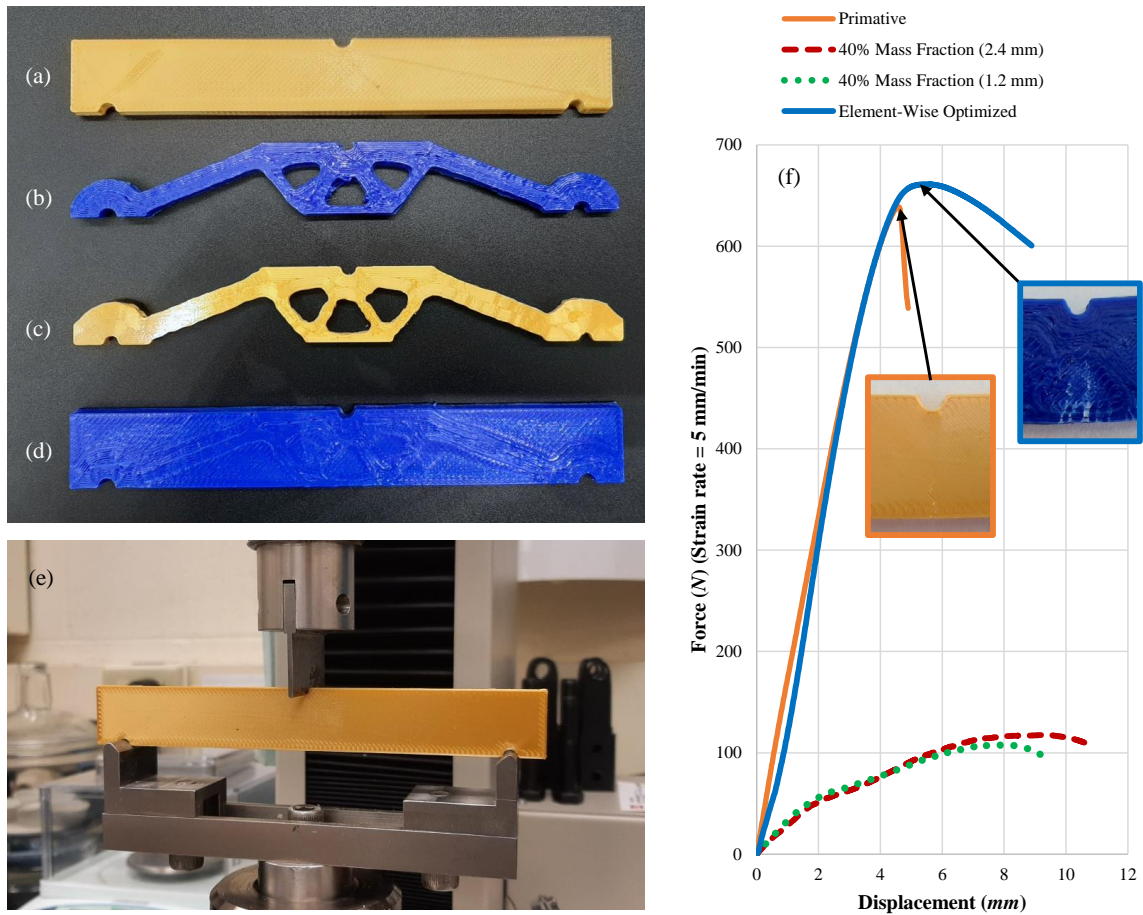


Figure 4.13: Case study 2 (a) printed basic primitive, (b) printed TO design for length scale = 2.4 mm, (c) printed TO design for length scale = 1.2 mm, (d) printed MPDSM, (e) experimental setup, and (f) experimental results.

Mechanical tests (3-point bend with a strain rate of 5 mm/min) were carried out to verify the success of the design, including the TO solutions on their own without embedding. Figure 4.13e shows the experimental setup used for all four cases. The performance is shown in Figure 4.13f. The two TO solutions behaved quite similarly, with the one having the higher minimum length scale performing slightly better; this is likely due to the fact that the larger length scale further reduced the probability of manufacturing defects even beyond what would be predicted by the standard manufacturability constraints. Looking at the performance of the MPDSM itself, it is very clear that it is a far superior design to the basic primitive, in spite of the fact that they are both made from the same material and have the same nominal density and printing parameters. As shown in Figure 4.13f, not only

is the MPDSM mechanically stronger (while maintaining about the same stiffness as the primitive) but also much tougher. Upon further analysis, it was found that the primitive (Figure 4.13, orange inset) began to fail by cracking with very little plastic deformation once it reached its peak strength. On the other hand, the MPDSM (blue inset) began to slowly relax, dissipating the energy more effectively through crazing and fiber relaxation, aided by a spring-like effect from the new part.

Overall, this was a very successful example of the process for creating MPDSMs using automated design tools (topology optimization in this case) and a clear demonstration of the benefits. In spite of nearly identical properties and processing (the other difference being color), the performance (especially the toughness) was greatly enhanced simply by arranging the manufacturable FDM-produced material elements. This problem could have been done several other ways, perhaps as successfully, including manual layout and using design rules. The use of the automated method (TO) to design the optimized region was a choice by the author to demonstrate this approach for creating good structural MPDSMs.

4.5.3 Case 3: Re-Design of Consumer Product

The final case study in this chapter on the creation and fabrication of general MPDSMs is the re-design of a consumer product. As shown in Figure 4.14a-b, a small clip (part of a harness) is subjected to an axial load during use. The team re-designing it as an MPDSM is told that it is made from PLA, has a designed strength of 250 pounds (approximately 1100N), and is normally made via FDM using a simple raster-45° pattern with a nozzle size of 0.6 mm and layer thickness of 0.2 mm. The design team is also told that the clip is subject to failure by fracturing in the regions shown in Figure 4.14c, but it is not specified at what load or under what conditions they normally fail (a common scenario during re-design). Finally, it is specified that the external shape, size, and material cannot be changed without changing the design of the whole system (the harness) to which it belongs. Therefore, the only design freedom given is in the design of the element layout. Using some basic design rules taken from standard engineering practice and from the knowledge about FDM provided in Chapter 3, the clip can be re-designed as an MPDSM to improve both its strength and toughness.

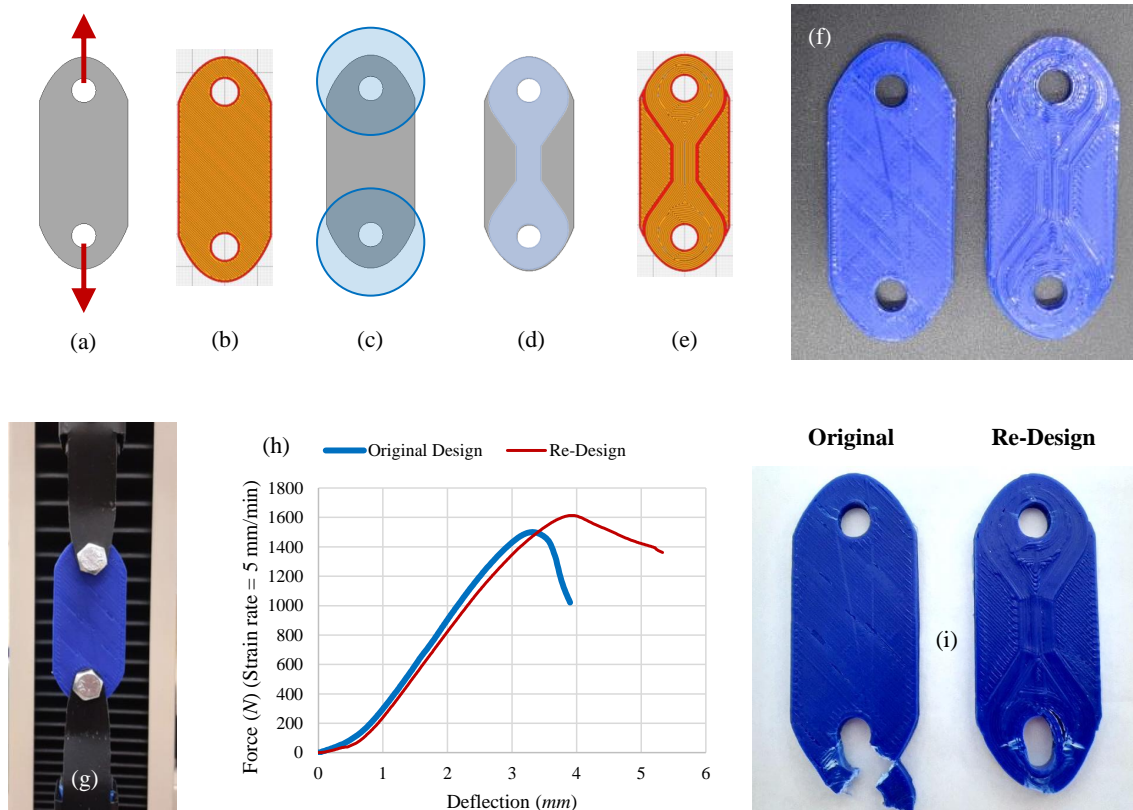


Figure 4.14: Case study 3 (a) design problem, (b) standard manufacturing layout, (c) failure-prone re-design space, (d) new conceptual design, (e) new design manufacturing layout, (f) printed specimens of each case, (g) experimental setup, (h) experimental results, and (i) post-experimental failure analysis.

Given the information about the basic geometry and loading (Figure 4.14a), the normal manufacturing approach (Figure 4.14b), and the potential trouble areas (Figure 4.14, re-design as an MPDSM can begin. After reflection, it was determined by the design team that there were three fundamental design properties (assuming a 2.5-D problem) at play in this problem:

1. Since all of the loading is at the holes, the thinnest areas need the best reinforcement.
2. The design space is symmetric, so only one side needs to be designed and then mirrored to the other side.
3. If the holes are reinforced, this could have a flow-down effect of increasing the chance for the middle section to fail if it is not also reinforced in some way, while trying to change the fundamental design as little as possible.

A very obvious solution to the problem is to simply print with the entire geometry printed as a series of concentric circles. However, there are three major issues with this approach for the problem at hand:

1. First, the having all of the fibers facing in the same direction of the load may decrease the stiffness of the clip significantly due to fiber relaxation and pullout.
2. Next, every layer in the structure would be a series of concentric rings, so any small manufacturing defects or fiber relaxation could case it to collapse.
3. PLA has a low glass transition temperature (60-70°C typically) and the MPDSM structure could weaken as the temperature rises, causing creep (in the best case) or disintegration (in the worst case). This is the reason that the raster-45° configuration is commonly used for PLA; it is generally considered to be the most stable configuration [75–79].

After carefully considering these design properties and considerations, it was clear that the historical weak areas (around the holes) should be re-designed as a MPDSM to improve the part. Because of the geometry and an assumed possibility that the applied force (from a rope or wire) could be applied from any direction, it was decided that the best approach was to arrange the material immediately around the holes. This extended the edge of the design space in Figure 4.14c) into a concentric configuration. After this was done, to prevent simply moving the fracture zone closer to the center of clip, a connecting bridge between the two concentric region was added while leaving as much of the old structure intact on the edges as possible to mitigate the three issues described above. This way, the structure is not simply a stack of identical layers, instead being a hybrid between the older design and an ideal new design. The new design space is shown in Figure 4.14d and the element layout for this new design is shown in Figure 4.14e. To verify the effectiveness of the design change, the two designs were printed (Figure 4.14f) and tested using a standard setup for compact tension (CT) testing (Figure 4.14g) (strain rate of 5 mm/min) to reproduce the loading in the problem description. Results of the experiment are shown in Figure 4.14h; the new design is slightly less stiff (as expected) but performs significantly better than the

original design, both in raw strength and in toughness. The original design was found to have a factor of safety of 1.36, which was increased to about 1.50 for the re-designed clip. Observing the two specimens after testing (Figure 4.14i), the logical reason for the improvement became very clear: The original design was stiffer until its failure point, but then experienced total failure. On the other hand, the re-designed version experienced crazing, fiber pull-out, and local plastic deformation but mostly maintained its structural integrity. If these were in use, the original design would have caused the harness to fail completely; for the re-designed version, the harness would have been weakened but would not have failed without a significant amount of additional deformation in the clip.

4.6 Closing Remarks

This chapter explored the design and creation of MPDSMs to be made by scanning-type AM (ST-AM) processes (particularly fused deposition modeling). Both qualitative and quantitative aspects of the problem were explored in depth, as demonstrated by the three case studies. Unlike most work on design approaches for structured materials (such as that discussed by Kochmann et al. [80]), this work focuses primarily on manufacturability (since it is driven by MDD principles) and second on structure, performance, or other factors. The discussion is material-agnostic, but it is assumed that most of the practical applications for this proposed method will use standard thermoplastic polymers. A general framework for the design and manufacturing of MPDSMs by FDM (and by extension, other ST-AM processes) was developed using a primarily qualitative approach, with some major discussion of practical implementation. This framework, subject to the discussed restrictions, allows the bottom-up design and construction of a class of structured materials by starting with generic, homogeneous, isotropic/transversely isotropic material elements and using these to build useful 3-D MPDSMs which simultaneously have high manufacturability and the largest possible design space.

Copyright Acknowledgement: As of April 10, 2021, the work presented in this chapter has not been published not has the copyright been assigned to anyone but the author. All figures in this chapter are original or published under a CC-BY license and reproduced under the terms of this license.

Chapter 4 Bibliography

- [1] S. K. Patiballa and G. Krishnan, “On the design of three-dimensional mechanical metamaterials using load flow visualization,” *Mechanics Based Design of Structures and Machines*, pp. 1–26, Feb. 2020.
- [2] Z.-Y. Yuan and B.-L. Su, “Insights into hierarchically meso-macroporous structured materials,” *Journal of Materials Chemistry*, vol. 16, no. 7, pp. 663–677, 2006.
- [3] A. Duval and M. Lawoko, “A review on lignin-based polymeric, micro- and nano-structured materials,” *Reactive and Functional Polymers*, vol. 85, pp. 78–96, Dec. 2014.
- [4] J. Zhao, Y. Deng, F. Xu, and J. Zhang, “Effects of initial grain size of al-zn-mg-cu alloy on the recrystallization behavior and recrystallization mechanism in isothermal compression,” *Metals*, vol. 9, p. 110, Jan. 2019.
- [5] J. Liu, Y. Ma, A. J. Qureshi, and R. Ahmad, “Light-weight shape and topology optimization with hybrid deposition path planning for FDM parts,” *The International Journal of Advanced Manufacturing Technology*, vol. 97, pp. 1123–1135, Apr. 2018.
- [6] K. W. Hall, T. W. Sirk, S. Percec, M. L. Klein, and W. Shinoda, “Monodisperse polymer melts crystallize via structurally polydisperse nanoscale clusters: Insights from polyethylene,” *Polymers*, vol. 12, p. 447, Feb. 2020.
- [7] Borgue, Müller, Leicht, Panarotto, and Isaksson, “Constraint replacement-based design for additive manufacturing of satellite components: Ensuring design manufacturability through tailored test artefacts,” *Aerospace*, vol. 6, p. 124, Nov. 2019.
- [8] J. Barrios-Muriel, F. Romero-Sánchez, F. J. Alonso-Sánchez, and D. R. Salgado, “Advances in orthotic and prosthetic manufacturing: A technology review,” *Materials*, vol. 13, p. 295, Jan. 2020.
- [9] Y.-E. Yeh, “Prediction of optimized color design for sports shoes using an artificial neural network and genetic algorithm,” *Applied Sciences*, vol. 10, p. 1560, Feb. 2020.

- [10] A. E. Patterson, “Image: Design relevant level definitions for structured materials,” Technical Report 109141, University of Illinois at Urbana-Champaign, Urbana, IL, USA, Jan. 2021. <https://www.ideals.illinois.edu/handle/2142/109141>.
- [11] G. Alaimo, S. Marconi, L. Costato, and F. Auricchio, “Influence of meso-structure and chemical composition on FDM 3D-printed parts,” *Composites Part B: Engineering*, vol. 113, pp. 371–380, Mar. 2017.
- [12] X. Ren, R. Das, P. Tran, T. D. Ngo, and Y. M. Xie, “Auxetic metamaterials and structures: a review,” *Smart Materials and Structures*, vol. 27, p. 023001, Jan. 2018.
- [13] D. D. Vescovo and I. Giorgio, “Dynamic problems for metamaterials: Review of existing models and ideas for further research,” *International Journal of Engineering Science*, vol. 80, pp. 153–172, July 2014.
- [14] T. Bückmann, N. Stenger, M. Kadic, J. Kaschke, A. Frölich, T. Kennerknecht, C. Eberl, M. Thiel, and M. Wegener, “Tailored 3d mechanical metamaterials made by dip-in direct-laser-writing optical lithography,” *Advanced Materials*, vol. 24, pp. 2710–2714, Apr. 2012.
- [15] K. Chynybekova and S.-M. Choi, “Flexible patterns for soft 3d printed fabrications,” *Symmetry*, vol. 11, p. 1398, Nov. 2019.
- [16] F. Liu, D. Zhang, P. Zhang, M. Zhao, and S. Jafar, “Mechanical properties of optimized diamond lattice structure for bone scaffolds fabricated via selective laser melting,” *Materials*, vol. 11, p. 374, Mar. 2018.
- [17] Y. Zhao, Y. Endo, Y. Kanamori, and J. Mitani, “A computational design method for tucking axisymmetric origami consisting of triangular facets,” *Symmetry*, vol. 10, p. 469, Oct. 2018.
- [18] S. Weiner and H. D. Wagner, “THE MATERIAL BONE: Structure-mechanical function relations,” *Annual Review of Materials Science*, vol. 28, pp. 271–298, Aug. 1998.
- [19] M. J. Olszta, X. Cheng, S. S. Jee, R. Kumar, Y.-Y. Kim, M. J. Kaufman, E. P. Douglas, and L. B. Gower, “Bone structure and formation: A new perspective,” *Materials Science and Engineering: R: Reports*, vol. 58, pp. 77–116, Nov. 2007.
- [20] Y.-J. Liang, D. Liu, and H.-M. Wang, “Microstructure and mechanical behavior of commercial purity Ti/Ti-6Al-2Zr-1Mo-1V structurally graded material fabricated by laser additive manufacturing,” *Scripta Materialia*, vol. 74, pp. 80–83, Mar. 2014.
- [21] A. Orlov, V. Sufiiarov, E. Borisov, I. Polozov, D. Masaylo, A. Popovich, M. Chukovenkova, A. Soklakov, and D. Mikhaluk, “Numerical simulation of the inelastic behavior of a structurally graded material,” *Letters on Materials*, vol. 9, no. 1, pp. 97–102, 2019.
- [22] A. S. Gladman, E. A. Matsumoto, R. G. Nuzzo, L. Mahadevan, and J. A. Lewis, “Biomimetic 4d printing,” *Nature Materials*, vol. 15, pp. 413–418, Jan. 2016.

- [23] F. Momeni, S. M. Hassani.N, X. Liu, and J. Ni, “A review of 4d printing,” *Materials & Design*, vol. 122, pp. 42–79, May 2017.
- [24] M. Domingo-Espin, J. M. Puigoriol-Forcada, A.-A. Garcia-Granada, J. Llumà, S. Borros, and G. Reyes, “Mechanical property characterization and simulation of fused deposition modeling polycarbonate parts,” *Materials & Design*, vol. 83, pp. 670–677, Oct. 2015.
- [25] G. Kasperovich, J. Haubrich, J. Gussone, and G. Requena, “Correlation between porosity and processing parameters in TiAl6V4 produced by selective laser melting,” *Materials & Design*, vol. 105, pp. 160–170, Sept. 2016.
- [26] H. Cui, R. Hensleigh, D. Yao, D. Maurya, P. Kumar, M. G. Kang, S. Priya, and X. R. Zheng, “Three-dimensional printing of piezoelectric materials with designed anisotropy and directional response,” *Nature Materials*, vol. 18, pp. 234–241, Jan. 2019.
- [27] B. Schönfisch, “Anisotropy in cellular automata,” *Biosystems*, vol. 41, pp. 29–41, Jan. 1997.
- [28] M. Pelanconi and A. Ortona, “Nature-inspired, ultra-lightweight structures with gyroid cores produced by additive manufacturing and reinforced by unidirectional carbon fiber ribs,” *Materials*, vol. 12, p. 4134, Dec. 2019.
- [29] J. Reinbold, T. Frenzel, A. Münchinger, and M. Wegener, “The rise of (chiral) 3d mechanical metamaterials,” *Materials*, vol. 12, p. 3527, Oct. 2019.
- [30] H. Chen, X. Zhou, H. Fujita, M. Onozuka, and K.-Y. Kubo, “Age-related changes in trabecular and cortical bone microstructure,” *International Journal of Endocrinology*, vol. 2013, pp. 1–9, 2013.
- [31] J. G. Bralla, *Design for Manufacturability Handbook (2nd Edition)*. McGraw-Hill Education, 1998.
- [32] A. R. Venkatachalam, J. M. Mellichamp, and D. M. Miller, “A knowledge-based approach to design for manufacturability,” *Journal of Intelligent Manufacturing*, vol. 4, pp. 355–366, Oct. 1993.
- [33] A. E. Patterson and J. T. Allison, “Generation and mapping of minimally-restrictive manufacturability constraints for mechanical design problems,” in *Volume 4: 24th Design for Manufacturing and the Life Cycle Conference; 13th International Conference on Micro- and Nanosystems*, American Society of Mechanical Engineers, Aug. 2019.
- [34] S. L. Vatanabe, T. N. Lippi, C. R. de Lima, G. H. Paulino, and E. C. Silva, “Topology optimization with manufacturing constraints: A unified projection-based approach,” *Advances in Engineering Software*, vol. 100, pp. 97–112, 2016.

- [35] H. Li, P. Li, L. Gao, L. Zhang, and T. Wu, "A level set method for topological shape optimization of 3d structures with extrusion constraints," *Computer Methods in Applied Mechanics and Engineering*, vol. 283, pp. 615–635, 2015.
- [36] I. Ferrer, J. Rios, and J. Ciurana, "An approach to integrate manufacturing process information in part design phases," *Journal of Materials Processing Technology*, vol. 209, no. 4, pp. 2085–2091, 2009.
- [37] M. Gries, "Methods for evaluating and covering the design space during early design development," *Integration, the VLSI Journal*, vol. 38, no. 2, pp. 131–183, 2004.
- [38] M. Iyengar and A. Bar-Cohen, "Design for manufacturability of SISE parallel plate forced convection heat sinks," *IEEE Transactions on Components and Packaging Technologies*, vol. 24, no. 2, pp. 150–158, 2001.
- [39] K. He, H. Wang, and H. Hu, "Approach to online defect monitoring in fused deposition modeling based on the variation of the temperature field," *Complexity*, vol. 2018, pp. 1–13, Sept. 2018.
- [40] S. L. Messimer, A. E. Patterson, N. Muna, A. P. Deshpande, and T. R. Pereira, "Characterization and processing behavior of heated aluminum-polycarbonate composite build plates for the FDM additive manufacturing process," *Journal of Manufacturing and Materials Processing*, vol. 2, p. 12, Feb. 2018.
- [41] Y. Zhou, T. Nyberg, G. Xiong, and D. Liu, "Temperature analysis in the fused deposition modeling process," in *2016 3rd International Conference on Information Science and Control Engineering (ICISCE)*, IEEE, July 2016.
- [42] J. Zhang, X. Z. Wang, W. W. Yu, and Y. H. Deng, "Numerical investigation of the influence of process conditions on the temperature variation in fused deposition modeling," *Materials & Design*, vol. 130, pp. 59–68, Sept. 2017.
- [43] C. Kousiatza and D. Karalekas, "In-situ monitoring of strain and temperature distributions during fused deposition modeling process," *Materials & Design*, vol. 97, pp. 400–406, May 2016.
- [44] A. E. Patterson, S. L. Messimer, and P. A. Farrington, "Overhanging features and the SLM/DMLS residual stresses problem: Review and future research need," *Technologies*, vol. 5, no. 2, p. 15, 2017.
- [45] C. Li, Z. Liu, X. Fang, and Y. Guo, "Residual stress in metal additive manufacturing," *Procedia CIRP*, vol. 71, pp. 348–353, 2018.
- [46] O. Fergani, F. Berto, T. Welo, and S. Y. Liang, "Analytical modelling of residual stress in additive manufacturing," *Fatigue & Fracture of Engineering Materials & Structures*, vol. 40, pp. 971–978, Dec. 2016.

- [47] B. Wu, Z. Pan, D. Ding, D. Cuiuri, H. Li, J. Xu, and J. Norrish, “A review of the wire arc additive manufacturing of metals: properties, defects and quality improvement,” *Journal of Manufacturing Processes*, vol. 35, pp. 127–139, Oct. 2018.
- [48] H. Taheri, M. R. B. M. Shoaib, L. W. Koester, T. A. Bigelow, P. C. Collins, and L. J. Bond, “Powder-based additive manufacturing - a review of types of defects, generation mechanisms, detection, property evaluation and metrology,” *International Journal of Additive and Subtractive Materials Manufacturing*, vol. 1, no. 2, p. 172, 2017.
- [49] H. Masuo, Y. Tanaka, S. Morokoshi, H. Yagura, T. Uchida, Y. Yamamoto, and Y. Murakami, “Influence of defects, surface roughness and HIP on the fatigue strength of ti-6al-4v manufactured by additive manufacturing,” *International Journal of Fatigue*, vol. 117, pp. 163–179, Dec. 2018.
- [50] B. Yao, F. Imani, A. S. Sakpal, E. W. Reutzler, and H. Yang, “Multifractal analysis of image profiles for the characterization and detection of defects in additive manufacturing,” *Journal of Manufacturing Science and Engineering*, vol. 140, Jan. 2018.
- [51] E. G. Gordeev, A. S. Galushko, and V. P. Ananikov, “Improvement of quality of 3d printed objects by elimination of microscopic structural defects in fused deposition modeling,” *PLOS ONE*, vol. 13, p. e0198370, June 2018.
- [52] M. Shofner, F. Rodriguez-Macias, R. Vaidyanathan, and E. Barrera, “Single wall nanotube and vapor grown carbon fiber reinforced polymers processed by extrusion freeform fabrication,” *Composites Part A: Applied Science and Manufacturing*, vol. 34, pp. 1207–1217, Dec. 2003.
- [53] S.-H. Ahn, M. Montero, D. Odell, S. Roundy, and P. K. Wright, “Anisotropic material properties of fused deposition modeling ABS,” *Rapid Prototyping Journal*, vol. 8, no. 4, pp. 248–257, 2002.
- [54] A. Cattenone, S. Morganti, G. Alaimo, and F. Auricchio, “Finite element analysis of additive manufacturing based on fused deposition modeling: Distortions prediction and comparison with experimental data,” *Journal of Manufacturing Science and Engineering*, vol. 141, Nov. 2018.
- [55] J. F. Rodríguez, J. P. Thomas, and J. E. Renaud, “Mechanical behavior of acrylonitrile butadiene styrene fused deposition materials modeling,” *Rapid Prototyping Journal*, vol. 9, pp. 219–230, Oct. 2003.
- [56] R. Hague, S. Mansour, N. Saleh, and R. Harris, “Materials analysis of stereolithography resins for use in rapid manufacturing,” *Journal of Materials Science*, vol. 39, pp. 2457–2464, Apr. 2004.
- [57] Y. Li, S. Peng, J.-T. Miao, L. Zheng, J. Zhong, L. Wu, and Z. Weng, “Isotropic stereolithography resin toughened by core-shell particles,” *Chemical Engineering Journal*, vol. 394, p. 124873, Aug. 2020.

- [58] S. Wang, Y. Ma, Z. Deng, K. Zhang, and S. Dai, "Implementation of an elastoplastic constitutive model for 3D-printed materials fabricated by stereolithography," *Additive Manufacturing*, vol. 33, p. 101104, May 2020.
- [59] B. AlMangour, D. Grzesiak, and J.-M. Yang, "Scanning strategies for texture and anisotropy tailoring during selective laser melting of TiC/316l stainless steel nanocomposites," *Journal of Alloys and Compounds*, vol. 728, pp. 424–435, Dec. 2017.
- [60] S. Cahill, S. Lohfeld, and P. E. McHugh, "Finite element predictions compared to experimental results for the effective modulus of bone tissue engineering scaffolds fabricated by selective laser sintering," *Journal of Materials Science: Materials in Medicine*, vol. 20, pp. 1255–1262, Feb. 2009.
- [61] F. Geiger, K. Kunze, and T. Etter, "Tailoring the texture of IN738lc processed by selective laser melting (SLM) by specific scanning strategies," *Materials Science and Engineering: A*, vol. 661, pp. 240–246, Apr. 2016.
- [62] J. Gardan, A. Makke, and N. Recho, "A method to improve the fracture toughness using 3D printing by extrusion deposition," *Procedia Structural Integrity*, vol. 2, pp. 144–151, 2016.
- [63] J. Gardan, "Method for characterization and enhancement of 3D printing by binder jetting applied to the textures quality," *Assembly Automation*, vol. 37, no. 2, pp. 162–169, 2017.
- [64] J. Gardan, A. Makke, and N. Recho, "Improving the fracture toughness of 3d printed thermoplastic polymers by fused deposition modeling," *International Journal of Fracture*, vol. 210, no. 1-2, pp. 1–15, 2017.
- [65] C. C. Seepersad, M. R. Haberman, and C. B. Morris, "Design exploration of additively manufactured metamaterials," *The Journal of the Acoustical Society of America*, vol. 146, pp. 2757–2757, Oct. 2019.
- [66] C. R. Garcia, J. Correa, D. Espalin, J. H. Barton, R. C. Rumpf, R. Wicker, and V. Gonzalez, "3d printing of anisotropic metamaterials," *Progress In Electromagnetics Research Letters*, vol. 34, pp. 75–82, 2012.
- [67] M. Bodaghi, A. Damanpack, G. Hu, and W. Liao, "Large deformations of soft metamaterials fabricated by 3d printing," *Materials & Design*, vol. 131, pp. 81–91, Oct. 2017.
- [68] S. Babaei, J. Shim, J. C. Weaver, E. R. Chen, N. Patel, and K. Bertoldi, "3d soft metamaterials with negative poisson's ratio," *Advanced Materials*, vol. 25, pp. 5044–5049, July 2013.
- [69] M. Ruiz-Montiel, J. Boned, J. Gavilanes, E. Jiménez, L. Mandow, and J.-L. P. de-la Cruz, "Design with shape grammars and reinforcement learning," *Advanced Engineering Informatics*, vol. 27, pp. 230–245, Apr. 2013.

- [70] C. J. Kim, Y.-M. Moon, and S. Kota, “A building block approach to the conceptual synthesis of compliant mechanisms utilizing compliance and stiffness ellipsoids,” *Journal of Mechanical Design*, vol. 130, Jan. 2008.
- [71] S. Kota, J. A. Hetrick, R. Osborn, D. Paul, E. Pendleton, P. Flick, and C. Tilmann, “Design and application of compliant mechanisms for morphing aircraft structures,” in *Smart Structures and Materials 2003: Industrial and Commercial Applications of Smart Structures Technologies* (E. H. Anderson, ed.), SPIE, Aug. 2003.
- [72] S. Orsborn, J. Cagan, R. Pawlicki, and R. C. Smith, “Creating cross-over vehicles: Defining and combining vehicle classes using shape grammars,” *Artificial Intelligence for Engineering Design, Analysis and Manufacturing*, vol. 20, pp. 217–246, June 2006.
- [73] T. Knight and G. Stiny, “Making grammars: From computing with shapes to computing with things,” *Design Studies*, vol. 41, pp. 8–28, Nov. 2015.
- [74] P. Wang, W. Sin, M. Nai, and J. Wei, “Effects of processing parameters on surface roughness of additive manufactured Ti-6Al-4V via electron beam melting,” *Materials*, vol. 10, p. 1121, Sept. 2017.
- [75] A. E. Patterson, T. R. Pereira, J. T. Allison, and S. L. Messimer, “IZOD impact properties of full-density fused deposition modeling polymer materials with respect to raster angle and print orientation,” *Proceedings of the Institution of Mechanical Engineers, Part C: Journal of Mechanical Engineering Science*, p. 095440621984038, Apr. 2019.
- [76] A. Ahmed and L. Susmel, “Additively manufactured PLA under static loading: strength/cracking behaviour vs. deposition angle,” *Procedia Structural Integrity*, vol. 3, pp. 498–507, 2017.
- [77] Y. Song, Y. Li, W. Song, K. Yee, K.-Y. Lee, and V. Tagarielli, “Measurements of the mechanical response of unidirectional 3D-printed PLA,” *Materials & Design*, vol. 123, pp. 154–164, June 2017.
- [78] I. Cuesta, E. Martinez-Pañeda, A. Díaz, and J. Alegre, “The Essential Work of Fracture parameters for 3D printed polymer sheets,” *Materials & Design*, vol. 181, p. 107968, Nov. 2019.
- [79] E. A. Papon and A. Haque, “Fracture toughness of additively manufactured carbon fiber reinforced composites,” *Additive Manufacturing*, vol. 26, pp. 41–52, Mar. 2019.
- [80] D. M. Kochmann, J. B. Hopkins, and L. Valdevit, “Multiscale modeling and optimization of the mechanics of hierarchical metamaterials,” *MRS Bulletin*, vol. 44, pp. 773–781, Oct. 2019.

Chapter 5

FRACTURE MECHANICS AND DESIGN KNOWLEDGE

Collaborator Acknowledgement: The author gratefully acknowledges the contributions, advice, direction, and feedback from the following people on the work presented in this chapter: **Charul Chadha** (collaborator on literature review discussion about standards and experimental approaches); **Dr. Iwona M. Jasiuk** (extensive discussion and advice on experimental methods, assumptions, and data interpretation).

This chapter may contain previously published text and figures, which are reproduced with the permission of the copyright holders. See the copyright statement and list of references at the end of the chapter.

5.1 Introduction

The fracture behavior of materials has significant implications for practical design and manufacturability decisions, as it is often a major limiting factor for applications and processing plans [1, 2]. Defects in materials can serve as crack initiators and lead to premature failure of the part. When brittle materials are used, cracks can lead to catastrophic fracture at

lower loads than those predicted by standard material properties [3–5]. In ductile materials, the internal defects may not cause an immediate failure but the plastic behavior of the material under load may be modified, affecting the structural integrity and stability of the material [6, 7]. The influence of uncertainties in material response (caused by natural and induced defects, environmental factors, load magnitude and location uncertainties, and other issues have traditionally been offset by using a “Factor of Safety” (FoS) during design process [8–10]. Choosing an appropriate FoS is essential, as a low one may still lead to unplanned failure but one that is too high can result in over-design and waste. It is also likely that the FoS will need to be locally calculated in order to ensure the most effective and efficient design. Fracture mechanics can give more precise information on material properties and relates these properties to the component behavior. It provides guidance on the size, shape, and locations of any inclusions, defects, cracks, or other stress concentrators; this perspective can also better help determine the magnitude of the load that can be safely applied for a given material or structure to withstand fracture [3, 11].

In current practice, advanced materials are extensively considered while designing. These materials are often complex, structured, and hierarchical systems (e.g., advanced composites [12, 13], architected [14, 15] and functionally-graded materials [16]). By studying the fracture behavior of these materials and structures, a large amount of *design knowledge* [17–19] can be extracted that can guide design decisions. Rigorous experiments are thus essential to understand the response of materials. Unlike many other types of mechanical testing, the effects of fracture mechanics can be directly observed, in real time with a relatively low cost and time investment. Fracture-driven design knowledge can not only be used to determine limitations and constraints, but also to expand the design space and guide development of new design methodologies.

These may take the form of discrete layers, sintered powder particles, deposited beads of material, and other similar elements. AM-driven inclusion/void creation in the material structure may be inter-layer, intra-layer, or both. This depends mainly on the type of process used; scanning-type (ST-AM) processes (such as fused deposition modeling (FDM) and laser powder bed fusion (LPBF)) typically deposit and fuse material in the form of beads or elements (also called “roads” in some literature) while non-ST-AM processes could

deposit and fuse entire layers at a time (such as the case with digital light processing (DLP)) or may print in a inkjet-like fashion (such as Polyjet or binder jetting (BJ)). The most common and well-refined class of additively manufactured materials are those based on standard thermoplastic and resin-based thermoset polymers [20–22]. Of the involved processes, FDM is the one with the most extensive history in the literature and the best-known material properties and mechanical behavior. In the past few years, a fairly extensive literature has been developed on the standard mechanical properties of many AM-processed materials, helping to advance them as engineering or commodity materials. However, no standard guidance has been developed on fracture testing of these AM-processed materials, which has resulted in variety of test processes and methodologies being used. This has led to high variance in details and rigor of reported results. ASTM and ISO standards are not always used for these tests and it has been an open question about which standards to use, if available, and how to interpret the collected data.

Fracture mechanics as a mechanical load or design driver is a major theme of this dissertation and will be discussed extensively in the next several chapters. In this chapter, a deep literature review is presented to show the state-of-the-art for fracture testing of FDM-processed materials. From this review, a large amount of information about the materials, testing methods, and standards used (Section 5.2) is shown to help drive decisions for the work presented in upcoming chapters. In addition to the raw information about the testing, perspectives on design knowledge and information were also collected and refined (Section 5.3) from the set of references, providing a more qualitative view of the literature from the perspective of an expert in mechanical design. After an extensive exploration of the literature, some practical implementation considerations are developed and presented in Section 5.4. Finally, some closing remarks are offered in Section 5.5. The purpose of this chapter was not only to review the literature, but to provide context and motivation for the study of fracture related to mechanical design which will be explored in upcoming chapters.

5.2 Review: Fracture Methods, Materials, and Standards for FDM Materials

This section presents the results of an extensive literature review meant to establish the state of the art regarding fracture testing of FDM-processed materials. The focus of the review was on fracture testing methods used previously, the list of materials that have been successfully tested, and the ASTM/ISO standards (if any) that were used to guide the work. More details about the review approach and details are given in Appendix G.

5.2.1 Fracture Testing Methods - FDM

The fracture testing methods identified during the review fit into four categories: (1) basic mechanical tests used to gather fracture information, (2) quasi-static fracture tests, (3) impact tests, and (4) dynamic tests. Note that all of the impact tests found were defined by only a single strike of the sample and that the dynamic tests did not involve fatigue analysis or measurement. Figure 5.1 shows the approximate distribution within the reviewed literature of each of the tests discussed in Table 5.1.

Table 5.1: Testing methods found during the survey for quasi-static, impact, and dynamic tests. Impact tests were considered to be those that applied the full load to the material suddenly, while dynamic tests applied the load in a slower but non-steady-state or non-static way. FLX, ONSENB, and SENB tests may have used 3-point or 4-point loading. Standard tensile test specimens may be solid or have internal defects but are not mechanically notched.

Test	Studies		
Standard Mechanical Tests	SCT	Standard compression test	[23, 24]
	STT	Standard tensile test	[24–32]
	FLX	Standard flexure test	[24, 29]
Quasi-Static Fracture Tests	CT	Compact tension test	[28, 33–36]
	DCB	Double cantilever beam test	[37–40]
	SENB	Single-end notch bending test	[26, 36, 39, 41–51]
	SENT	Single-end notch tension test	[27, 52–55]
	DDEN	Deep double edge notch test	[55, 56]
	ENF	End-notched flexure test	[38]
	MMB	Mixed-mode bending test	[38]
	ONSENB	Offset-notch SENB test	[26, 44]
Impact Tests	TTT	Trouser tear test	[57]
	CIT	Charpy impact test	[24, 58–61]
	IDT	Impact drop test	[59]
Dynamic Tests	IIT	IZOD impact test	[30, 62, 63]
	CB	Cantilever beam dynamic test	[64]
	SHPB	Split-Hopkinson pressure bar	[45]

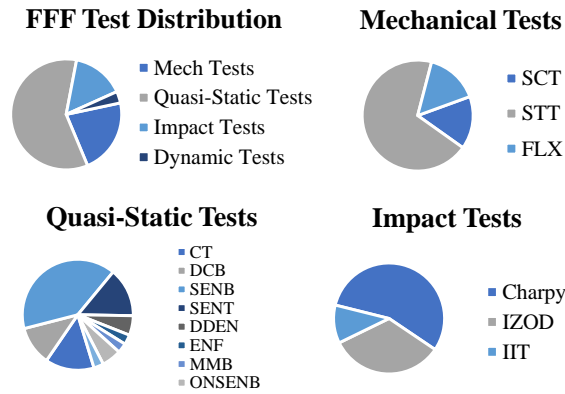


Figure 5.1: Distribution of the standard mechanical tests focusing on fracture behavior, the quasi-static fracture tests, the dynamic tests, and the impact tests performed in the reviewed literature. Specific tests within each category are also shown. It should be noted that many of the reviewed papers utilized multiple testing methods. Separate chart not shown for the dynamic tests, as there was only one study involving each of the two methods.

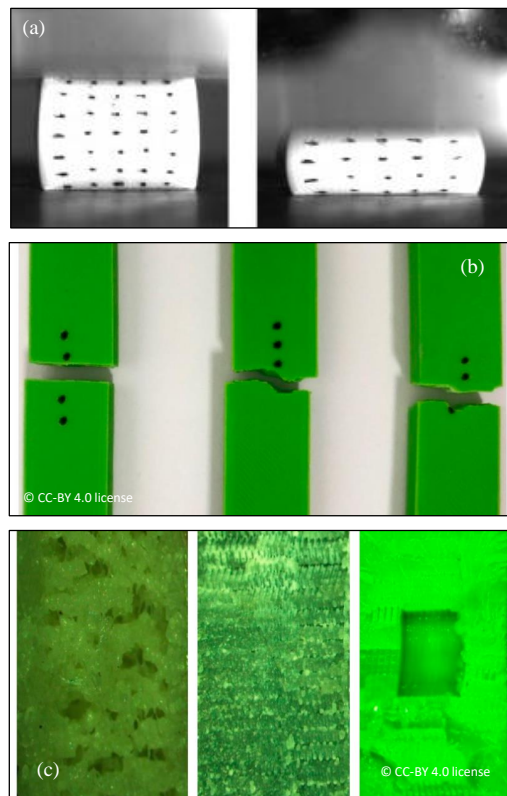


Figure 5.2: Fracture testing based on standard mechanical characterization tests: (a) Compression testing of FDM ABS [23], (b) fractured standard tensile testing FDM PLA samples, and (c) PLA fracture surface detail [25]. Panel (a) © Elsevier B.V., reproduced with permission. Panels (b) and (c) reproduced under CC-BY license terms.

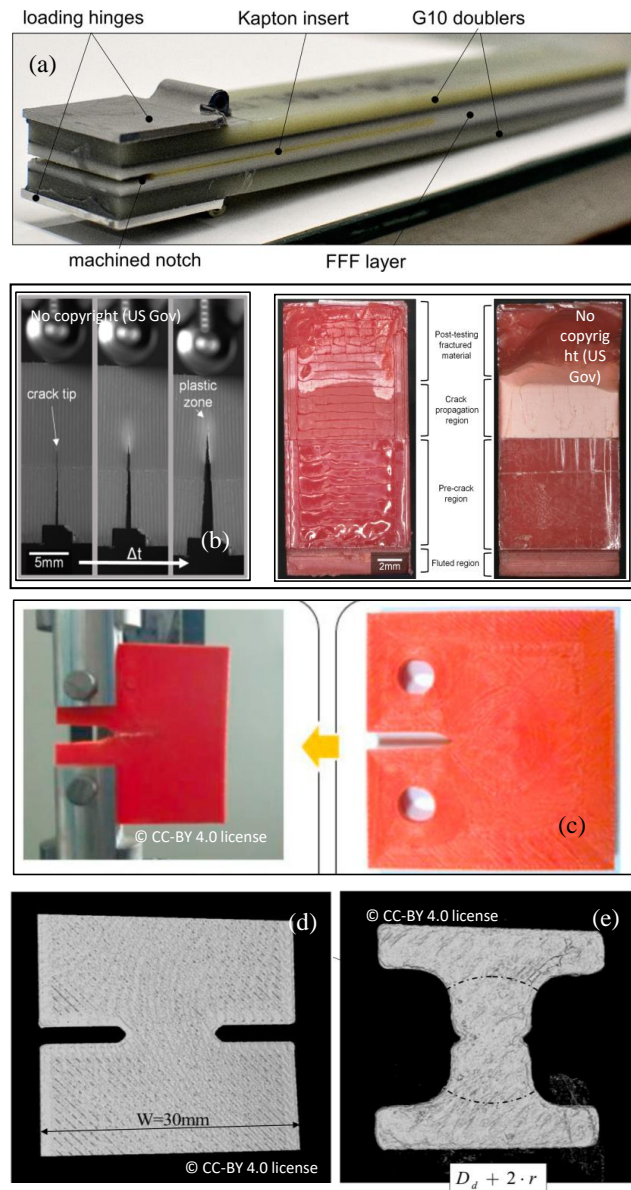


Figure 5.3: Quasi-static fracture tests: (a) Double cantilever beam (DCB) testing setup using FDM ABS [39], (b) single-edge notch bending (SENB) testing using FDM ABS and polycarbonate [49], (c) CT testing of FDM ABS [33], and deep double edge notched (DDEN) testing scheme under (d) tension and (e) punching [56] for FDM nylon. Panel (a) © Elsevier B.V., reproduced with permission. Panel (b) from US Government document and not subject to copyright. Panels (c-e) reproduced under CC-BY license terms.

The most common testing methods used in the reviewed literature were single-edge notch bending tests (SENB), single-edge notch tensile tests, compact tension tests (CT), Charpy impact tests, and standard tensile tests with fracture-related interpretations of the observed material behavior. The standard mechanical tests identified as being used to study

the fracture behavior of AM-processed polymer materials included standard compression (for example, Figure 5.2a completed by Guessasma *et al.* [23] on FDM ABS), tensile (Figures 5.2b and 5.2c observed for fracture behavior by Mourad *et al.* [25] using FDM PLA), and flexure tests (such as the study done by Spoerk *et al.* [29]).

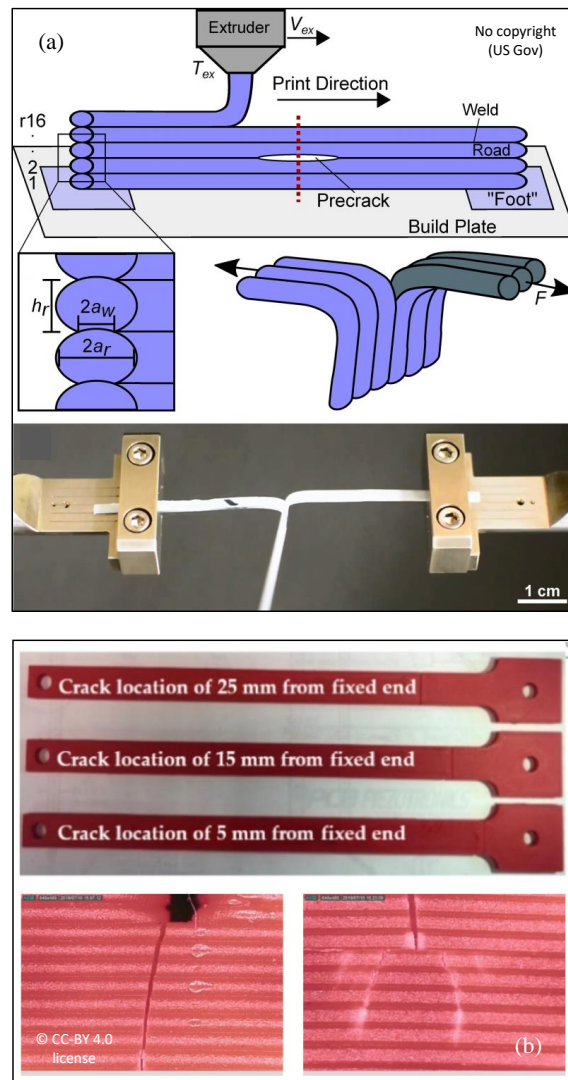


Figure 5.4: Dynamic and quasi-static fracture tests: (a) trouser tear test [57] on FDM ABS and (b) Dynamic cantilever beam test [64] for FDM ABS. Panel (a) from US Government document and not subject to copyright. Panel (b) reproduced under CC-BY license terms.

The experiments completed with quasi-static tests could be divided into two categories, namely the “common” setups most often used in fracture mechanics testing and those

that are more specialized and used to find specific information. The common tests that were found to have been used were the double cantilever beam (DCB) test (an example of this test from Young *et al.* [39] is shown in Figure 5.3a), single-edge notch bending (SENB) (Figure 5.3b as presented by Dunn *et al.* [49]), single-edge notch tensile (SENT), and compact tension tests (CT) (for example, Figure 5.3c from a study by Gardan *et al.* [33]). Of the quasi-static tests, the four common ones described here were used in the vast bulk of the experiments, with SENB by far the most common. The remaining studies used the more obscure and specialized tests, with Cuesta *et al.* [56] employing deep double edged notch (DDEN) tests for tensile (Figure 5.3d) and punch (Figure 5.3e) loadings, Khan *et al.* studying end-notch flexure (ENF) and mixed-mode bending (MMB), and Davis *et al.* [57] used trouser tear testing (TTT) to examine the in-layer strength of FDM ABS (Figure 5.4a). Finally, some SENB tests were completed by Lanzillotti *et al.* [26, 44] which used offset loadings and notches (ONSENB).

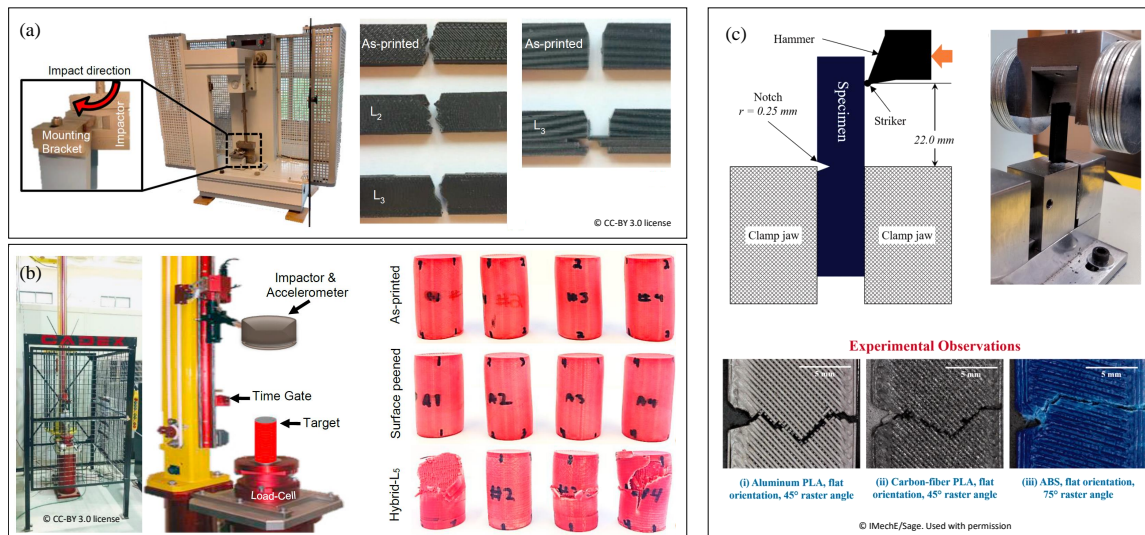


Figure 5.5: (a) Examples of a Charpy testing machine and samples [59], (b) drop testing device and tested samples [59], and (c) Type-E (reversed notch) IZOD [62] tests with results. Panels (a) and (b) reproduced under CC-BY license terms. Panel (c) © IMechE/Sage, reproduced with permission.

Finally, six different types of impact and dynamic tests were found in the reviewed literature. It should be noted that the dynamic tests referenced here were not fatigue tests and were used to evaluate other properties such as natural frequency changes in response to cracks (as explored by Baqasah *et al.*, [64], with the experimental samples shown in

Figure 5.4b), and testing the dynamic stress-strain relationship of the fractured material using a Split-Hopkinson pressure bar as done by Rabbi *et al.* [45]. With the exception of the drop impact experiment by Hadidi *et al.* [59] (Figure 5.5b), all of the impact tests found during the survey were standard Charpy and IZOD tests. Charpy tests (such as those by Hadidi *et al.* [59] (Figure 5.5a) and Caminero *et al.* [60]) were standardized and followed essentially the same procedure. Most of the IZOD tests (for example, Peng *et al.* [30]) used the Type A IZOD setup (notch in tension), but one very large study by Patterson *et al.* [62] (Figure 5.5c) used the Type E (notch in compression) IZOD setup to better explore the growth behavior of the cracks instead of simply characterizing the studied materials.

5.2.2 FDM-Processed Materials

As with the testing methods, more than one material or process may have been examined in a single reviewed article. For each of the studies, a list of studied materials was collected and tabulated (Table 5.2). The FDM process is reliant on the stable and predictable melting of the raw materials, so all of the discussed materials are thermoplastic polymers. A total of ten different thermoplastic materials (Table 5.2) were identified, in addition to multi-material or structural composites (MM-SC). The most widely studied materials were acrylonitrile butadiene styrene (ABS), polyamide/nylon (PA), and polylactic acid (PLA).

Table 5.2: FDM-processed materials examined in the literature

Thermoplastic Materials	FDM
Acrylonitrile butadiene styrene (ABS)	[23, 26, 32–35, 37–45, 47, 52, 53, 56–59, 62–64]
High-impact polystyrene (HIPS)	[62]
Polyamide/nylon (PA)	[31, 54, 56, 60–62]
Polycarbonate (PC)	[62, 63]
PC-ABS blend	[63]
Polyether ether ketone (PEEK)	[24]
Polyethylene terephthalate glycol (PETG)	[62]
Polylactic acid (PLA)	[25, 27, 28, 36, 38, 46, 51, 55, 56, 62]
Polypropylene (PP)	[29, 56]
Polyetherimide (ULTEM)	[48, 63]
Multi-material/structural composite (MM-SC)	[30, 49, 50]

5.2.3 Testing Standards - FDM

As previously discussed, 17 different fracture testing methods were identified during the review. In the majority of the experiments, ASTM and ISO testing standards were followed. In most cases, these were useful in helping to set up the experiments and interpreting the results; however, some standards that not been traditionally applied to AM materials were found to have been used. The list of standards found is given in Table 5.3. It should also be noted that a number of the studies did not specify a standard or only used standards for part of the study. Cases were also found where ASTM and ISO standards were mixed in the same article (such as Hadidi et al. [59] and Hart et al. [42,43]). It was not always clearly specified which version of a standard was followed, so for the references in this review, it was assumed that the currently binding standard was the one in use. Figure 5.6 shows the relative distribution of the relevant ASTM and ISO standards in the surveyed literature.

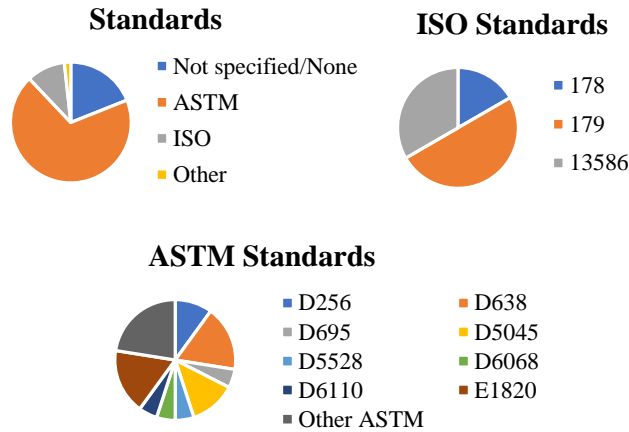


Figure 5.6: *Distribution of standards used in the reviewed literature. It should be noted that some papers used more than one standard and that many either used no standard or didn't specify which standard was followed*

Some of the standards followed are very commonly seen in the AM polymer literature (e.g., ASTM D256 [65], ASTM D638 [66], ASTM D695 [67], ASTM D790 [68], ASTM D6110 [69], ISO 178 [70], and ISO 179 [71] for general hard polymer material characterization studies. Similarly, standards such as the impact testing standards mentioned above along with ASTM D5045 [72], ASTM D6068 [73], ASTM E1820 [74], ASTM STP1359 [75], and ISO 13586 [76] are typical “general” fracture testing standards. More specialized frac-

ture standards (ASTM D1708 [77], ASTM D1876 [78], and ASTM D1938 [79]) were also found to be applied to the testing of AM polymer materials. All of these should be expected to be used during fracture testing of these materials and so their presence is not a surprise.

On the other hand, several standards were used that relate directly to polymer matrix composites (specifically ASTM D3039 [80], ASTM D3518 [81], ASTM D5528 [82], ASTM D6671 [83], and ASTM D7905 [84]). These do not seem particularly applicable to AM polymer fracture testing and their use and assumptions were not explained by the authors in most cases. These are clearly not applicable for AM-processed pure materials (especially in the case of thermoplastics), but this is also true in the case where the AM material uses a filler or fiber since the standards assume that the polymer matrix is well-understood and the only source of uncertainty is from the added composite material or fibers. In the case of all the polymer AM processes, this is not true since the structure of the AM material itself could introduce phenomena into the test results, making it difficult or impossible to accurately test the effect of the composite.

Table 5.3: Utilized standards from ASTM, ISO, and PN. Some studies did not specify a standard. For many studies, the exact version of the standard followed was not clear, so standard citations refer to the active or latest version as of May 2020.

Standard		Ref	Studies
ASTM D256	Standard Test Methods for Determining the Izod Pendulum Impact Resistance of Plastics	[65]	[30, 47, 62, 63]
ASTM D638	Standard Test Method for Tensile Properties of Plastics	[66]	[24-27, 30, 31, 54]
ASTM D695	Standard Test Method for Compressive Properties of Rigid Plastics	[67]	[24, 59]
ASTM D790	Standard Test Methods for Flexural Properties of Unreinforced and Reinforced Plastics and Electrical Insulating Materials	[68]	[24]
ASTM D792	Standard Test Methods for Density and Specific Gravity (Relative Density) of Plastics by Displacement	[85]	[37]
ASTM D1708	Standard Test Method for Tensile Properties of Plastics by Use of Microtensile Specimens	[77]	[27]

ASTM D1938	Standard Test Method for Tear-Propagation Resistance (Trouser Tear) of Plastic Film and Thin Sheet- ing by a Single-Tear Method	[79]	[57]
ASTM D3039	Standard Test Method for Tensile Properties of Poly- mer Matrix Composite Materials	[80]	[54]
ASTM D3518	Standard Test Method for In-Plane Shear Response of Polymer Matrix Composite Materials by Tensile Test of a +/- 45 Laminate	[81]	[38]
ASTM D5045	Standard Test Methods for Plane-Strain Fracture Toughness and Strain Energy Release Rate of Plas- tic Materials	[72]	[28, 35, 36, 39, 51]
ASTM D5528	Standard Test Method for Mode I Interlaminar Frac- ture Toughness of Unidirectional Fiber-Reinforced Polymer Matrix Composites	[82]	[38, 39]
ASTM D6068	Standard Test Method for Determining J-R Curves of Plastic Materials	[73]	[42, 43]
ASTM D6110	Standard Test Method for Determining the Charpy Impact Resistance of Notched Specimens of Plastics	[69]	[24, 60]
ASTM D6671	Standard Test Method for Mixed Mode I-Mode II Interlaminar Fracture Toughness of Unidirectional Fiber Reinforced Polymer Matrix Composites	[83]	[38]
ASTM D7905	Standard Test Method for Determination of the Mode II Interlaminar Fracture Toughness of Unidirectional Fiber-Reinforced Polymer Matrix Composites	[84]	[38]
ASTM E1820	Standard Tests Method for Measurements of Fracture Toughness	[74]	[33, 34, 41, 47-49, 52]
ASTM STP1359	Mixed-Mode Crack Behavior	[75]	[26]
ISO 178	Plastics – Determination of flexural properties	[70]	[29]
ISO 179	Plastics – Determination of Charpy impact properties	[71]	[29, 59, 61]
ISO 13586	Plastics – Determination of fracture toughness (GIC and KIC) - Linear elastic fracture mechanics approach	[76]	[42, 43]
PN 10045	Metallic Materials – Charpy Impact Test	[86]	[58]
Not specified			[23, 24, 32, 40, 44-46, 50, 53, 56, 64]

5.2.4 Remarks on Literature Review

In this review, the collection and discussion of information on the methods, materials, and standards provided four major outcomes which will be helpful for the remainder of this present Chapter as well as the following chapters:

- The collection and cataloging of the available data for FDM-processed polymers. This is useful immediately to help guide efforts in design-for-manufacturability (DFM) and design-for-AM (DFAM). This dataset is obviously incomplete and needs far more work, both in the collection of data and the standardization of assumptions and reporting.
- Noting and identifying gaps in the currently available fracture testing methods and data for FDM polymers.
- The demonstration of how to recognize and collect this information for other studies and domains. This will be useful for designers when reviewing experimental results or performing screening/proof-of-concept studies during design.
- To identify areas where improvements can be made in the design and reporting of fracture tests to ensure the collected information is useful for designers. From the mechanics side, better alignment with the needs of designers will also help to make the experiments more consistent and well understood by all users.

These purposes were refined during the review process and were not fully established at the beginning of the review since it was not certain what information could be found. In conclusion, this review provides a significant amount of data on the state-of-the-art of fracture testing of FDM-processed polymer materials which will help derive a logical and clear perspective on how to use this data in design practice.

In addition to more rigorous and design-focused fracture testing of other materials and standards development, there are several areas where more attention should be paid in the future. From the reviewed studies, it is clear that the most important areas are:

- Other polymer AM materials and processes, especially the common and rapidly-developing processes such as digital light processing (DLP). There is still much that is

not known about the behavior of projection-based thermoset processes and studying these from a design-under-fracture perspective could provide very useful information.

- While not covered in detail in this study, the size effect of AM materials should be studied more deeply, especially those processed using scanning-type (ST-AM) processes. There has been some research done in this area, as shown earlier in this review, but much is still not known.
- The influence of processing parameters on the fracture behavior from a design perspective.
- Material characterization and modeling of fracture behavior.
- Fracture properties of the materials relative to the number of samples and/or experimental replications, including the production of confidence intervals relevant to design.
- The true performance of commercial raw materials relative to that reported in company data sheets. Future efforts should focus on collecting the experimental information from suppliers and commercial producers and ensuring that standards and best practices are followed.
- The common testing methods discussed in this review seem to be well-represented and appropriate for AM polymers (with the current testing standard paradigm) but further development in the area of experimental design is needed. Considerations could be sampling points, the appropriateness of Taguchi, factorial, and parametric experimental designs, the minimum required number of testing specimens, reasonable expected variance in testing results, testing speeds, correction factors based on the AM-driven size effects, biases and distributions of collected data, and effective data analysis methods (parametric, such as ANOVA, or non-parametric methods).
- A rigorous analysis of the range of validity for the small-scale yielding assumption for AM polymer materials.

- Finally, the areas of research excluded from this review, especially fatigue (for which enough information exists relative to AM polymers for a separate review paper), the fracture behavior of polymer-non-polymer composites, biomaterials, adhesives, and soft or hyperelastic materials.

5.3 Design Information Gathering from Fracture Studies

5.3.1 Design Knowledge and Fracture Data

One way to define *design knowledge* is verified information, practices, and processes that enable engineers and other designers to effectively design products and systems. There are several major domains of potentially useful design knowledge that can be extracted from the results of fracture mechanics tests. As with any type of design knowledge, these can be classified as *constraints* (limitations of the design space), *advantages* (expansions of the design space), and *best practices* (expert advice, lessons-learned, or soft constraints). In this context, the term *design space* can be understood as the set of feasible final designs available to solve a particular problem; they all satisfy the objectives and each design candidate often represents different trade-offs within the design space. In the literature review presented in Section 5.2, seven areas of study were identified as potentially benefiting from the design knowledge that can be extracted from fracture data and studies [23, 27, 28, 30]:

1. *Design of material structures*: Material layout design and structural optimization for anisotropic, structured, and functionally graded standard materials and metamaterials
2. *Realistic damage assessment and prediction*
3. *Manufacturing process effects*: The influence and effect of manufacturing process-induced defects and uncertainties in materials
4. *Proper environmental use conditions*
5. *New manufacturing process development*: The need for new manufacturing processes and process variations to mitigate or take advantage of material phenomena observed during fracture testing

6. *Design quality evaluation*: Realistic performance analysis metric development, including verification/validation and design evaluation (both destructive and non-destructive)
7. *Material characterization*: Rigorous material and material system characterization

Designing with materials processed via AM can especially benefit from these perspectives. Regardless of which AM process or material is used, some anisotropy and structure at meso-scale exists in the final product [20–22]. In practice, the meso-scale features in AM materials exist between macro- and micro-scale features and are determined primarily by their relative size [27, 40].

5.3.2 From the Literature

As discussed in the introduction, fracture mechanics data can be extremely useful to consider in design, since the fracture properties are sometimes more realistic and limiting than properties such as yield stress (generally the mean value over a large number of tests). This is especially true for AM polymer materials, due to their natural structures and tendency to be more brittle than equivalent molded or machined materials. The seven domains of design knowledge offered by fracture testing data can be summarized as shown in Table 5.4.

Table 5.4: Design knowledge areas related to fracture mechanics data/experiments, with the related studies reviewed in this chapter

Domain	Description	Related Studies
Material layout design and optimization	The design of new material structures and composites, better designed and optimized using information from the observed fracture behavior. This can include both modeling of the new material structures and experimental analysis under realistic condition. The applications of this are not only in the design of structured materials, but in the use of these structured materials for more general design problems (such as the design of aerospace or medical device parts).	[26, 27, 30, 32–34, 38–40, 44, 45, 47, 49–54, 57, 60, 62, 63]

<p>Damage assessment and prediction</p>	<p>The realistic assessment of how the design under evaluation may fail from damage or how much damage can be sustained without failure. For many problems, a fracture mechanics perspective will provide a more realistic view of damage effects than basic mechanical tests and stress analysis can provide while being far easier and more practical than formal fatigue tests for many problems.</p>	<p>[23,64]</p>
<p>Influence of process-induced material defects</p>	<p>Extremely important for structured materials, since the small variations of material layout could have very dramatic effects on reliability and behavior. This can also drive the selection of manufacturing processes during design, since each process has different mechanics and some could be more appropriate for particular designs than others.</p>	<p>[27,63]</p>
<p>Environmental use conditions</p>	<p>Since basic fracture mechanics relies more on the response of the material to the input of energy [3] than the total strength of the basic material, the environmental conditions the material will experience can drastically affect its applicability and usefulness in final products. Fracture testing may be more useful in evaluating this than standard mechanical testing of the materials and products.</p>	<p>[25,51,59]</p>
<p>Design-driven process development</p>	<p>It has been observed several times in this review (e.g., Peng et al. [30], Hart et al. [43], and Hadidi et al. [59]) that the fracture behavior seen in a material or part necessitated the creation of new manufacturing processes. With the additional knowledge available using a design-driven process, this process can be used more effectively and reliably. This knowledge can be used to create processes which both take advantage of positive effects and mitigate negative ones.</p>	<p>[30,43,49,50,52,59].</p>

<p>Practical AM product performance analysis</p>	<p>Both when developing realistic design rules or heuristics and when performing verification and validation of designs, effective, clear, and consistent metrics are vital. Fracture behavior observations can be used to produce these metrics and design more effective and reliable performance tests (both destructive and non-destructive).</p>	<p>[30, 40, 49, 59]</p>
<p>New material and material system behavior characterization</p>	<p>Fracture testing methods can be used to quickly, cheaply, and reliably test new materials and material systems or composites; this is useful for both general characterization and for exploration during the product design process. Characterization methods that explore specific questions related to a design could be especially useful.</p>	<p>[24, 28, 29, 31, 35–37, 40–42, 46, 48, 51, 55–58, 61]</p>

The two main areas of contribution found represented in the reviewed literature were the material layout and design and the material characterization domains, followed by the design-driven process development. It should be noted that the reviewed papers on characterization of AM polymer materials provided more information and insight than simply reporting datasheet properties for the materials (as many characterization studies do). The structural effects of AM-processed materials (such as raster patterns and layer fusing quality), the crack growth patterns and their effects on properties, the repeatability of fracture behavior, and other important considerations were all presented. Also, it could be said that this extra layer of information collected is one of the main benefits of using fracture testing data in design, as the extra detail in inputs provides better design knowledge. In addition to the general principles discussed in Table 5.4, four other major aspects need to be considered specifically for AM polymer material design, namely (1) the design freedom, (2) the process mechanics, (3) the cost of polymer additive manufacturing and experiments, and (4) the nature and evolution of AM processes.

5.3.2.1 AM-Driven Design Freedom

The (often) near-net-shape design freedom of most AM processes allows the practical manufacturing of a wide variety of metamaterials, functionally graded materials (FGMs), lattices, solutions for 3-D topology optimization problems, and other difficult design problems. The processes do have significant manufacturability constraints, but these can be considered as constraints on the design. These constraints, the material behavior during processing, the effects of defects, and the elastic-plastic behavior of the AM polymer materials are all well understood and easily interpreted and applied during design. This aspect was widely seen in the reviewed literature, but was especially clear in the studies that dealt with the design of structured materials such those by Allum *et al.* [27], Peng *et al.* [30], Lenti [47], Gardan *et al.* [33,34,52], McLouth *et al.* [35], and Hart *et al.* [50]. The optimized layouts shown in Figure 5.7a were generated by Lenti [47] (other studies from the same research group on similar problems were found in references [26,33,34,44,52]); in this case, the designs were based on the free arrangement of the material elements deposited by FDM; only a single material was used.

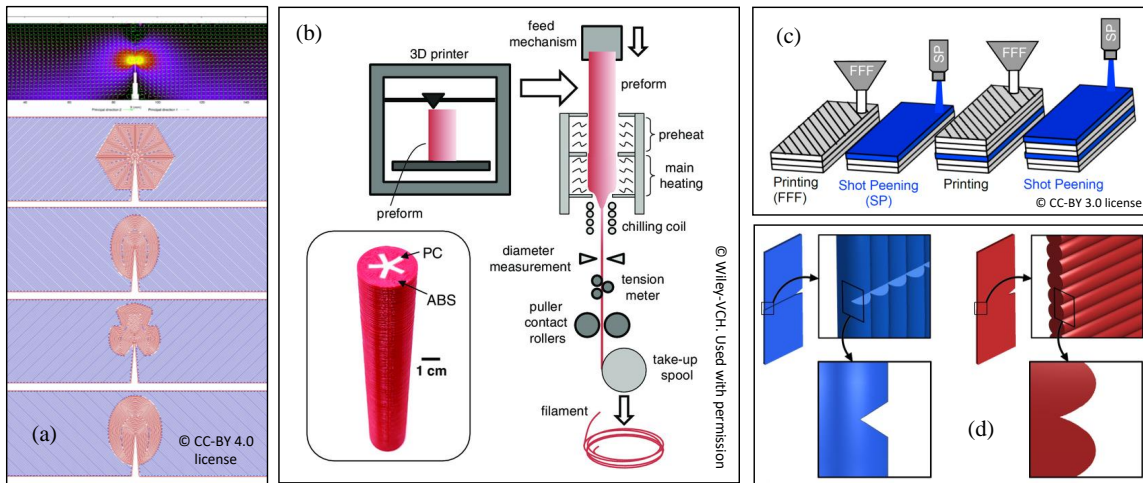


Figure 5.7: (d) Optimal material structure layouts under various objective functions [47], (b) Composite filament developed to build structural composites more efficiently [50], (c) new FDM-based manufacturing process which utilized shot peening on some layers to better control the print structure and toughen the material [59], and (d) process-induced material structure and features and their effect on fracture mechanics [27]. Panel (b) © Wiley-VCH, reproduced with permission. Panels (a) and (c) reproduced under CC-BY license. Panel (d) © Elsevier B.V., reproduced with permission.

5.3.2.2 Process Mechanics

The mechanics of AM (often best understood when using polymer AM processes due to cost and technical understanding) introduce small voids, other defects, and anisotropy into the final parts and this must be understood and accounted for during design. Different processes introduce various types of defects and knowledge of this could help drive the manufacturing process selection as well as drive design decisions. While the concept was present in several studies, the work by Allum *et al.* [27] specifically looked at the small-to-medium scale features and natural structure of FDM-fabricated materials and examined the effects on fracture mechanics. Some of the examined structural problems encountered are demonstrated in Figure 5.7d. It was found in this study that the structure of the elements (driven completely by the process mechanics of FDM) has a larger influence on the fracture behavior of the material in many cases than either the natural anisotropy of FDM materials or the polymer welding quality between the layers and elements.

5.3.2.3 Manufacturing and Experimental Costs

The cost of polymer-based AM (both in terms of raw materials and processing equipment) is much lower than for other AM materials, making it very practical and efficient to rely on experimental data to drive design instead of models and simulations. In many of the studies reviewed in this article, the large number of samples (over 1000 samples in one case) tested demonstrates this well. Therefore, evaluating the response of AM polymer materials to damage (whether fatigue is considered or not), the effects of the use environment, and realistic performance analysis using experimental results (especially fracture testing results) can provide a very detailed and effective view for designers. One of the main areas of AM technology yet to be developed is in the standards, verification/validation, and certification process for end-user parts; due to the wealth of extractable knowledge, fracture testing may have a very important role to play in developing this area, especially with the relatively low cost of physical experiments using these materials and processes.

5.3.2.4 AM Process Nature and Evolution

Design-driven process development is one of the most interesting things discovered during this review, as it is not an obvious place to look for design knowledge. However, the studies reviewed made an excellent case for the necessity of this; many AM processes exist but there are still large gaps in what is needed for specific design problems. Most AM processes are combinations and small-scale automations of traditional manufacturing processes [20–22] and therefore are not necessarily novel in themselves. For example, FDM is a combination of a traditional wire extrusion process with precise mechanical positioners (such as linear rail positioner and delta robotic arms) and control software; similarly, SLS is similar to powder metallurgy where the dense powder bed acts as the “tool” and the heat is applied selectively with a laser instead of tool pressure to generate the green parts. Therefore, as additional complex design problems are identified, new process combinations and modifications, in addition to new software and control schemes for old processes, can be developed. Refinements of existing processes can be performed as well to address problems and take advantage of potential benefits discovered. Two examples of this found in the reviewed literature were completed by Hart *et al.* [50] (Figure 5.7b) and Hadidi *et al.* [59] (Figure 5.7c). In the first case, the standard FDM process was modified slightly to deposit a dual-material filament effectively to build a structured material from two thermoplastic materials simultaneously. These two materials can have significantly different optimal processing temperatures. Once effective settings were found and the parts were post-processed, the mechanical properties (both bulk and fracture properties) were greatly improved, allowing ABS parts to be made which took advantage of the AM design freedom while also having near-molded-value mechanical properties. In the second case, a new process was developed which combined FDM with a shot-peening process; this helped to ensure that the layers were more effectively bonded and voids were reduced, greatly increasing the toughness of the printed material.

5.4 Practical Implementation in Design

As discussed throughout this chapter, a large amount of useful design knowledge and data can be extracted from fracture mechanics literature on FDM (and likely other AM processes

as well). In addition to the obviously valuable performance data offered by studying the fracture behavior of materials (especially materials that are difficult to characterize, as are most AM-processed materials), a significant amount of information valuable for decision-making is available. Most of the collected information from Table 5.4 falls into this category. From better learning how to take advantage of the process-induced material effects, to more accurate damage prediction, to illuminating the need for new manufacturing processes, and all the other important considerations, these data points can be very valuable for designers.

However, the FDM fracture experiments and their documentation could be improved in several areas in order to provide more value to practicing designers. In addition to the general recommendation to consider gaps in the literature when selecting testing methods, materials, and processes, some recommendations for future FDM fracture studies are:

1. ASTM and ISO standards were used in the majority of the reviewed studies, but the standards used did not always align well with the testing needs of AM materials. Care should be taken to use only the most applicable standards or to very carefully describe the experimental methods used (perhaps as supplemental materials) in lieu of using a standard which may not match the conditions of the experiment. Testing standards for these materials need to be developed and best practices during testing should be recorded carefully in publications to serve as a basis for new standards.
2. Some studies reported values for material properties which are questionable based on the standards followed. Most standards contain criteria for sample geometry, behavior, and performance that must be met to validly use the standard. While not calling out any specific works, there were several cases encountered which failed to fully test the criteria for validity before reporting data. While the standards may not accurately collect or test the behavior of the AM-processed materials, it is important that the standards either be followed exactly or not used at all to avoid any confusion and inaccurate data in the literature.
3. The general variability in properties is very high for AM materials, so some initial work should be done before any new experiment to understand the expected range of performance. This should be carefully compared with the actual data and suspected

or observed reasons for the variability reported with the data set. If the results are extreme outliers (as observed in the property tables in the Supplemental Materials) (such as an order of magnitude lower than expected), this may indicate mistakes in the experimental procedure or execution. At a minimum, additional replications of the experiments should be done to verify the unexpected value. It is expected over time that researchers and practitioners will converge on accepted confidence intervals for AM properties; however, the field is clearly far from this point and so everything should be checked and all experiments should be started by understanding the range of expected property values.

4. It was observed that in many cases, experimental standards were used to set up experiments and provide sample geometry, but were not used to interpret the results. A number of the standards also provide correction factors and sensitivity analyses (ASTM D256 [65] is a good example) which were not used and could have enhanced the rigor of the studies if used.
5. When possible, the mixing of ASTM and ISO standards in a single study should be avoided as they sometimes ask for different perspectives, numbers of samples, and interpretation guidelines.
6. When standards are used, this should always be reported. Likewise, when a standard is not used, this should be explicitly and prominently disclosed.
7. It was noted in a large number of the reviewed studies that the full experimental details were not given (it was especially problematic that many studies did not explicitly state how many samples were actually tested), preferring to focus the main discussion on other aspects of the study. It is vital for the generation of useful design knowledge that all the details are given when reporting the study.
8. It was noted in several studies that FDM has a sample-size effect but this was not considered by most of the other studies. Therefore, details such as the shell-infill ratio for ST-AM processes and the layer thicknesses should be given in every study. It should also be considered by experimenters that smaller samples will have larger

material elements (such as the beads or roads in FDM) relative to the whole sample size; this should be accounted for or large samples should be used.

9. It was observed in some of the studies that the shown samples had unnecessary manufacturing defects due to poor tuning or poor quality raw filament, which increased the variability of the observed properties. FDM machines should be tuned properly and the samples should be inspected before testing.
10. It is well known that different raw material sources vary considerably in quality; if characterization studies cannot be carried out for each batch of samples or set of parameters, effort should be made to ensure that the same material and supplier are used so the results will at least be correct relative to each experiment. All details regarding material source, quality, and such information should be carefully recorded and reported along with the experimental results.
11. It was not explicitly stated in many of the studies how and under what conditions the samples were conditioned prior to testing. This is vital information for FDM samples and should always be observed. Most of the standards for testing of polymer materials have specific and clear instructions for conditioning the samples before testing, which generally involved keeping them a stable temperature, humidity, and pressure for a specified number of hours between preparation and testing.

5.5 Closing Remarks

One of the best ways to collect useful design data, guided by the discussion presented in this chapter, is via carefully-designed physical experiments. When this is possible to do for a specific design process or life cycle, it can provide extremely high-quality design data that is set up from the beginning to answer specific questions. While literature reviews are very useful and provide great insight into design questions at minimal cost to the stakeholders (other than time cost), it is very rare that the collected data will be able to exactly answer the design questions. In order to explore this further and provide a useful and high-quality data set for the design problems in this dissertation, Part 2 of this work on fracture mechanics will be presented in Chapter 6.

Copyright Acknowledgement: As of April 10, 2021, the main text of this chapter has not been officially published nor has the copyright been assigned to anyone but the author. Some individual figures are the property of their copyright owners and are reproduced here with permission. See the official copyright permission forms attached in the supplemental materials.

- Figure 5.2a © Elsevier B.V. and reproduced with permission. The official copyright permission form can be found in the supplemental materials.
- Figure 5.3a © Elsevier B.V. and reproduced with permission. The official copyright permission form can be found in the supplemental materials.
- Figure 5.5c © IMechE/Sage. According to the Sage copyright license terms, authors of original materials do not need a specific copyright clearance to reuse their own figures as long as the owner of the copyright is clearly specified and the published paper cited.
- Figure 5.7b © Wiley-VCH and reproduced with permission. The official copyright permission form can be found in the supplemental materials.
- Figure 5.7d © Elsevier B.V. and reproduced with permission. The official copyright permission form can be found in the supplemental materials.
- All other figures in this chapter were originally published under a CC-BY license and appropriately cited, were original to this work, or were from official US Government documents and therefore not subject to copyright in the United States.

Chapter 5 Bibliography

- [1] N. V. Banichuk, S. Y. Ivanova, and F. Ragnedda, “Design of fracture resistant structures,” *International Journal of Fracture*, vol. 150, pp. 213–220, Mar. 2008.
- [2] C. Brooks and A. Choudhury, *Failure Analysis of Engineering Materials*. Blacklick, OH, USA: McGraw-Hill, 2002.
- [3] T. Anderson, *Fracture Mechanics: Fundamentals and Applications*. Boca Raton, FL, USA: CRC Press, 4th ed., 2012.
- [4] M. Ishikawa, H. Ogawa, and I. Narisawa, “Brittle fracture in glassy polymers,” *Journal of Macromolecular Science, Part B*, vol. 19, pp. 421–443, June 1981.
- [5] A. Pineau, A. Benzerga, and T. Pardoen, “Failure of metals I: Brittle and ductile fracture,” *Acta Materialia*, vol. 107, pp. 424–483, Apr. 2016.
- [6] A. Dasgupta and J. Hu, “Failure mechanism models for plastic deformation,” *IEEE Transactions on Reliability*, vol. 41, pp. 168–174, June 1992.
- [7] R. Lapovok, A. Pougis, V. Lemiale, D. Orlov, L. S. Toth, and Y. Estrin, “Severe plastic deformation processes for thin samples,” *Journal of Materials Science*, vol. 45, pp. 4554–4560, Mar. 2010.
- [8] C. Mischke, “A method of relating factor of safety and reliability,” *Journal of Engineering for Industry*, vol. 92, pp. 537–541, Aug. 1970.
- [9] J.-C. Sagot, V. Gouin, and S. Gomes, “Ergonomics in product design: safety factor,” *Safety Science*, vol. 41, pp. 137–154, Mar. 2003.
- [10] N. Crilly, J. Moultrie, and P. Clarkson, “Seeing things: consumer response to the visual domain in product design,” *Design Studies*, vol. 25, pp. 547–577, Nov. 2004.
- [11] X. Teng, H. Mae, Y. Bai, and T. Wierzbicki, “Pore size and fracture ductility of aluminum low pressure die casting,” *Engineering Fracture Mechanics*, vol. 76, pp. 983–996, May 2009.
- [12] C. Zweben, “Overview of advanced composites for thermal management,” in *Proceedings of the 4th International Symposium on Advanced Packaging Materials Processes, Properties and Interfaces (Cat. No.98EX153)*, IEEE, 1998.

- [13] N. Shah, M. Ul-Islam, W. A. Khattak, and J. K. Park, "Overview of bacterial cellulose composites: A multipurpose advanced material," *Carbohydrate Polymers*, vol. 98, pp. 1585–1598, Nov. 2013.
- [14] M. Osanov and J. K. Guest, "Topology optimization for architected materials design," *Annual Review of Materials Research*, vol. 46, pp. 211–233, July 2016.
- [15] S. Shan, S. H. Kang, J. R. Raney, P. Wang, L. Fang, F. Candido, J. A. Lewis, and K. Bertoldi, "Multistable architected materials for trapping elastic strain energy," *Advanced Materials*, vol. 27, pp. 4296–4301, June 2015.
- [16] S. Natarajan and G. Manickam, "Bending and vibration of functionally graded material sandwich plates using an accurate theory," *Finite Elements in Analysis and Design*, vol. 57, pp. 32–42, Sept. 2012.
- [17] D. Moritz, C. Wang, G. L. Nelson, H. Lin, A. M. Smith, B. Howe, and J. Heer, "Formalizing visualization design knowledge as constraints: Actionable and extensible models in draco," *IEEE Transactions on Visualization and Computer Graphics*, vol. 25, pp. 438–448, Jan. 2019.
- [18] G. Peng, H. Wang, H. Zhang, Y. Zhao, and A. L. Johnson, "A collaborative system for capturing and reusing in-context design knowledge with an integrated representation model," *Advanced Engineering Informatics*, vol. 33, pp. 314–329, Aug. 2017.
- [19] A. Drechsler and A. R. Hevner, "Utilizing, producing, and contributing design knowledge in DSR projects," in *Designing for a Digital and Globalized World*, pp. 82–97, Springer International Publishing, 2018.
- [20] N. Guo and M. C. Leu, "Additive manufacturing: technology, applications and research needs," *Frontiers of Mechanical Engineering*, vol. 8, no. 3, pp. 215–243, 2013.
- [21] I. Gibson, D. Rosen, and B. Stucker, *Additive Manufacturing Technologies: 3D Printing, Rapid Prototyping, and Direct Digital Manufacturing*. Springer, 2016.
- [22] M. K. Thompson, G. Moroni, T. Vaneker, G. Fadel, R. I. Campbell, I. Gibson, A. Bernard, J. Schulz, P. Graf, B. Ahuja, and F. Martina, "Design for additive manufacturing: Trends, opportunities, considerations, and constraints," *CIRP Annals*, vol. 65, no. 2, pp. 737–760, 2016.
- [23] S. Guessasma, S. Belhabib, H. Nouri, and O. B. Hassana, "Anisotropic damage inferred to 3D printed polymers using fused deposition modelling and subject to severe compression," *European Polymer Journal*, vol. 85, pp. 324–340, Dec. 2016.
- [24] K. M. Rahman, T. Letcher, and R. Reese, "Mechanical properties of additively manufactured PEEK components using fused filament fabrication," in *Volume 2A: Advanced Manufacturing*, American Society of Mechanical Engineers, Nov. 2015.

- [25] A.-H. I. Mourad, A. H. Idrisi, J. V. Christy, D. T. Thekkuden, H. A. Jassmi, A. S. Ghazal, M. M. Syam, and O. D. A. A. A. Qadi, “Mechanical performance assessment of internally-defected materials manufactured using additive manufacturing technology,” *Journal of Manufacturing and Materials Processing*, vol. 3, p. 74, Aug. 2019.
- [26] P. Lanzillotti, J. Gardan, A. Makke, and N. Recho, “Enhancement of fracture toughness under mixed mode loading of ABS specimens produced by 3D printing,” *Rapid Prototyping Journal*, vol. 25, pp. 679–689, May 2019.
- [27] J. Allum, A. Gleadall, and V. V. Silberschmidt, “Fracture of 3D-printed polymers: Crucial role of filament-scale geometric features,” *Engineering Fracture Mechanics*, vol. 224, p. 106818, Feb. 2020.
- [28] E. A. Papon and A. Haque, “Fracture toughness of additively manufactured carbon fiber reinforced composites,” *Additive Manufacturing*, vol. 26, pp. 41–52, Mar. 2019.
- [29] M. Spoerk, C. Savandaiah, F. Arbeiter, G. Traxler, L. Cardon, C. Holzer, and J. Sapkota, “Anisotropic properties of oriented short carbon fibre filled polypropylene parts fabricated by extrusion-based additive manufacturing,” *Composites Part A: Applied Science and Manufacturing*, vol. 113, pp. 95–104, Oct. 2018.
- [30] F. Peng, Z. Zhao, X. Xia, M. Cakmak, and B. D. Vogt, “Enhanced impact resistance of three-dimensional-printed parts with structured filaments,” *ACS Applied Materials & Interfaces*, vol. 10, pp. 16087–16094, Apr. 2018.
- [31] H. Li, S. Zhang, Z. Yi, J. Li, A. Sun, J. Guo, and G. Xu, “Bonding quality and fracture analysis of polyamide 12 parts fabricated by fused deposition modeling,” *Rapid Prototyping Journal*, vol. 23, pp. 973–982, Oct. 2017.
- [32] A. Khatri and A. Adnan, “Effect of raster orientation on fracture toughness properties of 3D printed ABS materials and structures,” in *Volume 9: Mechanics of Solids, Structures and Fluids; NDE, Diagnosis, and Prognosis*, American Society of Mechanical Engineers, Nov. 2016.
- [33] J. Gardan, A. Makke, and N. Recho, “A method to improve the fracture toughness using 3D printing by extrusion deposition,” *Procedia Structural Integrity*, vol. 2, pp. 144–151, 2016.
- [34] J. Gardan, “Method for characterization and enhancement of 3D printing by binder jetting applied to the textures quality,” *Assembly Automation*, vol. 37, no. 2, pp. 162–169, 2017.
- [35] T. D. McLouth, J. V. Severino, P. M. Adams, D. N. Patel, and R. J. Zaldivar, “The impact of print orientation and raster pattern on fracture toughness in additively manufactured ABS,” *Additive Manufacturing*, vol. 18, pp. 103–109, Dec. 2017.
- [36] F. Arbeiter, M. Spoerk, J. Wiener, A. Gosch, and G. Pinter, “Fracture mechanical characterization and lifetime estimation of near-homogeneous components produced by fused filament

- fabrication,” *Polymer Testing*, vol. 66, pp. 105–113, Apr. 2018.
- [37] N. Aliheidari, R. Tripuraneni, A. Ameli, and S. Nadimpalli, “Fracture resistance measurement of fused deposition modeling 3D printed polymers,” *Polymer Testing*, vol. 60, pp. 94–101, July 2017.
- [38] A. S. Khan, A. Ali, G. Hussain, and M. Ilyas, “An experimental study on interfacial fracture toughness of 3-D printed ABS/CF-PLA composite under mode I, II, and mixed-mode loading,” *Journal of Thermoplastic Composite Materials*, p. 089270571987486, Sept. 2019.
- [39] D. Young, N. Wetmore, and M. Czabaj, “Interlayer fracture toughness of additively manufactured unreinforced and carbon-fiber-reinforced acrylonitrile butadiene styrene,” *Additive Manufacturing*, vol. 22, pp. 508–515, Aug. 2018.
- [40] N. Aliheidari, J. Christ, R. Tripuraneni, S. Nadimpalli, and A. Ameli, “Interlayer adhesion and fracture resistance of polymers printed through melt extrusion additive manufacturing process,” *Materials & Design*, vol. 156, pp. 351–361, Oct. 2018.
- [41] R. Ghandriz, K. Hart, and J. Li, “Extended finite element method (XFEM) modeling of fracture in additively manufactured polymers,” *Additive Manufacturing*, vol. 31, p. 100945, Jan. 2020.
- [42] K. R. Hart and E. D. Wetzel, “Fracture behavior of additively manufactured acrylonitrile butadiene styrene (ABS) materials,” *Engineering Fracture Mechanics*, vol. 177, pp. 1–13, May 2017.
- [43] K. R. Hart, R. M. Dunn, J. M. Sietins, C. M. H. Mock, M. E. Mackay, and E. D. Wetzel, “Increased fracture toughness of additively manufactured amorphous thermoplastics via thermal annealing,” *Polymer*, vol. 144, pp. 192–204, May 2018.
- [44] P. Lanzillotti, J. Gardan, A. Makke, and N. Recho, “Strengthening in fracture toughness of a smart material manufactured by 3D printing,” *IFAC-PapersOnLine*, vol. 51, no. 11, pp. 1353–1358, 2018.
- [45] M. Rabbi, V. Chalivendra, and D. Li, “A novel approach to increase dynamic fracture toughness of additively manufactured polymer,” *Experimental Mechanics*, vol. 59, pp. 899–911, Mar. 2019.
- [46] A. E. Patterson and J. T. Allison, “Manufacturability constraint formulation for design under hybrid additive-subtractive manufacturing,” in *ASME IDETC: Volume 4: 23rd Design for Manufacturing and the Life Cycle Conference*, ASME, 2018.
- [47] A. Lenti, “Fracture toughness assessment using digital image correlation in additive manufacturing,” Master’s thesis, Polytechnic of Turin, Turin, Italy, 2019. Masters Thesis - Mechanical Engineering.

- [48] G. Taylor, S. Anandan, D. Murphy, M. Leu, and K. Chandrashekhara, “Fracture toughness of additively manufactured ULTEM 1010,” *Virtual and Physical Prototyping*, vol. 14, pp. 277–283, Dec. 2018.
- [49] R. M. Dunn, K. R. Hart, and E. D. Wetzel, “Improving fracture strength of fused filament fabrication parts via thermal annealing in a printed support shell,” *Progress in Additive Manufacturing*, vol. 4, pp. 233–243, Apr. 2019.
- [50] K. R. Hart, R. M. Dunn, and E. D. Wetzel, “Tough, additively manufactured structures fabricated with dual-thermoplastic filaments,” *Advanced Engineering Materials*, p. 1901184, Dec. 2019.
- [51] Y. Song, Y. Li, W. Song, K. Yee, K.-Y. Lee, and V. Tagarielli, “Measurements of the mechanical response of unidirectional 3D-printed PLA,” *Materials & Design*, vol. 123, pp. 154–164, June 2017.
- [52] J. M. Djouda, D. Gallitelli, M. Zouaoui, A. Makke, J. Gardan, N. Recho, and J. Crépin, “Local scale fracture characterization of an advanced structured material manufactured by fused deposition modeling in 3D printing,” *Frattura ed Integrità Strutturale*, vol. 14, p. 534–540, Dec. 2019.
- [53] J. Li, S. Yang, D. Li, and V. Chalivendra, “Numerical and experimental studies of additively manufactured polymers for enhanced fracture properties,” *Engineering Fracture Mechanics*, vol. 204, pp. 557–569, Dec. 2018.
- [54] F. Akasheh and H. Aglan, “Fracture toughness enhancement of carbon fiber-reinforced polymer composites utilizing additive manufacturing fabrication,” *Journal of Elastomers & Plastics*, vol. 51, pp. 698–711, Dec. 2018.
- [55] A. Ahmed and L. Susmel, “Additively manufactured PLA under static loading: strength/cracking behaviour vs. deposition angle,” *Procedia Structural Integrity*, vol. 3, pp. 498–507, 2017.
- [56] I. Cuesta, E. Martinez-Pañeda, A. Díaz, and J. Alegre, “The Essential Work of Fracture parameters for 3D printed polymer sheets,” *Materials & Design*, vol. 181, p. 107968, Nov. 2019.
- [57] C. S. Davis, K. E. Hillgartner, S. H. Han, and J. E. Seppala, “Mechanical strength of welding zones produced by polymer extrusion additive manufacturing,” *Additive Manufacturing*, vol. 16, pp. 162–166, Aug. 2017.
- [58] F. Gorski, W. Kuczko, and R. Wichniarek, “Impact strength of ABS parts manufactured using fused deposition modeling technology,” *Archives of Mechanical Technology and Automation*, vol. 34, no. 1, pp. 3–12, 2014.
- [59] H. Hadidi, B. Mailand, T. Sundermann, E. Johnson, G. Madireddy, M. Negahban, L. Delbreilh, and M. Sealy, “Low velocity impact of ABS after shot peening predefined layers during additive

- manufacturing,” *Procedia Manufacturing*, vol. 34, pp. 594–602, 2019.
- [60] M. Caminero, J. Chacón, I. García-Moreno, and G. Rodríguez, “Impact damage resistance of 3D printed continuous fibre reinforced thermoplastic composites using fused deposition modelling,” *Composites Part B: Engineering*, vol. 148, pp. 93–103, Sept. 2018.
- [61] E. Yasa, “Anisotropic impact toughness of chopped carbon fiber reinforced nylon fabricated by material-extrusion-based additive manufacturing,” *Anadolu University Journal of Science and Technology-A Applied Sciences and Engineering*, vol. 20, pp. 195–203, June 2019.
- [62] A. E. Patterson, T. R. Pereira, J. T. Allison, and S. L. Messimer, “IZOD impact properties of full-density fused deposition modeling polymer materials with respect to raster angle and print orientation,” *Proceedings of the Institution of Mechanical Engineers, Part C: Journal of Mechanical Engineering Science*, p. 095440621984038, Apr. 2019.
- [63] D. A. Roberson, A. R. T. Perez, C. M. Shemelya, A. Rivera, E. MacDonald, and R. B. Wicker, “Comparison of stress concentrator fabrication for 3D printed polymeric izod impact test specimens,” *Additive Manufacturing*, vol. 7, pp. 1–11, July 2015.
- [64] H. Baqasah, F. He, B. A. Zai, M. Asif, K. A. Khan, V. K. Thakur, and M. A. Khan, “In-situ dynamic response measurement for damage quantification of 3d printed ABS cantilever beam under thermomechanical load,” *Polymers*, vol. 11, p. 2079, Dec. 2019.
- [65] ASTM, “D256 - 10(2018): Standard Test Methods for Determining the Izod Pendulum Impact Resistance of Plastics,” standard, ASTM International, West Conshohocken, PA, 2018.
- [66] ASTM, “ASTM D638 - 14: Standard Test Method for Tensile Properties of Plastics,” standard, ASTM International, West Conshohocken, PA, 2014.
- [67] ASTM, “D695 - 15: Standard Test Method for Compressive Properties of Rigid Plastics,” standard, ASTM International, West Conshohocken, PA, 2015.
- [68] ASTM, “D790 - 17: Standard Test Methods for Flexural Properties of Unreinforced and Reinforced Plastics and Electrical Insulating Materials,” standard, ASTM International, West Conshohocken, PA, 2017.
- [69] ASTM, “D6110 - 18: Standard Test Method for Determining the Charpy Impact Resistance of Notched Specimens of Plastics,” standard, ASTM International, West Conshohocken, PA, 2018.
- [70] ISO, “178:2019: Plastics — Determination of flexural properties,” standard, International Organization for Standardization, Geneva, CH, 2019.
- [71] ISO, “179:2010: Plastics — Determination of Charpy impact properties,” standard, International Organization for Standardization, Geneva, CH, 2010.

- [72] ASTM, “D5045 - 14: Standard Test Methods for Plane-Strain Fracture Toughness and Strain Energy Release Rate of Plastic Materials,” standard, ASTM International, West Conshohocken, PA, 2014.
- [73] ASTM, “D6068 - 10(2018): Standard Test Method for Determining J-R Curves of Plastic Materials,” standard, ASTM International, West Conshohocken, PA, 2018.
- [74] ASTM, “E1820 - 20: Standard Test Method for Measurement of Fracture Toughness,” standard, ASTM International, West Conshohocken, PA, 2020.
- [75] ASTM, “STP1359: Mixed-Mode Crack Behavior,” standard, ASTM International, West Conshohocken, PA, 1999.
- [76] ISO, “13586:2018: Plastics – Determination of fracture toughness (GIC and KIC) – Linear elastic fracture mechanics (LEFM) approach,” standard, International Organization for Standardization, Geneva, CH, 2018.
- [77] ASTM, “D1708 - 18: Standard Test Method for Tensile Properties of Plastics by Use of Microtensile Specimens,” standard, ASTM International, West Conshohocken, PA, 2018.
- [78] ASTM, “D1876 - 08(2015)e1: Standard Test Method for Peel Resistance of Adhesives (T-Peel Test),” standard, ASTM International, West Conshohocken, PA, 2015.
- [79] ASTM, “D1938 - 19: Standard Test Method for Tear-Propagation Resistance (Trouser Tear) of Plastic Film and Thin Sheeting by a Single-Tear Method,” standard, ASTM International, West Conshohocken, PA, 2019.
- [80] ASTM, “D3039/D3039M - 17: Standard Test Method for Tensile Properties of Polymer Matrix Composite Materials,” standard, ASTM International, West Conshohocken, PA, 2017.
- [81] ASTM, “D3518/D3518M - 18: Standard Test Method for In-Plane Shear Response of Polymer Matrix Composite Materials by Tensile Test of a $\pm 45^\circ$ Laminate,” standard, ASTM International, West Conshohocken, PA, 2018.
- [82] ASTM, “D5528 - 13: Standard Test Method for Mode I Interlaminar Fracture Toughness of Unidirectional Fiber-Reinforced Polymer Matrix Composites,” standard, ASTM International, West Conshohocken, PA, 2013.
- [83] ASTM, “D6671/D6671M - 19: Standard Test Method for Mixed Mode I-Mode II Interlaminar Fracture Toughness of Unidirectional Fiber Reinforced Polymer Matrix Composites,” standard, ASTM International, West Conshohocken, PA, 2019.
- [84] ASTM, “D7905/D7905M - 19e1: Standard Test Method for Determination of the Mode II Interlaminar Fracture Toughness of Unidirectional Fiber-Reinforced Polymer Matrix Composites,” standard, ASTM International, West Conshohocken, PA, 2019.

- [85] ASTM, “D792 - 13: Standard Test Methods for Density and Specific Gravity (Relative Density) of Plastics by Displacement,” standard, ASTM International, West Conshohocken, PA, 2013.
- [86] PN, “EN 10045:1994: Metallic Materials - Charpy Impact Test,” standard, International Organization for Standardization, Geneva, CH, 1994.

Chapter 6

FDM FRACTURE MECHANICS - PHYSICAL EXPERIMENTS

Collaborator Acknowledgement: The author gratefully acknowledges the contributions, advice, direction, and feedback from the following people on the work presented in this chapter: **Charul Chadha** (assistance with some of the experiments and discussion about standards and experimental approaches); **Dr. Iwona M. Jasiuk** (extensive discussion and advice on experimental methods, assumptions, and data interpretation); **Tais Rocha Pereira** (for helping complete the Series VII experiments).

This chapter may contain previously published text and figures, which are reproduced with the permission of the copyright holders. See the copyright statement and list of references at the end of the chapter.

6.1 Introduction

Continuing from the theoretical discussion and background exploration in Chapter 5, this chapter presents the results of a set of physical experiments. The experiments had three main goals, namely to (1) collect material properties, (2) observe the fracture behavior

in various structured FDM-processed materials (from both qualitative and quantitative perspectives), and (3) derive a set of assumptions and design rules which will be used to design thermoplastic FDM-driven MPDSMs in Chapter 7 and Chapter 8. As previously discussed, the materials selected were ABS, polycarbonate, and PLA (Table 6.1). The print settings shown in Table 6.2 were used for all prints unless otherwise specified for a particular experiment. All samples were conditioned according to typical ASTM standards for a minimum of 40 hours in a room at a temperature of 22 – 24° C and relative humidity of 40 – 60% unless otherwise noted for a particular experiment.

Table 6.1: Material and source.

Material	Source	Color	Vendor
Acrylonitrile butadiene styrene (ABS)	Hatchbox	Red	Amazon.com
Polycarbonate (PC)	Hatchbox	Grey	Amazon.com
Polylactic acid (PLA)	Hatchbox	Dark blue	Amazon.com

Table 6.2: Basic printing parameters for most experiments in Chapter 6.

Parameter	ABS	PC	PLA
Extrusion Temperature (°C)	235	250	210
Bed Temperature (°C)	70	70	60
Print Speed (mm/s)	50	50	50
Nominal Density (%)	100%	100%	100%
Acceleration (mm/s^2)	400	400	400
Jerk (mm/s^2)	8	8	8

In most characterization studies on FDM-processed materials, all three of the associated printing orientations are studied. In this dissertation, the main objective is to develop useful design methods for MPDSMs under fracture and so the appropriate printing orientation or orientations offer significant design freedom. Most standard mechanical testing samples (such as those shown in Figure 6.1) are much thinner than they are tall. It is possible in some cases to design the mesostructure for the horizontal orientation (at least for plane strain conditions), but often the shell is too large and makes this impossible. It is not usually possible to design the structure in the vertical print direction, beyond perhaps changing the contact area between layers. Therefore, given the geometric considerations and objectives of the work, it was decided that the experiments which will be used to col-

lect design knowledge or data should be done using the flat orientation only. This allows the most design freedom, allows easier testing and observation of the fracture behavior, and is more efficient and less wasteful with materials and experimental time. For the main experiments examining the solid materials, ASTM 5045 [1] was used; for this standard, both the compact tension (CT) and single-edge notched bending (SENB) tests were available and can provide essentially the same information. Since limited time was available (due to COVID-19-related campus access restrictions), as well as a limited amount of raw filament and print bed size restrictions, it was decided that the ASTM D5045 tests should be done using flat-printed CT samples.

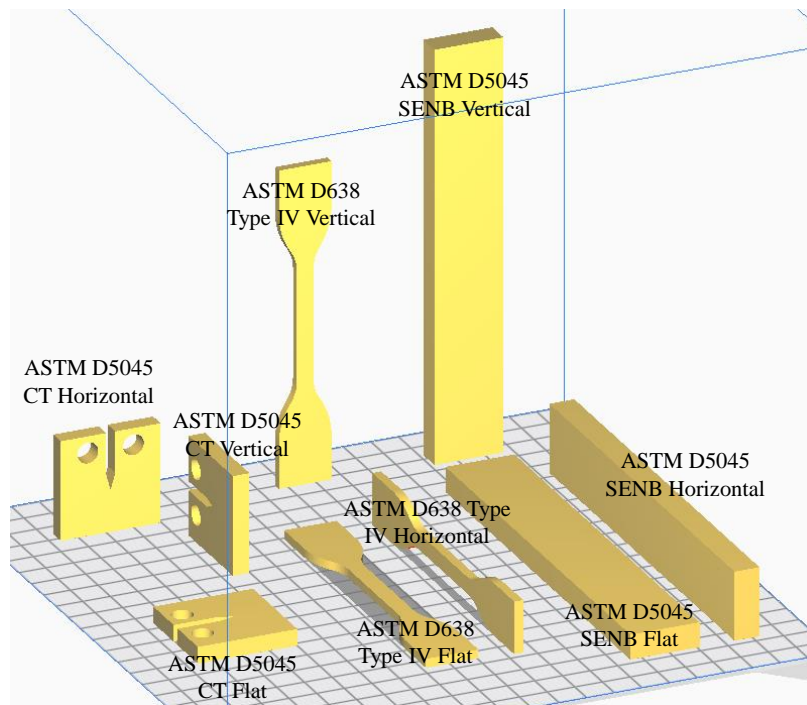


Figure 6.1: Some example common mechanical testing samples in the standard print orientations.

This chapter was mainly focused on documenting all of the experimental setups, the equipment used, and the experimental results, beginning with descriptions of the standard and new equipment used (Section 6.2). The testing series completed are then described: Series I on basic material characterization (Section 6.3), Series II on the properties of FDM-printed fibers (Section 6.4), Series III on FDM-printed thin films (Section 6.5), Series IV on sample size sensitivity (Section 6.6), Series V on pre-cracking sensitivity (Section 6.7), Series

VI on the fracture behavior versus element layout (Section 6.8), and Series VII on impact testing (Section 6.9). Finally, Section 6.10 provides some closing remarks for the chapter. Since this chapter is mainly concerned with collecting and presenting the experimental data, the bulk of the discussion and exploration of the results will be done in Chapter 7, where it will be useful for deriving design rules for the three materials in use.

6.2 Hardware, Equipment, and Software Used

6.2.1 FDM Printers

Two printers were used for various experiments (never mixed on an experiment), a standard aluminum-frame Prusa i3 with an expanded print bed and a Prusa i4 in a non-heated enclosure (see Section 6.2.2). The printers are shown in Figure 6.2.

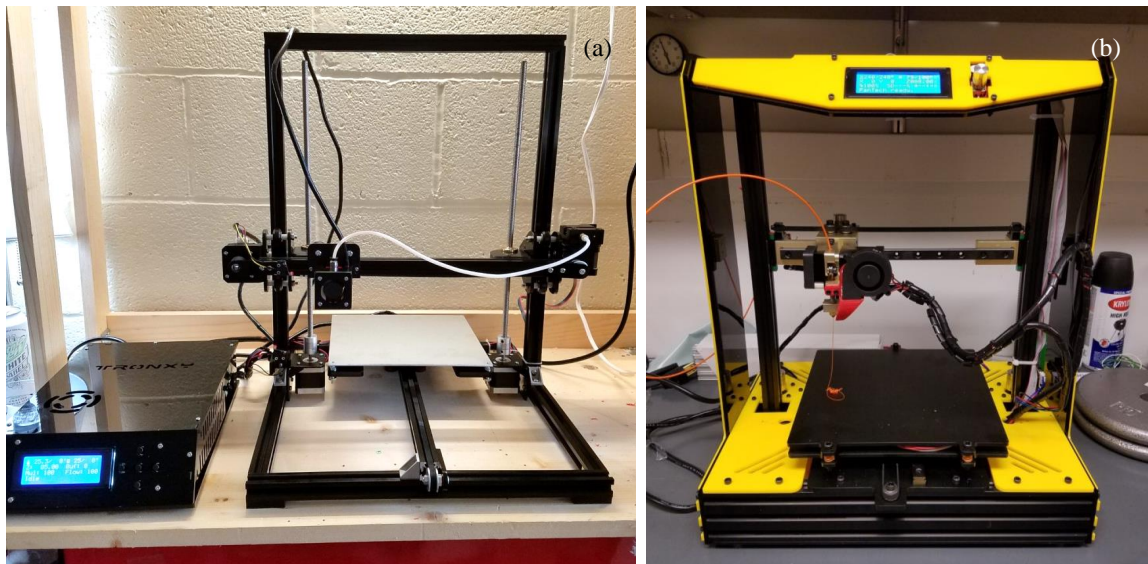


Figure 6.2: (a) Prusa i3 and (b) Prusa i4 FDM machines used in this chapter.

6.2.2 Printing Enclosure

To provide a secure environment for the printing of the samples, prevent warping and residual stress development, and make the printing safer in an area where other people were working (especially when printing ABS), an enclosure was built (Figure 6.3). This enclosure was well-insulated, well-sealed when the doors were closed, and had the capacity

to be heated during use. However, it was found that heating (beyond the printer heat itself) was not necessary and so no additional heat was used. All of the CT and tensile testing samples described in this chapter were printed inside of this enclosure, while the films and fibers study specimens and many of the other case studies in this dissertation were printed using the Prusa i3. The enclosure was set up in the author's home to ensure access to printing over several months when campus access was limited.



Figure 6.3: Printing enclosure.

6.2.3 Modeling and Design Software

As discussed extensively in Chapter 1, one of the major requirements for the work described in this dissertation was that only commercially-available software was to be used. This requirement was put in place to ensure that all of the presented results are easily applicable and reproducible by practicing engineers and engineering students. For all of the computer-aided design (CAD) work, including making testing specimens and models for figures, was

done using Autodesk[®] Inventor[®] 2020 Professional. This was supplemented as needed with the Autodesk Nastran (for finite element analysis) and Autodesk[®] Shape Generator (for topology optimization) tools. All of the pre-processing was done using Ultimaker[®] Cura[®] 4.2.1. G-code generation was done using the Autodesk and Cura tools in conjunction; a full tutorial on setting up and running the g-code layout method shown in this dissertation is provided in Appendix B.

6.2.4 Notching and Pre-Cracking

Notching of the samples was done either by printing the notch into the sample (Figure 6.4a) or by machining it into the sample later using a standard milling machine with a 30° engraving bit (Figure 6.4c). Samples that were printed retained their shell around the notch and those that were machined had the infill of each sample exposed; this distinction was intentional and will be discussed later in this chapter and in Chapter 7.

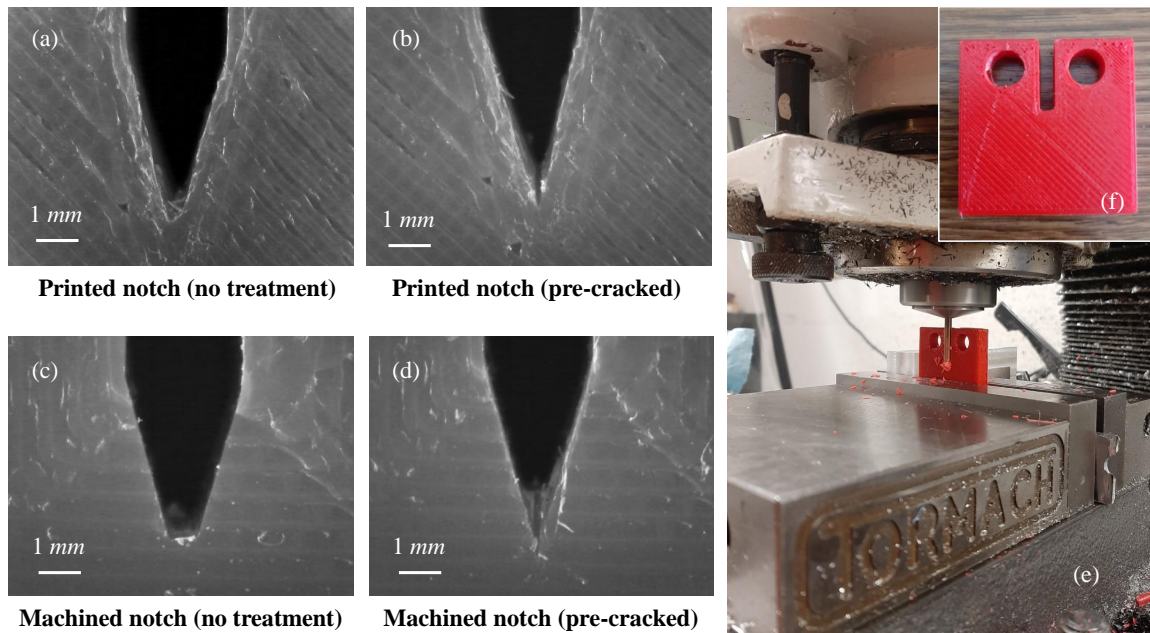


Figure 6.4: Example notches, (a) printed with no treatment, (b) printed and pre-cracked, (c) machined with no treatment, (d) machined and pre-cracked, and (e) notch machining process with (f) example ABS specimen before notching.

Pre-cracking of samples (when needed) was done using a standard razor blade with

the pre-cracks gently cut into the material. Originally, a desktop-sized pre-cracking device (described in [2]) was developed to help with this task but it was found to be unreliable with the polycarbonate samples since the material was so brittle. Therefore, the very gentle hand-held razor blade method was used to ensure consistency. For future work using more ductile materials, the device described above (or similar) should be used. Figures 6.4b and 6.4d show examples pre-cracking for printed and machined notches, respectively. A sample in the process of being machined is shown in Figure 6.4e. Different methods were developed specifically for the film and impact testing experiments since they needed specialized notches; these notching device are discussed in Section 6.5 and 6.9, respectively.

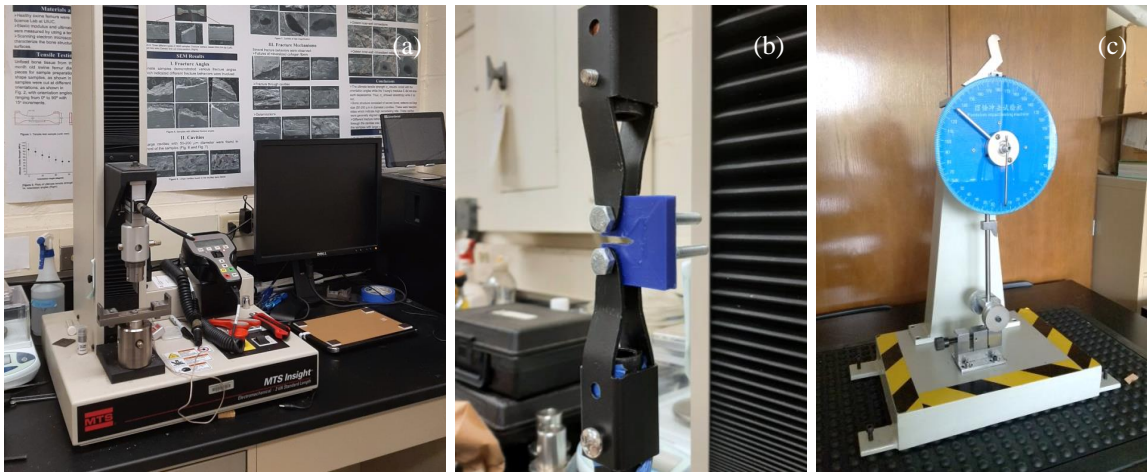


Figure 6.5: (a) MTS universal testing machine, (b) compact tension (CT) sample tool, and (c) impact testing machine with IZOD testing clamps.

6.2.5 Mechanical Testing

All mechanical testing was done using an MTS universal testing machine (Figure 6.5a) fitted with a 2 KN load cell and standard clamps for tensile testing and film testing, an extensometer, and 3-point bend tooling. To accommodate the CT samples, a CT testing fixture (Figure 6.5b) was designed and built by the author to fit with the MTS machine. The MTS Elite software provided with the machine was used to collect data, which was backed up on a UBS drive and on the University of Illinois Box cloud, as well as the parent computer, during testing to ensure accurate collection of all data. It was discussed that a larger tensile testing machine (10 KN or higher) should be used to allow the testing of

larger samples; however, due to campus closures, access issues, and other considerations during COVID-19, the 2 KN MTS machine was the only one to which the author could gain consistent access to during the research period. Therefore, it was used for all mechanical testing series.

6.2.6 Impact Testing

Impact testing was done using a standard 2.7J pendulum IZOD testing machine (from ASR Instruments) to complete ASTM D256 tests. The testing machine is shown in Figure 6.5c and discussed extensively in Section 6.9.

6.2.7 Analysis Tools

Some computational work was done within the MTS Elite software driving the testing machine but all other work was done using Microsoft Excel and Minitab. Figures were created using a combination of Excel, Microsoft PowerPoint, Minitab, and Adobe Creative Cloud.

6.2.8 Print Beds and Treatment

Both machines were outfitted with tempered borosilicate glass plates held on with small clamps to allow quick and easy plate replacement. This sped up the printing process significantly, as it was not required that the printer and parts cool off before being removed. It also allowed the printer to stay warm during periods of intense printing, helping to reduce stress on the components and helping extend its life. The plates had limited life spans and would eventually crack or chip and need to be replaced. For all the testing series described in this dissertation, about 12 plates were needed, including 5 that needed to be replaced during the process. Bed treatment was necessary for the specimens since the three materials used do not stick well to bare glass even when heated. For the polycarbonate parts, 3D Systems Cube Glue was used (this is no longer manufactured and the product used was left over from past printing projects). Bed Weld from Layerneer was used for the ABS and PLA specimens. In all cases, the plates were pre-heated and then carefully cleaned using isopropyl alcohol wipes before applying the necessary bed treatments.

6.3 Test Series I: Basic Characterization

6.3.1 Opening Remarks and Notes on Series I

The purpose of Series 1 was to establish the baseline mechanical properties for the three materials used in this dissertation under the established conditions and parameters. Type IV samples were used as defined in ASTM D638 [3]. While most of the other experiments in this chapter used only the flat print orientation (as explained in Section 6.1), this characterization used both the flat and horizontal orientations (Figure 6.6). Only the 45° and 0/90° raster orientations were used, as these are generally the strongest and weakest (respectively) orientations in the AM literature. Coupled with the two orientations, it was expected that the average of the four combinations of layout/orientation would give the best “average” values for the standard properties.

6.3.2 Series I Experimental Design

The experimental design for Series I is given in Table 6.3.

Table 6.3: Experimental design for Test Series I (ASTM D638). Each case was replicated five times for a total of $n = 60$.

Combination	Material	Print Orientation	Raster Angle
1	ABS	Flat	45°
2	PC	Flat	45°
3	PLA	Flat	45°
4	ABS	Horizontal	45°
5	PC	Horizontal	45°
6	PLA	Horizontal	45°
7	ABS	Flat	90°
8	PC	Flat	90°
9	PLA	Flat	90°
10	ABS	Horizontal	90°
11	PC	Horizontal	90°
12	PLA	Horizontal	90°

6.3.3 Series I Materials and Methods

6.3.3.1 Sample Configuration and Manufacturing

Standard Type IV specimens (Figure 6.6) as described in ASTM D638 were used due the size of the tensile testing machine available. All specimens were printed using a 0.6 mm extrusion nozzle. Larger samples would have been ideal for this type of anisotropic material, but this was the best option available for testing due to limited equipment access and time due to COVID-19 restrictions at the University of Illinois.

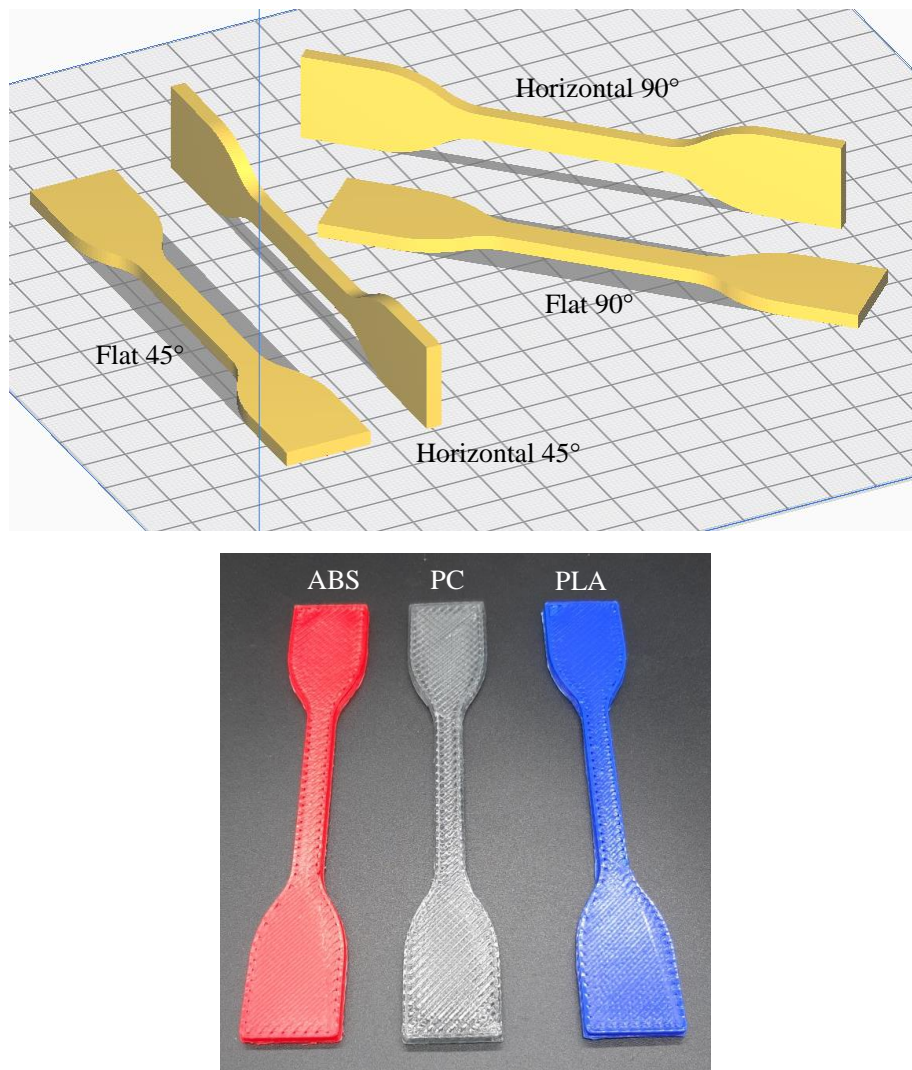


Figure 6.6: Sample printing orientations with examples of successful prints for Series 1

6.3.3.2 Sample Conditioning

Per standard ASTM conditioning guidelines for polymer materials, the specimens were conditioned in the same ambient environment (described in Section 6.1) as the tests were planned. The conditioning time was at least 40 hours for all specimens.

6.3.3.3 Experimental Setup

Standard tensile tests were completed using the MTS testing machine and standard clamps at a strain rate of 5 mm/min until sample rupture. Clamp distance was 80 mm and an extensometer with a 25 mm length was used to measure elongation. The machine setup is demonstrated in Figure 6.7.

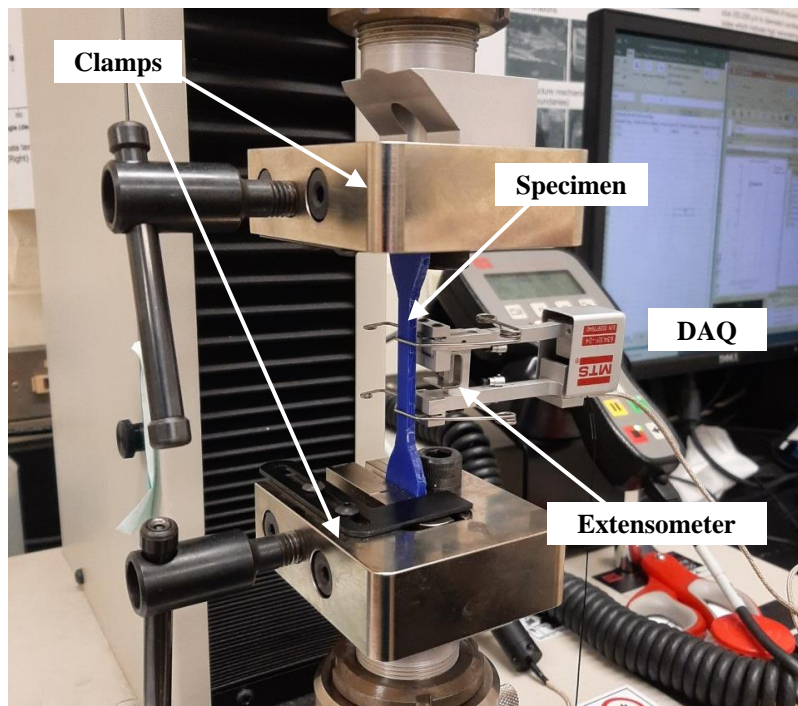


Figure 6.7: Series I experimental setup

6.3.4 Series I Results

Figure 6.8 shows example experimental (force vs deflection) curves for the different materials, orientations, and raster angles. These twelve curves were randomly selected from

the 60 experimental runs in Series I. The raw data from this experiment is archived and discussed in Appendix E. The values of the yield stress, the modulus of elasticity, and the elongation were automatically calculated using the MTS software based on input of the sample geometry. Table 6.4 gives the calculated material properties, the most important of which (relative to the other experiments in this chapter) is the yield strength.

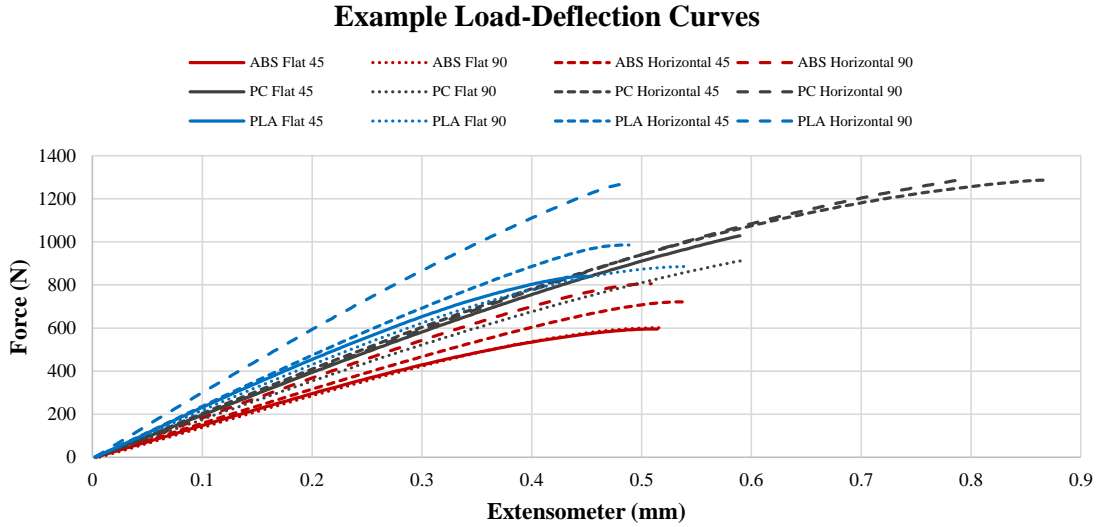


Figure 6.8: Examples of force-deflection curves for each of the 12 cases. One curve for each was randomly selected for each combination from the five replications of the experiment.

Table 6.4: Calculated material properties relevant to the future experiments and design problems in this dissertation. Calculated automatically in the MTS software during testing.

Material	n	Yield Stress (MPa)		Young's Mod (GPa)		Elongation (Yield) (%)	
		Mean	Stdev	Mean	Stdev	Mean	Stdev
ABS	20	32.36	4.54	2.01	0.19	1.96	0.09
PC	20	54.23	9.17	2.36	0.15	3.11	0.78
PLA	20	47.84	5.79	2.97	0.34	2.47	1.84

6.3.5 Series I Statistical Analysis

Since the purpose of this testing series was to collect and archive material properties for the three materials in use and not to provide direct design knowledge, no statistical analysis was done for Series I.

6.4 Test Series II: FDM-Processed Fibers

6.4.1 Opening Remarks and Notes on Series II

The most basic component of FDM-processed materials, and the most essential component of FDM-driven MPDSMs, is the deposited material element. When reviewing the literature on FDM, it was clear that no specific studies on the properties of the elements or fibers produced by FDM have been done beyond a few tests in the early development of FDM (before 2005) described in [4, 5]. Since this information is vital for understanding how to design MPDSMs (especially for fracture problems), a study was completed and is described in this section.

6.4.2 Series II Experimental Design

The experimental designs for these cases are shown in Tables 6.5, 6.6, and 6.7, respectively. The collected response was the highest load before fiber failure. The extruded fibers were tested to explore the properties between the extruder head and the build plate before and during printing, the single deposited fibers provided information about behavior after printing, and the series fibers showed the effect of having several elements printed in parallel in the same layer. The obvious expansion of this (to printed films) will be examined in Section 6.5.

Table 6.5: Experimental design for extruded fibers in Test Series II. Each case was replicated five times for a total of $n = 45$.

Combination	Material	Diameter (mm)
1	ABS	0.4
2	PC	0.4
3	PLA	0.4
4	ABS	0.8
5	PC	0.8
6	PLA	0.8
7	ABS	1.75
8	PC	1.75
9	PLA	1.75

Table 6.6: Experimental design for single deposited fibers in Test Series II. Each case was replicated five times for a total of $n = 30$.

Combination	Material	W/H Ratio
1	ABS	2
2	PC	2
3	PLA	2
4	ABS	3
5	PC	3
6	PLA	3

Table 6.7: Experimental design for series deposited fibers in Test Series II. Each case was replicated three times for a total of $n = 45$. For these cases, $W/H = 2$ with $d = 0.4$ mm.

Combination	Material	# of Printed Fibers
1	ABS	2
2	PC	2
3	PLA	2
4	ABS	4
5	PC	4
6	PLA	4
7	ABS	6
8	PC	6
9	PLA	6
10	ABS	8
11	PC	8
12	PLA	8
13	ABS	10
14	PC	10
15	PLA	10

6.4.3 Series II Materials and Methods

6.4.3.1 Sample Configuration and Manufacturing

To best understand the mechanical behavior of the printed material elements, this test series explored three different types of specimens:

1. *Extruded fibers*: Individually extruded directly from the nozzle but not deposited
2. *Deposited fibers*: Fibers that were extruded and deposited onto a heated glass plate
3. *Series fibers*: Sets of fibers printed in parallel (in groups of 2-10)

The extruded samples were made by raising the z-axis of an FDM machine such that at least 10 inches of extruded filament could freely drop (Figure 6.9) and disabling the other axes. G-code was then used to control the extrusion. Once the extruded fibers were completed, the printer motors were re-enabled and the deposited fibers were simply printed onto a glass plate by inputting the necessary g-code into the printer; they were later removed by soaking the plate in warm water to prevent damage to the fibers. The sets of fibers were printed in the same way as the individual ones, except that the machine was allowed to print multiple parallel tracks. Examples of each case are shown in Figure 6.10. Note that the 1.75 mm extruded samples are samples of raw filament from the roll; since the materials are thermoplastics, it was decided that they would give a good comparative baseline.

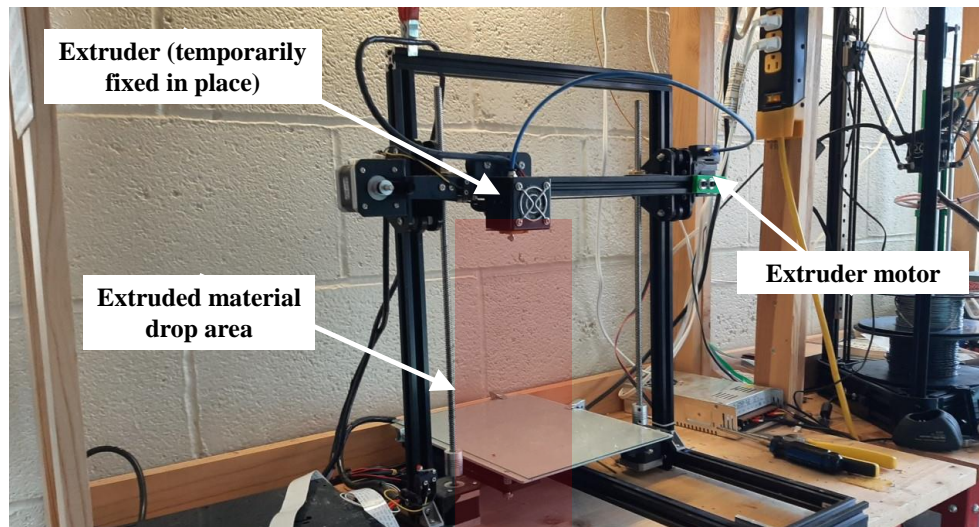


Figure 6.9: Setup for making the extruded fibers

Once all of the fiber samples were made, they were carefully glued into card stock, since the cut-paper method (Figure 6.11) was to be used to clamp and test the samples. In this method, the samples are carefully fixed via paper or card stock at both ends, with the thick card or paper end being placed in the clamp to prevent any damage to the fiber being tested. The effective tested length of all fibers and fiber series was 4 inches. As shown in Figure 6.11, a 2 × 4 inch business card cutter from Fiskars was used to prepare the card stock fiber holders to ensure consistency and accuracy.

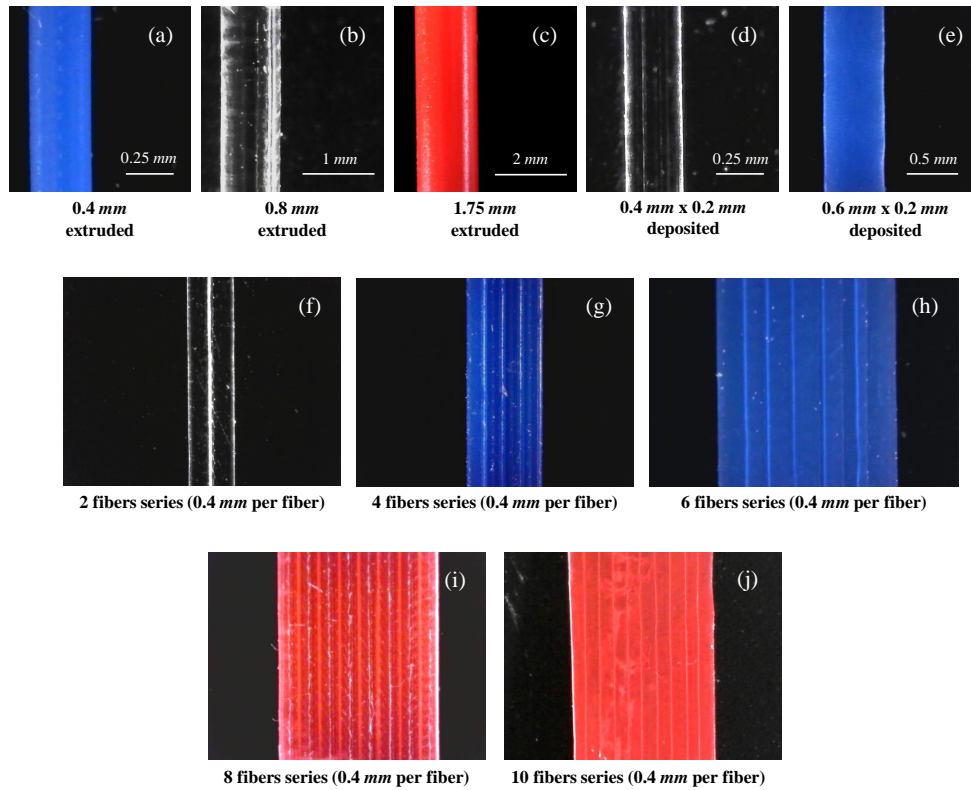


Figure 6.10: Examples of (a)-(c) extruded fibers, (d)-(e) deposited fibers, and (f)-(j) series fibers. Red fibers = ABS, grey/transparent fibers = PC, blue fibers = PLA.

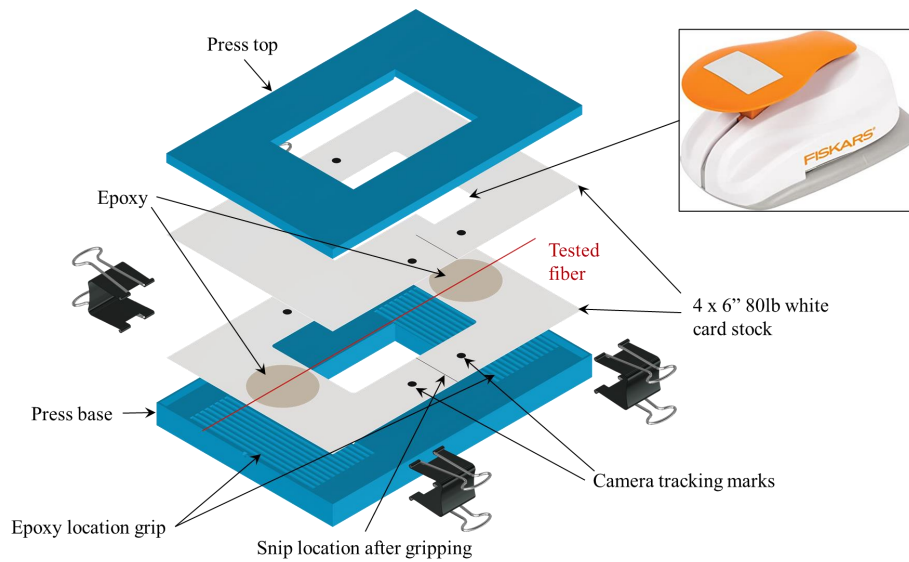


Figure 6.11: Setup for cut-paper method for tensile testing fibers

6.4.3.2 Sample Conditioning

Per standard ASTM conditioning guidelines for polymer materials, the specimens were conditioned in the same ambient environment (described in Section 6.1) as the tests were planned. The conditioning time was at least 40 hours for all specimens.

6.4.3.3 Experimental Setup

Figure 6.12 shows the experimental setup, including the cut locations in the paper after clamping. Standard tensile testing was done at a strain rate of 50 mm/min until sample breakage. Since no extensometer that could clamp onto a fiber was available, recorded data was based on cross head distance.

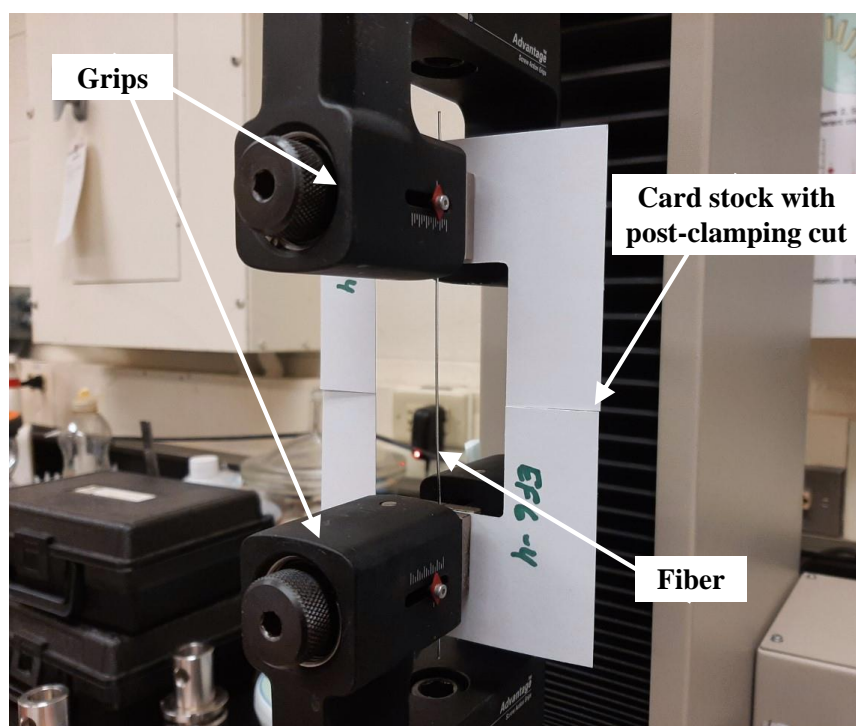


Figure 6.12: Experimental setup for Series II

6.4.4 Series II Results

The results from the three tests are shown in Table 6.8, Table 6.9, and Table 6.10 below. Data availability is discussed in Appendix E.

Table 6.8: Experimental results for extruded fibers testing.

Combination	Material	Diameter (mm)	n	Tensile Strength (N)	
				Mean	Stdev
1	ABS	0.4	5	7.37	0.14
2	PC	0.4	5	9.46	1.17
3	PLA	0.4	5	8.21	1.63
4	ABS	0.8	5	23.92	2.85
5	PC	0.8	5	40.90	6.23
6	PLA	0.8	5	35.57	0.78
7	ABS	1.75	5	84.02	20.69
8	PC	1.75	5	150.15	16.68
9	PLA	1.75	5	125.61	3.60

Table 6.9: Experimental results for deposited fibers testing.

Combination	Material	W/H Ratio	n	Tensile Strength (N)	
				Mean	Stdev
1	ABS	2	5	2.89	0.10
2	PC	2	5	3.52	0.24
3	PLA	2	5	3.57	0.59
4	ABS	3	5	3.40	0.96
5	PC	3	5	5.17	1.40
6	PLA	3	5	9.55	0.77

Table 6.10: Experimental results for series fibers testing.

Combination	Material	# of Fibers	n	Tensile Strength (N)	
				Mean	Stdev
1	ABS	2	5	4.74	0.52
2	PC	2	5	5.38	2.05
3	PLA	2	5	8.65	0.39
4	ABS	4	5	9.48	1.24
5	PC	4	5	12.30	2.54
6	PLA	4	5	19.80	8.02
4	ABS	6	5	14.36	0.37
5	PC	6	5	22.72	4.35
6	PLA	6	5	24.72	4.60
4	ABS	8	5	24.16	7.42
5	PC	8	5	30.13	8.02
6	PLA	8	5	27.76	4.67
4	ABS	10	5	35.10	12.60
5	PC	10	5	39.69	19.26
6	PLA	10	5	42.44	8.15

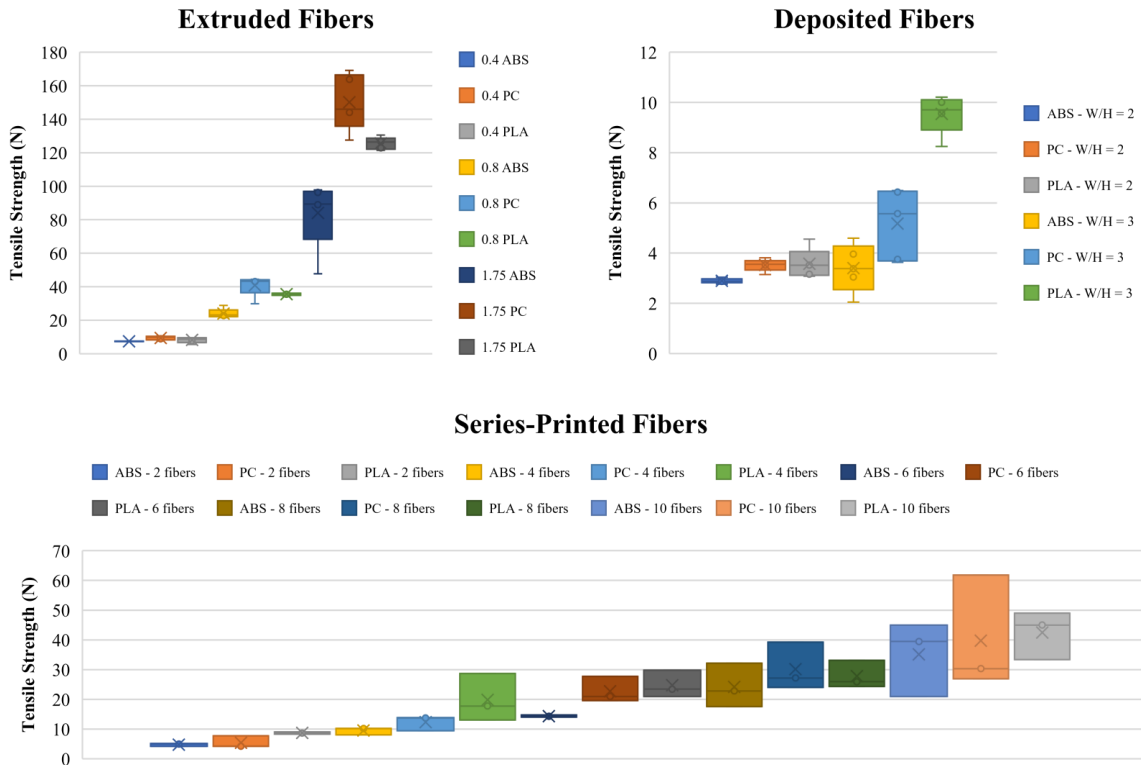


Figure 6.13: Box plot representations of the collected data on the tensile strength of the extruded, deposited, and series fibers.

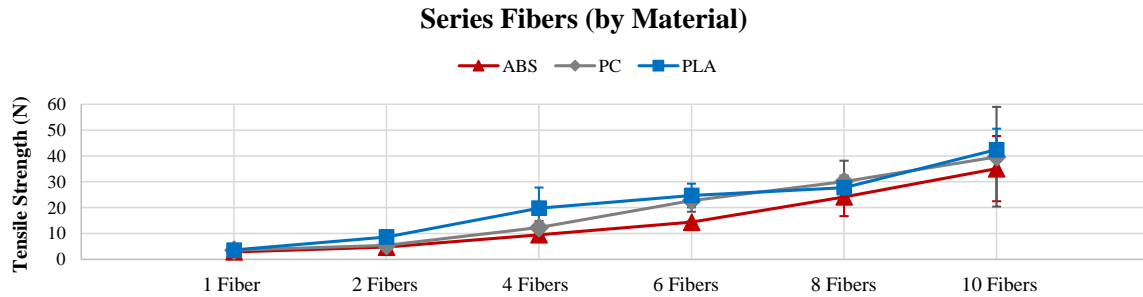


Figure 6.14: Tensile strength pattern of series fibers by material

6.4.5 Series II Statistical Analysis

Since the purpose of this testing series was to collect and archive material behavior/properties for the three materials in use and help derive design rules, no statistical analysis was done for Series II.

6.5 Test Series III: FDM-Processed Films

6.5.1 Opening Remarks and Notes on Series III

Given that the basic elements (“fibers”) produced by FDM are the building blocks of FDM-printed parts and material structures, the next level in the material hierarchy is the thin film. Expanding on from the series fibers, these films represent whole layers or sets of layers from which a part would be made. Printed in the flat orientation (Section 6.1), these can be made up of designed element patterns to serve as building blocks for FDM-driven MPDSMs.

6.5.2 Series III Experimental Design

The experimental design for Series III is shown in Table 6.11. The design was used for both notched and un-notched cases. Three replications were done for each case for a total of 108 tests in Series III. As for the fiber tests in Section 6.4, the experimental response was the tensile strength of the film.

Table 6.11: Experimental design for thin films (notched and un-notched) in Test Series III. Each case was replicated three times for a total of $n = 108$.

Combination	Material	# of Layers	Element Layout
1	ABS	1	R45
2	PC	1	R45
3	PLA	1	R45
4	ABS	2	R45
5	PC	2	R45
6	PLA	2	R45
7	ABS	1	Gyroid
8	PC	1	Gyroid
9	PLA	1	Gyroid
10	ABS	2	Gyroid
11	PC	2	Gyroid
12	PLA	2	Gyroid
13	ABS	1	Concentric
14	PC	1	Concentric
15	PLA	1	Concentric
16	ABS	2	Concentric
17	PC	2	Concentric
18	PLA	2	Concentric

6.5.3 Series III Materials and Methods

6.5.3.1 Sample Configuration and Manufacturing

The specimens used for this series were created based on the specifications for ASTM D882. They were printed using the same setup as the series fibers in Section 6.4, except that specific element layouts were used, as shown in Table 6.11 and Figure 6.15. All specimens were printed using a 0.6 mm extrusion nozzle. In addition to the variable layouts, the thickness was also varied by printing one or two layers. In addition, the experiment (Table 6.11) was run once for raw samples as described in ASTM D882 and once for notched samples. Notching was done using a hand-held film jig and razor blade (Figure 6.16) to produce the notched sample geometry shown in Figure 6.15.

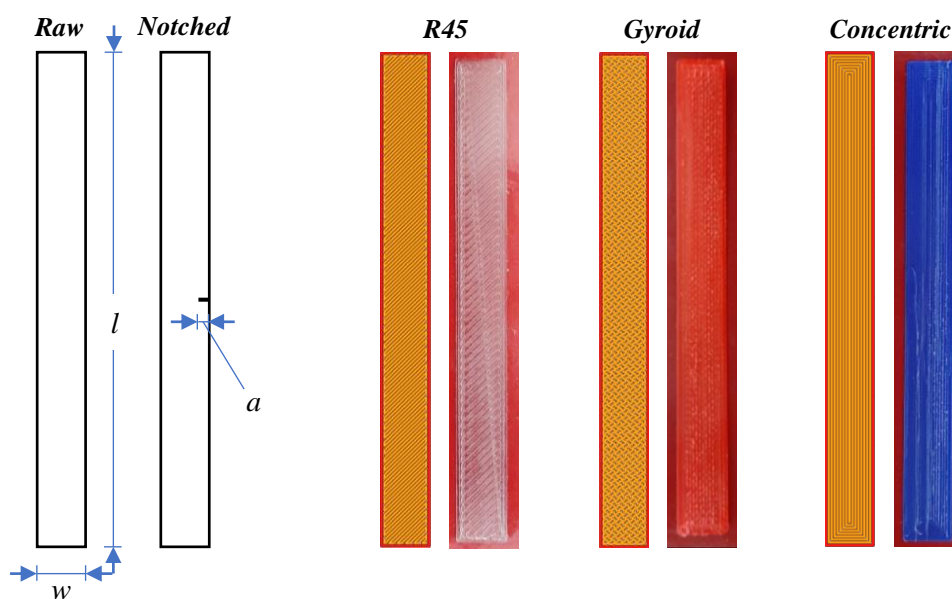


Figure 6.15: Specimen configurations for Series III. The dimensions $l = 100$ mm, $w = 10$ mm, and $a = 2$ mm were used for all samples.

6.5.3.2 Sample Conditioning

Per standard ASTM conditioning guidelines for polymer materials, the specimens were conditioned in the same ambient environment (described in Section 6.1) as the tests were planned. The conditioning time was at least 40 hours for all specimens. Notched specimens were conditioned both before and after notching.

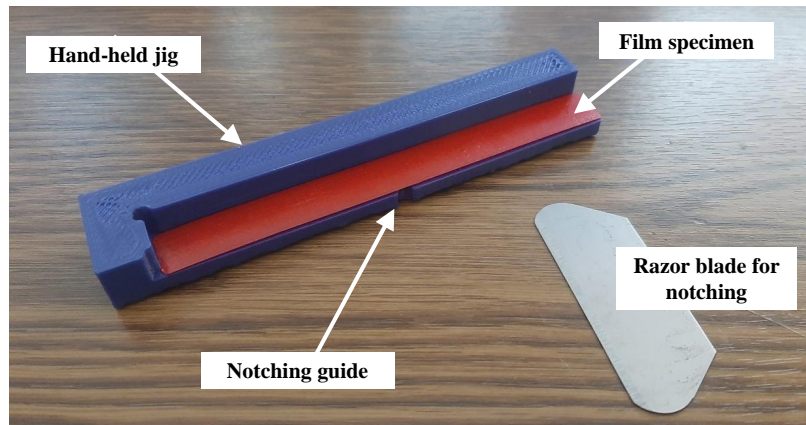


Figure 6.16: Film notching jig

6.5.3.3 Experimental Setup

The experimental setup for Series III is shown in Figure 6.17. A strain rate of 50 mm/min was used according with the recommendations of ASTM D882.

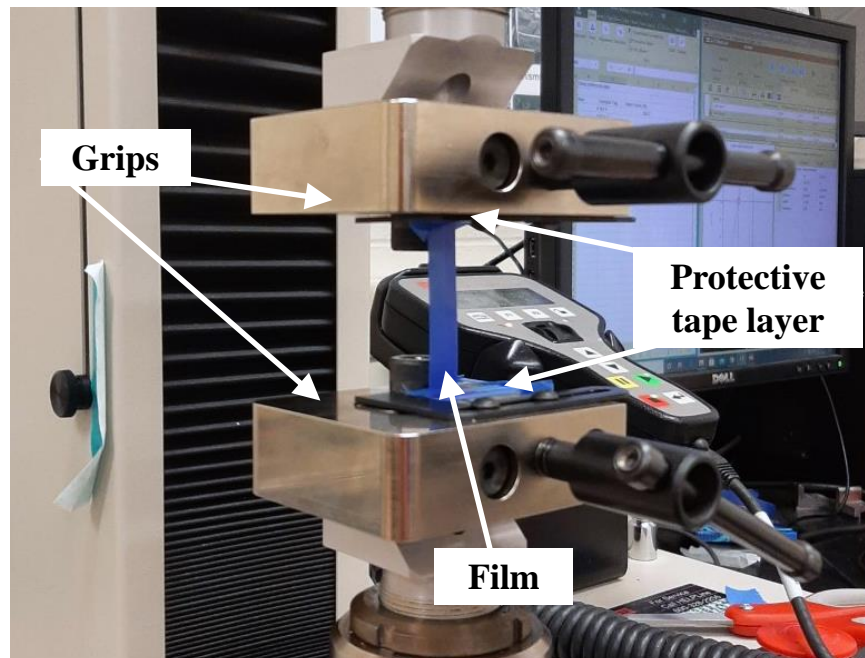


Figure 6.17: Series III experimental setup

Several layers of blue painter's tape were placed between the jaws and the samples to prevent cutting or damaging of the samples by the fixture. The tape was replaced every 25

samples to ensure it was effective. The samples were marked with a Sharpie pen to check for slippage, but none was observed on any of the samples using this setup.

6.5.4 Series III Results

The results from Series III are shown in Table 6.12 and Figure 6.18. Data availability is discussed in Appendix E.

Table 6.12: Experimental results for raw and notched FDM film testing. $n = 3$ for all cases in this table.

Combination	Material	Layers	Layout	TS - Raw (N)		TS - Notched (N)	
				Mean	Stdev	Mean	Stdev
1	ABS	1	R45	75.2	5.1	59.5	5.7
2	PC	1	R45	81.0	40.1	53.6	7.9
3	PLA	1	R45	90.8	5.0	62.2	9.6
4	ABS	2	R45	178.8	1.3	139.1	5.0
5	PC	2	R45	223.4	7.7	161.5	27.3
6	PLA	2	R45	217.4	2.0	177.8	4.3
7	ABS	1	Gyroid	73.0	2.7	59.6	6.9
8	PC	1	Gyroid	116.2	4.9	89.0	11.6
9	PLA	1	Gyroid	116.1	4.9	90.6	3.9
10	ABS	2	Gyroid	151.2	7.6	131.7	14.9
11	PC	2	Gyroid	211.0	19.5	184.4	34.8
12	PLA	2	Gyroid	230.6	7.8	175.5	2.0
13	ABS	1	Concentric	66.5	1.1	72.2	3.6
14	PC	1	Concentric	112.8	0.6	83.4	19.1
15	PLA	1	Concentric	127.7	6.8	99.8	5.5
16	ABS	2	Concentric	136.2	4.9	123.2	13.8
17	PC	2	Concentric	156.0	31.2	154.2	25.5
18	PLA	2	Concentric	236.3	0.2	179.6	10.5

6.5.5 Series III Statistical Analysis

Since the purpose of this testing series was to collect and archive material behavior/properties for the three materials in use and help derive design rules, no statistical analysis was done for Series III.

6.5.6 Series III Sensitivity Analysis

When examining the results of Series III, especially the large differences between the notched and raw samples, the question could be raised about the effect of the shell on the results.

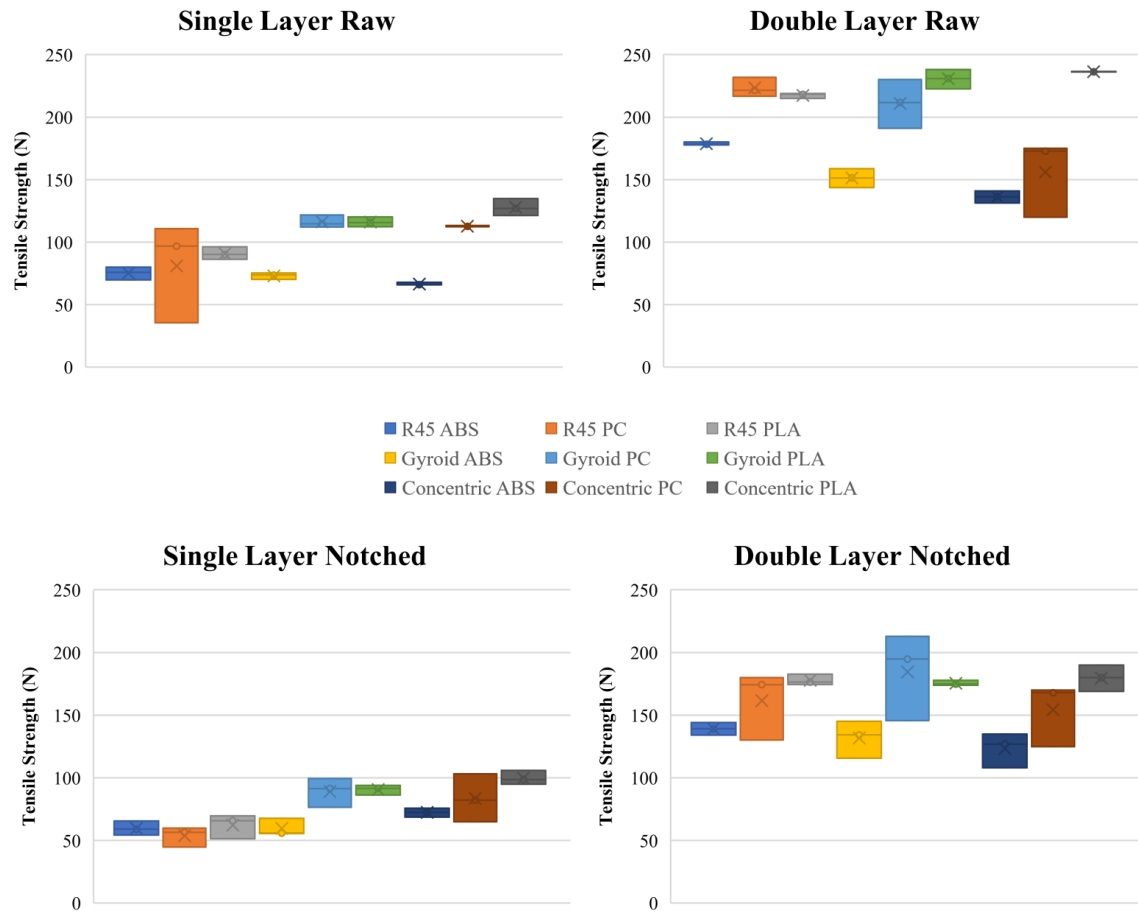


Figure 6.18: Series III experimental results for single and double layer cases with raw and notched samples

Table 6.13: Experimental design for thin films sensitivity analysis in Test Series III. Each case was replicated three times for a total of $n = 36$.

Combination	Material	Layers	Layout	Tensile Strength (N)	
				Mean	Stdev
1	ABS	1	R45	62.2	4.6
2	PC	1	R45	66.6	23.0
3	PLA	1	R45	85.1	1.9
4	ABS	2	R45	164.9	5.3
5	PC	2	R45	203.1	11.6
6	PLA	2	R45	193.6	9.5
7	ABS	1	Gyroid	63.2	2.3
8	PC	1	Gyroid	94.9	13.0
9	PLA	1	Gyroid	107.8	9.8
10	ABS	2	Gyroid	137.6	17.8
11	PC	2	Gyroid	210.0	16.1
12	PLA	2	Gyroid	208.2	7.7

Therefore, a simple sensitivity analysis was done where samples were tested without shells. The results were then transformed to correct for the difference in width (8.8 mm instead of 10 mm) and compared. The corrected data is shown in Table 6.13. Only the R45 and gyroid samples were analyzed, as the removal of the shell for the concentric cases (Figure 6.15) would clearly have little to no impact on the outcome. As shown in the sensitivity analysis plots (Figure 6.19), there is not a very large difference between the samples with shells and those without. A statistical analysis using the Kruskal-Wallis test produced p-values of 0.062 and 0.054 for the single and double layer cases, respectively. Using the typical $\alpha = 0.05$, there is not a statistically significant difference between using the shell or not for the thin films observed.

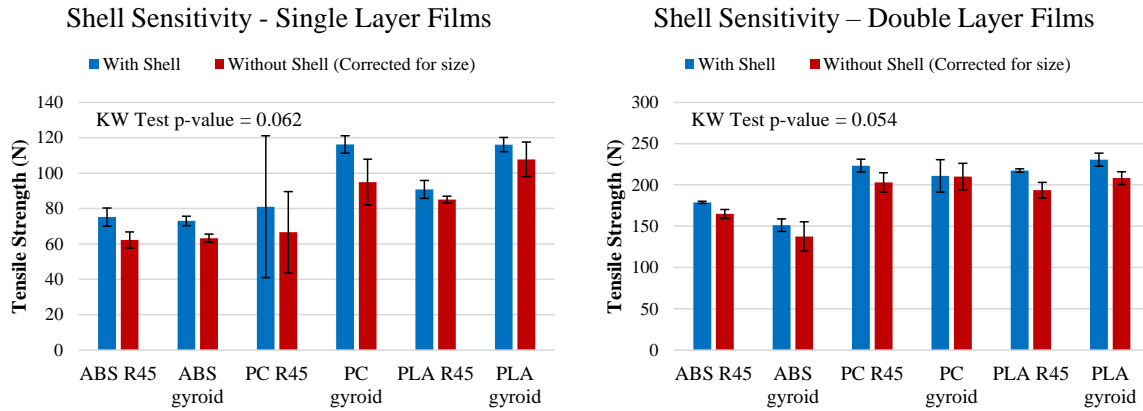


Figure 6.19: Sensitivity analysis regarding the use of a shell or not for the 1 and 2 layer thin film cases. Analysis indicates no statistically significant difference. $n = 3$ for all cases.

6.5.7 Series III Crack Pattern Analysis

Figure 6.20 shows some examples of typical crack patterns observed in the tested film samples for each combination. The behavior of the cracks was fairly consistent with the expectation that the layout pattern would cause a patterned crack to follow the pattern. Panel (a) shows an example of an ABS gyroid with the shell removed (from the sensitivity study); similarly to the gyroid patterns in panels (e) and (f), the crack is jagged but relatively straight. Looking at the difference between (a) and (e-f), it is clear that the shell made a difference on how controlled the crack was, even if it did not have a statistically

significant impact on the tensile strength. Panels (b) and (d) show a similar relationship for 2-layer R45 ABS samples, where the crack grows along the raster; again, the presence of the shell certainly had some effect on the crack behavior even if the differences in tensile strength were not statistically significant at the film level.

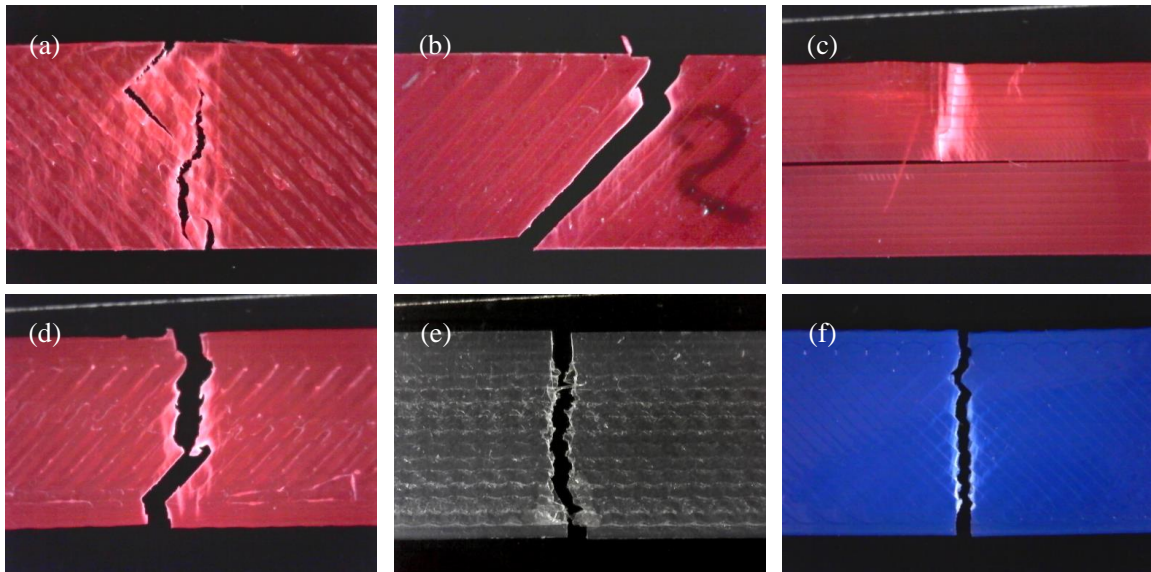


Figure 6.20: Examples of typical crack patterns for FDM-processed thin films

6.6 Test Series IV: ASTM D5045 CT Sample Size Sensitivity

6.6.1 Opening Remarks and Notes on Series IV

Up to this point in the present chapter, the basic macro-scale material properties and the properties of the fibers and films which serve as building blocks for FDM-processed materials were collected. With Series IV tests, the analysis of meso-scale materials begins. As previously described, the flat-printed ASTM 5045 CT sample will be the standard specimen for these cases. The first order of business is to select the sample size, which is not an easy task for FDM-processed materials. There is no consensus in the literature about the appropriate size to use and the samples used often do not meet all of the established requirements for plane strain fracture toughness K_{Ic} (i.e., independence from sample size effects, as least for isotropic, homogeneous polymer materials [1]). To judge the appropriate size to test for

this series, a short literature review was done for CT tests on FDM-processed materials; the results are shown in Table 6.14.

Table 6.14: Examples of CT testing on FDM-processed materials in the literature. Collected to help guide choice of specimen size for this dissertation.

Study	Material	W (mm)	B (mm)
[6]	PLA	40	8
[7]	PLA	30	6
[8]	ABS	60	12.7
[9]	PLA	19	9.4
[10]	Polyether ether ketone (PEEK)	15	7.5
[11, 12]	ABS	70	4
[13]	PC	30	4
[14]	Onyx (nylon + carbon fiber)	32	10

Since the experimental equipment available for these tests were limited to a 2 KN load (and recommended to stay well below this load), it was estimated that samples larger than $W = 50$ mm were not feasible without a larger testing machine, especially since the ASTM 5045 standard recommends a thickness of 10 mm for a $W = 50$ mm specimen. For this specimen, it was roughly estimated (using data sheet properties) that 1500-1700 N would be required to handle this sample size (note: As shown later in this chapter, the maximum observed load for this sample size was 1531 N). The sample size selected *must allow a significant amount of distance between the fracture load and the capacities of the machine, as later work on designing the layouts will increase the breaking strength of the specimens.* If the necessary load to break the raw sample is too close to the machine capacity, the machine may not be able to test the new/improved designs.

Reviewing the available information for this problem and keeping in mind the design objectives of this study, it was also decided that a sample smaller than $W = 30$ mm and $B = 6$ mm was also infeasible. While smaller samples could easily be manufactured and tested (and would save time and material), they would not present a large enough area around the crack tip to serve as an effective design space for element layout. Therefore, it was determined that the smallest feasible sample size for the three materials in use was $W = 30/B = 6$ mm and the largest $W = 50/B = 10$ mm.

Without extensive previous experimental data to rely on, it is impossible to predict

how the samples will behave and if the criteria for K_{1c} will be satisfied until after some tests have been done. If the criteria is not satisfied, larger samples can be used or a different measure of material behavior should be used (such as the conditional fracture toughness K_Q or simply the maximum load before fracture). When advanced testing capacities are available (such as very high-speed cameras and crack-tip-opening-displacement (CTOD) sensors), the R-curve and strain energy release rate can be measured in order to allow the J-integral to be used. Unfortunately, the present research project did not have access to the advanced testing capabilities and so was limited to completing ASTM D5045 tests which depend on reporting K_Q and K_{1c} values or standard mechanical properties.

6.6.2 Series IV Experimental Design

Given the information from the previous discussion, it was decided that the two extreme samples sizes and the average one between them should be tested. Therefore, the three sizes were $W = 30/B = 6$ mm, $W = 40/B = 8$ mm, and $W = 50/B = 10$ mm. The design is shown in Table 6.15.

Table 6.15: Experimental design for sample size sensitivity in Test Series IV (ASTM D5045). Each case was replicated three time for a total of $n = 27$.

Combination	Material	W (mm)	B (mm)
1	ABS	30	6
2	PC	30	6
3	PLA	30	6
4	ABS	40	8
5	PC	40	8
6	PLA	40	8
7	ABS	50	10
8	PC	50	10
9	PLA	50	10

6.6.3 Series IV Materials and Methods

6.6.3.1 Sample Configuration and Manufacturing

Standard flat-printed ASTM D5045 CT samples using the dimensions in Table 6.15 were manufactured for testing. Based on preliminary observations in other experiments, a printed

notch with a pre-crack (Figure 6.4) was selected. The crack length used was $a = W/2$ as recommended by the standard. Figure 6.21 shows examples of each size from each material. A standard raster printing pattern was used with a raster angle of 45° and a single shell.

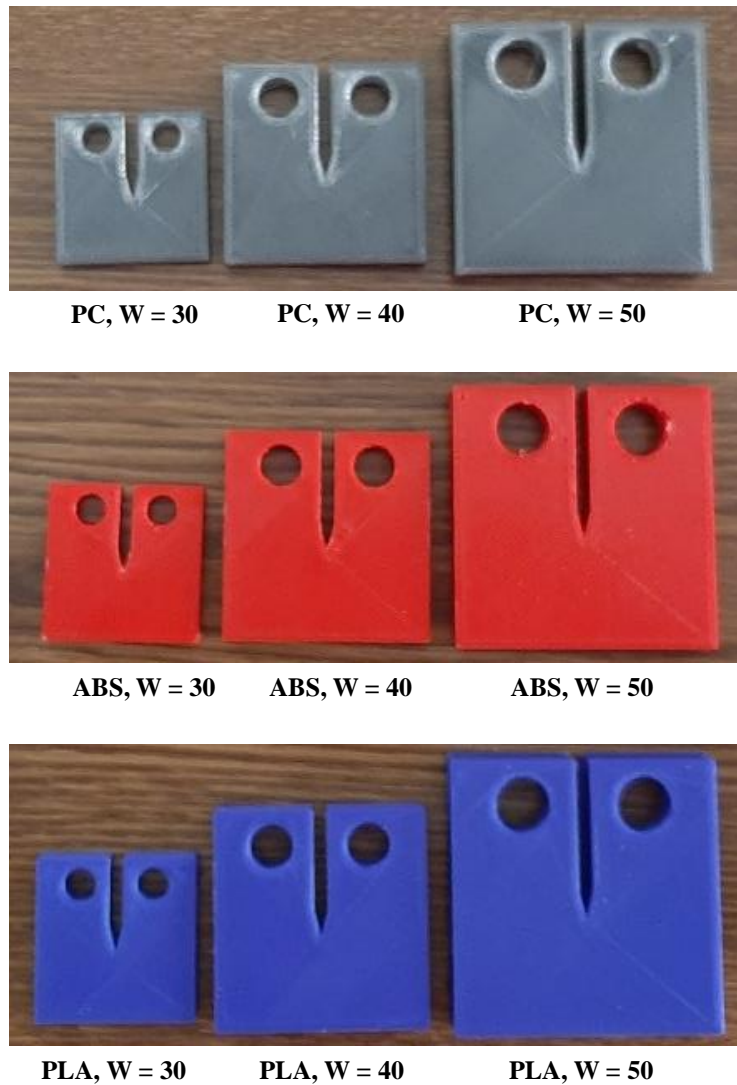


Figure 6.21: Examples of printed test specimens for Series IV

6.6.3.2 Sample Conditioning

Per standard ASTM conditioning guidelines for polymer materials, the specimens were conditioned in the same ambient environment (described in Section 6.1) as the tests were planned. The conditioning time was at least 40 hours for all specimens.

6.6.3.3 Experimental Setup

The experimental setup is shown in Figure 6.5b at the beginning of the paper. A strain rate of 10 mm/min was used as recommended by ASTM D5045.

6.6.4 Series IV Results

In Table 6.16, the mean fracture load at failure is shown for each case. In Table 6.17, the calculated values of K_Q are provided, in addition to the required sample thickness, crack, and ligament lengths to meet the K_{1c} criteria; the calculation process shown in ASTM D5045 was followed exactly for this. Data availability is discussed in Appendix E. Appendix D shows example calculations for K_Q from this section.

Table 6.16: Experimental results (fracture load) from Series IV

Combination	Material	W (mm)	B (mm)	Fracture Load (N)	
				Mean	Stdev
1	ABS	30	6	326.2	6.8
2	PC	30	6	579.1	55.5
3	PLA	30	6	587.5	34.0
4	ABS	40	8	554.9	39.4
5	PC	40	8	852.1	95.8
6	PLA	40	8	998.8	70.4
7	ABS	50	10	739.7	48.3
8	PC	50	10	1070.4	250.4
9	PLA	50	10	1468.2	67.7

Table 6.17: Conditional fracture toughness K_Q from Series IV

Combination	Material	W (mm)	B (mm)	K_Q (MPa · m ^{0.5})		
				R1	R2	R3
1	ABS	30	6	2.72	2.77	2.80
2	PC	30	6	4.79	5.35	5.54
3	PLA	30	6	5.24	5.03	4.68
4	ABS	40	8	3.05	3.13	3.31
5	PC	40	8	4.72	5.27	4.90
6	PLA	40	8	5.38	5.34	5.92
7	ABS	50	10	3.04	3.10	2.97
8	PC	50	10	3.44	4.84	5.37
9	PLA	50	10	5.82	6.02	5.56

Table 6.18: Length of B, crack length, and ligament (mm) to meet ASTM D5045 criteria for pure plane strain fracture toughness K_{Ic} . Values of σ_y taken from Table 6.4.

Combination	Material	W (mm)	B (mm)	$2.5 \left(\frac{K_Q}{\sigma_y} \right)^2$ (mm)		
				R1	R2	R3
1	ABS	30	6	17.6	18.2	18.7
2	PC	30	6	19.5	24.3	26.2
3	PLA	30	6	30.0	27.7	24.0
4	ABS	40	8	22.2	23.3	26.0
5	PC	40	8	18.9	23.7	20.5
6	PLA	40	8	31.7	31.2	38.4
7	ABS	50	10	22.1	22.9	20.9
8	PC	50	10	10.0	20.0	24.6
9	PLA	50	10	37.1	39.6	33.8

Given the values of K_Q , the pure plane strain criteria can be calculated for each case. As seen in Table 6.18, none of the samples satisfy the criteria and so values of K_{Ic} cannot be reported from this experiment. This is typical of FDM materials and discussed in depth in several of the papers shown in Table 6.14. The plotted results for K_Q are shown in Figure 6.22.

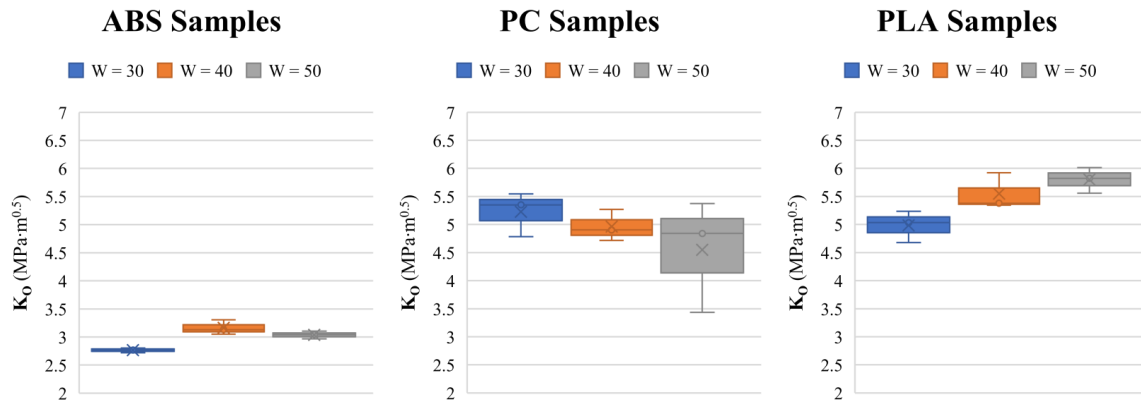


Figure 6.22: Observed K_Q values from Series IV

6.6.5 Series IV Statistical Analysis

Since the conclusions made from Series IV will be used to drive decision and testing approaches for the following several experimental series, a standard ANOVA test (Figure 6.23) was done on the collected data in order to better understand the results. Reviewing the plots in Figure 6.22, there does not appear to be a large effect on the results from the

sample size. As seen in the ANOVA results, the difference between sample sizes was not statistically significant.

Analysis of Variance

Source	DF	Adj SS	Adj MS	F-Value	P-Value
Material	2	30.0652	15.0326	69.75	0.000
Size	2	0.2485	0.1242	0.58	0.570
Error	22	4.7416	0.2155		
Lack-of-Fit	4	1.7448	0.4362	2.62	0.069
Pure Error	18	2.9969	0.1665		
Total	26	35.0553			

Figure 6.23: ANOVA results for Series IV

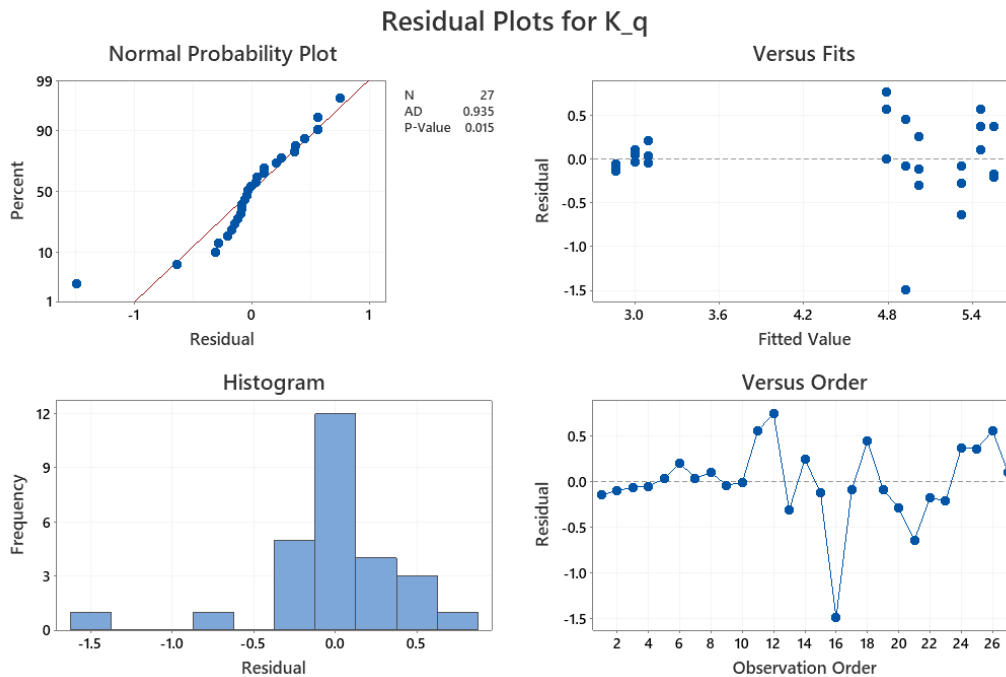


Figure 6.24: 4-in-1 residual plot for Series IV

However, before this result can be accepted the standard Fisher assumptions must be checked. First, the Anderson-Darling (AD) test was done to check for residual normality (Figure 6.24); the resulting p-value of 0.015 indicates that the normality assumption is invalid. Since the p-value was in the same order of magnitude as one that would be significant, the AD test was run again using the optimal Box-Cox transformation (this was done

automatically in Minitab), producing a p-value of $0.026 < 0.05$, so the normality assumption is violated and so a standard ANOVA cannot be relied on. In addition, it is obvious from Figure 6.24 (Versus Fits plot) that the equal variances assumption is violated even without testing it formally. However, visual analysis of the main effects and interactions plots (Figure 6.25) hold up the conclusions from the ANOVA quite well.

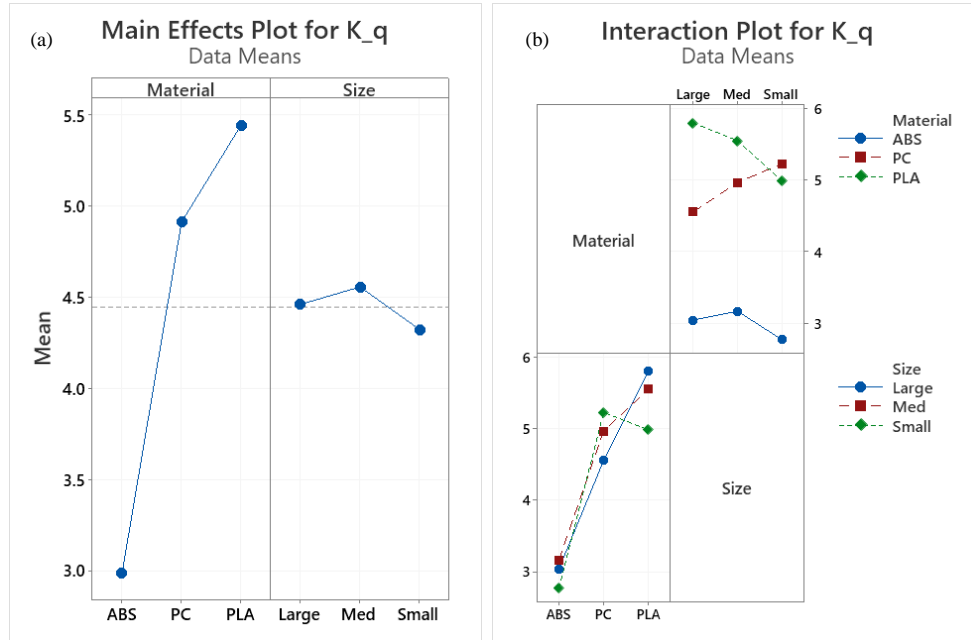


Figure 6.25: (a) Main effects and (b) interaction plots for Series IV

To mathematically address the failure of these assumptions and verify the conclusions of the failed ANOVA, a non-parametric method must be used. In many cases, the two methods will agree even if the normality and equal variances assumptions are violated but not always so this must be checked when the ANOVA assumptions fail. The test selected was the Kruskal-Wallis test, the results of which are shown in Figure 6.26. As seen in the figure, the results from the ANOVA were solid enough to hold up even when the two assumptions were invalid. Therefore, it can be safely assumed that *in the range tested and for the three materials in use, the sample size does not have a statistically significant impact on the value of the K_Q* . This suggests that the FDM-processed materials reached the point of plane strain with smaller samples than would be expected for molded samples, but this

needs more research before a solid conclusion could be reached.

Kruskal-Wallis Test: K_q versus Material

Descriptive Statistics

Material	N	Median	Mean Rank	Z-Value
ABS	9	3.043	5.0	-4.17
PC	9	4.903	16.2	1.03
PLA	9	5.380	20.8	3.14
Overall	27		14.0	

Test

Null hypothesis H₀: All medians are equal
 Alternative hypothesis H₁: At least one median is different

DF	H-Value	P-Value
2	18.84	0.000

Kruskal-Wallis Test: K_q versus Size

Descriptive Statistics

Size	N	Median	Mean Rank	Z-Value
Large	9	4.842	15.2	0.57
Med	9	4.903	15.0	0.46
Small	9	4.785	11.8	-1.03
Overall	27		14.0	

Test

Null hypothesis H₀: All medians are equal
 Alternative hypothesis H₁: At least one median is different

DF	H-Value	P-Value
2	1.06	0.588

Figure 6.26: Kruskal-Wallis test results for Series IV

6.6.6 Series IV Plane Strain Size Sensitivity Analysis

Given the conclusions from this testing series, it makes the most sense to go forward with the rest of the experiments using CT samples of $W = 30$ mm and $B = 6$ mm. As one final check to establish the validity of using these samples, the standard definition for plane strain and plane stress was consulted (Figure 6.27)

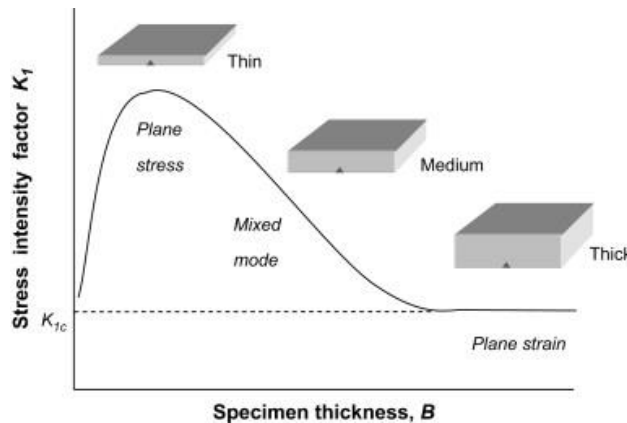


Figure 6.27: Plane stress to plane strain transition curve. From [15] and reproduced under the terms of the CC-BY license from the original publication of this figure.

As shown in the figure, the lack of statistical significance between the sample sizes strongly

suggests that plane strain has been reached (and therefore $K_Q = K_{1c}$), since the difference in K_Q (or K_I in this figure) between plane stress and plane strain may be an order of magnitude for polymers. As a final check, two more specimens of each material were made using the $W = 30$ mm dimension, but with $B = 3$ mm, which is half the original thickness and the thinnest CT sample that the author was able to test successfully without sample buckling. Ideally, a $B < 3$ mm should be used to capture plane stress more effectively but the samples have been observed to buckle at thinner dimensions than that. This sample dimensions clearly does not fit the requirements for ASTM D5045 (and therefore are not necessarily valid for testing) but are useful for a sensitivity analysis. Calculating the K_Q for these thinner samples and comparing them to the original (Figure 6.28) continues to show that there is no major impact from sample thickness as expected from plane stress-plane strain theory shown in Figure 6.27.

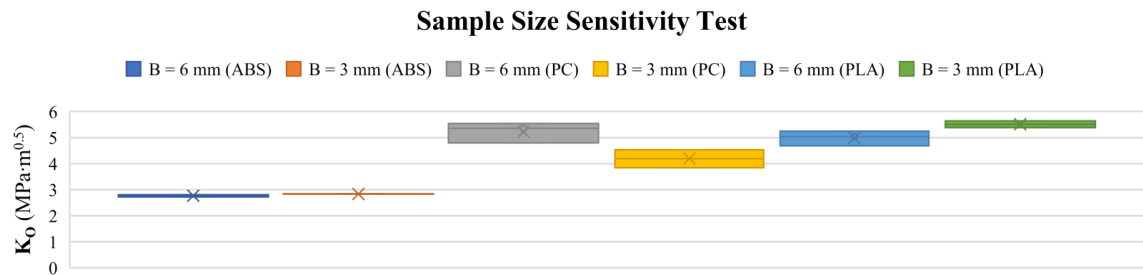


Figure 6.28: Thickness sensitivity observations during sensitivity study

The only material with some difference is PC, but it is in the opposite direction as expected if there was a sample size effect and PC has been shown to be quite variable and sometimes unpredictable throughout this chapter. This apparent lack of a dramatic sample size effect with FDM materials an interesting point that has not been observed with these materials in the past and certainly warrants further study in the future.

6.6.7 Data Reporting after Series IV

Based on the very clear results of Series IV, it was decided that future experiments using CT samples will report the fracture load (N) instead of a fracture toughness value (or both together). This will prevent controversy over the results and will provide several

major advantages from the perspective of design. Note also that this is not an uncommon approach and can be observed in a number of studies on the fracture mechanics of FDM materials, such as Refs [11, 12, 16–23] and others.

1. This will save time since it is not trivial to calculate K_Q values, especially when there are many of them. It is usually not possible to automate this and still get a very accurate solution.
2. Fewer steps in calculation will reduce errors.
3. Reporting fracture load instead of fracture toughness will give a more understandable and easier to apply metric to judge results.
4. Reporting fracture load instead of fracture toughness make it easier to use sample size and material as independent variables in design decisions. K_Q and K_{1c} are heavily dependent on sample size and material ductility, respectively. In addition, once the material element layouts are designed, the fracture toughness will vary significantly for the same sample size, material, etc. simply from the difference in layout.

6.7 Test Series V: ASTM D5045 CT Notch Sensitivity

6.7.1 Opening Remarks and Notes on Series V

Following up on the sample size sensitivity study, it was determined that the sensitivity to pre-cracking and notching method was also an important consideration. It was concluded in the last section that ASTM D5045 CT samples with $W = 30$ mm and $B = 6$ mm could be validly used, so they were used in this study as well. This test series was not meant to be as extensive or in-depth as the previous one as its conclusions only drive the decision about notching and pre-cracking methods for the final fracture analyses in Section 6.8.

6.7.2 Series V Experimental Design

The experimental design for testing the sensitivity to notching method and pre-cracking is shown in Table 6.19.

Table 6.19: Experimental design for pre-crack sensitivity in Test Series V (ASTM D5045). Each case was replicated three time for a total of $n = 27$.

Combination	Material	Notch Style
1	ABS	Printed, no treatment
2	PC	Printed, no treatment
3	PLA	Printed, no treatment
4	ABS	Printed + razor blade treatment
5	PC	Printed + razor blade treatment
6	PLA	Printed + razor blade treatment
7	ABS	Machined, raw
8	PC	Machined, raw
9	PLA	Machined, raw
10	ABS	Machined + razor blade treatment
11	PC	Machined + razor blade treatment
12	PLA	Machined + razor blade treatment

6.7.3 Series V Materials and Methods

6.7.3.1 Sample Configuration and Manufacturing

The sample configuration and manufacturing was identical to that described in Section 6.6 except for the notch preparation. Half the samples were printed with notches included and half were printed as shown in Figure 6.4f at the beginning of the chapter and notched later with a milling machine (as described in Section 6.2).

6.7.3.2 Sample Conditioning

Per standard ASTM conditioning guidelines for polymer materials, the specimens were conditioned in the same ambient environment (described in Section 6.1) as the tests were planned. The conditioning time was at least 40 hours for all specimens.

6.7.3.3 Experimental Setup

The experimental setup was identical to that described in Section 6.6. Note that the results from Section 6.6 on razor-blade treated samples with printed notches were reused here in this section. This gives a good and consistent baseline for the results in the previous section and this one and makes them easier to compare for making design decisions. Since the setup and processing procedures of the samples for the two testing series were identical, this was

not anticipated to introduce any uncertainty into the experimental results. In fact, it was expected to remove uncertainty since a clear connection could be made between the two data sets.

6.7.4 Series V Results

The results for Series V are shown in Table 6.20. The necessary information for this experimental section is available without the need to plot the results in this case. Data availability is discussed in Appendix E. As discussed in Section 6.6, the reported response for this test series is the fracture load (N) since it is more useful and clear response for the design work described in this dissertation than conditional fracture toughness K_Q or other material properties would be.

Table 6.20: Experimental results (fracture load) from Series V. $n = 3$ for all cases in this table.

Combination	Material	Notch Style	Fracture Load (N)	
			Mean	Stdev
1	ABS	Printed, no treatment	300.1	15.2
2	PC	Printed, no treatment	502.8	23.7
3	PLA	Printed, no treatment	561.7	68.4
4	ABS	Printed + razor blade treatment	326.2	6.8
5	PC	Printed + razor blade treatment	579.1	55.5
6	PLA	Printed + razor blade treatment	578.5	34
7	ABS	Machined, raw	380.6	31.1
8	PC	Machined, raw	658.9	51.0
9	PLA	Machined, raw	692.3	19.7
10	ABS	Machined + razor blade treatment	348.9	21.7
11	PC	Machined + razor blade treatment	648.5	48.6
12	PLA	Machined + razor blade treatment	683.3	42.8

It is very obvious from the experimental results that the notching style used has a very large impact on the fracture load of the samples for all materials. To better explore and attempt to explain the effect, a statistical analysis was done on the collected data.

Analysis of Variance

Source	DF	Adj SS	Adj MS	F-Value	P-Value
Material	2	613160	306580	194.29	0.000
Notch Style	3	86571	28857	18.29	0.000
Error	30	47340	1578		
Lack-of-Fit	6	10563	1761	1.15	0.365
Pure Error	24	36776	1532		
Total	35	747070			

Figure 6.29: ANOVA results for Series V

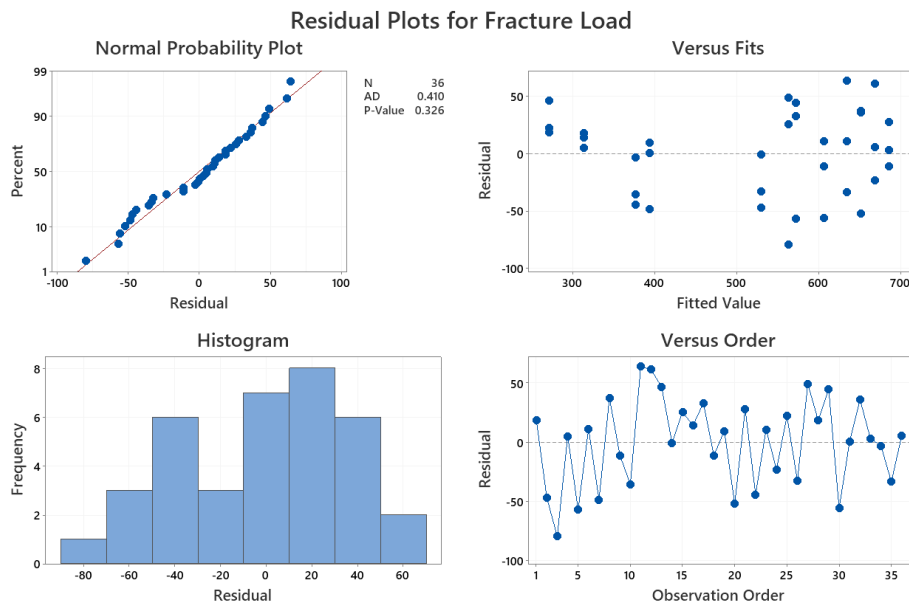


Figure 6.30: 4-in-1 residual plot for Series V.

6.7.5 Series V Statistical Analysis

A standard ANOVA was done using Minitab on the collected experimental data, the results of which can be seen in Figure 6.29. Checking the ANOVA for validity, it was found that the Anderson-Darling (Figure 6.30) test p-value was $0.326 \gg 0.05$, showing that the residuals are normally distributed as expected. Checking the equal variances assumption, the Multiple Comparisons test and Levene's test give p-values of 0.244 and 0.939, respectively. Therefore, the equal variances assumption is valid. Finally, observing the Versus Order plot in Figure 6.30, no clear or obvious patterns exist in the data. Therefore, it is safe to conclude that the ANOVA results are correct and valid.

6.7.6 Selection of Notching Method

Given that the verified ANOVA results show that the notching method had a statistically significant impact on the results, further analysis is needed before moving forward to future experiments. A notching method must be selected, but its selection must be justified in the light of the experimental results. To establish context, some observations should be made:

- The most variation in fracture load observed is about 15%, which is relatively small compared with the up to 60% variability observed in the literature for some materials simply from arranging the material elements [11, 12, 16–20, 22–25].
- For the non-pre-cracked cases, the difference can easily be explained by notch geometry (as seen in Figure 6.4), as it is clear that the printers used to complete the work of this dissertation were capable of printing sharper natural notches than the milling machine was able to make. ASTM D5045 recommends always machining the samples but does not give a standard machining method or tool for this.

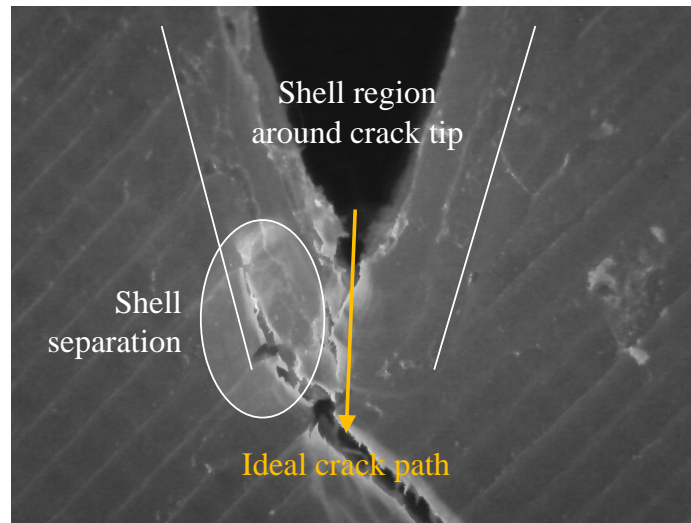


Figure 6.31: Extra cracks and shell separation observed in the printed notches which did not have pre-cracks.

- It was observed when looking at the samples after testing that all had clean breaks with single cracks except a few of the printed notches which were not pre-cracked. In these cases (such as the one shown in Figure 6.31), there were multiple cracks or

small areas of shell separation from the infill. These effects likely explain the major differences between the printed and print + pre-crack samples. Note again that this effect was *not* observed (after a search specifically looking for it) in the printed notches which had also been pre-cracked. Therefore, this observation does not question the validity of the results from Section 6.6.

- Upon review of the experimental samples to understand the difference between the printed and machined notches, it was concluded that the shell in the printed notches was the main contributor. Examining the crack tips (Figure 6.4), the shell around the crack tip is in tension and helps to make the sample more stiff during testing. Therefore, the stress concentration provided by the pre-crack and the extra stress concentration combined likely explains the effect observed. When the notches are machined, the shell is removed completely and the infill area is able to absorb slightly more energy before failing since it will be more flexible without the shell.

Based on these observations, it was concluded that the results of three of the cases (printed notch + pre-crack and the two machined notch cases) were valid and the differences in performance are easily explainable. For the fourth case, some crack tip effects from the shell caused some strange results which need to be further explored. Until this effect is better understood, raw printed notches should not be used for fracture testing FDM-processed materials. From a design perspective, it does not matter much which of the three valid methods are used (as long as the selected method is used consistently) since the point of design-driven fracture tests is to collect comparative information and design knowledge, not build constitutive material models. With these observations, the data provided by this section, and the recommendations of ASTM D5045, it was decided that future experiments related to these materials should use machine-notched samples with pre-cracks.

6.8 Test Series VI: Fracture Behavior vs Element Layout

6.8.1 Opening Remarks and Notes in Series VI

The purpose of this test series was to quantitatively and qualitatively collect information on the impact of various standard material element layouts on the fracture behavior. This data set will be used to drive design rules in Chapter 7.

6.8.2 Series VI Experimental Design

The experimental design for Series VI is shown in Table 6.21. Four different layouts are studied with two different extrusion nozzle sizes.

Table 6.21: Experimental design for CT sample testing with various layouts in Test Series VI. Each case was replicated three times for a total of $n = 72$.

Combination	Material	Nozzle Size	Layout Pattern
1	ABS	0.6	R45
2	PC	0.6	R45
3	PLA	0.6	R45
4	ABS	0.8	R45
5	PC	0.8	R45
6	PLA	0.8	R45
7	ABS	0.6	R90
8	PC	0.6	R90
9	PLA	0.6	R90
10	ABS	0.8	R90
11	PC	0.8	R90
12	PLA	0.8	R90
13	ABS	0.6	Gyroid
14	PC	0.6	Gyroid
15	PLA	0.6	Gyroid
16	ABS	0.8	Gyroid
17	PC	0.8	Gyroid
18	PLA	0.8	Gyroid
19	ABS	0.6	Concentric
20	PC	0.6	Concentric
21	PLA	0.6	Concentric
22	ABS	0.8	Concentric
23	PC	0.8	Concentric
24	PLA	0.8	Concentric

6.8.3 Series VI Materials and Methods

6.8.3.1 Sample Configuration and Manufacturing

The sample configurations and manufacturing were identical to those described in Section 6.6 except for the layout patterns and nozzle sizes. Figure 6.32 shows eight different layouts and corresponding samples for each.

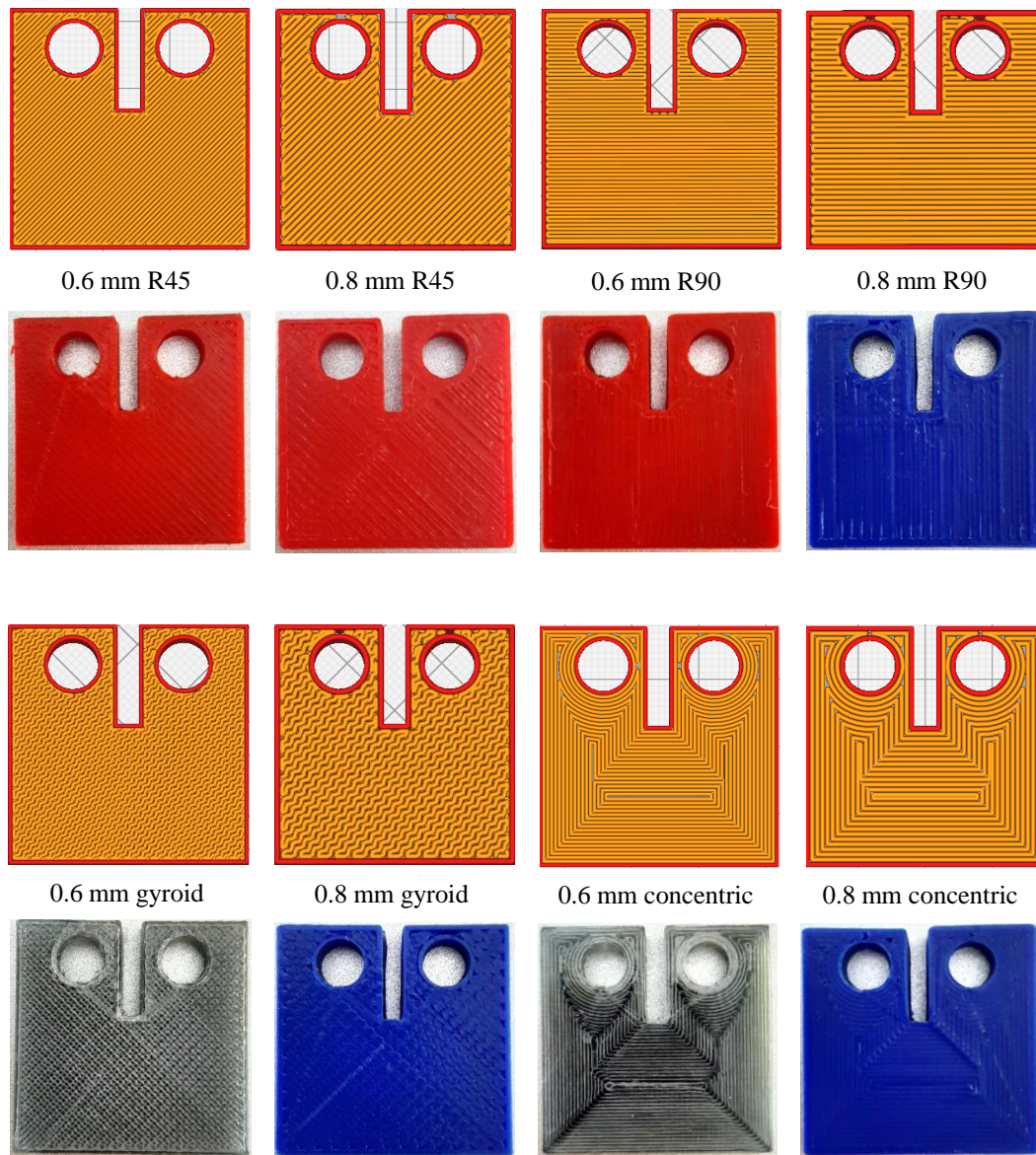


Figure 6.32: Material layouts and nozzle sizes for Series VI. Note that these are shown before notching.

6.8.3.2 Sample Conditioning

Per standard ASTM conditioning guidelines for polymer materials, the specimens were conditioned in the same ambient environment (described in Section 6.1) as the tests were planned. The conditioning time was at least 40 hours for all specimens.

6.8.3.3 Experimental Setup

The experimental setup was identical to that described in Section 6.6.

6.8.4 Series VI Results

Experimental results for Series VI are shown in Table 6.22 and Figure 6.33.

Table 6.22: Experimental results for Test Series VI. Each case was replicated three times for a total of $n = 72$.

Combination	Material	Nozzle Size	Layout Pattern	Fracture Load (N)	
				Mean	Stdev
1	ABS	0.6	R45	384.6	14.1
2	PC	0.6	R45	621.3	58.5
3	PLA	0.6	R45	688.6	23.4
4	ABS	0.8	R45	490.4	11.9
5	PC	0.8	R45	583.7	53.8
6	PLA	0.8	R45	766.5	32.9
7	ABS	0.6	R90	452.9	12.6
8	PC	0.6	R90	542.4	67.4
9	PLA	0.6	R90	672.8	55.3
10	ABS	0.8	R90	387.8	34.0
11	PC	0.8	R90	582.2	12.2
12	PLA	0.8	R90	650.1	30.3
13	ABS	0.6	Gyroid	338.1	7.8
14	PC	0.6	Gyroid	525.0	14.2
15	PLA	0.6	Gyroid	563.1	16.6
16	ABS	0.8	Gyroid	335.1	22.7
17	PC	0.8	Gyroid	557.9	11.1
18	PLA	0.8	Gyroid	579.9	35.7
19	ABS	0.6	Concentric	538.6	36.4
20	PC	0.6	Concentric	361.2	153.0
21	PLA	0.6	Concentric	828.2	24.9
22	ABS	0.8	Concentric	524.2	35.3
23	PC	0.8	Concentric	752.4	44.6
24	PLA	0.8	Concentric	850.6	26.8

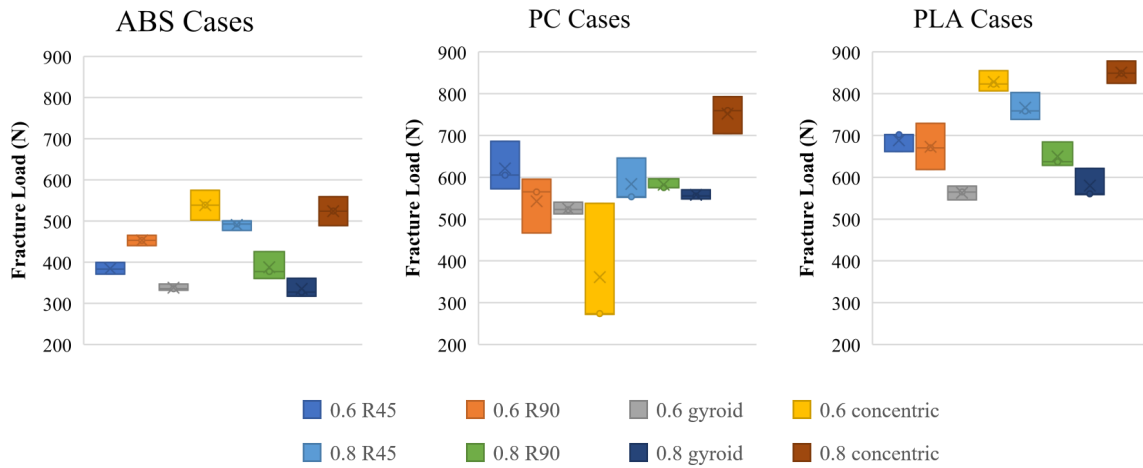


Figure 6.33: Experimental results for Series VI

6.8.5 Crack Analysis

Some of the important observed crack patterns are shown in Figures 6.34-6.37. The crack patterns observed for different materials and layouts were very consistent (and clearly had a major impact on the failure load, unlike what was seen for the films).

- For the R45 samples (Figure 6.34) the cracks followed the raster, occasionally experiencing a 90° turn to follow the raster of a different layer.
- The R90 samples (Figure 6.35) all had straight cracks from the notch tip toward the edge.
- The gyroid samples showed behavior similar to R45, except that the cracks were far more jagged and irregular (Figure 6.36).
- Of all the geometries, the concentrically printed samples were the only ones that showed specific dependence on the material. As shown in Figure 6.37, the ABS crack dissipated sideways into the structure (guided by the contour), the PLA crack tended to split into branches and cause crazing, and the PC samples remained stiff until the crack hit a contour and then failed in fast fracture.

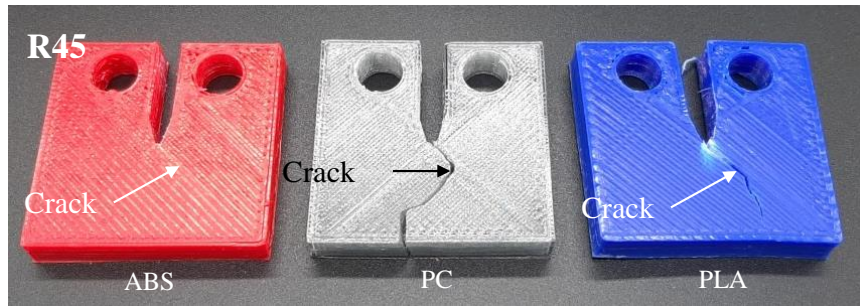


Figure 6.34: Typical crack patterns for R45 samples

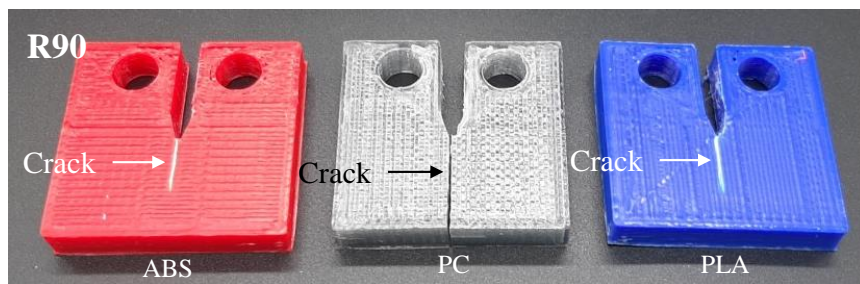


Figure 6.35: Typical crack patterns for R90 samples

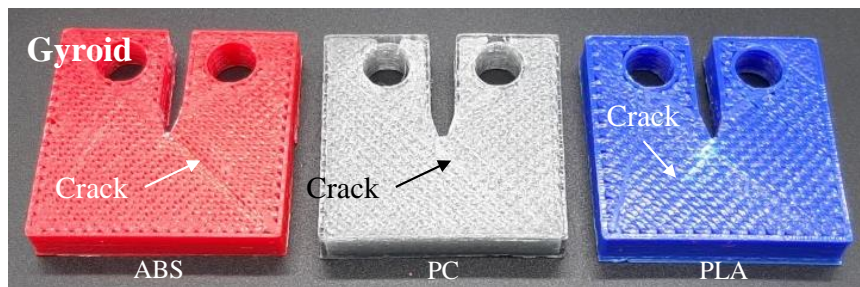


Figure 6.36: Typical crack patterns for gyroid samples

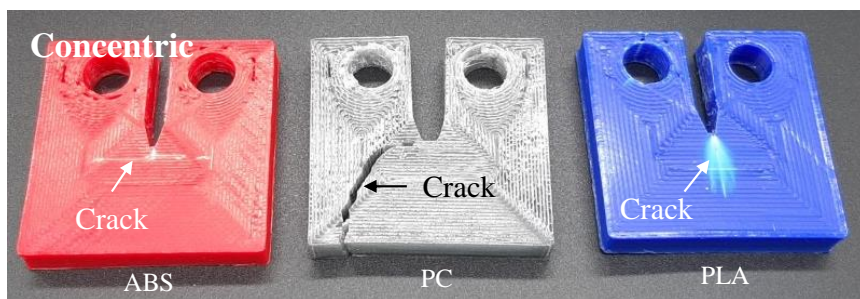


Figure 6.37: Typical crack patterns for concentric samples

6.9 Test Series VII: IZOD Impact Testing

6.9.1 Opening Remarks and Notes on Series VII

In this section, some experiments using IZOD testing samples were completed to explore the resulting properties as a function of raster angle. The Type E (notch compression) test was used to better explore the resulting crack patterns. For many of the tests described in the present chapter, the standard nozzle size was 0.6 mm. In this experimental series, a nozzle size of 0.4 mm was used. For the impact testing series, samples were made using various nozzle sizes and the larger sizes (0.6 mm at above) were too rough for the small standard ASTM D256 samples and left gaps in the structure; for context, standard IZOD samples are 10% (or less) the volume of many other specimens described in this chapter. In addition, the small samples were much more difficult to notch correctly with a larger element size, so a smaller nozzle size was required. For the rest of the experiments, it was found that the 0.6 mm and larger sizes were ideal for exploring crack patterns, as the fracture behavior was more obvious. Series VI (Section 6.8) examined the impact of the nozzle size, so some of the discussion in Chapter 7 regarding the IZOD tests will address this and examine if the change to a smaller nozzle size had a significant impact in the outcome. Based on the results seen in Sections 6.8, it is unlikely that changing the nozzle size had a significant impact since the samples were printed at 100% density.

The experimental details reported here were a portion of a much larger study (the full study is reported in [24]) and only parts of it relevant to the dissertation were reported. Details, figures, and text from the published study by the author are reproduced in this chapter with the permission of the copyright holder. Finally, it should be noted that the original experimental series explored three different printing orientations, but this section will only discuss the flat configuration for the three relevant materials, as it is the one in which the raster angles can be controlled to influence properties; therefore, it is the only orientation that will give useful design information instead of simple characterization or statistical analysis.

6.9.2 Series VII Materials and Methods

6.9.2.1 Sample Configuration and Manufacturing

As previously discussed, only information relevant to the three materials under study in this dissertation are reported here. The experimental design for the three materials and the seven raster angles relevant to the current dissertation is given in Table 6.23. Since only one print orientation was used and the five required replications for each case, the total number of tests recorded here is $n = 105$.

Table 6.23: Experimental design for IZOD testing (ABS, PC, and PLA) in Test Series VII (ASTM D256). Each case was replicated five time for a total of $n = 105$.

Combination	Material	Raster Angle
1	ABS	0°
2	PC	0°
3	PLA	0°
4	ABS	15°
5	PC	15°
6	PLA	15°
7	ABS	30°
8	PC	30°
9	PLA	30°
10	ABS	45°
11	PC	45°
12	PLA	45°
13	ABS	60°
14	PC	60°
15	PLA	60°
16	ABS	75°
17	PC	75°
18	PLA	75°
19	ABS	90°
20	PC	90°
21	PLA	90°

Figure 6.38 shows the specimen configuration for all cases. Due to the potential for shrinkage or dimensional errors when processing the FDM materials (some of which have not yet been characterized fully in the literature), it was decided to establish a nominal sample thickness of 3.25 mm. This allowed some shrinkage, while ensuring that all samples are at least 3.00 mm thick as required by ASTM D256 [26]. Rectangular (instead of square) cross-section samples were used as this is the most common configuration and the one most often

shown in the testing literature. The precautions taken to prevent bending and buckling of the samples during the test will be discussed in a later section. The true thickness of each of the tested samples was recorded and used to calculate the impact resistance and impact energy at the level of each sample. The sample size and dimensional accuracy distribution is the same as that reported in Chapter 3 under Dimensional Accuracy.

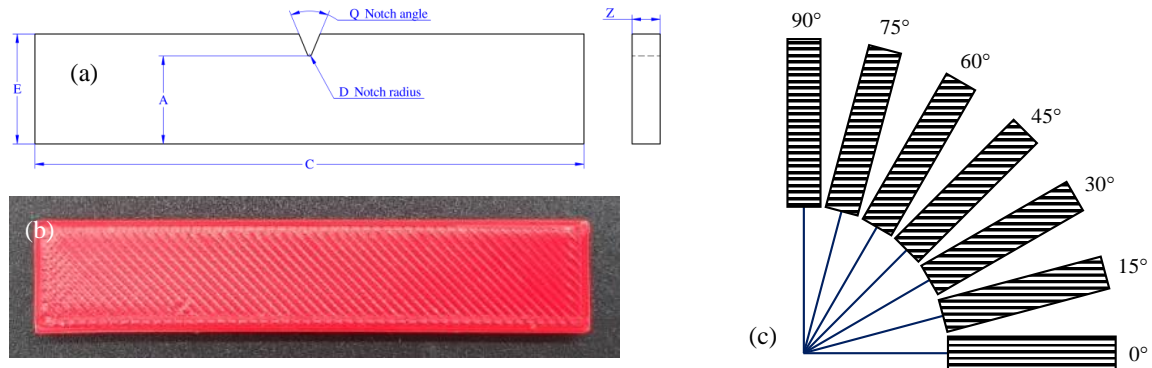


Figure 6.38: (a) ASTM D256 specimen configuration (nominal dimensions were $E = 12.70$ mm, $A = 10.16$ mm, $C = 63.50$ mm, $Z = 3.25$ mm, $Q = 45^\circ$, and $D = 0.25$ mm), (b) printed sample before notching, and (c) raster angle configurations.

6.9.2.2 Sample Notching

Several different notching methods for the FDM parts were attempted during the initial work on this experiment, including with a milling machine, router, and with a file. All of these methods were observed to severely damage the samples, making them unreliable for testing and out-of-spec with the standard. The impact testing experiments discussed in the FDM literature (at the date of experiment performance) did not focus on a feasible method for generating reliable and consistent notches, so a standard and reliable method has not been agreed upon by researchers in practice.

Because of a lack of a standard method for notching FDM samples that does not destroy the specimens, a custom method was developed by the author which proved to be effective. Figure 6.39a shows the tool built for this purpose, which uses a strong stand and rotary tool with a 0.25 mm tip 45 degree steel engraving bit (Figure 6.39c) to make the basic notches in a vertical configuration. The function was similar to a miniature high-speed

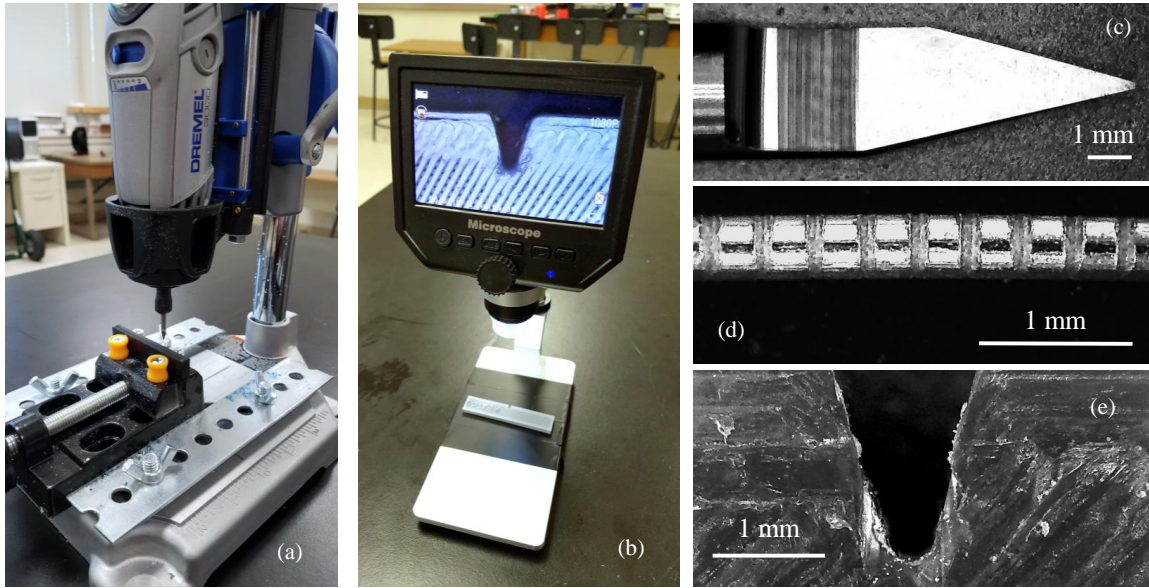


Figure 6.39: (a) Notcher, (b) inspection station, (c) main notch cutter, (d) notch rounding file, and (e) example notch after cutting and polishing

milling machine with a clamp that slid only in the Y-axis to ensure that the samples were held securely during the notching process. The steel engraving tool was very sharp and rotated at a speed of 35,000 rpm, allowing a very fast notch cut and no observed sample damage due to melting or chipping when checked using a microscope. In order to make the notches conform to the requirements of the ASTM standard, a final finishing of each notch was done using a 0.5 mm guitar bridge file (Figure 6.39d). Note that each sample was notched using a backing block. A microscopic inspection station (Figure 6.39b) was used to ensure that the notches were good quality; each sample was checked, even though the ASTM standard only requires checking each 100 – 500 samples. Figure 6.39e shows an example notch under a optical microscope.

6.9.2.3 Sample Conditioning

As required by the standard, the samples were conditioned in an ambient environment (Section 6.1) after notching for 48-60 hours before impact testing.

6.9.2.4 Experimental Setup

The impact test chosen to be performed was the ASTM D256 Type E test, which used a reversed notch (Figure 6.40a). This is one of the four standard IZOD tests described in the standard and the one that was anticipated to provide both the most consistent tests and the best comparative information related to performance versus the element layouts. Often, un-notched tests are used to study highly anisotropic materials [27–29] but it was found during preliminary tests that the un-notched samples did not behave consistently for several of the materials. The preliminary work consisted of manufacturing several samples of each material (including notching and conditioning) for each orientation (raster angles of 0° and 90°) and running mock IZOD tests using them. None of the preliminary test samples were counted as true data points and were used only to tune and test the IZOD machine. It was clear from the preliminary work that a stress concentrator was necessary to gain consistent results and reliable sample breaks; the Type E test provided the ability to test the influence of the raster angle and shell easily.

The IZOD machine from ASR Instruments was used for the experiments. Before the tests, the machine was completely refurbished, during which all of the bearings and essential fasteners were replaced and the provided weights were replaced using ones that were carefully calibrated to ensure accuracy. The dial assembly for the machine was also re-built and carefully tuned. The machine was oiled every 30 impact tests and checked for calibration regularly. Pointer calibration and error measurement was done according to Section 10.3 of ASTM D256. This was done at the beginning of the tests and repeated after each material to insure that the machine remained calibrated. It was found that the pointer energy loss was consistent throughout the test series at approximately 1.11% with a small 2.7J pendulum, which will be accounted for in the friction and windage correction factors.

6.9.2.5 Friction and Windage Correction

As required by the standard, a correction factor was calculated to determine the effects of friction and windage on the experimental results. A single factor cannot be calculated for

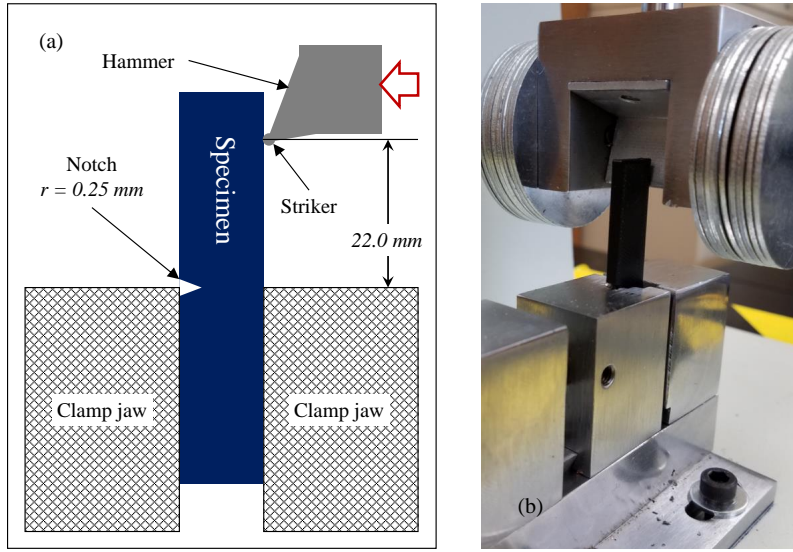


Figure 6.40: ASTM Type E IZOD machine/sample setup (a) diagram and (b) hardware

the whole experiment and must be calculated for each sample. As described in the previous sections, careful calibration of the machine was done before any tests were completed, so the friction and windage effect is inherent in the machine design and not due to wear or degradation of the machine. The values called for in Section A2 of the ASTM D256 standard are shown in Table 6.24 below; the values are the mean and standard deviation of 10 runs with the freshly calibrated machine. Clearly, the energy lost from the friction and windage are very small but they are still worth considering in this experiment to ensure the most accurate data possible. Per the standard, these values can be used to calculate the correction energies for each specimen. The maximum angle β_{max} of one swing was measured from the machine as the value of $\alpha_1 = 143.9^\circ$ in Table 6.24.

Table 6.24: Friction and windage correction input values

Variable		Value
E_M	Pendulum energy (J)	2.7
h_M	Pendulum mass height at start (m)	0.600
L	Length of pendulum (m)	0.322
θ	Starting angle ($^\circ$)	150.0
α_1	Angle for E_A ($^\circ$) (mean [stdev])	143.9 [0.57]
E_A	Energy lost through friction (J)	0.0153
β_1	Angle for E_B ($^\circ$) (mean [stdev])	145.3 [0.48]
E_B	Energy lost through windage (J)	0.0008

For each sample, the angle β_{sample} is measured and used to calculate the uncorrected energy E_S . For each reading, the total correction energy is:

$$E_{TC} = \left(E_A - \left(\frac{E_B}{2} \right) \right) \left(\frac{\beta_{sample}}{\beta_{max}} \right) + \left(\frac{E_B}{2} \right) \quad (6.1)$$

The impact resistance for each sample is calculated as:

$$I_R = \frac{E_S - E_{TC}}{t} \quad (6.2)$$

where t is the sample thickness. Similarly, the impact energy is calculated to be:

$$I_E = \frac{E_S - E_{TC}}{At} \quad (6.3)$$

where t is the sample thickness and A is the thickness of material under the notch.

6.9.2.6 Sample Clamping and Dimensional Measurement

Measurement of the samples was completed using a pair of digital vernier calipers with a resolution of 0.01 mm, using the microscopic inspection station to verify notch depth as needed. The samples were clamped into the IZOD machine (see Figure 6.40b for the hardware setup), taking extreme care to ensure that they were straight and correctly aligned. The notch was positioned using a thin, flat, blunted blade to ensure that it was positioned correctly relative to the clamp. Clamping was done only finger-tight to provide a secure base for the sample while providing consistent clamping pressure, since impact tests are very sensitive to clamping pressure and method.

6.9.3 Series VII Results

Using the procedure in ASTM D256 and the correction factors calculated previously, the impact strength (Figure 6.41a) and the impact energy (Figure 6.41b) were found for each sample. The calculated values are shown in Table 6.25. As previously noted, the two sets were not exactly equivalent since the thicknesses of the specimens varied somewhat (within the tolerances established in the standard; in all cases, the true specimen thickness was

used to calculate the impact energy.

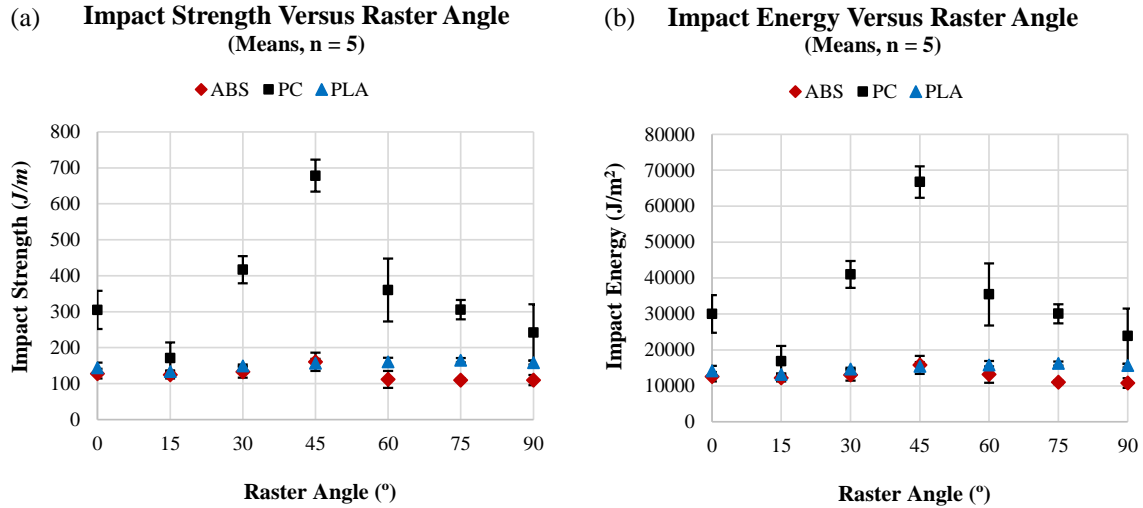


Figure 6.41: Series VII results for (a) impact strength and (b) impact energy. Data points shown represent means for $n = 5$, with corresponding standard deviations shown as error bars.

Analysis of Variance

Source	DF	Adj SS	Adj MS	F-Value	P-Value
Material	2	1073944	536972	88.77	0.000
Raster Angle	6	330880	55147	9.12	0.000
Error	96	580717	6049		
Lack-of-Fit	12	480342	40028	33.50	0.000
Pure Error	84	100375	1195		
Total	104	1985541			

Figure 6.42: ANOVA results for Series VII

6.9.4 Series VII Statistical Analysis

To better understand the results and better use the collected data for design decisions, a statistical analysis was completed on the data using Minitab (Version 19.2020.1). Figure 6.42 shows the initial analysis of variance (ANOVA) calculations, showing that both the material choice and raster angle had a statistically significant impact on the impact strength. Note that, while the two data sets for impact strength and impact energy are not exactly equivalent due to variance in sample thickness, they are similar enough so that

Table 6.25: Experimental results for IZOD testing of Series VII. Each case was replicated five time for a total of $n = 105$.

Combination	Material	Raster Angle	n	I_R (J/m)		I_E (J/m^2)	
				Mean	Stddev	Mean	Stddev
1	ABS	0°	5	127.7	13.6	12,558	1,335
2	PC	0°	5	305.0	53.2	30,017	5,211
3	PLA	0°	5	144.2	14.1	14,184	1,385
4	ABS	15°	5	124.4	10.0	12,238	981
5	PC	15°	5	171.2	43.1	16,855	4,255
6	PLA	15°	5	133.7	3.1	13,150	301
7	ABS	30°	5	132.8	16.3	13,070	1,607
8	PC	30°	5	416.8	37.8	41,028	3,746
9	PLA	30°	5	149.4	3.9	14,688	378
10	ABS	45°	5	160.9	25.5	15,819	2,508
11	PC	45°	5	678.3	44.6	66,707	4,380
12	PLA	45°	5	156.5	12.2	15,402	1,197
13	ABS	60°	5	111.7	23.4	13,151	2,302
14	PC	60°	5	360.1	87.5	35,437	8,637
15	PLA	60°	5	160.4	11.3	15,787	1,113
16	ABS	75°	5	109.8	4.7	10,991	462
17	PC	75°	5	305.4	27.0	30,061	2,656
18	PLA	75°	5	164.8	6.0	16,224	581
19	ABS	90°	5	109.8	14.1	10,797	1,374
20	PC	90°	5	242.4	78.0	23,852	7,667
21	PLA	90°	5	158.6	5.1	15,617	512

a regular statistical analysis will produce the same conclusions for each. Therefore, it was decided that analysis would only be completed on one of them.

To confirm that the ANOVA produced valid conclusions, the Fisher Assumptions were tested. In Figure 6.43, the set of residual plots for the data is shown. The p-value for the Anderson-Darling test fails to show normality of the residuals. Checking the equal variances assumption (Figure 6.44), it was also found that the assumption failed using both the multiple comparisons test and Levene’s test. Since both assumptions failed, it is not possible to use a transformation or parametric analysis tool. Therefore, it was necessary to recalculate the experiment p-values using a non-parametric method. For this series, the Kruskal-Wallis test was the easiest to use; the results are shown in Figure 6.45. The non-parametric test technically gave the same conclusion as the original ANOVA, but it should be noted that the weights of each of the factors is quite different. The impacts of this on design decisions and effective design-driven experimentation will be discussed in depth in

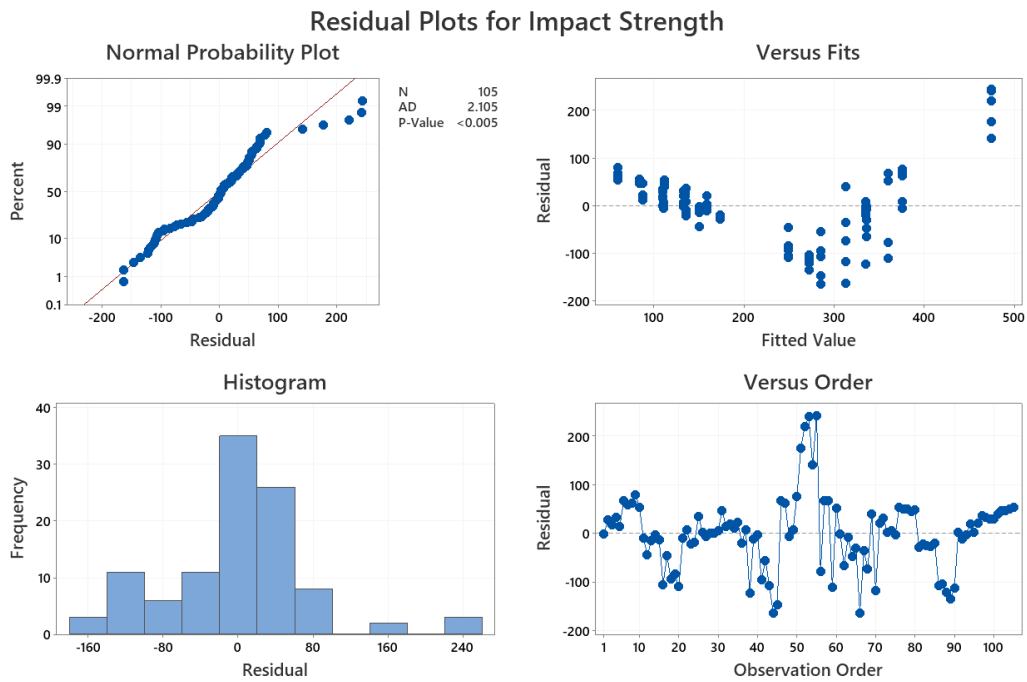
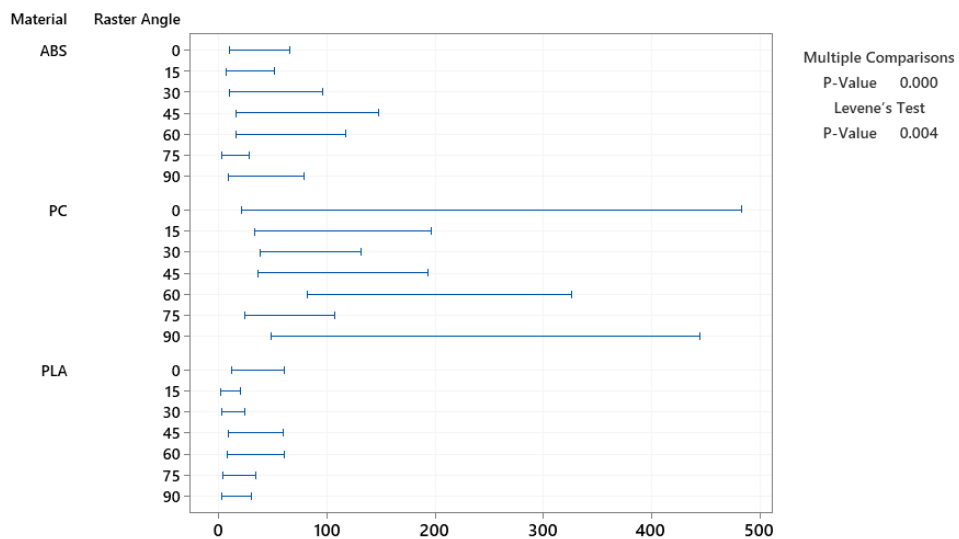


Figure 6.43: 4-in-1 residual plot for Series VII

Chapter 7.

Test for Equal Variances: Impact Strength vs Material, Raster Angle

Multiple comparison intervals for the standard deviation, $\alpha = 0.05$



If intervals do not overlap, the corresponding stdevs are significantly different.

Figure 6.44: Equal variances test results for Series VII

Kruskal-Wallis Test: Impact Strength versus Material

Descriptive Statistics

Material	N	Median	Mean Rank	Z-Value
ABS	35	125.354	24.8	-6.71
PC	35	328.542	84.5	7.48
PLA	35	154.049	49.7	-0.78
Overall	105		53.0	

Test

Null hypothesis H₀: All medians are equal
 Alternative hypothesis H₁: At least one median is different

Method	DF	H-Value	P-Value
Not adjusted for ties	2	67.72	0.000
Adjusted for ties	2	67.73	0.000

Kruskal-Wallis Test: Impact Strength versus Raster Angle

Descriptive Statistics

Raster Angle	N	Median	Mean Rank	Z-Value
0	15	142.385	49.6	-0.46
15	15	133.841	33.8	-2.63
30	15	148.249	57.5	0.61
45	15	165.618	70.6	2.42
60	15	160.525	59.7	0.92
75	15	164.744	53.0	-0.00
90	15	157.738	46.7	-0.86
Overall	105		53.0	

Test

Null hypothesis H₀: All medians are equal
 Alternative hypothesis H₁: At least one median is different

Method	DF	H-Value	P-Value
Not adjusted for ties	6	12.84	0.046
Adjusted for ties	6	12.84	0.046

Figure 6.45: Kruskal-Wallis test results for Series VII

After completion of the formal statistical analysis, two more plots were created from the data: (1) the main effects plot (Figure 6.46a) and (2) the interaction plot (Figure 6.46b). These plots are useful for graphically interpreting how each factor may affect the experiment response and how the factors may interact with each other. These are very important tools for collecting and interpreting design knowledge and will be discussed further in Chapter 7.

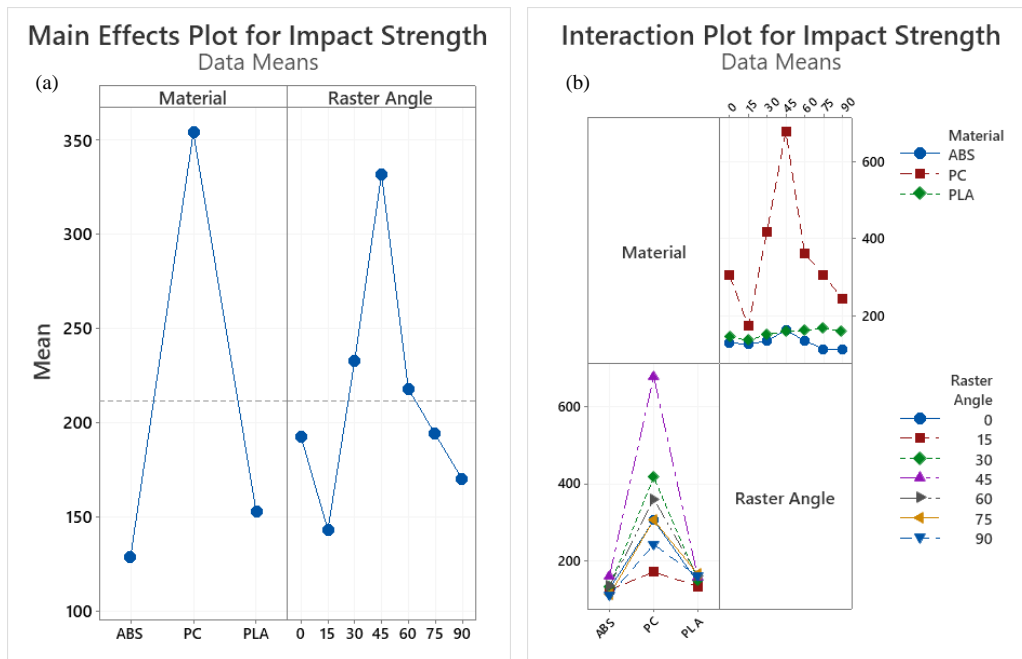


Figure 6.46: (a) Main effects and (b) interaction plots for Series VII

6.10 Closing Remarks

This chapter covered a wide range of physical experiments related to the fracture behavior of FDM-processed materials. Following the same bottom-up approach as the MPDSM design method described in this dissertation, these experiments began with a basic set of material characterizations to establish a baseline. The individual elements, in the form of fibers, were then tested. This was followed by the study of films (representing layers) and several different aspects of meso- and macro-scale fracture behavior.

Numerous important and interesting conclusions for each of the experiments were found, most especially that FDM materials did not show a sample size effect when tested, even though typical samples fail to meet the criteria for plane strain established by ASTM D5045. It was found that the materials were extremely sensitive to the notching method, which contradicts some published literature, such as in [25]. A final very important observation from these experiments is that the strength of fibers in series and layers is that the strength of the bundle or layer may be much less than the sum of the strengths seen in individual fibers.

Future iterations and replications of these experiments should consider using a much larger testing machine and J-integral methods. The work presented here is the best that could be accomplished given the circumstances and available resources, but additional experiments following the approach and principles laid out in this chapter would certainly improve understanding and design knowledge collection methods in the future.

Copyright Acknowledgement: As of April 10, 2021, much of the text in Section 6.9, as well as Figures 6.38, 6.39, and 6.40 and Table 6.24 are © IMechE/Sage and published in the following paper:

Patterson, A.E., Rocha Pereira, T., Allison, J.T., Messimer, S.L. (2019). IZOD impact properties of full-density fused deposition modeling polymer materials with respect to raster angle and print orientation. *Proceedings of the Institution of Mechanical Engineers, Part C: Journal of Mechanical Engineering Science*. DOI: 10.1177/0954406219840385

According to the Sage copyright agreement, the original authors of works do not need specific copyright permissions to reproduce their work in other venues as long as the original paper is cited and the owner of the copyrighted material is given clear attribution.

Chapter 6 Bibliography

- [1] ASTM, “D5045 - 14: Standard Test Methods for Plane-Strain Fracture Toughness and Strain Energy Release Rate of Plastic Materials,” standard, ASTM International, West Conshohocken, PA, 2014.
- [2] A. E. Patterson, C. Chadha, I. M. Jasiuk, and J. T. Allison, “Design and repeatability analysis of desktop tool for rapid pre-cracking of notched ductile plastic fracture specimens,” *Engineering Fracture Mechanics*, vol. 217, p. 106536, Aug. 2019.
- [3] ASTM, “ASTM D638 - 14: Standard Test Method for Tensile Properties of Plastics,” standard, ASTM International, West Conshohocken, PA, 2014.
- [4] J. F. Rodríguez, J. P. Thomas, and J. E. Renaud, “Mechanical behavior of acrylonitrile butadiene styrene fused deposition materials modeling,” *Rapid Prototyping Journal*, vol. 9, pp. 219–230, Oct. 2003.
- [5] A. Bellini and S. Güçeri, “Mechanical characterization of parts fabricated using fused deposition modeling,” *Rapid Prototyping Journal*, vol. 9, pp. 252–264, Oct. 2003.
- [6] F. Arbeiter, M. Spoerk, J. Wiener, A. Gosch, and G. Pinter, “Fracture mechanical characterization and lifetime estimation of near-homogeneous components produced by fused filament fabrication,” *Polymer Testing*, vol. 66, pp. 105–113, Apr. 2018.
- [7] E. A. Papon and A. Haque, “Fracture toughness of additively manufactured carbon fiber reinforced composites,” *Additive Manufacturing*, vol. 26, pp. 41–52, Mar. 2019.
- [8] T. D. McLouth, J. V. Severino, P. M. Adams, D. N. Patel, and R. J. Zaldivar, “The impact of print orientation and raster pattern on fracture toughness in additively manufactured ABS,” *Additive Manufacturing*, vol. 18, pp. 103–109, Dec. 2017.
- [9] J. Torres, M. Cole, A. Owji, Z. DeMastry, and A. P. Gordon, “An approach for mechanical property optimization of fused deposition modeling with polylactic acid via design of experiments,” *Rapid Prototyping Journal*, vol. 22, pp. 387–404, Mar. 2016.

- [10] M. Arif, S. Kumar, K. Varadarajan, and W. Cantwell, "Performance of biocompatible PEEK processed by fused deposition additive manufacturing," *Materials & Design*, vol. 146, pp. 249–259, May 2018.
- [11] J. Gardan, A. Makke, and N. Recho, "Fracture improvement by reinforcing the structure of acrylonitrile butadiene styrene parts manufactured by fused deposition modeling," *3D Printing and Additive Manufacturing*, vol. 6, pp. 113–117, Apr. 2019.
- [12] J. Gardan, A. Makke, and N. Recho, "A method to improve the fracture toughness using 3D printing by extrusion deposition," *Procedia Structural Integrity*, vol. 2, pp. 144–151, 2016.
- [13] M. Z. Huang, J. Nomai, and A. K. Schlarb, "The effect of different processing, injection molding (IM) and fused deposition modeling (FDM), on the environmental stress cracking (ESC) behavior of filled and unfilled polycarbonate (PC)," *Express Polymer Letters*, vol. 15, no. 3, pp. 194–202, 2021.
- [14] D. Yavas, Z. Zhang, Q. Liu, and D. Wu, "Fracture behavior of 3d printed carbon fiber-reinforced polymer composites," *Composites Science and Technology*, vol. 208, p. 108741, May 2021.
- [15] L. Ruiz-Pérez, G. J. Royston, J. P. A. Fairclough, and A. J. Ryan, "Toughening by nanostructure," *Polymer*, vol. 49, pp. 4475–4488, Oct. 2008.
- [16] J. Gardan, "Method for characterization and enhancement of 3D printing by binder jetting applied to the textures quality," *Assembly Automation*, vol. 37, no. 2, pp. 162–169, 2017.
- [17] J. Gardan, A. Makke, and N. Recho, "Improving the fracture toughness of 3d printed thermoplastic polymers by fused deposition modeling," *International Journal of Fracture*, vol. 210, no. 1-2, pp. 1–15, 2017.
- [18] P. Lanzillotti, J. Gardan, A. Makke, and N. Recho, "Strengthening in fracture toughness of a smart material manufactured by 3D printing," *IFAC-PapersOnLine*, vol. 51, no. 11, pp. 1353–1358, 2018.
- [19] P. Lanzillotti, J. Gardan, A. Makke, and N. Recho, "Enhancement of fracture toughness under mixed mode loading of ABS specimens produced by 3D printing," *Rapid Prototyping Journal*, vol. 25, pp. 679–689, May 2019.
- [20] A. Lenti, "Fracture toughness assessment using digital image correlation in additive manufacturing," Master's thesis, Polytechnic of Turin, Turin, Italy, 2019. Masters Thesis - Mechanical Engineering.
- [21] A.-H. I. Mourad, A. H. Idrisi, J. V. Christy, D. T. Thekkuden, H. A. Jassmi, A. S. Ghazal, M. M. Syam, and O. D. A. A. A. Qadi, "Mechanical performance assessment of internally-defected materials manufactured using additive manufacturing technology," *Journal of Manufacturing and Materials Processing*, vol. 3, p. 74, Aug. 2019.

- [22] R. M. Dunn, K. R. Hart, and E. D. Wetzel, "Improving fracture strength of fused filament fabrication parts via thermal annealing in a printed support shell," *Progress in Additive Manufacturing*, vol. 4, pp. 233–243, Apr. 2019.
- [23] J. M. Djouda, D. Gallitelli, M. Zouaoui, A. Makke, J. Gardan, N. Recho, and J. Crépin, "Local scale fracture characterization of an advanced structured material manufactured by fused deposition modeling in 3D printing," *Frattura ed Integrità Strutturale*, vol. 14, p. 534–540, Dec. 2019.
- [24] A. E. Patterson, T. Rocha Pereira, J. T. Allison, and S. L. Messimer, "IZOD impact properties of full-density fused deposition modeling polymer materials with respect to raster angle and print orientation," *Proceedings of the Institution of Mechanical Engineers, Part C: Journal of Mechanical Engineering Science*, p. 095440621984038, Apr. 2019.
- [25] D. A. Roberson, A. R. T. Perez, C. M. Shemelya, A. Rivera, E. MacDonald, and R. B. Wicker, "Comparison of stress concentrator fabrication for 3D printed polymeric izod impact test specimens," *Additive Manufacturing*, vol. 7, pp. 1–11, July 2015.
- [26] ASTM, "D256 - 10(2018): Standard Test Methods for Determining the Izod Pendulum Impact Resistance of Plastics," standard, ASTM International, West Conshohocken, PA, 2018.
- [27] H.-S. Yang, H.-J. Kim, J. Son, H.-J. Park, B.-J. Lee, and T.-S. Hwang, "Rice-husk flour filled polypropylene composites: Mechanical and morphological study," *Composite Structures*, vol. 63, pp. 305–312, feb 2004.
- [28] D. Plackett, T. L. Andersen, W. B. Pedersen, and L. Nielsen, "Biodegradable composites based on l-poly lactide and jute fibres," *Composites Science and Technology*, vol. 63, pp. 1287–1296, jul 2003.
- [29] V. C. Shunmugasamy, H. Anantharaman, D. Pinisetty, and N. Gupta, "Unnotched Izod impact characterization of glass hollow particle/vinyl ester syntactic foams," *Journal of Composite Materials*, vol. 49, pp. 185–197, dec 2013.

Chapter 7

DESIGN RULE DEVELOPMENT FOR FRACTURE-DRIVEN FDM MPDSMs

This chapter may contain previously published text and figures, which are reproduced with the permission of the copyright holders. See the copyright statement and list of references at the end of the chapter.

7.1 Introduction

Up to this point, several essential sources of design knowledge for the design fracture-driven MPDSMs have been carefully explored or developed, including those which have not been covered in the engineering literature before. The careful mapping and enforcement of constraints, new ideas for problem formulations, a deep understand of the manufacturing process being used, a new design perspective on what it means to design structured materials, a conceptual and experimental exploration of these materials under fracture, the meaning of design knowledge in terms of engineering design - all have been discussed in depth so far in this dissertation. Now, a way to apply these and other important design concepts and principles (within the MDD context) to real-world design problems is needed. This chapter brings these concepts together into one place and uses them to develop useful and practical design rules for fracture-driven FDM MPDSMs. These design rules will

be applied to several major design studies in Chapter 8 and to develop a practical design guide for practicing engineers, engineering students, and other designers who have a basic knowledge of material behavior and mechanics but are not experts in the specific technical areas explored in this dissertation.

This chapter is structured into several major sections, first exploring (Section 7.2) why developing design rules under MDD is advantageous and why this is a large improvement over classic design-for-manufacturing methods in the context of modern design techniques. Section 7.3 discusses the three major design objectives for fracture-driven FDM MPDSMs. This is followed up in Section 7.4 with a short but rigorous definition of design knowledge and how to use it in the context of this work. Several potentially valuable sources of information are presented, with the focus on giving the reader both the information and guidance on where and how to look for more if needed in the future. In Section 7.5, the formal design rules are laid out, each one explored and explained in detail with as many references to previous work and definitions as possible. Some final remarks are given in Section 7.6 in preparation for the design studies presented in Chapter 8.

7.2 Design Rules under MDD

As described in Chapters 2 and 4, manufacturability-driven design (MDD) is the design perspective in which manufacturability is the prime or co-prime design requirement. When done correctly and with good-quality models and good information about the process-material interactions, the design space can be limited to only manufacturable designs from the conceptual design phase [1–3]

This chapter brings all these topics together, along with some additional important sources of relevant design knowledge. It uses them all to derive a set of rigorous design rules for FDM-driven MPDSMs under fracture conditions. These design rules will be used by practicing engineers and designers to produce useful MPDSMs which will help address numerous design-manufacturing mismatch problems. These design rules will be useful for both driving problem formulations (for example, for setting up optimal design problems) and as an expert-driven design method on their own. As previously stated, the approach taken here goes far beyond classic design for manufacturing (DFM) principles. In particular, this

manufacturing-driven design (MDD) based approach (developed in Chapter 2 and Chapter 4), offers several major benefits for fracture-driven FDM MPDSM design:

- This MDD design rule approach is far more data-driven and model-driven than classic DFM and far less reliant on expert experience. Much of the data needed to make important design decisions can be modeled and cataloged.
- The design constraints generated using this approach are far more clear and specific than those that would be generated using classic DFM on a general scale.
- This approach does not penalize design complexity, but only limits it enough to ensure manufacturability.
- Any solution method (optimal design, expert intuition, topology optimization, and such) can be used in conjunction with the developed design rules

7.3 Fracture Driven FDM MPDSM Design Objectives

Given the crack tip and loading shown in Figure 7.1a, inputting additional energy into the material will eventually result in crack extension through the shown fields [4–7]. If the material is homogeneous, isotropic, and the specimen is consistent in size, it is reasonable to assume that the crack will grow in a straight line from the crack tip to the boundary. However, if the material is not perfect or is structured, then it should be expected that the crack may branch out or turn to follow the path of least resistance through the material. Therefore, the region where the crack could possibly grow after it starts looks like a contour; generally, the stress or strain field shape around the crack tip indicates its most likely direction [5, 7–9]. Good representations of these contours relative to position around the crack tip are given in Figures 7.1b and 7.1c.

One of the basic principles of fracture mechanics is that cracks are formed as a way to quickly and efficiently dissipate energy from the material [4, 7]. This is especially true if the material is brittle and cannot plastically deform (or deform enough) to dissipate the energy input. With this in mind, it is reasonable to assume that preventing or stopping cracks will produce a tougher material, while increasing the number and speed of cracks will increase the rate at which energy is dissipated from the system.

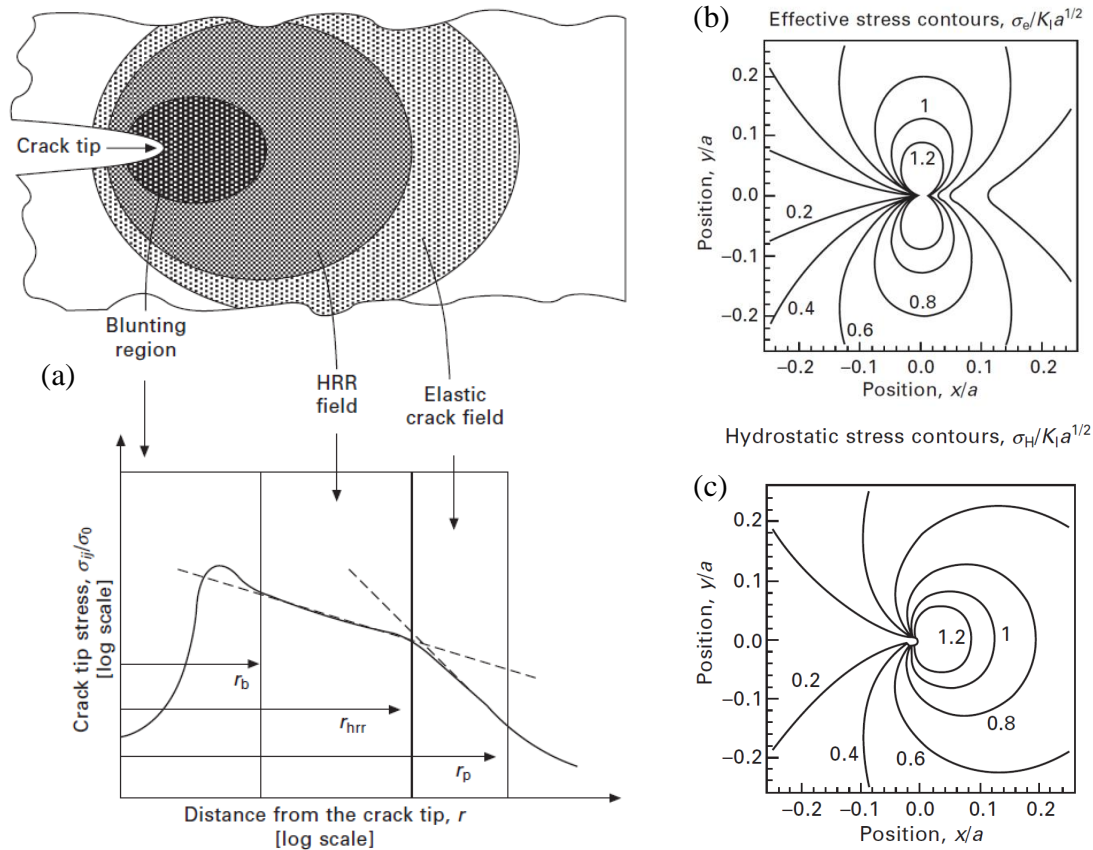


Figure 7.1: (a) A representation of a crack tip and the field zones around it in terms of distance and (b-c) example stress contours around the crack tip, which are useful in determining which material layout strategies should be used. All figures from [5] and © Elsevier B.V., reproduced with permission.

From the results of the fracture experiments and literature reviews, it is clear that a structured contour of material around the crack tip has the best chance of presenting a 90° (normal) wall to the crack as it grows, making it break the contour in order to continue growing and dissipating the maximum energy while stopping, preventing further growth. Inverting this, the contour can be used to steer the crack or to cause it to accelerate. Therefore, from the perspective of any fracture-driven design problem, there are three possible design objectives:

1. **Crack arrest:** A fracture exists or is possible in a material structure and the designer wants to prevent or stop the crack. This is the most common case and the objective of most fracture-based design since fracture is one of the common failure modes for materials (along with yielding and buckling). Therefore, it is common for

structural design and structural integrity problems to try to prevent or stop cracks in the structure.

2. **Crack acceleration:** Material fracturing to generate new surface energy [4] is one of the most efficient and fast ways to dissipate excess energy from a system. Therefore, there are numerous design problems (such as sacrificial structural members) which would benefit from rapid fracture. In this case, two different approaches are possible: (1) make the material as weak as possible to guarantee fast crack growth or (2) make the material structurally sound but encourage the crack to grow in the most efficient path. These two objectives compete, as making the material weak will speed up the crack but reduce the amount of energy dissipated in the process. The second option has the opposite effect.
3. **Crack pattern control:** There are many cases where crack pattern control is needed (for example, as explored in Refs. [10–14]). In this case, the same objectives are available as for the crack acceleration option. In fact, it could be said that the crack acceleration objective is a special case of crack pattern control where the crack is designed to follow the shortest and most efficient path to the boundary.

7.4 Design Knowledge Drivers

One of the prerequisites for producing a set of solid, consistent, and reproducible design rules is a good source or set of sources to collect design knowledge. Often, only modeling and problem formulation are considered when producing design rules but this dissertation explored many more in previous chapters. This section explores some of the most important ones in order to show the source and rigor of the design rules which will be generated in this chapter. A graphical representation is shown in Figure 7.2.

7.4.1 General Problem Understanding

It is extremely important for the designer and other stakeholders to understand the design problem well. Not only so that reasonable expectations can be set and the proper resources provided, but because the early project requirements will drive the quality of the design.

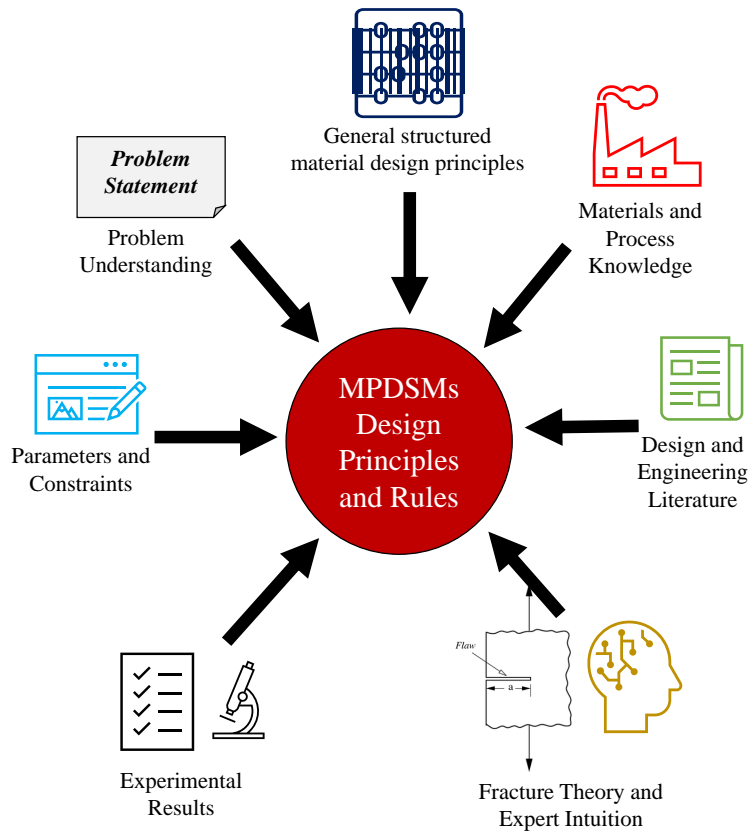


Figure 7.2: Design rule major sources

This is especially true when using an MDD-focused method; while MDD provides a wide range of benefits (as discussed in Chapter 4), one of its major drawbacks is that it is much more difficult to change design requirements and approach later in the design life cycle. Therefore, the requirements must be solid and show the true possible design space that can be explored.

7.4.2 Structured Material Principles

Another source of information, discussed in Chapter 4 and Chapter 5, is the fundamental design principles behind existing structured materials and metamaterials. Since many of the basic design principles will be the same (with MPDSMs being subjected to more specific constraints but having more design freedom in other areas), it can save time and work to study at least the basic principles. This was done in Chapter 4 and Chapter 5.

7.4.3 Material and Manufacturing Process Knowledge

The materials used in this dissertation are standard thermoplastic hard polymers (also often called engineering plastics or commodity plastics). ABS and PC are amorphous, while PLA is semi-crystalline. The polymer chemistry is similar for FDM, but the properties and realistic behavior of the materials during printing can certainly vary. The effects of the material selection and the manufacturing process was discussed and explored extensively in Chapter 2, Chapter 3, Chapter 4, and Chapter 5. Some of the major observations that could be made by a designer who is not an expert in polymer science are:

- Semi-crystalline thermoplastics are far more dense and less brittle than amorphous plastics. As seen in some of the crack images in Chapter 6, the semi-crystalline PLA is far more likely to send out webs of small cracks and craze before fracturing, while the amorphous materials showed fast brittle fracture, especially in the case of PC.
- While the polymerization reaction is complex and far beyond the scope of this dissertation, it can be easily observed that amorphous polymers shrink in a more uniform manner than semi-crystalline ones do. This helps increase the possible effective density significantly for amorphous materials (this effect was observed in [15] and other studies). This can help the material to be more homogeneous than it might otherwise be and therefore a tougher material in many cases.
- Amorphous materials have much higher structural stability at elevated temperature, as demonstrated by the differences in glass transition temperature between them.

7.4.4 FDM Parameters and Constraints

Chapter 3 presented a rigorous and solid set of manufacturability constraints was derived. The ones that are relevant to the design and fabrication of FDM MPDSMs are:

- Constraint 4: Extruder temperature
- Constraint 6: Printing speed
- Constraint 7: Build plate temperature

- Constraint 8: Jerk and acceleration
- Constraint 9: Degree of crystallinity
- Constraint 10: Shrinkage limit
- Constraint 11: Defect tolerance
- Constraint 12: Degree of structural homogeneity
- Constraint 13: Realistic packing density
- Constraint 17: Nozzle size
- Constraint 19: Element width
- Constraint 20: Layer height
- Constraint 22: Element dimensional ratio
- Constraint 25: Stand-alone element length
- Constraint 26: Element corner radius
- Constraints 27-30: Element on previous material length
- Constraints 31 and 34-35: Bridge and overhang distance
- Constraint 33: Shell-infill ratio
- Constraints 38-42: Small feature geometric restrictions
- Constraint 51: Length scale

7.4.5 Experimental Results

Chapter 6 of this dissertation was dedicated to experimentally exploring a large number of aspects related to the development and manufacturing of MPDSMs. The design knowledge was collected and used to drive many of the design rules presented in the next section. Crack pattern behavior, as discussed in Chapter 6, was especially important.

7.4.6 Fracture Mechanics Theory and Expert Intuition

While it was not necessary to outline detailed fracture mechanics theory, since it was explored previously from theory (Section 7.3), the literature (Chapter 5) and experimentally (Chapter 6), it should be noted that it certainly had an impact on the design rules. Given the extensive experience of the authors related to fracture mechanics, the concepts behind this field are represented in many areas of the dissertation. The study of fracture mechanics was one of the major driving forces behind the genesis of this project in the first place and motivation to continue it to completion.

7.4.7 Design and Engineering Literature

As discussed in Chapter 5, the engineering literature is an excellent place to start looking for design knowledge or expand it. As shown in Chapter 5, several major areas (not related directly to design) can be explored for useful information. Re-stating these in terms of what is needed for MPDSMs:

- Guidance on material element layout and material structure optimization
- Damage mechanics as the structured materials fail
- Understanding the process-material effects and synergy
- Effects of environmental effects
- The need for new manufacturing processes to deal with new design problems
- Realistic performance metrics
- Techniques for effect material and material system characterization and evaluation

7.5 Design Rules

This section describes the essential design rules which govern the design of fracture-driven FDM MPDSMs described in this dissertation. These rules come from a combination of the sources discussed in Section 7.4 and the other tools and themes developed in previous chapters of this work. In addition to driving a successful and straight-forward design process, these rules are formulated such that:

1. That there are as few rules as possible and that every possible rule has been turned into a guideline or best practice in order to maximize design freedom.
2. The designers and stakeholders using these rules do not need to be experts in fracture mechanics, additive manufacturing, or classic structured materials. Every effort was made to describe them in such a way that competent designers and engineers of any experience level (including senior engineering students) can make use of them effectively.
3. All of the described processes and techniques can be accomplished using standard commercial software. No specialized or complex design tools are required.
4. The design process can be as manual or as automated as the designer wishes to set it up to be by selection of the solution method.

These design rules, distilled from the work of this dissertation, will provide many benefits however, three things should be noted

1. The element layouts produced are at the meso-scale only. The conclusions may be applicable to other scales but this will need to be established through another study.
2. The set of design rules here are the smallest possible set in order to provide the largest possible design freedom. It is possible that some additional rules or guidelines would need to be produced and used for some special cases.
3. Due to the requirement in this dissertation that only commercially-available software and design tools be used, some additional improvements may be accomplished if the designer is willing to produce more specialized tools.

7.5.1 Design Rules: Feasibility and Applicability

When setting up any design problem where MDD may be used, the first important step is to make sure that the MDD approach is both feasible and applicable to the problem at hand. In addition to a clear problem statement, five basic requirements should be met.

1. The most important (or co-prime) requirement must be manufacturability. This requires that the stakeholders understand and accept that some (usually minor) trade-offs in performance, geometric freedom, and mathematical optimality may be required to accomplish this.
2. A specific manufacturing process or well-defined group of processes must be selected as early in the design life cycle as possible. Ideally this should be done during requirements definition and ideation but it is absolutely required by the conceptual design phase [1].
3. The selection of the manufacturing process early in the life cycle may limit the range of available materials for the final design. This must be integrated into the design requirements and understood by the stakeholders.
4. The selected process must be well-understood or well-documented by the design team OR a team or designer with the appropriate expertise must be available to map and define the manufacturability constraints.
5. For any application of MDD, there will likely be a clear process-design-material interaction. This must be understood and accepted by the stakeholders and must either be an acceptable trade-off OR part of the design objective. In the case where some kind of lattice, truss systems, structured material or material system (such as a composite), or something else for which structure drives system mechanical properties is being designed, there must be a well-defined and designable meso-structure.

Applying these general rules to fracture-driven FDM MPDSM design, the selected process is FDM and the range of materials available would be pure or composite thermoplastic engineering materials. The mapping of manufacturability constraints was done in Chapter 3, so

the process can be considered to be well-documented and well-understood by stakeholders. Finally, the process-design-material interaction produces the useful, designable matrix of isotropic or transversely isotropic material elements which make MPDSMs via FDM possible. In this case, MDD is both a design method to ensure manufacturability and a way to capture these useful meso-scale effects.

7.5.2 Design Rules: Problem Formulation

Assuming that the design problem at hand is applicable and feasible with MDD, as well as an appropriate problem to solve by using a fracture-driven FDM MPDSM, the next step is to establish the problem formulation. In particular, this involved defining the problem and imposing the design objectives and constraints. This step does not involve selecting a solution method directly, but in many cases the consideration of a solution method may simplify problem formulation. Now that a problem type and objectives are selected, more specific rules can be established. The main ones at this level are:

1. The mesoscale (“design scale”) must be carefully defined in terms of FDM. In this case, the meso-scale is the matrix of elements, which makes the micro-scale level the elements themselves and the macroscale is the whole part for which the mesostructure is being designed. Since FDM is an additive manufacturing process, the number of design degrees of freedom will be the number for the printer minus 1. For a standard FDM machine, this represents two dimensions of complete design freedom within each layer (subject to constraints on the elements). Very good 3-D MPDSMs can be designed and built, but this will be the result of a stacking of carefully-designed 2-D components and not of true 3-D design.
2. Carefully defining the objective function for the problem and understanding the rules which accompany this. In this current work, three objectives are possible and each one will have its own set of design rules.
3. In general, the manufacturability constraints and the performance design objectives will provide the constraints on the problem. In this case, the FDM constraints, constraints on the raw materials, and constraints on the fracture variables will provide

all of these problem constraints. These must be carefully defined in consistent and clear terms.

4. Select the printing parameters and settings for FDM as early as possible. Carefully define each one as a parameter (to be controlled during printing), a constant, or a constraint.
5. Select materials very carefully; the results in Chapter 6 show the massive difference in performance and controllability for various materials. In addition, it must be considered that AM-processed materials often behave very differently than molded ones. It is best to try to understand material performance on the element/microstructural level, as this is a better predictor than macroscale tested properties.
6. Any stress concentrators that will be placed in the system should follow the guidelines for notching and pre-cracking established in Chapter 6. Therefore, any notches must be able to be machined with a mill, router, saw, broach or other method without damaging or interfering with the rest of the part or material structure.
7. For fracture-related problems (as discussed in Section 7.4 and in the next subsection), the best material layout will almost always be a concentric or contoured layout designed to help steer cracks where they are intended to grow and away from areas (or dissipated) when not intended to grow. This may not be mathematically optimal from the perspective of the whole part, but it makes the most sense when looking from the perspective of the crack tip and resulting stress/strain fields.
8. Based on experiments in Chapter 4, it has been noted in this dissertation that adding newly designed regions to help deal with fracture objectives can help make the resulting material structure much more tough but it also makes it less stiff. The stakeholders must account for this when trying to design or redesign regions.
9. Re-design as little of the part as possible. It is tempting to simply turn the entire part into a concentrically-printed shape with no design but this is a mistake. While toughening the material to an extreme degree, it also greatly decreases the structural stability and makes the structure far more compliant. One way to prevent this is to

design or re-design only the areas that are necessary to meet the fracture objectives print the rest using the strong raster-45 pattern with alternating layer directions. Of course, a full re-design may be necessary in some cases.

10. Make sure that the part shell encloses both original and new regions to avoid cracking and separation in non-designed regions.
11. Keep in mind that each layer of the part can be examined as if it was a very dense truss made up on the material elements. This knowledge must guide the design layouts.
12. Follow relevant manufacturability constraints - when using Cura or similar, this is easy since you can input restrictions on angle, element length, bridge length, etc directly into the software. Not only is automation of this very easy with the right software, it will prevent printing errors and problems later.
13. Follow as many of the soft manufacturability constraints as practical with the given resources.
14. When setting up the areas (if not the whole part) to be designed or re-designed, make sure that the re-designed part has at least one one connection to a constraint point to prevent the part from possibly delaminating or shattering early. There may be more than one area to be re-designed (especially for 3-D problems) but they should all be connected to a solid boundary condition or connected into one mass.
15. Selecting the means of identifying the areas the designed or re-designed, linear elastic CAD and FEA models should only be used with a very fine mesh and only when it is reasonable to assume that the material is LEFM as well.
16. Similarly to other structured materials, the FDM MPDSMs are strongest in compression. If given the choice, the designer should strive to have as much compression load (versus tension, torsion, ect.) on the designed structure as possible. For FDM MPDSMs, the printing orientation may affect this significantly and should be considered prior to fabrication.

17. Avoid using support material of any kind when constructing an MPDSM, as it will likely be impossible to actually remove the supports after printing.

7.5.3 Design Rules: Fracture Mechanics

Based on the previous discussion of fracture mechanics theory and its impact on the design, some simple, logic-based design rules can be applied which do not require specific expertise in fracture mechanics. These include:

1. The largest and best design space for fracture-driven problems is the face through which the crack is growing or may grow. This is an important consideration when selecting a printing orientation for the part.
2. Some regions of the part may need reinforcement to prevent fracturing or yielding outside of the designed zone (or where the crack is designed to grow), depending on the load. This may take the form of bolts or other mechanical reinforcement that may involve post-processing (coatings, resin pours, annealing, etc).
3. For non-experts in fracture mechanics who must design fracture-driven problems, the following problem statements are useful for setting up the problem and making decisions:
 - If the crack is growing or may grow and the material structure needs to prevent this (i.e., “crack arrest”), the best way to do this is to dissipate the fracture energy. This is best done by presenting many obstacles to the crack growth, such as material elements or contours placed normally to the possible crack path.
 - If the crack is growing or may grow and the structure needs to accelerate it, the opposite should be done as with crack arrest; the shortest and most efficient path to the boundary should be determined and the material structure designed to facilitate and guide this growth.
 - If the crack needs to grow in a specific pattern, the material elements need to guide it, as with crack acceleration, but with the material around the crack remaining structurally sound.

7.5.4 Design Rules: Solution Method Selection

- If the output of the design process is a directly-manufacturable product, then the final product should be in the form of g-code. Otherwise, it can be output as a model or other product. This decision needs to be made as early as possible, as it will drive the solution method selected.
- It is very unlikely that only one solution will be best and different driver software packages may produce different g-code. This is not a problem as long as the final design makes sense in the context of the problem.

7.5.5 Design Rules: Manufacturing

1. While all of the printing parameters are important and should be carefully controlled, the build plate temperature is one of the most important. For amorphous materials, proper control of this parameter can help prevent residual stress build up in the material structure. For semi-crystalline materials, the build plate temperature can have a direct impact on the degree of crystallinity in the final polymer. For both types of material, a build plate temperature that is too low can lead to cracking and premature failure in the parts, while one that is too high can exceed the glass transition temperature of the polymer and cause it to settle or yield, destroying dimensional accuracy.

7.5.6 Design Rules: Post-Solution Check

1. User must check to make sure that the produced g-code actually meets the requirements. Making a simple “logical” checklist during design can be very helpful. For example, a simple check could be:
 - *If the problem requires stopping a crack, does the element layout present as many obstacles (ideally walls or contours normal to crack direction) as possible to dissipate the fracture energy?*
 - *If an accelerated crack is desired, does the element layout help guide it along*

the best and shortest path to the boundary with the smallest possible amount of interference?

- *If the problem needs to design a crack path, does the layout support this path growth while still allowing the rest of the material to be structurally sound?*

7.5.7 Verification and Validation

Before any product or design can be used in the real world, it must undergo a certification process. At the current time, this is a major future work direction for the AM community. However, the pre-certification verification and validation process can be explored. Using the standard definitions, *verification* is the process of making sure that the design requirements are met at a minimal level while *validation* ensures that the requirements truly captured the needs of the project or design. There is a lot of designer freedom here regarding FDM MPDSMs, but two simple rules should still be followed during this process:

1. Both destructive and non-destructive evaluation techniques are useful for final verification and validation processes. This must be planned for during design.
2. For mechanical testing, the strain rate used is extremely important and must be adjusted according to the problem, which may require some experimentation. A strain rate that is too slow will allow the material to relax, while one that is too high will cause dynamic effects.

7.6 Closing Remarks

This chapter was the compilation of the previous five chapters, in which the design knowledge collected from modeling, from literature reviews, from physical experiments, and from expert intuition were converted into a set of clear and simple design rules which may easily be understood by practicing engineers, engineering students, and designers who are not experts in fracture mechanics, additive manufacturing, or structured materials. This chapter ends the collection and modeling part of the dissertation. The next and final major chapter will set up, demonstrate, and experimentally verify four design studies to show these rules and concepts in practice.

Copyright Acknowledgement: As of April 10, 2021 the work presented in this chapter has not been published nor has the copyright been assigned to anyone but the author with the exception of Figure 7.1. This figure came from a cited article (Ref [5]) which is © Elsevier B.V. and was reproduced in this chapter with permission. The copyright permission form can be found in the appendix.

Chapter 7 Bibliography

- [1] NASA, *NASA Systems Engineering Handbook: NASA/Sp-2016-6105 Rev2 - Full Color Version*. 12th Media Services, 2017.
- [2] G. Pahl, W. Beitz, J. Feldhusen, and K. H. Grote, *Engineering Design: A Systematic Approach (3rd Edition)*. Springer, 2007.
- [3] G. Boothroyd, “Product design for manufacture and assembly,” *Computer-Aided Design*, vol. 26, no. 7, pp. 505–520, 1994.
- [4] T. Anderson, *Fracture Mechanics: Fundamentals and Applications*. Boca Raton, FL, USA: CRC Press, 4th ed., 2012.
- [5] M. Begley, J. Begley, and C. Landis, “Continuum mechanics modeling of hydrogen embrittlement,” in *Gaseous Hydrogen Embrittlement of Materials in Energy Technologies*, pp. 286–325, Elsevier, 2012.
- [6] B. Moran and C. F. Shih, “A general treatment of crack tip contour integrals,” *International Journal of Fracture*, vol. 35, pp. 295–310, Dec. 1987.
- [7] T. C. Hufnagel, U. K. Vempati, and J. D. Almer, “Crack-tip strain field mapping and the toughness of metallic glasses,” *PLoS ONE*, vol. 8, p. e83289, Dec. 2013.
- [8] J. Gardan, A. Makke, and N. Recho, “A method to improve the fracture toughness using 3D printing by extrusion deposition,” *Procedia Structural Integrity*, vol. 2, pp. 144–151, 2016.
- [9] J. Gardan, A. Makke, and N. Recho, “Improving the fracture toughness of 3d printed thermoplastic polymers by fused deposition modeling,” *International Journal of Fracture*, vol. 210, no. 1-2, pp. 1–15, 2017.
- [10] J. Huang, B. C. Kim, S. Takayama, and M. D. Thouless, “The control of crack arrays in thin films,” *Journal of Materials Science*, vol. 49, pp. 255–268, Sept. 2013.
- [11] J.-H. Pu, X. Zhao, X.-J. Zha, W.-D. Li, K. Ke, R.-Y. Bao, Z.-Y. Liu, M.-B. Yang, and W. Yang, “A strain localization directed crack control strategy for designing MXene-based customizable sensitivity and sensing range strain sensors for full-range human motion monitoring,” *Nano Energy*, vol. 74, p. 104814, Aug. 2020.

- [12] D. Ren, *Optimisation of the Crack Pattern in Continuously Reinforced Concrete Pavements*. PhD thesis, 2015.
- [13] A. Nakahara, Y. Shinohara, and Y. Matsuo, “Control of crack pattern using memory effect of paste,” *Journal of Physics: Conference Series*, vol. 319, p. 012014, Sept. 2011.
- [14] A. BINDL, H. LUTHY, and W. H. MORMANN, “Thin-wall ceramic CAD/CAM crown copings: strength and fracture pattern,” *Journal of Oral Rehabilitation*, vol. 33, pp. 520–528, July 2006.
- [15] A. E. Patterson, T. R. Pereira, J. T. Allison, and S. L. Messimer, “IZOD impact properties of full-density fused deposition modeling polymer materials with respect to raster angle and print orientation,” *Proceedings of the Institution of Mechanical Engineers, Part C: Journal of Mechanical Engineering Science*, p. 095440621984038, Apr. 2019.

Chapter 8

DESIGN STUDIES

8.1 Introduction

In this chapter, the principles and design rules developed in this dissertation are explored and demonstrated through a series of design studies. The three standard objectives of fracture-driven design are covered (crack arrest, crack acceleration, and crack pattern control) using a variety of different design perspectives. Four case studies are presented, all following the design rules from Chapter 7 and using various strategies for laying out the elements to meet the objectives of the problem. These do not represent all the possible approaches or design problems, but do a good job showing the concepts and applications of the concepts developed in this dissertation. Realistic applications were prioritized, so the majority of the problems focused on strengthening or toughening (as explored in Chapter 7) but some work demonstrating crack path control and crack acceleration is also presented, especially in Design Study 3.

1. **Design Study 1:** A sampling experiment using box plot optimization is used to explore three factors related to the toughness of a set of compact tension samples. Layouts are driven from the use of 2-D primitives and no modifications are made based on specific fracture knowledge. This study simulates a simple screening study, similar to one that would be done as a proof-of-concept or to identify significant factors for a large and expensive designed experiment.

2. **Design Study 2:** This case is the opposite of Design Study 1; in this study, the layouts are driven directly by Von Mises criterion for a 2-D plane stress (thin sample) case and the element layout patterns used are direct mapping of the stress fields for each material.
3. **Design Study 3:** This case is similar in approach and objectives to the simple 2-D ones presented in some previous studies (such as Refs. [1–7]) but with a more complex geometry and the imposition of the specific design rules. In this case, a linear elastic finite element model (used since it was concluded in Chapter 7 that the materials in use behave in an approximately linear elastic manner) is used to create a Von Mises stress map of the geometry based on percentages of the yield stress of the material. This map was then directly traced (with some minor modifications due to design rules) and used as the basis for the contour layout.
4. **Design Study 4:** The fourth design study has the same goals and approach as Design Study 3, except in 3-D. A notched cantilever beam with a combined bending and torsional load is the subject of this study.

Some notes and assumptions should be documented for these case studies in order to ensure that the full context is clear to the reader, especially for anyone trying to reproduce these case studies:

1. As explored in Chapter 7, the most appropriate (if not necessarily mathematically optimal for every element) layout for fracture problems is almost always a contour-based arrangement of elements based on where the crack may be predicted to grow. While the fracture mechanics theory behind the concept can be complex (though not as complex as some mechanics problems), the conclusions are relatively simple:
 - When crack arrest is desired, the contours should present a “wall” or normal obstacle to it so that the material can dissipate some of its excess energy into breaking the contour (perhaps through crazing or crack branching between the elements normal to the crack), thus starving the crack of its energy to keep growing before it affects the boundaries of the part or system.

- When crack acceleration is needed, the contour should help guide it to the nearest boundary as quickly as possible using the most efficient route while trying to dissipate its energy by the time it reaches the boundary; excess energy at the end may result in shattering or other dangerous behavior, as observed some of the fracture tests in Chapter 6 which used polycarbonate.
 - Crack pattern control requires a combined approach, as the crack both needs to be steered in the desired direction while dissipating the fracture energy as quickly as possible and as far from the boundary as possible.
2. One of the requirements for the investigation described by the chapters in this dissertation was that only commercially-available software and design tools; the purpose of this rules was to make sure that the methods and approaches described can easily be applied and reproduced by practicing engineers, engineering students, and designers who are not assumed to be experts in fracture mechanics, polymer additive manufacturing, or in structure materials. Therefore, a combination of Ultimaker Cura and Autodesk Inventor were used for the layout designs; a full tutorial on how to accomplish this using these standard software packages is provided in Appendix A. Cura is especially useful for doing such design, as it not only allows control of the element layouts (both directly and indirectly), but also allows direct input of the manufacturability constraints to ensure that any designs produced meet the definitions of an MPDSM.

8.2 Design Study 1: ASTM D5045 CT Layout using Cube Plot Optimization

8.2.1 Overview and Objectives

Cube plot optimization allows quick and low-cost screening of physical experiments for various things, most commonly potentially significant factors to be studied using more rigorous statistical methods in large and expensive designed experiments. Cube plot optimization allows a 2-level experimental design to be examined for up to 8 factors (2 will be explored in this case study), providing a graphical solution to help designers identify statistically

significant factors and very quickly select the best combination of factors. The objective is typically very simple, something similar to “which combination of factors produces the largest (or smallest) value of the response?” In this case, the objective function is to find two combinations of material choice and two design factors, one that provides the toughest structure and the one that fractures the most easily. The MPDSM patterns are arbitrarily-chosen primitive shapes (circle and diamond), which are connected to the tension points as recommended by Chapter 7.

8.2.2 Design Approach and Results

For this case study, the experimental design is shown in Table 8.1 and the specimen layouts shown in Figure 8.1 (before notching). The responses are (1) the maximum load before fracture and (2) the lowest load before of standard ASTM D5045 CT samples ($W = 30$ mm, $B = 6$ mm) tested at a strain rate of 10 mm/min.

Table 8.1: Case study 1 experimental design for each material (ABS, PC, and PLA)

Combination	Infill Primitive	Primitive Size (mm)	Fill Pattern
1	Circle	5	R45
2	Diamond	5	R45
3	Circle	20	R45
4	Diamond	20	R45

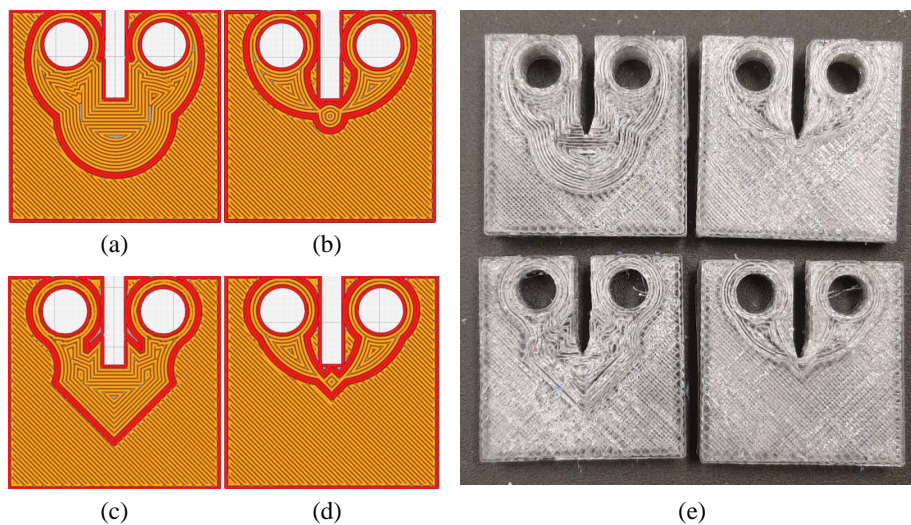


Figure 8.1: Case study 1 layouts with printed examples (PC after notching)

8.2.3 Experimental Validation

All three of the materials for this dissertation are considered. A total of 12 samples (one for each material - factor set combination) were printed, conditioned, notched, and tested as described in Chapter 6. The results were used to generate the cube plots shown in Figure 8.2. One cube plot was generated for each of the materials.

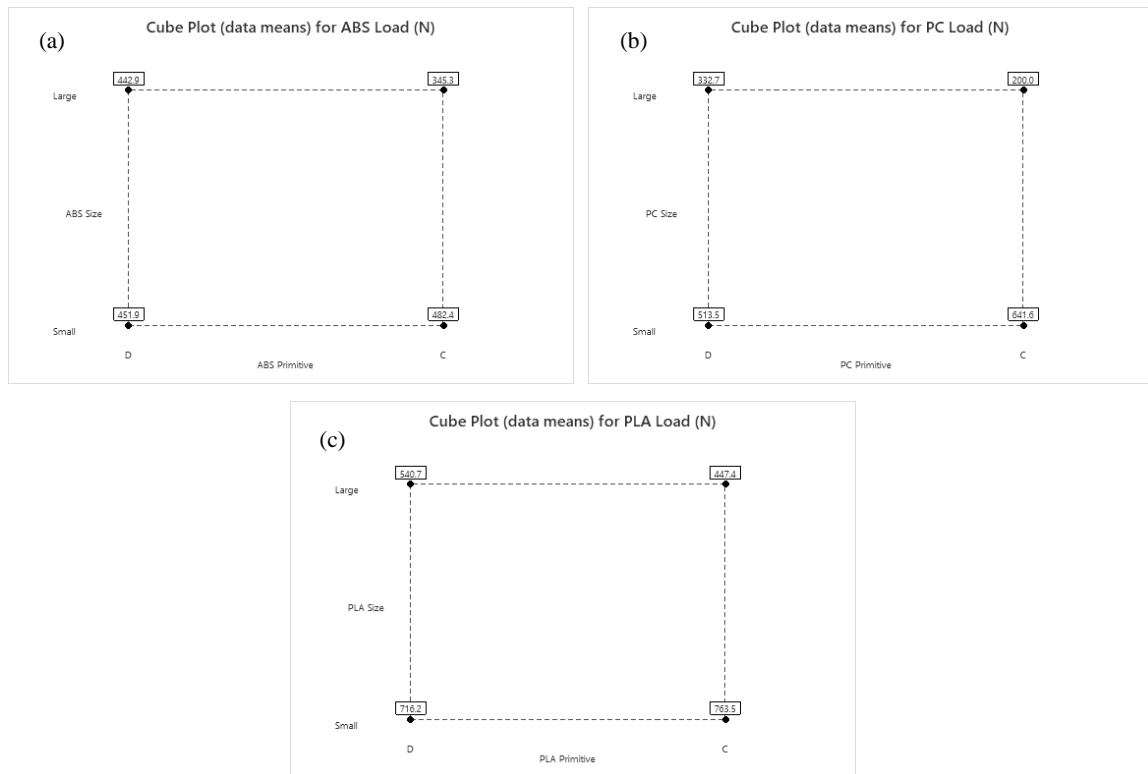


Figure 8.2: 2-factor cube plots for each of the materials generated in Minitab

While only a single run of the experiment was done in this design study, it would be standard to perform several runs and let the boxes represent means instead of raw data. No data analysis is needed from these (assuming that a real design study would have more complex data distributions); simple inspection of the boxes will answer the objective functions: The best combination for toughness is PLA with a small circle (fractured at 763.5 N) and the best for low fracture strength is PC with a large circle, which fractured at just 200 N.

8.2.4 Discussion

This design knowledge collection and design method (experimentally demonstrated above) is extremely simple, but valuable. To better show the value of such a screening experiment to aid in making design decisions, ANOVA and main effects analysis were done for each material. As shown in Figure 8.3, none of the factors are statistically significant at the normal $\alpha = 0.05$ level of significance. Therefore, a classic data analysis for design will not provide any valuable information. However, the box plot optimization method clearly gives fast and straight-forward answers to the objective functions. It should also be noted that the main effects plots shown below also show the results of the box plot optimization, even though the effect was not calculated to be statistically significant using regular methods.

Analysis of Variance

Source	DF	Adj SS	Adj MS	F-Value	P-Value
ABS Primitive	1	1126	1126	0.27	0.693
ABS Size	1	5336	5336	1.30	0.458
Error	1	4102	4102		
Total	3	10564			

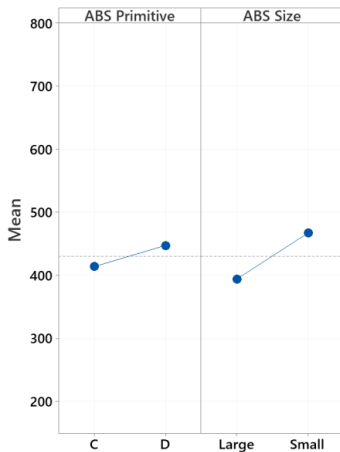
Analysis of Variance

Source	DF	Adj SS	Adj MS	F-Value	P-Value
PC Primitive	1	5	5.3	0.00	0.989
PC Size	1	96845	96845.4	5.70	0.253
Error	1	17004	17004.2		
Total	3	113855			

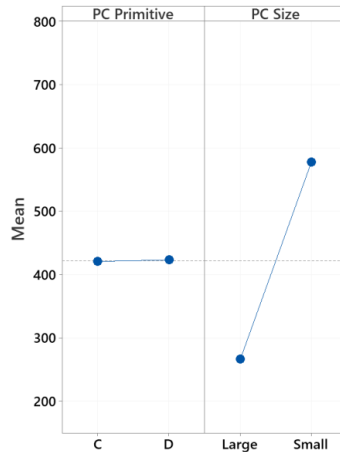
Analysis of Variance

Source	DF	Adj SS	Adj MS	F-Value	P-Value
PLA Primitive	1	529.0	529.0	0.11	0.799
PLA Size	1	60417.6	60417.6	12.23	0.177
Error	1	4942.1	4942.1		
Total	3	65888.7			

Main Effects Plot for ABS Load (N)
Data Means



Main Effects Plot for PC Load (N)
Data Means



Main Effects Plot for PLA Load (N)
Data Means

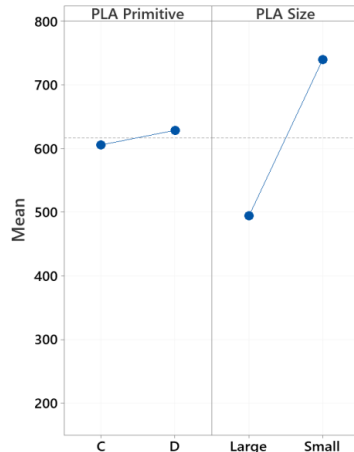


Figure 8.3: ANOVA and main effects analysis results for Design Study 1

8.3 Design Study 2: Plane Stress Field Trace

8.3.1 Overview and Objectives

In the previous design study, primitive shapes were used to reinforce the areas around the cracks, giving best performing examples for both the maximum fracture load and the minimum fracture load. In this case study, the layout is calculated based on the plane stress field using Von Mises criterion for establishing the field size and geometry. The objective for this study was to show that the stress fields could be accurately calculated from the basic equations and reproduced to solve a practical design problem. A thin ASTM D5045 CT sample is used for this test with dimensions $W = 30$ mm and $B = 3$ mm.

8.3.2 Design Approach and Results

Given the Von Mises yield criterion (σ values are principle stresses),

$$2\sigma_{yield}^2 = (\sigma_1 - \sigma_2)^2 + (\sigma_2 - \sigma_3)^2 + (\sigma_3 - \sigma_1)^2 \quad (8.1)$$

Knowing that for the plane stress $\sigma_3 = 0$, this equation reduces to

$$2\sigma_{yield}^2 = (\sigma_1 - \sigma_2)^2 + \sigma_2^2 + \sigma_1^2 = \frac{K_I^2}{2\pi r} \cos^2\left(\frac{\theta}{2}\right) \left(6 \sin^2\left(\frac{\theta}{2}\right) + 2\right) \quad (8.2)$$

Solving for the r (distance from crack tip to field edge),

$$r = \frac{K_I^2}{4\pi\sigma_{yield}^2} (1 + \cos(\theta) + 3/2 \sin^2(\theta)) \quad (8.3)$$

Finding the stress intensity factor around the crack for a CT sample,

$$K_I = \frac{P}{B} \sqrt{\frac{\pi}{W}} (16.7(a/W)^{1/2} - 104.7(a/W)^{3/2} + 369.9(a/W)^{5/2} - 573.8(a/W)^{7/2} + 360.5(a/W)^{9/2}) \quad (8.4)$$

Assuming $P = 150$ N, $a/W = 0.5$ (as recommended by ASTM D5045), and using the yield

stress values for each material measured in Chapter 6, the Von Mises stress fields for each material are shown in Figure 8.4. The resulting field traces for each CT sample are shown in Figure 8.4.

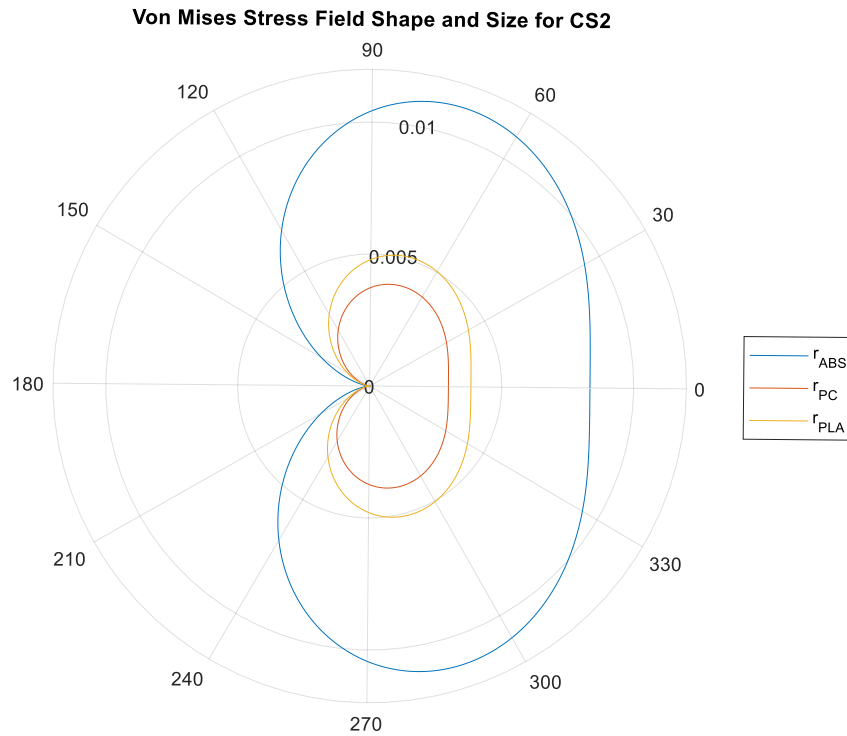


Figure 8.4: Von Mises stress fields for ABS, PC, and PLA based on the mechanical properties measured in Chapter 6. The fields and plot were produced in Matlab using the derived equations.

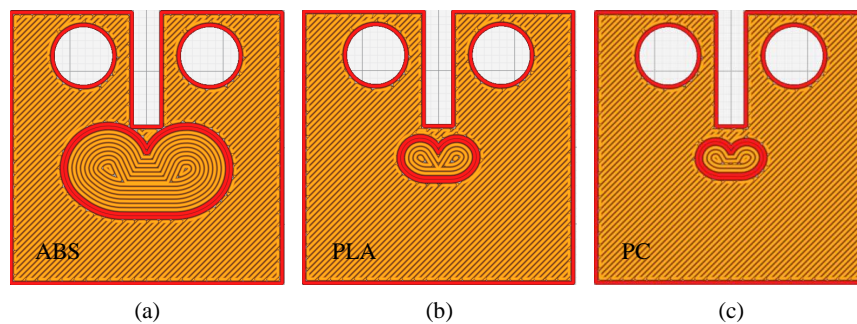


Figure 8.5: Case study 2 layouts

8.3.3 Experimental Validation

While the samples for this design study were not mechanically tested, they were printed to show that the stress fields could be easily calculated and transferred into design geometry with no special tools or software. The prints (under a microscope) are shown in Figure T

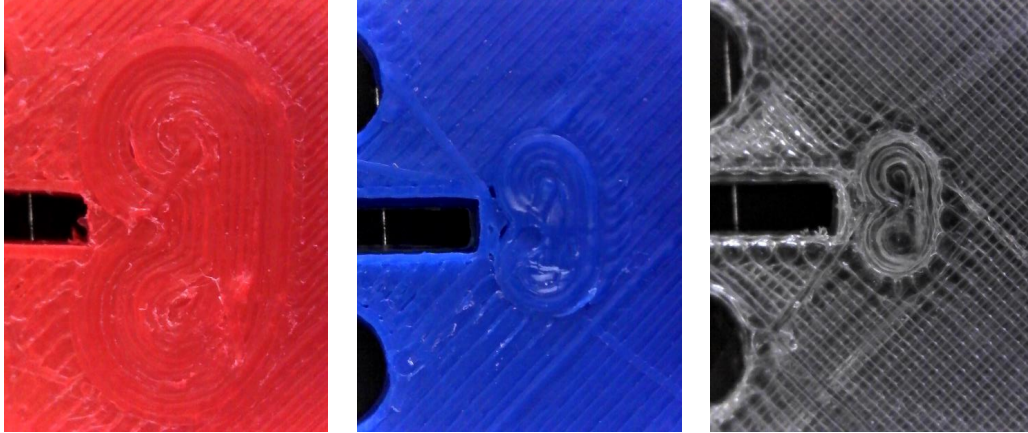


Figure 8.6: Printed stress fields for each material (samples not notched), which match Figure 8.4 very well.

8.3.4 Discussion

The purpose of Case Study 2 was to explore the creation of MPDSMs around an analytically-calculated stress field. This field was reproduced in the design very easily, showing that such an approach could be an excellent alternative to finite element analysis. Note that the printed field are not notched, but if they were to be notched with a mill, router, saw, or other method, the calculated CT dimensions (with $a/W = 0.5$) would automatically place the beginning of the pre-crack exactly in the nexus of the fields.

8.4 Design Study 3: 2-D Eccentric Beam Re-Design

8.4.1 Overview and Objectives

In this case study, an eccentric beam with two notches subject to a tensile load (Figure 8.7), where one notch is in tension and one in compression. The out-of-plane cross-section is uniform, as is the loading, so the solution is in 2-D. This is typical of the few similar problems in the engineering literature, such as those cited earlier in this chapter. The

beam is to be made from PLA and two designs must be produced: One which significantly increases the fracture load of the beam and one in which a guided crack causes the beam to fracture quickly and dissipate energy as quickly as possible. Therefore, two designs must be produced and compared with the baseline beam. Suppose the maximum predicted load of the beam is 2000 N (including the factor of safety, but the designers were told that its actual capacity is much less than this, without being given specific information.

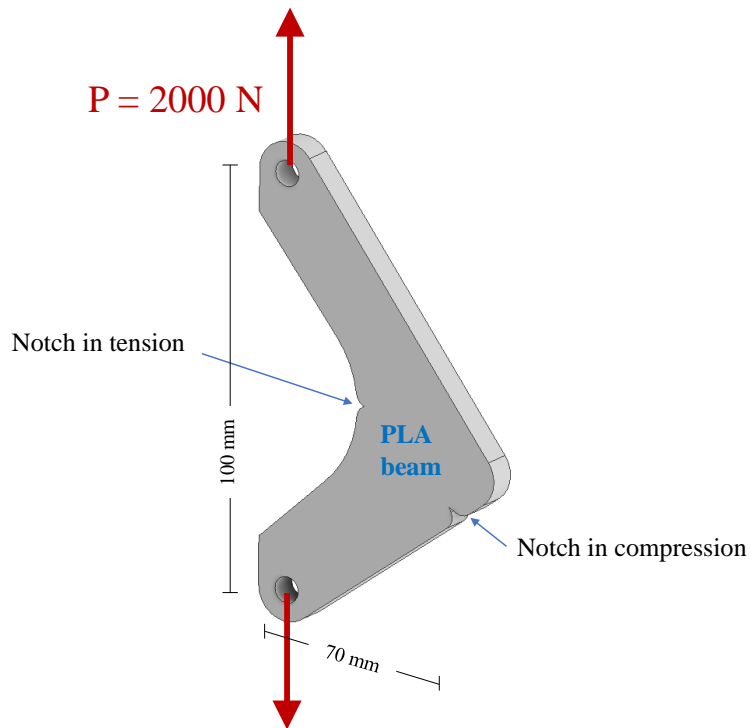


Figure 8.7: Case study 3 setup and loading

8.4.2 Design Approach and Results

This beam is part of a system and will be difficult and expensive to re-design the geometry itself, so better controlling its performance through using MPDSM principles will be attempted in this design study. To begin, the basic geometry was subjected to a 2000 N worst-case load, resulting in a the stress field show in Figure 8.8. The material properties of PLA from Chapter 6 were used and input manually. A linear elastic finite element model (Autodesk[®] NASTRAN[®]) was used with an average mesh size of 1.5 mm.

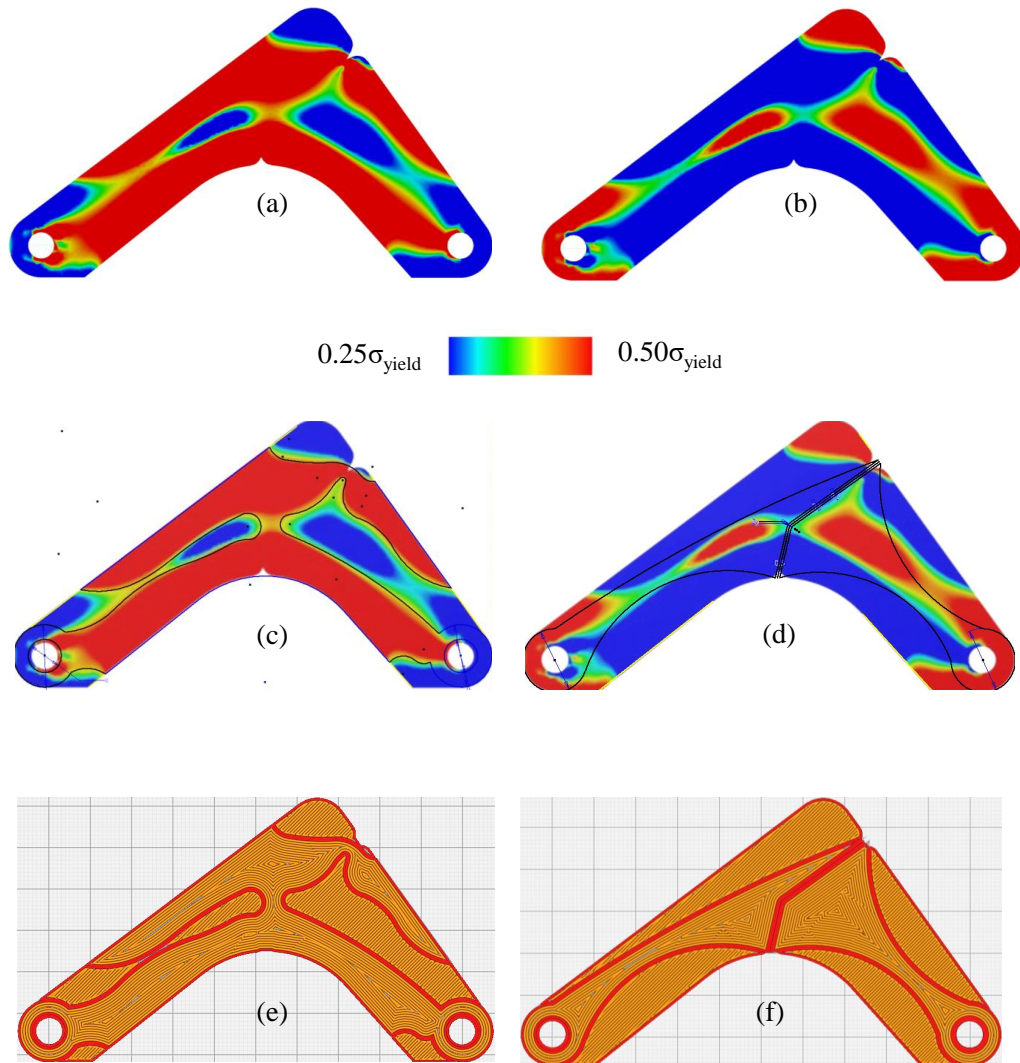


Figure 8.8: Case study 3 tools and designs. (a) Stress field for the given loading and material, (b) inverted stress field to find the areas where a crack may grow easily, (c-d) the stress field traces (modified for Chapter 7 rules) for (a-b), and (e-f) manufacturable final designs with element layout.

Figure 8.8a shows the stress field relative to a percentage of the yield stress of PLA, while Figure 8.8c shows the field trace (i.e., area to be re-designed) to toughen the structure. Inverting the field (Figure 8.8b), the weaker areas are exposed, which will help the designers use expert intuition to guide a crack through the most efficient path in order to quickly dissipate energy if needed. The crack path can be seen clearly in the trace in Figure 8.8d. These designs follow the rules and guidelines for fracture-driven MPDSMs, though the full checklist from Chapter 7 will not be repeated here. Two points that should be highlighted,

however, were that even though the needed reinforcement (as shown by the FEA model) around the cracks did not necessarily reach a boundary condition or connection. Therefore, as shown in several parts of Figure 8.8, small bridging areas and connections to the pin joints were added to meet the requirements outlines in Chapter 7. This was done manually by the designer, not automatically by any program or model.

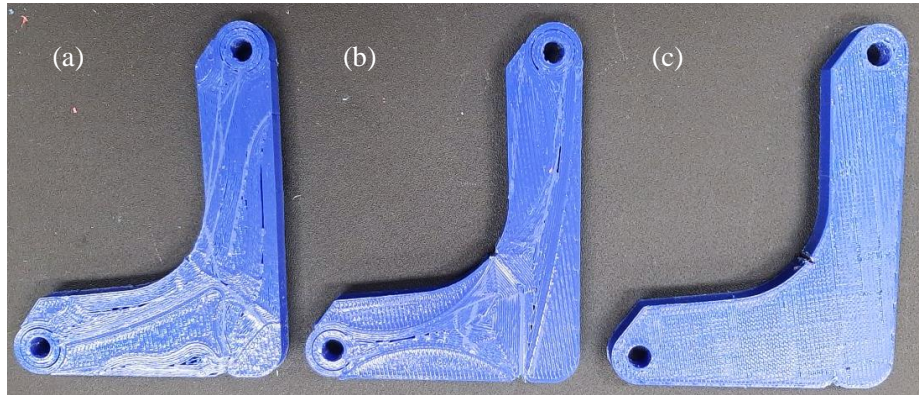


Figure 8.9: Case study 3 samples. (a) toughened MPDSM, (b) designed crack MPDSM, and (c) baseline

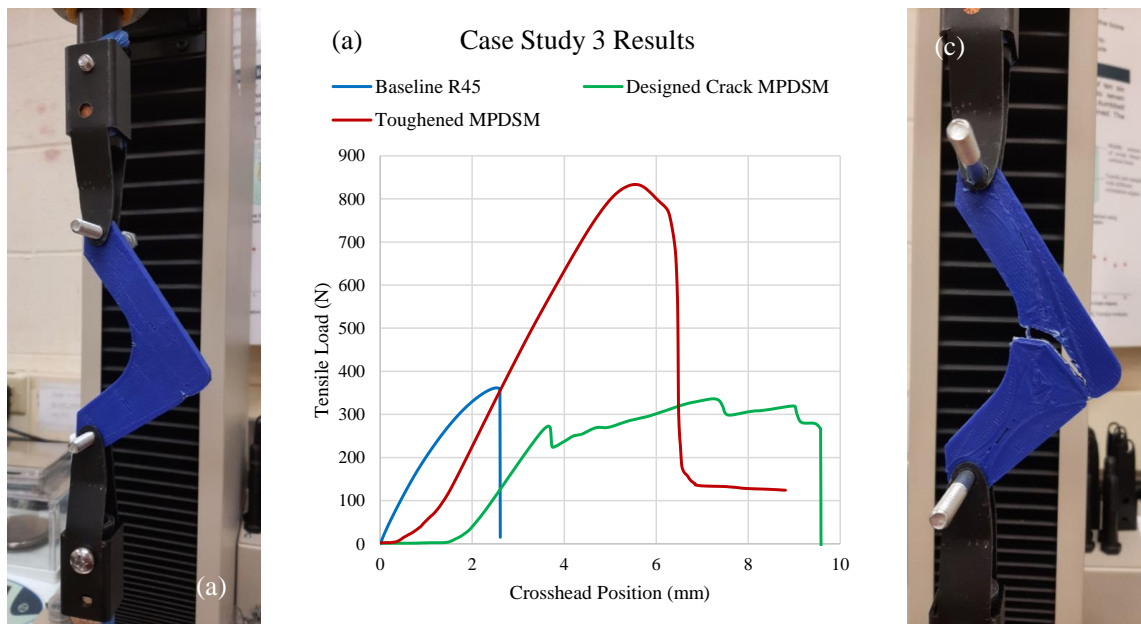


Figure 8.10: Case study 3 (a) experimental setup (strain rate was 5 mm/min), (b) force-deflection curves for the three cases, and (c) successful crack-control design after testing.

8.4.3 Experimental Validation

After re-design and conversion of the two cases, manufacturable forms (g-code), as shown in Figure 8.8e and 8.8f, were produced and printed (Figure 8.9). The same geometry, but using a full R45 infill, was printed to serve as the baseline to compare the performance of the other two. Next, the samples were tensile tested using the MTS machine and equipment described in Chapter 6. The experimental setup and results are shown in Figures 8.10a and 8.10b, respectively. Figure 8.10c shows the successful designed crack which behaved so erratically during the test but which dissipated a lot more energy than the R45 baseline.

8.4.4 Discussion

While the performance of the re-designed beams was not as good as hoped by the designers (the best load was about 850 N, not the 2000 N that would have been ideal), the improvement was very dramatic, increasing the strength nearly 300% simply by laying out the elements. This suggests that the designers will have to change the geometry or material to achieve the desired capability, but that the required changes will be less severe due to the availability of this design method. The design space is now wider, so it is more likely that the stakeholders will be able to find a solution with a much less dramatic and less expensive re-design of the system to which it belongs. One more note should be made here in the context of the other materials and their performance observed throughout this dissertation: It is likely that this large improvement was only going to be observed in PLA (and similar materials), as it is far more dense (40% more than ABS) and tougher than ABS or PC. This design is also a poor application for PC, as it is too brittle to survive this loading pattern based on its behavior in Chapter 6 and Design Study 1. This problem is a more complex version of some layout re-design problems in the literature (such as seen in [1–7]), but it remains a 2-D problem; the next design study extends the ideas to 3-D.

8.5 Design Study 4: 3-D Beam Design under Bending and Torsion Load

8.5.1 Overview and Objectives

For this case, a cantilever beam clamped on one end and eccentrically loaded on the other needs to be toughened without changing the macro-scale geometry of the beam or the material. This problem is very similar to Design Study 3, except that the design problem is in 3-D and it made from ABS. Polycarbonate was considered for this case, but after reviewing its performance in Chapter 6, it was decided that PC was not a suitable material. Figure 8.11 shows the scenario, loading and major dimensions. In addition, the model results are shown; the model was made using the same steps as in Case Study 3.

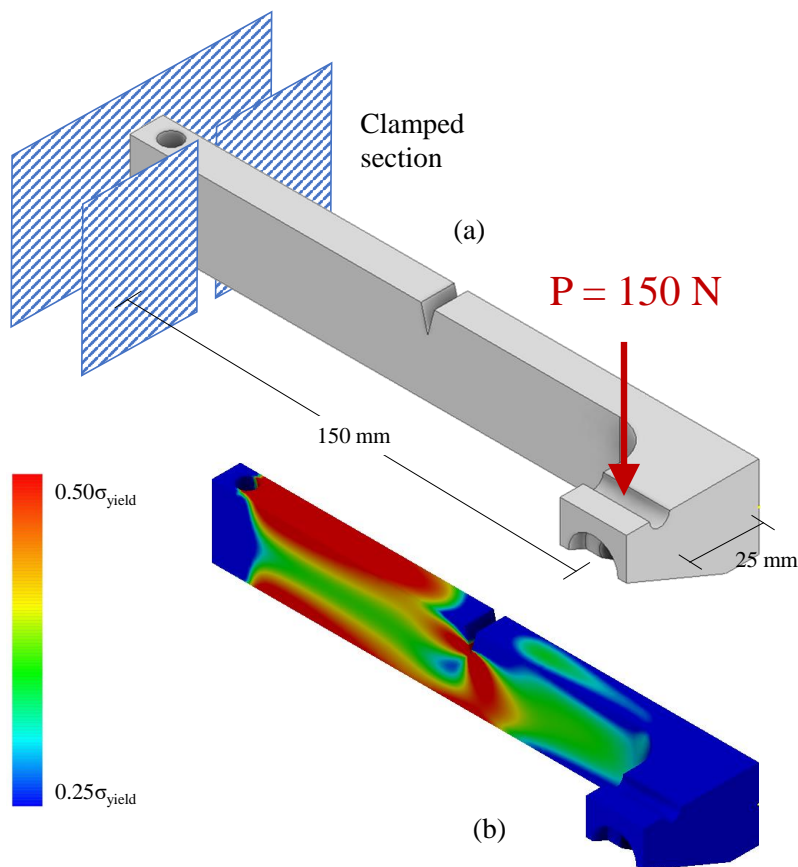


Figure 8.11: Case study 4 setup

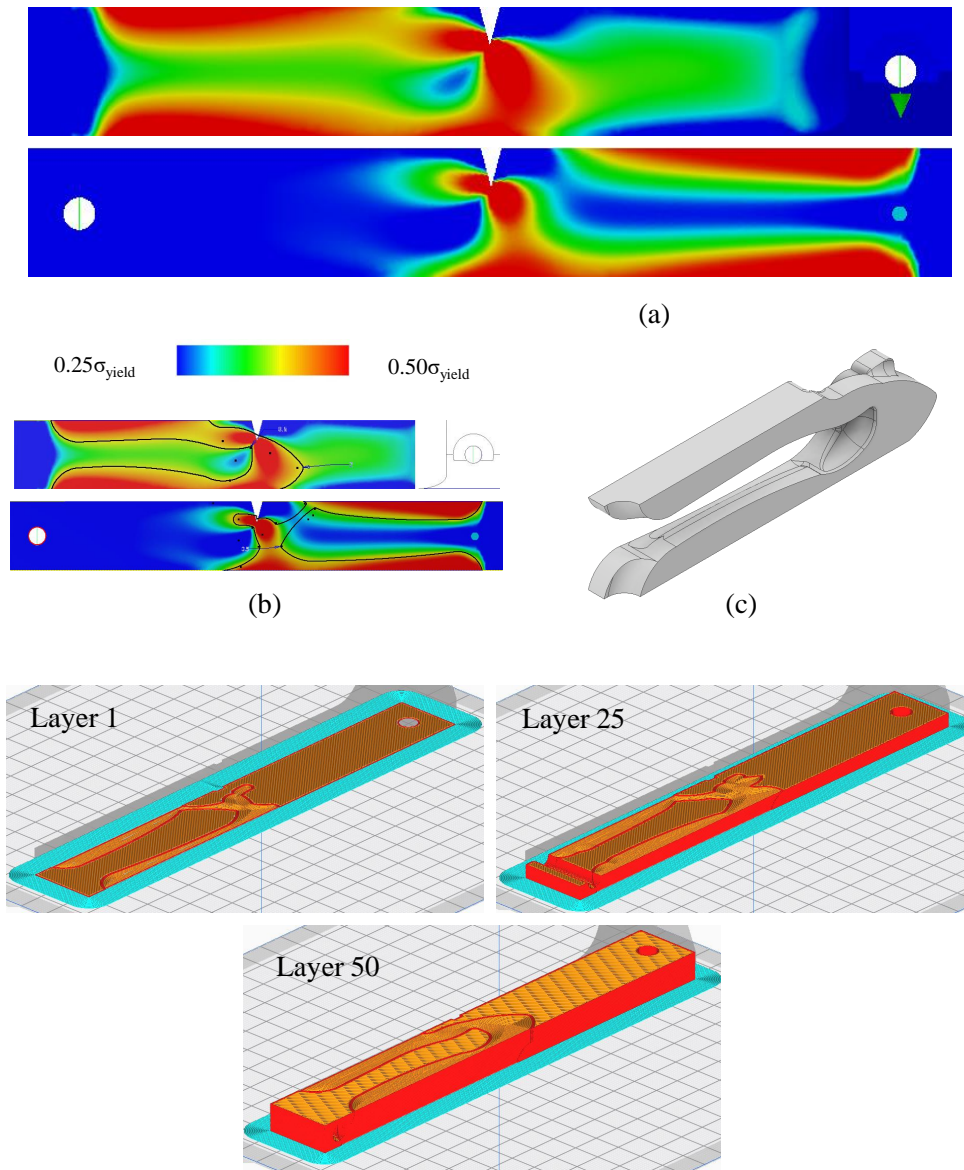


Figure 8.12: Case study 4 (a) model sides, (b) traces, (c) design solution, (d) layers

8.5.2 Design Approach and Results

The design approach taken was the same one described in Design Study 3, except that it was done from both sides of the model (Figure 8.12a and 8.12b) and the results joined in the middle (Figure 8.12c) via a combine function in Autodesk Inventor. After inputting the original geometry and the newly designed region into Cura, slicing was one and every layer was inspected to make sure that there would be no manufacturing problems or unexpected

stress concentrations. Originally, a loft feature was attempted to create a more “average” MPDSM geometry throughout the thickness of the beam, but due to the complexity of the stress fields it was not able to be produced digitally. If the fields were more simple or more similar in size, the loft approach most likely would produce a design that is even better than the one shown here. Note that since this was a 3-D problem that every layer was unique; Figure 8.12d shows images of the first layer, the 25th layer, and the 50th layer.

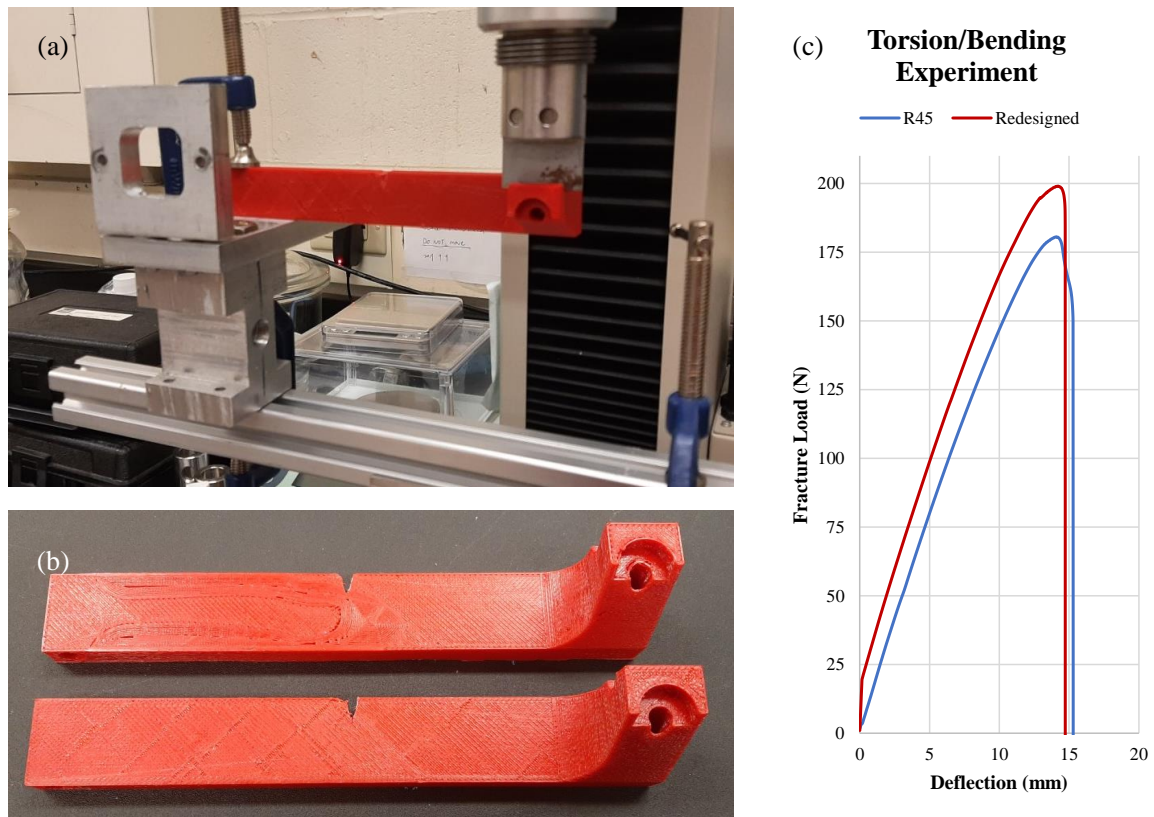


Figure 8.13: Case study 4 (a) model sides, (b) traces, (c) design solution, (d) layers

8.5.3 Experimental Validation

To test the quality and effectiveness of the design, two specimens were printed from ABS (Figure 8.13), conditioned, notched, and pre-cracked like the CT samples used in previous sections. A simple cantilever system (Figure 8.13a) made from scrap metal and clamps was used to hold the sample while it was tested in compression in the MTS machine at a strain rate of 5 mm/min. The recorded results are shown in Figure 8.13c.

8.5.4 Discussion

While the effect of the designed area is clear, the benefits are not nearly as dramatic as seen in Design Case 3. It is likely a combination of using softer material, the much more severe mechanical load, and the fact that larger samples are more likely to contain small undetectable defects. The reason for the really high stiffness for the first new Newtons of force applied to the redesigned case is unknown, but it is suspected that this was when the pre-crack was beginning to release in the material. Note that the strain rate was slow, so it took a significant amount of time to reach a significant load so it also possible there was some fiber relaxation effects as well. It was discussed that the experiment should be re-done using PLA but this was not done due to time constraints, a low supply of material, and the fact that the behavior of PLA was already well-established in previous design studies. Future replications and extension of this problem should focus on testing different strain rates and materials.

8.6 Closing Remarks

The purpose of this chapter was to demonstrate and experimentally validate the design method and rules developed throughout this dissertation. As such, it is the final chapter and close of the investigation into this new design approach for creating manufacturable structured materials that are designed relative to fracture problems. It should be noted once again that these design studies, while clear and comprehensive, do not represent or test all of the possible design scenarios or variations on the design rules. Further development is needed for other types of mechanical design problems and other materials. Of the three materials considered during these design case studies, PLA performed by far the best in almost every case. This is important knowledge for future designers, as PLA is an environmentally-friendly, non-toxic, and biomass-generated engineering plastic. It is not nearly as common as the hydrocarbon-based engineering plastics such as ABS and PC, but this could change quickly if designers are convinced to seriously consider it as a material option. Based on the results of these case studies, this appears to be a feasible reality in the near future.

Chapter 8 Bibliography

- [1] J. Gardan, A. Makke, and N. Recho, “A method to improve the fracture toughness using 3D printing by extrusion deposition,” *Procedia Structural Integrity*, vol. 2, pp. 144–151, 2016.
- [2] J. Gardan, “Method for characterization and enhancement of 3D printing by binder jetting applied to the textures quality,” *Assembly Automation*, vol. 37, no. 2, pp. 162–169, 2017.
- [3] J. Gardan, A. Makke, and N. Recho, “Improving the fracture toughness of 3d printed thermoplastic polymers by fused deposition modeling,” *International Journal of Fracture*, vol. 210, no. 1-2, pp. 1–15, 2017.
- [4] J. Gardan, A. Makke, and N. Recho, “Fracture improvement by reinforcing the structure of acrylonitrile butadiene styrene parts manufactured by fused deposition modeling,” *3D Printing and Additive Manufacturing*, vol. 6, pp. 113–117, Apr. 2019.
- [5] P. Lanzillotti, J. Gardan, A. Makke, and N. Recho, “Strengthening in fracture toughness of a smart material manufactured by 3D printing,” *IFAC-PapersOnLine*, vol. 51, no. 11, pp. 1353–1358, 2018.
- [6] P. Lanzillotti, J. Gardan, A. Makke, and N. Recho, “Enhancement of fracture toughness under mixed mode loading of ABS specimens produced by 3D printing,” *Rapid Prototyping Journal*, vol. 25, pp. 679–689, May 2019.
- [7] A. Lenti, “Fracture toughness assessment using digital image correlation in additive manufacturing,” Master’s thesis, Polytechnic of Turin, Turin, Italy, 2019. Masters Thesis - Mechanical Engineering.

Chapter 9

CONCLUSIONS AND FUTURE WORK

This dissertation explored the idea of using a manufacturing process-material-mechanics interaction (i.e., the natural bottom-up construction of parts and products by laying out material elements) as a new design method for producing manufacturable structured materials under fracture load. The process used was fused deposition modeling, a well-developed and common additive manufacturing process for thermoplastic polymers. This is an excellent problem for exploring the interfaces and synergies between solid mechanics (not limited to fracture), manufacturing science, and mechanical design methods. Exploring this problem effectively required consideration of perspectives from all of these domains. This also involved refining methods, definitions, and tools to support this new design perspective. Most importantly, all of the proposed methods, approaches, rules, and design tools were experimentally validated.

In addition to some additional tools and processes (discussed throughout the document), six major contributions were made toward this problem in the course of this dissertation, including (1) a very extensive literature review on several major topics, (2) the development and validation of a method for capturing and mapping manufacturability constraint, (3) a full application of the constraint mapping method to a new manufacturing process, (4) the full development and validation of a new bottom-up design method for producing manufacturable structured materials (MPDSMs) based on the material-process effects of FDM, (5) the completion of a very large course of fracture mechanics experiments,

some of which have not been presented in the literature in any form before, and finally (6) the compilation of all other contributions and tools to develop a new method for designing and manufacturing MPDSMs under fracture conditions.

Future work will focus on several major areas, including but not limited to:

- Applying the design rules and principles developed in this dissertation to other material configurations, including bio-inspired materials and composites.
- Further refinement of the MPDSMs concept specifically for application to current aerospace and automotive design problems.
- Refining and developing an MPDSM perspective for other AM processes, especially nylon selective laser sintering and metal-based processes.
- Further refinement of the design rules presented by scientifically comparing them with other design methods and different perspectives.
- Further development of major design studies which expose the developed principles to more intellectual risk (both to validate the method more completely and to explore which types of problems are applicable and which are not).
- Development of a graduate-level course on this topic, as well as undergraduate-level modules which can be integrated into advanced undergraduate mechanics or design courses.
- Better design automation
- More design-valuable fracture testing approaches, including standards development, more rigorous experimental methods, and better reporting standards for results.

Appendix A

PRELIMINARY DESIGN GUIDE

Introduction

This appendix expands the design rules from Chapter 7 and provides guidance for practical implementation, as well as guidance on when the methods proposed in this dissertation are applicable. This guide is meant to be used by practicing engineers and engineering students who are not experts in fracture mechanics, structured materials, or advanced mechanics but need to use the presented methods in real-world design.

Feasibility and Applicability

When using the MPDSMs approach for design, it is applicable and practical to use only when five conditions are met. If it does not meet these conditions, then the design approach must be modified or a different method used.

1. The most important (or co-prime) requirement must be manufacturability. It is very important this this be very clear to the design team and stakeholders, as it will likely require some trade-offs to accomplish. Some important things that the designer should keep in mind are:

- Manufacturability does need to be the most important requirement, since the successful application of the MPDSMs concept requires that the process-material interactions be captured and taken advantage of. However, a compromise could be made if necessary so that another requirement (say, geometry or performance) is equally important with manufacturability. As long as the formulation of the problem allows both the restriction of the design space to manufacturable designs AND allows the process-material effects to be controlled or captured, this requirement should be satisfied. This determination should be made before the establishment of any design requirements if possible for the most effective use of the MPDSMs concept.
2. A specific manufacturing process or well-defined group of processes must be selected as early in the design life cycle as possible. Ideally this should be done during requirements definition and ideation but it is absolutely required by the conceptual design phase.
 - Since in MDD the mechanics of the process influence so much of the design and many of the design decisions, it is extremely important that the process be selected as early as possible. This will help to focus the design effort and make the design process more efficient. However, there is a trade-off: Once the design moves out of the very early design phases, it is very difficult to change the design approach or (in many cases) the material since the design decisions up to that point were largely influenced by the process choice.
 3. The selection of the manufacturing process early in the life cycle may limit the range of available materials for the final design. This must be integrated into the design requirements and understood by the stakeholders.
 - Within the range of the selected process, this is not as limiting of a factor as the selection of the process itself. For example, selecting machining or FDM or investment casting still leaved a wide range of materials available. On paper, it is extremely important to document and maintain the material catalog within the

process capabilities, but in practice this is not a huge design problem for many manufacturing processes. In fact, this consideration could influence the selection of the process. For example, would the stakeholders rather take advantage of a process which is specific and limited but offers a lot of design freedom (many AM processes) or rather keep the material flexibility and give up some of the design freedom?

4. The selected process must be well-understood or well-documented by the design team OR a team or designer with the appropriate expertise must be available to map and define the manufacturability constraints.

- Basic requirement when putting together the team. Since this design approach is heavily dependent on the manufacturing method, someone very familiar with that method (or an excellent digital twin or dataset) is essential for the design team.

5. For any application of MDD, there will likely be a clear process-design-material interaction. This must be understood and accepted by the stakeholders and must either be an acceptable trade-off OR part of the design objective. In the case where some kind of lattice, truss systems, structured material or material system (such as a composite), or something else for which structure drives system mechanical properties is being designed, there must be a well-defined and designable meso-structure.

- In most cases, the practicing engineer can determine if this rule is satisfied or not by simple inspection of the proposed design or design problem. In more complex cases, this can be determined experimentally or may be artificially defined to be part of the design.

Design Rules: Problem Formulation

Assuming that the applicability rules are satisfied, the next step is to establish the problem formulation. Specifically, this involved defining the problem and imposing the design objectives and constraints. This step does not involve selecting a solution method (such

as topology optimization or other method) directly, but in many cases the consideration of a solution method may simplify problem formulation. Of all the design rules for fracture-driven FDM MPDSMs, the problem formulation is the concern of the largest number of rules. In most cases, these rules are simple to establish and self-explanatory.

1. The mesoscale (“design scale”) must be carefully defined in terms of FDM. In this case, the meso-scale is the matrix of elements, which makes the micro-scale level the elements themselves and the macroscale is the whole part for which the mesostructure is being designed. Since FDM is an additive manufacturing process, the number of design degrees of freedom will be the number for the printer minus 1. For a standard FDM machine, this represents two dimensions of complete design freedom within each layer (subject to constraints on the elements). Very good 3-D MPDSMs can be designed and built, but this will be the result of a stacking of carefully-designed 2-D components and not of true 3-D design.
2. Carefully defining the objective function for the problem and understanding the rules which accompany this. In this current work, three objectives are possible and each one will have its own set of design rules.
 - For general mechanical problems (as discussed in Chapter 4), a much larger number of objective functions are possible depending on the needs and goals of the designers.
3. In general, the manufacturability constraints and the performance design objectives will provide the constraints on the problem. In this case, the FDM constraints, constraints on the raw materials, and constraints on the fracture variables will provide all of these problem constraints. These must be carefully defined in consistent and clear terms.
 - The way that the MPDSMs concept is defined in this dissertation is compatible with the systems engineering theory and approach structure proposed in the NASA Systems Engineering Handbook. This would be an excellent reference to use along with this design guide. Organizing the constraints according to the

ISRC technique discussed in Chapter 2 and in the NASA Handbook can be a very helpful, simple, and effective way to handle large problems.

4. Select the printing parameters and settings for FDM as early as possible. Carefully define each one as a parameter (to be controlled during printing), a constant, or a constraint.
5. Select materials very carefully; the results in Chapter 6 show the massive difference in performance and controllability for various materials. In addition, it must be considered that AM-processed materials often behave very differently than molded ones. It is best to try to understand material performance on the element/microstructural level, as this is a better predictor than macroscale tested properties.
6. Any stress concentrators that will be placed in the system should follow the guidelines for notching and pre-cracking established in Chapter 6. Therefore, any notches must be able to be machined with a mill, router, saw, broach or other method without damaging or interfering with the rest of the part or material structure.
7. For fracture-related problems, the best material layout will almost always be a concentric or contoured layout designed to help steer cracks where they are intended to grow and away from areas (or dissipated) when not intended to grow. This may not be mathematically optimal from the perspective of the whole part, but it makes the most sense when looking from the perspective of the crack tip and resulting stress/strain fields.
8. Based on experiments in Chapter 4, it has been noted in this dissertation that adding newly designed regions to help deal with fracture objectives can help make the resulting material structure much more tough but it also makes it less stiff. The stakeholders must account for this when trying to design or redesign regions.
9. Re-design as little of the part as possible. It is tempting to simply turn the entire part into a concentrically-printed shape with no design but this is a mistake. While toughening the material to an extreme degree, it also greatly decreases the structural stability and makes the structure far more compliant. One way to prevent this is to

design or re-design only the areas that are necessary to meet the fracture objectives print the rest using the strong raster-45 pattern with alternating layer directions. Of course, a full re-design may be necessary in some cases.

10. Make sure that the part shell encloses both original and new regions to avoid cracking and separation in non-designed regions.
 - In practice, this rule is an ideal that should strived for but may not always be feasible or realistic. The designer should inspect the final design and make sure that there are at least no regions which could easily separate away from the intended stress field. This is especially important when a part would be under a tensile stress or the load is applied normal to the print orientation.
11. Keep in mind that each layer of the part can be examined as if it was a very dense truss made up on the material elements. This knowledge must guide the design layouts.
12. Follow relevant manufacturability constraints - when using Cura or similar, this is easy since you can input restrictions on angle, element length, bridge length, etc directly into the software. Not only is automation of this very easy with the right software, it will prevent printing errors and problems later.
13. Follow as many of the soft manufacturability constraints as practical with the given resources.
14. When setting up the areas (if not the whole part) to be designed or re-designed, make sure that the re-designed part has at least one one connection to a constraint point to prevent the part from possibly delaminating or shattering early. There may be more than one area to be re-designed (especially for 3-D problems) but they should all be connected to a solid boundary condition or connected into one mass.
15. Selecting the means of identifying the areas the designed or re-designed, linear elastic CAD and FEA models should only be used with a very fine mesh and only when it is reasonable to assume that the material is LEFM as well.

16. Similarly to other structured materials, the FDM MPDSMs are strongest in compression. If given the choice, the designer should strive to have as much compression load (versus tension, torsion, ect.) on the designed structure as possible. For FDM MPDSMs, the printing orientation may affect this significantly and should be considered prior to fabrication.
 - In practice, this may require some experimentation and/or expert intuition in order to accomplish and there may be some design trade-offs involved.
17. Avoid using support material of any kind when constructing an MPDSM, as it will likely be impossible to actually remove the supports after printing.

Design Rules: Fracture Mechanics

Based on the previous discussion of fracture mechanics theory and its impact on the design, some simple, logic-based design rules can be applied which do not require specific expertise in fracture mechanics. These include:

1. The largest and best design space for fracture-driven problems is the face through which the crack is growing or may grow. This is an important consideration when selecting a printing orientation for the part.
2. Some regions of the part may need reinforcement to prevent fracturing or yielding outside of the designed zone (or where the crack is designed to grow), depending on the load. This may take the form of bolts or other mechanical reinforcement that may involve post-processing (coatings, resin pours, annealing, etc).
3. For non-experts in fracture mechanics who must design fracture-driven problems, the following problem statements are useful for setting up the problem and making decisions:
 - If the crack is growing or may grow and the material structure needs to prevent this (i.e., “crack arrest”), the best way to do this is to dissipate the fracture energy. This is best done by presenting many obstacles to the crack growth, such as material elements or contours placed normally to the possible crack path.

- If the crack is growing or may grow and the structure needs to accelerate it, the opposite should be done as with crack arrest; the shortest and most efficient path to the boundary should be determined and the material structure designed to facilitate and guide this growth.
- If the crack needs to grow in a specific pattern, the material elements need to guide it, as with crack acceleration, but with the material around the crack remaining structurally sound.

Design Rules: Solution Method Selection

- If the output of the design process is a directly-manufacturable product, then the final product should be in the form of g-code. Otherwise, it can be output as a model or other product. This decision needs to be made as early as possible, as it will drive the solution method selected.
- It is very unlikely that only one solution will be best and different driver software packages may produce different g-code. This is not a problem as long as the final design makes sense in the context of the problem.

Design Rules: Manufacturing

1. While all of the printing parameters are important and should be carefully controlled, the build plate temperature is one of the most important. For amorphous materials, proper control of this parameter can help prevent residual stress build up in the material structure. For semi-crystalline materials, the build plate temperature can have a direct impact on the degree of crystallinity in the final polymer. For both types of material, a build plate temperature that is too low can lead to cracking and premature failure in the parts, while one that is too high can exceed the glass transition temperature of the polymer and cause it to settle or yield, destroying dimensional accuracy.

Design Rules: Post-Solution Check

1. User must check to make sure that the produced g-code actually meets the requirements. Making a simple “logical” checklist during design can be very helpful. For example, a simple check could be:
 - *If the problem requires stopping a crack, does the element layout present as many obstacles (ideally walls or contours normal to crack direction) as possible to dissipate the fracture energy?*
 - *If an accelerated crack is desired, does the element layout help guide it along the best and shortest path to the boundary with the smallest possible amount of interference?*
 - *If the problem needs to design a crack path, does the layout support this path growth while still allowing the rest of the material to be structurally sound?*

Appendix B

CURA-BASED G-CODE GENERATOR TUTORIAL

Overview

This tutorial demonstrates how to complete element layouts in Ultimaker[®] Cura. It should be noted that Cura is used only for implementing the layout and is not an optimization or design software in itself. The region to be re-designed or optimized (including its shape), the manufacturability constraints, and the other inputs must be independently input into Cura. It is recommended that Cura be paired with Autodesk[®] NASTRAN or the Autodesk[®] Shape Generator tool for the best design outcomes. As with other implementation software, bad inputs will result in bad outputs so care must be taken to ensure that the design is sound before implementation.

Inputs

The basic inputs will be two or more STL files (one for the primitive to describe the design space and at least one for the MPDSM region), the FDM manufacturability constraints for the process settings and materials used, and any other relevant settings and printing parameters.

Process Steps

Setting Up the Workspace

Open Cura, making sure that any needed updates have been completed. The version used in this dissertation was Cura 4.2.1. Make sure to use a native Cura build and not one that is customized for a particular printer or brand.

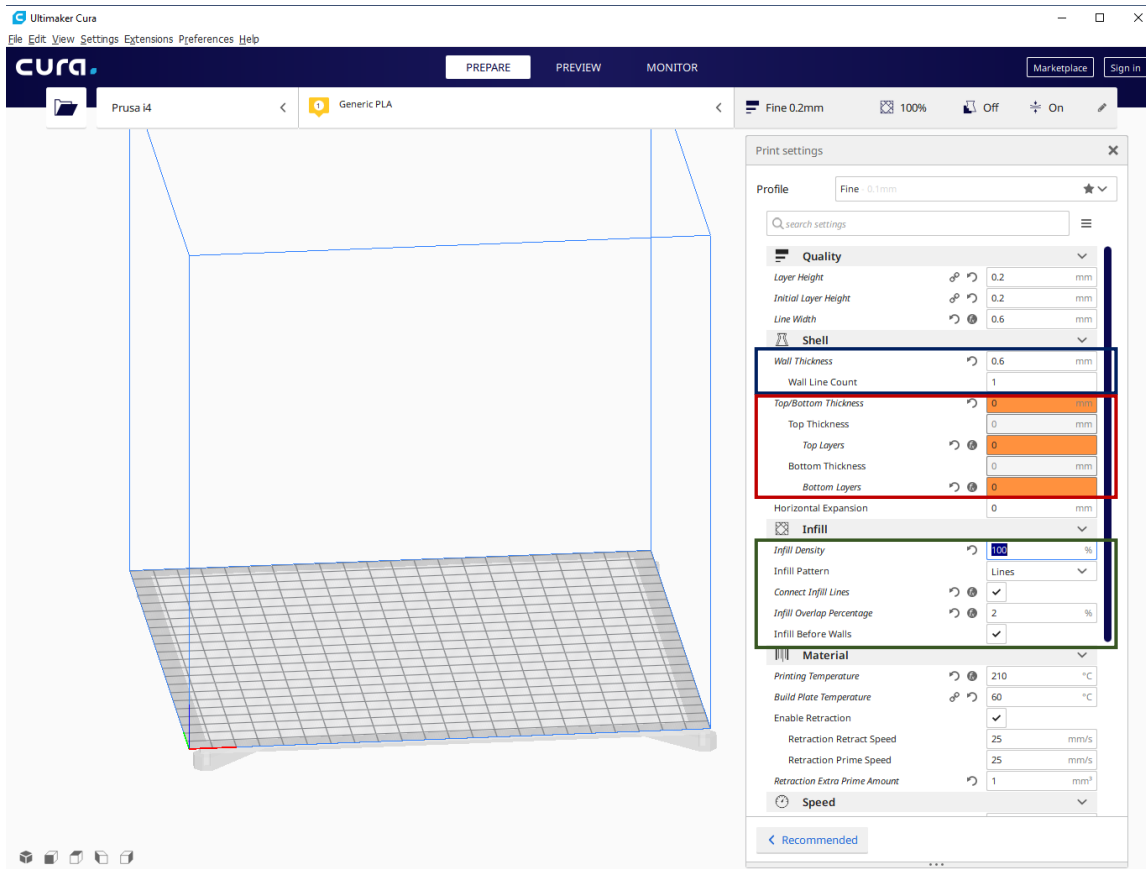


Figure B.1: Initial Cura setup.

As shown in Figure B.1, some initial settings should be carefully considered. First, Cura should be put into manual mode (or custom selection mode, depending on the version). At a minimum, the settings shown in the figure should be turned on (see Figure B.2 for the button to modify setting visibility). Note that this is also the main gateway into the settings catalog, which is the best way to input and enforce manufacturability constraints during the layout process. The designers should add as many settings as needed to the control window in order to account for all the manufacturability constraints.

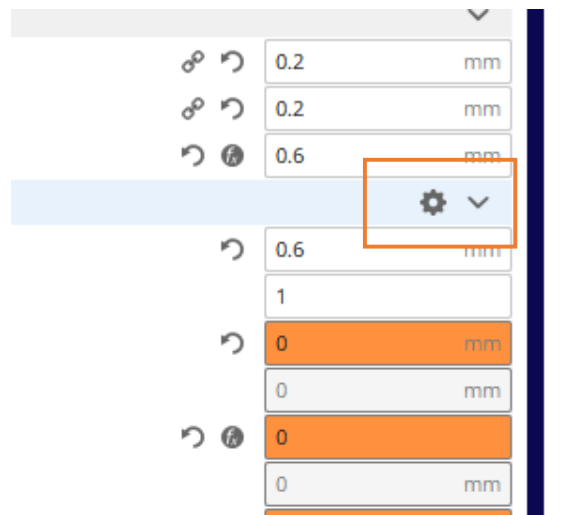


Figure B.2: Button to access setting visibility in Cura manual mode.

The following should be set:

1. Wall thickness should be set to the nozzle size and the wall line count should be set according to the need of the designer. In this setting configuration, one shell can be sufficient but more can be used as needed. It should be noted that the more shells used, the smaller the design area for the MPDSM or MPDSM region will be.
2. Very importantly, the bottom and top thickness (and layers) values should be set to zero. These layers are difficult to control and setting them to zero allows the designer to use only designable layers for the whole build. The horizontal expansion setting is optional and up to the designer and has little effect on the layouts; it is mainly used to account for shrinkage in the cases where severe residual stresses are present.

3. The initial infill density and pattern (“Lines” gives the standard raster configuration in Cura) should be input.
4. Connect infill lines and the overlap settings should be activated in order to make sure the laid out elements connect well.
5. Finally, it is recommended that the walls be printed last before the infill. In the experience of the author, this is the best way to produce good quality layouts while still maintaining good macro-scale dimensional accuracy.

Importing STL Files

Once the work space is set up, the various STL files (at least the primitive and the file describing the designed or re-designed region) should be imported (Figure B.3) and checked for errors.

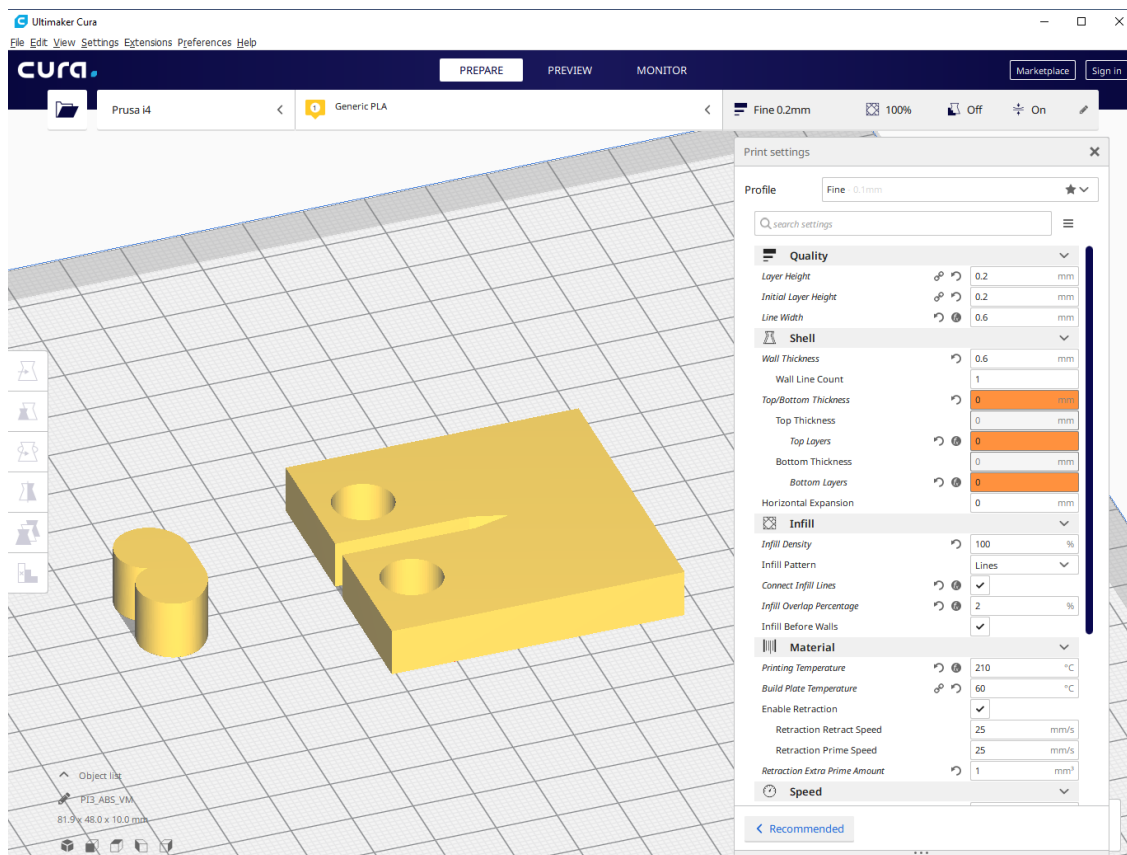


Figure B.3: Imported STL files.

The designer should ensure that both parts land flat on the build plate in the correct orientation relative to each other and made any needed adjustments. While not required, it is often helpful to scale the part representing the designed area in one direction so that it extends above the other part; make sure to turn off the uniform scaling requirement so that the important dimensions are not affected by this. The results of this scaling is shown in Figure B.3 and Figure B.5.

Relative Settings

First, set the primitive part as the base and overlap the designed area part as shown in Figure B.4. This should look like the primitive + designed region from the analysis or model from BEFORE the Cura input of the two regions.

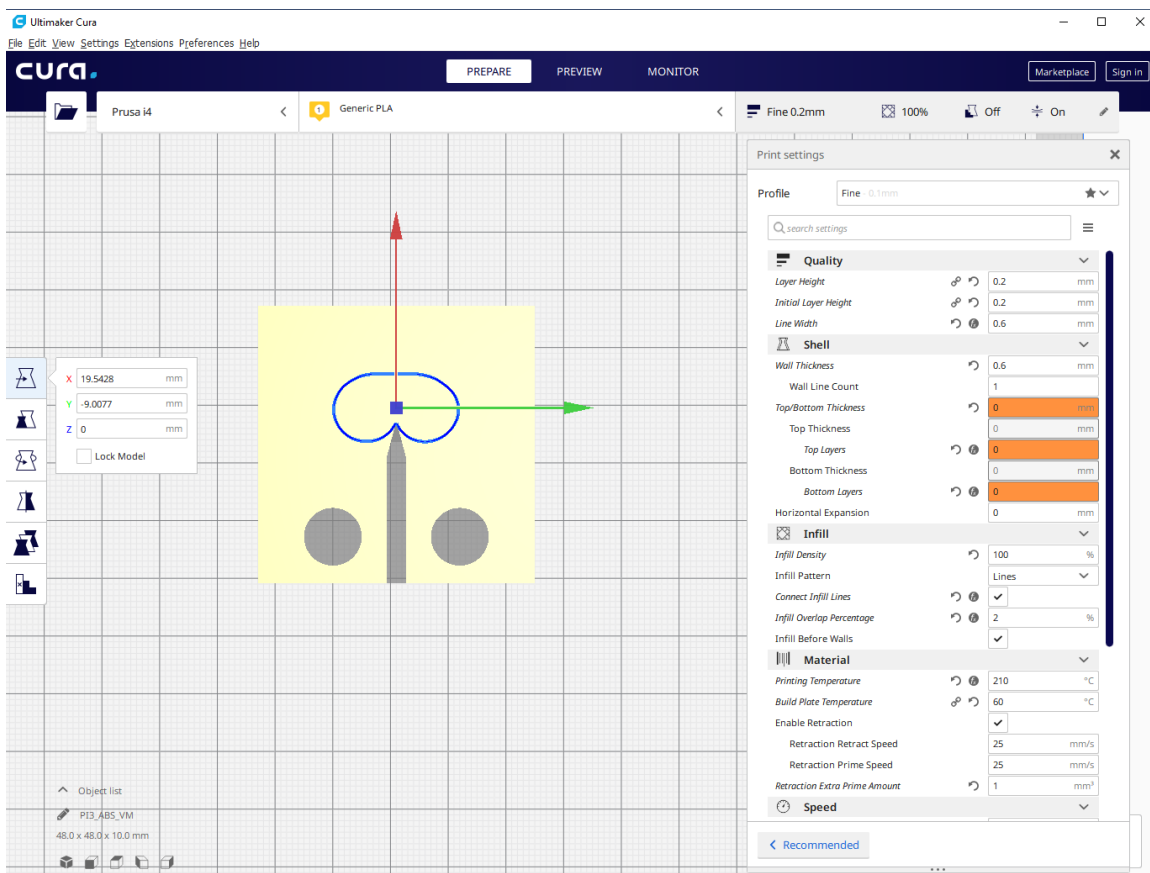


Figure B.4: Relative placement of the primitive and designed region STL files.

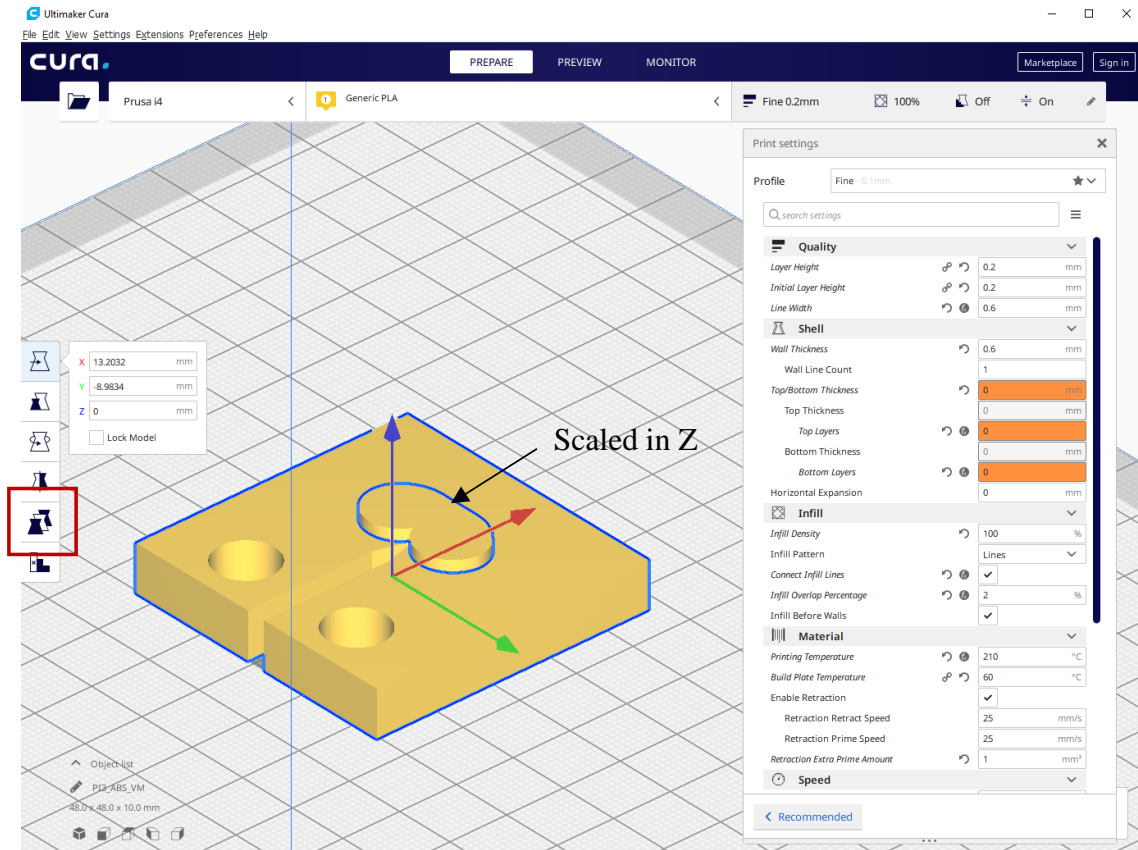


Figure B.5: Select Per Model Settings.

Next, select the primitive and select the Per Model Setting (Figure B.5). From there, make sure that the primitive is set as “Normal Model”. Select settings (Figure B.6, Figure B.7, and Figure B.8) and ensure they are the basic settings needed for the primitive for the regions that are not designed or re-designed. As a test, slice the model (Figure B.9); at this point, both regions should have the same settings.

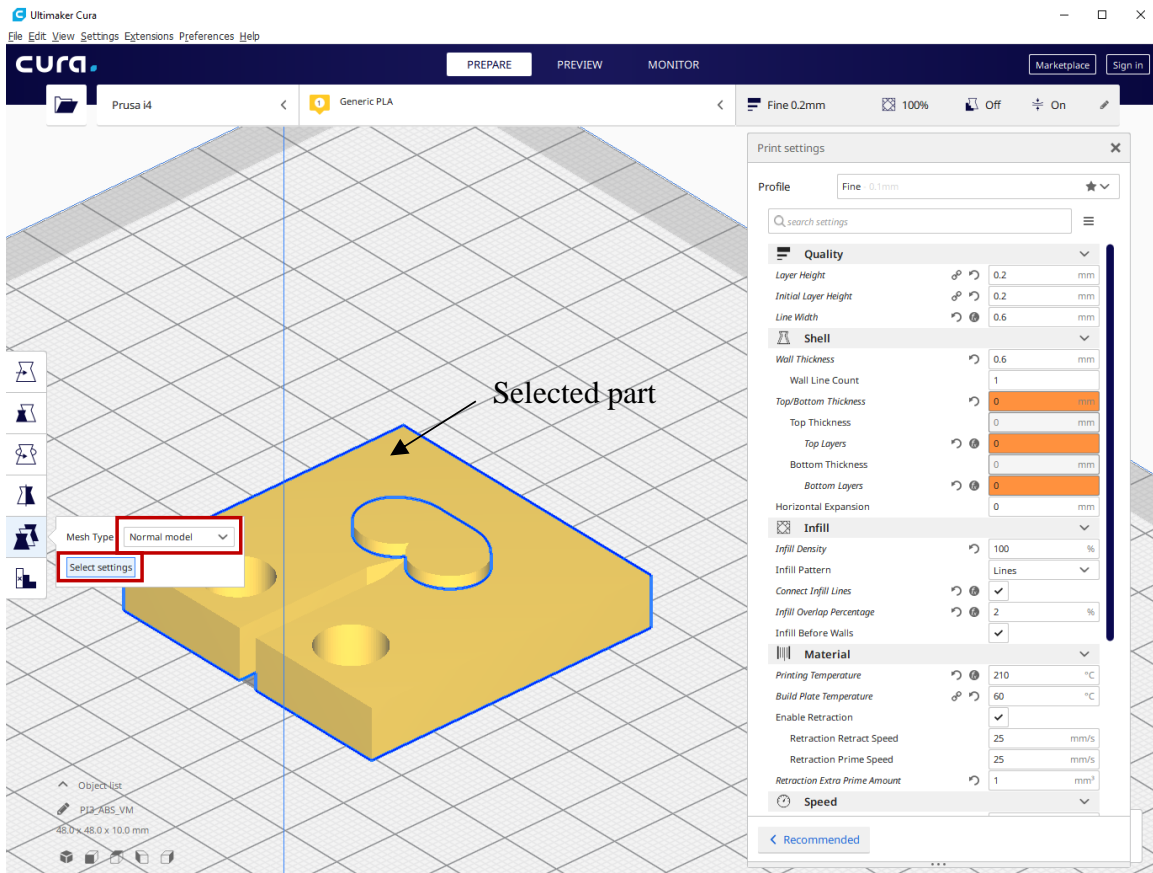


Figure B.6: Confirm primitive settings, Step 1.

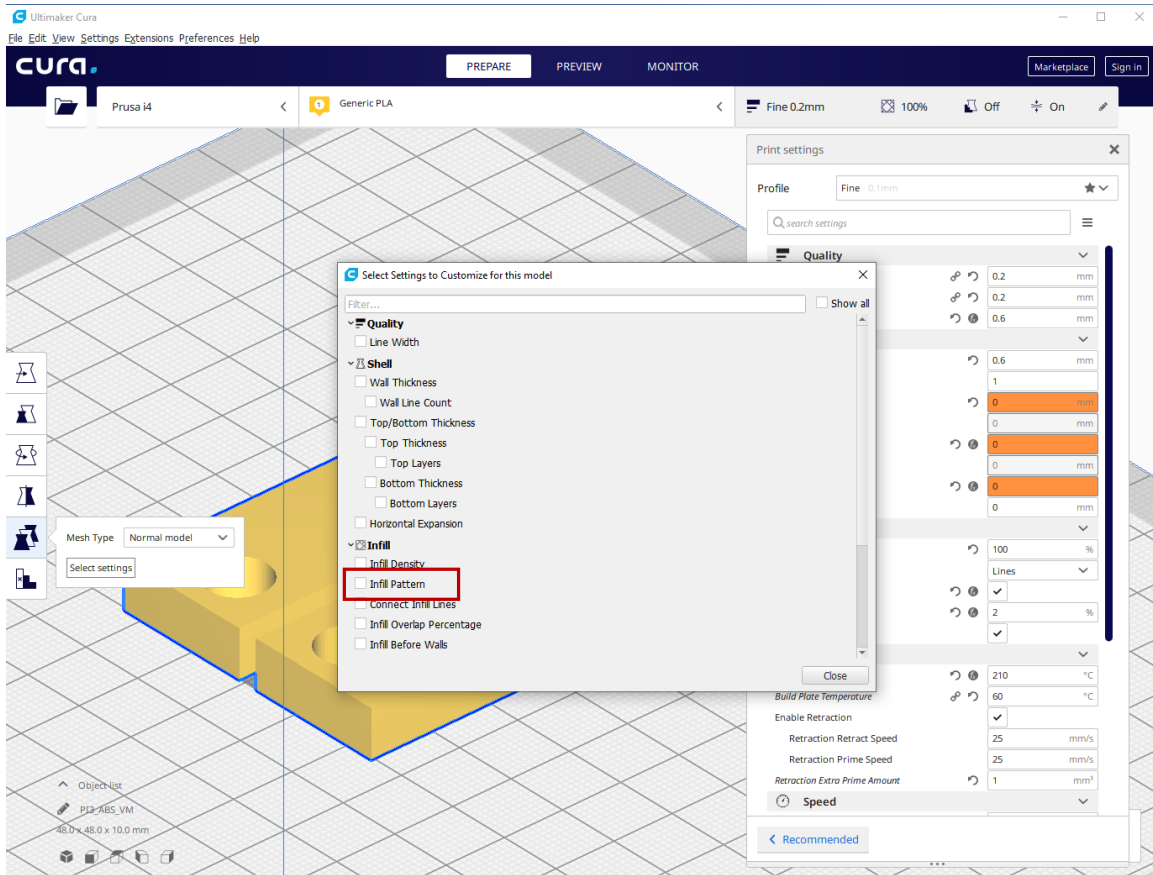


Figure B.7: Confirm primitive settings, Step 2.

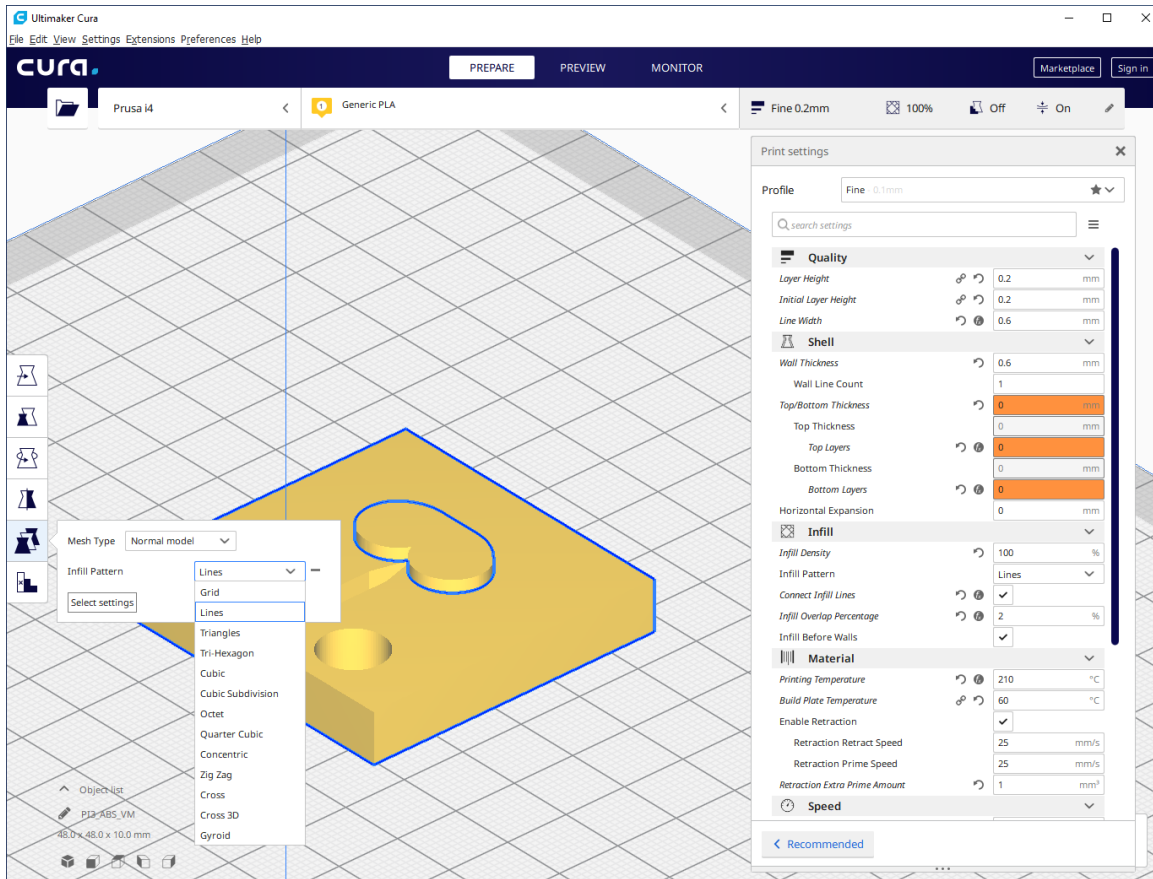


Figure B.8: Confirm primitive settings, Step 3.

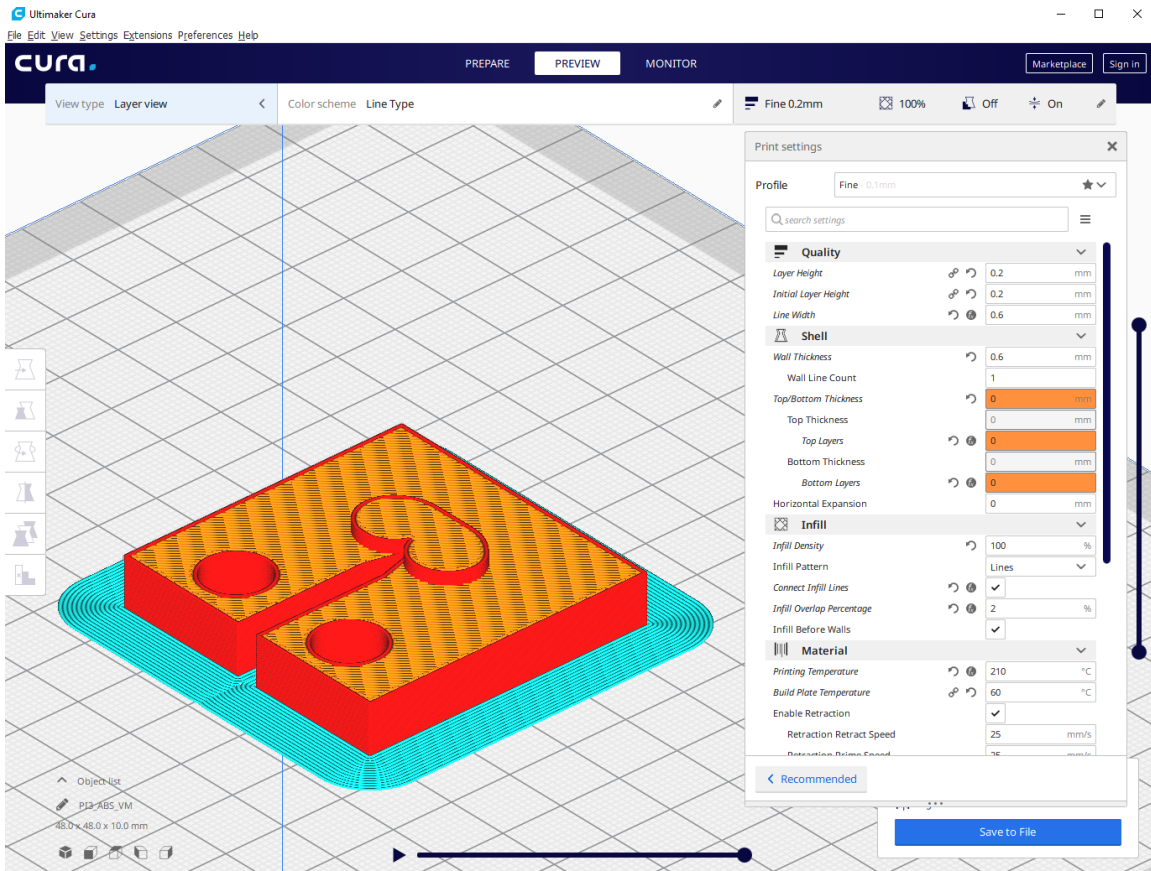


Figure B.9: Test slice.

New Designed Region

Given that the primitive is now finalized and ready to print, the designed region layout should be done. As shown in Figure B.10, the designed region part should be active. Again select the Per Model Setting and select Modify Settings for Overlap with Other Models (Figure B.11).

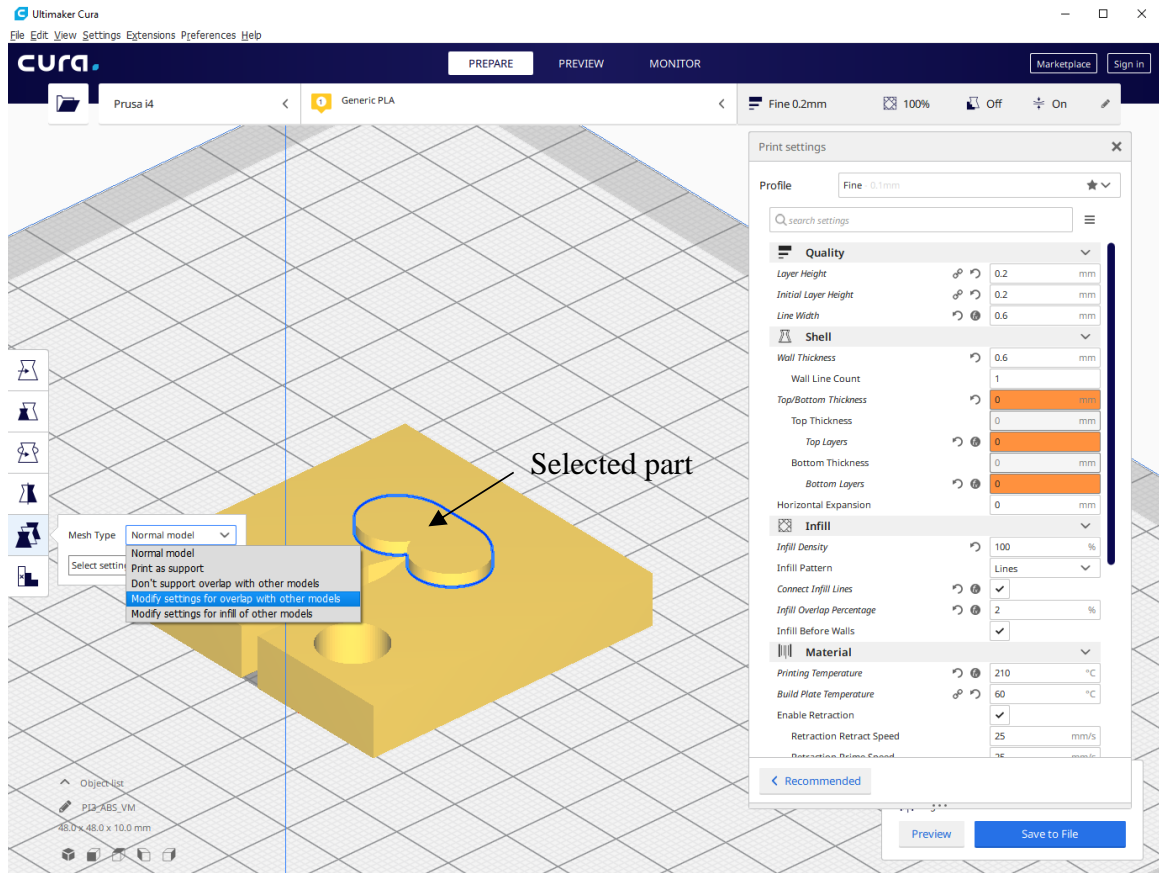


Figure B.10: Design of the laid out region.

Select the desired layout pattern (usually will be concentric, at least for fracture problems) (Figure B.11 and Figure B.12).

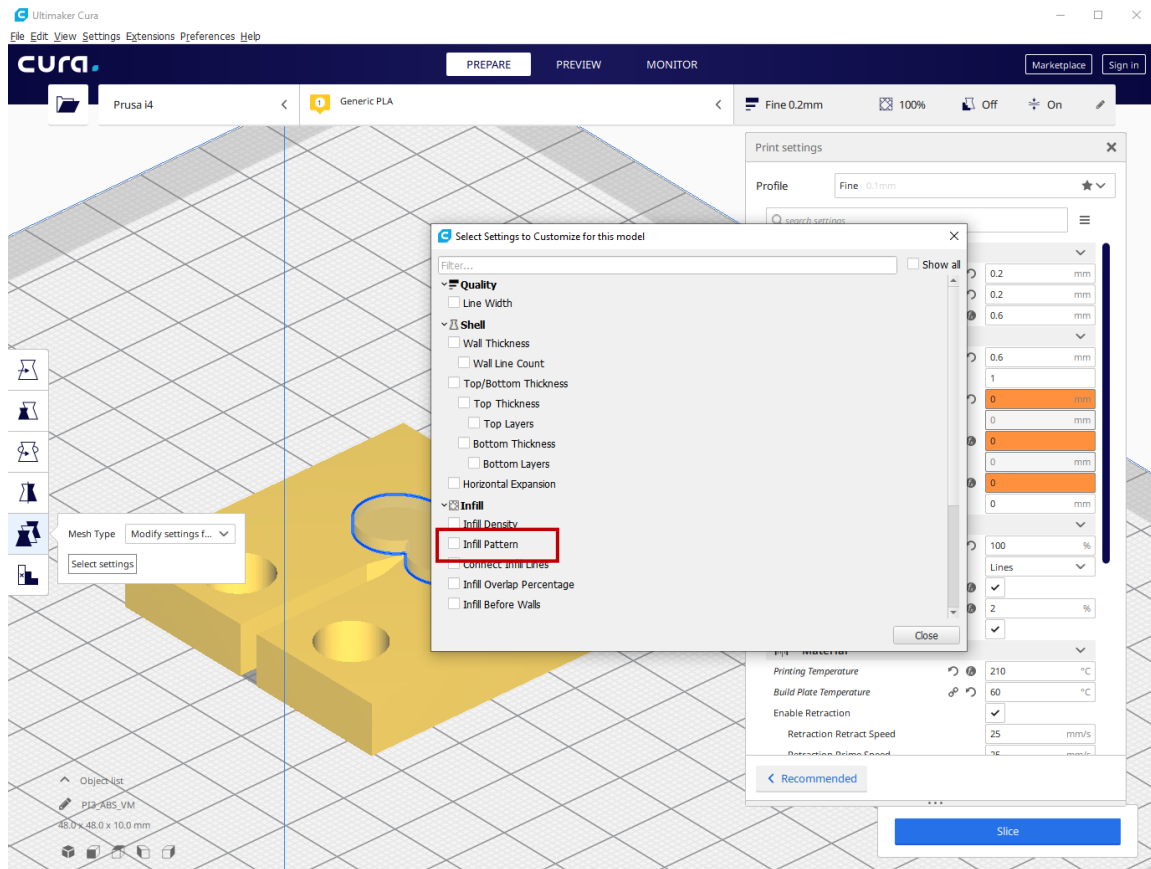


Figure B.11: Select layout pattern for designed region.

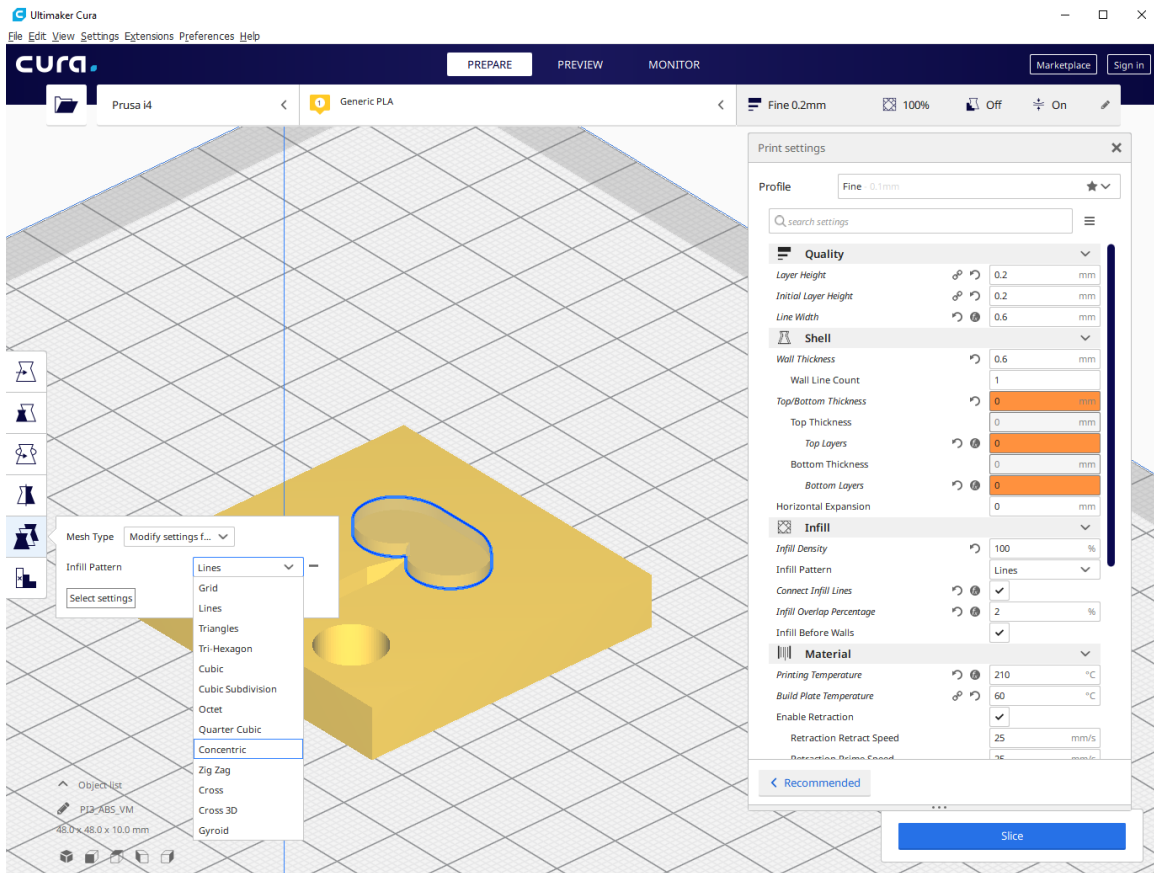


Figure B.12: Concentric layout selection

Output

Figure B.13 shows a successful output after slicing. From here, the g-code can be output directly to the printer. If desired, an animation of the build layer-by-layer can be produced using the print animation tool (Figure B.14)

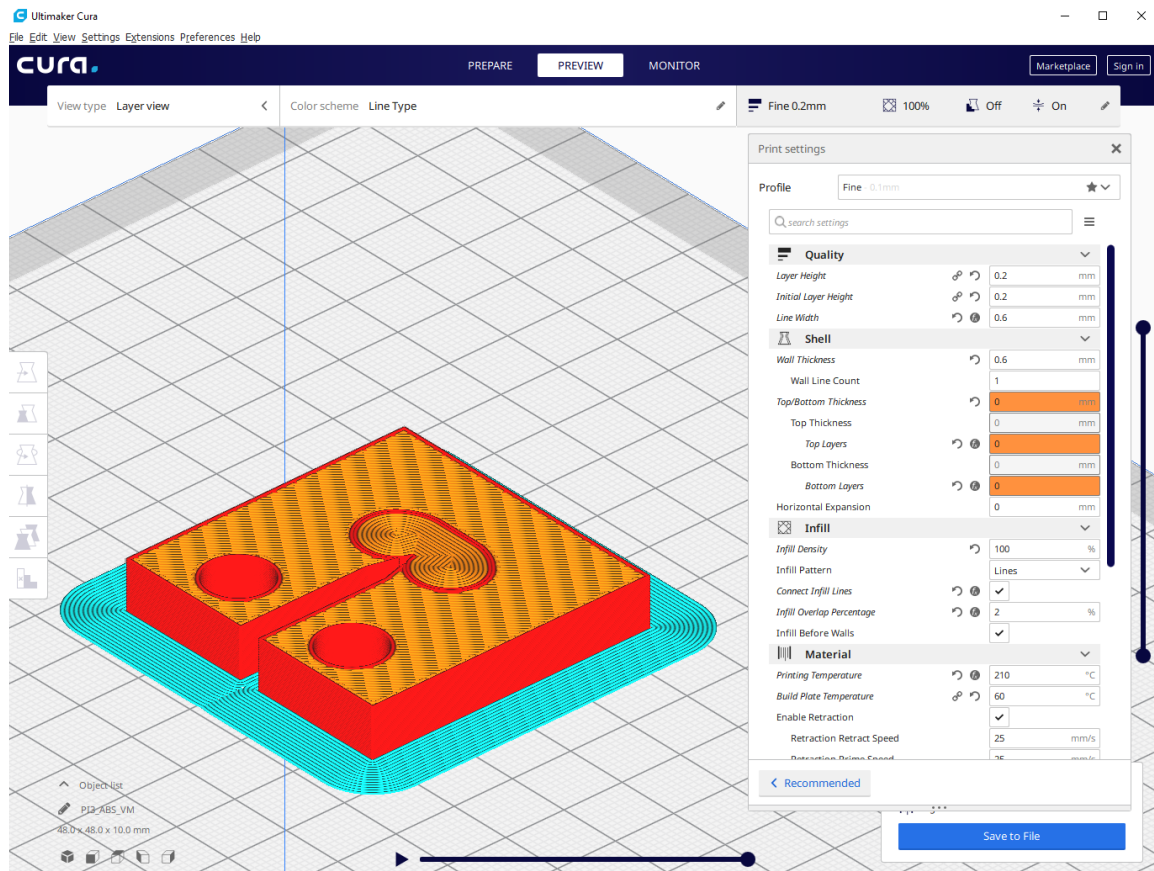


Figure B.13: Caption

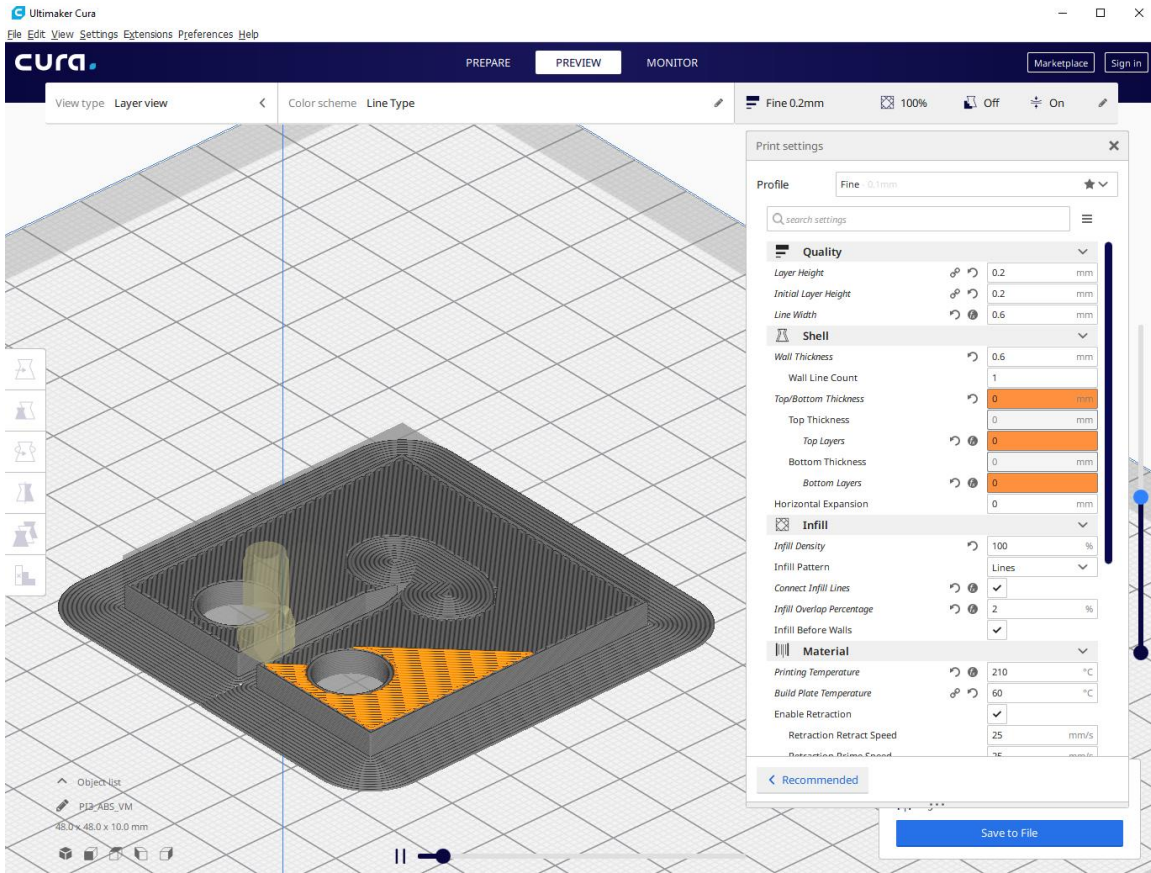


Figure B.14: Caption

Appendix C

CONVERTING G-CODE BACK TO STL WITH VOXEL MESH

It is standard practice to use pre-processing software to prepare parts for printing. These tools (such as Ultimaker Cura) take STL files as input, slice them into layers, and generate g-code based on the given inputs plus the inputs provided by the user. Some programs are very basic (such as those which come from proprietary printer manufacturers and only work with one machine or small family of machines), while some (such as Cura) are very advanced. The more advanced pre-processing software packages allow the direct input of design and manufacturability constraints, custom materials, and allow direct control of the g-code presented. From the additive manufacturing perspective, the pre-processing software packages available are powerful and reliable and are usable by anyone from a beginning hobbyist to manufacturing engineers working with advanced MPDSMs (Chapter 4).

One of the main features of manufacturability-driven design (Chapters 3 and 4) that the final output of the design process is a directly manufacturable design. For the cases where AM is used, this generally will consist of g-code. While this gives a practicing engineer a directly manufacturable design without having to worry about further analysis or processing, this is not always a good outcome. In the cases where further design analysis is desired or the printed part needs to be simulated as part of the verification, validation, and accreditation process, it would be very useful to have a means for outputting a digital part instead of g-code.

There are several ways to do this, including producing both a final model and g-code as design outputs. However, this can be extremely computationally expensive. A much more simple way to accomplish it is to convert the g-code itself into a solid model when needed. The best way to do this is to use a tool which converts the toolpath instructions (both the travel path and the cross-section element design) into a voxel-based mesh. Voxel meshes are the easiest way to accomplish this outcome in general, as they are simple to apply and the elements are all of a consistent size. The trade-off for this is a slightly less dimensionally-accurate digital model but one that is simple and low-cost to produce.

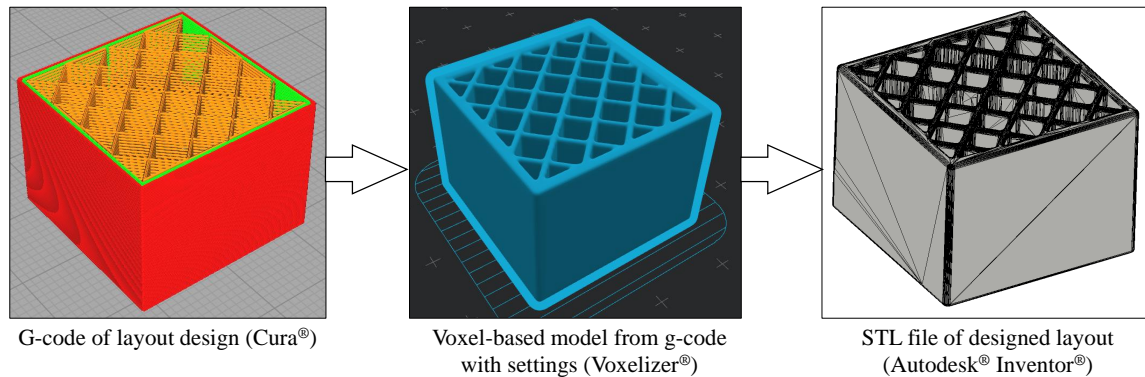


Figure C.1: Example conversion of a g-code layout (with printing parameters and manufacturability constraints imposed) into a useful STL file using the Voxelizer tool to translate the toolpaths to equivalent solid geometry. The STL file can easily be further converted into a STEP or Parasolid file for finite element analysis.

In practice, the best tool to use for this will be Voxelizer (Voxelizer.com), which can accept g-code (including all the information about the cross-section of elements) and convert it into an STL file. This file can then be converted (using Autodesk Inventor or similar) into a parasolid or STEP file for inputting into a finite element solver. Figure C.1 shows an example where this was done successfully. Some notes from the author on how to do this more effectively and with less risk of failure:

- Standard Voxelizer and other similar softwares will start with the outer shell when building the voxel mesh. Therefore, if the internal printed geometry is to be reproduced, it should be outside of a shell in the g-code
- It is recommended that in Voxelizer that no roof or floor layers be used, as this will

more accurately reproduce any internal geometry

- The largest mesh that should be used should be such that at least 3 voxels cover the cross section of each printed element. If computational cost is not too high, it should be more than this. The smaller the voxels, the more accurate the final model will be.

Appendix D

CALCULATION PROCESS FOR K_Q AND K_{1c} IN CHAPTER 6

This appendix demonstrates the calculation process for finding K_Q and K_{1c} from experimental data. The specimen used is a CT specimen with $W = 50$ mm, $B = 10$ mm, and $a/W = 0.5$. The specimen was made from PLA and printed using an R45 configuration. Figure 1 shows the specimen and the force-deflection data collected during the test.

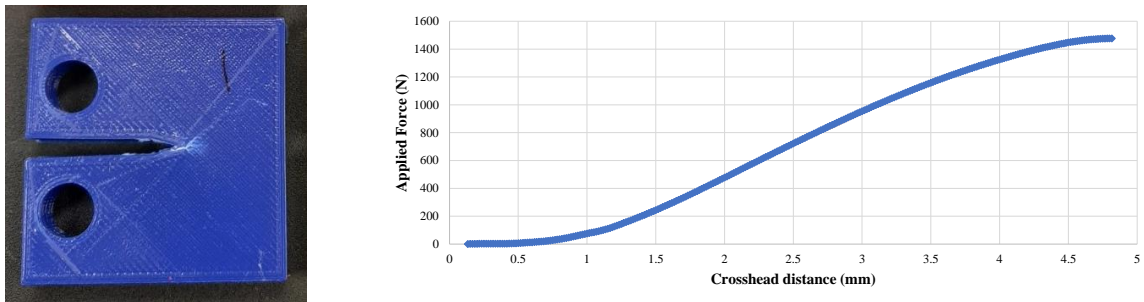


Figure D.1: Example specimen and testing data

The calculation procedure follows the guidelines from the ASTM D5045 standard. First, calculating the tangent line (Figure 2), the following equation can be approximated:

$$y = 457.38x - 433.04 \quad (1)$$

Finding the value of C (inverse slope):

$$C = 1/457.38 = 0.002186 \quad (2)$$

Finding the 1.05C line,

$$y = 435.59x - 433.04 \quad (3)$$

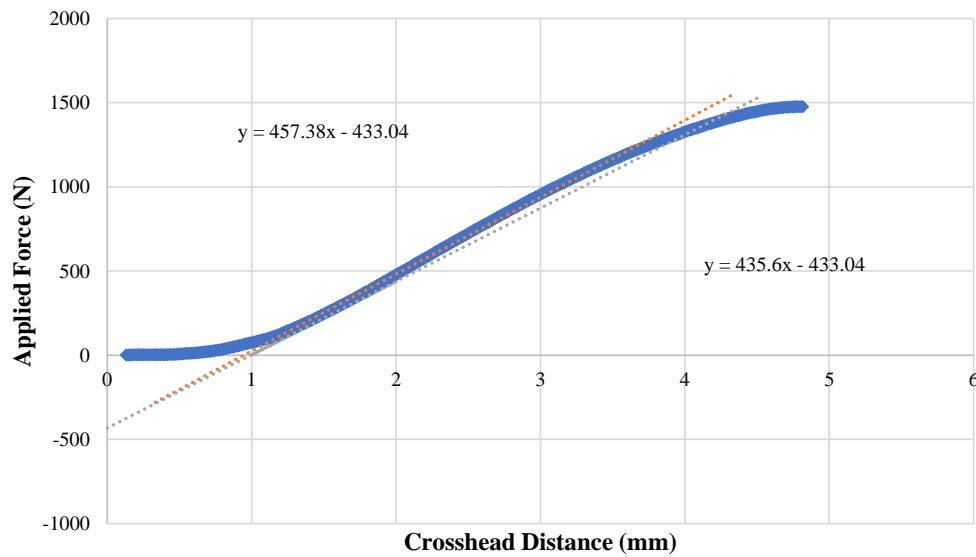


Figure D.2: Calculations and intercept lines

This provides a value of $P_Q = 1349$ N. Inspecting the dataset, $P_{max} = 1477$ N. Therefore,

$$\frac{P_{max}}{P_Q} = 1.094 < 1.1 \rightarrow \text{Valid test} \quad (4)$$

Given the values and dimensions above ($f(x) = 9.65$ from ASTM D5045),

$$K_Q = f(x) \left(\frac{P_Q}{BW^{1/2}} \right) = 5.82 \text{MPa}\sqrt{m} \quad (5)$$

Given that the measured yield stress for PLA is $\sigma_y = 47.8$ MPa,

$$2.5 \left(\frac{K_Q}{\sigma_y} \right)^2 = 37.1 \text{ mm} \quad (6)$$

Since B , a , and $(W - a)$ are all smaller than the required sample size, it is not possible to conclude that $K_Q = K_{1c}$ and K_Q should be reported as the conditional fracture toughness.

Appendix E

EXPERIMENTAL DATA SHARING AND AVAILABILITY

All of the experimental data generated during this course of this investigation is archived and is available upon request to the author at pttrsnv2@illinois.edu or aepatterson12@gmail.com. Upon publication of all the related articles from this dissertation, the data will be publicly archived and available under a CC-BY licence. To allow time to publish the related work, the data will be kept from public disclosure until April 30, 2023.

Appendix F

INTERESTING EXPERIMENTAL FIGURES

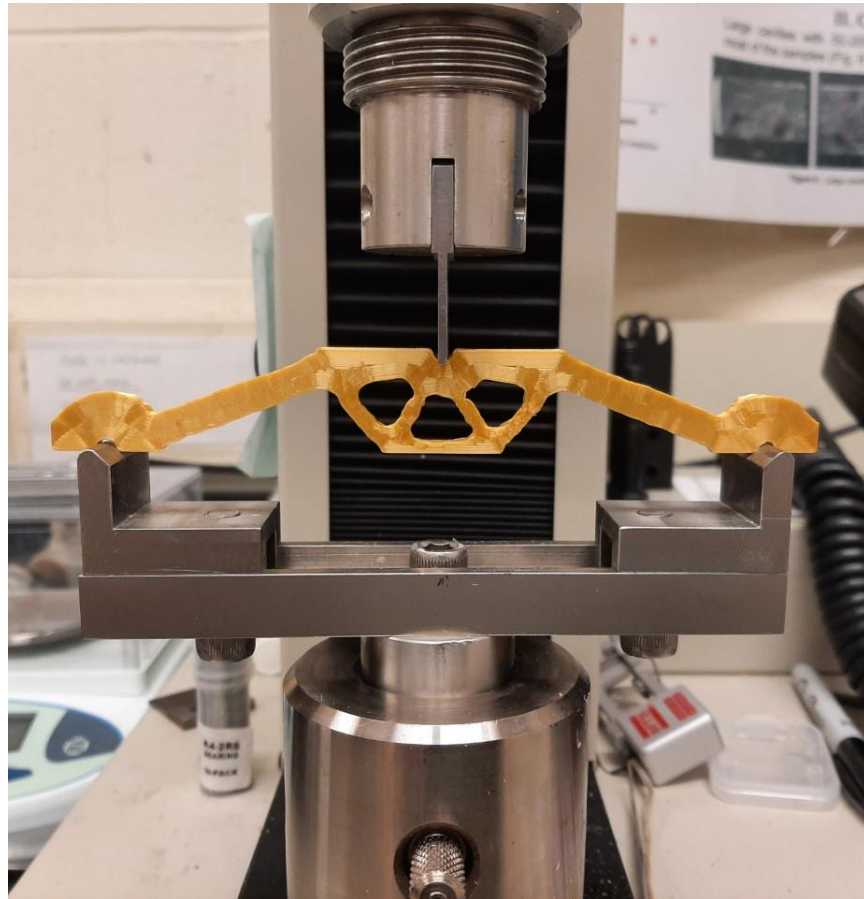


Figure F.1: 3-point bend testing of one of the topology optimization solutions from the design studies in Chapter 4.

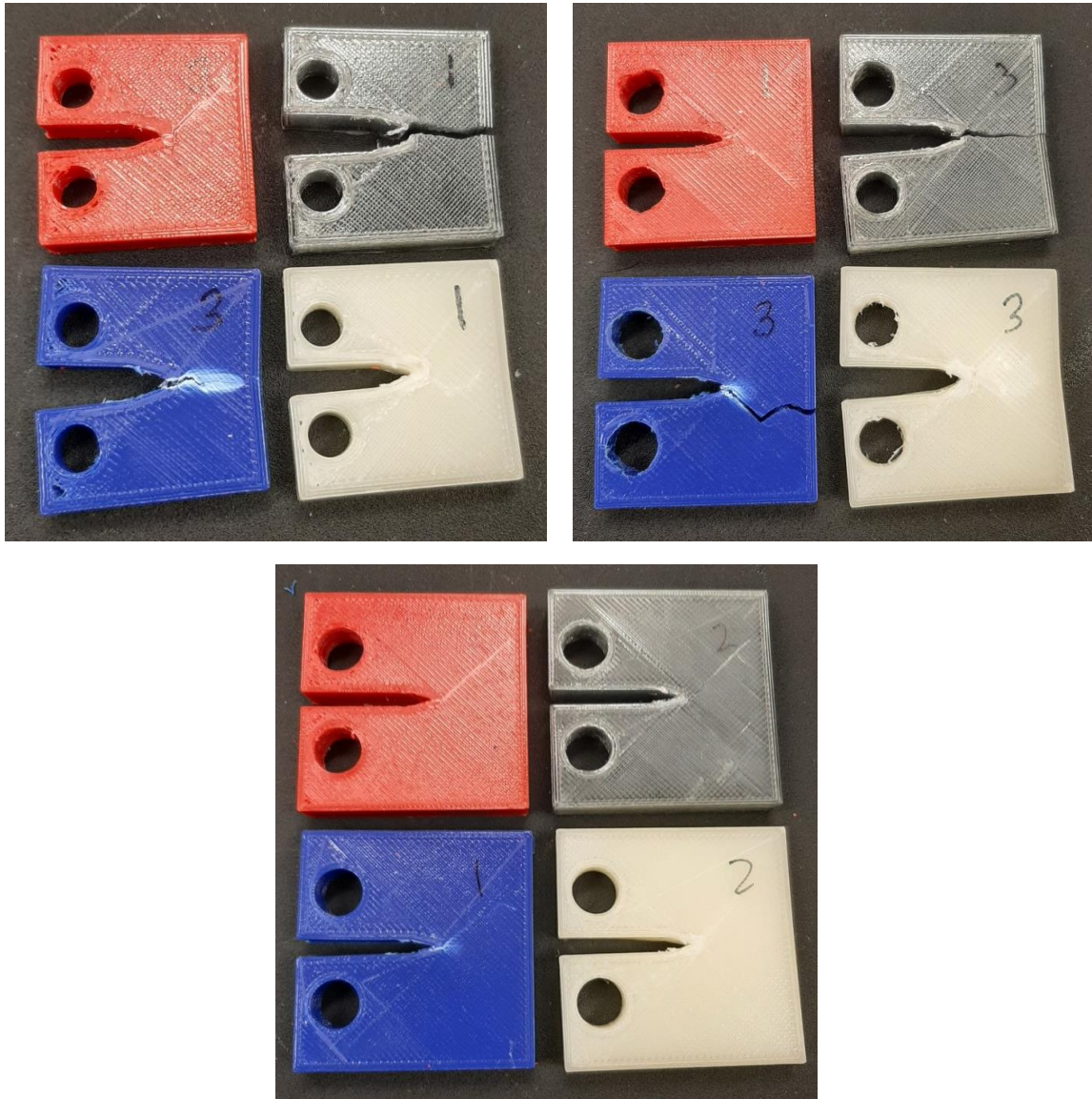


Figure F.2: Fracture samples from the sample size sensitivity study, including some trial nylon (white) samples which were not used in the final study.

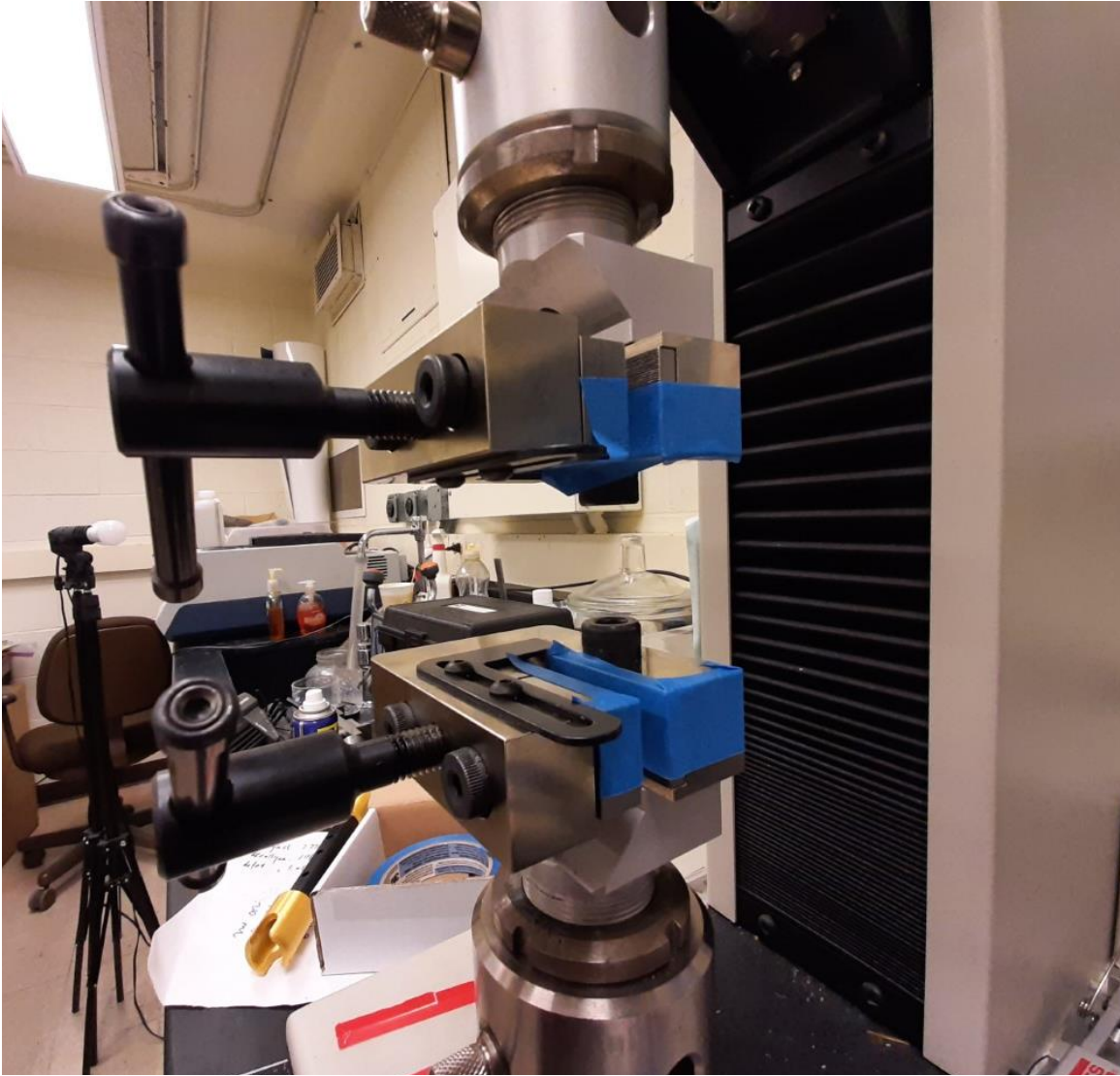


Figure F.3: Grip setup (with blue tape) for the tensile film testing.

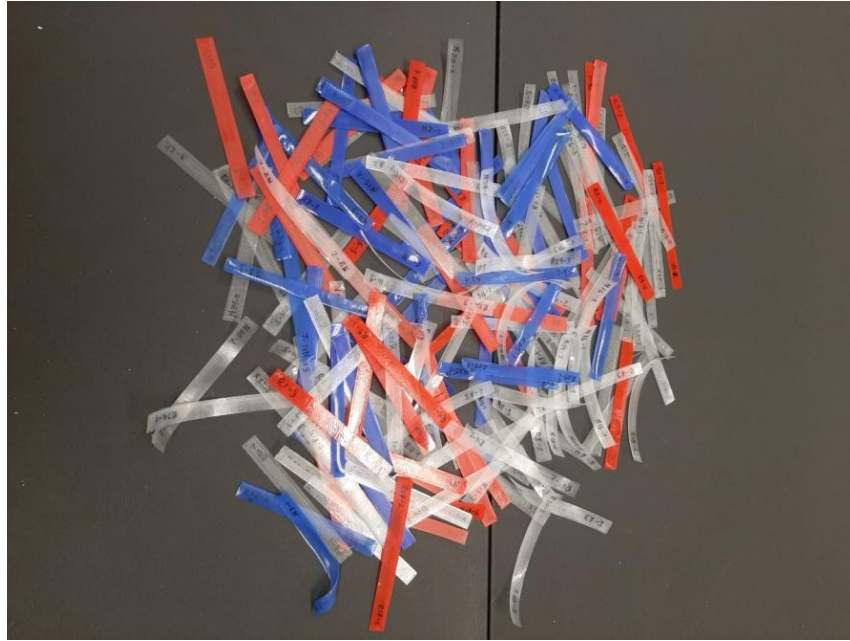


Figure F.4: Film sample set pre- and post-testing. Includes some nylon testing samples that were not used in the final study.

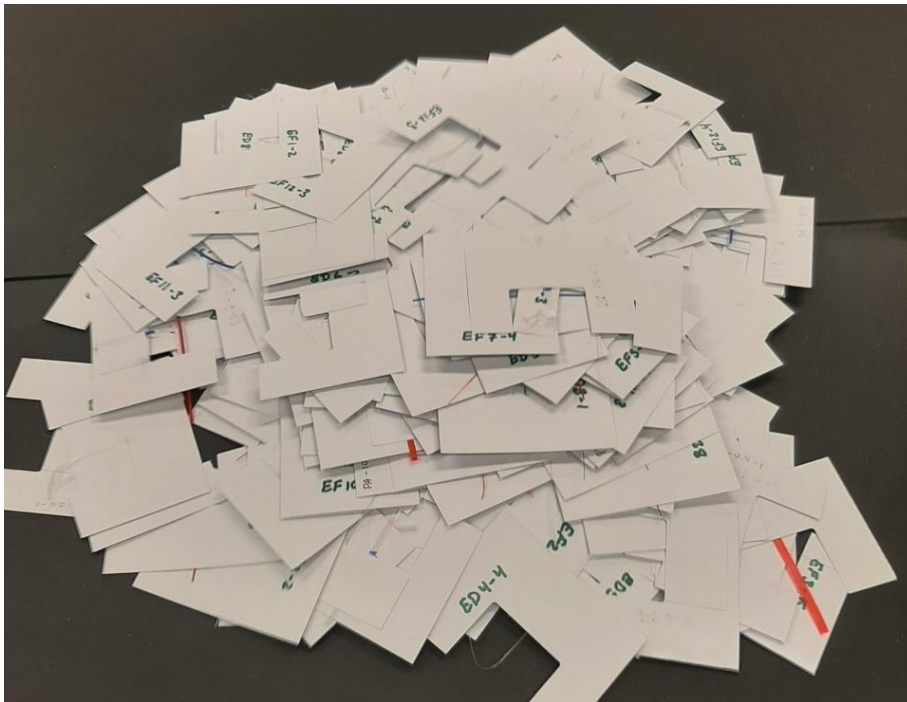


Figure F.5: Fiber sample set pre- and post-testing. Includes some nylon testing samples that were not used in the final study.

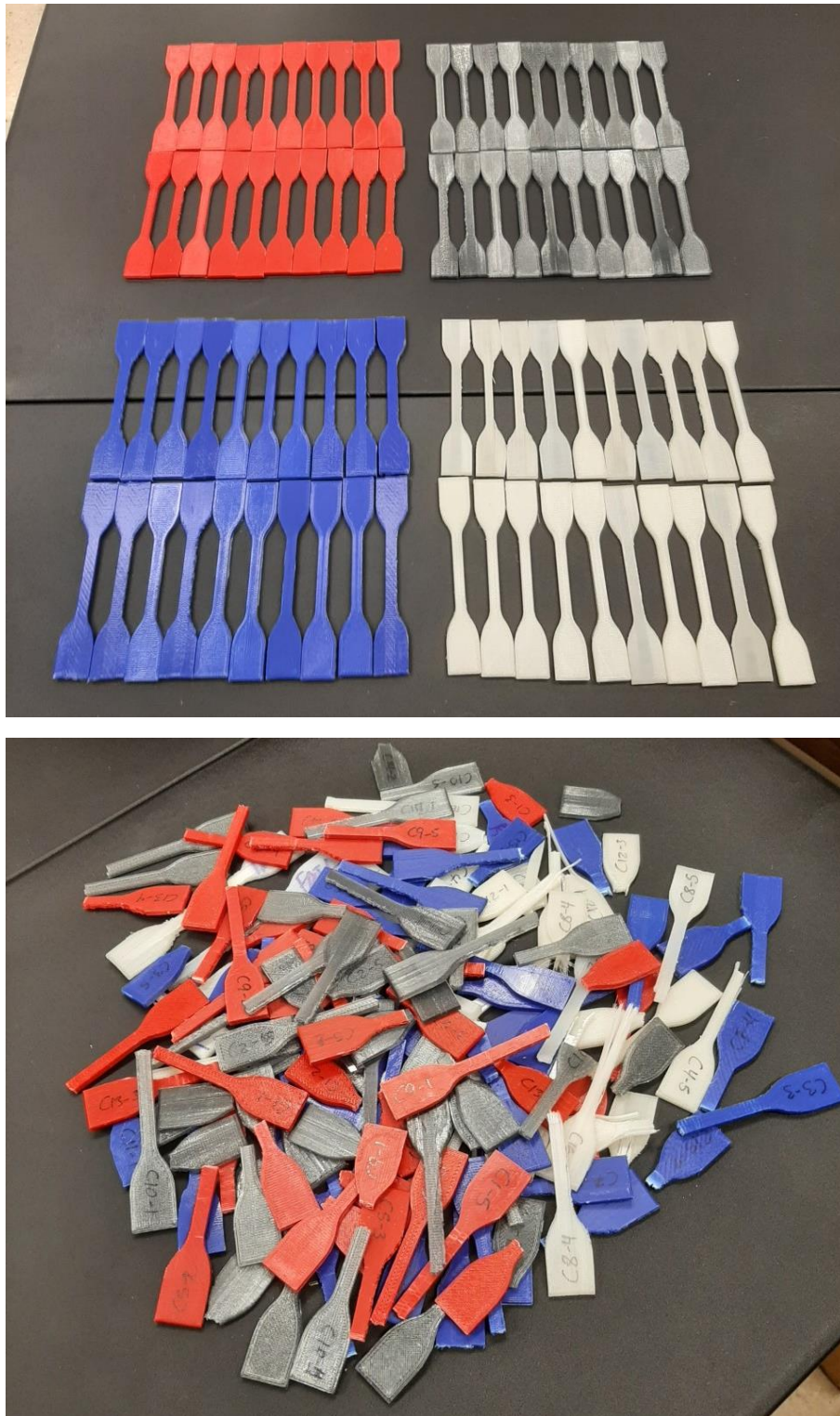


Figure F.6: Basic characterization sample set pre- and post-testing. Includes some nylon testing samples that were not used in the final study.

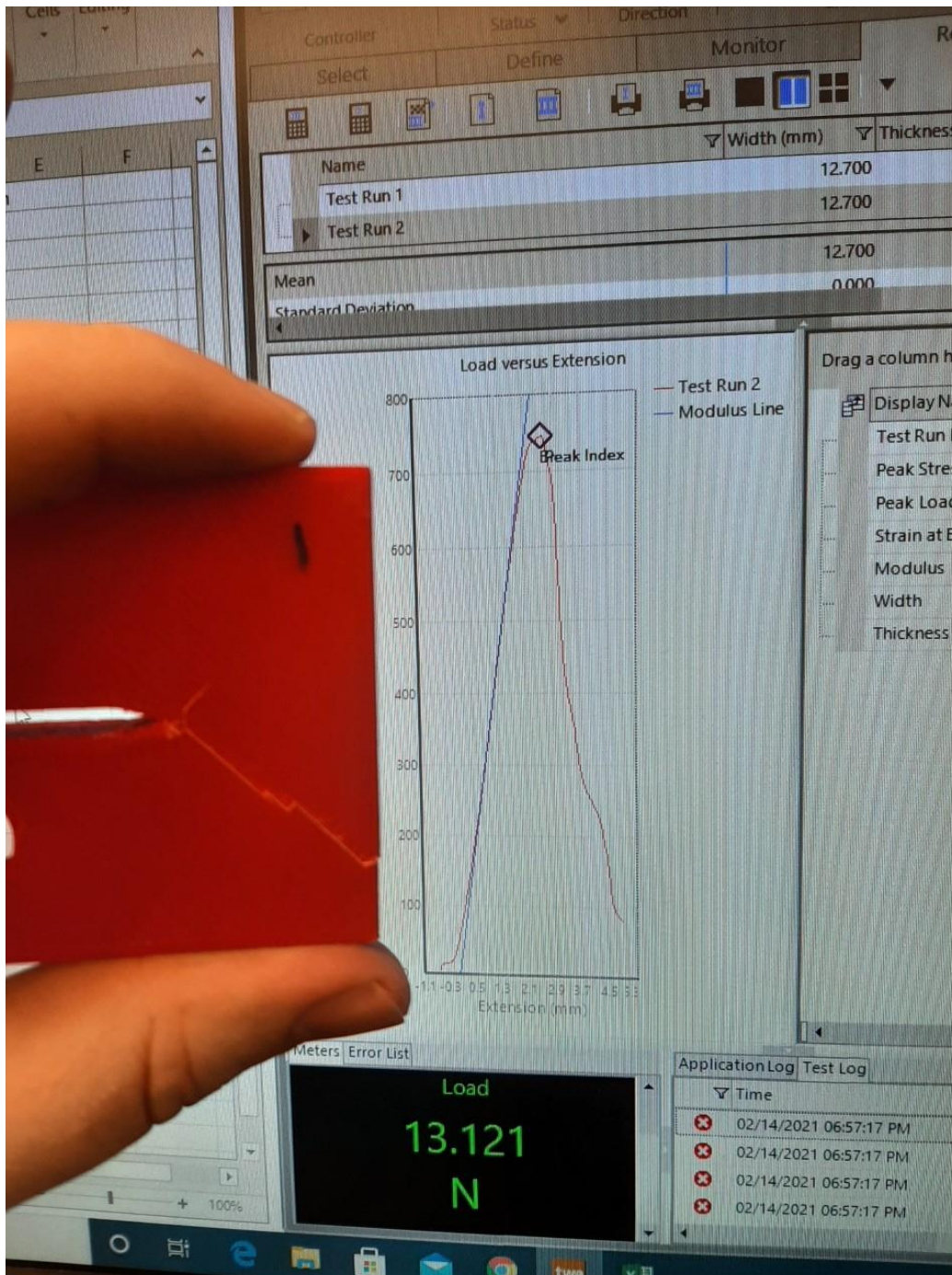


Figure F.7: Fractured sample compared shown next to the collected data from testing it.

Appendix G

DETAILED REVIEW APPROACHES FOR CHAPTER 2 AND CHAPTER 5

Chapter 2 Review

Chapter 2 Detailed Survey Approach and Design

While this project was intended as a detailed survey and not a meta-analysis review, every effort was made to include all the relevant literature and provide an accurate view of the topic under study within the limitations discussed in the main paper. It should be noted that the collection of references for this survey had some limitations in scope, specifically excluding references in the following categories:

- Papers not published in English
- Most review papers where the authors could not find new and unique information not available from the primary sources
- Patent literature, editorials, posters, and viewpoint papers except those reporting major field problems and/or experimental results
- Technical reports and theses published before 2005 (more than 15 years old)
- Conference papers for which a later journal version was published and available

- Conference papers published before 2000 (which did not have a journal version), were not hosted by a major society (such as IEEE, ASME, IISE, ESIS, AIAA, etc.), or were not indexed (such as in ACS and Scopus).
- Any paper from an online-only mega-journal (which publishes papers without a focus on a specific field), with the exception of papers from IEEE Access, Scientific Reports (Nature), AIP Advances, and PLOS One.
- Any paper from a journal considered to be possibly predatory (failure of the Think-Check-Submit test [<https://thinkchecksubmit.org/>], an unknown publisher, a publisher on Beall's List [https://en.wikipedia.org/wiki/Beall%27s_List], or a combination of these)

These exclusions were made to ensure that only credible works which could be competently evaluated by the authors were included in the survey and that works were counted only once (in the case of excluding earlier conference versions of journal papers). It should be noted that small, new, or national-level journals or conferences were considered legitimate if the authors could establish credibility and they were not widely suspected to be predatory.

To begin the survey, a set of relevant keywords were compiled by the authors, which were then used to search for literature in both major indexes which hold engineering-related papers (Google Scholar and Scopus); in each case, the search was ended when reaching the third page with no useful results. The results were sorted based on relevance and no date restrictions were placed on the search criteria. In addition to the standard indexes, a set of peer-reviewed journals and major international conferences related to manufacturing and design were specifically queried.

A total of 180 unique potentially useful papers were found, based on title and abstract, after the search. The papers were then subjected to a review of reference sections to uncover any additional references that were missed in the search; 15 more were found, bringing the total to 195. The set of papers were then subjected to the standard quality screening employed by the authors when completing review papers, screening out any papers that fall into one or more of the categories described above. The final list of papers was then screened carefully for relevance to the topic of this review. After both screenings, 52 papers

were excluded from the review. Therefore, a total of 143 papers were explored and discussed in this review. In addition to papers directly on the topic of the review, an additional 108 papers were found to support the review, such as papers describing manufacturing processes or design needs or papers providing information needed to understand the context of the review. These papers were specifically searched for and only the best 1-2 found on each topic were included in the reference section. With these additional papers, the total number of references for the main paper stands at 251.

Chapter 2 Search Keywords

- Design for manufacturing
- Manufacturability
- Manufacturing constraints
- Manufacturing design constraints
- Manufacturing considerations
- Manufacturability constraints
- Additive manufacturing
- Subtractive manufacturing
- Formative manufacturing
- Tooling design
- Manufacturing design
- Manufacturing system
- Systems engineering manufacturing
- Top-down design
- Bottom-up design

- Product design
- Product design manufacturing
- Sustainable manufacturing
- Sustainability manufacturing
- Green manufacturing
- Macro design, macro design + constraint
- Meso design, meso design + constraint
- Micro design, micro design + constraint
- Sub-micro design, sub-micro design + constraint
- In addition, the names of each of the most common subtractive, additive, and formative manufacturing processes followed by “design”, “constraints”, and “optimization” were also queried.

Chapter 2 List of Journals and Conferences Queried

- ASME Journals
 - Journal of Manufacturing Science and Engineering
 - Journal of Mechanical Design
- Elsevier Journals
 - Additive Manufacturing
 - Advances in Engineering Software
 - CIRP Annals – Manufacturing Technology
 - Composites Part B: Engineering
 - Computer Aided Design
 - Engineering Fracture Mechanics

- International Journal of Machine Tools and Manufacture
- Journal of Cleaner Production
- Journal of Manufacturing Processes
- Journal of Manufacturing Systems
- Journal of Materials Processing Technology
- Manufacturing Letters
- Materials & Design
- Procedia CIRP
- Procedia Structural Integrity
- Robotics and Computer-Integrated Manufacturing
- Emerald Journals
 - Assembly Automation
 - Rapid Prototyping Journal
- Liebert Journals
 - 3D Printing and Additive Manufacturing
- MDPI Journals
 - Journal of Manufacturing and Materials Processing
 - Designs
 - Machines
 - Materials
- Sage Journals
 - Concurrent Engineering
 - Proceedings of the Institution of Mechanical Engineers, Part B: Journal of Engineering Manufacture

- Proceedings of the Institution of Mechanical Engineers, Part C: Journal of Mechanical Engineering Science
- Springer-Nature Journals
 - International Journal of Advanced Manufacturing Technology
 - International Journal of Fracture
 - JOM
 - Journal of Intelligent Manufacturing
 - Progress in Additive Manufacturing
 - Structural and Multidisciplinary Optimization
- Taylor & Francis Journals
 - IISE Transactions
 - International Journal of Computer Integrated Manufacturing
 - International Journal of Production Research
 - Journal of Engineering Design
 - Machining Science and Technology
 - Virtual & Physical Prototyping
- Wiley Journals
 - International Journal for Numerical Methods in Engineering
- Independent Journals
 - International Journal of Bioprinting
- Conference Proceedings
 - Solid Freeform Fabrication (SFF) Symposium: An Additive Manufacturing Conference
 - ASME International Mechanical Engineering Congress and Exposition (IMECE)
 - ASME International Design Engineering Technical Conferences & Computers and Information in Engineering Conference (IDETC/CIE)

Chapter 5 Review

Chapter 5 Detailed Survey Approach and Design

While this project was intended as a survey and not a formal review paper, every effort was made to include all the relevant literature and provide an accurate view of the topic. Note that only papers published in English were included in the survey. To begin the survey, a set of 38 relevant keywords were compiled by the authors, which were then used to search for literature in both major indexes which hold engineering-related papers (Google Scholar and Scopus); in each case, the search was ended when reaching the third page with no useful results. The results were sorted based on relevance and no date restrictions were placed on the search criteria. The only exclusion from the search was for patent literature, as it was not anticipated to be useful for this review. In addition to the standard indexes, a set of 19 peer-reviewed journals and two major international conferences related to AM and fracture mechanics were specifically queried.

A large set of unique potentially useful papers were found, based on title and abstract, after the search. The vast majority of the works found were published in peer-reviewed journals since 2014, with only a handful of conference papers, theses, and technical reports found on the topic. The papers were then subjected to a review of reference sections to uncover any additional references that were missed in the search; several more were found, bringing the total to 112. The set of papers were then subjected to the standard quality screening employed by the authors when completing review papers, screening out any papers that fall into one or more of the following categories:

- Technical reports and theses published before 2005 (more than 15 years old at the time of the start of the review)
- Review papers in which no new information could be found in addition to the original works
- Conference papers published before 2008 (which did not have a journal version), are not hosted by a major society (such as IEEE, ASME, IISE, ESIS, AIAA, etc.), or were not indexed (such as in ACS and Scopus)

- Any paper from an online-only mega-journal (which publishes papers without a focus on a specific field), with the exception of papers from IEEE Access, Scientific Reports, AIP Advances, and PLOS One.
- Any paper from a journal considered to be possibly predatory (failure of the Think-Check-Submit test [<https://thinkchecksubmit.org/>], an unknown publisher, a publisher on Beall's List [https://en.wikipedia.org/wiki/Beall%27s_List], or a combination of these)

It should be noted that small, new, or national-level journals or conferences were considered legitimate if the authors could establish credibility and they were not known to be predatory. After screening using the above categories, two papers were removed from consideration and are given at the end of this document for the reader to evaluate. After screening, the final list contained 84 articles for deeper review. The final list of 84 papers were then screened carefully for their relevance to the topic of this review, with 21 papers being removed due to not being directly related to the topic or providing no useful information relative to the research questions for this review. The remaining papers were divided into two categories:

1. Direct relevance and included in the review (40 papers – given in the main paper)
2. Interesting information, but not directly related to the research questions and were therefore not included in the main review (26 papers). Earlier iterations (including pre-expansion conference versions) of papers included in the review were also included in this category.

Other supporting works for the main survey (to supply definitions, to back up claims in the introduction, to supply standards, etc.) were also found, bringing the total cited works to 86 in the main manuscript and an additional 26 in these supplemental materials.

Chapter 5 Search Keywords

Google Scholar, Scopus, and the queried journals/conferences were searched for relevant literature using the following 38 keywords related to the topic of this literature survey:

- Additive manufacture charpy
- Additive manufacture crack
- Additive manufacture crack propagation
- Additive manufacture CTOD
- Additive manufacture fracture
- Additive manufacture IZOD
- Additive manufacture notch
- Additive manufacture precrack
- Additive manufacturing digital image correlation
- Additive manufacturing failure analysis
- Additive manufacturing fracture energy
- Additive manufacturing fracture toughness
- Additive manufacturing LEFM
- Additive manufacturing linear elastic fracture
- mechanics
- Additive manufacturing testing method
- AM CTOD
- AM charpy
- AM crack
- AM crack propagation
- AM digital image correlation
- AM failure analysis

- AM fracture
- AM fracture energy
- AM fracture test
- AM fracture toughness
- AM IZOD
- AM LEFM
- AM mechanical testing method
- AM notch
- AM precrack
- FDM crack
- FDM fracture
- Fused deposition modeling crack
- Fused deposition modeling fracture
- Polymer additive manufacture crack
- Polymer additive manufacture fracture
- Polymer AM crack
- Polymer AM fracture

Chapter 5 List of Journals and Conferences Queried

In addition to the index searches in Google Scholar and Scopus, the following journals and conferences were specifically queried using the same keywords as described in the previous section.

1. Rapid Prototyping Journal (Emerald)

2. International Journal of Advanced Manufacturing Technology (Springer-Nature)
3. Virtual & Physical Prototyping (Taylor & Francis)
4. Additive Manufacturing (Elsevier)
5. Progress in Additive Manufacturing (Springer-Nature)
6. JOM (TMS/Springer-Nature)
7. Materials & Design (Elsevier)
8. 3D Printing and Additive Manufacturing (Liebert)
9. Journal of Manufacturing Science and Engineering (ASME)
10. Materials (MDPI)
11. Journal of Manufacturing and Materials Processing (MDPI)
12. Polymers (MDPI)
13. Polymer Testing (Elsevier)
14. Engineering Fracture Mechanics (Elsevier)
15. Procedia Structural Integrity (Elsevier)
16. International Journal of Fracture (Springer-Nature)
17. Journal of Materials Processing Technology (Elsevier)
18. Proceedings of the Institution of Mechanical Engineers, Part B: Journal of Engineering Manufacture (Sage)
19. Proceedings of the Institution of Mechanical Engineers, Part C: Journal of Mechanical Engineering Science (Sage)
20. Solid Freeform Fabrication (SFF) Symposium: An Additive Manufacturing Conference (2008 to present)
21. ASME IMECE (2008-present)

Chapter 5 Excluded But Potentially Relevant References

The following references were excluded from the review but were evaluated to possibly be of interest to the readers of this survey. They were excluded for a variety of reasons, as explained in the introduction to this section. All are rigorous and reliable sources from reputable publication venues.

1. Ahmed, A.A. & Susmel, L. (2017). On the use of length scale parameters to assess the static strength of notched 3-D printed PLA. *Frattura ed Integrità Strutturale*, 41: 252-259.
2. Chacon, J.M., Caminero, M.A., Garcia-Plaza, E., et al. (2017). Additive manufacturing of PLA structures using fused deposition modelling: Effect of process parameters on mechanical properties and their optimal selection. *Materials and Design*, 124: 143-157.
3. Damodaran, V., Castellanos, A.G., Milostan, M., et al. (2018). Improving the Mode-II interlaminar fracture toughness of polymeric matrix composites through additive manufacturing. *Materials and Design*, 157: 60-73.
4. Dizon, J.R., Espera Jr, A.H., Chen, Q., et al. (2018). Mechanical characterization of 3D printed polymers. *Additive Manufacturing*, 20: 44-67.
5. Dong, Y., Milentis, J., & Pramanik, A. (2018). Additive manufacturing of mechanical testing samples based on virgin poly(lactic)(PLA) and PLA/wood fibre composites. *Advances in Manufacturing*, 6: 71-82.
6. Dowoud, M., Taha, I., & Ebeid, S.J. (2016). Mechanical behavior of ABS: An experimental study using FDM and injection moulding techniques. *Journal of Manufacturing Processes*, 21: 39-45.
7. Durgun, I. & Ertan, R. Experimental investigation of FDM process for improvement of mechanical properties and production costs. *Rapid Prototyping Journal*, 20(3): 228-235.

8. Garg, A. & Bhattacharya, A. (2017). An insight to the failure of FDM parts under tensile loading: finite element analysis and experimental study. *International Journal of Mechanical Sciences*, 120: 225-236.
9. Goh, G.D., Dikshit, V., Nagalingam, A.P., et al. (2018). Characterization of mechanical properties and fracture mode of additively manufactured carbon fiber and glass fiber reinforced thermoplastics. *Materials and Design*, 137: 79-89.
10. Hill, N. & Haghi, M. (2014). Deposition direction-dependent failure criteria for fused deposition modeling polycarbonate. *Rapid Prototyping Journal*, 20(3): 221-227.
11. Hoskins, T.J., Dearn, K.D., & Kukureka, S.N. (2018). Mechanical performance of PEEK produced by additive manufacturing. *Polymer Testing*, 70: 511-519.
12. Islam, M.S. & Prabhakar, P. (2017). Interlaminar strengthening of multidirectional laminates using polymer additive manufacturing. *Materials and Design*, 133: 332-339.
13. Liao, G., Li, Z., Cheng, Y., et al. (2018). Properties of oriented carbon fiber/polyamide 12 composite parts fabricated by fused deposition modeling. *Materials and Design*, 139: 283-292.
14. Miguel, M., Leite, M., Ribeiro, A.M.R., et al. (2019). Failure of polymer coated nylon parts produced by additive manufacturing. *Engineering Failure Analysis*, 101: 485-492.
15. Patterson, A.E., Chadha, C., Jasiuk, I.M., et al. (2019). Design and repeatability analysis of desktop tool for rapid pre-cracking of notched ductile plastic fracture specimens. *Engineering Fracture Mechanics*, 217: 106536.
16. Riddick, J.C., Haile, M.A., Von Wahlde, R., et al. (2016). Fractographic analysis of tensile failure of acrylonitrile-butadiene-styrene fabricated by fused deposition modeling. *Additive Manufacturing*, 11: 49-59.
17. Slotwinski, J. & Moylan, S. (2014). Applicability of existing materials testing standards for additive manufacturing materials. NIST Report # NISTIR 8005. DOI: 10.6028/NIST.IR.8005.

18. Spoerk, M., Arbeiter, F., Cajner, H., et al. (2017). Parametric optimization of intra- and inter-layer strengths in parts produced by extrusion-based additive manufacturing of poly(lactic acid). *Journal of Applied Polymer Science*, 134(41): 45410.
19. Spoerk, M., Arbeiter, F., Raguz, I., et al. (2018). Polypropylene filled with glass spheres in extrusion-based additive manufacturing: Effect of filler size and printing chamber temperature. *Macromolecular Materials and Engineering*, 303: 1800179.
20. Studart, A.R. (2016). Additive manufacturing of biologically-inspired materials. *Chemical Society Reviews*, 45: 359.
21. Torrado Perez, A.R., Roberson, D.A., Wicker, R.B. (2014). Fracture surface analysis of 3D-printed tensile specimens of novel ABS-based materials. *Journal of Failure Analysis and Prevention*, 14: 343-353.
22. Torres, J., Cole, M., Owji, A., et al. 2016. An approach for mechanical property optimization of fused deposition modeling with polylactic acid via design of experiments. *Rapid Prototyping Journal*, 22(2): 387-404.
23. Tronvoll, S.A., Welo, T., & Elverum, C.W. (2018). The effect of voids on structural properties of fused deposition modelled parts: A probabilistic approach. *The International Journal of Advanced Manufacturing Technology*, 97: 3607-3618.
24. Uddin, M.S., Sidek, M.F.R., Faizal, M.A., et al. (2017). Evaluating mechanical properties and failure mechanisms of fused deposition modeling acrylonitrile butadiene styrene parts. *Journal of Manufacturing Science and Engineering*, 139: 081018.

The following papers were identified as being clearly presented and containing potentially useful data (even if the using obsolete methods or standards), but the publication venues could not be verified, were excluded due to criteria established in the introduction, or and have been called out as being predatory publishers. Readers should review these carefully before citing or using these as references to guide research decisions. Note that the inclusion of these on this list is in no way a personal criticism of the paper authors; their work should be evaluated and judged based on its own merit.

1. Patel, N.D. & Patel, B.B. (2015). Fracture analysis of FDM manufactured acrylonitrile butadiene styrene using FEM. *International Journal of Recent Research in Civil and Mechanical Engineering*, 2(1): 84-90.
2. Patel, R., Shah, H.N., & Kumari, S.V. (2015). Experimental investigation of fracture of ABS materials by ASTM D-5045 for different crack length & layer of orientation using FDM process. *International Journal of Mechanical and Industrial Technology*, 3(1): 79-83.

Appendix H

COPYRIGHT PERMISSION FORMS

Chapter 2 Figure Copyright Permissions

Note on copyright permissions from ASME. The journal paper that was submitted and in review at the time of this thesis deposit required the signing of copyright forms (see email below). However, upon further analysis and speaking with ASME, the copyright remains with the author until and if the paper is accepted for publication. The collection of the copyright forms at the beginning of the process is for the convenience of the publisher. Albert E. Patterson retains all rights and copyright to the paper MANU-21-1143 until and if the paper is accepted for publication by ASME. As of April 14, 2021 the paper is being reviewed but no decision has been made about publication. If the paper is eventually accepted, the copyright on the material in it (from Chapter 2) will be assigned to ASME by the author of this dissertation at that time. Therefore, no permission is needed at this time for that paper. Written permissions to reuse the other four papers can be seen in the following permission email.

4/14/2021

Mail - Patterson, Albert Edward V - Outlook

RE: Permissions for Paper Reuse in Dissertation

Beth Darchi <DarchiB@asme.org>

Wed 4/14/2021 9:18 AM

To: Patterson, Albert Edward V <pttrsnv2@illinois.edu>

Dear Mr. Patterson,

It is our pleasure to grant you permission to use **all or any part** of the following ASME papers:

- Patterson, A.E., Lee, Y-H., Allison, J.T. (2021). Generation and enforcement of process-driven manufacturability constraints: A survey of methods and perspectives for product design. Journal of Mechanical Design, 2021
- Patterson, A.E., Allison, J.T. (2019). Generation and mapping of minimally-restrictive manufacturability constraints for mechanical design problems, Paper number DETC2019-97386.
- Patterson, A.E., Lee, Y-H., Allison, J.T. (2019). Overview of the development and enforcement of process-driven manufacturability constraints in product design. Paper number DETC2019-97384.
- Patterson, A.E., Allison, J.T. (2018). Manufacturability constraint formulation for design under hybrid additive-subtractive manufacturing. Paper number DETC2018-85637

cited in your letter for inclusion in a dissertation to be published by University of Illinois at Urbana-Champaign.

Permission is granted for the specific use as stated herein and does not permit further use of the materials without proper authorization. Proper attribution must be made to the author(s) of the materials. **Please note:** if any or all of the figures and/or Tables are of another source, permission should be granted from that outside source or include the reference of the original source. ASME does not grant permission for outside source material that may be referenced in the ASME works.

As is customary, we request that you ensure full acknowledgment of this material, the author(s), source and ASME as original publisher.

As per ASME policy, we cannot grant permission to use any or all of the works of your journal paper "Minimally-restrictive manufacturability constraints in mechanical design: Mapping and enforcement" until after full publication with ASME. Once the paper has been published, you can then send a request for permission to use this paper. **PLEASE NOTE**, that we do not keep these requests on file. Once you have presented/published your paper then send the request for permission to [Permissions](#).

Many thanks for your interest in ASME publications.

Sincerely,

Beth Darchi
Publishing Administrator
ASME
2 Park Avenue
New York, NY 10016-5990

From: Patterson, Albert Edward V <pttrsnv2@illinois.edu>

Sent: Thursday, April 8, 2021 6:06 PM

To: permissions@asme.org

Subject: Permissions for Paper Reuse in Dissertation

WARNING: This Message Came From Outside of ASME. Do not click on links or attachments unless you know the content to be safe.

Dear ASME Permissions Office,

Re: Permission requests for ASME-copyrighted papers

<https://outlook.office.com/mail/inbox/id/AAQKAGFiMjAyZmY0LTlYnZgtNDgxNy1iZTlyLWQ2YjY0YWMwYjU4ZgAQAMPe3D8Fg1LoFJ%2Bp3qIkUk%3D> 1/3

4/14/2021

Mail - Patterson, Albert Edward V - Outlook

Before sending this email, I made a serious attempt to submit my request through the normal copyright permission system, but my requests were rejected. The error messages told me to email your office about my inquiry.

I have just completed my doctoral degree at the University of Illinois at Urbana-Champaign and am putting the final polishes on the dissertation before deposit, including gathering copyright permissions. One of my key chapters was built from work which I published (with the intention of using to satisfy dissertation requirements) in ASME conferences and journals from 2018 to present:

Patterson, A.E., Lee, Y-H., Allison, J.T. (2021). Generation and enforcement of process-driven manufacturability constraints: A survey of methods and perspectives for product design. *Journal of Mechanical Design* (not yet assigned to an issue). DOI: 10.1115/1.4050740.

Patterson, A.E., Allison, J.T. (2019). Generation and mapping of minimally-restrictive manufacturability constraints for mechanical design problems. ASME IDETC - 24th ASME Design for Manufacturing and the Life Cycle Conference, August 18-21, 2019, Anaheim, CA, USA. DOI: 10.1115/DETC2019-97386.

Patterson, A.E., Lee, Y-H., Allison, J.T. (2019). Overview of the development and enforcement of process-driven manufacturability constraints in product design. ASME IDETC - 24th ASME Design for Manufacturing and the Life Cycle Conference, August 18-21, 2019, Anaheim, CA, USA. DOI: 10.1115/DETC2019-97384.

Patterson, A.E., Allison, J.T. (2018). Manufacturability constraint formulation for design under hybrid additive-subtractive manufacturing. ASME IDETC - 23rd ASME Design for Manufacturing and the Life Cycle Conference, August 26-29, 2018, Quebec City, QC, Canada. DOI: 10.1115/DETC2018-85637.

And in one paper which is currently in review but for which we signed the copyright to ASME during submission:

Patterson, A.E., Allison, J.T. Minimally-restrictive manufacturability constraints in mechanical design: Mapping and enforcement. Currently under review with *Journal of Manufacturing Science and Engineering*. #MANU-21-1143. Copyright assigned to ASME on submission.

I am the main and corresponding author on all five of these papers. I am requesting official permission to reproduce the content of these papers (except for any figures to which ASME does not own the copyright) in my final dissertation. This dissertation will not be published officially outside of the normal university repository after deposit. The last page of the chapter in the final dissertation will clearly lay out that the work is copyrighted by ASME and reproduced with permission.

Thank you for your time!

Respectfully,

Albert E. Patterson
PhD Candidate (Industrial Engineering: Design and Manufacturing)

2020-2021 UIUC College of Engineering Mavis Future Faculty Fellow
TA - SE-311 Engineering Design Analysis

Engineering Systems Design Lab, Transportation Building 405
Department of Industrial and Enterprise Systems Engineering



<https://outlook.office.com/mail/inbox/id/AAQkAGFiMjAyZmY0LTlyNzgtNDgxNytiZTlyLWQ2YjY0YWMwYjU4ZgAQAMPe3D8Fg1LoFJ%2Bp3qIkUk%3D> 2/3

ELSEVIER LICENSE
TERMS AND CONDITIONS

Apr 10, 2021

This Agreement between Mr. Albert Patterson ("You") and Elsevier ("Elsevier") consists of your license details and the terms and conditions provided by Elsevier and Copyright Clearance Center.

License Number	5044431181633
License date	Apr 08, 2021
Licensed Content Publisher	Elsevier
Licensed Content Publication	Advances in Engineering Software
Licensed Content Title	Topology optimization with manufacturing constraints: A unified projection-based approach
Licensed Content Author	Sandro L. Vatanabe,Tiago N. Lippi,Cicero R. de Lima,Glaucio H. Paulino,Emilio C.N. Silva
Licensed Content Date	Oct 1, 2016
Licensed Content Volume	100
Licensed Content Issue	n/a
Licensed Content Pages	16
Start Page	97
End Page	112
Type of Use	reuse in a thesis/dissertation
Portion	figures/tables/illustrations
Number of figures/tables/illustrations	2
Format	both print and electronic
Are you the author of this Elsevier article?	No

ELSEVIER LICENSE
TERMS AND CONDITIONS

Apr 10, 2021

This Agreement between Mr. Albert Patterson ("You") and Elsevier ("Elsevier") consists of your license details and the terms and conditions provided by Elsevier and Copyright Clearance Center.

License Number	5045480094056
License date	Apr 10, 2021
Licensed Content Publisher	Elsevier
Licensed Content Publication	Computer Methods in Applied Mechanics and Engineering
Licensed Content Title	A level set method for topological shape optimization of 3D structures with extrusion constraints
Licensed Content Author	Hao Li, Peigen Li, Liang Gao, Li Zhang, Tao Wu
Licensed Content Date	Jan 1, 2015
Licensed Content Volume	283
Licensed Content Issue	n/a
Licensed Content Pages	21
Start Page	615
End Page	635
Type of Use	reuse in a thesis/dissertation
Portion	figures/tables/illustrations
Number of figures/tables/illustrations	1
Format	both print and electronic
Are you the author of this Elsevier article?	No

ELSEVIER LICENSE
TERMS AND CONDITIONS

Apr 10, 2021

This Agreement between Mr. Albert Patterson ("You") and Elsevier ("Elsevier") consists of your license details and the terms and conditions provided by Elsevier and Copyright Clearance Center.

License Number	5045480298292
License date	Apr 10, 2021
Licensed Content Publisher	Elsevier
Licensed Content Publication	Computer-Aided Design
Licensed Content Title	Minimum void length scale control in level set topology optimization subject to machining radii
Licensed Content Author	Jikai Liu,Huangchao Yu,Yongsheng Ma
Licensed Content Date	Dec 1, 2016
Licensed Content Volume	81
Licensed Content Issue	n/a
Licensed Content Pages	11
Start Page	70
End Page	80
Type of Use	reuse in a thesis/dissertation
Portion	figures/tables/illustrations
Number of figures/tables/illustrations	1
Format	both print and electronic
Are you the author of this Elsevier article?	No

ELSEVIER LICENSE
TERMS AND CONDITIONS

Apr 10, 2021

This Agreement between Mr. Albert Patterson ("You") and Elsevier ("Elsevier") consists of your license details and the terms and conditions provided by Elsevier and Copyright Clearance Center.

License Number	5045480574020
License date	Apr 10, 2021
Licensed Content Publisher	Elsevier
Licensed Content Publication	CIRP Journal of Manufacturing Science and Technology
Licensed Content Title	Design for Additive Manufacturing—Element transitions and aggregated structures
Licensed Content Author	Guido A.O. Adam,Detmar Zimmer
Licensed Content Date	Jan 1, 2014
Licensed Content Volume	7
Licensed Content Issue	1
Licensed Content Pages	9
Start Page	20
End Page	28
Type of Use	reuse in a thesis/dissertation
Portion	figures/tables/illustrations
Number of figures/tables/illustrations	1
Format	both print and electronic
Are you the author of this Elsevier article?	No

ELSEVIER LICENSE
TERMS AND CONDITIONS

Apr 10, 2021

This Agreement between Mr. Albert Patterson ("You") and Elsevier ("Elsevier") consists of your license details and the terms and conditions provided by Elsevier and Copyright Clearance Center.

License Number	5045480826276
License date	Apr 10, 2021
Licensed Content Publisher	Elsevier
Licensed Content Publication	Additive Manufacturing
Licensed Content Title	Powder bed fusion metrology for additive manufacturing design guidance
Licensed Content Author	Jared Allison,Conner Sharpe,Carolyn Conner Seepersad
Licensed Content Date	Jan 1, 2019
Licensed Content Volume	25
Licensed Content Issue	n/a
Licensed Content Pages	13
Start Page	239
End Page	251
Type of Use	reuse in a thesis/dissertation
Portion	figures/tables/illustrations
Number of figures/tables/illustrations	1
Format	both print and electronic
Are you the author of this Elsevier article?	No

ELSEVIER LICENSE
TERMS AND CONDITIONS

Apr 10, 2021

This Agreement between Mr. Albert Patterson ("You") and Elsevier ("Elsevier") consists of your license details and the terms and conditions provided by Elsevier and Copyright Clearance Center.

License Number	5045481006690
License date	Apr 10, 2021
Licensed Content Publisher	Elsevier
Licensed Content Publication	Robotics and Computer-Integrated Manufacturing
Licensed Content Title	Systematic approach for automated determination of parting line for die-cast parts
Licensed Content Author	Ranjit Singh,Jatinder Madan
Licensed Content Date	Oct 1, 2013
Licensed Content Volume	29
Licensed Content Issue	5
Licensed Content Pages	21
Start Page	346
End Page	366
Type of Use	reuse in a thesis/dissertation
Portion	figures/tables/illustrations
Number of figures/tables/illustrations	1
Format	both print and electronic
Are you the author of this Elsevier article?	No

Chapter 5 Figure Copyright Permissions

4/10/2021

RightsLink Printable License

ELSEVIER LICENSE
TERMS AND CONDITIONS

Apr 10, 2021

This Agreement between Mr. Albert Patterson ("You") and Elsevier ("Elsevier") consists of your license details and the terms and conditions provided by Elsevier and Copyright Clearance Center.

License Number	5045700073136
License date	Apr 10, 2021
Licensed Content Publisher	Elsevier
Licensed Content Publication	European Polymer Journal
Licensed Content Title	Anisotropic damage inferred to 3D printed polymers using fused deposition modelling and subject to severe compression
Licensed Content Author	Sofiane Guessasma,Sofiane Belhabib,Hedi Nouri,Omar Ben Hassana
Licensed Content Date	Dec 1, 2016
Licensed Content Volume	85
Licensed Content Issue	n/a
Licensed Content Pages	17
Start Page	324
End Page	340
Type of Use	reuse in a thesis/dissertation
Portion	figures/tables/illustrations
Number of figures/tables/illustrations	1
Format	both print and electronic
Are you the author of this Elsevier article?	No

ELSEVIER LICENSE
TERMS AND CONDITIONS

Apr 10, 2021

This Agreement between Mr. Albert Patterson ("You") and Elsevier ("Elsevier") consists of your license details and the terms and conditions provided by Elsevier and Copyright Clearance Center.

License Number	5045700339946
License date	Apr 10, 2021
Licensed Content Publisher	Elsevier
Licensed Content Publication	Additive Manufacturing
Licensed Content Title	Interlayer fracture toughness of additively manufactured unreinforced and carbon-fiber-reinforced acrylonitrile butadiene styrene
Licensed Content Author	Devin Young,Nelson Wetmore,Michael Czabaj
Licensed Content Date	Aug 1, 2018
Licensed Content Volume	22
Licensed Content Issue	n/a
Licensed Content Pages	8
Start Page	508
End Page	515
Type of Use	reuse in a thesis/dissertation
Portion	figures/tables/illustrations
Number of figures/tables/illustrations	1
Format	both print and electronic
Are you the author of this Elsevier article?	No

JOHN WILEY AND SONS LICENSE
TERMS AND CONDITIONS

Apr 10, 2021

This Agreement between Mr. Albert Patterson ("You") and John Wiley and Sons ("John Wiley and Sons") consists of your license details and the terms and conditions provided by John Wiley and Sons and Copyright Clearance Center.

License Number 5045691268657

License date Apr 10, 2021

Licensed Content Publisher John Wiley and Sons

Licensed Content Publication Advanced Engineering Materials

Licensed Content Title Tough, Additively Manufactured Structures Fabricated with Dual-Thermoplastic Filaments

Licensed Content Author Eric D. Wetzel, Ryan M. Dunn, Kevin R. Hart

Licensed Content Date Dec 17, 2019

Licensed Content Volume 22

Licensed Content Issue 4

Licensed Content Pages 7

Type of use Dissertation/Thesis

Requestor type University/Academic

Format Print and electronic

Portion Figure/table

Chapter 7 Figure Copyright Permissions

4/12/2021

RightsLink Printable License

ELSEVIER LICENSE TERMS AND CONDITIONS

Apr 12, 2021

This Agreement between Mr. Albert Patterson ("You") and Elsevier ("Elsevier") consists of your license details and the terms and conditions provided by Elsevier and Copyright Clearance Center.

License Number	5046641034426
License date	Apr 12, 2021
Licensed Content Publisher	Elsevier
Licensed Content Publication	Elsevier Books
Licensed Content Title	Gaseous Hydrogen Embrittlement of Materials in Energy Technologies
Licensed Content Author	M.R. Begley, J.A. Begley, C.M. Landis
Licensed Content Date	Jan 1, 2012
Licensed Content Pages	40
Start Page	286
End Page	325
Type of Use	reuse in a thesis/dissertation
Portion	figures/tables/illustrations